Norrin Signaling in Norrie Disease and Allelic Disorders

Dissertation

zur

Erlangung der naturwissenschaftlichen Doktorwürde (Dr. sc. nat.)

vorgelegt der

Mathematisch-naturwissenschaftlichen Fakultät

der

Universität Zürich

von

Nikolaus F. Schäfer

aus

Deutschland

Promotionskomitee

Prof. Dr. Stephan Neuhauss (Vorsitz)

Prof. Dr. Wolfgang Berger (Leitung der Dissertation)

Prof. Dr. Christian Grimm

Zürich, 2009

Declaration

I declare that the present thesis was composed by myself and the enclosed experimental work was performed on my own as indicated in the respective chapters.
This dissertation has not been submitted for any other degree or professional qualification except as specified.

Nikolaus F. Schäfer, Zürich 2009

Für meine Familie

Abbreviations

5-HT	5-hydroxytryptamine; serotonin
A	adenine
aa	amino acid
Aass	*aminoadipate-semialdehyde synthase*
Abcb1a	*ATP-binding cassette, sub-family B (MDR/TAP), member 1A*
Actb	*beta actin*
ad	autosomal dominant
Adm	*adrenomedullin*
Agtrl1	*angiotensin receptor-like 1*
AMD	age related macula degeneration
ApoD	*apolipoprotein D*
ar	autosomal recessive
ARVO	Association for Research in Vision and Ophthalmology
β-ME	2-mercaptoethanol
BCA	bicinchoninic acid
BLAST	Basic Local Alignment Search Tool
BLAT	BLAST-Like Alignment Tool
Bmp4	bone morphogenetic protein 4
bp	basepair/s
BSA	bovine serum albumin
C	cytosine
Ctnnb1	β-catenin
CB	ciliary body
CD	Coats' disease
CDS	coding sequence
cDNA	complementary DNA
Centd3	*centaurin, delta 3*
ChAT	choline acetyltransferase
Cldn5	*claudin 5*
CNS	central nervous system
CNV	copy number variation
Ct	cycle threshold
ddH_2O	double distilled water
ddNTP	dideoxy nucleotide-triphosphate
DAPI	4',6-diamidino-2-phenylindole (fluorescent dye labeling DNA)
DEPC	diethylpyrocarbonate
DKK	dickkopf
DNA	deoxyribonucleic acid
DNase	deoxyribonuclease
dNTP	deoxy nucleotide-triphosphate
DTT	dithiothreitol / Cleland's reagent
EB	elution buffer (10 mM Tris-HCl, pH 8.5)
ED	Eales' disease
EDTA	ethylenediaminetetraacetic acid
EGF	epidermal growth factor
EJN	European Journal of Neuroscience
EM	electron microscope
ENU	N-ethyl-N-nitrosourea (a potent mutagen)
ERG	electroretinography
ESE	exonic splice enhancer

8 ABBREVIATIONS

ESR	exonic splicing regulatory elements
EtBR	ethidium bromide
EtOH	ethanol
EVR	exudative vitreoretinopathy
FEVR	familial exudative vitreoretinopathy
FPLC	fast protein liquid chromatography
fwd	forward
FZD4	frizzled homolog 4
G	guanine
Gapd	glyceraldehyde-3-phosphate dehydrogenase
gDNA	genomic deoxyribonucleic acid
HBM	high bone mass
HRP	horseradish peroxidase
IgG	immunoglobulin G
IHC	immunohistochemistry
IMAC	immobilized metal ion affinity chromatography
INL	inner nuclear layer
IOVS	Investigative Ophthalmology and Vision Research
IP	Incontinentia pigmentii
IPL	inner plexiform layer
IS	inner segment
kb	kilobasepair/s
kDa	kilo Dalton
ko	knockout
LB	Luria-Bertani broth, bacterial growth medium
Lef1	lymphoid enhancer binding factor 1
LRP5	low density lipoprotein receptor-related protein 5
LRP5L	low density lipoprotein receptor-related protein 5-like
M	methionine or molar
MAOA/B	mono amine oxidase A / B
MAPK	mitogen-activated protein kinase
MF	manifesting female
miRNA	micro RNA
min	minutes
MR	mental retardation
mRNA	messenger RNA
NCBI	National Center for Biotechnology Information
ND	Norrie Disease
NDP	Norrie disease pseudoglioma
Ndph	Norrie disease pseudoglioma homolog
NE	norepinephrine
NF	neurofilament
NFL	nerve fiber layer
NGS	normal goat serum
NMD	nonsense-mediated mRNA decay
NSS	non-specific serum
NV	neovascularization
OCT	optimal cutting temperature
OD_{562}	optical density at 562nm
OIR	oxygen induced retinopathy
OMIM	Online Mendelian Inheritance in Man
o/n	over night
ONL	outer nuclear layer
OPL	outer plexiform layer
OPPG	osteoporosis pseudoglioma syndrome
ORF	open reading frame

OS	outer segment
p7	postnatal day 7
PAS	polyadenylation signal
PBS	phospate buffered saline
PBST	phospate buffered saline with Tween® 20
PCR	polymerase chain reaction
pDNA	plasmid DNA
PI	propidium iodide
PFA	paraformaldehyde
Pfu	*Pyrococcus furiosus*
PFV	persistent fetal vasculature
PHPV	persistent hyperplastic primary vitreous
Plvap	plasmalemma vesicle associated protein
Pola2	*polymerase, alpha 2*
Prdm9	*VPR domain containing 9*
PRDX	primary retinal dysplasia, X-linked
PVDF	polyvinyliden difluoride
qRT-PCR	quantitative reverse transcription polymerase chain reaction
RB	retinoblastoma
rev	reverse
RGC	retinal ganglion cell layer
RIN	RNA integrity number
RIPA	radioimmunoprecipitation assay buffer
RNA	ribonucleic acid
RNase	ribonuclease
ROP	retinopathy of prematurity
RP	retinitis pigmentosa
RPE	retinal pigment epithelium
rpm	revolutions per minute
rRNA	ribosomal RNA
RS	retinoschisis
RT	room temperature
RT-PCR	reverse transcription polymerase chain reaction
SDS-PAGE	sodium dodecyl sulfate polyacrylamide gel electrophoresis
Slc38a5	solute carrier family 38, member 5
SNAT5	amino acid transporter system N2 (*Slc38a5* protein)
SNP	single nucleotide polymorphism
T	thymine or threonine
TAE	tris-acetate / EDTA
Taq	*Thermus aquaticus* polymerase
Tcf3	transcription factor 3 (*Tcf7l1*)
Tcf7l2	transcription factor 7-like 2 (*Tcf4*)
TE	tris-EDTA
TEMED	tetramethylethylenediamine
Tris	2-amino-2-hydroxymethyl-propane-1,3-diol / $(HOCH_2)_3CNH_2$
U	uracil
UTR	untranslated region (non-coding part of an exon)
VI	venous insufficiency
VPA	valproic acid
VRNI	Neovascular inflammatory vitreoretinopathy
Vwf	*von Willebrand factor homolog*
WB	Western blot
WGA	whole genome amplification
Wnt	wingless-related MMTV integration site family of genes
wt	wild type
Xl	X-linked

Summary

Norrie disease (ND) is an X-linked, recessive disorder that presents with congenital blindness, progressive deafness and, to a certain degree, mental retardation. It is caused by mutations in the Norrie disease pseudoglioma (*NDP*) gene, which has also been associated with a variety of other recessive and sporadic vitreoretinal diseases, including exudative vitreoretinopathy (EVR), retinopathy of prematurity (ROP, stages 4b and 5) and Coats' disease (CD). Mutations in norrin (the *NDP*–protein) cause a defect of vascular development in the retina, which secondarily leads to inner retinal hypoxia and the associated clinical features. Previously, norrin was shown to be a high affinity ligand of the receptor-pair FZD4 and LRP5, and to activate the canonical Wnt-pathway in cell culture, eventually leading to transcriptional regulation of target genes.

However, even though a possible molecular mechanism for Norrin signaling has been proposed, it is still unknown whether this pathway is actually affected *in vivo*, whether other pathways might be involved in the course of the pathogenesis, and how norrin contributes to the development of the retinal vasculature. To address these questions, several potential downstream target genes of norrin signaling were identified in the course of this thesis, differential Wnt-signaling was investigated in a mouse model, and a small patient group was screened for mutations in candidate genes. The results confirm norrin's role in blood vessel development, and help to explain not only the ocular, but also the brain phenotype. Expression of two genes, *Plvap* and *Slc38a5*, is considerably altered in retinal development of norrin knockout mice and may reflect or contribute to the pathogenesis of the disease. In particular, ectopic expression of Plvap is consistent with hallmark disease symptoms in mouse and man. Contrary to the cell culture findings, canonical Wnt-signaling could not be shown to be prominently involved. Instead, involvement of other pathways, such as the mitogen-activated protein kinase (MAPK) pathway and serotonin-mediated signaling, are discussed. Several potential modifying genes for ND were identified, and recombinant norrin protein was produced in eukaryotic cells to facilitate functional and structural analyses in the future.

Zusammenfassung

Die Norrie Krankheit ist eine X-chromosomal vererbte, rezessive Form angeborener Blindheit, die mit progressiver Schwerhörigkeit und in manchen Fällen mit geistiger Behinderung einhergeht. Sie wird durch Mutationen im *NDP*-Gen (Norrie disease pseudoglioma) hervorgerufen, die auch mit einigen anderen rezessiven und spontanen Vitreoretinopathien assoziiert wurden, unter anderem exsudativer Vitreoretinopathie, Frühgeborenenretinopathie (Stadien 4b und 5) und Morbus Coats'. Mutationen in Norrin (dem *NDP*-Protein) verursachen einen Defekt in der Entwicklung retinaler Blutgefässe, der sekundär zu Hypoxie in der inneren Netzhaut und den beobachteten klinischen Bildern führt. In Zellkulturexperimenten wurde zuvor gezeigt, dass Norrin ein hochaffiner Ligand für das Rezeptorenpaar FZD4 und LRP5 ist, und den kanonischen Wnt-Signalweg aktivieren kann, was schliesslich zur transkriptionellen Regulation von Zielgenen führt.

Doch obwohl ein möglicher molekularer Mechanismus für Norrin vorgeschlagen wurde, weiss man bisher nicht, ob dieser Signalweg auch tatsächlich *in vivo* betroffen ist, ob andere Kaskaden ebenfalls eine Rolle in der Pathogenese spielen, und wie Norrin zur Entwicklung des retinalen Gefässsystems beiträgt. Um diese Fragen zu beantworten, wurden im Laufe dieser Arbeit mehrere mögliche, durch Norrin regulierte Zielgene identifiziert, die Aktivität des Wnt-Signalwegs in einem Mausmodell analysiert, und eine kleine Patientengruppe auf Mutationen in Kandidatengenen untersucht. Die Ergebnisse bestätigen Norrins Rolle in der Blutgefässentwicklung und helfen nicht nur den Augen-, sondern auch den Gehirnphänotyp zu verstehen. Die deutlich veränderte Expression zweier Gene, *Plvap* und *Slc38a5*, während der Netzhautentwicklung in Norrin-knockout Mäusen könnte den Krankheitsverlauf widerspiegeln oder sogar eine Beteiligung an der Pathogenese der Krankheit nahelegen. Speziell die ektopische Expression von Plvap stimmt mit Hauptsymptomen in Maus und Mensch überein. Im Gegensatz zu den Zellkulturresultaten konnte keine bedeutende Mitwirkung des Wnt-Signalwegs gezeigt werden. Stattdessen wird die Beteiligung anderer Signalwege, wie z.B. der MAP-Kinase-Kaskade (mitogen-activated protein) oder Serotonin-vermittelter Signalübertragung, diskutiert. Mehrere mögliche Modifikatorgene für die Norrie Krankheit wurden identifiziert, und rekombinantes Norrin wurde in einem eukaryotischen Zellsystem hergestellt, um zukünftige funktionelle und strukturelle Analysen zu ermöglichen.

Table of Contents

1. Introduction

1.1 The eye

The eye probably is the most important sense organ for human beings. It enables us to detect light and provides us with rich and detailed vision, including the ability to detect location, size, shape, direction and speed of an object in our environment, to discriminate 10 million colors and, due to the binocular vision and the overlapping fields of sight, to perceive depth. Light enters the eye through the cornea, a specialized, transparent part of the sclera, which is the fibrous tissue that delineates and shapes the eyeball (Figure 1). It then passes the pupil, an opening that can be adjusted in size through contraction of a circular muscle (the iris) to admit more or less light to enter the eye depending on environmental conditions. The light is then projected through the lens and the vitreous (the gel-like content taking up most space in the eye) onto the retina, which is the sensory tissue lining the inner surface of the eye. Here, external light stimuli are translated into electrical pulses that are transmitted to the brain through the optic nerve.

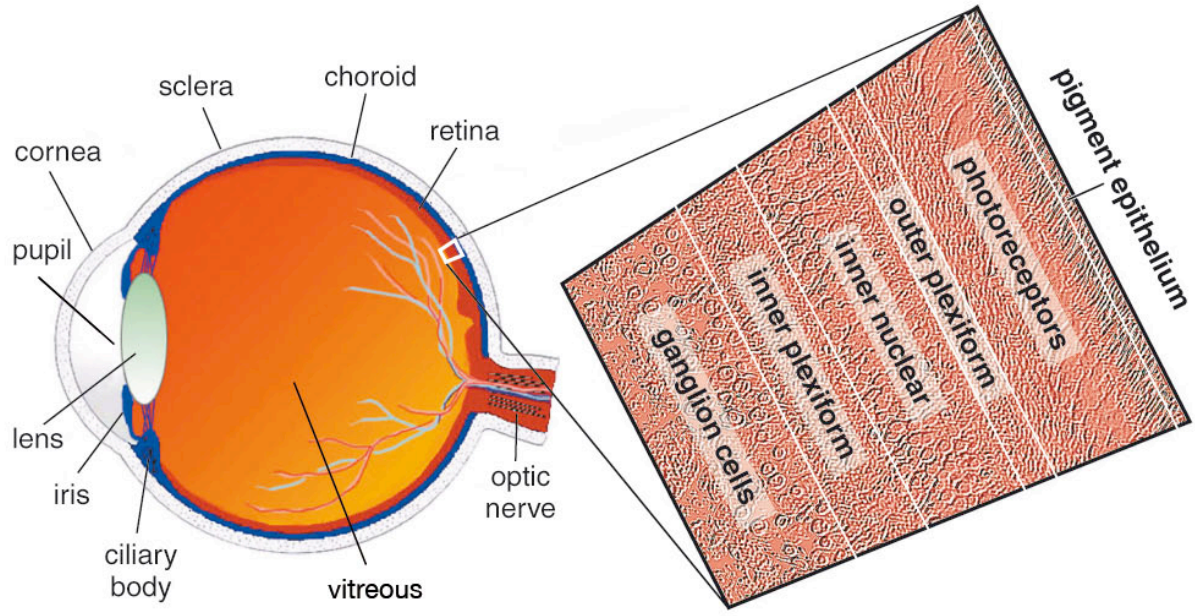

Figure 1 Schematic mid-sagittal cross-section of the human eye (Kolb, 2003). The enlargement on the right side shows the layered structure of the retina.

1.1.1 The retina

The retina (including the optic nerve) develops from outgrowths of the embryonic brain and thus is considered part of the central nervous system (CNS). It is a thin structure, not thicker than 0.5mm, which is organized in three neuronal and two synaptic (plexiform) layers. The outermost layer (outer nuclear layer; ONL) consists of two types of light sensitive photoreceptors: the rods and the cones. The ~120 million rods in the human retina are responsible for dim light vision, while the ~7 million cones are responsible for daylight and color vision. Curiously, the sensory cells in vertebrates are not located at the surface of the retina; in this inverted retina light has to pass through all downstream neurons before it reaches the light sensitve cells. One immediate reason

is that the photoreceptors have to be in contact with the light absorbing retinal pigment epithelium (RPE), which restores the photopigment retinal. Retinal, or vitamin A aldehyde, is necessary for the conversion of electromagnetic radiation (light) into neuronal (electric) impulses. Without the direct contact between photoreceptors and pigment epithelium cells, the ablity to perceive light could not be maintained. The pigment granules of the RPE further prevent photoreceptors from radiation damage by absorbing excessive light. In the outer plexiform layer, visual information is then relayed through synapses between photoreceptors and interneurons located in the inner nuclear layer (INL), the bipolar cells. First stages of image processing are already performed at this synaptic level. In the inner plexiform layer (IPL), the bipolar cells then connect to retinal ganglion cells (RGC), whose axons constitute the optic nerve and transmit axon potentials to the visual centers in the brain. There are, however, about 70 different cell types in the retina, and the retinal circuitry is far more complex than described here.

The retina has the highest oxygen demand of all human tissues and therefore needs a well-developed blood supply (Yu et al., 2001). Therefore, the retina is supported by two blood vessel systems: the choroid and the retinal vasculature. The choroid vessel system lies between the RPE and the sclera and nourishes RPE and photoreceptor cells. The inner retina (ganglion cells and bipolar cells) is supplied by the retinal vasculature. It consists of three networks: A superficial network in the nerve fiber layer (above the ganglion cell layer); a deep network at the border from the INL to the outer plexiform layer; and an intermediate network at the border from the INL to the inner plexiform layer (Figure 2).

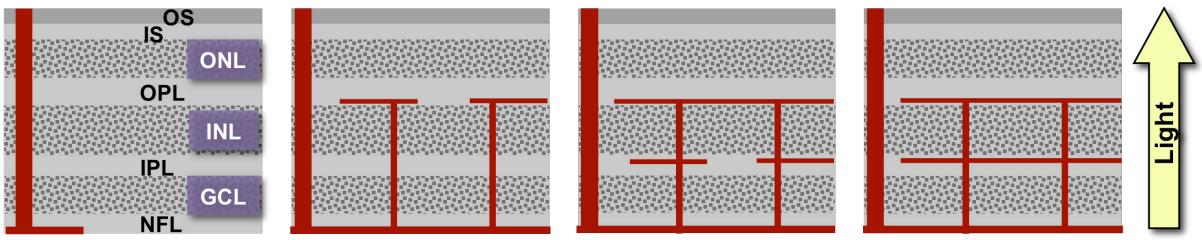

Figure 2 Schematic diagram of the development of the retinal vasculature (adapted from Xu and Wang et al., 2004). The superficial network emerges from the central artery/vein through radial outgrowth of vessels in the nerve fiber layer. Then, the deep vasculature starts to develop at the INL/OPL border after perpendicular sprouting of vessels into the retina. Finally, an intermediate plexus forms at the border of INL and IPL. *OS:* outer segment; *IS:* inner segment; *ONL:* outer nuclear (photoreceptor) layer; *OPL:* outer plexiform layer; *INL:* inner nuclear layer; *IPL:* inner plexiform layer; *GCL:* ganglion cell layer; *NFL:* nerve fiber layer

1.2 The brain

The brain is the center of the nervous system and integrates sensory information with memory to generate behaviour in response to the environment. While the function of single nerve cells and their synapses is considerably understood, comprehension of the complex neural network of ~100 billion neurons in the human is demanding, and is subject of uncounted studies investigating cognitive functions in development and disease. The brain can be divided in numerous areas that are morphologically and functionally distinct. In the following paragraph, I want to adress some selected regions that are of interest in this work (Figure 3).

The cortex is the outermost layer of the forebrain, and is important for awareness, consciousness, memory, thought, and language. It is the phylogenetically most recent part of the brain, and distinguishes mammals from lower vertebrates by facilitating enhanced cognitive functions. Further evolutionary gain of brain mass lead to folding of the cortex in higher mammals, which is a conspicuous difference between the human and the mouse brain. The hippocampus is a morphologically well defined structure of the forebrain, and is located beneath the cortical surface. It is primarily involved in long-term memory and spatial navigation. The part of the brain mainly known to be important for motion control and integration of sensory perception is the cerebellum, although it has also been shown to be involved in attention and memory. The olfactory bulb, the most rostral part of the murine brain, relays sensory information about odors from the nose to the brain, and is necessary for smelling. The brain stem is the evolutionary oldest part of the brain and in mammals is important for controlling and maintaining basic body functions, like regulation of cardiac and respiratory function, consciousness and the sleep-wake cycle. The pituitary gland is an endocrine gland located inferior to the hypothalamus, to which it is functionally linked, and regulates numerous body functions like growth or blood pressure through the production of hormones.

1.2.1 The cerebellum

The cerebellum receives input from the brainstem and engages in movement control by projecting to all upper motor neurons via the deep cerebellar nuclei. This information flow through the cerebellum is modulated by a feedback system located in the cerebellar cortex (Figure 3 D). In contrast to the cerebral neocortex, which is organized in six horizontal layers, the cerebellar cortex can be divided in three layers. The innermost layer is the granular layer, which contains granule and Golgi cells. The granule cells receive their excitatory input from Mossy fibers, which also signal on the deep cerebellar nuclei, and receive negative feedback through Golgi cells. Granule and Golgi cells project axons into the outermost cerebellar layer, the molecular layer. Projections of granule cells, also known as parallel fibers, form hundreds of thousands of glutamatergic synapses with Purkinje cell dendrites. These cells make up the middle layer of the cerebellar cortex, the Purkinje cell layer. They are exceptionally large and represent the main integrative neurons of the cerebellum, projecting back on the deep cerebellar nuclei to form inhibitory (GABAergic) synapses. Purkinje cells also receive direct input from the brain stem via climbing fibers, which in contrast to parallel fibers only contact a single Purkinje cell. Besides the enormous dendritc trees of the Purkinje cells, the

molecular layer further contains two inhibitory interneuron types, the stellate and the basket cells, which also make synapses with the Purkinje cells.

Although the cerebellum's classical role is movement control, cerebellar lesions can also result in mental retardation and often in epileptic seizures (Johnsen et al., 2002; Boltshauser, 2004).

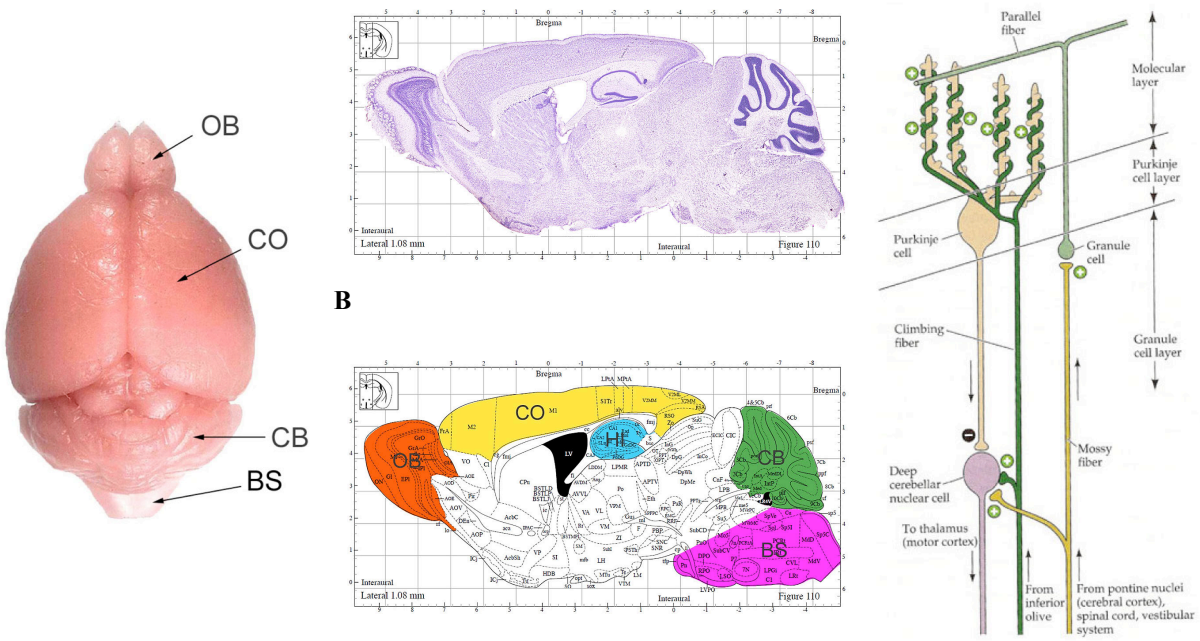

A **C** **D**

Figure 3 The mouse brain. **(A)** Superior view of an isolated mouse brain (source: www.nervenet.org). Note the smooth appearance of the cortex, which in contrast is folded in humans. **(B)** Nissl-stained sagittal section through a mouse brain. Rostral is on the left, superior is on top. **(C)** Scheme of the section presented in (B). Brain areas mentioned in this work are highlighted. *BS*: brain stem; *CB*: cerebellum; *CO*: cortex; *HI*: hippocampus; *OB*: olfactory bulb. (modified from Paxinos and Franklin, 2001, and adapted from Masterthesis Hänseler, 2008) **(D)** Neuronal circuitry scheme of the cerebellum. Movement related information is transferred from the brain stem to motor areas in the neocortex through the deep cerebellar nuclei. These signals are modulated in the three-layered cerebellar cortex through inhibitory signals from Purkinje cells, which integrate sensorimotor information from hundreds of thousands of granule cells. This cell type is the most abundant in the CNS, accounting for about 70% of all neurons (Source: Purves et al., 2004).

1.3 Norrie disease and allelic disorders

1.3.1 Blindness

Blindness (amaurosis) is a severe handicap that affects between 0.3% (legally blind) and 1.2% (low vision) of the European population (WHO report 2008; http://www.who.int/mediacentre/factsheets/fs282/en). About 10% of all blindness cases in industrial nations are congenital, mainly caused by hereditary retinochoroidal dystrophies. The incidence of these usually monogenic disorders has been estimated 1:4000 in Germany (Kellner et al., 2004). While most forms of blindness (cataract, glaucoma, corneal opacity, diabetic retinopathy, vitamin A deficiency, infectious causes like trachoma and onchocerciasis) can be treated or prevented, treatment of hereditary forms is limited. Thus, the primal mission for handling of these diseases is an unambiguous differential diagnosis through molecular genetic testing, followed by investigation of the pathophysiology. This may ultimately lead to the development of new therapeutic strategies like gene therapy (Bainbridge et al., 2008). At present, genetic counseling and follow-up examinations is all that can be provided to patients immediately.

1.3.2 Norrie disease and allelic disorders

In this thesis, I aimed to add further knowledge to the understanding of the pathogenesis of a subgroup of hereditary retinal diseases that are caused by variants in the Norrie disease pseuoglioma (*NDP*) gene and that may be subsumed under the umbrella term "exudative vitreoretinopathies" (EVR). This group of diseases is characterized by a high phenotypic variability, which complicates the diagnosis and the prediction of the impact of the disease on the individual patient.

The common feature of EVRs is retinal hypoxia, which secondarily leads to tissue damage. It is likely caused by a defect development of the retinal blood vessel system, ranging from symptom-free, small avascular peripheral regions to nearly complete avascularity of the retina (Berger and Ropers, 2001). The existing vessels become leaky, and intra- and subretinal lipid accumulation may ultimately lead to exudative retinal detachment. In addition, regression of the hyaloid vessel system, a transient network nourishing the developing lens, is often impaired. Remainders of these vessels may appear as retrolental structures that can exert tractional forces on the retina, which can lead to tractional retinal detachment. Many clinical descriptions of patients have been published with slightly different symptoms, often postulating a distinct disease, although it later could be shown that all patients harbour mutations in the *NDP* gene. However, exudative vitreoretinopathies are heterogenous. At present, two other genes have been associated with this group: the seven-transmembrane-domains receptor Frizzled-4 (*FZD4*), and the gene for the low-density lipoprotein receptor-related protein 5 (*LRP5*), while more, possibly disease-modifying genes will likely be identified in the future. In the following paragraph, I want to address the different clinical pictures that are associated with *NDP* mutations.

1.3.2.1 Norrie disease (ND)

Norrie disease (ND) first has been described by the Danish ophthalmologist Gordon Norrie in 1927, who examined a pair of brothers who suffered from congenital blindness (Norrie, 1927). The disease was given his name by Mette Warburg in 1961 (Warburg, 1961), further reporting on a Danish family with 7 affected males suffering from pseudotumour of the retina. In contrast to the patients described by Norrie himself, Warburg found that 5 of her patients encountered progressive hearing loss in addition to their visual impairment, and 4 were also mentally retarded. Following her first report in 1961, Warburg examined 8 more families in the years after (Warburg, 1963; Warburg, 1966; Warburg, 1968), and showed that the disease is inherited X-chromosomal recessive. She also noted a high variability of the clinical presentation. In 1992, linkage analysis and subsequent positional cloning lead to the identification of a locus on the short arm of chromosome X that co-segregated with the disease and henceforth was termed *NDP* – Norrie disease pseudoglioma (Berger et al., 1992; Chen et al., 1992). Prevalence of Norrie disease is rare, with only one in 100'000 individuals affected (Chen et al., 1992).

The first visible symptom and hallmark feature of Norrie disease is bilateral leukocoria, which can be recognized by a yellowish, opaque pupillary reflex soon after birth (Figure 4A). It is caused by retrolental masses of fibrovascular tissue, which at first glance are hard to differentiate from a retinal tumour and thus are commonly referred to as pseudoglioma (Figure 4B). In a progressed stage of the disease, the eye becomes atrophic and the globe shrinks (Figure 4C).

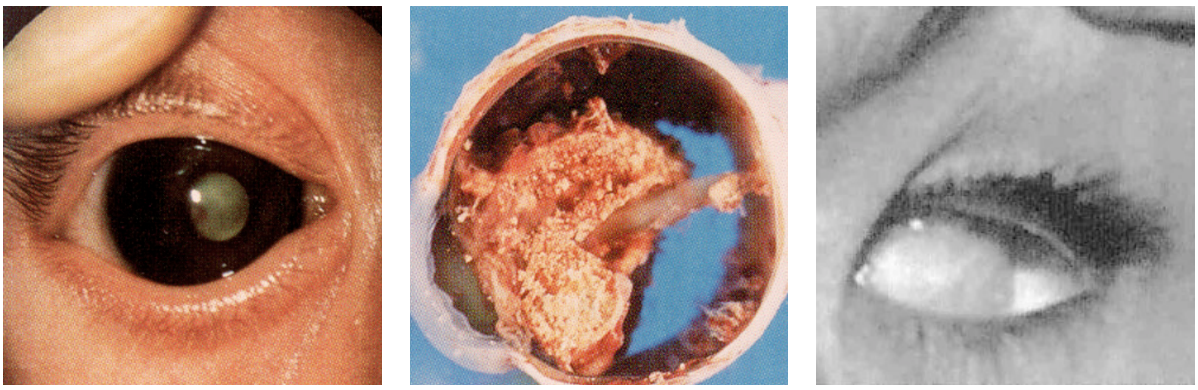

A **B** **C**

Figure 4 Clinical presentation of the ocular ND phenotype. **(A)** The hallmark feature and first visible clinical sign of ND is leukocoria, a yellowish pupillary reflex (Chynn et al., 1995). The image shows the affected eye of an 1-month-old patient. **(B)** The same eye as in (A) after it has been enucleated at the age of 2 months due to suspicion of retinoblastoma. **(C)** Eye of a 10-year-old patient showing shrinkage of the eye bulb (phthisis bulbi) (Khan et al., 2004).

In a less severe form, these retrolental masses can also resemble persistent fetal vasculature (PFV), which includes remaining hyaloid vessels and vitreoretinal hemorrhages. Additional ocular features include retinal folding and retinal detachment, which have been described in detail in a publication reporting on a histopathologic examination of an ND patient's eye that has been enucleated at the age of 6 months (Schroeder et al., 1997). Fibrovascular proliferation in the vitreous, but not in the retina,

seemed to cause progressive hypoplasia and disorganization of the inner retinal layers. The authors postulated that formation of rosette-like structures in the photoreceptor cell layer, retinal folding, and retinal detachment resulted from tractional forces caused by these fibrovascular masses.

Secondarily, a cataract may develop, and the cornea, iris, ciliary body, and retinal pigment epithelium also become involved.

In addition to the hallmark ocular features, deafness and mental retardation (MR) are frequently noted. MR manifests in up to fifty percent of the patients early in childhood, whereas progressive hearing loss typically is first diagnosed in the second or third decade of life. Warburg estimated the prevalence of the latter in about one third of the patients (Warburg, 1966), but a recent report suggests a (variable) penetrance of 100% (Halpin et al., 2005). A possible explanation for this discrepancy could be the late on-set of hearing impairment, and a lack of follow-up studies on ND patients.

1.3.2.2 Coats' disease (CD)

Coats' disease (CD) first has been described by George Coats in 1908. The classical form is defined through a sporadic, unilateral form of abnormal retinal vascular development (retinal telangiectasis) that results in exudative retinal detachment (Figure 5). It almost exclusively affects males. An excellent review of the literature has been published by Muletarow who states, "The general assumption is that CD is a connatal ophthalmologic disease with no familial occurrence and no manifestation of vascular anomalies in other organs." (Muletarow et al., 2004). However, 192 of 283 patients described until 2004 showed additional pathologic features. This group exhibited no gender predisposition, and further presented mainly with a bilateral eye phenotype. This suggests the conclusion that CD is often diagnosed only on the basis of the morphologic definition, and thus rather describes an eye phenotype, not a disease, with Coats'-like unspecific alterations of the retinal vasculature.

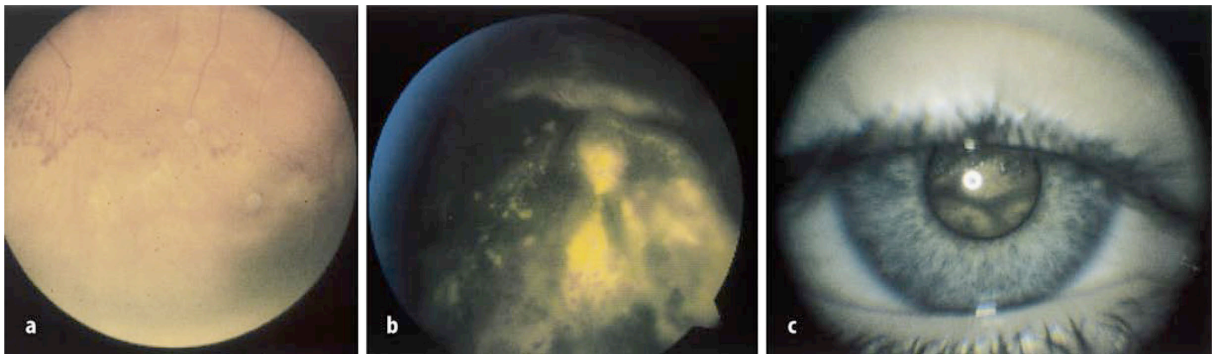

Figure 5 Coats' disease. **(A)** The fundus picture shows telangiectatic vessels and an avascular periphery. **(B)** Retinal exudates in the proximity of abnormal vessels. **(C)** Leukocoria as a result of exudative retinal detachment. (Source: Muletarow et al., 2004)

For example, CD has been diagnosed in patients who in addition to their eye phenotype exhibited alterations in the brain, such as calcifications of the white matter (Goutieres et

al., 1999; Révész et al., 1992; Rossazza et al., 1983; Tolmie et al., 1988), cerebellar atrophy (Kajtár et al., 1994), cerebellar ataxia (Goutieres et al., 1999; Révész et al., 1992; Tolmie et al., 1988), palsy of the 6th brain nerve (Gass et al., 1991), as well as changes in the cerebral vasculature, which were characterized by a reduced development of the deep venous system in favor of a prominent superficial venous plexus (Robitaille et al., 1996). Further, CD patients suffering from epileptic seizures (Blum et al., 1994; Goutieres et al., 1999; Rossazza et al., 1983; Scholz et al., 1997; Tolmie et al., 1988; Wilensky et al., 1976) and mental retardation have been described (Burch et al., 1980; Folk et al., 1981; Matsuzaka et al.; 1986; Révész et al., 1992; Rossazza et al., 1983; Scholz et al., 1997; Skuta et al., 1987; Small, 1968). Growth delay was described in 6 CD patients (reviewed in Muletarow et al., 2004).

CD also has been proposed to be a secondary effect to retinitis pigmentosa (RP), which has been diagnosed in 58 of the 283 CD patients (Koshibu et al., 1979; Witschel, 1974). This might be a direct effect of the degenerating retina on the vasculature through release of factors that trigger the increased vessel leakiness, or an indirect effect secondary to inflammation.

Taken together, many of the patients diagnosed with CD who exhibit extraocular symptoms in the brain or ear could possibly also be described as ND patients. This hypothesis has been supported by the finding of an *NDP*-mutation in the enucleated eye of a Coats' patient (Black et al., 1999). Linking the diagnosis of CD to the morphological features, those authors postulated that Coats' disease can be considered as a unilateral, non-syndromic form of Norrie disease that is likely caused by a somatic *NDP* mutation in the affected eye (Black et al., 1999). In the case of patients without gender predisposition and with a bilateral phenotype, I suspect that FEVR would be a better diagnosis.

1.3.2.3 Episkopi blindness

A large greek family with an X-linked form of blindness living in Episkopi, Cyprus, has been described in 1959 (Taylor et al., 1959). Warburg speculated already in her first publication about ND (Warburg, 1961) that this clinical entity could be another, non-syndromic presentation of Norrie disease. In 1992, this presumption could be substantiated, when it was shown that Episkopi blindness and ND mapped to the same genomic region (Wolff et al., 1992).

1.3.2.4 X-linked recessive primary retinal dysplasia (PRDX)

X-linked recessive primary retinal dysplasia (PRDX) is another clinical description that has been linked to Norrie disease locus (Ravia et al., 1993; Zhu and Hussels-Maumanee, 1994). PRDX describes a condition characterized by abnormal proliferation of retinal tissue, most likely neurons or glial tissue, that leads to retinal folds or glioma, but has no extraocular symptoms. It was diagnosed in a family with five affected males, who only presented with an eye phenotype, and two carrier females with minimal symptoms. Because of the lack of extraocular features and the penetrance in the carrier females, ND was initially rejected as diagnosis (Godel and Goodman, 1981). However, linkage analysis of the family later suggested that the PRDX gene and *NDP* map to the same genetic region (Ravia et al., 1993), suggesting that PRDX could be caused by mutations in

NDP. In addition, the description of the retinal phenotype correlates well with the hypoplastic and disorganized inner retina found in a patient with an *NDP* mutation (Schroeder et al., 1997).

1.3.2.5 Persistent hyperplastic primary vitreous (PHPV) / Persistent fetal vasculature (PFV)

Persistent hyperplastic primary vitreous (PHPV) often has been described as a disease. However, it has been suggested that it rather describes a symptom, which in addition should more accurately be termed persistent fetal vasculature (PFV) (Figure 6; Goldberg, 1997). The classical description includes white, vascularized tissue covering all or part of the posterior part of the lens; centrally dragged ciliary processes; intravitreal hemorrhages; persistence of the hyaloid artery; secondary glaucoma caused by swelling of the lens; and retinal detachment. Corneal opacifications, cataract, and persistence of the papillary membrane are also often observed. PFV has often been mentioned in the clinical description of patients diagnosed with ND or similar diseases, and *NDP*, *FZD4*, and *LRP5* mutations have been found in patients diagnosed with PHPV/PFV (Gong et al., 2001; Wu et al., 2007; Aponte et al., 2009; Robitaille et al., 2009).

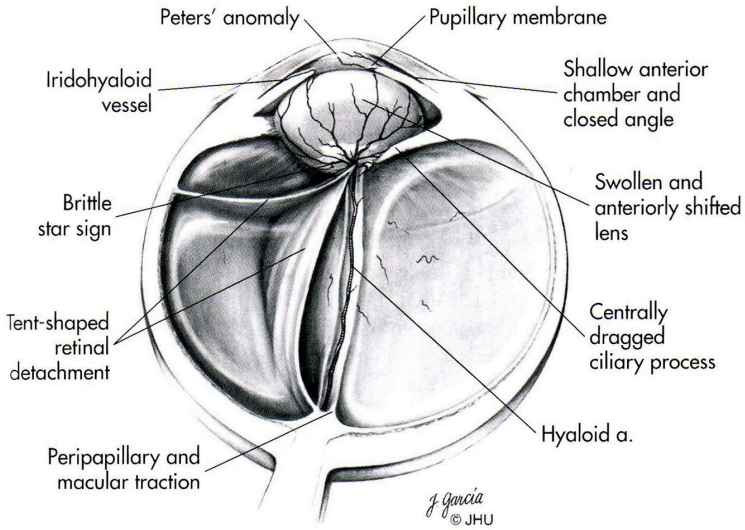

Figure 6 Spectrum of clinical features summarized under the term „persistent fetal vasculature" (PFV). (Picture taken from Goldberg, 1997)

1.3.2.6 Familial exudative vitreoretinopathy (FEVR)

Familial exudative vitreoretinopathy (FEVR), or Criswick-Schepens syndrome, is a slowly progressive congenital blinding disorder characterized by an incomplete peripheral vascularization of the retina (Criswick and Schepens, 1969) and vitreous abnormalities resembling ROP. This defect in blood vessel development entails a highly variable phenotype due to secondary complications like vitreoretinal traction, retinal folds, or hemorrhages, which can range from symptom-free conditions to severe retinal detachment (Canny and Oliver, 1976; Laqua et al., 1980). High phenotypic similarity of FEVR to mild forms of ND lead to the statement that „clinically, Norrie Disease and XEVR appear to be different progressed stages of the same disease" (Kellner et al., 1996). Most

cases are autosomal dominant, but X-linked recessive and sporadic cases have also been reported. Indeed, in case of X-linked inheritance, FEVR can be synonymous with non-syndromic ND, as mutations in *NDP* have been associated with FEVR (EVR2; Chen et al., 1993). In addition, two autosomal genes have been associated with FEVR: Frizzled-4 (*FZD4;* EVR1; Robitaille et al., 2002), and low-density lipoprotein receptor-related protein 5 (*LRP5;* EVR4; Toomes et al., 2004), while a fourth locus has been linked to 11p13-p12 without knowing the gene involved (EVR3; Downey et al., 2001) (Figure 21).

In contrast to *FZD4*, mutations in *NDP* and *LRP5* have been associated with additional diseases and extra-ocular symptoms. Mutations in *NDP* often present with defects in the brain and inner ear, and recessive mutations in *LRP5* have been associated with osteoporosis pseudoglioma syndrome (OPPG), further presenting with bone abnormalities (Gong et al., 2001; Ai et al., 2005). Thus, it is difficult to describe phenotypic differences between FEVR and ND, when part of the reported FEVR cases are in fact non-syndromic, mild ND cases due to mutations in the *NDP* gene. The same applies to differences between FEVR and OPPG, because both are associated with mutations in *LRP5*.

Concentrating only on the FEVR cases with dominant mutations in *FZD4*, the following clinical observations have been made: Peripheral retinal avascularity (mainly temporal), severe retinal exudates, retinal peripheral neovascularization, peripheral fibrovascular mass, macular ectopia, retinal fold, retinal detachment, and vitreal hemorrhage (Qin et al., 2005). In addition, stretched temporal vessels, myopia, vitreofoveal traction, mature cataract, secondary strabism, PFV or PFV-like features, and microphthalmos have been noted (Robitaille et al., 2002; Müller et al., 2007; Robitaille et al., 2009) (Figure 7). No extraocular symptoms like progressive hearing loss, mental retardation, or altered bone density have been reported so far.

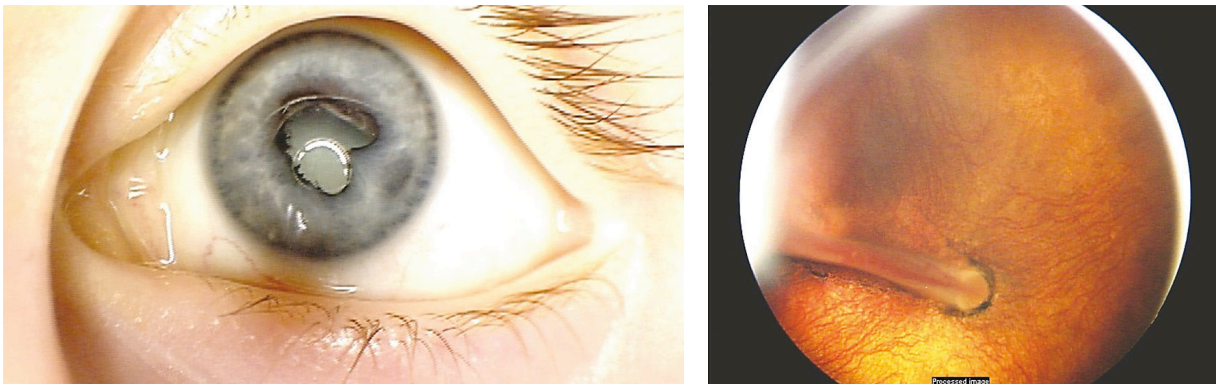

A **B**

Figure 7 Cinical presentation of a female FEVR patient with a small deletion in *FZD4* (p.M493_W494del). **(A)** The left eye is conspicuous with a hypoplastic iris with posterior synechiae (adherence of the iris to the lens) and leukocoria. **(B)** In the right eye, retinal vessels are prominently lacking in the dysplastic retina, and a fibrovascular stalk extends from the optic disc to the inferotemporal aspect of the lens, reminiscent of PFV. (Source: Robitaille et al., 2009)

1.3.2.7 Retinopathy of prematurity (ROP)

Retinopathy of prematurity (ROP) is a major cause of blindness in children despite current surgical treatment in the late-stage of the disease (Chen and Smith, 2007). ROP was originally described in the 1940s as retrolental fibroplasia that occured in premature infants (Terry, 1942; Terry, 1944). Its hallmark feature is development of retinal neovascularization due to transient local ischemia, mainly in the temporal periphery of the eye. Secondary complications are highly variable, ranging from no effect on vision to bilateral, total blindness. The younger and smaller the premature children, the higher the risk of desastrous ROP (Ashton et al., 1953; Palmer et al., 1991).

In the 1950s, supplementary oxygen was suspected as cause for the development of ROP. It was soon found that only the incompletely vascularized retina is susceptible to oxygen, and the more immature the vasculature, the greater the pathologic response to oxygen (Ashton et al., 1954). Thus, the temporal retina is predisposed for ROP, because it is the last part of the retina that becomes vascularized.

The pathogenesis of ROP can be divided into two phases. The primary stage is characterized by vasoconstriction of immature retinal vessels, which can progress to vascular occlusion. It has been proposed that this mechanism could protect the neural retina during phases of elevated oxygen pressure (Flower, 1985). When the oxygen pressure normalizes, e.g. through return of the patient to ambient air, the disease enters phase 2, which can be identified by retinal neovascularization through proliferation of endothelial cells that are adjacent to the areas of ablated retinal capillaries. These events become clinically relevant when the proliferating cells penetrate the inner limiting membrane and blood vessels start to grow on the retinal surface and into the vitreous, especially in the central part of the retina. Therefore, ROP is internationally classified by the retinal areas that are involved (anterioposterior zones I-III, where I represents the center around the optic disc and the macula and III is the temporal periphery), and the grade of pathogenic progression.

The extent of ROP can be classified in five stages (Figure 8). The first visible sign is the appearance of a demarcation line, a sharp border between the vascularized, central retina and the avascular periphery (Stage 1; Figure 8A). When the disease progressed to stage 2, this demarcation line appears elevated in centripetal direction within the eye globe; a ridge has formed (Figure 8B). In stage 3, extraretinal fibrovascular tissue proliferates from the ridge (Figure 8C). The next stage of severity is characterized by partial retinal detachment. Depending on foveal involvement, this stage can be classified in 4A (without foveal involvement) and 4B (with foveal involvement) (Figure 8D). Stage 5 finally, the most severe form of ROP, is characterized by total retinal detachment (Figure 8E).

The different stages of ROP bear similarities to other clinical entities. Classic, severe ND is similar to ROP stage 5, PRDX has been suggested to characterize ROP grades 3 and 4, and FEVR is similar to the milder ROP grades 1 and 2 (Table 1; Mintz-Hittner et al., 1996). An important differential diagnosis for stages 4 and 5 further is retinoblastoma, and atypical cases of Coats' disease (CD), Eales' disease (ED), and retinoschisis can also resemble the clinical picture of ROP (Palmer et al., 2001).

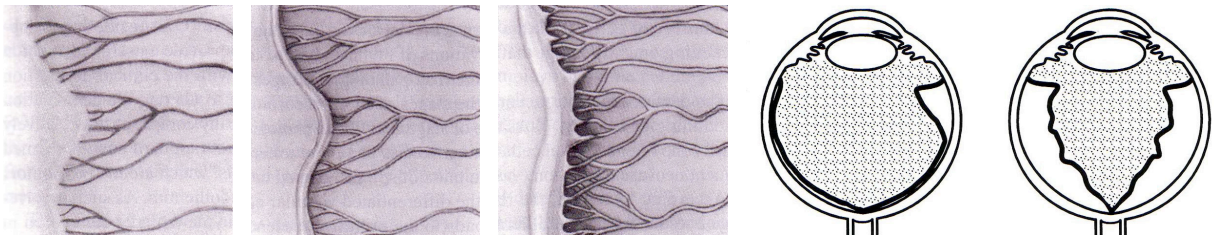

A ROP Stage 1 **B** ROP Stage 2 **C** ROP Stage 3 **D** ROP Stage 4A **E** ROP Stage 5

Figure 8 Diagrams showing the classification of ROP stages. **(A)** Stage 1. A demarcation line separates the mature, vascularized part of the retina (*right*) from the avascular periphery (*left*). **(B)** Stage 2. The characteristic ridge becomes visible along the demarcation line. **(C)** Stage 3. Along the ridge, proliferation of extraretinal fibrovascular tissue is evident. **(D)** Stage 4A. Subtotal detachment of the retina without involvement of the fovea. **(E)** Stage 5. Total retinal detachment with anterior and posterior open funnel. (modified after figures presented in Palmer et al., 2001)

ROP Stage	Characteristic	Corresponds to
1	Demarcation line	FEVR; CD; ED; RS
2	Ridge	FEVR; CD; ED; RS
3	Ridge with extraretinal fibrovascular proliferation	PRDX; CD; ED
4A	Subtotal retinal detachment (extrafoveal)	PRDX; RB; PFV; ED
4B	Subtotal retinal detachment (including the fovea)	PRDX; RB; PFV; ED
5	Total retinal detachment	ND; RB; PFV; ED

Table 1 Classification of ROP stages. A „plus“ is added to each stage when marked vascular changes are present (enlargement of posterior veins, increased tortuosity of arterioles, iris vascular engorgement, pupillary rigidity, and vitreous haze). (Source: Palmer et al., 2001)

While the oxygen-based hypothesis commonly is the most accepted, the etiology of ROP is not clear and appears to be multifactorial. Prematurity, low birth weight, and prolonged oxygen supplementation have long been established as main risk factors. Recently, insulin-like growth factor (*IGF-1*) has been found to act indirectly as a permissive factor for vessel growth. Lack of IGF-1 in preterm infants prevents normal retinal vascular growth in phase I of ROP. Rising levels of IGF-1 in phase II then allow pathological neovascularization (Chen and Smith, 2007). IGF serum levels in the developing child depend heavily on the mother's serum levels, and low *IGF-1* serum levels in the mother may pose another risk factor for ROP. However, no genetic variations in the *IGF-1* gene have been associated with ROP so far. In contrast, mutations in *NDP* have been found to predispose for a higher risk to develop ROP (Shastry et al., 1997; Hiraoka et al., 2001). However, the occurence of these mutations and the low gestational age could be coincident, opening the question whether these patients suffered from ROP or were just pre-term babies who suffered from ND.

Although cryotherapy and laser photocoagulation of the avascular retina became available in the 1980s and 1990s, these ablation treatments reduce the incidence of blindness only by 25% in infants with late-stage disease. Understanding of the molecular basis of the disease would be the prerequisite for a better and more comprehensive treatment.

1.3.3 Differential diagnosis

In addition to the clinical entities that have been associated with mutations in the *NDP* gene, several other conditions with a similar phenotype have been described that may be related through a common pathogenic molecular pathway.

1.3.3.1 Osteoporosis pseudoglioma syndrome (OPPG)

Osteoporosis pseudoglioma syndrome (OPPG) is an autosomal recessive disorder presenting with juvenile skeletal fragility and congenital or early-onset visual loss. The ocular phenotype is variable and resembles ND and FEVR, including the presence of congenital retinal folds and exudates, avascular periphery, PFV, pseudoglioma, phtisis bulbi, and cataract (Figure 9). The disease is usually bilateral, but unilateral eye involvement has been reported (Ai et al., 2005). In addition, muscular hypotonia, ligamentous laxity, and mental retardation were noted (Balemans and van Hul, 2007). Cognitive impairment of varying degree has been estimated to occur in 27% (8 of 30) of all OPPG patients (Ai et al., 2005).

Importantly, skeletal disease often was not recognized during the first 2 years of life (only in less than half of the cases) (Ai et al., 2005). In several asymptomatic infants, skeletal anomalies were found incidentally when radiographs were obtained for other reasons. Thus, depending on the degree or diagnosis of bone involvement, patients suffering from OPPG can also be diagnosed as FEVR or ND patients (especially when mental retardation is evident).

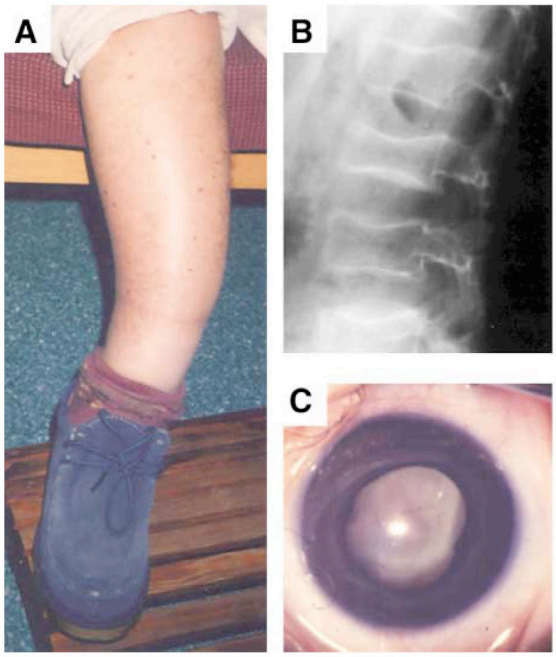

Figure 9 (A) Right leg of a 40-year-old female OPPG patient with angular deformity of the tibia and fibula, the consequence of multiple fractures occurring during childhood. **(B)** Abnormal flattening and concavity of the lumbar vertebrae of a 10-year-old male OPPG patient shown in a lateral radiograph. **(C)** The right eye of a 3-month-old male patient presents with leukocoria. (Source: Gong et al., 2001)

OPPG has been associated with mutations in the low-density lipoprotein receptor-related protein 5 (*LRP5*) (Gong et al., 2001), which later has also been associated with FEVR (Toomes et al., 2004), substantiating the close similarity of the ocular phenotype.

1.3.3.2 Retinoblastoma

The retrolental masses and/or pseudoglioma observed in ND and allelic disorders are often confused with a malignant tumor (Figure 10). In a CT scan, retinoblastomas can be diagnosed by a high degree of calcifications, which are only rare in pseudogliomas. Further, pseudogliomas seen in ND and allelic diseases are usally not solid, as can be observed by MRT (Scholz et al., 1997). Finally, differentiation can be achieved by genetic analysis, since hereditary retinoblastoma has been shown to be caused by mutations in the tumor-suppressor gene *RB1* located at 13q14.2 (Lee et al., 1987).

Figure 10 Retinoblastoma in a patient aged 3 years and 5 months. Note the characteristic leukocoria. (Source: Meier et al., 2006)

1.3.3.3 Reese retinal dysplasia

Reese retinal dysplasia is the characteristic eye phenotype of trisomy 13 (Iwig, 1969). The ocular presentation is similar to ND regarding the malformation of the retina and persistence of fetal vitreous vessels. However, it is accompanied by many visceral manifestions and other extra-ocular symptoms like polydactyly and cleft lip and palate (Reese and Straatsma, 1958) (Figure 11).

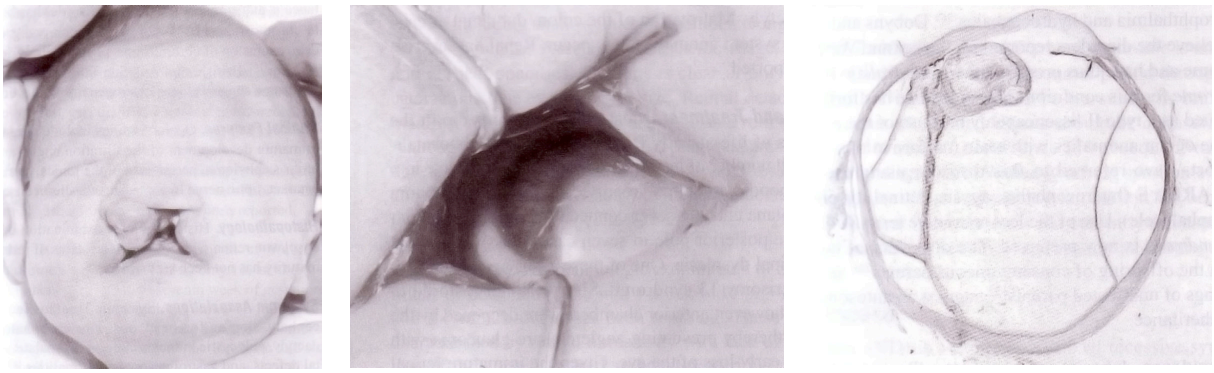

A **B** **C**

Figure 11 Trisomy 13 in a full-term neonate. **(A)** Bilateral nasolabial cleft lip and palate. **(B)** Microphthalmos, corneal leukoma, and iris coloboma. **(C)** Section of the enucleated eye exhibiting cataract, PFV, retinal dysplasia and detachment. (Source: de Juan, Jr. et al., 2001)

1.3.3.4 Familial retinoschisis (RS)

X-linked retinoschisis (RS) is a common juvenile macular dystrophy diagnosed in boys. It is characterized by intraretinal splitting that may lead to bilateral retinal folds and detachment that can be difficult to differentiate from other causes of retinal detachment. X-linked juvenile retinoschisis has been linked to the Xp22.2-p22.1 interval and lead to the discovery of the *XLRS1* gene (Sauer et al., 1997). RS typically occurs with hyperopia and is only slowly progressive. Further reduction of visual acuity only occurs in the infrequent case of intravitreal hemorrhages. However, RS mainly affects the central, not peripheral part of the retina, and is not associated with a defect in blood vessel development (Kellner et al., 2004) (Figure 12). A possible pathogenic mechanism could be based on a developmental defect of retinal Müller cells. Concurrent presence of temporal retinoschisis cavities reminiscent of RS and nasal telangiectatic vessels typical for CD have been described in two unrelated patients. However, sequencing of the exonic regions of the *NDP* and *XLRS1* genes have not revealed any disease-causing mutations (Berinstein et al., 2001), opening the possibility for yet another gene involved in a CD/RS-like phenotype.

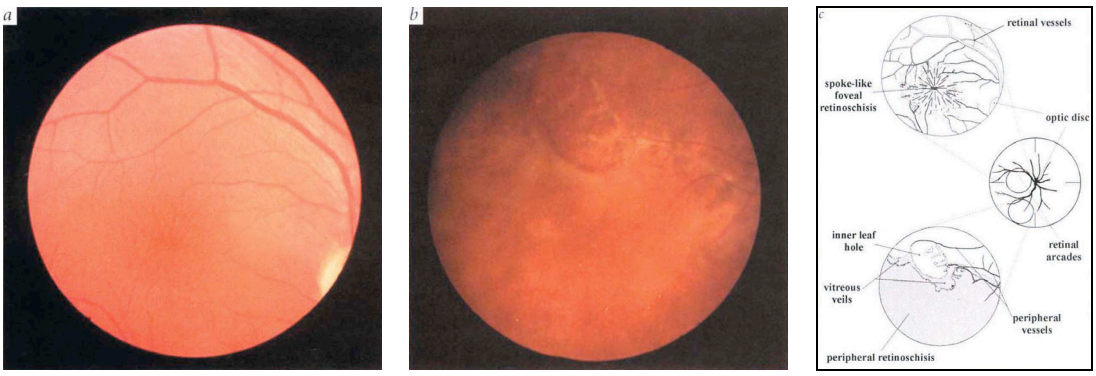

Figure 12 Fundus images from an 11-year-old RS patient. **(A)** Foveal retinoschisis produces the characteristic spoke-like macular appearance. **(B)** Inferotemporal retinoschisis with a large inner leaf hole and vitreous veils. **(C)** Schematic drawing of (A) and (B) and their position in the retina. (Source: Sauer et al., 1997)

1.3.3.5 Incontinentia pigmenti (IP)

Familial incontinentia pigmenti (IP; Bloch-Sulzberger syndrome) is an X-linked dominant, bilateral, but asymmetric disorder of pigmentary skin abnormalities with associated ocular, central nervous, and dental abnormalities that has first been described in 1926 (Bloch, 1926; Sulzberger, 1927). It is caused by mutations in the NF-kappa-B essential modulator gene (*NEMO/IKBKG*) at Xq28 (Smahi et al., 2000).

Ocular findings are very similar to ND and allelic diseases. Proliferating fibrovascular material in the periphery can lead to tractional retinal detachment (Cole and Cole, 1959). The vasculature is markedly impaired and presents with peripheral microaneurysms, arteriovenous shunts, neovascularization in a peripheral avascular zone (Francois, 1984), dilated retinal and choroidal vessels (Laqua, 1980), macular aneurysms (Jain and Willetts, 1978), optic disc neovascularization (Shah et al. 1997), persistence of fetal vasculature, and vitreous hemorrhage (Fard and Goldberg, 1998)

(Figure 13). Further phenocopying ND, IP may occur with congenital cataract (Carney, 1976) and corneal opacities (Cole and Cole, 1959).

Sporadic cases due to somatic mutations in *NEMO/IKBKG* only in ocular precursor cells would be difficult to differentiate ophthalmologically from ND and allelic diseases.

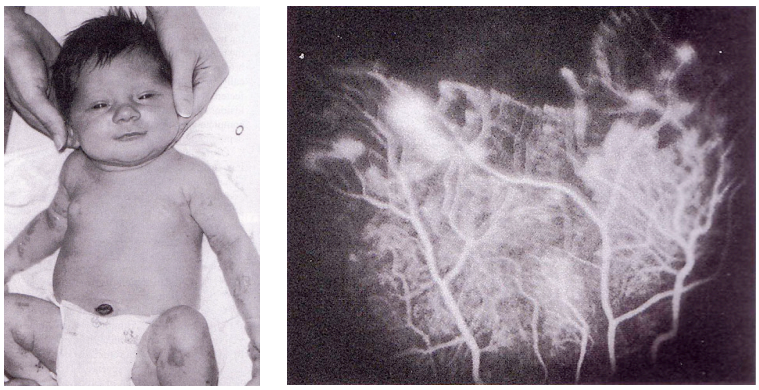

A B

Figure 13 Clinical findings of incontinentia pigmenti (IP). **(A)** Erythematous vesicles and papules in a 3-week-old girl. **(B)** Avascular periphery, arteriovenous shunts, vessel dilations, neovascularization, and leakage of fluorescein seen in the angiogram of a 10-month-old girl. (Source: de Juan, Jr. et al., 2001; pictures courtesy of Molton Goldberg)

In two sporadic cases, a de novo X-autosome translocation t(X;9)(p11;q34) was found, which suggested that another IP gene may be at Xp11 (Hodgson et al., 1985; Gilgenkrantz et al., 1985). However, it has been argued that these and other sporadic cases are not confluent with incontinentia pigmenti at all, since none of them matched the (syndromic) diagnostic criteria (Sybert, 1994). It could be possible, though, that these chromosomal rearrangements affected the *NDP* locus at Xp11.3, which thus could explain the ocular similarities to IP.

The eponymous pigmentary disturbances of the RPE have been postulated to be the cause of the retinovascular changes (Mensheha-Manhart and Rodrigues, 1975). But also the opposite, namely a vascular basis for the disease, has been suggested (Watzke and Stevens, 1976). So far, the exact pathogenetic mechanism is unknown, although a unifying hypothesis was formulated proposing that vascular abnormalities are the result of a generalized type II (antibody-mediated) cytotoxic inflammatory response to an abnormal gene product (Catalano, 1990).

1.3.3.6 Eales' disease (ED)

Eales' disease (ED) is named after Henry Eales, who first noted recurrent hemorrhages and abnormal retinal veins in otherwise healthy young men (Eales, 1880). Today, it is described as a primary retinal periphlebitis (inflammation of the outer coat of a vein or the tissues surrounding it), which secondarily leads to retinal ischemia (mainly in the periphery), finally culminating in retinal neovascularization, recurrent haemorrhages, and retinal detachment (Biswas et al., 2002). It predominantly affects healthy young males (97.6%) in India and the Middle East with a mean age of onset of 26 years,

although one study from North America did not detect any gender differences (reviewed by Biswas et al., 2002).

Retinal nonperfusion can lead to tortuous veins that closely resemble the vascular phenotype seen in ND/CD patients. Vascular sheating can be seen in 80% of the patients (Gieser and Murphy, 2001; Figure 14 A). In addition, the border between perfused and nonperfused retina is sharply demarkated (Spitznas et al., 1975; Figure 14 B).

The etiology of ED is unclear and appears to be multifactorial. The primary events seem to involve ocular inflammation associated with immunologic phenomena. Leukocyte antigen, retinal autoimmunity, mycobacterial tuberculosis, and free radical–mediated damage seem to influence the pathogenesis of the disease (reviewed by Biswas et al., 2002). However, no evidence for a genetic basis has been presented so far.

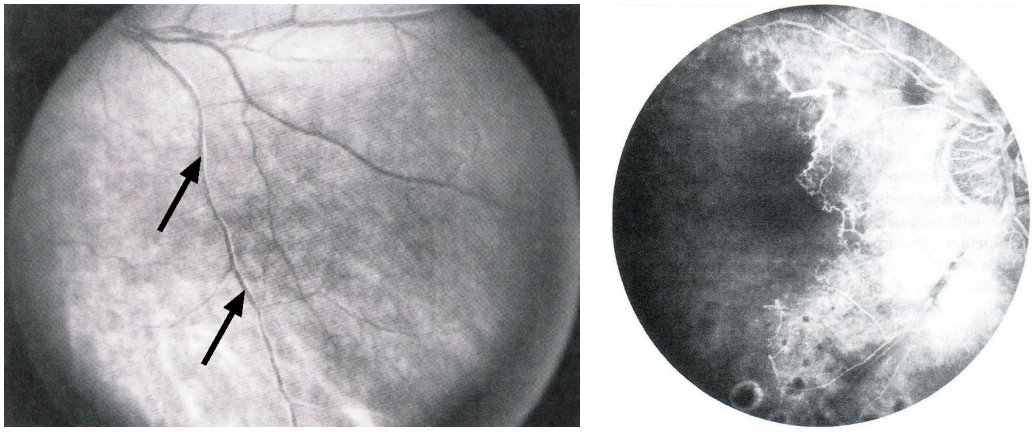

A B

Figure 14 Fluorescein angiograms of Eales' disease patients. **(A)** Venular sheathing. Note the thin, continous white lines encompassing the vein (arrows). **(B)** The junction of perfused and nonperfused retina is obvious. (Source: Gieser and Murphy, 2001)

1.3.3.7 Neovascular inflammatory vitreoretinopathy (VRNI)

Neovascular inflammatory vitreoretinopathy is an autosomal dominant blinding disorder characterized by neovascularization, vitreous hemorrhage, retinal detachment, and symptoms of ocular inflammation. It has been mapped to chromosome 11q13, the region containing *FZD4* and *LRP5* (Sheffield et al., 1992; Stone et al., 1992). Sheffield et al. argued against the hypothesis that FEVR and VRNI are allelic, mainly on the basis of phenotypic differences. However, these differences might not exist on second sight (e.g., the authors claimed the presence of vitreous cells to be exclusive for VRNI; a statement that cannot be sustained with regard to the published findings of the last 17 years). Consistency with another retinal disease, Best vitelliform macular dystrophy (VMD), which also maps to 11q13, has been dismissed, because VMD has been associated with a gene 10cM apart, bestrophin 1 (*BEST1*) (Sheffield et al., 1992).

1.3.4 Animal models

To elucidate the molecular pathogenic mechanisms of human diseases and to investigate the efficacy of therapeutic strategies, animal models are often used under the assumption that findings can be generalized to human biology. Mice have become the major model used in medical research, primarily due to the ability to selectively turn genes on or off in so-called transgenic or knockout mice, respectively (recently recognized by the award of the Nobel prize in Physiology or Medicine for 2007 to M.R. Capecchi, M.J. Evans, and O. Smithies for the development of the knockout technology). In addition, murine organ development and morphology are highly comparable to humans. With regard to the eye, some differences have to be kept in mind, though: Typical for a nocturnal animal, the cornea, lens, and vitreous are relatively large. The retina is rod-dominated, and only two cone-types (in contrast to three in humans) are present. However, one of the cone pigments is maximally responsive to ultraviolet (UV) light, thereby shifting the spectrum of perceivable light to shorter wave lenghts. Although no fovea (the retinal region in humans with the highest density of cones and lack of rods or retinal neurons; responsible for sharp, central vision) is present, the functional organization of the retinal network is largely similar.

Further, the timing of events in retinal development is comparable, although the retinal vasculature in humans develops around mid-gestation, and only postnatally in mice. This is important concerning the use of mouse models in ND research, because it allows easy accessibility during retinal vessel development, and allows generalization to human physiology. The murine retinal vasculature is also organized in three distinct layers. The superficial plexus, located within the ganglion cell / nerve fiber layer (GCL/NFL), starts at the optic nerve head and spreads radially towards the periphery between postnatal days 3 (p3) and p17. Around p7, blood vessels start to sprout perpendicular into the retina to form the deep retinal network at the border between outer plexiform layer (OPL) and inner nuclear layer (INL). The third, intermediate plexus starts to develop at p12, forming between the superficial and the deep networks at the border between inner plexiform layer (IPL) and INL (Fruttiger, 2007).

1.3.4.1 The Ndph knockout mouse

The human *NDP* gene and the murine orthologue *Ndph* (Norrie disease pseudoglioma homolog) are highly conserved (95% sequence identity on the amino acid level), and similar transcriptional activity in eye, brain, and ear suggested an *Ndph* knockout mouse as a suitable model to study ND. The ko mouse was generated through targeted replacement of the coding part of exon 2 with a reverse oriented neomycin cassette, resulting in the deletion of the first 56 aa from the gene, including the signal peptide (Berger et al., 1996). The initial phenotypic characterization revealed an obvious involvement of ocular tissues. The vitreous of hemizygous $Ndph^{y/-}$ mice contained a fibrovascular mass, and the retina appeared to be dysmorphic, with prominent disorganization of the ganglion cell layer. Heterozygous female carriers were asymptomatic. Electroretinography (ERG) measurements conducted to investigate retinal function revealed a more severe involvement of the inner retina. The b-wave amplitudes generated by second order neurons were markedly reduced in hemizygous $Ndph^{y/-}$ mice, while the a-waves (generated by the photoreceptors in the outer retina) were indistinguishable at lower light intensities, and only became conspicuous with increasing stimulus strength (Rüther et al., 1997). This finding was supported by a

global gene expression study investigating retinal transcription in older mice, which revealed late degeneration of photoreceptor cells (Lenzner et al., 2002).

The primary event in the pathogenesis of ND in the mouse seems to be the development of the retinal vasculature, as abberant morphology has been reported several times (Richter et al., 1998; Rehm et al., 2002; Luhmann et al., 2005a,b). The superficial vessel growth is delayed and never completed, leaving the retinal periphery avascular, and the deeper networks entirely fail to develop (Figure 15; Figure 16; Figure 50). Since the astrocytic scaffold, which precedes vascular development and is important for vessel guidance, appears to be intact, a primary effect of the *Ndph* ko allele on endothelial cells has been suggested, resulting in a defect in sprouting angiogenesis (Luhmann et al., 2005a). In addition, regression of the fetal hyaloid vessel system is delayed and incomplete, resembling PFV. Detailed analysis of the early retinal development specifically focused on the vasculature in *Ndph* knockout mice revealed two phases of disease progression *in vivo* (Luhmann et al., 2005a): In the early phase, the absence of functional Norrin (*Ndph*–protein) causes a defect in sprouting angiogenesis and thus leads to a delayed outgrowth of the superficial vessels and prevents the formation of the deep capillary networks in the retina. Then, in the later phase, the developmental lack of the deep vasculature leads to inner retinal hypoxia. This pathological hypoxia may explain the observed clinical features of Norrie disease and might also be responsible for the similarities of the clinical phenotypes of the allelic diseases (Luhmann et al., 2005a).

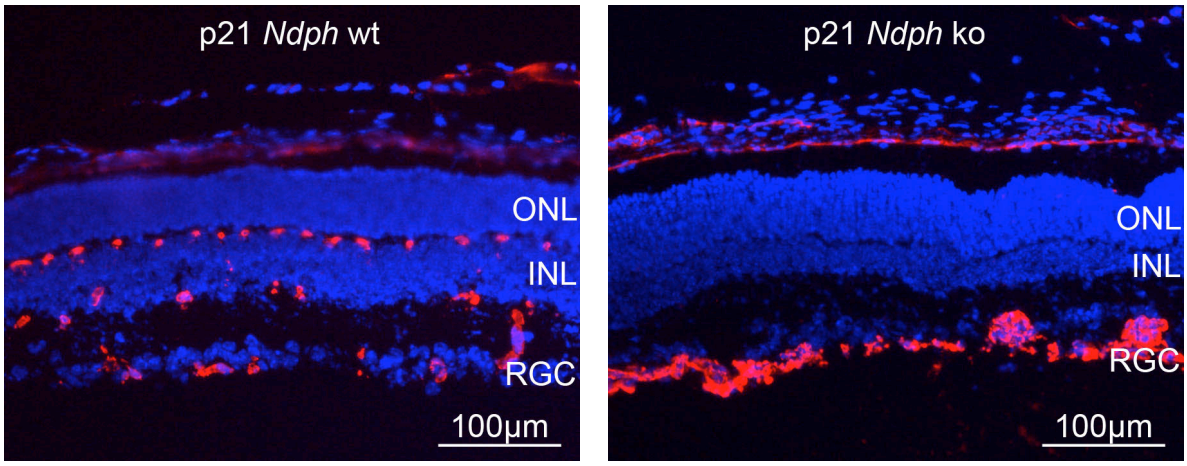

Figure 15 Sections of p21 *Ndph* wt and knockout retinas. Vessels have been stained with an antibody against collagen IV (*red*), nuclei were labeled with DAPI (*blue*). **(A)** All three retinal networks have developed in the wt retina, located in the RGC and in both plexiform layers adjacent to the INL. A connective vessel between the superficial and the intermediate network is visible on the right. **(B)** In the *Ndph*$^{y/-}$ retina, the deep and the intermediate vasculature are lacking. The superficial vasculature appears to be enlarged and forms occasional vessel clumps that can infiltrate the inner plexiform layer (visible on the right). *INL*: inner nuclear layer; *ONL*: outer nuclear layer; *RGC*: retinal ganglion cell layer.

In situ hybridization revealed *Ndph* expression in the three nuclear layers of the retina (RGC, INL, ONL), in the cochlea, olfactory bulb, hippocampus, cortex, and in the granular and Purkinje cell layers of the cerebellum (Chen et al., 1995; Berger et al., 1996; Hartzer et al., 1999). Thus, *Ndph* is expressed in all organs or tissues affected in ND.

In concordance, *Ndph* ko mice also resemble the human phenotype with regard to the auditory system, exhibiting a progressive hearing loss that first affects the high frequencies (age 3-4 months), but later progresses to a loss at all frequencies (15 months) (Rehm et al., 2002). Auditory perfomance correlated with progressive degeneration of the cochlea. Similar to the retina, the most obvious changes occured in the vasculature, especially in the stria vascularis. Vessels appeared to be enlarged, and their number decreased progressively, resulting in a loss of outer hair cells and later

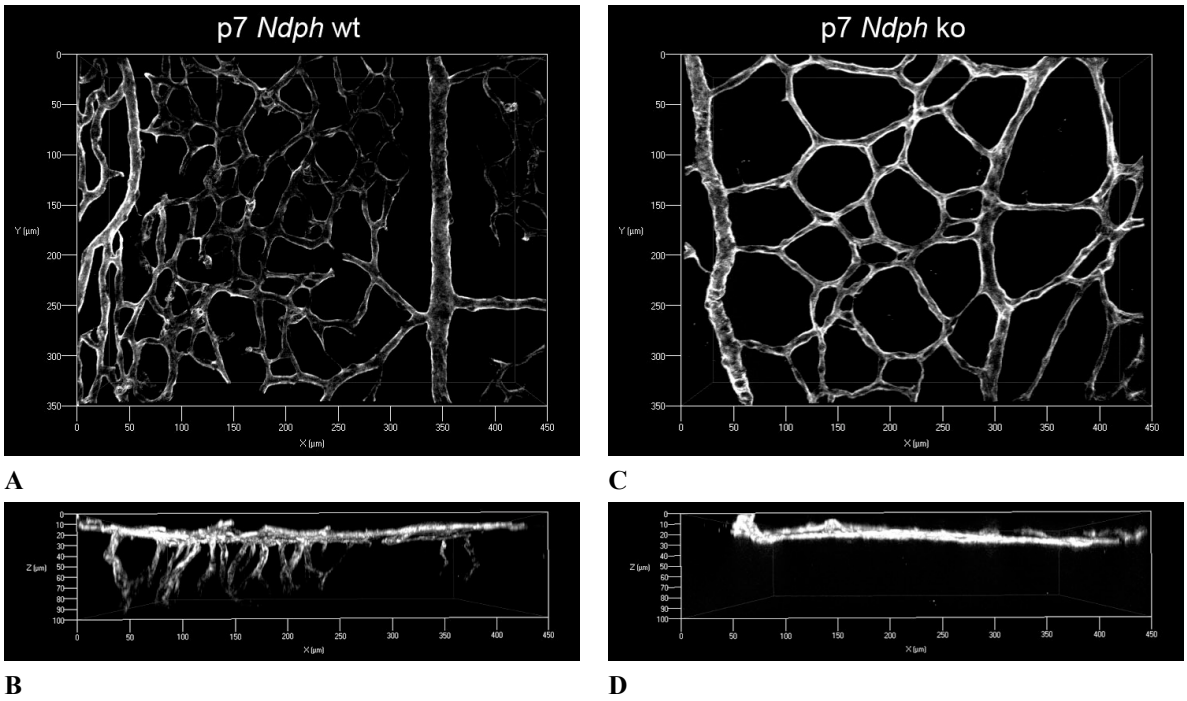

Figure 16 Flatmounted retinas of p7 *Ndph* wt mice in comparison to ko. Images compiled from a Z-Stack of pictures acquired with a Zeiss ApoTome™. To visualize the retinal vasculature, an antibody against collagen IV was used. **(A)** Top view of the wt superficial vasculature. **(B)** Same image as a in (A), but rotated 90°. The superficial vasculature is located at the top. Deeper networks start to develop from angiogenic sprouts, mainly from veins and capillaries. **(C)** Topview of the ko retina. Outgrowth of the superficial capillary network appears to be much sparser, and **(D)** no developing deeper network could be detected in the 90° rotated view.

neurons of the spiral ganglion. But in contrast to the developmental defect in the eye, vessels in the inner ear at first seemed to develop normally, and pathologic changes only occured progressively during the adult life, hinting at a defect in homeostasis. Thus, norrin probably has a different effect on vasculature in eye and ear, affecting development in the first, and maintenance in the latter.

In addition, *Ndph* transcripts were also detected in the endometrium of pregnant mice and in human placenta (Luhmann et al., 2005b). A human phenotype in female reproduction has not been reported so far, but female mice homozygous for the *Ndph* ko allele are completely infertile due to a defect in decidualization, i.e. remodeling of the endometrium (the inner membrane of the uterus) upon implantation of the embryo, probably as a result of impaired angiogenesis similar to the defects in eye and ear (Luhmann et al. 2005b).

No brain phenotype in the *Ndph* ko mouse has been described so far. However, in contrast to the eye, ear, and reproduction anomalies, assessment of mental retardation or developmental delay is more complicated. Since impairment of angiogenic remodeling seems to be the common cause of the respective phenotypes, it is tempting to speculate that it is also affected in cerebral tissues, especially since *Ndph* mRNA expression has been shown in cortex, hippocampus, and cerebellum.

The ocular *Ndph* knockout phenotype could be rescued by ectopic overexpression of norrin in the lens (Ohlmann et al., 2005).

1.3.4.2 The Fzd4 knockout mouse

The human and murine *Fzd4* genes are highly homologous, sharing 96% sequence identity on the amino acid level. The *Fzd4* knockout mouse was generated through targeted replacement of the coding region of the *Fzd4* locus with a knock-in construct containing a β-galactosidase reporter and a neomycin resistance cassette, resulting in the near-complete deletion of the *Fzd4* coding sequence (CDS; excluding the 3'-most 70bp) (Wang et al., 2001). *Fzd4* is widely expressed during development, and in the adult, *LacZ* activity of the knock-in reporter revealed expression in many CNS tissues, including brain, retina, and inner ear. In the cerebellum, LacZ expressivity was constrained to the Purkinje cells, while in the retina, uniform staining was found in the photoreceptor layer, and punctate staining was found in the inner nuclear and ganglion cell layers (Figure 17 C).

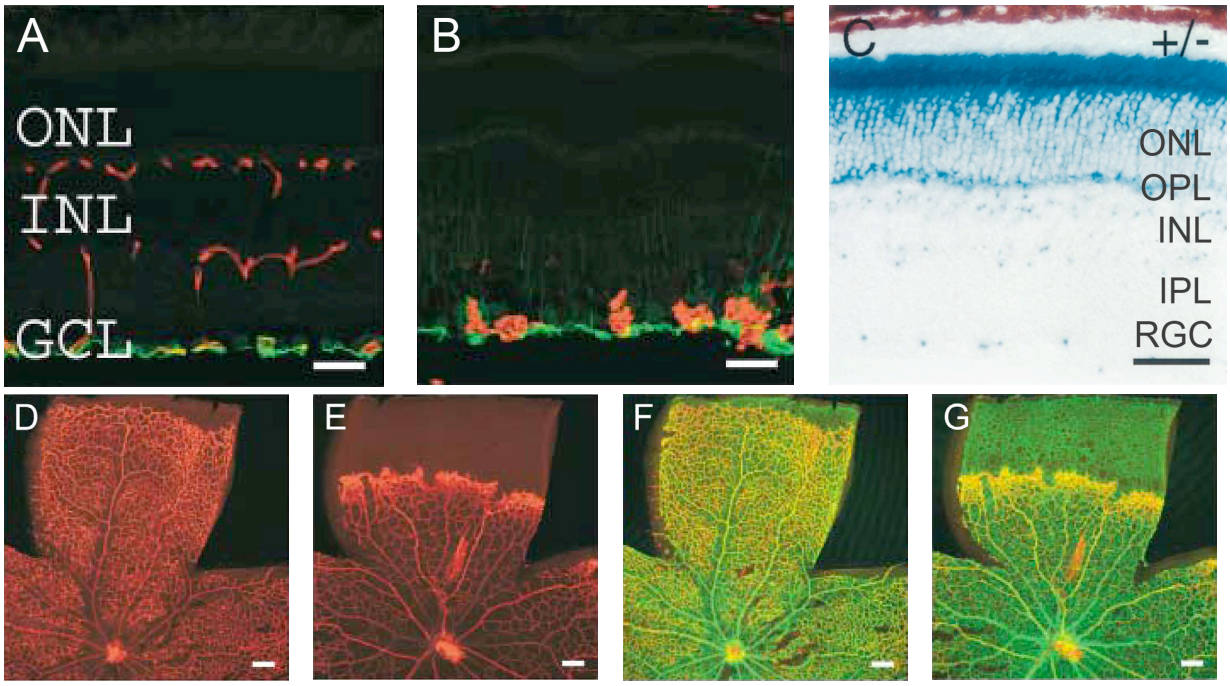

Figure 17 (A, B) Retinal sections from p17 *Fzd4* wt and *Fzd4*$^{-/-}$ mice (Source: Xu and Wang et al., 2004). **(A)** The astrocytic network in the ganglion cell layer (GCL), labeled with an antibody against GFAP (*green*), and the three retinal blood vessel networks, stained with lectin (*red*), appeared normal in the wt mouse. **(B)** While the astrocytic network was similar to the wt, the *Fzd4*$^{-/-}$ retina obiously lacks the deep and intermediate vasculature, and vessels of the superficial plexus appeared sparser and enlarged. **(C)** Spatial expression of *Fzd4* was investigated by X-Gal staining of the adult *Fzd4*$^{+/-}$ retina. Intenese staining in the

photoreceptor layer, with uniform staining especially in the inner segments, and scattered, punctate staining in the inner nuclear and ganglion cell layers was observed (Source: Wang et al., 2001). (D-G) Retinal flatmounts of p10 *Fzd4* wt and ko mice. Vessels were stained as in A & B (Source: Xu and Wang et al., 2004). **(D**) In the p10 wt, the superficial vasculature has reached the retinal periphery. **(E)** In the *Fzd4*$^{-/-}$ retina, the superficial vasculature is sparser, and a characteristical clustering of endothelial cells at the sprouting front has formed, reminiscent of the fibrovascular ridge seen in ROP patients, separating the vascularized retina from the avascular periphery. (F, G) Same pictures as D & E, but with additional GFAP staining (*green*). **(F)** In the wt retina, close association of the astrocytic scaffold and the vasculature can be seen (*yellow*). **(G)** The astrocytic network in the *Fzd4*$^{-/-}$ retina is similar to the wt, extending to the retinal periphery.

Homozygous *Fzd4*$^{-/-}$ knockout mice exhibit several distinct defects that closely resemble that of the *Ndph* ko mouse (Wang et al., 2001; Xu and Wang et al., 2004). The two intraretinal vessel systems are not developed, and the capillary bed of the superficial vasculature is only sparse, while the major arteries and veins are enlarged and tortuous (Figure 17). In further concordance with the *Ndph* ko phenotpye (Figure 50), outgrowth of the superficial vasculature is delayed, and a clustering of endothelial cells reminiscent to the characteristic fibrovascular ridge in ROP patients (Figure 8) forms at the front of the sprouting vessels (Figure 16). Many vessels in the nerve fiber layer are fenestrated, correlating with frequently observed retinal hermorrhages, and the hyaloid vessels in the vitreous fail to regress (Xu and Wang et al., 2004). However, in contrast to the *Ndph*$^{y/-}$ mouse, no obvious disorganization or degeneration of retinal neurons was noted in early adulthood.

In addition to the ocular phenotype, progressive deafness was found, caused by a defect in the peripheral auditory system. The stria vascularis presented with enlarged vessels, and loss of outer hair cells was noted at 4.5 months of age. In 11-month-old *Fzd4*$^{-/-}$ mice, the stria vascularis was completely degenerated and no vessels remained. Concomitantly, nearly complete loss of outer and inner hair cells was noted. Importantly, initial development of the inner ear seems to be similar to wt, thus Fzd4 may be necessary for cochlear maintenance and survival (Wang et al., 2001), similar to norrin (Rehm et al., 2002).

Loss of normal vascular morphology was further observed in the cerebellum, where it seems to correlate with progressive cerebellar degeneration. Beginning in the third postnatal week, *Fzd4*$^{-/-}$ mice exhibit an anormal gait and characteristical wide stance, which is a sign of severe cerebellar ataxia (Wang et al., 2001). Vessels become sparser, and by 6 months of age, the network appears disturbed, with enlarged vessels and frequent small hemorrhages (Figure 18), while the vasculature elsewhere in the brain seems to be normal (Xu and Wang et al., 2004).

Like the *Ndph* ko homozygous females, *Fzd4* ko homozygous female mice were reported to be infertile. However, the defect seems to involve corpora lutea formation, causing a failure in implantation, in contrast to impaired decidualization in *Ndph* ko mice (Hsieh et al., 2005).

In addition, growth delay, reduced viability, and the absence of a skeletal muscle sheath around the lower esophagus have been noted. Also, the coat color of homozygous knockout mice is lighter, suggesting that *Fzd4* may play a role in the expansion or migration of melanocyte precursors from the neural crest or the differentiation and survival of melanocytes (Wang et al., 2001).

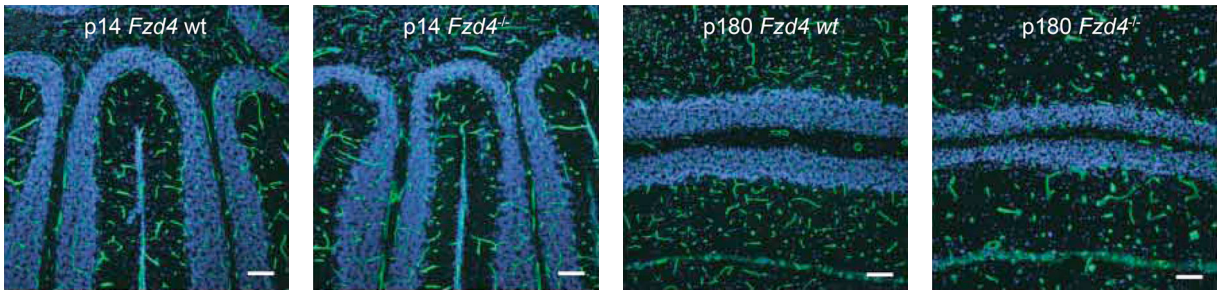

Figure 18 Cerebellar sections of *Fzd4* wt and ko mice stained with an antibody against collagen IV (*green*) and DAPI (*blue*). **(A)** Cerebellar vasculature in the p14 wt is similar to **(B)** the *Fzd4*$^{-/-}$ vasculature. **(C)** Vessels in the cerebellum of a 6-month-old wt present with a different pattern than **(D)** cerebellar vessels in the *Fzd4*$^{-/-}$ mouse. Vessels are sparser, enlarged, and irregularly patterned, and the granule cell layer (*blue*) appears thinner than in the wt. (Source: Xu and Wang et al., 2004)

Taken together, the phenotypic similarity between *Fzd4* and *Ndph* knockout mice is striking. The auditory and cerebellar phenotypes of *Fzd4*$^{-/-}$ mice implicate Fzd4 signaling in maintenance of viability and integrity of the nervous system, which is in constrast to the observed ocular developmental defect and the commonly presumed role associated with Wnts, early cell proliferation and patterning effects (Wang et al., 2001). An interesting difference to human patients with mutations in *Fzd4* is the observed heterozygous insufficiency. Only one (severe) FEVR case with a homozygous mutation has been published (Kondo et al., 2003; Kondo et al., 2007), while all other cases are heterozygous. Thus, mutations in *Fzd4* are considered to be dominant, while the heterozygous mouse apparently shows no differences to wt littermates. Further, no extraocular symptoms have been described in patients with *FZD4* mutations, which maybe only manifest in homozygous cases.

1.3.4.3 The Lrp5 knockout and r18 mutant mice

Lrp5 is a 23 exon gene that like norrin shares 95% sequence identity between human and mouse on protein level (Hey et al., 1998). *Lrp5* is very broadly expressed in most mouse tissues (Kato et al., 2002). Two different knockout mice (Kato et al., 2002; Fujino et al., 2003), and a mouse with a frameshift mutation, derived through induced mutagenesis (Xia et al., 2008), have been established.

The first *Lrp5* ko mouse was generated through insertion of an IRES-*LacZ*-Neomycin cassette at amino acid residue 373 in exon 6 (Kato et al., 2002). This deletion of exon 6 did not lead to exon skipping, and thus created a functional ko, although a truncated 5'-transcript and resulting N-terminal peptide were detected.

Heterozygous *Lrp5*$^{+/-}$ mice were phenotypically normal. *Lrp5*$^{-/-}$ mice were viable and fertile, but had a higher mortality rate, presumably due to fractures. They presented with a failure of macrophage-mediated apoptosis of the hyaloid vessels (Kato et al., 2002), although the number of macrophages associated with wt and *Lrp5*$^{-/-}$ hyaloid vessels did not differ. LacZ expression of the knock-in construct was detected in macrophages (Kato et al., 2002) and closely associated vitreal microvasculature endothelial cells (Lobov et al., 2005). In addition to the persistance of the hyaloid

vasculature, a mild delay in regression was noted for the pupillary membrane and the tunica vasculosa lentis. No delay in hyaloid vessel regression was detected in *Lrp5*$^{+/-}$ (Kato et al., 2002). The retinal phenotype again was very similar to that observed in *Ndph* and *Fzd4* knockout animals. Only the superficial vasculature was developed, while secondary and tertiary intraretinal networks were absent in the *Lrp5*$^{-/-}$ mouse (Figure 19) (Xia et al., 2008). Fluorescein angiography further revealed leakiness of the remaining vessels.

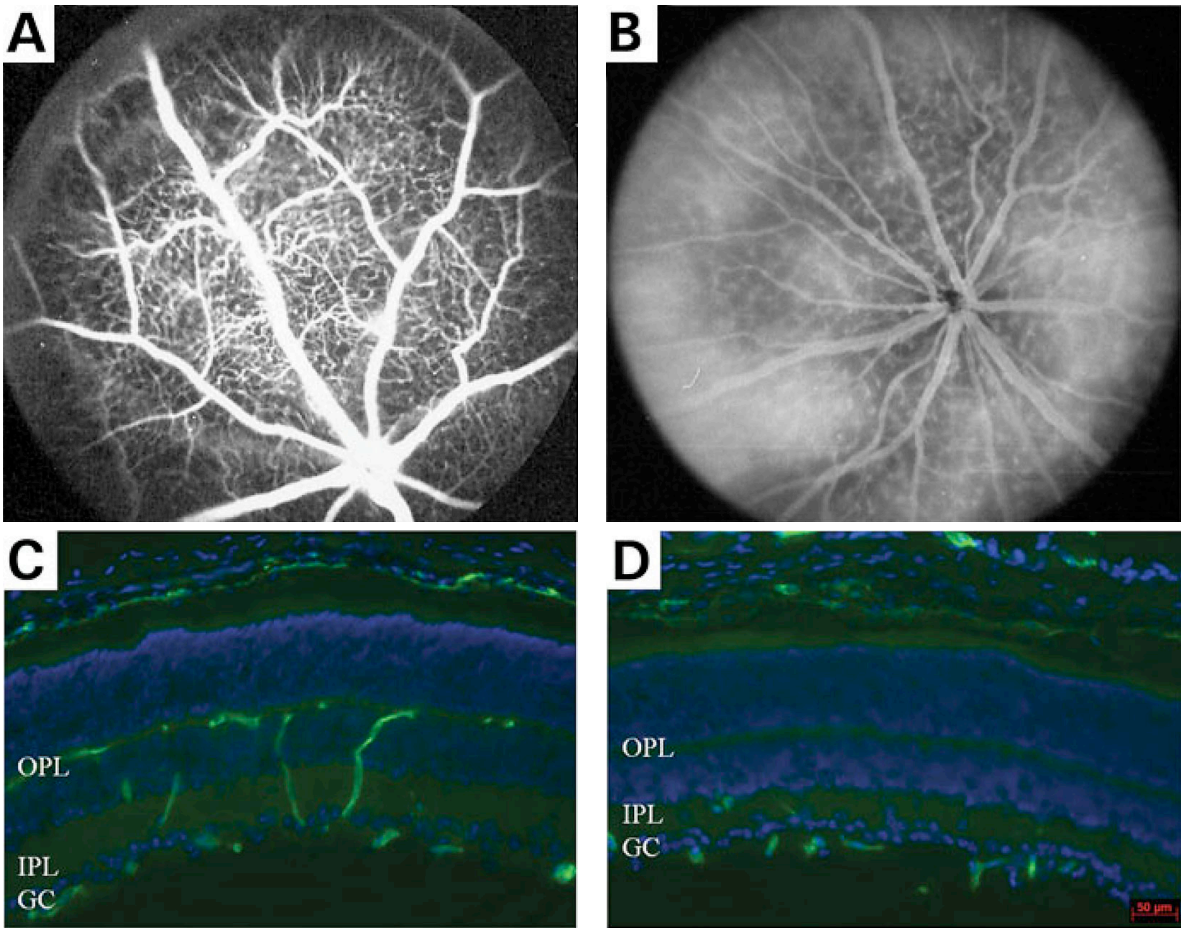

Figure 19 Retinal vasculature in 1-month-old *Lrp5* knockout mice. **(A)** Normal fluorescein angiogram of an *Lrp5*$^{+/-}$ retina. **(B)** The angiogram of the *Lrp5*$^{-/-}$ retina reveals increased background fluorescent signals due to hyperpermeable vessels. **(C)** A normal, three-layered vasculature was found in this *Lrp5*$^{+/-}$ retinal section labeled with an antibody against CD31 (PECAM; an endothelial cell marker; *green*). **(D)** In the *Lrp5* null retina, only the superficial network was labeled similarly. The deep plexus in the outer plexiform layer (OPL) was not developed, and vessels in the IPL were reduced. (Source: Xia et al., 2008)

Another OPPG mouse model was generated through ENU (N-ethyl-N-nitrosourea)-induced mutagenesis (Xia et al., 2008). Whole-genome linkage analysis of offspring presenting with an eye phenotype similar to FEVR lead to the localization of the *r18* mutant allele in the *Lrp5* gene. A single nucleotide insertion in exon 23 was found, causing a frame shift and resulting in the replacement of the C-terminal 39 amino acid residues by 20 new amino acids.

Hetero- and homozygous *r18* mice were viable and fertile. Homozygous *Lrp5*$^{r18/r18}$ mice presented with pale, attenuated retinal arteries, hypopigmentation, and frequently

displayed hemorrhages. The retinal vasculature was described to be leaky and contained fewer small vessels and capillaries. The development was not as sharply impaired as in the *Lrp5* ko mice generated by Kato et al., but also presented with a lack of retinal vasculature, especially in the outer plexiform layer (Figure 20). Some of the capillaries in the inner plexiform layer failed to develop a lumen, and endothelial cells were wrapped in a thicker basal membrane.

No effects on brain or hearing system were reported from any of the mouse models yet.

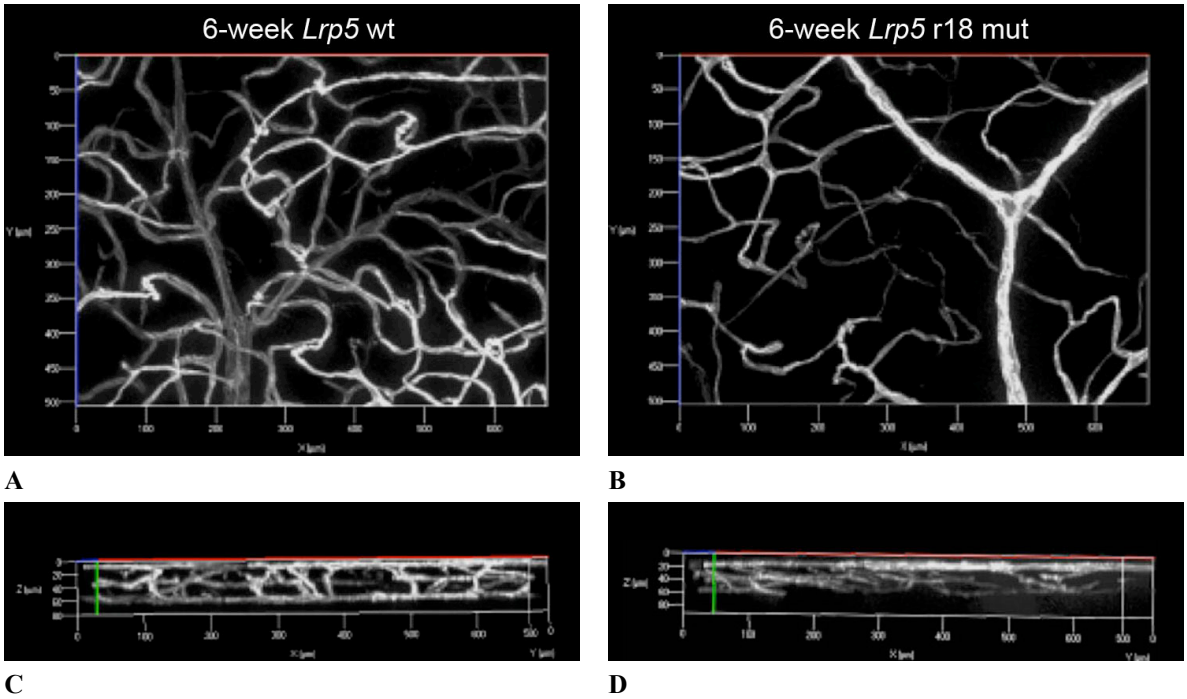

Figure 20 Three dimensional images of fluorescent-dye labeled retinal vessels in 6-week-old *Lrp5 r18* mutant hetero- and homozygous littermates. (A) A normal, three-layered vasculature is present in the heterozygous $Lrp5^{+/r18}$ retina. (B) The retinal blood vessel system of the homozygous $Lrp5^{r18/r18}$ mutant is disorganized and attenuated. (C, D) These panels correspond to the images above, but are rotated 90°. (Source: Xia et al., 2008)

Instead, extensive analyses have concentrated on the bone phenotype. Decreased bone mass in $Lrp^{-/-}$, but also to a lesser extent in $Lrp5^{+/-}$, were shown to be the result of a functional defect of osteoblasts (Kato et al., 2002). Decrease in osteoblast proliferation and subsequent reduction of bone matrix deposition resulted in impaired bone formation postnatally. Since this phenotype was also evident in heterozygotes, the bone phenotype was proposed to be a dominant effect of the mutation, while the ocular features are recessive (Kato et al., 2002). This observation correlates well with the description of OPPG patients (Gong et al., 2001; Ai et al., 2005).

Another *Lrp5* deficient mouse was generated through insertion of a neomycin cassette in exon 18, thereby disrupting a ligand binding repeat (Fujino et al., 2003). In contrast to the other *Lrp5* mouse models, no apparent histological anomalies in bone or eye were reported. However, Lrp5 and canonical Wnt signaling were shown to be required for glucose-induced insulin secretion. Thus, this finding may provide a link between exudative vitreoretinopathies (caused by mutations in *NDP*, *FZD4*, and *LRP5*) and diabetic retinopathy.

1.3.5 The molecular basis of Norrie disease and allelic disorders

From a geneticist's point of view, the definite diagnosis for a certain exudative vitreoretinopathy can only be made when a causative gene mutation has been found. I suggest the diagnosis of Norrie disease, if a mutation in *NDP* were found; OPPG, if the mutation in *LRP5* is recessive, and HBM, if it is dominant. A little complex and confusing is the diagnosis of FEVR, since mutations in *FZD4*, *NDP*, and *LRP5* have been described as causes for FEVR, maybe due to the high variability of the diseases and the difficulties to establish definite morphological and clinical definitions. I suggest that the diagnosis of FEVR is only used when mutations in *FZD4* have been found, although the term "familial exudative vitreoretinopathy" could equally apply to all disorders caused by inherited mutations in *NDP*, *FZD4*, and *LRP5*.

Prompted by the similar symptoms in patients harboring mutations in either *NDP*, *FZD4*, or *LRP5* (Figure 21), and the close phenotypic appearance of the respective mouse models, Norrin has been found to be a high-affinity ligand of the FZD4/LRP5 receptor pair (Xu and Wang et al., 2004).

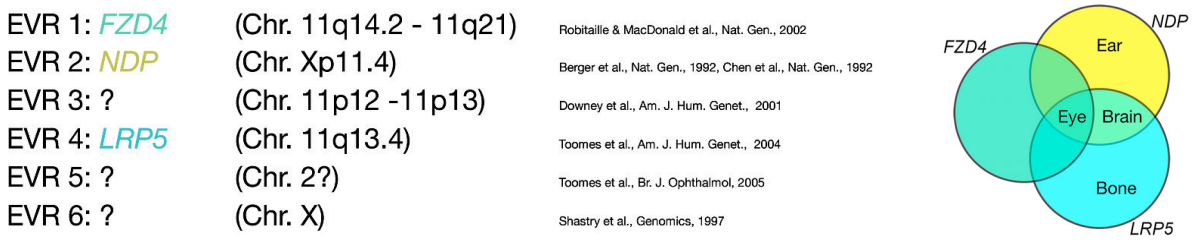

Figure 21 Loci and phenotypes associated with familial exudative vitreoretinopathy. Mutations in 3 genes have been associated with FEVR so far, while evidence has been published for at least 3 additional loci.

1.3.5.1 Wnt-signaling

FZD4 and LRP5 are known receptors for wingless type (Wnt) proteins. Members of this family are highly conserved and play important roles in multiple developmental processes, including mesoderm induction, tissue patterning, cell fate determination, and cell proliferation (Logan and Nusse, 2004). Wnt-induced signaling generally is thought to be limited to the immediate vicinity of the site of synthesis and secretion, presumably as a consequence of the tight binding of Wnts to extracellular matrix molecules (Wang et al., 2001). Although norrin is not part of the Wnt-family of proteins, it shares a number of common features, like asscociation with the extracellular matrix (Perez-Villar and Hill, 1997), and the ability to induce canonical Wnt-signaling (Figure 22) through binding to FZD4/LRP5 (Xu and Wang et al., 2004).

Canonical Wnt-signaling (or "Wnt/β-catenin signaling") probably is the most investigated and best understood Wnt pathway (reviewed in Lad et al., 2008). In the absence of Wnt-proteins, a destruction complex consisting of adenomatous polyposis coli (*APC*) and AXIN1 causes casein kinase 1 and glycogen synthase kinase 3 (GSK3β) to phosphorylate β-catenin, thereby targeting it for ubiquitination and subsequent

degradation by the proteosome. Upon binding of Wnts to the Frizzled/LRP-receptor complex, activation of the phosphoprotein disheveled (*DVL*) leads to translocation of the GSK3-complex to the cell membrane, where AXIN1 binds to LRP5/6 and becomes degraded. As a result, the GSK3-complex dissociates, stablizing cytoplasmic β-catenin and allowing it to translocate to the nucleus. It then interacts with transcription factors of the TCF/LEF-family and initiates the transcription of target genes (Figure 22).

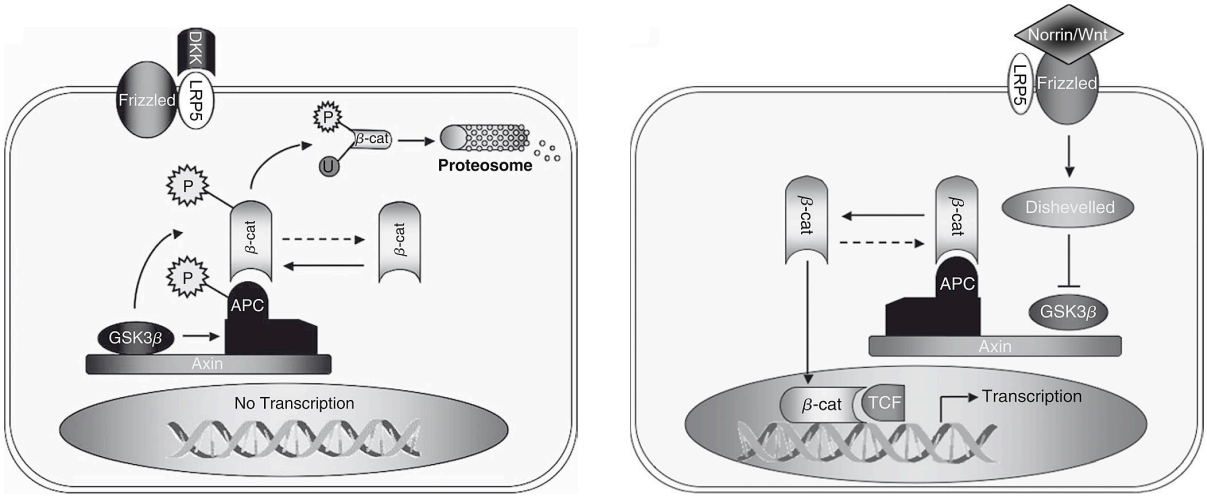

A **B**

Figure 22 Canonical Wnt-pathway. **(A)** In absence of Wnts or norrin, cytoplasmic β-catenin is phosphorylated by a GSK3β complex (containing GSK3β, Axin1, APC, and casein kinase 1), leading to ubiquitination and degradation by the proteosome. **(B)** Binding of norrin or Wnt-proteins to frizzled and LRP5/6 receptors activates the phosphoprotein disheveled, which subsequently inhibits GSK3β, and leads to binding of Axin1 to LRP5/6. As consequence, the GSK3β destruction complex is degraded, and β-catenin becomes stabilized and is able to translocate to the nucleus, where it binds to transcription factors of the TCF/LEF family, leading to transcription of target genes (modified after Lad et al., 2008).

Based on the finding that norrin activates canonical Wnt-signaling, the most likely pathogenic molecular mechanism for *NDP, FZD4,* and *LRP5*-associated diseases would be altered signaling activity. This hypothesis was supported by experiments, in which signaling efficacy was measured for 18 *NDP* missense mutations in cells co-transfected with *Fzd4*, *Lrp5*, and a Luciferase reporter under the control of Wnt-/β-catenin signaling (the so called "Super TOP-FLASH" reporter). For 17 mutations, reduced signaling efficacy was found (Table 2). 11 mutations even show less than half of the wt activity. In contrast, one mutation (p.K58N) showed 2-fold enhanced activity in comparison to the wt construct (Xu and Wang et al., 2004).

Thus, Wnt-target genes affected by altered signaling activity of the NDP/FZD4/LRP5 complex would be ideal candidates for further mutation screening in ND/EVR patients negative for mutations in the three known genes (Figure 21).

In the following paragraph, I want to give an overview over the known genetic basis of ND and allelic diseases by reviewing the molecular properties of *NDP*, *FZD4*, and *LRP5*, and all disease-associated mutations reported so far.

1.3.5.2 NDP

Linkage analyses of ND patient families lead to localization of the disease locus to the short arm of the X-chromosome at Xp11.4-p11.3 (Bleeker-Wagemakers et al., 1985). In 1992, the causative gene was isolated through positional cloning (Berger et al., 1992; Chen et al., 1992), and was termed Norrie disease pseudoglioma (*NDP*) thereafter. It spans a genomic region of 28 kb and is organized in 3 exons (separated by two introns of 15 and 9 kb) that encode a 1.8 kb RNA transcript. The open reading frame, located in exons 2 and 3, codes for a 133aa protein including a 24aa signal peptide that later has been named norrin (Figure 23 A). Norrin is highly conserved among species, with 95% identity on the amino acid level with rat, mouse, and dog, especially with regard to 11 cysteine residues (Berger, 2008). *In silico* modeling revealed a 3-D structure similar to transforming growth factor-β (TGF-β) (Figure 23 B, C) (Meitinger et al., 1993), and subsequently norrin has been put into a superfamily of cystine-knot-containing growth

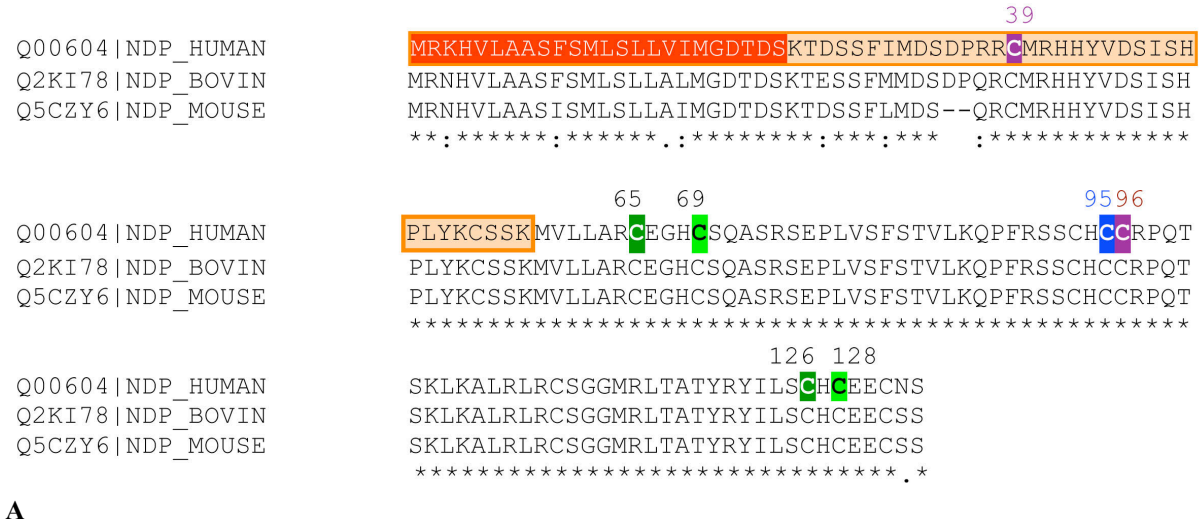

A

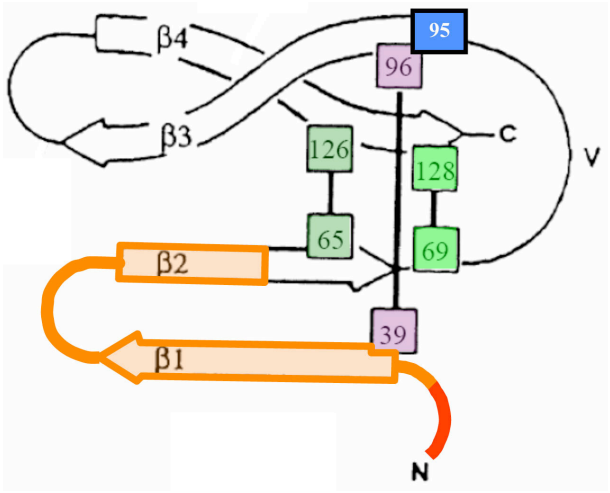

B

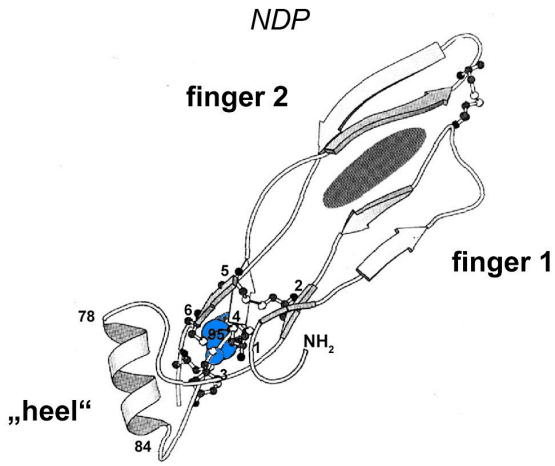

C

Figure 23 Sequence and structure of norrin. **(A)** Multiple alignment of human, cow, and mouse norrin shows strong conservation. Six cysteine residues are important for the cystine-knot structure. Specific domains are highlighted: *orange*: amino acids encoded by exon 2; *red*: signal peptide; *green, magenta*: intramolecular disulfide bridge-forming cysteins; *blue*: cysteine involved in dimerisation or oligomerisation. **(B)** Putative NDP tertiary structure, forming a cystine-knot (adapted from Meitinger et al., 1993). Color scheme is equal to the one used in (A). **(C)** 3D model of monomeric Norrin. An α-helix ("heel") is shown instead of the v-loop in (B), and the two anti-parallel β-sheets are designated as "fingers" (from Meitinger et al., 1993). (Figure adapted from: Masterthesis Zürcher, 2007, and W. Berger, personal communication)

factors that also include platelet-derived growth factor-β (PDGF-β), nerve growth factor (NGF), vascular endothelial growth factor (VEGF), placental growth facor (PlGF), and von-Willebrand-factor (VWF) (McDonald and Hendrickson, 1993).

A total of 116 different *NDP* mutations have been described so far (Table 2). These include 16 gross chromosomal aberrations leading to entire or partial deletion of the *NDP* locus. The remaining mutations are small insertions, deletions, or point mutations. 91 different mutations lie inside the reading frame, 5 mutations are located in exon 1, 1 mutation is in intron 1, 5 mutations are in intron 2, and 1 mutation has been located in the 3'-UTR. Point mutations alone account for an amino acid exchange at 49 different positions.

All mutations have been associated with visual impairment, although Norrie disease was not always suspected. Due to the high variability of the clinical presentation, even within one family (Zaremba et al., 1998), diagnoses also included Coats' disease (CD), (familial) exudative vitreoretinopathy (F)EVR, persistent fetal vasculature (PFV/PHPV), X-linked recessive primary retinal dysplasia (PRDX), retinopathy of prematurity (ROP), retinoblastoma (RB), and retinoschisis (RS). In the case of 29 mutations (25%), variable degrees of hearing impairment have been reported in addition. No mention about hearing impairment has been made for 22% of the *NDP* mutations. In the remaining 53%, signs of progressive deafness might have been missed, since late onset and slow progression of the hearing loss may mask its presence and thereby limit formal assessment (Schuhback et al., 1995). While Warburg initially estimated 30% (Warburg, 1966) of the patients suffer from deafness, Halpin and Rehm proposed that penetrance is 100% (Rehm et al., 2002; Halpin et al., 2005), and nearly all patients have detectable hearing impairment after puberty. Although this might be technically right, it is of great importance to be aware what these numbers mean for the blind patients, and to be careful how to confront them with the diagnosis.

Mental retardation has been described in association with 40 mutations (35%). Here again, high variability has been observed, ranging from low IQ and learning difficulties to severe MR, growth failure, autistic features, and seizures. In contrast to the progressive nature of the hearing impairment, mental features usually present very early in life, and thus the estimated value of 35% may be a good estimate for the penetrance. However, it could be difficult to differentiate between an *NDP*-related mild MR and a developmental delay that is often observed in congenitally blind patients. In addition to vision loss, blind patients often encounter problems with their circadian rhythm (depending on the severity of damage to their melanopsin-containing ganglion cells). If learning depends on a regular sleep routine (which is a popular hypothesis), developmental delay could easily be explained with a disturbed sleep/wake cycle alone.

Black et al. suggested that Coats' disease (CD) is caused by a somatic *NDP* mutation within cells of neuroectodermal origin at a stage of development that results in a segment of the retina carrying the mutant allele (Black et al., 1999). This hypothesis of a genetic mosaic could explain the typical unilateral appearance and high phenotypic variability of CD.

Manifesting carriers have been described for 8 mutations (7%). One of those patients was diagnosed with Coats' disease as only one of her eyes was affected. Interestingly, she then gave birth to an affected son, who presented with a full ND phenotype. In this case, a possible explanation could be a non-random X-inactivation, or a second, somatic

mutation in the *NDP* gene in the mother's affected eye. Such a situation was found in an enucleated eye of another, unrelated CD patient (Black et al., 1999). In the case of a manifesting carrier with a p.C69S mutation (Chen et al., 1993), a 70:30 X-inactivation ratio in favor of the mutant allele has been found. In another 2 cases, genetically healthy female offspring of an *NDP* mutation-carrying mother presented with an ND phenotype, indicating a transplacental role of Norrin might affect penetrance in females (Mintz-Hittner et al., 1996).

Different attempts have been made to assign certain mutations to a specific clinical presentation. Gross deletions and nonsense mutations have been assigned exclusively to ND (first noted by Wong et al., 1993; Chynn et al., 1996). Further, more severe phenotypes have been described if one of the structurally relevant six cysteine residues (39, 65, 69, 96, 126, 128) constituting the cystine-knot-motif is involved (Meitinger et al., 1993; Schuback et al., 1995). Initially, it was suggested that mutations in *NDP* only account for the ocular phenotype, since no signs of mental retardation (MR) were found in a patient with a 150kb deletion encompassing the entire *NDP* gene, but not the neighboring *MAO-A* and *MAO-B* genes. In contrast, patients with gross deletions including these genes were mentally challenged (Berger et al, 1992). However, since then many point mutations have been described in patients with features of ND including MR, substantiating a role for norrin in the development of MR (e.g. Joos et al., 1994; Lev et al., 2007; Table 2). Further, it has been proposed that myoclonus epilepsy and growth retardation were never seen in association with point mutations and thus must be ascribed to functional defects in other genes or non-genic factors (Berger et al., 1992). However, a patient with a p.S75P mutation has been described who suffered from tonic-clonic epilepsy and frontal motor seizures, indicating that epilepsy is part of the phenotypic spectrum of ND, in the case concurrent non-genic factors can be excluded (Yamada et al., 2001).

Phenotype	Exon	cDNA	Protein	Reference	Age	Deafness	MR	MF
Gross deletions including NDP:								
ND		4 different deletions (complete, partial, 4bp and single)		Zhu, 1994	?	?	?	
ND / FEVR		xp11.4invq22		Pettenati, 1993	~	+	+	
ND	1-3	entire NDP deletion, as well as MAOA & MAOB; 2-2.5 Mb		Suarez-Merino, 2001	~	?	seizures	
ND	2	partial NDP deletion, 4kb		Chen, 1993	?	?	?	
ND	2	partial NDP deletion, 5kb		Chen, 1993	?	?	?	
ND	2	partial NDP deletion, 2-10kb		Chen, 1993	2	-	-	
ND	2	partial NDP deletion		Schuback, 1995	2	-	-	
ND	2-3	partial NDP deletion		Schuback, 1995	5	-	-	
ND	3	partial NDP deletion; MAOA/MAOB del >20kb		Chen, 1993	2	-	microcephaly, seizures	
ND	3	partial NDP deletion; 7kb; part of exon 3		Chen, 1993	?	?	?	
ND	3	partial NDP deletion		Schuback, 1995	<1	-	-	
ND	3	partial NDP deletion		Schuback, 1995	36	+	seizures	
ND	3	partial NDP deletion; 3'-UTR of ex3 incl. PAS		Rivera-Vega, 2005	~	-	22%	
Small deletions, insertions, and point mutations in NDP:								
ROP	1	c.-391_-380delinsGTCTCTC	5´-UTR	Talks, 2001	1	-	-	+
ROP	1	c.-386_-310del	5´-UTR	Talks, 2001	<1	?	?	
ND, ROP	1	ins 12 bp (CT repeat)	5´-UTR	Hiraoka, 2001; Wu, 2007	<1	-	-	
ND	1	ins 10 bp (CT repeat)	5´-UTR	Schuback, 1995	~	+	50%	
ROP, RS	1	del 14 bp (CT repeat)	5´-UTR	Hiraoka, 2001; Dickinson, 2006; Wu, 2007	<1	-	-	
ND	IVS 1	c.-208+1G>A		Fuchs, 1996	9	+	+	
ND	2	c.1A>G	p.M1V	Isashiki, 1995; Gal, 1996; ZH, unpublished	~	50%	50%	
ND	2	c.2_3delTG	p.M1KfsX22	Caballero, 1996	10	-	-	
ND	2	c.2T>G	p.M1R	Schuback, 1995	20	+	autistic features	
ND?	2	c.27_28insATCC	p.F10IfsX17	Berger, 1992	~	-	-	
ND	2	c.38T>G	p.L13R*	Fuchs, 1994	~	78%	45%	
ND	2	c.44T>G	p.L15R	Berger, 2008	11	?	?	
ND	2	c.47T>C	p.L16P	Yamada, 2001	~	-	seizures (20%)	
ND	2	c.50_51insT	p.V17fsX8	Gal, 1996	~	?	seizures	
ND, FEVR	2	c.53T>A	p.I18K	Kondo, 2007; Shima, 2009	<1	-	-	
ND	2	c.65delC	p.T22KfsX9	Schuback, 1995	12	+/-	-	
ND	2	c.86C>G	p.S29X	Meindl, 1992	~	?	+	
ND	2	c.103delG	p.D35TfsX6	Chynn, 1996	<1	-	-	
ND	2	c.109C>T	p.R37X	Ott, 2000	6	-	-	
ND, FEVR, PHPV	2	c.112C>T	p.R38C	Royer, 2003; Riveiro-Alvarez, 2005	~	-	-	
ND	2	c.115T>C	p.C39R	Joos, 1994; Wu, 2007	~	50%	microcephaly (50%)	
EVR	2	c.122G>A	p.R41K*	Shastry, 1997	?	-	-	
PFV	2	c.123G>C	p.R41S	Wu, 2007	<1	-	-	
PFV	2	c.123G>T	p.R41S	Dhingra, 2006	<1	-	-	
FEVR, EVR	2	c.125A>G	p.H42R*	Shastry, 1997; Wu, 2007	~	-	-	
ND	2	c.128_129insA	p.H43QfsX13	Caballero, 1996	<1	-	-	
ND	2	c.128A>G	p.H43R	Dickinson, 2006	5	+	-	
ND	2	c.129C>G	p.H43Q	Royer, 2003	~	-	+	
ND	2	c.131A>G	p.Y44C	Meindl, 1992	26	-	++	
ND, PHPV, sporadic	2	c.131_132insA	p.Y44X	Hatsukawa, 2002	~	-	-	
ND	2	c.133G>A	p.V45M	Royer, 2003	18	-	+	
ND, MR	2	c.134T>A	p.V45E	Lev, 2007	<2	?	seizures	
ND	2	c.136delG	p.D46IfsX58	Schuback, 1995	22	+	-	
ND	2	c.142_145delATCA	p.I48VfsX55	Zhu, 1994 Meeting abstract	?	?	?	
ND, FEVR	2	c.162G>C	p.K54N	Hoefsloot, 2000; Kondo, 2007; Boonstra, 2009	~	-	?	+
ND	2	c.170C>G	p.S57X	Berger, 1992	?	+	+	
ND, EVR	2	c.174G>T	p.K58N†	Fuentes, 1993; Shastry, 1997	~	+/-	50%	
ND	IVS 2	c.174+1G>T	?	ZH, unpublished	?	?	?	
ND	IVS 2	c.174+1G>C	?p.K58fsX49?	Fuchs, 1996	2	-	-	
ND	IVS 2	c.174+5G>C	?p.K58fsX49?	Berger, 1992; Fuchs, 1996	?	-	+	
ND	IVS 2	c.175-1G>C	?	Royer, 2003	~	+	40%	
ND, FEVR	IVS 2	c.175-1G>A	?	Kondo, 2007	1	-	-	
ND	3	c.179T>A	p.V60E*	Meindl, 1992	11	-	+/-	
ND, VI	3	c.181C>T	p.L61F	Berger, 1992; Rehm, 1997	~	+	-	
FEVR	3	c.181C>A	p.L61I	Wu, 2007	<1	-	-	
ND	3	c.182T>C	p.L61P*	Schuback, 1995	14	-	-	
ND	3	c.185T>C	p.L62P	Zhu, 1994 Meeting abstract	?	?	?	
ND	3	c.187G>T	p.A63S	Novelli, 1999	?	?	?	
ND	3	c.188C>A	p.A63D*	Schuback, 1995	14	-	-	
ND	3	c.194G>A	p.C65Y	Strasberg, 1995; Wu, 2007	~	+	+	
ND	3	c.195C>G	p.C65W	Schuback, 1995	?	?	?	
PFV (unilateral)	3	c.196G>A	p.E66K	Aponte, 2009	<1	-	-	

Phenotype	Exon	cDNA	Protein	Reference	Age	Deafness	MR	MF
ND	3	c.205delT	p.C69AfsX35	Schuback, 1995	45	+	+	
ND	3	c.206G>C	p.C69S	Chen, 1993	~	+	66%	+
ND	3	c.218C>A	p.S73X	Walker, 1997	<1	-	-	
ND, FEVR	3	c.220C>T	p.R74C	Berger, 1992; Fuchs, 1996; Allen, 2006	?	+/-	-	
ND	3	c.223T>C	p.S75P	Yamada, 2001	~	-	seizures (40%)	
ND	3	c.224C>G	p.S75C	Berger, 1992	?	+	+	
ND	3	c.226G>T	p.E76X	Hutcheson, 2005	?	?	?	
ND	3	c.236_240delTGTCG	p.V78fsX67	Riveiro-Alvarez, 2005	?	+	+	
ND	3	c.267_268insCTC	p.F89_R90insL	Hutcheson, 2005	?	?	?	
ND	3	c.268C>T	p.R90C	Royer, 2003	~	-	75%	
ND	3	c.269G>C	p.R90P*	Berger, 1992	?	-	-	
ND	3	c.282_286delinsATGCCTCG	p.H94_C96delinsQCLG	Schuback, 1995	17	+	autistic features	
ND (severe)	3	c.283T>C	p.C95R	Isashiki, 1995	16	-	-	
ND (severe)	3	c.284G>T	p.C95F	Khan, 2004	~	-	-	
ND (severe)	3	c.285C>A	p.C95X	Wu, 2007	<1	50%	?	
ND, EVR	3	c.287G>A	p.C96Y	Berger, 1992; Meindl, 1992; Shastry, 1999	~	-	+	+
ND, CD	3	c.288C>G	p.C96W	Black, 1999	~	-	-	+
ND	3	c.290delG	p.R97RfsX6	Berger, 1992	?	?	+	
ND	3	c.290G>C	p.R97P	Rivera-Vega, 2005; Kondo, 2007	~	-	33%	
ND, PHPV (mild)	3	c.302C>T	p.S101F*	Walker, 1997	~	-	-	
FEVR	3	c.307C>G	p.L103V	Dickinson, 2006	?	-	-	
ND (mild)	3	c.310A>C	p.K104Q*	Meindl, 1995	3	?	-	
ND	3	c.312G>T	p.K104N	Riveiro-Alvarez, 2006	?	?	?	
ND	3	c.313G>A	p.A105T*	Torrente, 1997	~	-	-	
ROP	3	c.323T>C	p.L108P*	Shastry, 1997	1	-	-	
ND	3	c.325C>T	p.R109X	Schuback, 1995; Mintz-Hittner, 1996	~	50%	50%	(+)*
ND	3	c.328T>C	p.C110R	Zhu, 1993; Fuchs, 1996	~	+	-	
FEVR	3	c.328T>G	p.C110G*	Torrente, 1997	~	-	-	
ND	3	c.328T>A	p.C110S	ZH, unpublished		?	?	
ND	3	c.330C>A	p.C110X	Berger, 1992	?	-/+	-	
ND	3	c.333delA	p.S111fsX150	Hutcheson, 2005	?	?	?	
FEVR (highly variable)	3	c.335G>A	p.G112E	Allen, 2006	~	-	-	
FEVR	3	c.344G>T	p.R115L	Kondo, 2007	21	-	-	
ND	3	c.353C>A	p.A118D	Shastry, 1999	~	+	-	+
EVR	3	c.359A>G	p.Y120C*	Shastry, 1997	?	-	-	
ND	3	c.360C>A	p.Y120X	Riveiro-Alvarez, 2005	?	+	+/-	
ND	3	c.360_368delCCGGTACAT	p.R121_I123del	Schuback, 1995	1	-	-	
ND, PRDX	3	c.361C>G	p.R121G	Zhu, 1994 Meeting Abstract	?	?	?	
ND, ND (mild), FEVR, ROP	3	c.361C>T	p.R121W	Meindl, 1995; Shastry, 1995; Kellner, 1996; Shastry, 1997; Wu, 2007	~	-	-	+
ND, ND (mild), FEVR	3	c.362G>A	p.R121Q*	Fuentes, 1993; Meindl, 1995; Riveiro-Alvarez, 2005; Boonstra, 2009	~	-	-	
FEVR (highly variable)	3	p.362G>T	p.R121L*	Johnson, 1996; Mintz-Hittner, 1996	~	-	-	(+)*
ND	3	c.368T>A	p.I123N*	Schuback, 1995	~	50%	seizures	
FEVR	3	c.370C>T	p.L124F*	Chen, 1993	~	-	-	
ND	3	c.377G>C	p.C126S	Gal, 1996	~	+	seizures	
ND	3	c.378T>A	p.C126X	Fuchs, 1996; Keller, 1996	~	-	-	+
ND	3	c.382T>C	p.C128R	Royer, 2003	3	-	-	
ND	3	c.383_384delinsAA	p.C128X	Wong, 1993; Hutcheson, 2005	~	-	autistic features	
ND	3	c.384C>A	p.C128X	Schuback, 1995	<1	?	+	
ND	3	c.397delT	p.S133PfsX129	Berger, 1992	?	?	+	
ND	3	c.399delC	p.S133fsX128	Riveiro-Alvarez, 2008	?	?	?	
FEVR	3	c.*716T>C	3´-UTR	Wu, 2007	<1	-	-	

Table 2 List of all *NDP* mutations published so far. Numbering according to reference sequence NC_000023.9, GI: 89161218. The A of the ATG start codon lies at position +1. *Age:* age at first examination; tilde symbol (~): varying, i.e. the same patient was examined at different ages, or several different patients have been described. Penetrance of the mutation is given in percent, where described. Mutations marked with * have been shown to have reduced efficacy to induce Wnt-/β-catenin signaling in cell culture, while the p.K58N mutation (†) has 2-fold increased efficacy (Xu and Wang et al., 2004). *CD:* Coats' disease; *EVR:* exudative vitreoretinopathy (sporadic); *FEVR;* familial exudative vitreoretinopathy; *MF:* manifesting female; *MR:* mental retardation; *ND:* Norrie disease; *PAS:* polyadenylation signal; *PHPV:* persistent hyperplastic primary vitreous; *PFV:* persistent fetal vasculature; *PRDX:* primary retinal dysplasia, X-linked; *ROP:* retinopathy of prematurity; *RS:* retinoschisis; *VI:* venous insufficiency. *indicated manifesting females were genetically healthy (wt) offspring of a heterozygous mother; this may indicate a transplacental effect of *NDP* mutations.

1.3.5.3 FZD4

The first locus for autosomal dominant FEVR has been mapped to the long arm of chromosome 11 at 11q13-q23 (Li et al., 1992). Ten years later, the seven-pass transmembrane receptor Frizzled-4 (*FZD4; CD344*) was identified as the disease-causing gene, thereby associating a Wnt-receptor with human disease for the first time (Robitaille et al., 2002). *FZD4* is a 2-exon gene consisting of 7,382 bps (separated by a 2,330bps intron), producing a 537aa protein, and spans a 9,711bps genomic region at 11q14.2 (Figure 24). *FZD4* is highly conserved, with 96% identity on the amino acid level with rat and mouse.

A total of 27 different mutations have been described so far (Figure 24; Table 3). Most common are missense mutations (18), followed by frameshift (5) and nonsense (3) mutations. Although mutations in the *FZD4* gene have been defined to follow dominant inheritance, which is in contrast to the mouse model (Wang et al., 2001), penetrance and phenotypic variablility are high. Kondo et al. (2003) described 2 families with a p.R417Q exchange in 7 members, yet only 4 were diagnosed with FEVR (58%). In the case of the p.M105V and p.G488D alterations, only one of two family members carrying one of the mutations was clinically affected (50%). The same applies to the p.M342V and p.W335C mutations, which only have been found in one of two mutation-carrying family members (Yoshida et al., 2004; Qin et al., 2005). Penetrance of the p.W319CfsX5 frameshift

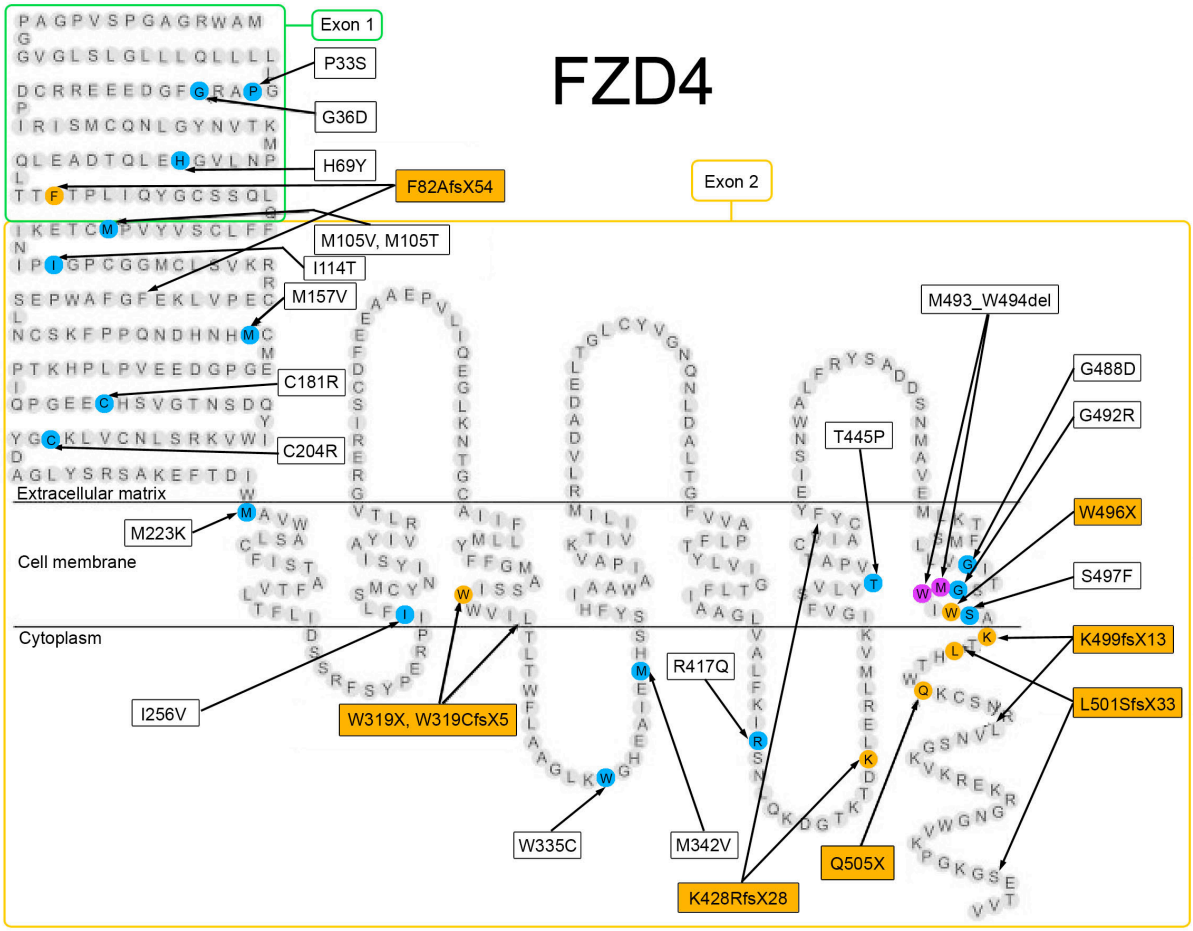

Figure 24 Amino acid sequence and schematic structure of FZD4. The first 95aa are encoded in exon 1 (*green box*), the remaining 442aa in exon 2 (*orange box*). All mutations known to date are depicted: Truncating nonsense or frameshift mutations (*orange*), missense mutations (*blue*), and the small deletion (*purple*) (adapted from Toomes et al., 2004).

Phenotype	Exon	cDNA	Protein	Reference	Age
FEVR	1	c.97C>T	p.P33S†	MacDonald, 2005; Nallthambi, 2006; Boonstra, 2009	~
FEVR	1	c.107G>A	p.G36D	Toomes, 2004	
FEVR	1	c.205C>T	p.H69Y	Omoto, 2004	
FEVR	1	c.244_251del8ins27	p.F82AfsX54	Nallathambi, 2006	
FEVR	2	c.313A>G	p.M105V	Kondo, 2003	
FEVR	2	c.314C>T	p.M105T	Toomes, 2004	
ND; FEVR; PFV	2	c.341T>C	p.I114T	Robitaille, 2009	
FEVR	2	c.471A>G	p.M157V	Toomes, 2004	~
FEVR; PFV	2	c.541T>C	p.C181R	Omoto, 2004	
FEVR	2	c.610T>C	p.C204R	Nallathambi, 2006	~
FEVR	2	c.668T>A	p.M223K	Boonstra, 2009	
ROP	2	c.766A>G	p.I256V	MacDonald, 2005	?
FEVR	2	c.957G>A	p.W319X	Kondo, 2003	
FEVR	2	c.957delG	p.W319CfsX5	Toomes, 2004	<1
FEVR	2	c.1005G>C	p.W335C	Qin, 2005	
FEVR	2	c.1024A>G	p.M342V	Yoshida, 2004	
PHPV/severe FEVR*	2	c.1250G>A	p.R417Q	Kondo, 2003 / 2007	
FEVR	2	c.1286_1290delAGTTA	p.K428RfsX28	Müller, 2004	~
FEVR	2	c.1333A>C	p.T445P	Boonstra, 2009	
FEVR	2	c.1463G>A	p.G488D	Kondo, 2003	
FEVR	2	c.1474C>G	p.G492R	Müller, 2004	~
FEVR; PFV	2	c.1479_1484delGTGGAT	p.M493_W494del	Robitaille, 2002 / 2009	
FEVR	2	c.1488G>A	p.W496X	Boonstra, 2009	
FEVR	2	c.1490C>T	p.S497F	Toomes, 2004	
FEVR	2	c.1497delA	p.K499fsX13	Toomes, 2004	
FEVR	2	c.1501_1502delCT	p.L501SfsX33	Robitaille, 2002	
FEVR	2	c.1513C>T	p.Q505X	Toomes, 2004	

Table 3 List of all *FZD4* mutations published so far. Numbering according to reference sequence NC_000011.8, GI: 51511727. The A of the ATG start codon lies at position +1. *Age:* age at first examination; tilde symbol (~): varying, i.e. the same patient was examined at different ages, or several different patients have been described. *FEVR:* familial exudative vitreoretinopathy; *ND:* Norrie disease; *PHPV:* persistent hyperplastic primary vitreous; *PFV:* persistent fetal vasculature; *ROP:* retinopathy of prematurity. *The severe phenotype could be explained by the homozygousity of the mutation, the only one described so far. † Conflicting reports exist about the pathogenicity of this mutation, since it was not found to segregate with the disease in an FEVR family (Boonstra et al., 2009), but was found in a sporadic case (MacDonald et al., 2005) and in an Indian family (Nallathambi et al., 2006).

mutation was determined to be 33% (1/3). However, the patient's father and sibling had not undergone fluorescein angiography, leaving the possibility of subclinical affection. The truncation mutation p.Q505X had a penetrance of 75% (3/4) (Toomes et al., 2004). The mutations p.K428RfsX28 and p.G492R have been reported to show 100% penetrance, but variable expressivity (Müller et al., 2008), and non-penetrance for mutations in p.W319X was 53% (8/15) (Boonstra et al., 2009). The two variants p.P33S and p.P168S were found in cis in a sporadic EVR case (MacDonald et al., 2005). Since the p.P168S alteration was described as a benign rare sequence variant (p<0.3%) before (Toomes et al. 2004), the authors concluded that only the p.P33S variation is pathogenic. However, both variations on the same allele did not co-segregate with FEVR in a family recently described, further suggesting highly variable penetrance (Boonstra et al., 2009).

Taken together, although mutations in *FZD4* are dominantly inherited, no prediction can be made on the expressivity of a clinical phenotype, suggesting the involvement of additional modifiers. One such possible non-genic modifier was recently discussed in a family with 4 members carrying a p.I114T (Robitaille et al., 2009). The grandmother

harbored the mutation, but was asymptomatic. The mother also carried the mutation, but the phenotype was mild, with no avascular retinal areas and a retinal tear and possible hole being the only signs. In contrast, her two boys presented with a full blown FEVR phenotype with retinal detachments and low visual acuity. Of interest, the mother was treated with valproic acid for juvenile myoclonic epilepsy during pregnancy. Valproic acid has been shown to up-regulate genes in the Wnt-pathway (Duenas-Gonzales et al., 2008), and the authors thus speculated that development of a worse FEVR phenotype could in part be due to valproic acid in the presence of a *FZD4* mutation in the mother.

In addition to co-segregation with the disease, the effect of possible pathogenic alterations in *FZD4* was mainly supported with *in silico* analyses, e.g. by predicting an effect on the protein structure. In the case of the p.L501SfsX33 mutation, it could be experimentally shown that the mutation in the cytoplasmic tail inhibited the protein to translocate to the plasmamembrane (Robitaille et al., 2002).

Interestingly, and in contrast to *NDP* and *LRP5*, mutations in *FZD4* have been associated only with ocular features so far. This may be related to the almost exclusive heterozygous occurrence in FEVR patients. The homozygous *Fzd4* ko mouse, like the *Ndph* ko mouse, presented with progressive hearing loss and in addition showed signs of cerebellar ataxia. The lack of reports on homozygous *FZD4* mutations in patients might of course be due to the rare prevalence of the mutated alleles, but it is tempting to speculate that some extraoccular features could manifest in patients harboring a homozygous mutation. In the only case report of a homozygous patient published so far, the eye phenotype was severe and worse than in the heterozygous parents, but no mention about extraocular features was made (Kondo et al., 2007).

1.3.5.4 LRP5

Mutations in the low-density lipoprotein receptor-related protein 5 gene (*LRP5*) first have been associated with OPPG (Gong et al., 2001), then with high bone mass phenotypes (HBM; Little et al., 2002; Boyden et al., 2002), and later also with FEVR (Toomes et al., 2004). *LRP5* is located on 11q13.2 and spans a genomic region of 136.63 kb. The only known transcript (ENST00000294304) consists of 5,124 bps, is organized in 23 exons and codes for a 1,615 aa protein (Figure 92).

LRP5 functions as a Wnt co-receptor that can be divided into an extracellular, a single transmembrane, and a cytoplasmic domain. The large extracellular domain of LRP5 consists of a signal peptide followed by four six-bladed β-propeller domains (containing six YWDT motifs) separated by an EGF-like repeat each, and three LDL-Receptor repeats (Figure 25). WNT ligands bind to the first two β-propellers. The intracellular domain has been shown to bind Axin (*AXIN1*) and FRAT1 (frequently rearranged in advanced T-cell lymphomas) (Balemans and van Hul, 2006). The Wnt-inhibitor family dickkopf (*DKK*) initially has been proposed to bind to the third β-propeller (Mao et al., 2001), although additional evidence has been provided that DKK may bind to the first and second or the third and fourth β-propeller motifs (Zhang et al., 2004). This would correlate with the finding that DKK inhibition (besides inhibition through Sclerostin) is impaired in HBM associated alleles, which cluster in the first β-propeller (Semenov, 2006).

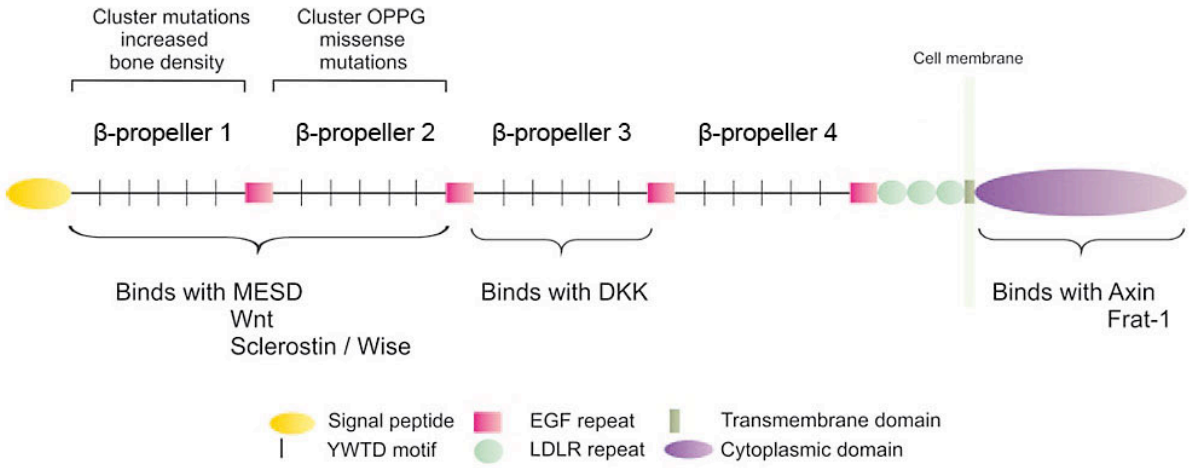

Figure 25 Illustration of the LRP5 protein showing the clustering of mutations causing HBM in the first β-propeller and the clustering of missense mutations causing OPPG in the second β-propeller. (modified from Balemans and van Hul, 2006)

A total of 85 different *LRP5* mutations have been described so far (Table 4). Two large deletions were reported: one gross deletion of 8kb due to non-homologous recombination between Alu repeats, leading to the removal of exons 14-16 (Chung et al., 2009), and one large deletion of 174bp involving parts of exon and intron 11 (Ai et al., 2005). The remaining mutations are small insertions, deletions, or point mutations. 81 different mutations lie inside the reading frame, 2 mutations are located in the 5'-UTR, 3 mutations are intronic. 70 mutations have been associated with an eye phenotype; the remaining 15 were only described in conjunction with bone anomalies. All 10 HBM associated mutations do not seem to have ocular effects (Boyden et al., 2002; Little et al.,

2002; van Wesenbeek et al., 2003; Boyden in response to Whyte et al., 2004; Rickels et al., 2005; Balemans et al., 2007).

Carriers of OPPG mutations show an increased incidence for osteoporotic fractures, indicating a dominant effect of *LRP5* on bone mass, but only a recessive influence on the ocular phenotype (van Wesenbeeck et al., 2003; Gong et al, 1996). This hypothesis correlates with the published data: All 15 bone-only-related mutations follow dominant inheritance, and 51 of the 70 eye-related mutations have been described as recessive. The cases of the divergent 19 mutations described as dominant have to be treated with care: In most cases, the respective mutation was also found heterozygously in non-affected relatives (Gong et al., 2001; Toomes et al., 2004; Ai et al., 2005), and the term „dominant" was used to describe the effect on the skeletal system, but not the eye.

Several compound heterozygous *LRP5* mutations were found (Gong et al., 2001; Ai et al., 2005; Cheung et al., 2006). Digenic inheritance of mutations in *LRP5* and *FZD4* was reported in one study, stating that the phenotype was more severe than with the dominant *FZD4* mutation alone (Qin et al., 2005). This finding opens up the possibility that digenic inheritance could have been missed in some of the cases with a supposed dominant effect of *LRP5* mutations on the eye.

The reported mutations might have different functional aspects. The most conclusive effect of deletions, frameshift, or nonsense mutations in OPPG patients is the lack of protein, because transcripts truncated in all but the last exon are likely a target of nonsense-mediated mRNA decay (NMD). Lack of LRP5 protein then results in decreased bone mass due to reduced canonical Wnt-signaling (Balemans and van Hul, 2006). Missense mutations could lead to impaired LRP5 function. In vitro studies showed that different mutated LRP5 proteins (p.T390K, p.T244M, p.G404R, p.D.434N, p.G610R) reached the cell surface in different amounts and had different affinities for the molecular chaperone MESD, which is important for folding and transportation (Ai et al., 2005). The mutants p.T244M, p.S356L, p.T390K, p.G520V were shown to be unable to transduce Wnt1, Wnt10b, or NDP signals, while the p.G404R p.D434N, and p.G610R variants had significantly reduced signaling activity (Ai et al., 2005). None of these mutants had a dominant negative effect on Wnt-signaling when co-expressed with the wt LRP5. These observations correlate with the finding that most missense mutations cluster in the second β-propeller domain, which has been shown to be required for binding to MESD or Wnts. In contrast, nonsense, frameshift and splice site mutations are scattered over all domains (Balemans and van Hul, 2006).

All HBM mutations reside near the top surface and central region of the first β-propeller domain. None of them was constitutively active in the absence of Wnts. However, HBM mutant LRP5 proteins have been shown to have reduced affinity to DKK1, an endogenous Wnt-inhibitor, and it was suggested that these mutations affect Wnt-signaling through diminished regulation by DKK1 (Boyden et al., 2002; Ai et al., 2005). In addition, some HBM mutations might selectively bind one Wnt-ligand better than the other, thereby shifting the specificity of LRP5.

Phenotype	AD/AR	Domain	Exon	cDNA	Protein	Reference
OPPG	AR	signal peptide	1	c.29G>A	p.W10X	Gong, 2001
OPPG	AR	signal peptide	1	c.43-60del	p.Leu15_Leu20del	Chung, 2009
Osteoporosis	AD	signal peptide	1	c.85G>A	p.A29T	Hartikka, 2005
OPPG	AR	β-propeller 1	2	c.209_210delinsAA	p.F70X	Ai, 2005
Osteopetrosis	AD	β-propeller 1	2	c.331G>T	p.D111Y	van Wesenbeek, 2003
FEVR, reduced BMD	AD	β-propeller 1	2	c.433C>T	p.L145F	Qin, 2005
HBM	AD	β-propeller 1	2	c.461G>T	p.R154M	Rickels, 2005
Osteopetrosis	AD	β-propeller 1	3	c.511G>C	p.G171R	van Wesenbeek, 2003
HBM	AD	β-propeller 1	3	c.512G>T	p.G171V	Little, 2002; Boyden, 2002
FEVR	AD	β-propeller 1	3	c.518C>T	p.T173M	Toomes, 2004
HBM	AD	β-propeller 1	3	c.593A>G	p.N198S	Whyte, 2004
OPPG	AR	β-propeller 1	3	c.607G>A	p.D203N	Ai, 2005
Endosteal hyperostosis, HBM	AD	β-propeller 1	3	c.640G>A	p.A214T	van Wesenbeek, 2003
Osteosclerosis	AD	β-propeller 1	3	c.641C>T	p.A214V	van Wesenbeek, 2003
Endosteal hyperostosis, Osteopetrosis	AD	β-propeller 1	4	c.724G>A	p.A242T	van Wesenbeek, 2003
OPPG	AR	β-propeller 1	4	c.731C>T	p.T244M	Ai, 2005
Osteopetrosis	AD	β-propeller 1	4	c.758C>T	p.T253I	van Wesenbeek, 2003
OPPG	AR	β-propeller 1	4	c.765G>A	p.W255X	Ai, 2005
OPPG	AR	β-propeller 1	4	c.789C>A	p.C263X	Ai, 2005
FEVR, reduced BMD	AR	β-propeller 1	4	c.803_812delGGGGGAAGAG	p.G268_R271delfsX4	Qin, 2005
HBM	AD	β-propeller 1	4	c.844A>G	p.M282V	Balemans, 2007
OPPG	AR	EGF1	5	c.920C>T	p.S307F	Ai, 2005
OPPG	AR	EGF1	5	c.1004_1005insAGGAC	p.T335fsX50	Ai, 2005
OPPG	AR	β-propeller 2	6	c.1042C>T	p.R348W	Ai, 2005
OPPG	AR	β-propeller 2	6	c.1058G>A	p.R353Q	Ai, 2005
OPPG	AR	β-propeller 2	6	c.1067C>T	p.S356L	Ai, 2005
OPPG	AD*	β-propeller 2	6	c.1169C>A	p.T390K	Ai, 2005
OPPG	AR	β-propeller 2	6	c.1199C>A	p.A400E	Ai, 2005
OPPG	AR	β-propeller 2	6	c.1210G>A	p.G404R	Ai, 2005
OPPG	AR	β-propeller 2	6	c.1225A>G	P.T409A	Streeten, 2008
OPPG	AR	β-propeller 2	6	?	p.W425X	Streeten, 2008
OPPG	AR	β-propeller 2	6	c.1282C>T	p.R428X	Gong, 2001
OPPG	AR	β-propeller 2	6	c.1300G>A	p.D434N	Ai, 2005
FEVR, reduced BMD	AD+	β-propeller 2	6	c.1330C>T	p.R444C	Qin, 2005
Osteoporosis	AD	β-propeller 2	6	c.1364C>T	p.S455L	Crabbe, 2005
OPPG	AR	β-propeller 2	6	c.1378G>A	p.E460K	Ai, 2005
OPPG	AR	β-propeller 2	7	c.1432T>A	p.W478R	Cheung, 2006
OPPG	AD*	β-propeller 2	7	c.1453G>T	p.E485X	Gong, 2001
OPPG	AR	β-propeller 2	7	c.1468delG	p.D490MfsX40	Gong, 2001
OPPG	AR	β-propeller 2	7	c.1481G>A	p.R494Q	Gong, 2001
OPPG	AR	β-propeller 2	7	c.1512G>T	p.W504C	Cheung, 2006
FEVR	AD	β-propeller 2	7	c.1532A>C	p.D511A	Boonstra, 2009
OPPG	AR	β-propeller 2	7	c.1559G>T	p.G520V	Ai, 2005
FEVR / Osteoporosis	AD	β-propeller 2	7	c.1564G>A	p.A522T	Qin, 2005
OPPG	AR	β-propeller 2	8	c.1592A>T	p.N531I	Barros, 2007
FEVR	AR	β-propeller 2	8	c.1604C>T	p.T535M	Qin, 2005
OPPG	AR	β-propeller 2	8	c.1708C>T	p.R570W	Gong, 2001
FEVR	AR	β-propeller 2	8	c.1709G>A	p.R570Q	Jiao, 2004
OPPG	AR	β-propeller 2	8	c.1750C>T	p.Q584X	Ai, 2005
FEVR, reduced BMD	AR	EGF 2	9	c.1828G>A	p.G610R	Qin, 2005
OPPG	AD*	EGF 2	9	c.1828G>C	p.G610R	Ai, 2005
FEVR	AR	EGF 2	9	c.1850T>G	p.F617C	Qin, 2005
reduced BMD	AD	β-propeller 3	9	c.1999G>A	p.V667M	Ferrari, 2004
OPPG	AR	β-propeller 3	9	c.2047G>A	p.D683N	Ai, 2005
OPPG	AR	β-propeller 3	10	c.2151_2152insT	p.D718X	Gong, 2001
OPPG	AR	β-propeller 3	10	c.2197T>C	p.Y733H	Ai, 2005
OPPG, reduced BMD	AD	β-propeller 3	10	c.2202G>A	p.W734X	Gong, 2001
OPPG	AR	β-propeller 3	10	c.2246delG	p.G749fsX48	Ai, 2005
FEVR	AR	β-propeller 3	10	c.2254C>G	p.R752G	Jiao, 2004
OPPG, reduced BMD	AD	β-propeller 3	10	c.2305delG	p.D769IfsX29	Gong, 2001
FEVR	AD	β-propeller 3	11	c.2392A>G	p.T798A	Qin, 2005
OPPG	AR	β-propeller 3	11	c.2409_2503+79del (174bp)	?	Ai, 2005

FEVR	AD	β-propeller 3	11	c.2413C>T	p.R805W	Boonstra, 2009
OPPG	AR	β-propeller 3	12	c.2557C>T	p.Q853X	Gong, 2001
OPPG	AR	EGF 3	12	c.2718_2721delTATG	p.C906fsX52	Ai, 2005
OPPG	AR	EGF 3	12	c.2737_2738insT	p.C913LfsX73	Ai, 2005; Hartikka, 2005
OPPG	AR	β-propeller 4	14-16	chr11:g.(13871447_1387511)_(13879636_13879700)del	p.P1010QfsX38	Chung, 2009
Osteoporosis	AD	β-propeller 4	14	c.3107G>A	p.R1036Q	Hartikka, 2005
OPPG	AR	β-propeller 4	14	c.3232C>T	p.R1078X	Ai, 2005
OPPG	AD*	β-propeller 4	15	c.3295G>T	p.D1099Y	Ai, 2005
OPPG	AR	β-propeller 4	15	c.3337C>T	p.R1113C	Ai, 2005
FEVR	AD	β-propeller 4	15	c.3361A>G	p.N1121D	Qin, 2005
FEVR	AD*	β-propeller 4	16	c.3502T>C	p.Y1168H	Toomes, 2004
OPPG	AR	LDLR repeat	17	c.3763+2T>C	?	Ai, 2005
OPPG	AR	LDLR repeat	18	c.3804delA	p.T1268fsX170	Gong, 2001
FEVR	AD*	LDLR repeat	19	c.4081T>G	p.C1361G	Toomes, 2004
FEVR	AR	LDLR repeat	19	c.4099G>A	p.Q1367K	Jiao, 2004
OPPG	AD*	LDLR repeat	19	c.4105_1406delAT	p.M1369VfsX2	Ai, 2005
FEVR	AD	LDLR repeat	20	c.4119_4120insC	p.K1374QfsX176	Toomes, 2004
OPPG	AR	transmembrane	20	c.4202G>A2	p.G1401D	Ai, 2005
FEVR	AD	Cytoplasmic	21	c.4488+2T>G	?	Toomes, 2004
OPPG	AR	Cytoplasmic	22	c.4512_4517delinsTGTACAACAT	p.P1504fsX46	Ai, 2005
OPPG	AR	Cytoplasmic	22	c.4586+2T>C	?	Ai, 2005
OPPG	AR	Cytoplasmic	23	c.4600C>T	p.R1534X	Ai, 2005
Osteoporosis	AD	Cytoplasmic	23	c.4609G>A	p.A1537T	Crabbe, 2005

Table 4 List of all *LRP5* mutations published so far. Numbering according to reference sequence NM_002335. The A of the ATG start codon lies at position +1. *AD:* autosomal dominant; *AR:* autosomal recessive; *BMD:* bone mass density; *FEVR:* familial exudative vitreoretinopathy; *HBM:* high bone mass; *OPPG:* osteoporosis pseudoglioma syndrome. * Heterozygous mutation not only in the patient, but also in clinically unconspicuous relatives. + patient is compound heterozygous with an additional *FZD4* mutation (p.R417Q), explaining the more severe phenotype.

1.4 Aim of the thesis

This thesis aimed to add further knowledge to the understanding of the pathogenesis of human blinding diseases caused by variants in the Norrie disease pseuoglioma (*NDP*) gene. To further elucidate the functional role of norrin (the *NDP* protein), the *Ndph* knockout mouse model was used, focussing on the early stages of postnatal eye development. I wanted to investigate norrin's proposed role as transcriptional regulator, especially of Wnt/beta-catenin target genes, and to investigate the activity of this pathway *in vivo.*

I further aimed to identify and sequence potential candidate genes in ND/EVR-patients, who were negative for mutations in *NDP* or its receptors *FZD4* and *LRP5.* To this end, I hypothesized that genes differentially transcribed in the retina of the *Ndph* ko mouse model would be attractive candidates.

2. Material and Methods

2.1 Animals

The research presented in this work was approved by the Veterinary Service of the State of Zurich (Switzerland).

2.1.1 Ndph knockout mouse

The *Ndph* knockout mouse line has been established in 1996 by homologous recombination (Berger et al., 1996). Exon 2 of the *Ndph* gene has partially been replaced with a reverse oriented neomycin cassette, resulting in a loss of about half the coding sequence, including the signal peptide for protein secretion. The gene targeting was performed in embryonic stem cells from the 129P2 strain, but the mutation has been kept on a C57BL/6 background. For all experimental work in this study, only males were used.

2.1.2 BATgal reporter mouse

A Wnt-signaling reporter mouse, the so-called BATgal reporter (Maretto et al., 2003), was obtained from the lab of Stefano Piccolo (Padua, Italy). The reporter was constructed by fusing seven TCF/LEF-binding sites upstream of the minimal promoter–TATA box of the anuran *siamois* gene, a known Wnt target (Brannon et al., 1997), to the bacterial *lacZ* gene. This reporter mouse, which was maintained on a B6D2F1 background, was subsequently crossed with the *Ndph* ko mouse line to create a cross-breed termed NDxBATgal.

2.1.3 Preparation and tissue isolation

For tissue preparation, mice were deeply anaesthetized with CO_2 (when they were older than p10), and sacrificed by cervical dislocation and subsequent decapitation (directly, when they were younger). A tail biopsy was taken for genotyping.

Eyes were enucleated by a forceps pull behind the eye, taking care to firmly grab the optic nerve to avoid any traction damage to the retina. Occasionally, especially when eyes were prepared from very young animals (p3, p5), which still have very delicate tissue structures, enucleation was performed with a scissor cut behind the eye. When eyes were prepared from stages with closed eyes (up to p14), eye lids were cut off before enucleation.

Retinas were prepared by two different methods, depending on the purpose they were used for: A “quick-and-dirty” method for RNA and protein extraction, and a more careful method for whole-mount preparations and microscopy.

For quick retina isolation, the eye, still *in situ*, was fixed with a forceps at the exit point of the optic nerve. The cornea was then opened with fine spring scissors. Then pressure was applied from the forceps behind the eye, and the lens and vitreous were squeezed out. After cautious removal with the scissors, the retina was stripped out off the eye by pulling the forceps gently forward. The retina was then briefly cleaned from remaining vitreous or retinal pigment cells, and then quickly transferred to a micro centrifuge tube and snap-frozen in liquid nitrogen.

For retinal whole-mount preparation, the eye was removed as described above. The eye was hold by the optic nerve remnant against the edge of a Petri dish lid, and the cornea was poked with a small, butterfly-type syringe to reduce eye pressure. Then it was transferred into a PBS-filled Petri dish. Beginning from the hole in the cornea, the eye was opened with spring scissors, cutting along the ora serrata. The cornea was removed, the spring scissors were inserted perpendicular to the corneal plane and 4-5 cuts were made to separate the eye globe in 4-5 sectors. Each of these sectors was then pulled to the bottom of the Petri dish, flattening the retina and sclera to a structure resembling a 4-5-foil cloverleaf (Figure 26).

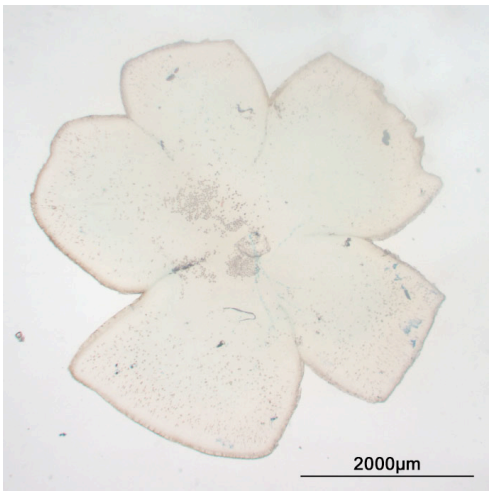

Figure 26 Cloverleaf-like retinal flatmount of a p15 BGND animal.

Then vitreous and lens were removed. Through gentle agitation of the tissue in the PBS, the retina was slowly dissociated from the retinal pigment epithelium. Occasionally, when the cut along the ora serrata was to precautious, the retina remained attached to the underlying sclera through the ciliary musculature. In this case, a fine cut between the peripheral retinal edge and the ciliary body was conducted. Finally, the spring scissors were carefully inserted between the retina and the pigment epithelium, and the optic nerve was cut directly beneath the optic disc, mostly resulting in a small hole in the middle of the retina. The retina now freely floated away from the pigment epithelium. After short cleaning of the retina from possible remainers of RPE, the retina was transferred into a micro centrifuge tube containing PBS or directly onto a microscope slide.

The brain was also prepared from part of the animals. Skin, muscle and fat tissue were cut off / stripped off in rostral direction. Also lateral tissue (ears) was removed, until the skull was completely exposed. If adult mice were prepared, scissors were inserted carefully into the foramen magnum, taking care to guide the blade only superficial to avoid any damage to the brain, and the skull was cut along the sagittal suture from caudal to rostral. Subsequently, two other cuts were performed along the lambdoid suture, from the median to each lateral side. Each parietal portion of the skull was then broken apart with sturdy forceps, followed by the frontal and occipital parts. If the animals were in their first postnatal weeks, the skull was punctured at the lambda point, the intersection of the central and the lambdoid sutures, and cut open analogous to the

procedure for adults, in order to avoid damage to the brain stem and cerebellum. The occipital part of the skull was then simply broken apart without a median cut. During the cutting and breaking procedure, great care had to be taken to avoid damage to the basis of skull. After the skull had been opened, the brain was lifted out of the skull, beginning at the olfactory bulbs, with a small spatula. In most cases, the brain was subsequently transferred in a Petri dish that was placed on ice, and sagitally cut into two halfs with a razor blade.

2.2 DNA techniques

2.2.1 DNA Isolation

2.2.1.1 DNA isolation from mouse-tail biopsies

Mouse-tail biopsies were used to isolate DNA for genotyping purposes. The tissue was digested by a proteinase K solution (Roche Diagnostics, Rotkreuz, Switzerland), and the nucleic acids were subsequently precipitated with isopropanol, washed with ethanol and resolved in TE buffer.

The required digestion buffer volume should be thrice the amount of buffer that barely overcasts the tail biopsy in the micro centrifuge tube. Typically, 500µl were used.

Proteinase K buffer	Stock conc.	Vol.	Final conc.
dH_2O		365µl	
Tris HCl pH 7.5	1M	50µl	100mM
EDTA pH 8.0	0.5M	5µl	5mM
SDS-solution	10%	10µl	0.2%
NaCl	5M	20µl	200mM
Proteinase K	10mg/ml	50µl	1mg/ml
Total:		**500µl**	

Table 5 Proteinase K digestion buffer for mouse-tail biopsies.

- Tail biopsies were digested in a heating block for 1-3h @ 55°C, 1200
- Tubes were centrifuged for 1h @ 4°C, 13000 rpm
- Supernatant was transferred into a new micro centrifuge tube and mixed with one volume (500µl) of 100% isopropanol
- Tubes were centrifuged for 30min @ 4°C, 13000 rpm
- Supernatant was carefully decanted and remaining alcohol at the edge of the tube was removed by spotting the tube on kim wipes
- The nucleic acid pellet was washed with 200µl 70% ethanol
- Tubes were centrifuged for 10min @ 4°C, 13000 rpm
- Supernatant was carefully removed by pipetting, and the pellet was air-dried in a heating block for 5-10min @ 37°C
- Finally, the pellet was resolved in 500µl TE buffer (pH 8) for 30 min @ 37°C or o/n @ 4°C for complete dissolving

2.2.1.2 DNA isolation from patient's blood or saliva

All patients were referred to the Institute of Medical Genetics for diagnostic purposes and informed consent according to the declaration of Helsinki and applicable Swiss law was obtained from all subjects involved in genetic testing. DNA samples were extracted from EDTA blood in the diagnostics division of our institute, from saliva samples collected with the OraGene™ kit (DNA Genotek, Ottawa, Ontario, Canada), or sent to us by approved foreign diagnostic laboratories. All samples obtained a five-digit identification (ID) number in order to anonymize personal patient data (Table 6). Additionally, 192 DNAs of patients who were referred to us and diagnosed with non-ND/EVR related diseases were used as internal controls to obtain allele frequencies for the new sequence variants found in the screening.

#	DNA	Sex	Clinical diagnosis	*NDP*	*FZD4*	*LRP5*
1	22277	m	ND	p.C110S	-	-
2	23081	m	ND	p.C128X	-	-
3	25775	m	ND	p.M1V	-	-
4	27019	m	ND	c.174+1G>T	-	-
5	27095	m	ND; PHPV	p.R74C	-	-
6	27118	f	CD, bilateral; FEVR	none	p.P33S, p.P168S	-
7	28786	f	CD	none	none	p.T672M
8	22439	f	CD, bilateral	none	none	none
9	24165	f	CD; retinal telangiectasia	none	none	none
10	24536	m	CD	none	none	c.2178C>T and c.3764-30G>A
11	25160	m	ND	none	none	none
12	25649	m	ND	none	none	none
13	27110	f	ND; FEVR; PHPV	none	none	none
14	27111	?	ND	none	none	none
15	27112	?	ND; RB	none	none	none
16	27113	?	ND	none	none	none
17	27116	?	ND	none	none	c.3427+10C>T
18	27188	m	ND	none	none	-
19	27735	m	CD; retinal telangiectasia	none	none	none
20	28931	m	ED	none	none	none
21	29550	f	FEVR	none	none	none
22	29833	m	ND	none	-	-

Table 6 Patients screened in this study. The first five patients have been shown to have mutations in the *NDP* gene by our diagnostic department, patient 27118 was shown to be heterozygous for 2 mutations in the *FZD4* gene (Masterthesis J. Zürcher, 2007), and patient 28786 harbors a missense mutation in the *LRP5* gene that may contribute to the disease phenotype (Masterthesis W. Hänseler, 2008). All patients were screened for mutations in the *LMO2*, *PLVAP*, and *SLC38A5* genes. Patient DNAs 27110 – 27118 were referred to us from Susanne Kohl and Bernd Wissinger (Universitätsklinikum Tübingen, Department für Augenheilkunde, Forschungsinstitut für Augenheilkunde, Molekulargenetisches Labor, Tübingen, Germany), DNA 29550 from Tanya Bardakjian (Albert Einstein Medical Center, Philadelphia, PA, USA). CD: *Coats' disease*; ED: *Eales' disease*; FEVR: *Familial exudative vitreoretinopathy*; ND: *Norrie disease*; PHPV: *Persistent hyperplastic primary vitreous*; RB; *Retinoblastoma*

DNA from patient's blood was isolated with a semi-automated DNA extraction robot (chemagic MSMI; Chemagen, Baesweiler, Germany; Figure 27) in our diagnostic

department. The extraction method is based on the usage of magnetic particles that bind to DNA. Isolation was performed according to the manufacturer's protocol.

Figure 27 Chemagic magnetic separation module I (MSM I).

Patient's DNA was also collected in form of saliva samples. For this purpose, the OraGene™ saliva DNA extraction kit (OG-250, DNA Genotek, Ottawa, Ontario, Canada) was applied. The extraction method is based on alcohol precipitation and was performed according to the manufacturer's protocol.

2.2.1.3 DNA isolation from agarose gels

DNA bands from electrophoresis gels were excised with a scalpel on a UV-transilluminator (TFX-20.M; Vilber Lourmat, Eberhardzell, Germany) and transferred into a microcentrifuge tube. After weighing of the sample, DNA was isolated with the column-based QIAquick® gel extraction kit (#28706; Qiagen, Hilden, Germany) according to the manufacturer's instructions.

2.2.1.4 Plasmid DNA (pDNA) isolation from bacterial cells

Plasmid DNA was isolated with a column-based kit according to the manufacturer's protocol. Depending on the amount of pDNA to be isolated, different kits were used: The QIAprep® Spin Miniprep Kit (Qiagen, Hilden, Germany; no. 27104/27106) for pDNA up to 20µg, ort h QIAGEN® Plasmid Maxi Kit (no. 12163) for pDNA up to 500µg.

2.2.1.5 DNA isolation from the yeast Pichia pastoris

DNA from *Pichia pastoris* was only needed for genotyping by PCR, so the extraction method was essentially only a break-up of the cell pellet. A single colony was picked with a sterile pipette tip or an inoculation loop and dissolved in 20µl TE/SDS-buffer (Table 7) by vortexing for a few seconds. The cell suspension was then heated to 100°C for 5min and vortexed again. After spin-down of the cell debris (14'000rpm/10min), 2.5µl of the supernatant were used as PCR template.

Yeast cell breakage-buffer	
Tris-HCl 1M, pH 8.0	500µl
EDTA 0.5M, pH 8.0	100µl
SDS 10%	50µl
ddH_2O	add 50ml

Table 7 TE/SDS-buffer for DNA isolation from yeast.

2.2.2 DNA quantification

DNA concentration was quantified with a NanoDrop® ND-1000 photospectrometer (NanoDrop Technologies/Thermo Scientific, Wilmington, DE, USA).

2.2.3 Polymerase chain reaction (PCR)

The polymerase chain reaction (PCR) at present is arguably the most important and often used technique in molecular biology (Mullis et al., 1986; Saiki et al., 1988). It was applied numerous times during the course of my thesis to amplify genomic regions of interest. A specific protocol is given in context with each respective experiment. Primers were designed with the web-based tool Primer 3 (http://frodo.wi.mit.edu/primer3/input.htm), VectorNTI 10.1.1 (Invitrogen, Carlsbad, CA, USA), Oligo 6.57 (Molecular Biology Insights, Cascade, CO, USA), or Primer Express 2.0 (Applied Biosystems, Foster City, CA, USA) and were ordered from Microsynth (Balgach, Switzerland). Primer sequences are given in the appendix. PCR reagents used were mainly from Solis BioDyne (Tartu, Estonia; HOT FIRETaq™ Polymerase, buffer B, dNTPs, S-solution) or Qiagen (Hilden, Germany; HotStarTaq® Polymerase, PCR-buffer, $MgCl_2$, Q-solution). For generation of long fragments (*P. pastoris* expression constructs), the Phusion™ High-Fidelity PCR Kit was used (#F-553S, New England Biolabs, Frankfurt am Main, Germany). The thermocyclers used in this study were from Applied Biosystems (Foster City, CA, USA; ABI 2720) or MJ Research (Oldendorf, Germany; MJR PTC-200, MJR PTC-225; Figure 28).

Figure 28 MJR PTC-225 thermocycler.

2.2.3.1 Mouse genotyping

The *Ndph* genotype was determined using a multiplex PCR (Berger et al., 1996; Table 8). Primers 179 and 180 flank exon 2 of the *Ndph* gene and amplify a 527bp product from the wild type allele. Primers 177 and 178 bind inside the neomycin cassette of the *Ndph* knockout allele and will yield 2 smaller PCR products in combination with primers 179 and 180: a 133bp product (178 with 180), and an amplicon of 271bp (177 with 179).

Ndph	Stock conc.	Vol.	Final conc.
ddH_2O		12.75µl	
Buffer B	10x	2.5µl	1x
$MgCl_2$	25mM	6µl	6mM
dNTPs (each)	20mM	0.25µl	200µM
DTT	100mM	1.25µl	5mM
Primer 177 (SL 105)	10µM	0.25µl	100nM
Primer 178 (SL 106)	10µM	0.25µl	100nM
Primer 179 (SL 107)	10µM	0.25µl	100nM
Primer 180 (SL 108)	10µM	0.25µl	100nM
HotFire™ Polymerase	5u/µl	0.25µl	0.05u/µl
DNA template	20ng/µl	1µl	0.8ng/µl
Total:		**25µl**	

Cycling conditions		
95°C	15min	
95°C	1min	35x
62°C	1min	
72°C	2min	
72°C	10min	
10°C	∞	

Table 8 PCR conditions ort he *Ndph* genotyping procedure.

To distinguish females and males, a PCR amplifying the *Sry* gene was used, which is the sex-determining region on the Y chromosome. Primers 188 and 189 generated a 406bp product only from males (Table 9).

Sry	Stock conc.	Vol.	Final conc.
ddH_2O		16µl	
Buffer B	10x	2.5µl	1x
$MgCl_2$	25mM	3µl	3mM
dNTPs (each)	20mM	0.25µl	200µM
Primer 188 (SL 120)	10µM	1µl	400nM
Primer 189 (SL 121)	10µM	1µl	400nM
HotFire™ Polymerase	5u/µl	0.25µl	0.05u/µl
DNA template	20ng/µl	1µl	0.8ng/µl
Total:		**25µl**	

Cycling conditions		
95°C	15min	
95°C	1min	35x
56°C	1min	
72°C	2min	
72°C	10min	
10°C	∞	

Table 9 PCR conditions ort he *Sry* genotyping procedure

Presence of the BATgal reporter gene, the bacterial *LacZ*, was determined with primers 54 and 55, resulting in a 450bp amplicon (Table 10).

LacZ	Stock conc.	Vol.	Final conc.
ddH_2O		16.5µl	
Buffer B	10x	2.5µl	1x
$MgCl_2$	25mM	2.5µl	2.5mM
dNTPs (each)	20mM	0.25µl	200µM
Primer 54 (LacZ1L20)	10µM	1µl	400nM
Primer 55 (LacZ1U20)	10µM	1µl	400nM
HotFire™ Polymerase	5u/µl	0.25µl	0.05u/µl
DNA template	20ng/µl	1µl	0.8ng/µl
Total:		**25µl**	

Cycling conditions		
95°C	15min	
95°C	1min	35x
59°C	1min	
72°C	2min	
72°C	10min	
10°C	∞	

Table 10 PCR conditions ort he *LacZ* genotyping procedure

2.2.3.2 Mutation analysis

Six different (candidate) genes were amplified from patient's DNA and sequenced afterwards. The PCR conditions for *NDP* (Table 11) have been established before in our diagnostic division and our technician Silke Feil has performed sequencing mainly. The conditions for *FZD4* (Table 12) were determined by Jurian Zürcher, who also did most of the *FZD4* screening, as part of his MSc thesis during the time of my thesis. Primer design for and sequencing of *LRP5* (Table 13) were performed mainly by Walther Hänseler as part of his MSc thesis, which he wrote under my supervision. The conditions for *SLC38A5* (Table 16) were established mainly by Karin Schläpfer, who did a 6-week internship at the institute also under my supervision, during which time she also conducted most of the *SLC38A5* sequencing bench work. The PCRs for *LMO2* (Table 14) and *PLVAP (*Table 15*)*, as well as the PCRs for the 3'-UTRs of *NDP* and *FZD4*, were exclusively designed by myself. Further, I did not only conduct sequencing of these genes, but did some sequencing of *NDP*, *FZD4*, *LRP5*, and *SLC38A5* by myself.

2.2.3.2.1 *NDP*

NDP	Stock conc.	Vol.	Final conc.
ddH_2O		13.35µl	
Buffer B	10x	2µl	1x
$MgCl_2$	25mM	1.2µl	1.5mM
dNTPs (each)	20mM	0.25µl	250µM
Primer fwd	10µM	1µl	500nM
Primer rev	10µM	1µl	500nM
HotFire™ Polymerase	5u/µl	0.2µl	0.05u/µl
DNA template	100ng/µl	1µl	5ng/µl
Total:		**20µl**	

Exon	Primer	Size [bp]
1	581/582	369
2	583/584	525
3	585/586	442
3.1	561/562	501
3.2	563/590	850

Cycling conditions		
95°C	15min	
95°C	1min	
58°C	1min	35x
72°C	1.5min	
72°C	10min	
10°C	∞	

Table 11 PCR conditions for amplification of exons 1, 2, and 3 of the *NDP* gene.

2.2.3.2.2 *FZD4*

FZD4	Stock conc.	Vol.	Final conc.
ddH_2O		17.55µl	
Buffer B	10x	2.5µl	1x
$MgCl_2$	25mM	1.5µl	1.5mM
dNTPs (each)	20mM	0.25µl	200µM
Primer fwd	10µM	1µl	400nM
Primer rev	10µM	1µl	400nM
HotFire™ Polymerase	5u/µl	0.2µl	0.04u/µl
DNA template	100ng/µl	1µl	4ng/µl
Total:		**25µl**	

Exon	Primer	Size [bp]
1	465/429	437
2a	430/450	440
2b	443/444	425
2c	445/447	473
2e	446/439	448

Cycling conditions Exon 1		
95°C	15min	
95°C	1min	
64°C	1min	35x
72°C	2min	
72°C	10min	
10°C	∞	

Cycling conditions Exon 2		
95°C	15min	
95°C	1min	
60°C	1min	35x
72°C	2min	
72°C	10min	
10°C	∞	

Table 12 PCR conditions for amplification of exons 1 and 2 (fragments a-e) of the *FZD4* gene. Fragment 2d does not exist.

2.2.3.2.3 *LRP5*

LRP5 all exons Δ1, 4	Stock conc.	Vol.	Final conc.
ddH_2O		16.5µl	
Buffer B	10x	2.5µl	1x
$MgCl_2$	25mM	2.5µl	2.5mM
dNTPs (each)	20mM	0.25µl	200µM
Primer fwd	10µM	1µl	400nM
Primer rev	10µM	1µl	400nM
HotFire™ Polymerase	5u/µl	0.2µl	0.04u/µl
DNA template	50ng/µl	1µl	2.5ng/µl
Total:		**25µl**	

Exon	Primer	Size [bp]
1.1	355/356	361
(1.2)†	361/290	270
2	291/292	613
3	293/294	609
4	295/296	468
5	297/298	555
6	299/300	789
7	301/302	563
8	303/304	428
9	305/306	712
10	344/345	438
11	309/310	538

Exon	Primer	Size [bp]
12	311/312	578
13	313/314	477
14	343/316	603
15	317/318	522
16	319/320	523
17	321/322	396
18	323/324	547
19	325/326	327
20	327/328	495
21	329/330	388
22	331/332	495
23	333/341	603

LRP5 exon 1	Stock conc.	Vol.	Final conc.
ddH_2O		13.55µl	
PCR-buffer*	10x	2.5µl	1x
Q-Solution™	5x	5µl	1x
$MgCl_2$	25mM	0.5µl	*2.0mM
dNTPs (each)	20mM	0.25µl	200µM
Primer fwd	10µM	1µl	400nM
Primer rev	10µM	1µl	400nM
HotFire™ Polymerase	5u/µl	0.2µl	0.04u/µl
DNA template	50ng/µl	1µl	2.5ng/µl
Total:		**25µl**	

LRP5 exon 4	Stock conc.	Vol.	Final conc.
ddH_2O		14µl	
Buffer B	10x	2.5µl	1x
S-Solution™	10x	2.5µl	1x
$MgCl_2$	25mM	2.5µl	2.5mM
dNTPs (each)	20mM	0.25µl	200µM
Primer fwd	10µM	1µl	400nM
Primer rev	10µM	1µl	400nM
HotFire™ Polymerase	5u/µl	0.2µl	0.04u/µl
DNA template	50ng/µl	1µl	2.5ng/µl
Total:		**25µl**	

Cycling conditions exons 2, 3, 6, 7, 11, 12, 14, 16, 17, 19, 21		
95°C	15min	
95°C	1min	
60°C	1min	35x
72°C	2min	
72°C	10min	
10°C	∞	

Cycling conditions exons 4, 5, 8, 9, 10, 13, 15, 18, 20, 22, 23		
95°C	15min	
95°C	1min	
64°C	1min	35x
72°C	2min	
72°C	10min	
10°C	∞	

Cycling conditions exon 1		
95°C	15min	
95°C	1min	
67°C	1min	35x
72°C	2min	
72°C	10min	
10°C	∞	

Table 13 PCR conditions for amplification of exons 1 to 23 of the *LRP5* gene. * Qiagen PCR-buffer contains 15mM $MgCl_2$. †Fragment 1.2 is designed as a nested PCR from amplicon 1.1 to reduce contamination by product derived from the highly similar *LRP5L* sequence from chromosome 22.

2.2.3.2.4 *LMO2*

LMO2 exons 1, 2, 5, 6.1	Stock conc.	Vol.	Final conc.
ddH_2O		13.4µl	
Buffer B	10x	2µl	1x
$MgCl_2$	25mM	1.6µl	2mM
dNTPs (each)	20mM	0.2µl	200µM
Primer fwd	10µM	0.8µl	400nM
Primer rev	10µM	0.8µl	400nM
HotFire™ Polymerase	5u/µl	0.2µl	0.05u/µl
DNA template	50ng/µl	1µl	2.5ng/µl
Total:		**20µl**	

Exon	Primer	Size [bp]
1	565/566	641
2	567/568	359
3-4	588/589	837
5	600/601	389
6.1	575/576	601

LMO2 exon 3-4	Stock conc.	Vol.	Final conc.
ddH_2O		9.4µl	
Buffer B	10x	2µl	1x
Q-Solution™	5x	4µl	1x
$MgCl_2$	25mM	1.6µl	2mM
dNTPs (each)	20mM	0.2µl	200µM
Primer fwd	10µM	0.8µl	400nM
Primer rev	10µM	0.8µl	400nM
HotFire™ Polymerase	5u/µl	0.2µl	0.05u/µl
DNA template	50ng/µl	1µl	2.5ng/µl
Total:		**20µl**	

Cycling conditions		
95°C	15min	
95°C	1min	35x
58°C	1min	
72°C	2min	
72°C	10min	
10°C	∞	

Table 14 PCR conditions for amplification of exons 1-6 (only CDS-containing part of exon 6) of the *LMO2* gene.

2.2.3.2.5 *PLVAP*

PLVAP	Stock conc.	Vol.	Final conc.
ddH_2O		13.4µl	
Buffer B	10x	2µl	1x
$MgCl_2$	25mM	1.6µl	2mM
dNTPs (each)	20mM	0.2µl	200µM
Primer fwd	10µM	0.8µl	400nM
Primer rev	10µM	0.8µl	400nM
HotFire™ Polymerase	5u/µl	0.2µl	0.05u/µl
DNA template	50ng/µl	1µl	2.5ng/µl
Total:		**20µl**	

Exon	Primer	Size [bp]
1.1	545/546	301
1.2	547/548	432
2	549/550	276
3.1	551/552	502
3.2	553/554	501
4-5	555/556	551
6.1	557/558	583
6.2	559/560	556

Cycling conditions exons 1.1, 2, 3.2		
95°C	15min	
95°C	1min	
58°C	1min	35x
72°C	2min	
72°C	10min	
10°C	∞	

Cycling conditions exons 1.2, 3.1, 4-5, 6.1, 6.2		
95°C	15min	
95°C	1min	
66°C	1min	35x
72°C	2min	
72°C	10min	
10°C	∞	

Table 15 PCR conditions for amplification of exons 1-6 of the *PLVAP* gene.

2.2.3.2.6 *SLC38A5*

SLC38A5	Stock conc.	Vol.	Final conc.
ddH_2O		18µl	
Buffer B	10x	2.5µl	1x
$MgCl_2$	25mM	2µl	2mM
dNTPs (each)	20mM	0.25µl	200µM
Primer fwd	10µM	0.5µl	200nM
Primer rev	10µM	0.5µl	200nM
HotFire™ Polymerase	5u/µl	0.25µl	0.05u/µl
DNA template	20ng/µl	1µl	0.8ng/µl
Total:		**25µl**	

Exon	Primer	Size [bp]
1a	604/605	500
1b	606/607	500
1c	608/609	489
2-3	610/611	499
4-5	612/613	495
6-7	614/615	548
8	616/617	389

Exon	Primer	Size [bp]
9-10	632/633	538
11	620/621	363
12	622/623	387
13	624/625	398
14-15	626/627	571
16a	628/629	484
16b	630/631	500

Cycling conditions all exons Δ 9-10		
95°C	15min	
95°C	1min	
60°C	1min	35x
72°C	2min	
72°C	10min	
10°C	∞	

Cycling conditions exon 9-10		
95°C	15min	
95°C	1min	
62°C	1min	35x
72°C	2min	
72°C	10min	
10°C	∞	

Table 16 PCR conditions for amplification of exons 1-16 of the *SLC38A5* gene.

2.2.3.3 Verification of Pichia pastoris *expression vector constructs*

To verify the presence of the correct constructs in *Pichia* clones used for recombinant protein expression, a PCR with primers against the *AOX1* gene was conducted (Table 17). The wt *AOX1* gene has a size of 2.2kb, and the expected C-terminal tagged *NDP* constructs placed under the control of the *AOX1* promoter have 1017bp. Thus, through usage of the appropriate extension time, only a PCR product from the *NDP* constructs was received.

P. pastoris expression vector	Stock conc.	Vol.	Final conc.
ddH_2O		14.5µl	
Buffer B	10x	2.5µl	1x
$MgCl_2$	25mM	3µl	3mM
dNTPs (each)	20mM	0.25µl	200µM
Primer 282 (AOX 5')	10µM	1µl	400nM
Primer 283 (AOX 3')	10µM	1µl	400nM
HotFire™ Polymerase	5u/µl	0.25µl	0.05u/µl
DNA template	?*	2.5µl	?*
Total:		**25µl**	

Product	Primer	Size [bp]
wt *AOX1*	282/283	2200
C-term construct	282/283	1017
N-term construct	282/283	1071

Cycling conditions		
95°C	15min	
95°C	1min	
54°C	1min	35x
72°C	2min	
72°C	10min	
10°C	∞	

Table 17 PCR reaction mix for *P. pastoris* expression vector constructs. *Supernatant of a crude cell breakage suspension was used as the PCR template.

2.2.4 Gel electrophoresis

The PCR products were separated by size using agarose gel electrophoresis. DNA was stained with ethidium bromide (EtBr; 0.5µg/ml), which intercalates into the DNA double helix (**Figure 29**), and was visualized on a UV transilluminator.

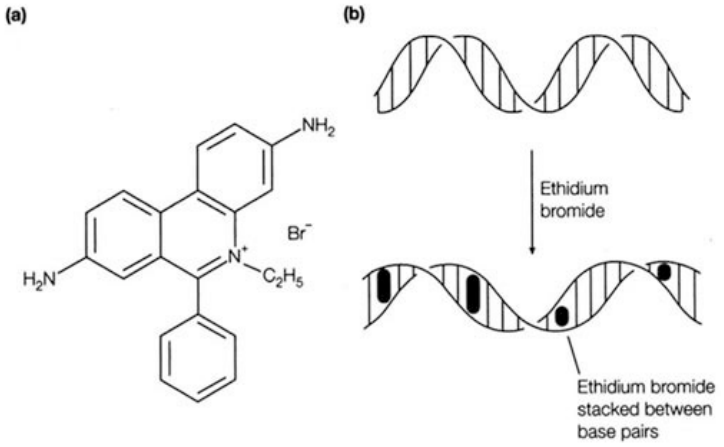

Figure 29 (a) Chemical structure of ethidium bromide; **(b)** Process of intercalation, illustrating the lengthening and untwisting of the DNA helix.

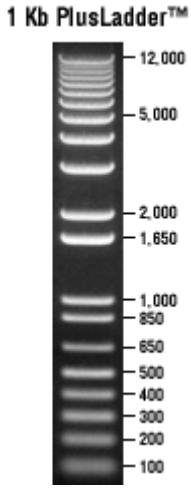

Figure 30 Band pattern of the Invitrogen 1Kb PlusLadder™ in base pairs.

For amplicons of medium size (~500bp), typically an 1.2% agarose gel was prepared. If the products were smaller, higher agarose concentrations were used (up to 2.0%), and contrary, lower agarose concentrations (down to 0.8%) were applied if large fragments had to be analysed. Such a gel was then run at 90-130V for 40min. Three different gel sizes (mini, midi, maxi) were used (Table 18). To estimate PCR product sizes, a reference DNA mix with known fragment sizes was loaded in the first lane (1Kb PlusLadder™, Invitrogen, Figure 30).

TAE-buffer 50x	
Tris-base	50g
Glacial acetic acid	57.1ml
EDTA 0.25M, pH 8.0	200ml
Glycerol	12.5ml

Loading-buffer 10x	
ddH_2O	add 50ml
Ficoll® 400	7.5g
Bromphenol blue	0.25mg
EDTA 0.5M, pH 8.0	1ml

Agarose gel 1.2%			
	Mini	**Midi**	**Maxi**
Electrophoresis chamber	Horizon® 58	Horizon® 11-14	Horizon® 20-25
TAE-Buffer 1x	25ml	100ml	250ml
Agarose	0.3g	1.2g	3.0g
EtBr 10mg/ml	1.25µl	5µl	12.5µl

Gel electrophoresis equipment	
1Kb Plus Ladder™	Invitrogen, Carlsbad, CA, USA
Acetic acid	Merck, Darmstadt, Germany
Agarose	Eurogentech, Seraing, Belgium
EDTA	Brunschwig, Basel, Switzerland
Ethidium bromide (EtBr)	Fluka, Buchs, Switzerland
Ficoll® 400	Pharmacia Biotech, Vienna, Austria
Glacial acetic acid	Merck, Darmstadt, Germany
Glycerol	Fluka, Buchs, Switzerland
Horizon® 11-14 gel electrophoresis chamber	GibcoBRL Life Technologies / Invitrogen
Horizon® 20-25 gel electrophoresis chamber	GibcoBRL Life Technologies / Invitrogen
Horizon® 58 gel electrophoresis chamber	GibcoBRL Life Technologies / Invitrogen
Image Master® VDS UV transilluminator	Pharmacia Biotech, Vienna, Austria
Standard Power Pack P25 Power Adapter	Biometra, Göttingen, Germany
Tris-Base	Merck, Darmstadt, Germany
Video Graphic Printer UP-895CE	Sony, Schlieren, Switzerland

Table 18 Gel electrophoresis equipment

2.2.5 Cloning of DNA fragments

The *Taq*-based polymerases used in this study (HOT FIREPol® from Solis Biodyne, Tartu, Estonia, and HotStarTaq® from Qiagen, Hilden, Germany) add single deoxyadenosine (A) overhangs to the 3'-end of the PCR amplicons. If necessary, these amplicons were subcloned with the TOPO TA Cloning® Kit using the pCR®II-TOPO® Dual promotor vector and OneShot® TOP10 chemically competent cells (Invitrogen, Carlsbad, CA, USA). Amplicons generated with the *Pfu*-based Phusion™ DNA polymerase were blunt-ended and have been cloned with the Zero Blunt® TOPO® PCR Cloning Kit (Invitrogen, Carlsbad, CA, USA). Reactions were performed according to the manufacturer's instructions. Transformed TOP10 *E. coli* cells were grown on LB agar plates (Table 19) with 50µg/ml ampicillin and clones were selected with X-gal (32µl per plate/50mg/ml; only in case of pCR®II-TOPO. The pCR®-Blunt II-TOPO® vector includes the lethal *ccdB* selection gene, and thus does not require X-Gal selection).

Positive clones were picked with a disposable inoculation loop (Nunc, Langenselbold, Germany) and incubated in 12ml culture tubes (Sarstedt, Nümbrecht, Germany) with 3ml LB medium (Table 19) containing 50µg/ml ampicillin at 37°C o/n at 220rpm in a lab incubator shaker (Innova™ 4400; New Brunswick Scientific, Edison, NJ, USA). The colonies were pelleted in a benchtop centrifuge (5810R; Eppendorf, Hamburg, Germany) for 10min at 4000rpm and the plasmid DNA was isolated (see page 63).

2.2.5.1 Restriction analysis of clones

Clones were analyzed for constructs of the expected size with an *EcoR*I restriction enzyme digestion prior to sequencing. 2µl of pDNA were digested in a 10µl-reaction (6µl ddH_2O, 1µl 10x buffer, 1µl *EcoR*I; Fermentas, St.-Leon-Rot, Germany) at 37°C for at least 1h, before DNA fragments were separated by size on an agarose gel (see page 70).

LB medium	
NaCl	10g 5g (low-salt)
Bacto Tryptone	10g
Bacto Yeast Extract	5g
dH_2O	1000ml

LB plates	
NaCl	10g
Bacto Tryptone	10g
Bacto Yeast Extract	5g
Bacto Agar	15g
dH_2O	1000ml

Cloning equipment	
5417R centrifuge	Eppendorf, Hamburg, Germany
5810R centrifuge	Eppendorf, Hamburg, Germany
Ampicillin	Sigma-Aldrich, Buchs, Switzerland
Bacto Agar	Brunschwig, Basel, Switzerland
Bacto Tryptone	Brunschwig, Basel, Switzerland
Bacto Yeast Extract	Brunschwig, Basel, Switzerland
Culture tubes / Snap-cap 12ml	Sarstedt, Nümbrecht, Germany
Disposable inoculation loops	Nunc, Langenselbold, Germany
*EcoR*I	Fermentas, St. Leon-Rot, Germany
Innova™ 4400 incubator shaker	New Brunswick Scientific, Edison, NJ, USA
One Shot® TOP10 competent cells	Invitrogen, Carlsbad, CA, USA
TOPO TA Cloning® Kit	Invitrogen, Carlsbad, CA, USA
X-Gal	Promega, Madison, WI, USA
Zero Blunt® TOPO® PCR Cloning Kit	Invitrogen, Carlsbad, CA, USA

Table 19 Reagents and equipment for cloning. LB medium was autoclaved after mixing. 1000ml LB Agar was sufficient for ~40 LB plates.

2.2.6 Sequencing

DNA sequencing was performed through the Sanger chain-termination method (Sanger et al., 1977). The principle behind it is random incorporation of fluorescently marked dideoxynucleotides (ddNTPs) into the DNA strand during amplification, which inhibits further elongation. When ddNTPs are mixed with an excess of dNTPs (1:100), a heterogenous population of fragments of all possible lengths is generated, one for each nucleotide of the sequence. Since each nucleotide is labeled with a unique fluorescent dye, it is possible to distinguish the different nucleotides and obtain the sequence information after size separation of the fragments by gel electrophoresis.

The sequencing in this study was performed with the ABI PRISM® BigDye™ Terminator v.3.1 Cycle Sequencing kit and a capillary gel electrophoresis-based sequencing machine (ABI PRISM® 3100 or ABI PRISM® 3730 Genetic Analyser; Applied Biosystems, Foster City, CA, USA).

2.2.6.1 PCR product purification

After PCR and before nucleotide labeling, small DNA fragments (<70bp) that otherwise could interfere with the sequencing reaction were removed through application of the ExoSAP-IT® PCR Clean-up method (#78200; USB, Cleveland, OH, USA). It is based on two enzymes: Exonuclease I (Exo) digests residual single-stranded primers and any irrelevant single-stranded DNA produced during the PCR reaction, and Shrimp Alkaline Phosphatase (SAP) removes unincorporated, remaining dNTPs.

5 µl of ExoSAP-IT® mix (0.1µl ExoSAP, 4.9µl EB buffer (Qiagen, Hilden, Germany)) were added to 0.6µl of PCR product and digested for 15 minutes at 37°C. The reaction was stopped by 15 minutes incubation at 80°C to inactivate the enzymes.

2.2.6.2 Nucleotide labeling

In contrast to a regular PCR, the cycle sequencing, as the the nucleotide labeling procedure is also called, only allows for one primer. To obtain the sequence information of both complementary strands, each PCR product was sequenced twiced, i.e. in the forward and the reverse direction. The reaction conditions are given in Table 20. Typically, the primers that were used for amplification of the product were also used for cycle sequencing; exceptions are highlighted in Table 21. The 0.6µl PCR reaction in the protocol is a good standard volume for PCR products that works in most cases. However, standard recommendations were 10ng/100bp PCR product or 200ng pDNA per cycle sequencing reaction.

Cycle sequencing	Vol.
ddH_2O	1.2µl
Sequencing buffer	1.6µl
ExoSAP / PCR-Product	5.6µl
Primer	0.8µl
BigDye™	0.8µl
Total:	**10µl**

Cycling conditions		
96°C	20s	
96°C	20s	25x
50°C	10s	
60°C	2min	
10°C	∞	

Table 20 Reaction mix and conditions ort he cycle sequencing reaction.

NDP		
Exon	Primer	
	fwd	rev
1	587	582
2	583	584
3	585	586
3.1	561	562
3.2	563	590

FZD4		
Exon	Primer	
	fwd	rev
1	465	429
2a	430	450
2b	443	444
2c	445	447
2e	446	439

LRP5		
Exon	Primer	
	fwd	rev
(1.2)†	361	290
2	291	292
3	293	294
4	295	296
5	297	298
6	336	300
	337	338
7	301	302
8	303	304
9	339	306
10	350	345
11	309	310

LRP5		
Exon	Primer	
	fwd	rev
12	311	12
13	313	13
14	343	14
15	317	15
16	319	16
17	321	17
18	323	18
19	325	19
20	327	20
21	329	21
22	331	22
23	333	341

LMO2		
Exon	Primer	
	fwd	rev
1	565	566
2	567	568
3-4	588	589
5	600	601
6.1	575	576

PLVAP		
Exon	Primer	
	fwd	rev
1.1	545	546
1.2	547	548
2	549	550
3.1	551	552
3.2	553	554
4-5	591	556
6.1	557	558
6.2	559	560

SLC38A5		
Exon	Primer	
	fwd	rev
1a	604	605
1b	606	607
1c	608	609
2-3	610	611
4-5	612	613
6-7	614	615
8	616	617

SLC38A5		
Exon	Primer	
	fwd	rev
9-10	632	633
11	620	621
12	622	623
13	624	625
14-15	626	627
16a	628	629
16b	630	631

Table 21 Primers used ort he cycle sequencing reaction. Special sequencing primers different from the PCR primers are highlighted.

2.2.6.3 Gel filtration

To avoid signal interference with the labeled fragments during the capillary gel electrophorsis, excess ddNTPs were removed from the cycle sequencing reaction by gel filtration with Sephadex® columns (Sephadex® G-50, no. S5897; Sigma-Aldrich, Buchs, Switzerland).

The Sephadex® powder was portioned with a 96-well molding tool and transferred into a 96-well filter plate. 350 µl ddH_2O were added to each well and the Sephadex® was allowed to expand for 3 hours at room temperature (or at 4°C o/n). Subsequently, the plate was centrifuged at 1500g for 1 minute, 170 µl ddH_2O were added and the plate was centrifuged for an additional 5 minutes at 950g. The cycle sequencing reaction was applied directly onto the Sephadex® columns, and the plate was centrifuged for 5 minutes at 910g. During this step, ddNTPs were retained in the pores of the the Sephadex® column, and the eluate was finally transferred into a 96-well sequencing plate. Prior to the capillary gel electrophoresis, the volume of the eluate was adjusted to 30µl (through addition of ddH_2O).

2.2.6.4 Capillary gel electrophoresis

The labeled DNA fragments were size-separated by capillary gel eletrophoresis with an ABI PRISM® 3100 (16 capillaries) or 3730 (48 capillaries) Genetic Analyser (Figure 31). The DNA sequence was determined by a laser detector, which measured the light emission of the fluorecently labeled fragments in dependence of run-time of the gel electrophoresis. This way, the sequence data was obtained nucleotide after nucleotide, and the collected output data was saved in an electropherogram.

Figure 31 ABI PRISM® 3730 48-capillary DNA analyzer (image from http://www.appliedbiosystems.com).

2.2.6.5 Analysis of sequence data

Analysis of the electropherograms was performed with the software Sequencing Analysis 5.2, SeqScape 2.6 (both Applied Bioscience, Foster City, CA, USA), and/or Sequence Pilot 3.1 (JSI Medical Systems GmbH, Kippenheim, Germany). Reference sequences were downloaded from Ensembl (http://www.ensembl.org) or NCBI (http://www.ncbi.nlm.nih.gov) (Table 22).

Gene	NCBI reference	Ensembl reference
NDP	NC_000023.9, GI:89161218	
FZD4	NC_000011.8, GI:51511727	
LRP5	NC_000011.8, GI:51511727	
LMO2		ENSG00000135363
PLVAP		ENSG00000130300
SLC38A5		ENSG00000017483

Table 22 Reference sequences of the investigated genes.

2.3 RNA techniques

2.3.1 RNA isolation

Total RNA was extracted with the RNeasy®-Kit (Qiagen, Hilden, Germany) according to the manufacturer's instructions. Lysis buffer (at least 100µl) was added to deep frozen (-80°C) tissue, and the sample was homogenized immediately with an Ultra-Turrax® high-performance disperser (Ika-Werke, Staufen, Germany). HEK293T cell pellets were homogenized with a shredder-column (QIAshredder Kit; Qiagen, Hilden, Germany).

Total RNA including small RNAs (e.g. miRNA) was extracted with the miRNeasy®-Kit (Qiagen, Hilden, Germany) according to the manufacturer's instructions.

2.3.2 RNA quantification

RNA quantity and quality was determined with a NanoDrop® ND-1000 (NanoDrop Technologies/Thermo Scientific, Wilmington, DE, USA) and a Bioanalyzer 2100 (Agilent Technologies, Santa Clara, CA, USA) according to the manufacturer's instructions. Only samples with a 260nm/280nm ratio between 1.8–2.1 and an RNA integrity number (RIN) higher than 9.0 were further processed.

2.3.3 Reverse transcription PCR (RT-PCR)

To determine absolute, local, or temporal expression of a gene, RT-PCR is applied. In contrast to a regular PCR, which amplifies specific DNA fragments, RT-PCR uses RNA as template. The procedure is nearly identical – the only difference is an initial RNA-to-DNA conversion procedure facilitated by an enzyme with reverse transcriptase activity.

2.3.3.1 DNase Treatment of RNA samples

To remove all possible remaining traces of DNA that would interfere with downstream applications such as quantitative RT-PCR, DNase digestion was applied either directly on-column during extraction with the RNeasy®-Kit (RNase-free DNase Set, cat. no. 79254, Qiagen, Hilden, Germany), the TURBO DNA-*free*™-Kit (#1907; Ambion, Austin, TX, USA), or separately after RNA extraction (RQ1 RNase-free DNase, p/n M610A, Promega, Madison, WI, USA) according to the manufacturer's instructions.

2.3.3.2 Synthesis of cDNA

1250ng total RNA were reverse transcribed in a 20µl reaction, using random hexamer primers pd(n)$_6$ (Amersham Biosciences / GE Healthcare Europe, Otelfingen, Switzerland) and the reverse transcriptase SuperScript™ III RT (Invitrogen, Carlsbad, CA, USA) according to the manufacturer's instructions. Before addition of the reverse transcriptase, RNA samples were heated to 65°C for 5 min to break down secondary structures. RNasin® Plus (#9PIN261; Promega, Madison, WI, USA) or RNaseOUT™ (#10777-019; Invitrogen, Carlsbad, CA, USA) RNase inhibitor was added to the reaction mix to prevent template degradation during the 1h / 50°C incubation step. For every RNA sample, a negative „-RT" control reaction without reverse transcriptase was run.

2.3.4 Microarrays

2.3.4.1 Whole genome cDNA microarray

Gene chip expression analysis has been carried out with RNA from p7 retinae of the ND mouse strain (wt: n=5, ko: n=5) using the Affymetrix GeneChip® Mouse Genome 430 2.0 array (Affymetrix Inc., Santa Clara, CA, USA). On this chip, over 34,000 genes and ESTs are represented by ~45,000 probe sets. The microarray experiment, from cDNA synthesis to raw data processing, was performed at the Functional Genomics Center Zurich (FGCZ) by Marzanna Künzli. A detailed description of the protocol is given in the IOVS publication.

2.3.4.2 Whole genome miRNA microarray

Total RNA including miRNA was isolated from *Ndph* wt (n=4) and ko (n=4) mice aged p5 and p21. The actual microarray experiments were conducted by Andrea Patrignani at the FGCZ with an Agilent Mouse miRNA 8 x 15K OligoMicroarray (#G4472A, Design ID 019119; Agilent Technologies, Santa Clara, CA, USA). This array contains probes for 567 mouse and 10 viral microRNAs from the Sanger database v10.1 (microrna.sanger.ac.uk).

Fluorescent miRNA with a sample input of 100ng of total RNA was generated. This method involves the ligation of one cyanine 3-pCp molecule to the 3' end of a RNA molecule using a kit (miRNA Complete Labeling and Hyb Kit; #5190-0456; Agilent, Waldbronn, Germany). The quality of Cy3-RNA was determined using a NanoDrop ND 1000. Only RNA samples with a dye incorporation rate >2 pmol/µg were considered for hybridization.

Cy3-labeled RNA samples were mixed with the kit blocking solution and resuspended in hybridization buffer. Target RNA samples (45µl) were hybridized on to the microarray chip for 20h at 55°C. Arrays were then washed using GE wash buffers 1 and 2 (#5188-5326; Agilent, Waldbronn, Germany) according to the manufacturer instructions (www.agilent.com). A microarray scanner (Agilent #G2565BA) was used to measure the fluorescent intensity emitted by the labeled target.

Raw data processing was performed using the Agilent Scan Control and the Agilent Feature Extraction Software Version 9.5.3.1. Quality control measures were considered before performing the statistical analysis. These included inspection of the array hybridization pattern (absence of scratches, bubbles, areas of non hybridization), proper grid alignment and number of green feature non uniformity outliers (below 100 for all samples). Expression values were imported and processed in the B-fabric database (http://fgcz-bfabric.uzh.ch/b-fabric/welcome). Hubert Rehrauer of the FGCZ performed the statistical analyses with the free software package R (http://www.r-project.org/).

2.3.5 Quantitative RT-PCR (qRT-PCR)

Quantitative RT-PCR was carried out in five replicates in an ABI PRISM® 7900HT system (Applied Biosystems, Foster City, CA, USA; Figure 32) using the recommended standard cycling conditions: 45 cycles of denaturation (15s/95°C) and annealing/extension (1min/60°C). Relative expression was calculated by the ΔΔCt (cycle threshold) method in two subsequent normalization steps:

1.) Normalization of target gene expression to endogenous control:

$$Ct_{\text{target gene}} - Ct_{\text{endogenous control}} = \Delta Ct$$

2.) Normalization of an individual sample to an arbitrary (e.g. mean of wt samples) calibrator sample:

$$\Delta Ct_{\text{sample}} - \Delta Ct_{\text{calibrator sample}} = \Delta\Delta Ct$$

With this method, fold change expression differences can be calculated with the formula: $2^{-\Delta\Delta Ct}$. Confidence intervals for wild type and knockout gene expression (or treated vs. untreated samples) were calculated on basis of the mean ΔΔ ct-values at a significance level of 95% using Student's t-test.

Two different transcript detection methods were applied, using either

- two target-recognizing primers and SYBR®-Green (a fluorescent dye that intercalates in doublestranded DNA),
- or using a TaqMan® probe (a third, fluorescently labeled primer that is only detectable when a target amplicon is generated).

For each target gene, the amount of template cDNA had to be empirically determined for each tissue. Ideally, Ct-values were between 25-30, since Ct values lower than 35 could also occur sporadically by chance. Candidate genes defined by the microarray experiment were verified by probes/primer pairs binding in the area that is recognized by the Affymetrix probes.

Figure 32 ABI PRISM® 7900HT qRT-PCR system (image from http://www.appliedbiosystems.com).

2.3.5.1 qRT-PCR with SYBR®-Green

Transcriptional analysis of several target genes (Table 23) was conducted using 0.5µM of a forward/reverse primer pair and SYBR®-Green PCR Mastermix (Applied Biosystems, Foster City, CA, USA) in a 10µl reaction volume (Table 24). In addition, in the case primers were not exon spanning, DNA contamination of the sample was checked by a –RT control reaction (a sample where no reverse transcription has been performed). Efficiency of the primer pair was tested with a cDNA dilution series and compared to the efficiency of several endogenous controls to determine the appropriate control for each target gene.

Gene	Primer pair	RNA
Bmp4	220 / 221	10ng
Isl-1	284 / 285	1ng
LacZ	230 / 231	1ng
Mdm2 (Int7)	200 / 201	10ng
Slc38a5	198 / 199	100ng
Syp	286 / 287	1ng
Endogenous controls:		
28S rRNA	202 / 203	0.025-0.1ng
Pol2ra	351 / 352	1ng

Table 23 SYBR®-Green qRT-PCR primer pairs used in this study.

SYBR®-Green reaction mix	
ddH_2O	3.5µl
Template	1.0µl
Primer 5' (10µM)	0.25µl
Primer 3' (10µM)	0.25µl
SYBR®-Green mastermix	5.0µl
Total:	10.0µl

Table 24 SYBR®-Green reaction mix.

2.3.5.2 qRT-PCR with TaqMan® probes

TaqMan® probes and TaqMan® Universal PCR Mastermix (Applied Biosystems, Foster City, CA, USA) were also used for relative quantification of mRNA expression. Reactions with a volume of 6µl were performed in 384-well plates (Table 25). TaqMan® probes and appropriate cDNA amounts used in this study are listed in Table 26.

TaqMan® reaction mix	
ddH_2O	1.7µl
Template	1.0µl
Primer/Probe (20x)	0.3µl
TaqMan® mastermix	3.0µl
Total:	6.0µl

Table 25 TaqMan® reaction mix.

Gene	TaqMan® probe	RNA
Aass	Mm00497118_m1	10ng
Abcb1a	Mm00440761_m1	10ng
Adm	Mm00437438_g1	10ng
Agtrl1	Mm00442191_s1	10ng
ApoD	Mm00431817_m1	10ng
Centd3	Mm00551866_m1	10ng
Cldn5	Mm00727012_s1	10ng
Ifnb1	Mm00439546_s1	65ng
Ndph Ex3	probe: 6FAM – CTG AGC CCT TGG TGT C - MGBNFQ fwd: CAC TGC AGC CAG GCA TCA C rev: AGG AAC GGA AAG GTT GCT TGA	1ng
Plvap	Mm00453379_m1	10ng
Prdm9	Mm00522708_m1	10ng
SLC38A5	Hs01012028_m1	10ng
Vwf	Mm00550376_m1	10ng
Endogenous controls:		
18S rRNA	p/n 4308329	0.1ng
Gapdh	p/n 4352339E	0.1ng
GAPD	Hs02786624_g1	0.1ng

Table 26 TaqMan® probes used in this study.

2.4 Protein techniques

2.4.1 Protein isolation

All protein working steps were performed on ice. Animal tissue or cell pellets were disrupted in freshly prepared RIPA buffer (Table 27; 1g tissue – 3ml buffer). To this end, deep frozen (dry ice) retinae were transferred in either a glass homogenizer (FB56673; Fisher Scientific, Wohlen, Switzerland) or a special microcentrifuge tube that was part of a single-use homogenizer kit. Without hesitation, the tissue was disrupted by up-down/rotary movements of the pestle for 30 seconds. All retinal samples in this study, regardless of their weight, were extracted in 100µl of buffer, since this was the minimal volume needed for proper functioning of the homogenizers.

Cell pellets and brain tissue were disrupted by sonication in a minimal volume of 200µl (Sonopuls HD 2200 with MS72 tip; Bandelin, Berlin, Germany). Ten 0.5s pulses with a maximum of 25% power were applied over the course of 10s.

The tissue lysate was placed on ice for 3h before it was centrifuged at 20000g for 30min at 4°C. The supernatant was transferred into a new microcentrifuge tube and stored until further use at -20°C together with the unsoluble pellet fractions (which could contain membrane proteins).

2.4.2 Protein quantification

Protein concentration was estimated with the bicinchoninic acid (BCA) protein assay kit (Sigma-Aldrich, Buchs, Switzerland) at 560nm. The assay was carried out in a 96-well optical plate (TechnoPlasticProducts, Trasadingen, Switzerland) with a protein sample volume of 20µl and 200µl of BCA solution (Table 27). The samples were incubated for 30min at 37°C (Heraeus function line incubator; Kendro, Zurich, Switzerland) and absorption was measured at 560nm with a 96-well microplate reader (ELx808™; Bio-Tek®, Bad Friedrichshall, Germany).

The protein amount of a sample was calculated through comparision to a series of bovine serum albumine (BSA) reference samples of known concentrations (50-1000ng/µl). Since this relative quantification is only valid within the linear range of the standard curve (OD_{560nm} between 0 and 1), two different sample dilutions (1:10, 1:20) were measured simultaneously. Each sample was run in duplicate.

2.4.3 SDS-Polyacrylamide gel electrophoresis (SDS-PAGE)

Proteins were separated by size with SDS-PAGE using a Mini-PROTEAN® 3 electrophoresis system (BioRad, Reinach, Switzerland; Figure 33). To remove possible traces of greasy residues, glass plates, combs, and sealings were cleaned with EtOH, and the setup was assembled to the manufacturer's instructions. The resolving gel solution was prepared dependent on the expected size of the proteins to be separated (Sambrook et al., 1989;Figure 34) and poured between the glass plates.

Figure 33 Components of the Mini-PROTEAN® Tetra system. **(A)** electrophoresis module, companion running module, tank, lid, and buffer dam; **(B)** glass plates and combs; **(C)** sample loading guides; **(D)** casting stand and casting frames (image from http://bio-rad.com).

To obtain a smooth and flat border, the gel was covered with 0.5ml isopropanol, which was removed with whatman paper after polymerization of the gel. Then the stacking gel was poured onto the resolving gel and filled to the top. To create the sample pockets, a comb was placed into the yet non-polymerized stacking gel. After polymerization, the comb was removed, and the gel was transferred into the electrophoresis chamber, which was filled with 1x SDS-PAGE running buffer (Table 27). To remove perturbing gel strands that may have formed during the preparation, sample pockets were flushed with 1x SDS-PAGE running buffer several times by pipetting up and down several times. Protein samples were heated for 5min at 95 °C with Lämmli loading buffer containing β-mercaptoethanol, which reduced disulfide bonds („reducing conditions"). All samples were centrifuged for 2 min at 10000 rpm and equal amounts of protein were loaded into the gel pockets (ideally, the loading volume was also adjusted with RIPA buffer to ensure comparable running characteristics; max. 20µl). Proteins were then separated for about 60 min at 200 V until the loading dye reached the bottom of the gel. Since protein mass can be determined only relatively by this method, a molecular mass marker was loaded in each gel in the first (and/or last) lane. Usually, the PageRuler™ Prestained Protein Ladder Plus (#SM1811; Fermentas, St. Leon–Rot, Germany) was used (Figure 34).

separation size range (kDa)	% acrylamide in resolving gel
10 – 60	15 %
30 – 120	10 %
50 – 200	8 %

Resolving gel 10% (10ml)	
H_2O	4.0 ml
30% acrylamide mix	3.3 ml
1.5M Tris (pH 8.8)	2.5 ml
10% SDS	0.1 ml
TEMED	5 µl
10% Ammonium Persulfate	0.1 ml

Stacking gel 5% (2ml)	
H_2O	1.4 ml
30% acrylamide mix	0.33 ml
1M Tris (pH 6.8)	0.25 ml
10% SDS	20 µl
TEMED	2 µl
10% Ammonium Persulfate	20 µl

A

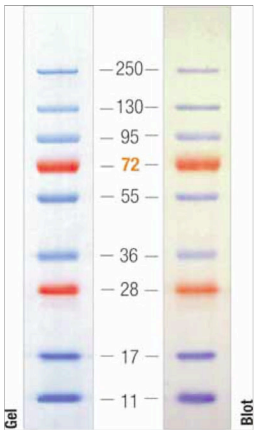

B

Figure 34 (A) SDS-PAGE protocols for resolving / stacking gels and **(B)** a 8-16% SDS-PAGE showing the PageRuler™ Protein Ladder #1811 (Fermentas, St.Leon-Rot, Germany).

2.4.4 Western blot

SDS-PAGE separated proteins were electrotransferred onto a polyvinylidene difluoride (PVDF) membrane (Roche Diagnostics, Rotkreuz, Switzerland) in a semi-dry blotting chamber (BioRad, Reinach, Switzerland). To make it hydrophilic, the PVDF membrane was soaked shortly in methanol, washed in ddH_20 for 5min and then prepared in blotting buffer for another 5min. The SDS-PA gel was incubated for 15min in blotting buffer. Three pieces of chromotography filter paper (Whatman®, GE Healthcare, Otelfingen, Switzerland) were soaked with blotting buffer and stacked on the anode of the blotting system, trying to avoid air bubbles in between. The PVDF membrane was put on top of the three filter papers, and the SDS-PA gel was carefully placed above it. The blot sandwich was completed with an additional three pieces of filter paper, and the blot chamber was closed with the cathode (Figure 35). Proteins were transferred for 20 min at 15V.

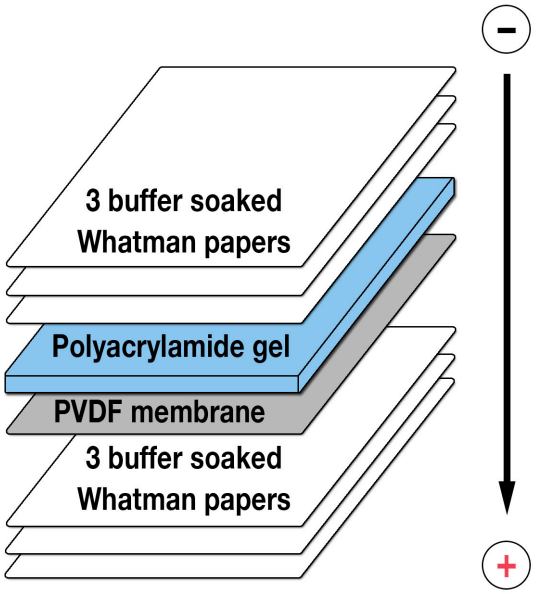

Figure 35 Blot sandwich setup.

RIPA buffer (10ml)	
Tris HCl pH 7.5 1M	500µl
NaCl 5M	300µl
EDTA pH 8.0 0.5M	20µl
Nonidet P40	20µl
ddH_2O	9160µl
Complete Protease Inhibitor (25x solution)	400µl

Lämmli Loading-buffer 5x	
1M Tris-HCl pH 6.8	2.5ml
Glycerol	2.5ml
ddH_2O	~2.5ml (add 10ml)
SDS	0.5g
Bromphenol blue solution	0.5ml
2-Mercaptoethanol	2ml

SDS running buffer 5x	
Tris/HCl pH 8.3	15.1g
Glycin	72g
SDS	5g
ddH_2O	ad 1000ml

BCA assay mix	
Solution A: BCA, Na_2CO_3, sodium tartrate, $NaHCO_3$ in 0.1N NaOH	196µl
Solution B: Copper (II) sulfate pentahydrate solution 4% (w/v)	4µl

Blotting buffer 5x	
Tris/HCl pH 8.3	29.1g
Glycin	14.65g
SDS	1.88g
ddH_2O	ad 1000ml

Bromphenol blue solution	
ddH_2O	10ml
Bromphenol blue	0.25mg

Protein fixation buffer (for 5ml gel)	
Ethanol	7.5ml
Glacial acetic acid	2.5ml
ddH_2O	15ml

Blotting buffer 1x (with MeOH)	
Blotting buffer 5x	20ml
Methanol	20ml
ddH_2O	60ml

Silver stain fixation buffer (for 5ml gel)	
Na_2CO_3	2.5g
Formaldehyde solution 37%	12.5µl
ddH_2O	25ml

Silver stain solution (for 5ml gel)	
$AgNO_3$ 20%	125µl
ddH_2O	25ml

SDS-PAGE / Western blot equipment	
2-Mercaptoethanol	Merck, Darmstadt, Germany
Ammonium Persulfate (#9592.3)	Carl Roth, Karlsruhe, Germany
BCA Protein Assay Kit	Sigma-Aldrich, Buchs, Switzerland
Bovine serum albumine (BSA) 1mg/ml protein standard (#P0914)	Sigma-Aldrich, Buchs, Switzerland
Bromphenol blue (#15375)	Serva, Heidelberg, Germany
Complete Protease Inhibitor Cocktail tablets (#04693116001)	Roche Diagnostics, Rotkreuz, Switzerland
Curix 60 film developer machine	AGFA, Köln, Germany
EDTA	Brunschwig, Basel, Switzerland
ELx808™ absorbance microplate reader	Bio-Tek®, Bad Friedrichshall, Germany
Gel dryer model 543	BioRad, Reinach, Switzerland
Glacial acetic acid	Merck, Darmstadt, Germany
Glycerol	Fluka / Sigma-Aldrich, Buchs, Switzerland
Imperial™ protein stain (#24615)	Pierce / Thermo Scientific, Rockford, IL, USA
Laboratory shaker (#3006)	GFL, Burgwedel, Germany
Mini-PROTEAN® 3 electrophoresis system	BioRad, Reinach, Switzerland
Nonidet P40 (#1754599)	Roche Diagnostics, Rotkreuz, Switzerland
Powerpack 200	BioRad, Reinach, Switzerland
PVDF Western blotting membrane (#03010040001)	Roche Diagnostics, Rotkreuz, Switzerland
Rotiphorese® Gel 30 acrylamide gel mix	Carl Roth, Karlsruhe, Germany
Roto-Torque® Heavy Duty rotator (#7637-10)	Cole-Parmer instruments, London, UK
Silver nitrate	Merck, Darmstadt, Germany
Sodium azide NaN_3 (#71290)	Fluka / Sigma-Aldrich, Buchs, Switzerland
TEMED (#87689)	Fluka / Sigma-Aldrich, Buchs, Switzerland
Trans-Blot® SD Semi-Dry Transfer Cell (Blotting chamber)	BioRad, Reinach, Switzerland
Tris-HCl	Merck, Darmstadt, Germany
Western Lightning™ Chemiluminescence Reagent Plus (NEL103)	Perkin Elmer, Boston, MA, USA
Whatman® Chromatography Paper 3mm, 46x57cm (#3030917)	GE Healthcare, Otelfingen, Switzerland

Table 27 Protein / SDS-PAGE / Western blot reagents and equipment.

2.4.5 Visualization of proteins

2.4.5.1 Antibody staining / chemiluminescence detection of proteins on PVDF membranes

After the blotting procedure, the PVDF membrane was shortly rinsed in PBST, and then blocked with 5 % milk powder in PBST for 1h at RT on a laboratory shaker (#3006; GFL, Burgwedel, Germany) to prevent unspecific antibody binding. The primary antibody was diluted (Table 28) in the blocking solution and the membrane was incubated o/n at 4°C on a laboratory rocker or rotator (Roto-Torque® Heavy Duty rotator, No 7637-10; Cole-Parmer instruments, London, UK). The blot was washed three times for 5 min in PBST at RT before it was incubated in the secondary antibody solution (Table 29) for 30min at RT. Unbound antibodies were removed thoroughly by washing three times for 10min with PBST. The horse radish peroxidase (HRP) labeled secondary antibodies were detected with the Western Lightning™ ECL plus system (NEL103; Perkin Elmer, Boston, MA, USA). With this method, membrane-bound proteins are detected by an enzymatic reaction that catalyzes chemiluminescence detection substrates to emit light, which then produces an image on photosensitive film. The substrates were prepared according to the manufacturer's protocol and added to the membrane, which was then placed between two transparent overhead sheets and transferred into a film cassette. A photosensitive film (Lumi-film; Roche, Mannheim, Germany) was then exposed to the membrane for different time spans and subsequently processed in a photo developer machine (Curix 60; AGFA, Köln, Germany). Usually, the blot was then incubated a second time to ensure equal loading through the detection of the household protein GAPDH. Before the second incubation round, the blot was „stripped", i.e. the activity of the horse radish peroxidase was terminated through incubation of the membrane in 0.1% NaN_3 (Fluka/Sigma-Aldrich, Buchs, Switzerland) in PBST for 1h at RT.

Antibody	Host	Company	Order no.	Dilution
α-c-myc	mouse	Roche	1667149	1 : 500
α-mouse β-catenin	mouse	BD Biosciences	610153	1 : 1,000
α-mouse Plvap/MECA-32	rat	Developmental Studies Hybridoma Bank	-	1 : 100
α-rat SNAT5 / Slc38a5	guinea pig	F. Zafra, Madrid	custom	1 : 4,000
α-rabbit GAPDH	mouse	Chemicon	MAB374	1 : 8,000
α-rat p44/42 MAP Kinase	rabbit	Cell Signaling	4695	1 : 1,000
α-human phospho p44/42 (Thr202/Tyr204) MAP Kinase	rabbit	Cell Signaling	9101	1 : 250

Table 28 Primary antibody dilutions for Western blots used in this study. Antibodies were diluted in PBST pH 7.2 with 5% milk powder.

Antibody	Host	Company	Order no.	Dilution
α-chicken/turkey IgG-HRP	rabbit	Zymed / Invitrogen	61-3120	1 : 10,000
α-guinea pig IgG-HRP	rabbit	Zymed / Invitrogen	61-4620	1 : 2,000
α-mouse IgG-HRP	goat	Dianova	115035062	1 : 10,000
α-rat IgG-HRP	mouse	Zymed / Invitrogen	80-9520	1 : 2,000

Table 29 Secondary antibody dilutions for Western blots used in this study. Antibodies were diluted in PBST pH 7.2 with 5% milk powder.

2.4.5.2 Ponceau staining of SDS-PAGE separated proteins on PVDF membranes

The membrane was washed shortly three times in PBS at RT. It was then incubated in 0.1% Ponceau S solution (P7110; Sigma, Buchs, Switzerland) for a few minutes until protein bands became visible. The membrane was quickly rinsed, and photographs were taken.

2.4.5.3 Coomassie staining of SDS-PAGE protein gels

The gel was washed three times in ddH_2O for 5min at RT. It was then incubated in 20ml staining solution (Imperial™ protein stain #24615; Pierce, Rockford, IL, USA) for 2h. The gel was washed in ddH_2O for another 2h before it was dried (Gel dryer model 543; BioRad, Reinach, Switzerland).

2.4.5.4 Silver staining of SDS-PAGE protein gels

Proteins were fixed through incubation of the gel in five volumes of an ethanol:glacial acetic acid:water (30:10:60) solution o/n at RT. After removal of the fixative, the gel was gently washed twice in five gel volumes of 30% EtOH for 30min at RT. The ethanol was removed and ten gel volumes of ddH_2O were added. This washing step was conducted twice for 10min at RT. After washing, the gel was stained in five gel volumes of a fresh 0.1% $AgNO_3$ solution for 30min at RT (gently shaking). The solution was discarded and both sides of the gel were washed under a stream of deionized water for 20s each. The gel was protected from light and five volumes of a freshly made fixing solution containing 2.5% sodium carbonate and 0.02% formaldehyde were added. The gel was incubated for a few minutes at RT, until protein bands became visible. The reaction was stopped through washing of the gel in a 1% acetic acid solution. Finally, the gel was washed in water three times for 10min and subsequently preserved by drying.

2.5 Histology

2.5.1 Cryosections

Eyes were dissected, fixed for 1h in PBS / 4% para-formaldehyde, washed in PBS and cryo-protected in succrose/PBS solution (30min in 10%, then o/n in 20%) at 4°C. Occasionally, the fixation step was omitted or fixation time was reduced, and the cryo-protection was also not performed during some experiments. The eyes were embedded in Tissue-Tek® O.C.T. Compound (Sakura Finetek, Zoeterwoude, Netherlands), submersed in liquid nitrogen, cut into 8µm sections with a Leica Cryostat CM 3050S (Leica, Heerbrugg, Switzerland) and transferred onto microscope glass slides.

2.5.2 Immunohistochemistry

After drying the sections for at least 3h, unspecific binding sites were blocked by incubation with 5% non-specific serum (goat, rabbit, or sheep, depending on the origin of the secondary antibody; Sigma Aldrich, Steinheim, Germany) in PBST for 1h. Slides were incubated with primary antibodies in blocking solution (o/n, 4°C) in a wet

chamber. Antibodies and used antiserum concentrations are listed in Table 30. Sections were washed and incubated with secondary antibodies in PBS (90min, RT); secondary antibodies and dilutions used are given in Table 31. Slides were washed a last time and finally mounted in a DAPI-containing medium (Vectashield® Mounting Medium for Fluorescence with DAPI H-1200, Vector Laboratories, Burlingame, CA, USA).

Antibody	Host	Company	Order no.	Dilution
α-mouse Plvap/MECA-32	rat	Developmental Studies Hybridoma Bank	-	1 : 16
α-mouse Collagen IV	rabbit	AbD Serotec	2150-1470	1 : 300
α-rat SNAT5 / Slc38a5	guinea pig	F. Zafra, Madrid	custom	1 : 250
α-mouse APJ / Agtrl1	chicken	abcam	ab15639	1 : 300
α-human APOD	rabbit	abcam	ab24808	1 : 200
α-E.coli β-galactosidase	rabbit	Molecular Probes	A-11132	1 : 500
Antibodies used in L. Galli-Restas lab in Pisa:				
α-mouse Synaptophysin/p38	mouse	Boehringer/Roche; E. Strettoi	?	1 : 500
α-mouse Islet-1/4D5	mouse	Sigma; L. Galli-Resta	?	1 : 50
α-mouse Vimentin (very old!)	mouse	Boehringer/Roche; L. Galli-Resta	?	1 : 5
α-mouse ChAT	goat	Chemicon	AB144P	1 : 200
α-mouse mGluR6	rabbit	E. Strettoi, Pisa	custom	1 : 1,000
α-mouse NF150	rabbit	Chemicon	AB1981	1 : 500
α-mouse calbindin 28kDa	rabbit	Swant; L. Galli-Resta	?	1 : 200

Table 30 Primary antibody dilutions for cryosections used in this study. Antibodies were diluted in blocking solution (PBST pH 7.2 with 10% normal goat/sheep serum).

Antibody	Host	Company	Order no.	Dilution
α-rabbit IgG Cy3™	goat	Jackson ImmunoResearch Europe	111-165-003	1 : 300
α-rat IgG AF®488	goat	Molecular Probes / Invitrogen	A-11006	1 : 1'000
α-guinea pig IgG AF®488	goat	Molecular Probes / Invitrogen	A-11073	1 : 300
α-chicken IgY Cy3™	donkey	Jackson ImmunoResearch Europe	703-166-155	1 : 300

Table 31 Secondary antibody dilutions for cryosections used in this study. Antibodies were diluted in blocking solution (PBST pH 7.2 with 10% normal goat/sheep serum)

2.5.3 X-Gal staining

After drying of the cryosections for 2h, the microscope slides were washed three times shortly (2-3min) with PBS. Then 300µl X-Gal staining solution (Table 32) were applied to each slide.

X-Gal staining solution	Stock	Final conc.	Volume
BetaBlue™ buffer	1x		292µl
X-Gal in DMSO	40µg/µl	1µg/µl	7.5µl
NP-40	10%	0.02%	0.6µl
Total per slide:			300µl

Table 32 Reaction mix for the X-Gal staining solution sufficient for one microscope slide. Kit ingrdients were from the BetaBlue™ Staining Kit (Novagen/Merck, Darmstadt, Germany).

Microscope slides were then incubated o/n at 37°C in a wet chamber. The staining solution was removed, and the slides were washed three times shortly (2-3min) with PBS. Sections were postfixed for 1h with 4% PFA in PBS, and washed again in PBS (5x3min). Finally, the sections were embedded in DAPI-containing mounting medium, or were further stained by immunohistochemistry.

2.5.4 Whole mount preparations

For retinal flatmounts, eyes were dissected and fixed for 15min in PBS/4% para-formaldehyde. Retinae were removed and post-fixed for additional 15min. After washing in PBS, unspecific binding was blocked by 10% non-specific serum in PBST for 1h. Samples were then incubated o/n with the primary antibodies. They were washed six times for 1h in PBST and incubated o/n with the secondary, fluorescently-labeled antibodies. After repetition of the washing procedure, the retinae were finally flatmounted on microscope slides in a DAPI-containing medium.

2.5.5 Paraffin sections

After dissection, tissue was fixed in Serras-fixative (Table 33) on ice for a few hours, during which time the liquid was agitated 2-3 times, because water leaking from the tissue has a higher density than the fixative. The sample was then placed at 4°C and fixed o/n.

On the next day, the Serras-solution was exchangend with ice-cold 70% isopropanol, and the tissue was dehydrated for about 2h. The step was repeated three times, and the last step was conducted o/n. The 70% solution was then changed to 100% isopropanol, (3x 2h), at which point the tissue could be stored at -20°C.

Corneas were removed, and the eyes were further dehydrated by ice-cold chloroform, which was exchanged once after 3h, before being placed at 4°C o/n. The tissue was then immersed in paraffin oil and placed into an incubator at 60°C. It was then transferred into liquid paraffin for 2h, which was exchanged two more times. The second paraffin step was conducted o/n. The tissue was then embedded in paraffin in a casting mold, carefully adjusting the eye's position in space with a micro-forceps, and the paraffin-block was stored o/n at 4°C. The embedded tissue was then cut into 7µm sections with a rotary microtome (RM2145; Leica, Heerbrugg, Switzerland). The sections were straightened in a flattening bath, transferred onto microscope slides, and dried o/n at 42°C on a heated flattening table.

„Serras“ fixative	
Ethanol	60%
Formaldehyde solution 37%	30%
Acetic acid	10%

4% PFA fixation solution	
Formaldehyde	2g
PBS buffer	50ml

Histology solutions & equipment	
AxioCam HRc digital camera	Carl Zeiss MicroImaging, Jena, Germany
AxioCam MRm digital camera	Carl Zeiss MicroImaging, Jena, Germany
Axioplan 2 microscope	Carl Zeiss MicroImaging, Jena, Germany
Chloroform (#102445.1000)	Merck, Darmstadt, Germany
Cold plate (#EG1140 C)	Leica, Heerbrugg, Switzerland
Cryostat (#CM 3050S)	Leica, Heerbrugg, Switzerland
Eosin staining solution 3% (Eosin B; #E8017)	Sigma Aldrich, Steinheim, Germany
Ethanol 95% (#1.00983)	Merck, Darmstadt, Germany
Flattening bath (#HI1210)	Leica, Heerbrugg, Switzerland
Flattening table (#HI1220)	Leica, Heerbrugg, Switzerland
Isopropanol (#109634)	Merck, Darmstadt, Germany
Mayer’s hemalum solution (#1.09249)	Merck, Darmstadt, Germany
Microtome blades type N35H, disposable: extreme hard (#207500007); hard(#207500006)	Leica, Heerbrugg, Switzerland
Paraffin (Histowax; #14 037432123)	Leica, Heerbrugg, Switzerland
Paraffin dispensing module, heated (#EG1140H)	Leica, Heerbrugg, Switzerland
Paraffin oil (#9190)	Carl Roth, Karlsruhe, Germany
Rotary microtome (#RM2145)	Leica, Heerbrugg, Switzerland
Roti Histokitt (#6638)	Carl Roth, Karlsruhe, Germany
Rotihistol (#6640) (Xylol alternative)	Carl Roth, Karlsruhe, Germany
Stereo microscope (#MZ6)	Leica, Heerbrugg, Switzerland
Superfrost / Plus microscope slides (#H867.1)	Carl Roth, Karlsruhe, Germany
Vectashield® Mounting Medium with DAPI (#H-1200)	Vector Laboratories, Burlingame, CA, USA

Table 33 Histology reagents, solutions, and equipment

2.5.6 Hematoxylin-eosin staining

Paraffin-embedded sections were then stained with hematoxylin-eosin. For that purpose, the sections were deparaffinized twice in Rotihistol (Carl Roth, Karlsruhe, Germany) for 10min, and subsequently hydrated in a descending alcohol series (2min each in 100%(2x), 90%, 70%, 50% isopropanol, ddH_2O). Then, staining of the cell nuclei was performed with hemalum solution (Mayer’s; Merck, Darmstadt, Germany) for 5min. The sections were washed twice quickly in ddH_2O, and were then subjected to an ascending alcohol series and eosin stain (which labels the cytoplasm):

- 50% EtOH (10 dips)
- 70% EtOH + NH_4OH (2 drops/50ml) (30s)
- 70% EtOH (quick)
- 95% EtOH (quick)
- 95% EtOH + 0.3% eosin (90s)
- 95% EtOH (quick)
- 95% EtOH (quick)

After preparation through submersion in Rotihistol III (5min) and Rotihistol IV (5min), sections were embedded with the Roti Histokitt (Carl Roth, Karlsruhe, Germany), and the slides were dried o/n.

2.5.7 Microscopy

Images were taken with an Axioplan 2 microscope equipped with AxioCam HRc (color) and MRm (monochrome) digital cameras (Carl Zeiss MicroImaging, Jena, Germany; Figure 36). Three-dimensional immunofluorescence images from retinal flatmounts were compiled from a Z-Stack of pictures acquired with a Zeiss ApoTome™.

During a 10-day internship in Lucia Galli-Restas lab in Pisa (Istituto di Neuroscienze, Consiglio Nazionale delle Ricerche), cryosections and wholemounts were examined under a confocal microscope (Leica TCS NT; Leica Microsystems S.p.A., Milano, Italy).

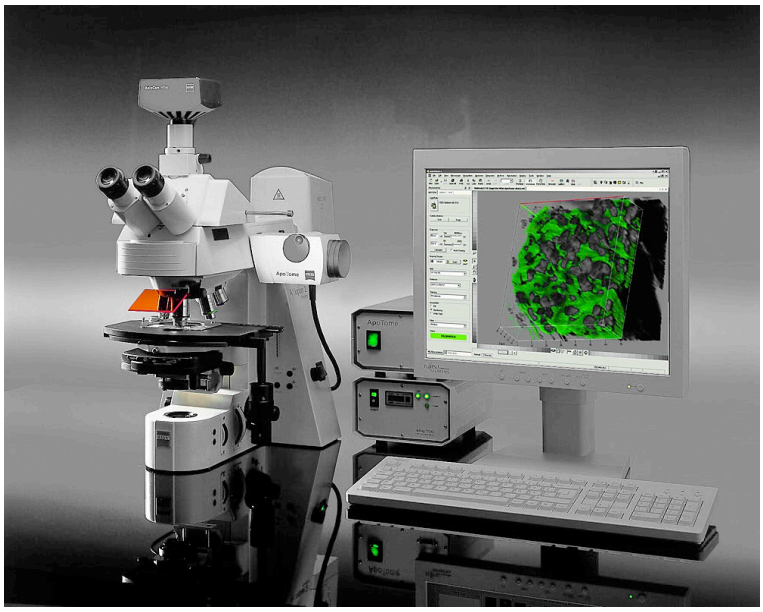

Figure 36 ApoTome imaging system on the basis of the fluorescence microscope Axioplan 2 (Carl Zeiss MicroImaging, Jena, Germany. Source: www.zeiss.de)

2.6 Recombinant protein expression in yeast

Recombinant norrin was engineered with the Multi-Copy *Pichia* expression kit (#K1750-01; Invitrogen, Carlsbad, CA, USA). The *NDP* constructs were placed under control of the *AOX1* promoter, which allows methanol-inducible high-level expression in *Pichia pastoris* cells. In addition, the *NDP* fragment was cloned behind an α–factor signal sequence, which facilitates secretion of the desired protein into the medium.

2.6.1 Generation of expression vectors

To generate the *P. pastoris* expression vectors, the Invitrogen Gateway® technology (#12535-019,12535-027; Invitrogen, Carlsbad, CA, USA) has been used. It consists of the following three steps:

1. Generation of an attB-flanked PCR product
2. Generation of an entry clone through an enzymatic recombination of the attB-PCR product and a donor vector
3. Generation of the expression clone through enzymatic recombination of the donor vector and the expression vector.

Donor and *P. pastoris* expression vectors have already been available and were provided by Rolf Jaussi (Paul-Scherrer-Institute, Villigen, Switzerland) (Figure 37), who also conducted the recombination reactions. Construction of the attB-flanked PCR product, verification of the constructs through sequencing, and also some of the recombination procedures were performed by myself and, to a minor extent, by Lucas Mohn. Four different constructs coding the mature form, i.e. without the first 24 signal-peptide coding amino acids, were generated: the human wild type Norrin and a C95R variant, which copies a known human mutation (Isashiki et al., 1995), either one tagged C- or N-terminally with c-myc and 6xHis.

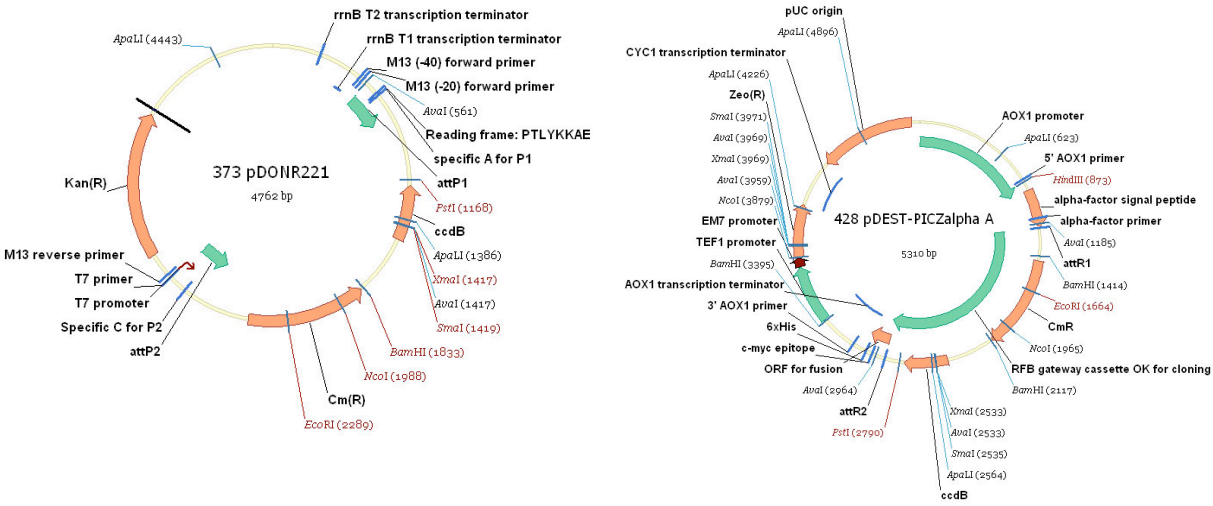

Figure 37 Donor (pDONR221; *left*) and *P. pastoris* expression (pDEST-PICZalpha A; *right*) vectors for the Invitrogen Gateway® system were provided by Rolf Jaussi (Paul-Scherrer-Institute, Villigen, Switzerland).

2.6.1.1 Generation of the attB-flanked PCR product

Gateway® attB recombination sites, tags, and flanking cleavage sites for thrombin (TCS) were introduced with elongated PCR primers (Figure 38; Figure 39). The inclusion of c-myc and 6xHis tags facilitates easy purification and antibody detection of the recombinant protein, and TCS sites allow for facultative removal of the tags, e.g. for structure crystallography. Plasmid DNAs nos. 82 and 84 containing the human wild type and C95R Norrin variant in the pBudCE4.1 mammalian expression vector (#V53220; Invitrogen, Carlsbad, CA, USA), respectively (provided by Ulrich Luhmann; see also PhD thesis Luhmann, 2005), served as template for the PCR. Phusion™ High-Fidelity DNA polymerase (#F-530s; New England Biolabs GmbH, Frankfurt am Main, Germany) was used to reduce the possibility of misincorporated bases (Table 34).

A nested PCR strategy was applied for the N-terminal constructs. Amplicons were excised from the gel after the first PCR, and DNA from the gel extractions was used as template for the nested PCR to create the N-terminally tagged constructs. For downstream processing, only DNA from excised bands was used (Figure 40).

hNDP – Constructs	Stock conc.	Vol.	Final conc.
ddH_2O		16.5µl	
Phusion HF buffer	5x	5µl*	1x
$MgCl_2$	25mM	0µl*	1.5mM
dNTPs (each)	20mM	0.25µl	200µM
Primer fwd	10µM	1.25µl	500nM
Primer rev	10µM	1.25µl	500nM
Phusion™ Polymerase	2u/µl	0.25µl	0.02u/µl
DNA template	20ng/µl	0.5µl	0.4ng/µl
Total:		**25µl**	

Product	Primer	Size [bp]
C-terminal	277/278	424
1st N-terminal	279/280	425
2nd N-terminal	281/280	478

Cycling conditions		
98°C	30s	
98°C	15s	35x
64°C	30s	35x
72°C	30s	35x
72°C	10min	
10°C	∞	

Table 34 PCR reaction mix for C- and N-terminally tagged constructs. *Phusion HF buffer contains 1.5mM $MgCl_2$

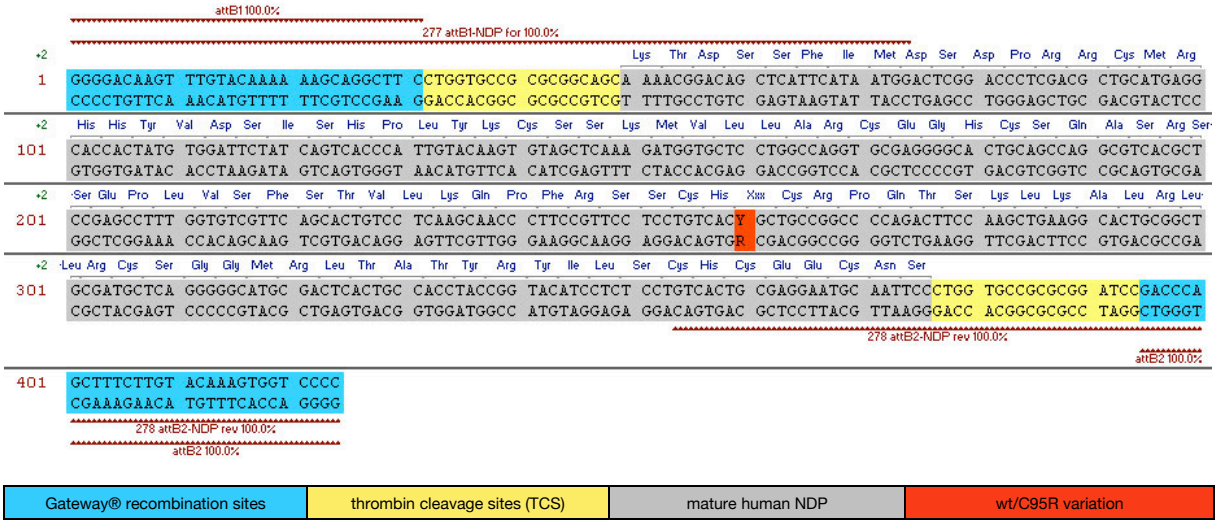

Figure 38 Sequence of the attB-flanked **PCR product of the C-terminal tagged constructs**. The c-myc and 6xHis tags were already present in the expression vector and had not to be added through PCR primers. Note that the endogenous Stop codon was removed from the *NDP* sequence. Primers 277 and 278 have been used to introduce the TCS sites and the attB sequences required for the Gateway® recombination reaction.

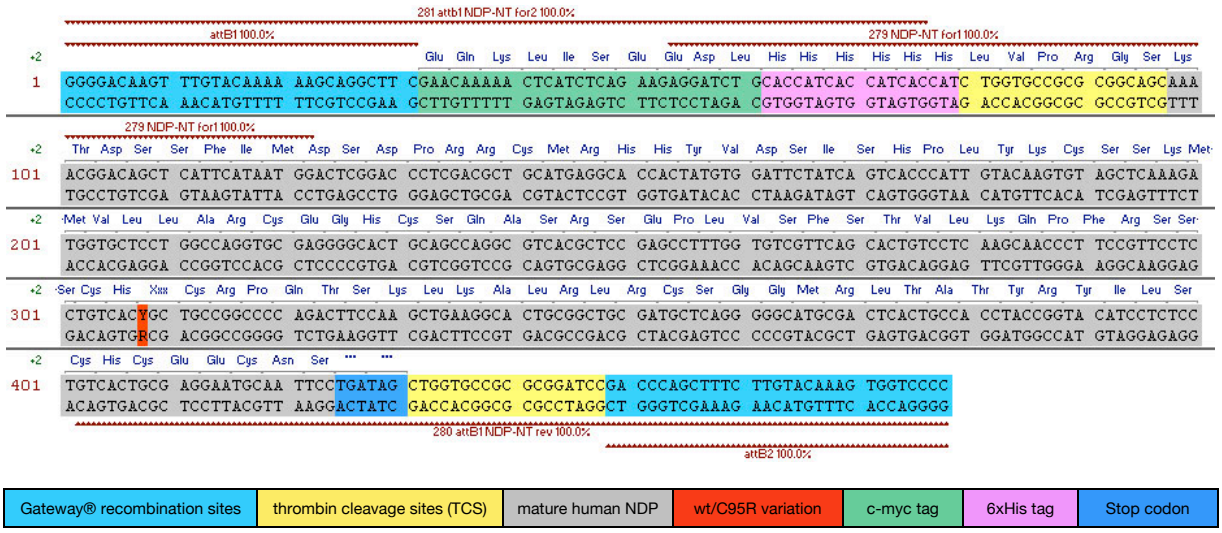

Figure 39 Sequence of the attB-flanked **PCR product of the N-terminal tagged constructs**. Primers 279 and 280 have been used in a first PCR, and primers 281 and 280 in the following nested PCR to introduce TCS sites, attB sequences required for the Gateway® recombination reaction, and the N-terminal c-myc and 6xHis tags. To ensure that no read-through occurs at the end of the coding sequence, a second Stop codon was added.

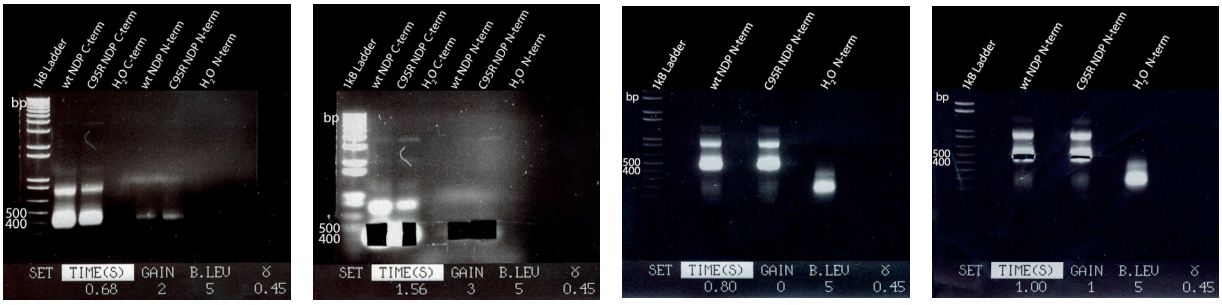

A **B** **C** **D**

Figure 40 Generation of the attB-flanked PCR products. **(A)** 1st PCR for C- and N-terminally tagged constructs. **(B)** Same gel as in (A) showing the position of the excised bands. **(C)** 2nd, nested PCR with DNA from the right two extractions (N-terminal constructs) of the gel shown in (B). **(D)** Same gel as in (C) showing the position of the excised bands.

2.6.1.2 Generation of entry vectors through enzymatic recombination of the attB-PCR product and the donor vector

DNA isolated from the electrophoresis gel was cloned into the Zero Blunt® TOPO® vector and constructs were verified by sequencing (clones no. 219-222). In a first attempt, this vector DNA was used as template for the Gateway® recombination reaction. However, as this vector features the same resistance genes as the donor and expression vectors (Kanamycin and Zeocin™), the recombined clones could not be obtained, and only the template Zero Blunt® vector was successfully selected. In a second attempt, Rolf Jaussi did a PCR on the Zero Blunt® template with *M13* primers (56/57) and lowered the background of the template vector through digestion with *Dpn*I (Fermentas/LabForce, Nunningen, Switzerland), which only cuts methylated, vector DNA. The BP recombination reaction was performed with the donor vector pDONR221 according to the manufacturer's instructions, and the Clonase™ enzyme mix

was digested with Proteinase K. DH10β cells (in 100µl SOC medium containing 10% glycerin) were transformed through electroporation (Gene Pulser™; BioRad, Reinach, Switzerland) at 1.7kV/200µF/200Ω in a 1mm cuvette (resulting in a time constant between 4.2 – 4.8 ms). Selection of positive entry vector clones (Figure 41) was performed on LB plates with Kanamycin (50µg/ml). After verification through sequencing with *M13* primers, one clone each was selected for the generation of the expression vector.

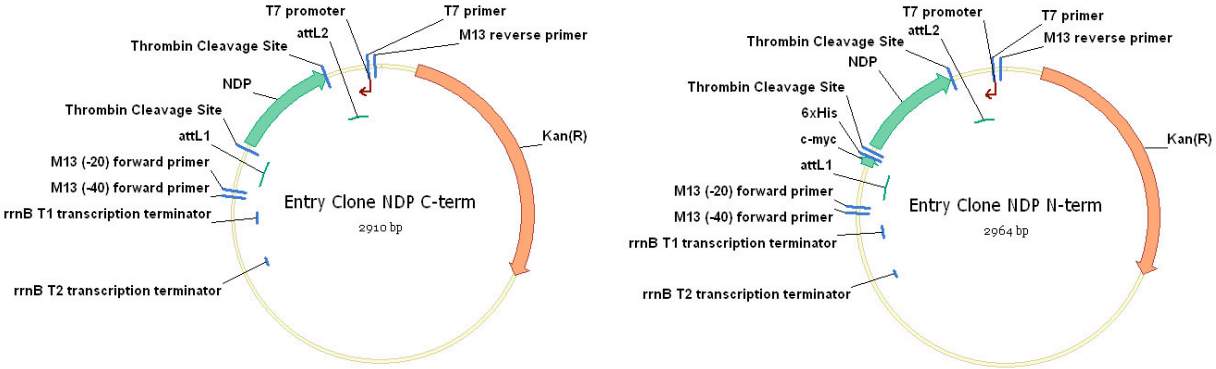

Figure 41 Entry vectors for the C-terminal (*left*) and N-terminal (*right*) tagged *NDP* constructs generated through enzymatic recombination of the attB-PCR product and the donor vector (pDONR221).

2.6.1.3 Generation of the expression vector through enzymatic recombination of the donor vector and the expression vector

The LR recombination reaction was performed with the expression vector pDEST-PICZalpha according to the manufacturer's instructions, and the Clonase™ enzyme mix was digested with Proteinase K. DH10β cells were transformed through electroporation, and selection of positive expression vector clones (Figure 42) was performed on low-salt LB plates (5g/l NaCl) with Zeocin™ (100µg/ml; #R250-01; Invitrogen, Carlsbad, CA, USA). Four clones were picked for each construct and verified through sequencing with *AOX1* primers (282/283). One clone each was selected for subsequent transformation of *Pichia* cells (clones no. 223-226; Figure 43; Figure 44).

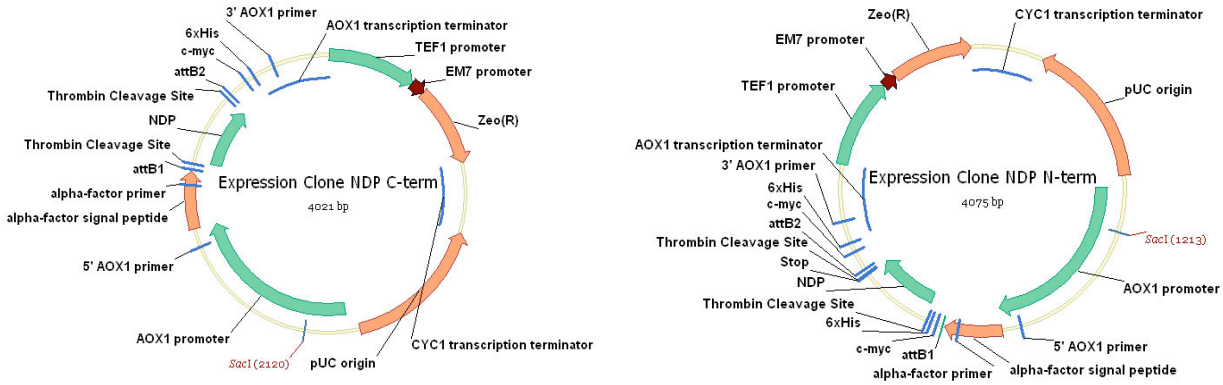

Figure 42 *P. pastoris* expression vectors for the C-terminal (*left*) and N-terminal (*right*) tagged *NDP* constructs generated through enzymatic recombination of the donor and the expression vector. A double Stop-codon was introduced between the *NDP* C-terminus and the vector-derived tags in the N-terminal constructs (*right*). *TCS*: Thrombin cleavage site

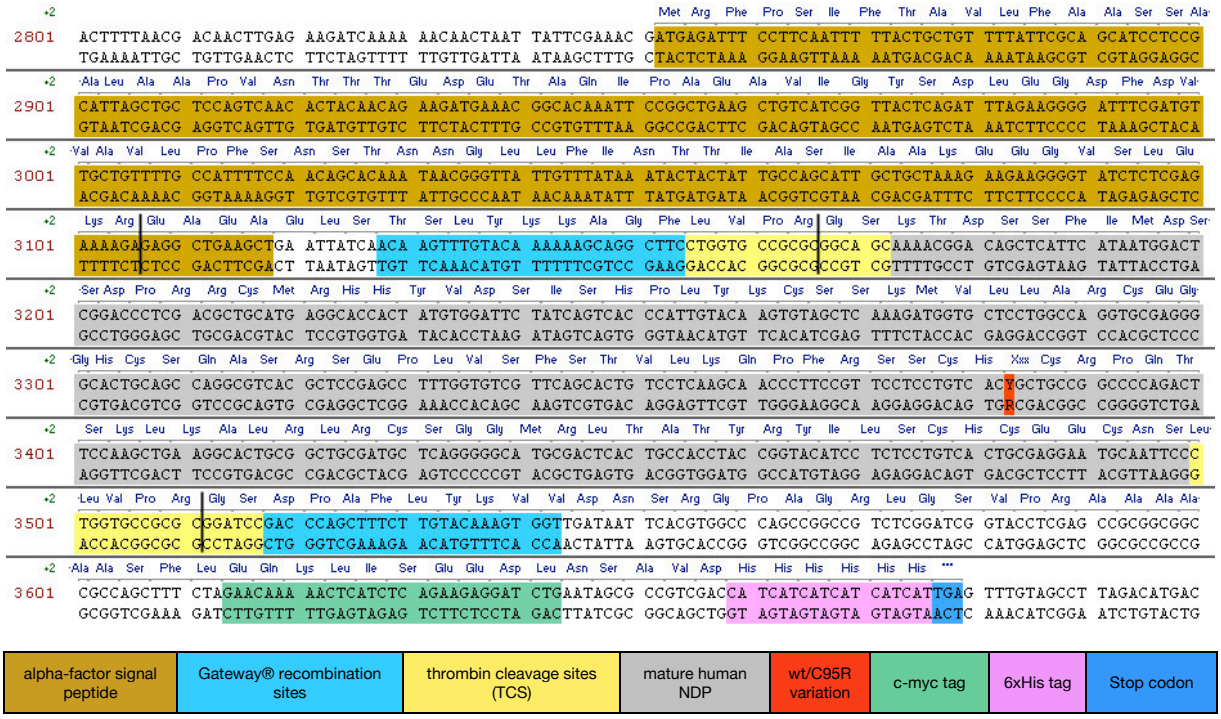

Figure 43 Sequence of the translated part of the **C-terminal tagged expression vector**. Different domains are color-coded. Enzymatic cleavage sites of KEX2 (inside the alpha factor signal peptide sequence) and thrombin (inside the TCS sites) are indicated by black bars. **Clone no. 223** contains the wt *NDP* variant, **clone no. 224** contains the C95R mutation.

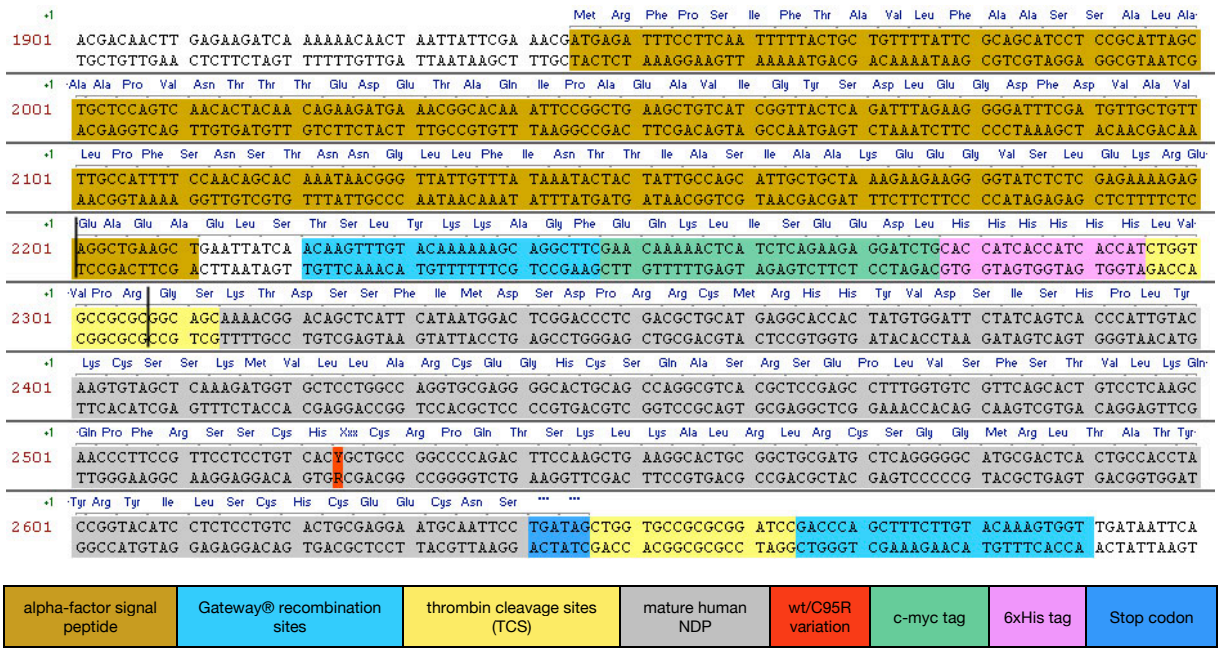

Figure 44 Sequence of the translated part of the **N-terminal tagged expression vector**. Different domains are color-coded. Enzymatic cleavage sites of KEX2 (inside the alpha factor signal peptide sequence) and thrombin (inside the TCS site) are indicated by black bars. **Clone no. 225** contains the wt *NDP* variant, **clone no. 226** contains the C95R mutation.

2.6.2 Recombinant protein expression in *Pichia pastoris*

Transformation of yeast cells and expression of recombinant protein was performed according to the manufacturer's instructions (Invitrogen #V195-20 and #K1750-01).

2.6.2.1 Transformation of Pichia cells

To obtain sufficient amounts of DNA for transformation of *Pichia pastoris* X-33 cells, colonies of the selected clones were cultured in 250ml low-salt LB medium and pDNA was isolated. Prior to transformation, the vector was linearized by 50-fold overdigestion with *Sac*I (Fermentas/LabForce, Nunningen, Switzerland) o/n at 37°C (Table 35). Complete digestion was verified by loading of 1µl onto a 0.9% agarose gel and the enzyme was heat-inactivated at 65°C for 20min.

Vector linearization	Stock conc.	Vol.
pDNA	0.17µg/µl	60µl
Buffer Ecl136II	10x	7.78µl
SacI	10u/µl	10µl
Total:		77.78µl

Table 35 Reaction mix for vector linearization.

Linearized vector DNA was then isolated by phenol-chloroform extraction (Carl Roth, Karlsruhe, Germany) and subsequent EtOH precipitation (containing 1/10 volume 3M sodium acetate). *Pichia pastoris* cells were transformed by Suzanne Kronenberg (Paul-Scherrer-Institute) by electroporation and 4 positive clones per construct were selected on YPDS plates containing 100, 200, 500, and 800µg/ml Zeocin™, and glycerol stocks were prepared for storage at -80°C according to the manufacturer's protocol (glycerol stock no. 5-20).

2.6.2.2 Induction of recombinant protein expression

Clones were incubated o/n in 5ml BMGY medium in 12ml culture tubes at 30°C / 180rpm. Cell number was estimated by photospectrometric measurement of the OD_{600}, and cultures were all diluted to an OD_{600} of 0.8 to ensure equal number of cells. Then, 4ml of the cultures were used to inoculate 46ml of BMGY medium in 300ml shaker flasks with baffles (Vitaris, Baar, Switzerland). Cultures were incubated for 24h at 30°C / 180rpm (growth phase). Then, cell numbers were normalized again through OD_{600} measurement, equal amounts of cells were pelleted and the medium was exchanged to BMMY (Expression phase). Induction of protein expression was maintained every 12h with 0.5% (250µl) 100% methanol over a total period of 4 days. Medium samples (500µl) were taken at each methanol-induction time point.

2.6.2.3 Concentration of recombinant protein

Culture supernatant was concentrated with Amicon® Ultra-4 10K filter columns (Millipore, Billerica, MA, USA) according to the manufacturer's instructions. These columns have a molecular weight cut-off of 10kDa, and concentrate 4ml input volume to 200µl elution volume (factor 20).

2.7 Cell culture of mammalian cells

A total of 8 HEK293T cell cultures were seeded in standard medium (DMEM; Sigma/Aldrich, Steinheim, Germany) and grown for 2 days in medium sized bottles (75cm^2, 12ml volume; TPP, Trasadingen, Switzerland) by Jurian Zürcher. Sodium chloride (control) or lithium chloride (induction of canonical Wnt-signaling) were added to the medium of four colonies each to a final concentration of 25mM. Cells were incubated o/n and harvested the next day by trypsination: After removal of the medium, cells were washed with 4ml phosphate buffered saline (PBS) to remove cell debris and Mg^{2+}. The cell monolayer was then enzymatically digested with trypsin (0.25%) for 2min at 37°C. The digest was stopped with the addition of 12ml DMEM. Cells were transferred to a centrifuge tube and pelleted at 300g for 5min.

After centrifugation, the cell pellets were split in order to isolate RNA for quantitative RT-PCR from one portion and protein for Western blot experiments from the other.

3. Results

3.1 Vascular changes in the cerebellum of Norrin ⁄ Ndph knockout mice correlate with high expression of Norrin and Frizzled-4

Ulrich F. O. Luhmann,[1,*,†] John Neidhardt,[1,†] Barbara Kloeckener-Gruissem,[1,2] Nikolaus F. Schäfer,[1] Esther Glaus,[1] Silke Feil[1] and Wolfgang Berger[1]

[1]Division of Medical Molecular Genetics & Gene Diagnostics, Institute of Medical Genetics, University of Zurich, Schorenstrasse 16, CH-8603 Schwerzenbach, Switzerland; [2]Department of Biology, ETH Zurich, Zurich, Switzerland; *Present address: Division of Molecular Therapy, UCL Institute of Ophthalmology, 11-43 Bath-Street, London EC1V 9EL, UK; †These authors contributed equally to this work.

Manuscript published in: *European Journal of Neuroscience, 2008* ***27****; pp. 2619–2628*

3.1.1 Abstract

X-linked Norrie disease, familial exudative vitreoretinopathy (FEVR), Coats' disease and retinopathy of prematurity are severe human eye diseases and can all be caused by mutations in the Norrie disease pseudoglioma gene. They all show vascular defects and characteristic features of retinal hypoxia. Only Norrie disease displays additional neurological symptoms, which are sensorineural hearing loss and mental retardation. In the present study, we analysed transcript levels of the ligand Norrin (*Ndph*) and its two receptors Frizzled-4 (*Fzd4*) and LDL-related protein receptor 5 (*Lrp5*) in six different brain regions (cerebellum, cortex, hippocampus, olfactory bulb, pituitary and brain stem) of 6- to 8-month-old wild-type and *Ndph* knockout mice by quantitative real-time PCR. No effect of the *Ndph* knockout allele on *Fzd4* or *Lrp5* receptor expression was found. Furthermore, no alterations of the transcript levels of three hypoxia-regulated angiogenic factors (*Vegfa*, *Itgrb3* and *Tie1*) were observed in the absence of Norrin. Interestingly, we identified significant differences in *Ndph*, *Fzd4* and *Lrp5* transcript levels in brain regions of wild-type mice and observed highest expression of Norrin and Frizzled-4 in cerebellum. Transcript analyses were correlated with morphological data obtained from cerebellum and immunohistochemical studies of blood vessels in different brain regions. Vessel density was reduced in the cerebellum of Ndph knockout mice but the number of Purkinje and granular cells was not altered. This provides the first description of a brain phenotype in Ndph knockout mice, which will help to elucidate the role of Norrin in the brain.

Keywords: brain, hypoxia, Lrp5, mental retardation, Norrie disease

3.1.2 Introduction

Mutations in the Norrie disease pseudoglioma gene (*NDP*) cause a variety of human eye diseases including Norrie disease, X-linked familial exudative vitreoretinopathy (FEVR), Coats' disease and severe retinopathy of prematurity (ROP) (Berger et al 92a;Berger et al 92b;Chen et al 92;Shastry et al 97b;Shastry et al 97a;Black et al 99). Among these, only Norrie disease can be accompanied by progressive hearing loss and mental retardation (for review see (Berger 98), but all four diseases exhibit similar vascular defects in the eye. Thus it was suggested that Norrin, the protein encoded by the *NDP* gene, has a role in ocular vascular development. This was supported by data from the respective mouse

model (Berger et al 96), which showed malformation of the retinal and hyaloid vasculature and abnormal vessels in the inner ear (Richter et al 98;Ohlmann et al 04;Rehm et al 02). Further examination of retinal vascular development revealed that Norrin plays a role in sprouting angiogenesis. Its absence causes the lack of deep retinal capillary networks and subsequent retinal hypoxia which is accompanied by a three- to fivefold increase of expression of the angiogenic factors *Vegfa, Itgb3 and Tie1*. Retinal hypoxia seems to be one major pathogenic mechanism in the eye and might explain the clinical similarities in patients with all four diseases (Luhmann et al 05).

Identification of FEVR causing mutations in the Wnt receptor Frizzled-4 (*FZD4*) and its co-receptor LDL related protein 5 (*LRP5*) (Robitaille et al 02;Toomes et al 04), together with high phenotypic similarities of *Ndph* and *Fzd4* knockout mice in eye and ear (Berger et al 96;Richter et al 98;Rehm et al 02;Wang et al 01;Xu et al 04) led to the finding that Norrin is a high affinity ligand of Fzd-4 and Lrp5 and activates the canonical Wnt-/beta-catenin signalling pathway (Xu et al 04). Furthermore, these studies suggested that defects in this signalling pathway are also responsible for the progressive hearing loss observed in both, mice and Norrie disease patients from early adulthood onwards (Berger et al 96;Wang et al 01;Halpin et al 05;Rehm et al 02;Richter et al 98). Findings in the brain of homozygous *Fzd4* knockout mice indicated the requirement of the Wnt-receptor *Fzd4* for normal neuronal development. Abnormal gait and progressive cerebellar ataxia with a dramatic loss of cerebellar granular cells and a progressive Purkinje cell loss have been found in this mouse line (Wang et al 01). At 6 month of age, these mice also showed sparse, enlarged and irregular blood vessels in the cerebellum (Xu et al 04), suggesting an additional role of *Fzd4* signalling for the brain vasculature. Here, we aim to complement the understanding of Norrin's role as a ligand of the Fzd4/Lrp5 receptor pair in the adult brain, and to identify potential pathogenic mechanisms for the mental retardation phenotype observed in Norrie disease patients. We therefore investigated the correlations between *Norrin* and its receptors by quantitative RT-PCR in different brain regions and explored whether degenerative and vascular defects as described for *Fzd4* knockout mice and subsequent hypoxia occur in the adult brain of *Ndph* knockout mice. We found that Norrin and its receptors were widely distributed in the brain and observed differences in their expression levels between brain regions. Highest levels for Norrin and Frizzled-4 were detected in the cerebellum where we also found a slight reduction in vessel density in *Ndph* knockout mice. We discuss a possible role of Norrin in maintenance of cerebellar blood vessels during adulthood.

3.1.3 Material and methods

3.1.3.1 Animals

The *Ndph* knockout mouse line and genotyping has been described previously (Berger et al 96). Male animals were obtained by breeding of heterozygous female mice with C57Bl/6 male mice. Whenever possible, siblings from the same litter were used for experimental procedures. The research was performed in accordance with the ARVO Statement for the Use of Animals in Ophthalmic and Vision Research.

3.1.3.2 Tissue preparation, fixation, histology and immunohistochemistry

Total brain or brain regions (olfactory bulb, cortex, cerebellum, brain stem, hippocampus, and pituitary) were dissected from male *Ndph* knockout mice and wild type littermates at the age of 6-8 months. For RNA isolation, tissue preparations were performed on ice and immediately frozen in liquid nitrogen. For immunohistochemistry the brain was embedded into O.C.T. compound (Tissue-Tek/ Sakura Finetek, Zoeterwoude, Netherlands) and frozen on dry ice. The brains were sagittally sectioned (8μm), transferred to SuperFrost slides (Roth, Reinach, Germany) and dried over night at room temperature for fixation. The brain sections were stained with a primary antibody against Collagen type IV (polyclonal Col IV antibody, rabbit anti-mouse (1:250), no.2150-1470, AbD Serotec/MorphoSys, Oxford, UK) and a secondary Cy-3-labeled anti rabbit antibody (1:200, no 111-165-003; Dianova, Hamburg, Germany).

For histological examination the tissue was transferred to Serra's fixative (60% ethanol, 11.1% (30% of 37%) formaldehyde, 10% acetic acid) and fixed over night at 4°C. Subsequently, the tissue was dehydrated in 70% and 100% isopropanol, embedded in paraffin, sectioned (7μm), and transferred onto SuperFrost Plus slides (Roth, Reinach, Germany). Histological staining was performed by hematoxylin-eosin staining procedure (Mayer's hemalum solution, Merck, Darmstadt, Germany). The slides were mounted with Rotihistokitt (Roth, Reinach, Germany) and observed under bright light illumination using a Zeiss Axioplan 2 microscope. Image collection was performed by using an AxioCam HRc digital camera (Carl Zeiss AG, Jena, Germany).

3.1.3.3 Quantitative examination of hematoxylin-eosin - or ColIV-stained sections

To quantify the cell number in the cerebellum, hematoxylin-eosin stained sagittal brain sections of five wild type (wt: $n = 5$) and five *Ndph* knockout mice (*Ndph*-ko: $n = 5$) were used. Within an individual cerebellum two groups of three images each were taken from two different sectioning planes differing by at least 140μm. The three images within a group were taken from the same sagittal section at defined positions. For quantitative analysis of cell numbers, all Purkinje cells per image were counted and granular cells were determined in two areas of 250μm^2. A mean value per image was calculated. Based on the mean values for both cell types in each animal, the mean cell number of Purkinje cells and the mean cell density for granular cells in the cerebellum were calculated.

Col IV stains the extracellular matrix of endothelial cells and was used to label blood vessels in the brain. Col IV stained cryosections (wt: $n = 6$; *Ndph*-ko: $n = 6$) were used to determine the vessel density in three different brain regions (cerebellum, cortex and hippocampus). The number of vessels was counted and normalized to the total area used for counting. Vessel density is given in number of blood vessels per 500μm^2 for each brain region.

3.1.3.4 RNA isolation, DNaseI treatment and quantitative RT-PCR (Real–Time –PCR)

Total RNA was isolated from dissected brain regions from animals of both genotypes (wt: $n = 6$; *Ndph*-ko: $n = 6$) using RNA extraction kits (RNeasy Mini kit: olfactory bulb, pituitary; RNeasy Midi kit: cerebellum, cortex, hippocampus, brain stem; Qiagen, Hilden, Germany). The RNA was treated with RQ1 RNAse-Free DNase I (Promega, Mannheim,

Germany) before concentration and integrity were checked on an Agilent Bioanalyzer 2100 (Agilent technologies, Basel, Switzerland). DNaseI-treated RNA (0,5 - 1 μg) was reverse transcribed using SuperScript III RNase H^- Reverse Transcriptase (Invitrogen, Basel, Switzerland) and random Hexamer Primers $pd(N)_6$ (Amersham Bioscience, Freiburg, Germany). Quantitative real-time-PCR in 384-well plate format was performed using a robotic aid for pipetting and the ABI PRISM 7900 Sequence Detection System with the published MGB-TaqMan probes for *Ndph*, *Fzd4*, *Lrp5*, *Itgb3*, *Tie1* and *Vegfa* (Luhmann et al 05). Five replicates for target genes and three replicates for the internal standard *18S* rRNA (TaqMan Ribosomal RNA Control Reagent, ABI, Rotkreuz, Switzerland) were included for each sample. The ΔC_t-method for relative quantification was used and data was normalized to the Norrin expression level in one individual wild type cortex. Data analysis was performed using the ABI Prism 7900HT SDS2.2 Software and a spreadsheet program. Based on the mean relative expression values for the technical replicates in each brain region, mean values for wild type and knockout groups were calculated and are shown with standard deviation (SD) error bars in the graphs. Since the technical reproducibility of the qRT results was very high, SD error bars reflect the inter-individual variability.

3.1.3.5 Statistical analysis

For statistical analysis the software package SPSS 14.0 for Windows (SPSS inc., Chicago, USA) was used. Real-time expression data were statistically analyzed by using ANOVA for repeated measurements treating brain regions as repeated measurements (dependent within subject factor) and defining the two groups of wt and *Ndph*-ko animals as independent between subject factors. For this test we used the ΔΔCt values for statistical analysis, as they are assumed to be normally distributed (Love et al 06). Subsequently, pair wise comparisons were used to identify groups with significant differences. For within subject data (brain regions), the parametric paired *t*-test or the non parametric Wilcoxon signed rank test was used, while for independent groups (wt versus *Ndph* knockout) either the parametric Student's *t*-test or the non parametric Mann Whitney U-test was applied.

As the ANOVA for repeated measurement analyses did not show significant differences between wild type and knockout animals for *Fzd4*, *Lrp5, Itgrb3, Tie1 and Vegfa* expression in all brain regions (see results), the statistical analysis for the pair wise comparison of expression levels between different brain regions were based on pooled data sets from 6 wild type and 6 knockout animals (total $n = 12$).

3.1.4 Results

3.1.4.1 Expression studies for Ndph, Lrp5 and Fzd4 revealed differences in various brain regions

We evaluated the relative expression levels of *Ndph*, *Frizzled-4* (*Fzd4)* and *LDL related protein 5* (*Lrp5)* in different brain regions by quantitative RT-PCR (Figure 45 and Table 36). When comparing the expression of all three genes in wild type and *Ndph* knockout animals, no significant differences were found, except the expected absence of the *Ndph* transcript in knockout animals [repeated-measurements ANOVA: WT, $n = 6$; *Ndph*-KO, *n*

= 6 (*Ndph*, $P < 0.01$; *Fzd4*, $P = 0.950$; *Lrp5*, $P = 0.397$)]. However, when comparing the expression levels in brain regions, significant differences were indicated for all three transcripts [*Ndph* ($n = 6$), *Fzd4* and *Lrp5* ($n = 12$): $P < 0.01$; Figure 45, Table 36]. To identify the differences in transcript levels in individual brain regions, both the parametric paired *t*-test analysis of the $\Delta\Delta C_t$ values and the non parametric Wilcoxon signed rank test analysis of the relative expression values (RQ) were used for pair wise comparison. For both tests significance was set to $P < 0.05$.

For *Ndph*, we observed the highest relative expression in the cerebellum (Figure 45). It was significantly higher than in olfactory bulb and brain stem. The latter two were not significantly different from each other, but were higher than those in cortex and hippocampus. In pituitary, only traces of *Ndph* expression have been detected (Figure 45, Table 36).

For *Fzd4* the highest level of expression was also found in cerebellum, which was significantly higher compared to all other brain regions ($n = 12$, paired *t*-test analysis of the $\Delta\Delta C_t$ values: $P < 0.05$; Figure 45). In contrast to *Ndph, Fzd4* showed its lowest relative expression level in olfactory bulb ($n = 12$, paired *t*-test and Wilcoxon signed rank test: $P < 0.05$). Other brain regions (cortex, hippocampus, pituitary and brain stem) showed intermediate transcript levels, which were statistically not distinguishable from each other (Figure 45, Table 36).

Interestingly, pituitary was the only brain region where both receptors (*Fzd4* and *Lrp5*) were expressed, whereas their ligand (*Ndph*) was virtually absent. This might suggest a Norrin-independent role of *Fzd4* in the pituitary.

For *Lrp5,* the lowest amount of transcript was found in cortex and the highest in pituitary (Table 36). Among the other regions, the expression level in cerebellum was significantly higher than that in hippocampus ($n = 12$; paired *t*-test and Wilcoxon signed rank tests $P < 0.05$). *Lrp5* in comparison to *Fzd4* showed an about 8-9 fold lower expression in cerebellum, cortex and hippocampus, while in olfactory bulb, pituitary and brain stem the reduction was only 4-5 fold (Table 36). This indicates that different brain regions express different Fzd4/Lrp5 receptor transcript ratios**.** Our data also suggested variable receptor/ligand ratios in different brain regions and revealed overlapping expression of *Ndph* with its two receptors *Lrp5* and *Fzd4* in all but one brain region.

3.1.4.2 Evaluation of hypoxia regulated angiogenic factors in brain regions of Ndph knockout mice

To assess potential hypoxic changes in the brain of *Ndph* knockout mice at the molecular level, we quantified the transcript levels of the three angiogenic factors integrin beta 3 (*Itgb3)*, tyrosine kinase receptor 1 (*Tie1*) and vascular endothelial growth-factor A (*Vegfa*) in the six brain regions by quantitative RT-PCR (Figure 46; Table 37). We chose these three factors as they are known to be transcriptionally up-regulated by hypoxia in Norrie disease mouse retinae (Luhmann et al 05). Comparison of wild type ($n = 6$) and *Ndph* knockout mice ($n = 6$) revealed no significant differences for the three angiogenic genes (ANOVA for repeated measurement analysis; *Itgb3*, $P = 0.764$; *Tie1*, $P = 0.620$; *Vegfa*, $P = 0.868$). Thus, we found no indication for hypoxia in *Ndph* knockout brains.

Gene	Brain region	Relative Expression ± S.D.	
		Wt	*Ndph* ko
Ndph	Cerebellum	3.06 ± 0.81	0.00 ± 0.00
	Cortex	1.22 ± 0.39	0.00 ± 0.00
	Hippocampus	0.97 ± 0.47	0.00 ± 0.00
	Olfactory bulb	2.19 ± 0.41	0.00 ± 0.00
	Pituitary	0.03 ± 0.02	0.01 ± 0.01
	Brain stem	1.85 ± 1.23	0.00 ± 0.00
Fzd4	Cerebellum	5.07 ± 1.32	4.53 ± 1.10
	Cortex	2.83 ± 0.75	3.00 ± 1.18
	Hippocampus	4.42 ± 2.47	3.33 ± 0.88
	Olfactory bulb	1.77 ± 0.38	2.13 ± 0.49
	Pituitary	3.45 ± 1.47	3.27 ± 0.72
	Brain stem	3.67 ± 2.14	3.61 ± 1.51
Lrp5	Cerebellum	0.59 ± 0.33	0.47 ± 0.30
	Cortex	0.33 ± 0.21	0.27 ± 0.14
	Hippocampus	0.48 ± 0.29	0.30 ± 0.11
	Olfactory bulb	0.45 ± 0.10	0.42 ± 0.16
	Pituitary	0.83 ± 0.27	0.64 ± 0.36
	Brain stem	0.64 ± 0.51	0.49 ± 0.20

Table 36 Relative Expression of *Ndph* and its two receptors *Fzd4* and *Lrp5* in different brain regions of wt and *Ndph* ko mice. Data ± SD were normalized to Norrin expression in the cortex of an individual animal.

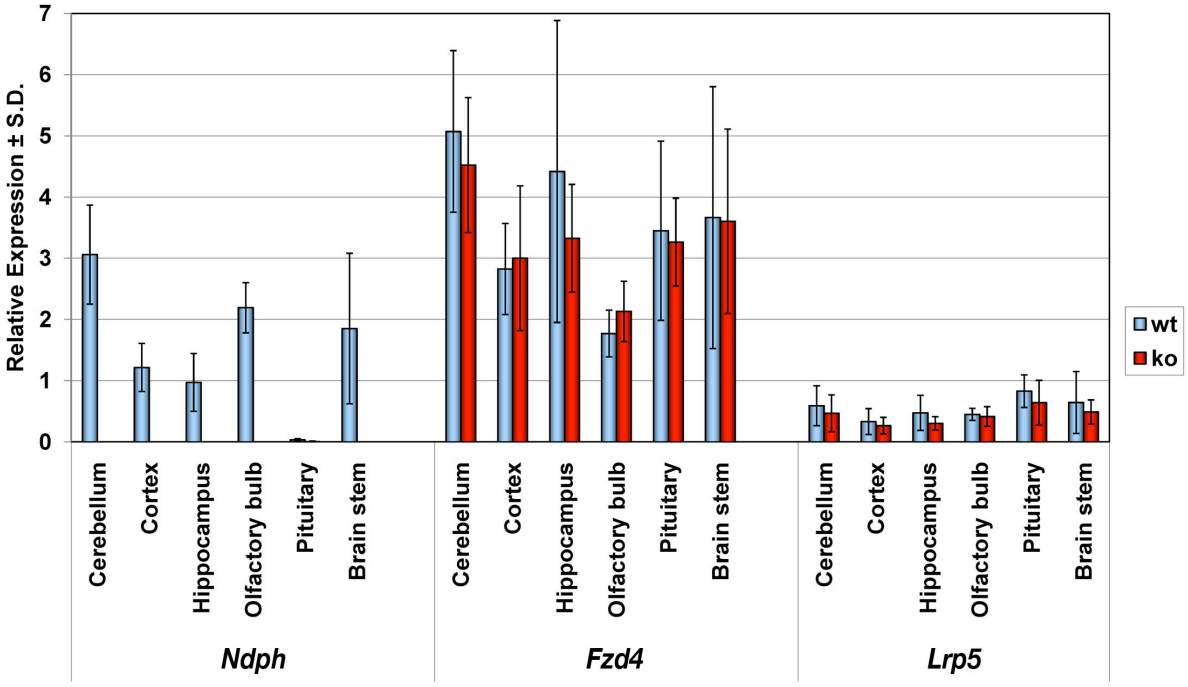

Figure 45 Differential expression of *Ndph*, *Lrp5* and *Fzd4* in six brain regions of mice. The relative expression (± SD) of these genes was determined by quantitative real-time PCR in *Ndph* wild-type and knockout mice (WT, $n = 6$; KO, $n = 6$). All relative expression values were normalized to an individual *Ndph* expression level in WT cortex.

Gene	Brain region	Relative Expression ± S.D.	
		Wt	*Ndph* ko
Itgb3	Cerebellum	0.22 ± 0.10	0.19 ± 0.06
	Cortex	0.46 ± 0.17	0.45 ± 0.06
	Hippocampus	0.24 ± 0.10	0.20 ± 0.03
	Olfactory bulb	0.24 ± 0.08	0.24 ± 0.06
	Pituitary	0.28 ± 0.09	0.26 ± 0.06
	Brain stem	0.40 ± 0.17	0.38 ± 0.13
Tie1	Cerebellum	2.96 ± 0.88	2.41 ± 0.35
	Cortex	1.94 ± 0.45	2.41 ± 0.63
	Hippocampus	1.73 ± 0.72	1.83 ± 0.56
	Olfactory bulb	1.65 ± 0.54	1.88 ± 0.47
	Pituitary	3.79 ± 1.00	3.72 ± 0.73
	Brain stem	3.62 ± 1.72	3.95 ± 1.76
Vegfa	Cerebellum	13.49 ± 3.53	12.70 ± 4.02
	Cortex	6.98 ± 0.63	7.88 ± 1.23
	Hippocampus	6.32 ± 3.01	5.92 ± 1.09
	Olfactory bulb	9.70 ± 2.21	8.97 ± 2.16
	Pituitary	3.46 ± 0.92	3.29 ± 1.51
	Brain stem	9.74 ± 5.15	9.62 ± 3.51

Table 37 Relative Expression three angiogenic factors in six brain regions of wt and *Ndph* ko mice. Data ± SD were normalized to Norrin expression in the cortex of an individual animal.

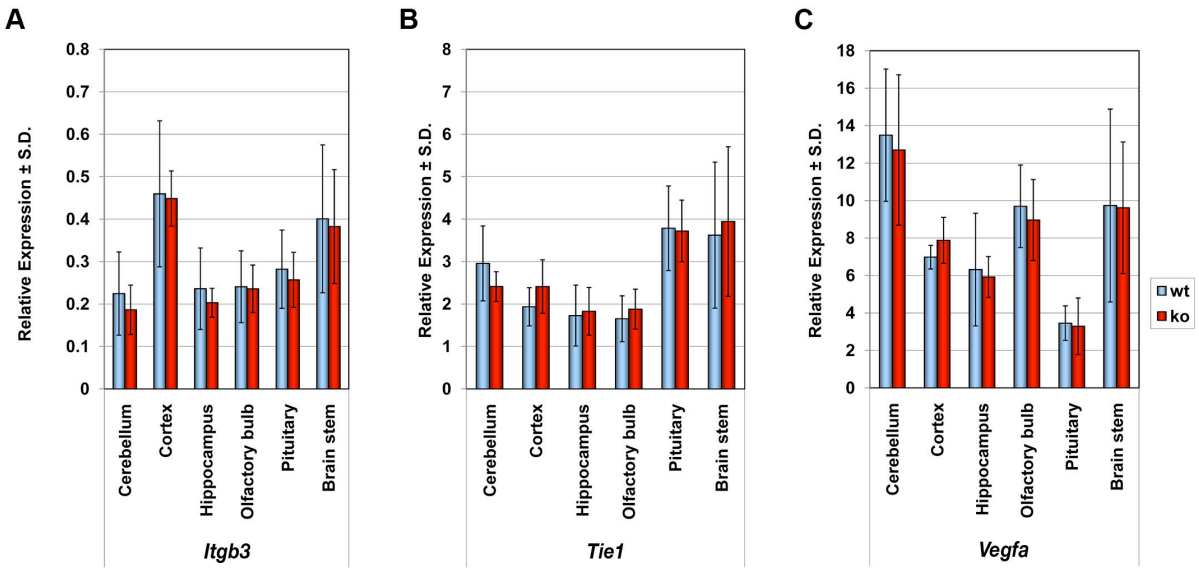

Figure 46 Expression of three hypoxia-regulated angiogenic factors. Quantitative analysis of transcript levels of integrin beta 3 (*Itgrb3*) **(A)**, tyrosine kinase receptor 1 (*Tie1*) **(B)** and vascular endothelial growth-factor A (*Vegfa*) **(C)** in six brain regions. The mean relative expression is presented ± SD (WT, *n* = 6; KO, *n* = 6). Note the differences in the scale of the axes for the three transcripts.

Nevertheless, when we analyzed transcript levels in different brain regions by using pair wise comparison on pooled data sets of wildtype and knockout data (n = 12), a significant difference was found (ANOVA for repeated measurement; $P < 0.01$).

Itgb3 was highest expressed in cortex and brain stem, while pituitary, olfactory bulb, hippocampus and cerebellum showed significantly lower levels (Figure 46A, Table 37; $P < 0.05$ for paired *t*-Test and Wilcoxon signed rank test). In contrast, *Tie1* mRNA showed highest amounts in pituitary and brain stem (Figure 46B).

The highest *Vegfa* expression level was found in the cerebellum, with successively decreasing levels in olfactory bulb, cortex, hippocampus, and pituitary (differences were significant in both, the Wilcoxon signed rank test and the paired *t*-test $P < 0.05$ (Figure 46C). While *Vegfa* expression in brain stem and olfactory bulb was at comparable levels, variability was less in the latter region. We note, that *Vegfa* and Norrin display a similar ratio of expression levels (approximately 5:1) in the various brain regions with the exception of pituitary. In this brain region Norrin expression was virtually absent, while *Vegfa* was found at considerable levels (Figure 45 and Figure 46C).

Taken together, our quantitative transcript analyses of angiogenic factors did not indicate hypoxia-induced transcriptional upregulation in *Ndph* knockout mice.

3.1.4.3 Analysis of cerebellar morphology in Ndph knockout mice

Because we observed highest *Ndph* and *Fzd4* expression in cerebellum we then examined the morphology of this brain region in 6–8-month-old wild type and *Ndph* knockout mice using hematoxylin-eosin stained sagittal sections (Figure 47). Since no gross morphological changes were observed in *Ndph* knockout mice (Figure 47A,B), we determined the number of cerebellar Purkinje and granular cells from five individual animals per genotype as an indicator for degenerative processes. Representative high-magnification images from wild type and knockout sections are shown in Figure 47C and D. No alterations were detected in the amount of Purkinje and granular cells (Mann Whitney U, $P = 0.138$, $P = 0.249$, respectively) (Figure 47E).

3.1.4.4 Characterization of the vasculature in cerebellum, hippocampus and cortex of wild type and Ndph knockout mice

To assess potential vascular changes in the brain of *Ndph* knockout mice, we applied immunohistochemistry. We stained for Collagen IV in sagittal sections of whole brains as a marker for the extracellular matrix of vascular endothelial cells (Figure 48A). No obvious differences in vessel size and morphology were noted in hippocampus, cortex and the cerebellum (Figure 48B). However, the distribution of blood vessels in the cerebellum of *Ndph* knockout mice occasionally seemed to be less dense compared to that in the wild type. Therefore, vessels in all three brain regions from wild type and *Ndph* knockout animals (n = 6) were counted and displayed as mean vessel density (Figure 49A). We found a significant reduction of 16.4% in the cerebellum, while an effect of the *Ndph* knockout on the vessel density in hippocampus and cortex was not detected (Figure 49A, ANOVA for repeated measurement ($P < 0.05$) and 2-tailed independent sample *t*-test ($P < 0.05$)).

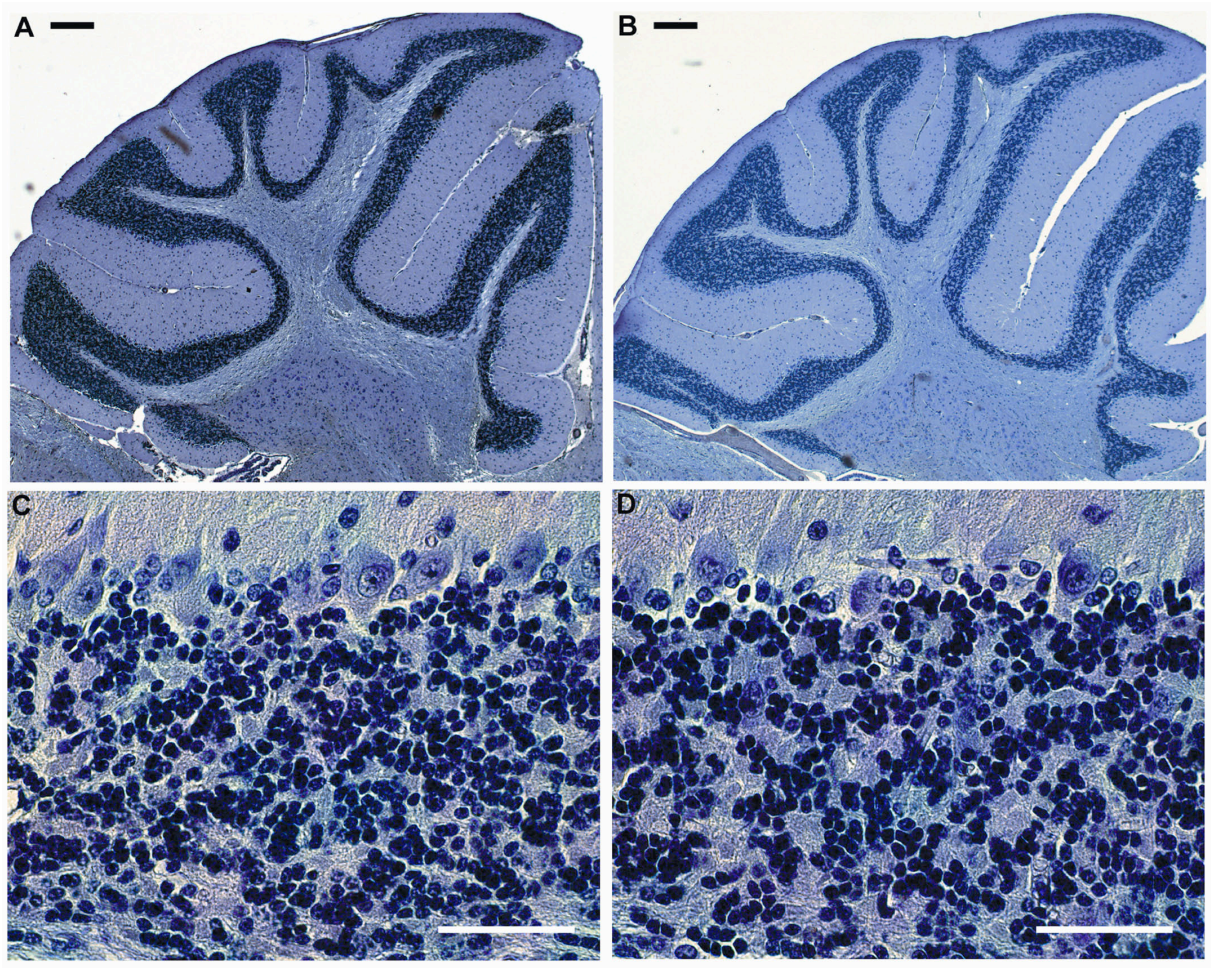

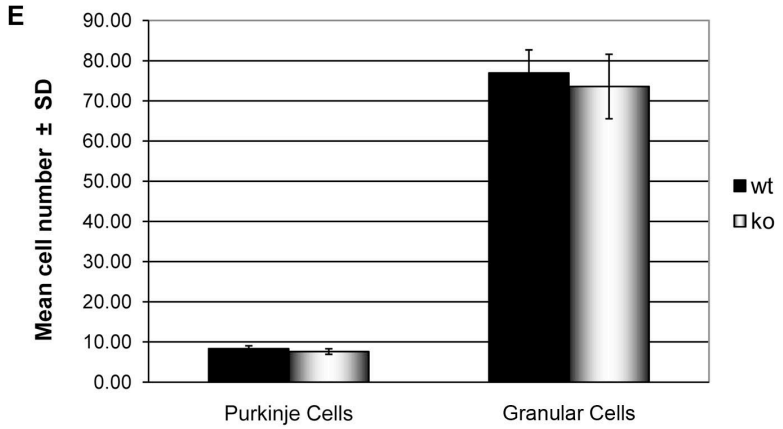

Figure 47 Gross morphology and cell number of Purkinje and granular cells are not altered in *Ndph*-KO mice. Haematoxylin–eosin stains of sagittally sectioned cerebellum from *Ndph* WT and knockout mice. **A** and **C**, wild-type; **B** and **D**, *Ndph*-KO; E, quantitative assessment of Purkinje and granular cell numbers in the cerebellum. Mean cell number (± SD) of Purkinje cells per section and granular cells per 250µm² (*n* = 5). Scale bars in A and B = 200µm, in C and D = 50µm.

In addition, we found for both genotypes that the vessel density of the cerebellum was significantly higher than in cortex and hippocampus (Figure 49A; ANOVA ($P < 0.01$); paired *t*-test and Wilcoxon signed rank test; $n = 6$; $P < 0.05$).

We attempted to localize the statistically significant reduction in the cerebellar vessel density to the layers of molecular, granular/Purkinje cell or white matter. We found that vessel density in the white matter layer (69.8% ± 16.3 % of Wt) was significantly reduced (2-tailed independent sample *t*-test ($P = 0.034$) (Figure 49B). In contrast, the trend of reduction in vessel densities of the molecular layer (86.0% ± 15.9 % of Wt) and the granular/Purkinje cell layer (86.8 % ± 22.8% of Wt) was not statistically significant (Figure 49B).

Taken together, our data suggested that the *Ndph* knockout had no general effect on the vascular system in the brain, but causes a mild reduction in vessel density in the white matter of the cerebellum.

3.1.5 Discussion

The data reported here expand our knowledge about the quantitative mRNA expression of Norrin and its two receptors Frizzled-4 and LDL related protein 5 in different brain regions of adult mice. Former studies located *Ndph* transcripts to retina and total brain. RNA *in situ* studies (Berger et al 96) showed, in good accordance with our quantitative data, signals in the olfactory bulb and in Purkinje cells of the cerebellum, where we found highest Norrin transcript levels. Our data now provide additional evidence that Norrin is more widely expressed in brain including now also cortex, hippocampus and brain stem, while in pituitary only traces of Norrin were detected. Similarly, significant expression differences between the brain regions were found for *Fzd4* and *Lrp5* and, like *Ndph*, the highest expression of *Fzd4* was detected in cerebellum. *Fzd4* and *Lrp5* were co-expressed in all brain regions in which *Ndph* was present. In combination with the observation that Norrin activates the Wnt-/beta-catenin signalling pathway via FZD4 and LRP5 in cell culture assays (Xu et al.04), our expression data are consistent with the potential modulatory role of Norrin for the Wnt signalling pathway via FZD4 and its co-receptor LRP5 in the brain.

The expression patterns further suggest Norrin-independent functions of FZD4 and LRP5 in the pituitary and raise the possibility of a regulation of Wnt-signalling by changes in the expression levels of the ligand Norrin across different brain regions. As indicated by our results, a regulation of this signalling may also occur by changes in the ratio of FZD4 to LRP5 levels in different brain regions, which we either found to be 8-9 in cerebellum, cortex and hippocampus or 4-5 in olfactory bulb, pituitary and brain stem.

Based on the similarity in expression patterns of Norrin and VEGFA across different brain regions, we hypothesize that concerted action of both factors may play a role in controlling brain angiogenesis. While the role of VEGFA and its signalling for this process is well established also in the cerebellum (Acker et al 01;Zachary and Gliki 01), the knowledge about Norrins role in angiogenesis is limited (Luhmann et al 05;Berger et al 96;Richter et al 98). Whether an interaction between Norrin and VEGFA signalling exists, requires further investigations.

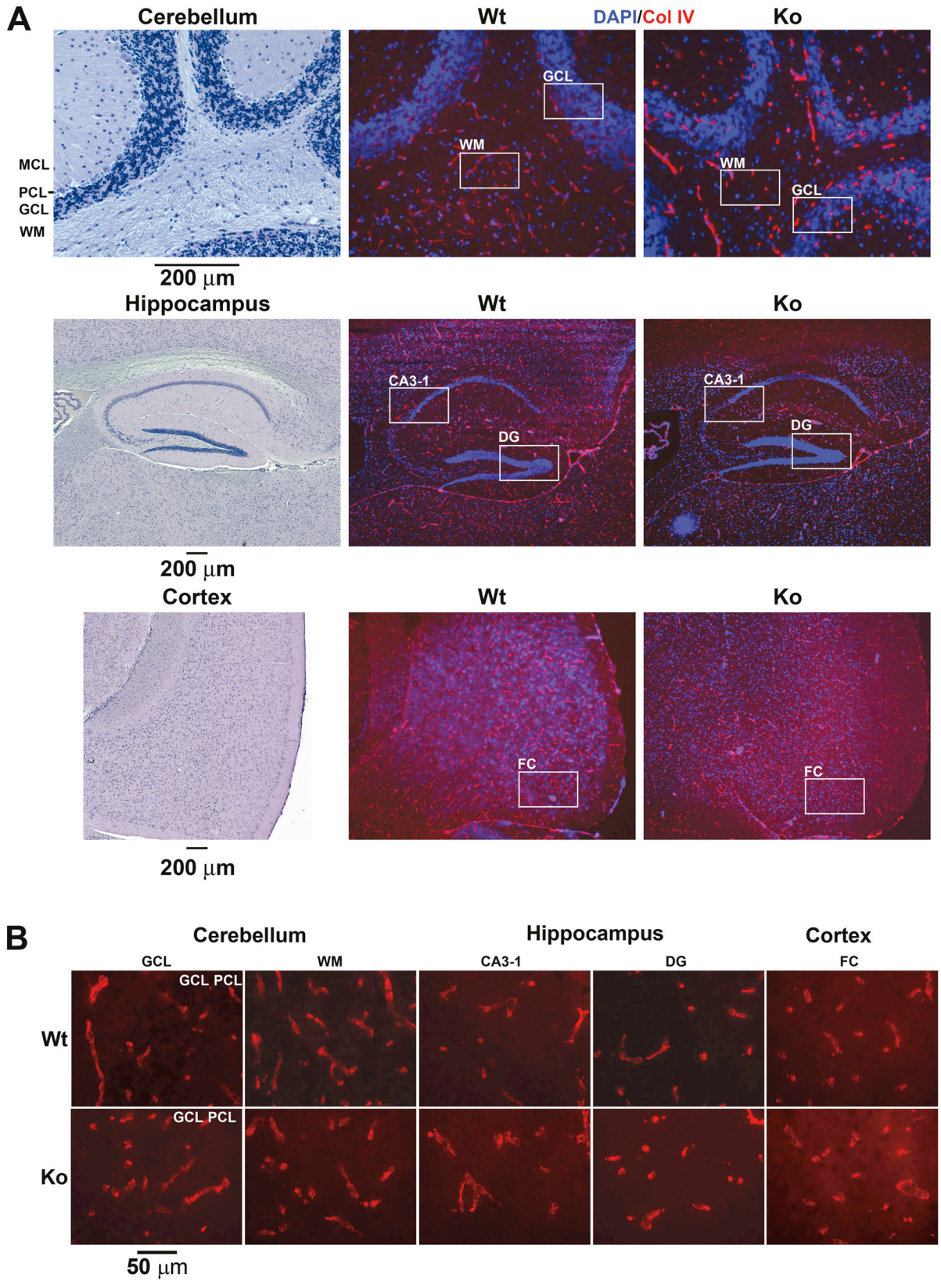

Figure 48 Vessel morphology in different brain regions. **(A)** Collagen IV immunohistochemistry of the vasculature in cerebellum, hippocampus and cortex of wild-type (WT) and *Ndph*-KO (KO) mice. Counter-staining was performed with DAPI. Representative haematoxylin–eosin-stained images are shown in the left column. **(B)** Higher magnification of Col IV immunohistochemistry without counterstaining to visualize the vessel morphology. The white frames indicate the areas from which images of higher magnification for B have been taken. *MCL*: molecular cell layer; *PCL*: Purkinje cell layer; *GCL*: granular cell layer; *WM*: white matter, CA3-1, CA3-1 region; *DG*: dentate gyrus; *FC*: frontal cortex.

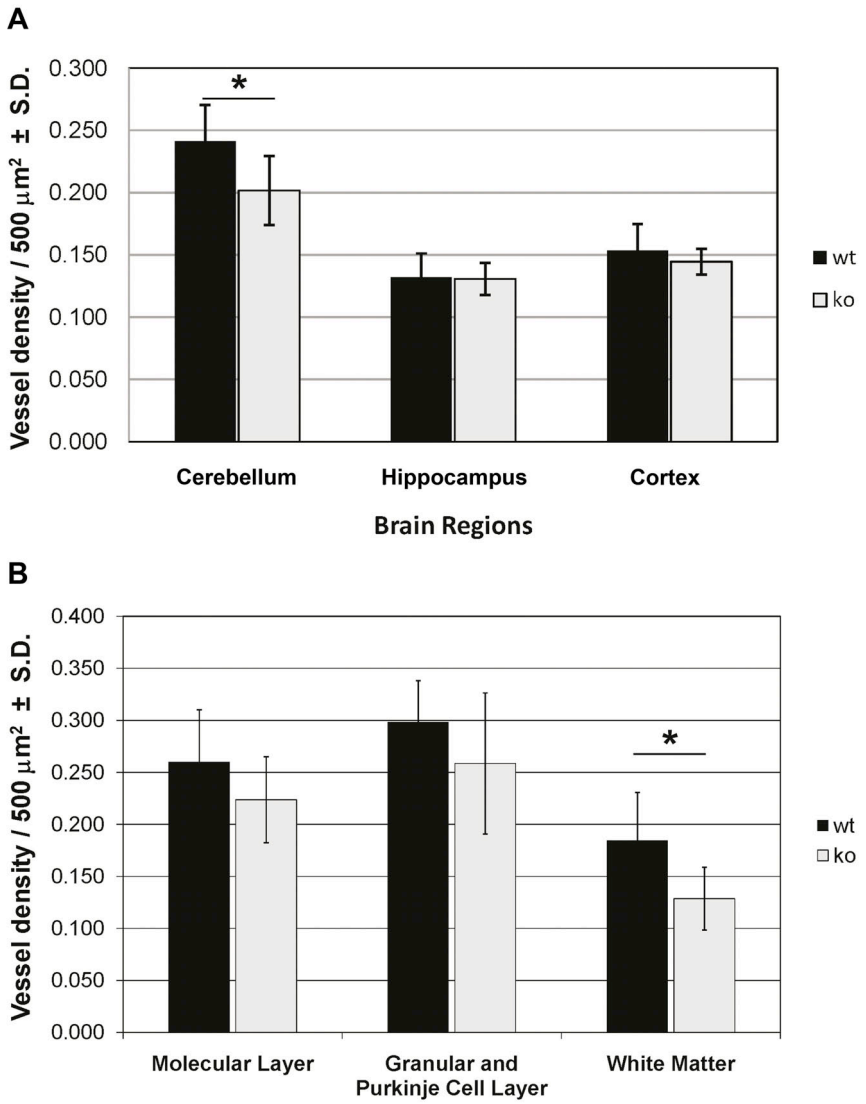

Figure 49 Quantitative assessment of vessel density in different brain regions and different layers of the cerebellum. **(A)** Col IV-stained vessel sections were evaluated in defined areas from six sections of each animal and brain region. The mean vessel density (± SD) per 500µm² is shown. The asterisk indicates statistical significance for the reduction in vessel density in *Ndph*-KO mice based on parametric tests (*$P <$ 0.05, anova for repeated measurements; between-subject test: $P = 0.037$, Student's *t*-test: $P = 0.037$). **(B)** Quantitative assessment of vessel density in the molecular layer, granular / Purkinje cell layer and white matter. The number of Col IV-stained vessels in each layer was counted and normalized to its area. The mean vessel density (± SD) per 500µm² for WT and *Ndph*-KO animals is shown. The asterisk indicates statistical significance in vessel density found in the white matter of *Ndph*-KO mice (Students *t*-test, $P =$ 0.034).

Homozygous *Fzd4* knockout mice show vascular defects in the retina, progressive hearing loss, growth retardation, abnormal gait and premature death (Xu et al 04;Wang et al 01). It was shown that these mice exhibit cerebellar degeneration, starting with a massive loss of granular cells between postnatal days p14 and p19 and a later reduction of Purkinje cells (Wang et al 01). In contrast to this mouse model, we detected no numerical reduction of these cells in the cerebellum of six- to eight-month-old *Ndph* knockout mice. This suggests that no degenerative changes leading to permanent cell loss are present up to this age although we can not exclude any transient changes during earlier development or age-related manifestations (Figure 47). We conclude that Norrin,

despite its high expression in the cerebellum (Figure 45), does not have a crucial role for the maintenance of neuronal cells, in particular the granular and Purkinje cells. This striking difference between *Ndph* and *Fzd4* knockout mouse lines suggests that Fzd4 requires additional ligands other than Norrin. Most likely these ligands are members of the Wnt family, the conventional ligands for Frizzled receptors, which are widely and commonly expressed in the brain and play important roles in neuronal development and synapse formation as well as in control of neuronal apoptosis and neurotrophin expression (Ciani and Salinas 05;Patapoutian and Reichardt 00).

However, we cannot exclude a direct effect of Norrin on neurons in different brain regions. During retinal development, the ectopic over-expression of Norrin in the lens led to an increased number in retinal progenitor cells *in vivo* and suggested a pro-proliferative effect on neuronal precursors of Norrin (Ohlmann et al 05). While we did not observe any indications for such a role in the adult brain, it remains to be elucidated, whether a similar Norrin function might be important during the development of the brain.

In addition to the neuronal degeneration of granular and Purkinje cells, progressive vascular enlargement and vascular disorganizations were described in the cerebellum of six-month-old homozygous *Fzd4* knockout mice. This vascular appearance was described as sparse, enlarged and irregular (Xu et al 04). While our examination of the hippocampal, cortical and cerebellar vasculature of *Ndph* knockout mice at comparable age, using comparable methods, did not show obvious differences in vascular morphology and size even at higher magnifications. the significant 16% reduction in vessel density in the cerebellum of *Ndph* knockout mice suggests a sparser vessel distribution. Furthermore, our data from the different cerebellar layers shows a general trend of reduced vessel density in all three layers, which reached significance in the white matter.

This mild reduction in vessel density might indicate a potential role of Norrin for the maintenance of the vasculature in the cerebellum and revealed the first phenotypic alterations in brain of *Ndph* knockout mice. Supportively, *Ndph* and *Fzd4* expression was highest in this brain region.

Norrin's role for the vascular system in brain appears only modulatory, while it is essential in the retina. Thus, it seems that the function of Norrin for the vasculature shows a tissue-specific effect. Tissue-specificity has been reported in eye and ear of *Ndph* knockout mice (Luhmann et al 05;Rehm et al 02). While the progressive hearing loss in Norrie disease patients and in *Ndph* knockout mice begins during early adulthood, the severe phenotype in the eye is already present shortly after birth (Rehm et al 02;Halpin et al 05;Warburg 66;Luhmann et al 05). Furthermore, the degeneration of the capillary network in the stria vascularis starts shortly after normal development suggesting a maintenance role for Norrin in the ear (Rehm et al 02). In contrast, development rather than maintenance is affected in the retina (Luhmann et al 05).

Hypoxic pathogenic processes as seen in *Ndph* knockout retinae were not indicated in the brain, since we did not find up-regulation of *Itgrb3*, *Vegfa* and *Tie1*. We chose these markers since they are significantly higher expressed in retinae of *Ndph* knockout mice under hypoxic conditions (Luhmann et al 05). In addition, *Vegfa* is upregulated by hypoxia in brain (Marti and Risau 98;Ozaki et al 99). Since we did not find differences between wildtype and knockout animals for these three markers in the cerebellum, we

conclude that the mild reduction in vessel density in *Ndph* knockout mice does not lead to a severe oxygen deficiency. Therefore, functional consequences of the reduced vessel density in the cerebellum remain uncertain at the molecular level. Future experiments will address Norrin's role in hypoxia-induced angiogenic responses and ischemic conditions in the brain.

This study provides initial evidence for a mild vascular defect in the brain of *Ndph* knockout mice. The brain can also be affected in patients with Norrie disease (Warburg 66) but the underlying processes are poorly characterized. The phenotypic features described in the brain vary and, consequently, it is difficult to understand the action of Norrin in the brain. The phenotype has often been described in general terms, such as "mental retardation". For example, in a large Cuban kindred with 46 affected members, 45% of the examined patients were described to show moderate or severe mental retardation (Fuchs et al 94). In other families severe developmental delay has been described, with some patients showing hypotonia or epileptic seizures (Schuback et al 95;Yamada et al 01;Lev et al 04;Fuentes et al 93). The observations suggest that these clinical symptoms can occur in Norrie disease and probably reflect a pleiotropic function of Norrin also in the brain. It is tempting to speculate that mild vascular changes, as observed in the *Ndph* knockout mouse model, might also occur in Norrie disease patients and lead to a higher susceptibility to seizures. This idea is supported by the findings that, in a rodent model, hypoxia has been shown to be epileptogenic in immature animals, but not in adults (Jensen et al 91). Therefore, the concept that absence of Norrin leads to vascular defects and to hypoxic insults in respective organs could be applicable not only to retina but also to the brain, although we cannot exclude the possibility that the function of Norrin may differ between mice and human.

Therefore, further clinical examinations in patients with Norrie disease, FEVR, ROP and Coats' disease, especially addressing extra ocular vessel manifestations, could help to clarify the role of the Norrin/Frizzled-4/Lrp5 signaling for vascular development or maintenance of vasculature in different tissues. To the best of our knowledge, e.g. FEVR patients show no clinical symptoms in brain or ear, which is in contrast to Norrie disease patients and to findings in the *Fzd4*-deficient mice (Xu et al 04). To further characterize these differences in phenotype between mouse and human and to understand pathogenic mechanisms, a more thorough examination especially in the cerebellum might be worth considering.

Although our study only showed a mild effect of the *Ndph* knockout on the vasculature in cerebellum, it might be worthwhile to examine different brain regions of patients for pathogenic changes. Vascular alterations might potentially help to explain the phenotypic variability of mental retardation seen in Norrie disease patients (Fuchs et al 94). In this context it is interesting to note that the cerebellum has been shown not only to be involved in motor function but also in certain aspects of cognition and affective functioning, including emotional reactivity and mood (Gordon 07). It was documented that patients with isolated cerebellar hypoplasia (incomplete or underdevelopment of the cerebellum) were predisposed to psychomotor delays and cognitive impairments, occasionally including epileptic seizures (Ventura et al 06). Furthermore, patients with cerebellar lesions in the posterior inferior artery showed deficits in mainly visual-spatial working and episodic memory as well as emotional withdrawal (Exner et al 04). This might suggest that any potential defect in the Norrin-Fzd4-Lrp5 signaling pathway affecting the cerebellum could possibly contribute to the mental retardation phenotype in Norrie disease patients.

3.1.6 Acknowledgement

We thank Catey Bunce for her advice regarding the statistical analysis of the expression data and are grateful for the funding by the Swiss National Science Foundation (SNF #3100-067786), the VELUX Foundation (WB, UL), and the EMDO Foundation Zurich (WB).

3.1.7 References

1. Acker,T., Beck,H. & Plate,K.H. (2001) Cell type specific expression of vascular endothelial growth factor and angiopoietin-1 and -2 suggests an important role of astrocytes in cerebellar vascularization. *Mechanisms of Development*, 108, 45-57.

2. Berger,W. (1998) Molecular dissection of Norrie disease. *Acta Anat.(Basel)*, 162, 95-100.

3. Berger,W., Meindl,A., van de Pol,T.J., Cremers,F.P., Ropers,H.H., Doerner,C., Monaco,A., Bergen,A.A., Lebo,R., Warburg,M., Zergollen,L., Lorenz,B., Gal,A., Bleeker-Wagemakers,E.M. & Meitinger,T. (1992a) Isolation of a candidate gene for Norrie disease by positional cloning. *Nat.Genet.*, 1, 199-203.

4. Berger,W., van de Pol,D., Bachner,D., Oerlemans,F., Winkens,H., Hameister,H., Wieringa,B., Hendriks,W. & Ropers,H.H. (1996) An animal model for Norrie disease (ND): gene targeting of the mouse ND gene. *Hum.Mol.Genet.*, 5, 51-59.

5. Berger,W., van de,P.D., Warburg,M., Gal,A., Bleeker-Wagemakers,L., de Silva,H., Meindl,A., Meitinger,T., Cremers,F. & Ropers,H.H. (1992b) Mutations in the candidate gene for Norrie disease. *Hum.Mol.Genet.*, 1, 461-465.

6. Black,G.C., Perveen,R., Bonshek,R., Cahill,M., Clayton-Smith,J., Lloyd,I.C. & McLeod,D. (1999) Coats' disease of the retina (unilateral retinal telangiectasis) caused by somatic mutation in the NDP gene: a role for norrin in retinal angiogenesis. *Hum.Mol.Genet.*, 8, 2031-2035.

7. Chen,Z.Y., Hendriks,R.W., Jobling,M.A., Powell,J.F., Breakefield,X.O., Sims,K.B. & Craig,I.W. (1992) Isolation and characterization of a candidate gene for Norrie disease. *Nat.Genet.*, 1, 204-208.

8. Ciani,L. & Salinas,P.C. (2005) Wnts in the Vertebrate Nervous System: From Patterning to Neuronal Connectivity. *Nat Rev Neurosci*, 6, 351-362.

9. Exner,C., Weniger,G. & Irle,E. (2004) Cerebellar lesions in the PICA but not SCA territory impair cognition. *Neurology*, 63, 2132-2135.

10. Fuchs,S., Xu,S.Y., Caballero,M., Salcedo,M., La,O.A., Wedemann,H. & Gal,A. (1994) A missense point mutation (Leu13Arg) of the Norrie disease gene in a large Cuban kindred with Norrie disease. *Hum.Mol Genet*, 3, 655-656.

11. Fuentes,J.J., Volpini,V., Fernandez-Toral,F., Coto,E. & Estivill,X. (1993) Identification of two new missense mutations (K58N and R121Q) in the Norrie disease (ND) gene in two Spanish families. *Hum.Mol.Genet.*, 2, 1953-1955.

12. Gordon,N. (2007) The cerebellum and cognition. *European Journal of Paediatric Neurology*, 11, 232-234.

13. Halpin,C., Owen,G., Gutierrez-Espeleta,G.A., Sims,K. & Rehm,H.L. (2005) Audiologic features of Norrie disease. *Ann Otol.Rhinol.Laryngol.*, 114, 533-538.

14. Jensen,F.E., Applegate,C.D., Holtzman,D., Belin,T.R. & Burchfiel,J.L. (1991) Epileptogenic effect of hypoxia in the immature rodent brain. *Ann.Neurol.*, 29, 629-637.

15. Lev, D, Hasan, M, Weigel, Y, Gak, E, Vinkler, C, Lerman-Sagie, T, and Watemberg, N. (2007) A novel missense mutation in the ND gene in a child with Norrie disease and severe neurological involvement. *Am.J.Hum.Genet.* 143A(9), pp. 921-924

16. Love,J.L., Scholes,P., Gilpin,B., Savill,M., Lin,S. & Samuel,L. (2006) Evaluation of uncertainty in quantitative real-time PCR. *J.Microbiol.Methods*, 67, 349-356.

17. Luhmann,U.F.O., Lin,J., Acar,N., Lammel,S., Feil,S., Grimm,C., Seeliger,M.W., Hammes,H.P. & Berger,W. (2005) Role of the Norrie Disease Pseudoglioma Gene in Sprouting Angiogenesis during Development of the Retinal Vasculature. *Invest.Ophthalmol.Vis.Sci.*, 46, 3372-3382.

18. Marti,H.H. & Risau,W. (1998) Systemic hypoxia changes the organ-specific distribution of vascular endothelial growth factor and its receptors. *PNAS*, 95, 15809-15814.

19. Ohlmann,A., Scholz,M., Goldwich,A., Chauhan,B.K., Hudl,K., Ohlmann,A.V., Zrenner,E., Berger,W., Cvekl,A., Seeliger,M.W. & Tamm,E.R. (2005) Ectopic Norrin Induces Growth of Ocular Capillaries and Restores Normal Retinal Angiogenesis in Norrie Disease Mutant Mice. *J.Neurosci.*, 25, 1701-1710.

20. Ohlmann,A.V., Adamek,E., Ohlmann,A. & Lutjen-Drecoll,E. (2004) Norrie Gene Product Is Necessary for Regression of Hyaloid Vessels. *Invest.Ophthalmol.Vis.Sci.*, 45, 2384-2390.

21. Ozaki,H., Yu,A.Y., Della,N., Ozaki,K., Luna,J.D., Yamada,H., Hackett,S.F., Okamoto,N., Zack,D.J., Semenza,G.L. & Campochiaro,P.A. (1999) Hypoxia inducible factor-1alpha is increased in ischemic retina: temporal and spatial correlation with VEGF expression. *Invest Ophthalmol Vis.Sci.*, 40, 182-189.

22. Patapoutian,A. & Reichardt,L.F. (2000) Roles of Wnt proteins in neural development and maintenance. *Current Opinion in Neurobiology*, 10, 392-399.

23. Rehm,H.L., Zhang,D.S., Brown,M.C., Burgess,B., Halpin,C., Berger,W., Morton,C.C., Corey,D.P. & Chen,Z.Y. (2002) Vascular defects and sensorineural

deafness in a mouse model of Norrie disease. *J.Neurosci.*, 22, 4286-4292.

24. Richter,M., Gottanka,J., May,C.A., Welge-Lussen,U., Berger,W. & Lutjen-Drecoll,E. (1998) Retinal vasculature changes in Norrie disease mice. *Invest.Ophthalmol.Vis.Sci.*, 39, 2450-2457.

25. Robitaille,J., MacDonald,M.L., Kaykas,A., Sheldahl,L.C., Zeisler,J., Dube,M.P., Zhang,L.H., Singaraja,R.R., Guernsey,D.L., Zheng,B., Siebert,L.F., Hoskin-Mott,A., Trese,M.T., Pimstone,S.N., Shastry,B.S., Moon,R.T., Hayden,M.R., Goldberg,Y.P. & Samuels,M.E. (2002) Mutant frizzled-4 disrupts retinal angiogenesis in familial exudative vitreoretinopathy. *Nat.Genet.*, 32, 326-330.

26. Schuback,D.E., Chen,Z.Y., Craig,I.W., Breakefield,X.O. & Sims,K.B. (1995) Mutations in the Norrie disease gene. *Hum.Mutat.*, 5, 285-292.

27. Shastry,B.S., Hejtmancik,J.F. & Trese,M.T. (1997a) Identification of novel missense mutations in the Norrie disease gene associated with one X-linked and four sporadic cases of familial exudative vitreoretinopathy. *Hum.Mutat.*, 9, 396-401.

28. Shastry,B.S., Pendergast,S.D., Hartzer,M.K., Liu,X. & Trese,M.T. (1997b) Identification of missense mutations in the Norrie disease gene associated with advanced retinopathy of prematurity. *Arch.Ophthalmol.*, 115, 651-655.

29. Toomes,C., Bottomley,H.M., Jackson,R.M., Towns,K.V., Scott,S., Mackey,D.A., Craig,J.E., Jiang,L., Yang,Z., Trembath,R., Woodruff,G., Gregory-Evans,C.Y., Gregory-Evans,K., Parker,M.J., Black,G.C., Downey,L.M., Zhang,K. & Inglehearn,C.F. (2004) Mutations in LRP5 or FZD4 underlie the common familial exudative vitreoretinopathy locus on chromosome 11q. *Am J Hum.Genet.*, 74, 721-730.

30. Ventura,P., Presicci,A., Perniola,T., Campa,M.G. & Margari,L. (2006) Mental Retardation and Epilepsy in Patients With Isolated Cerebellar Hypoplasia. *J Child Neurol*, 21, 776-781.

31. Wang,Y., Huso,D., Cahill,H., Ryugo,D., Nathans,J. (2001) Progressive Cerebellar, Auditory, and Esophageal Dysfunction Caused by Targeted Disruption of the frizzled-4 Gene. *J.Neurosci.*, 21, 4761-4771.

32. Warburg,M. (1966) Norrie's disease. A congenital progressive oculo-acoustico-cerebral degeneration. *Acta Ophthalmol.(Copenh)*, Suppl 89, 5-147.

33. Xu,Q., Wang,Y., Dabdoub,A., Smallwood,P.M., Williams,J., Woods,C., Kelley,M.W., Jiang,L., Tasman,W., Zhang,K. & Nathans,J. (2004) Vascular development in the retina and inner ear: control by Norrin and Frizzled-4, a high-affinity ligand-receptor pair. *Cell*, 116, 883-895.

34. Yamada,K., Limprasert,P., Ratanasukon,M., Tengtrisorn,S., Yingchareonpukdee,J., Vasiknanonte,P., Kitaoka,T., Ghadami,M., Niikawa,N. & Kishino,T. (2001) Two Thai families with Norrie disease (ND): association of two novel missense mutations with severe ND phenotype, seizures, and a manifesting carrier. *Am J Med Genet*, 100, 52-55.

35. Zachary,I. & Gliki,G. (2001) Signaling transduction mechanisms mediating biological actions of the vascular endothelial growth factor family. *Cardiovascular Research*, 49, 568-581.

3.1.8 Contributions of authors to the manuscript „Vascular changes in the cerebellum of Norrin/Ndph knockout mice correlate with high expression of Norrin and Frizzled-4“

U.F.L.: Conceptualization of the experiments, planning and administration of the mouse breeding, preparation of animals, preparation of sections, immunohistochemistry, morphometric analysis, preparation of RNA, qRT-PCR, Western blots, statistics, interpretation of data, writing of the manuscript

J.N.: Conceptualization of the experiments, interpretation of data, immunohistochemistry, morphometric analysis, editing of the manuscript

B.K.G.: Preparation of RNA, qRT-PCR, editing of the manuscript

N.F.S.: Morphometric analysis, Western blots, editing of the manuscript

E.G.: Technical assistance, immunohistochemistry, morphometric analysis

S.F.: Technical assistance, mouse genotyping

W.B.: Principal investigator (PI), conceptual planning, design and supervision of the entire study, interpretation of data, editing of the manuscript

3.2 Differential gene expression in Ndph knockout mice in retinal development

***Nikolaus F. Schäfer*[1], *Ulrich F.O. Luhmann*[1a], *Silke Feil*[1] *and Wolfgang Berger*[1]**

[1]Division of Medical Molecular Genetics & Gene Diagnostics, Institute of Medical Genetics, University of Zurich, Switzerland; [a]current address: Division of Molecular Therapy, UCL Institute of Ophthalmology, 11-43 Bath-Street, EC1V 9EL London, UK

Manuscript published in: *Investigative Ophthalmology & Visual Science, 2009* ***50*** *(2); pp. 906-16*

3.2.1 Abstract

PURPOSE. Mutations in the *NDP* gene impair angiogenesis in the eyes of patients diagnosed with a type of blindness belonging to the group of exudative vitreoretinopathies. With this study, we aimed to investigate differential gene expression caused by the absence of Norrin (the *NDP* protein) in the developing mouse retina to elucidate early pathogenic events.

METHODS. A comparative gene expression analysis was performed on p7 (postnatal day 7) retinae from a knockout mouse model for Norrie disease using Affymetrix microarrays. Subsequently, results were verified by quantitative real-time PCR analyses. Immunohistochemistry was performed for the vascular permeability marker Plasmalemma vesicle-associated protein (Plvap).

RESULTS. Our study identified expression differences in *Ndph*$^{y/-}$ vs. wild type mice retinae at p7. Gene transcription of the neutral amino acid transporter *Slc38a5*, apolipoprotein D (*ApoD*) and angiotensin II receptor-like 1 (*Agtrl1*) was decreased in the knockout, whereas transcript levels of adrenomedullin (*Adm*) and of the plasmalemma vesicle associated protein (*Plvap*) were increased in comparison to the wild type. In addition, we found ectopic expression of Plvap in the developing retinal vasculature of Norrin knockout mice on the protein level.

CONCLUSIONS. These data provide molecular evidence for a role of Norrin in the development of the retinal vasculature. Expression of two genes, *Plvap* and *Slc38a5*, is considerably altered in retinal development of Norrin knockout mice and may reflect or contribute to the pathogenesis of the disease. In particular, ectopic expression of Plvap is consistent with hallmark disease symptoms in mouse and man.

Key words: Vitreoretinopathy • Angiogenesis • Gene expression • Norrie Disease • Ndph • Plvap

3.2.2 Introduction

Norrie Disease (OMIM 310600; ND) is an X-linked, recessive neurological disorder that presents with congenital blindness, progressive deafness and mental retardation[1], and is caused by mutations in the Norrie disease pseudoglioma (*NDP*) gene[2,3,4]. The high phenotypic variability even within one family carrying the same mutation[5,6,7] suggests the involvement of modifier genes or other factors, which might explain why no clear genotype-phenotype correlation has been described so far. In addition, mutations in this gene have also been associated with a variety of other recessive and sporadic

vitreoretinal diseases, including exudative vitreoretinopathy (OMIM 133780; EVR), retinopathy of prematurity (ROP, stages 4b and 5) and Coats' disease (OMIM 300216)[8,9,10,11]. These allelic clinical entities show remarkable similarities in their ocular phenotype especially with regard to abnormalities in the retinal vasculature.

The human disease phenotype is strongly resembled by the Norrie disease pseudoglioma homolog (*Ndph*) knockout mouse[12,13]. Although the retinal vasculature in humans develops around mid-gestation, and only postnatally in mice, the timing of events is comparable. In mice, retinal blood vessels start to develop around birth at the optic disc and spread radially inside the nerve fiber layer across the retina, until they reach the periphery around postnatal day 9 (p9). In addition, vessels start to sprout into the deeper layers of the retina at p7 to form two additional networks in the plexiform layers, parallel to the superficial plexus. Contrary to the development of the retinal vasculature, the hyaloid vessel system, a transient developmental vasculature nourishing the developing lens, regresses. This process starts after its peak extension around p5 and lasts until p15, around which time the mice open their eyes and eye development is more or less complete[14]. In the *Ndph* knockout mouse, the inner retinal vessel development is severely impaired. The outgrowth of the superficial retinal vessel plexus is delayed and remains sparse, deep retinal vessels do not develop, and the regression of the hyaloid vasculature is delayed and incomplete. Furthermore, disorganization of the retinal ganglion cell layer and a reduction of retinal ganglion cells have been described[12,15,13]. However, proliferation of fibrovascular material in the vitreous cavity is not as massive as the pseudoglioma described in patients suffering from severe ND.

Different hypotheses have been postulated about the etiology of these symptoms. It has been discussed that the extended presence of hyaloid vessels might impair the development of the retinal vasculature[16,17]. However, blockage of the placental growth factor (PlGF) during early postnatal stages in the eye leads to delayed regression of the hyaloid vessel system, but not to changes in the retinal vasculature[18], indicating that persistence of the hyaloidea does not necessarily lead to defects in or lack of retinal vascularization. Another hypothesis was provided by a detailed analysis of the early development of the retinal vasculature in *Ndph* knockout mice, which suggested two phases of disease progression *in vivo*[15]: In the early phase, the absence of functional Norrin (*Ndph*–protein) causes a defect in sprouting angiogenesis, which leads to a delayed outgrowth of the superficial vessels and prevents the formation of deep capillary networks in the retina. Then, in the later phase, the developmental lack of the deep vasculature leads to inner retinal hypoxia. This pathologic hypoxia may explain the observed clinical features of Norrie disease and might also be responsible for the similarities of the clinical phenotypes of the aforementioned diseases[15]. In another study, the knockout phenotype could be completely rescued by ectopic overexpression of Norrin in the lens[19]. Their authors suggested a direct effect of Norrin on vascular proliferation, since proliferation of microvascular endothelial cells was increased after co-cultivation with the Norrin-expressing lenses[19].

Further, autosomal dominant and recessive forms of FEVR (familial exudative vitreoretinopathy), which are caused by mutations in Frizzled- 4 (*FZD4*) and LDL related protein 5 (*LRP5*) in approximately 35% of the patients[20,21], resemble the clinical pictures of the X-linked diseases[12,13,22]. Prompted by these findings and the phenotypic similarities between *Ndph* and *Fzd4* knockout mice, Xu et al. could provide the first hint for a possible cellular function of Norrin. They showed that Norrin is a high affinity

ligand of Frizzled-4 and activates the canonical Wnt/beta-catenin pathway in the presence of LRP5 in cell culture[23]. This pathway eventually leads to transcriptional regulation of target genes under the control of TCF/Lef-binding sites. In summary, these data suggest that Norrin has an influence on transcriptional regulation of Wnt-target genes, is required for early angiogenic sprouting in the retina and the regression of the hyaloid vessel system, and is necessary for the formation of deep retinal capillary networks around postnatal day 7 (p7)[15].

The main purpose of the experiment reported here was to find differently expressed genes in retinae of p7 *Ndph* knockout mice that are involved in the process of deep plexus formation and that could confirm Norrin's hypothesized role on Wnt target genes *in vivo*. Our findings support a role of Norrin in blood vessel development and provide evidence for a potential regulation of new target genes that were not considered so far. However, involvement of the Wnt/beta-catenin pathway could not be demonstrated by our experiments. One gene, the plasmalemma vesicle associated protein (*Plvap*), has been characterized in more detail. This gene was described as a major structural component of fenestrated blood vessels[24], and here was found to be up-regulated in the retinal vasculature in the absence of Norrin. Thus, we discuss the question whether or not Norrin could also be involved in blood vessel integrity and the formation or maintenance of the blood-retina-/blood-brain-barrier.

3.2.3 Materials And Methods

3.2.3.1 Animals

The *Ndph* knockout mouse line has been described before by Berger et al.[12]. Briefly, exon 2 of the *Ndph* gene has partially been replaced by homologous recombination with a reverse oriented neomycin cassette, resulting in a loss of about half the coding sequence, including the signal peptide for protein secretion. The mutation is kept on a C57BL/6 background. Genotyping was performed by PCR analysis of tail DNA[12]. The research was performed in accordance with the ARVO Statement for the Use of Animals in Ophthalmic and Vision Research and was approved by the Veterinary Service of the State of Zurich (Switzerland).

3.2.3.2 Tissue isolation and RNA preparation

Wild type and *Ndph*$^{y/-}$ mice of different developmental stages (p5, p7, p10, p15, p21) were sacrificed by cervical dislocation. Five animals of each genotype were prepared and the retinae were frozen in liquid nitrogen. Total RNA was extracted using the RNeasy®-Kit (Qiagen, Hilden, Germany) according to the manufacturer's instructions. DNase digestion was applied either directly on-column (p7 samples, RNase-free DNase Set, cat. no. 79254, Qiagen, Hilden, Germany), or separately after RNA extraction (RQ1 RNase-free DNase, p/n M610A, Promega, Madison, WI, USA). Both retinae of one animal were pooled into one tube of lysis buffer and homogenized with an Ultra-Turrax® high-performance disperser (Ika-Werke, Staufen, Germany). RNA quality was determined with a NanoDrop ND 1000 (NanoDrop Technologies, Delaware, USA) and a Bioanalyzer 2100 (Agilent Technologies, Santa Clara, CA, USA). RNA Integrity number of all samples was greater or equal to 9.3.

3.2.3.3 Microarray experiment

Gene chip expression analysis has been carried out with RNA from p7 retinae (wt: n=5, ko: n=5), using the Affymetrix GeneChip® Mouse Genome 430 2.0 array (Affymetrix Inc., Santa Clara, CA, USA). On this chip, over 34,000 genes and ESTs are represented by ~45,000 probe sets. The Microarray experiment, from cDNA preparation to raw data processing, was performed at the Functional Genomics Center Zurich. Briefly, total RNA samples (2µg each) were reverse-transcribed without additional amplification (one-cycle protocol), purified, labeled and hybridized to the chip according to the manufacturer's instructions. An Affymetrix GeneChip Scanner 3000 was used to measure the fluorescence intensity emitted by the labeled target.

Statistical analysis Raw data processing was performed using the Affymetrix GCOS 1.2 software (Affymetrix Inc., Santa Clara, CA, USA). After hybridization and scanning, probe cell intensities were calculated and summarized for the respective probe sets by means of the MAS5 algorithm[25]. To compare the expression values of the genes from chip to chip, global scaling was performed, which resulted in the normalization of the trimmed mean of each chip to a target intensity (TGT value) of 500 as detailed in the statistical algorithms description document of Affymetrix (2002). Quality control measures were considered before performing the statistical analysis. Differently expressed genes were calculated with the GeneSpring 7.2 software (Agilent Technologies, Santa Clara, CA, USA), filtered for presence (per Affymetrix presence/absence flags) in four of five samples in either one condition (wt or ko) and then subjected to a non-parametric test for differential expression (Mann-Whitney test without multiple testing correction ($p<0.01$), or with Benjamini-Hochberg multiple testing correction ($p<0.1$)).

Pathway analysis Pathway analysis was conducted with the online tool "Pathway express", which is part of the "Onto-Tools", hosted by the Wayne State University, Detroit, USA, using the default options[26].

Gene ontology annotations Gene ontology (GO) annotations are used to describe e.g. biological process or cellular component of a given gene product. Annotations for the top differently expressed genes (Table 40) were obtained from the Database for Annotation, Visualization and Integrated Discovery (DAVID) from the National Institute of Health[27].

3.2.3.4 Quantitative reverse transcription-PCR

Quantitative RT-PCR was performed not only to investigate differential expression during development, but also to verify the microarray results. For p7, the same samples as in the array experiment were used. Generation of cDNA was accomplished as follows: 1250ng total RNA were reverse transcribed in a 20µl reaction, using random hexamers $pd(n)_6$ (Amersham Biosciences / GE Healthcare Europe, Otelfingen, Switzerland) and SuperScript III RT (Invitrogen, Carlsbad, CA, USA). For expression analysis of *Slc38a5* and *Mdm2*, quantitative RT-PCR was conducted using 0.5µM of a forward/reverse primer pair (binding in the area that is recognized by the Affymetrix probes) and SYBR®-Green PCR Mastermix (Applied Biosystems, Foster City, CA, USA). TaqMan® probes and TaqMan® Universal PCR Mastermix (Applied Biosystems, Foster City, CA, USA) were used for quantification of *Aass*, *Centd3*, *ApoD*, *Cldn5*, *Agtrl1*, *Adm* and *Plvap* expression (Table 38). In each reaction, 10ng of transcribed total RNA were employed (except: *Slc38a5* / 100ng).

Quantitative RT-PCR was carried out in five replicates in an Applied Biosystems PRISM® 7900HT system using the recommended standard cycling conditions: 45 cycles of denaturation (15s/95°C) and annealing/extension (1min/60°C). *Gapdh* and 18S (TaqMan®) or 28S (SYBR®-Green) rRNA were used as endogenous controls. Confidence intervals for wild type and knockout gene expression were calculated on basis of the mean ΔΔ ct-values at a significance level of 95% using Student's t-test.

Gene	5' Primer	3' Primer
Mdm2	AAG ACA GGC TCT CAC TAT TAG CTA TGG	TGG GAG TTA AAG GTC TGC CTG AT
Slc38a5	CGA CCT TTG GAT ACC TCA CCT T	TGG GTG TAC ATT TCC AGC ATC T
28S rRNA	TTG AAA ATC CGC GGG AGA G	ACA TTG TTC CAA CAT GCC AG
Gapdh	AAC GAC CCC TTC ATT GAC	TCC ACG ACA TAC TCA GCA C

Gene	TaqMan® probe	Gene	TaqMan® probe
Aass	Mm00497118_m1	*Adm*	Mm00437438_g1
Agtrl1	Mm00442191_s1	*Plvap*	Mm00453379_m1
ApoD	Mm00431817_m1	*18S rRNA*	p/n 4308329
Centd3	Mm00551866_m1	*Gapdh*	p/n 4352339E
Cldn5	Mm00727012_s1		

Table 38 Primers for SYBR®-Green assays and part no. of TaqMan® assays used in this study (Applied Biosystems, Foster City, CA, USA).

3.2.3.5 Immunohistochemical staining and histology

Cryosections were prepared from male *wt* and *Ndph*$^{y/-}$ mice aged p3, p5, p7, p10, p15 and p21. Eyes were dissected, fixed for 1h in PBS / 4% para-formaldehyde, washed in PBS and cryo-protected in Succrose (30min in 10%, then o/n in 20%) at 4°C. They were embedded in Tissue-Tek® O.C.T. Compound (Sakura Finetek, Zoeterwoude, Netherlands), submersed in liquid nitrogen, cut into 8µm sections with a Leica Cryostat CM 3050S (Leica, Heerbrugg, Switzerland) and transferred onto microscope glass slides. After drying the sections for at least 3h, unspecific binding sites were blocked by incubation with 5% normal sheep serum (Sigma Aldrich, Steinheim, Germany) in PBST for 1h. Slides were incubated with primary antibodies in blocking solution (o/n, 4°C) in a wet chamber. Antiserum concentrations were 1µg/ml for anti-Plvap/MECA-32 (rat anti-mouse, Developmental Studies Hybridoma Bank) and 7µg/ml for anti-Collagen IV (polyclonal Col IV antibody, rabbit anti-mouse, no. 2150-1470, AbD Serotec/MorphoSys, Oxford, UK). Sections were washed and incubated with secondary antibodies in PBS (90min, RT). Cy3™-conjugated anti-rabbit IgG serum (Jackson ImmunoResearch Europe, Newmarket, Suffolk, UK) was used at a concentration of 5µg/ml, Alexa Fluor® 488-labelled anti-rat IgG/M (no. A11006, Molecular Probes, Leiden, Netherlands) was used at 2µg/ml. Slides were washed a last time and finally mounted in a DAPI-containing medium (Vectashield® Mounting Medium for Fluorescence with DAPI H-1200, Vector Laboratories, Burlingame, CA, USA). Images were taken with an Axioplan 2 microscope equipped with an AxioCam HRc digital camera (Carl Zeiss MicroImaging, Jena, Germany). Contrast in Plvap/AF 488 images was enhanced after acquisition with a photo-editing program.

For retinal flatmounts, eyes were dissected and fixed for 15min in PBS/4% para-formaldehyde. Retinae were removed and post-fixed for additional 15min. After

washing in PBS, unspecific binding was blocked by 10% normal sheep serum in PBST for 1h. Samples were then incubated o/n with the Collagen IV antibody. They were washed six times for 1h in PBST and incubated o/n with the secondary Cy3-labeled antibody. After repetition of the washing procedure, the retinae were finally flatmounted on microscope slides.

Sections (8µm) of paraffin-embedded eyes were hematoxylin-eosin stained as described elsewhere[15] and observed under bright-light illumination.

3.2.4 Results

In this study, we used the *Ndph* knockout mouse to investigate molecular pathways involved in early angiogenic sprouting in the retina and the formation of deep retinal capillary networks at around postnatal day 7 (p7)[15]. We hypothesized that Norrin is required for these processes, probably by transcriptional regulation of Wnt/beta-catenin target genes and/or other pathways.

3.2.4.1 Retinal morphology at p7

At p7, conventional microscopy of HE stained retinal sections did not reveal apparent differences in the retinal morphology of wild type and *Ndph* knockout mice (Figure 50a,b). In contrast, ColIV immunohistochemistry revealed that the retinal vasculature of the *Ndph* knockout was strikingly altered, showing an intermediate phenotype to what we earlier observed at p5 and p10[15]. The superficial vessel system appeared much sparser than in the wild type, its outgrowth was delayed, and missing vascular sprouts indicated a lacking development of deep retinal vessels (Figure 50c-e). Since we argue that the vascular phenotype is the earliest and most obvious retinal defect caused by the absence of *Ndph*, we used this developmental stage to investigate the initial pathologic events on the molecular level, i.e. to identify genes involved in the initiation of the deep retinal capillary network by sprouting angiogenesis, which may be regulated by Norrin directly or indirectly.

3.2.4.2 Microarray gene expression analysis

To identify differently expressed genes in the retina of *Ndph* knockout mice, we took a global gene expression approach using microarrays. The gene chip experiment resulted in 26'817 expressed probe sets in p7 retinae. Differences in the overall expression levels between *Ndph*$^{y/-}$ and wild type retinae were rather moderate, both in absolute number and fold-change. In microarray studies, usually an arbitrary fold-change cut-off of 2.0 has been applied[28], still resulting in dozens or hundreds of differently expressed genes. Yet, expression changes of highly expressed genes may still be biologically relevant

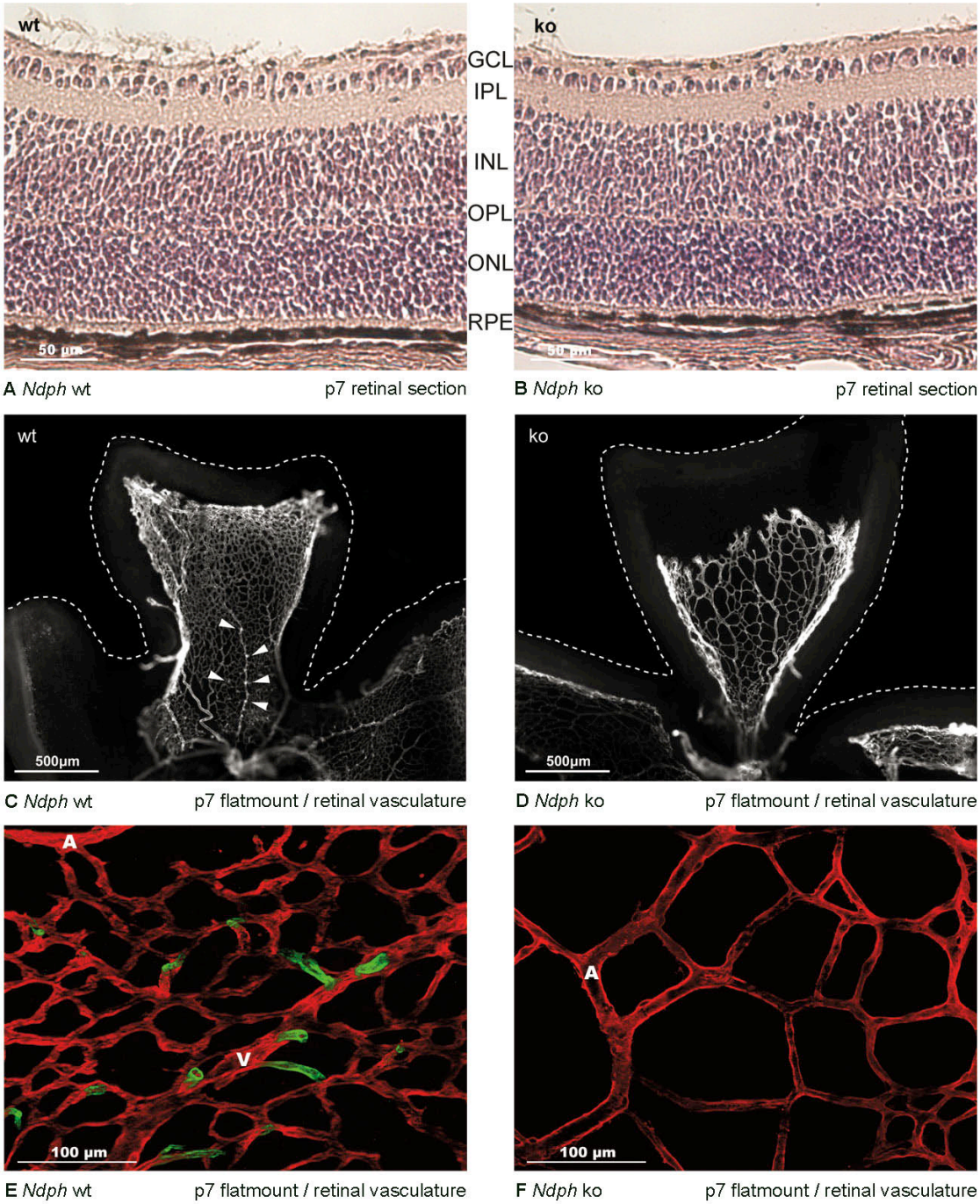

Figure 50 Retinae of p7 *Ndph*$^{y/-}$ mice in comparison to wild type. **(A,B)** Hematoxylin-eosin (HE) stained central sections of paraffin embedded retinae. No obvious difference in retinal organization could be detected. **(C,D)** Immunofluorescence images from retinal flatmounts. Images compiled from a Z-Stack of pictures acquired with a Zeiss ApoTome™. To visualize the retinal vasculature, an antibody against Collagen IV was used. In the wild type p7 retina, deeper networks start to develop from veins and capillaries, but not arteries, as has been shown by other authors[14] (arrowheads). In contrast, outgrowth of the superficial capillary network in the knockout is delayed, appears to be much sparser, and no developing deeper network could be detected. **(E,F)** Higher magnification of ApoTome™ images from c,d. Superficial vasculature is shown in red, deep vasculature in green. *GCL: ganglion cell layer; IPL: inner plexiform layer; INL: inner nuclear layer; OPL: outer plexiform layer; ONL: outer nuclear layer; A: artery; V: vein*

despite a fold-change lower than 2.0, while weakly expressed transcripts may show a fold-change higher than 2.0 due to their greater inherent measurement error[28]. In this study, we reasoned that a cut-off of 1.6 might still be valid considering our use of five biological replicates (instead of the standard three) while giving us a decent list of differently expressed genes.

The list of expressed probe sets was subjected to a non-parametric Mann-Whitney test with multiple testing correction (Benjamini-Hochberg, $p<0.1$). This resulted in a list of 450 probe sets (with 10% = 45 false positives), thirty-four of which showed a fold-change of at least 1.6. Each of the thirty-four represents a different gene (Table 40), including five currently unknown cDNAs. Sixteen transcripts show an elevated expression in the knockout, while levels of eighteen genes are decreased.

Since only one of these 34 genes (*Apcdd1*) has been associated with the Wnt-signaling pathway so far, we attempted to find evidence for its involvement with a pathway analysis. Because the list of 34 genes was too small for this purpose, we subjected the list of expressed probe sets to a non-parametric Mann-Whitney test ($p<0.01$), but this time without multiple testing correction and fold-change cut-off. This resulted in a list of 872 probe sets (730 genes or ESTs) to be considered differently expressed between wild type and knockout. We then performed a pathway analysis based on these 730 genes by utilizing the online tool "Pathway express"[26]. Also here, an involvement of Wnt-signaling was not striking. The five most prominent affected pathways were: the MAP-Kinase pathway, focal adhesion, calcium-signaling, tight junction, and only then, Wnt-signaling (Table 39). Due to the low statistical power of this analysis, these results must be treated with caution. While they might provide clues for future research activities, they have to be verified first by independent experiments. In the study presented here, we decided to concentrate on the list of the 34 most differently expressed genes (Table 40).

Rank	Pathway Name	Impact Factor	Genes in Pathway	Input Genes in Pathway	Pathway Genes on Chip	% Input Genes in Pathway
1	MAPK signaling pathway	23.79	233	11	231	1.51
2	Focal adhesion	20.00	156	7	143	0.96
3	Calcium signaling pathway	18.93	180	8	172	1.10
4	Tight junction	13.67	125	7	114	0.96
5	Wnt signaling pathway	12.77	141	6	139	0.82
	Genes mapped to pathways:	75				
	cDNAs:	868				

Table 39 Top 5 involved pathways. Results of a pathway analysis performed with the online tool "Pathway express", which is part of the "Onto-Tools", hosted by the Wayne State University, Detroit, USA[26]. Only 10% of the input genes could be mapped to a pathway based on the KEGG Pathway Database.

As expected for a knockout, the *Ndph* gene appears in the list of lower expressed genes. However, its expression is only decreased by the factor of two. One possible explanation could be the general low retinal *Ndph* expression in the wild type, so the indicated fold-change could be the result of a measurement error. Second, the knockout is not a complete null-allele, but rather lacks most of exon 2, resulting in the loss of about half its

Increased	Symbol	Name	Gene Ontology (GO)		Affymetrix ID
			Biological Process (BP)	Cellular Component (CC)	
3.06	*Mdm2*	Transformed mouse 3T3 cell double minute 2	traversing start control point of mitotic cell cycle, protein ubiquitination	cytoplasm, nucleus	1457929_at
2.79	*Wdr67*	WD repeat domain 67			1442286_at
2.47	*Seh1l*	SEH1-like (S. Cerevisiae)			1441857_x_at
2.03	*Adm*	Adrenomedullin		extracellular space	1447839_x_at
2.00	*Lilrb4*	Glycoprotein 49 B			1420394_s_at
1.95	*Arhgap10*	Rho GTPase activating protein 10	cytoskeleton organization and biogenesis		1442967_at
1.88	*Iqsec2*	IQ motif and Sec7 domain 2			1448063_at
1.86	*Plvap*	Plasmalemma vesicle associated protein		integral to membrane	1418090_at
1.84	*Foxp1*	Forkhead box P1	regulation of transcription	nucleus	1446280_at
1.81	*A2m*	Alpha-2-macroglobulin	protease inhibitor activity (MF)		1434719_at
1.80	*Gabarapl2*	GABA-A receptor-associated protein-like 2	intra-Golgi vesicle-mediated transport	Golgi, cytoskeleton	1459477_at
1.76	*Sync*	Syncoilin	intermediate filament-based process	cytoplasm, intermediate filament, Z-disc, synapse	1432350_at
1.67	*Acta2*	Actin, alpha 2, smooth muscle, aorta	cytoskeleton organization and biogenesis	Actin filament, cytoskeleton	1416454_s_at
		Unknown genes			
2.30		A130078K24Rik			1444482_at
2.04		E330034G19Rik			1433798_a_at
1.66		AW492805			1457729_at

Decreased	Symbol	Name	Gene Ontology (GO)		Affymetrix ID
			Biological Process (BP)	Cellular Component (CC)	
14.03	*Slc38a5*	Solute carrier family 38, member 5	amino acid transport, oxygen transport	integral to membrane	1454622_at
2.57	*Panx2*	Pannexin 2		gap junction, integral to membrane	1440350_at
2.44	*Mfsd2*	major facilitator superfamily domain containing 2		integral to membrane	1428223_at
2.13	*Aass*	Aminoadipate-semialdehyde synthase	response to oxidative stress, electron transport	mitochondrion	1423523_at
2.06	*Apod*	Apolipoprotein D	transport	extracellular space	1416371_at
2.05	*Centd3*	Centaurin, delta 3	regulation of cell shape and GTPase activity, negative regulation of cell migration	cytoplasm, lamellipodium, ruffle, nucleus	1419833_s_at
2.03	*Cldn5*	Claudin 5	cell-cell adhesion	tight junction, integral to membrane	1417839_at
2.01	*Ndph*	Norrie disease homolog		extracellular space	1449251_at
1.92	*Agtrl1*	Angiotensin receptor-like 1	G-protein coupled receptor protein signaling pathway	integral to membrane	1438651_a_at
1.85	*Plekhh1*	Pleckstrin homology domain containing, family H (with MyTH4 domain) member 1	cell adhesion	cytoskeleton	1435053_s_at
1.85	*Sh2d3c*	SH2 domain containing 3C	intracellular signaling cascade	cytoplasm	1430098_at
1.76	*Zfp206*	Zinc finger protein 206			1438787_at
1.72	*Eltd1*	EGF, latrophilin seven transmembrane domain containing 1	G-protein coupled receptor protein signaling pathway, neuropeptide signaling pathway	integral to membrane	1418059_at
1.67	*Vwa1*	von Willebrand factor A domain containing 1		extracellular space	1426399_at
1.66	*Apcdd1*	Adenomatosis polyposis coli down-regulated 1			1418383_at
1.62	*Slc7a1*	Solute carrier family 7 (cationic aa transporter, y+ system), 1	amino acid transport	integral to membrane	1454992_at
		Unknown genes			
1.89		6230424C14Rik			1441972_at
1.88		2310015A05Rik			1436104_a_at

Table 40 Genes with the most change in expression. GO terms listed may not include all annotations for each gene, but rather only parent or main annotations to facilitate a first impression of possible gene function.

coding region. Since the probes of the Affymetrix Mouse Genome 430 2.0 array predominantly target the 3'-region and a signal was detected in the knockout, it is possible that a transcript including this region is present in the retina of *Ndph*$^{y/-}$ mice. In fact, a ko-allele derived, low expressed artificial transcript has been isolated from the brain of *Ndph*$^{y/-}$ mice. Partial sequencing of this transcript revealed that no functional Norrin can be translated from this RNA, as almost half of the open reading frame, including the signal peptide, is missing and no start codon is present in the relevant transcript area (data not shown[29]).

3.2.4.3 Verification of differential expression by qRT-PCR

To validate the microarray results, qRT-PCR was performed for three of the most upregulated and six of the most downregulated transcripts using the same p7 retina RNA samples that were used for the array experiment. Relative quantification values were determined with *18S* or *28S rRNA* and *Gapdh* (not shown) as endogenous controls. Expression values in general seemed to correlate with the microarray results (Figure 51). Five genes were proven to be significantly differentially expressed. Three genes showed a decreased expression in the knockout: The neutral amino acid transporter *Slc38a5* (24x less), apolipoprotein D (*ApoD*; 2.4x less) and angiotensin II receptor-like 1 (*Agtrl1*; 2x less). Increased expression was found for the plasmalemma vesicle-associated protein (*Plvap*; 4.2x higher) and adrenomedullin (*Adm*; 2.7x higher).

Despite the low fold-change threshold of 1.6 for our microarray statistical analysis, we were able to confirm differential expression of more than half the genes examined.

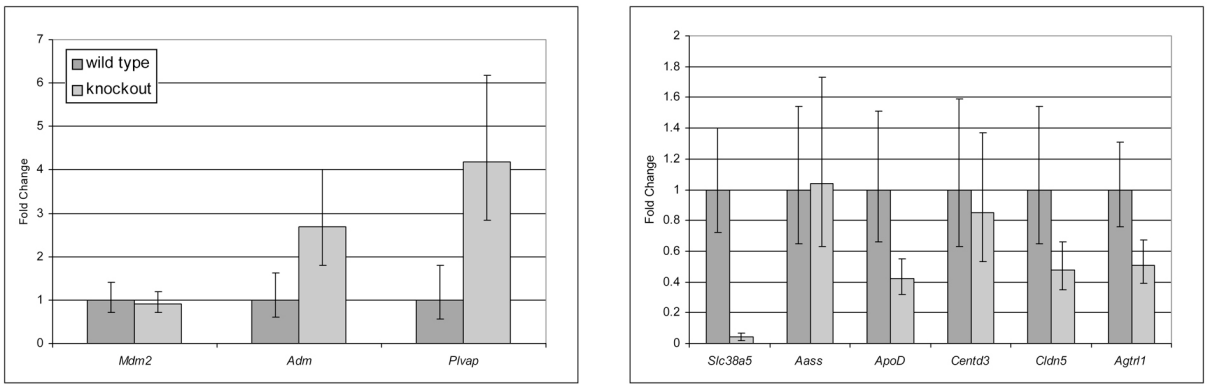

A increased expression at p7 **B** decreased expression at p7

Figure 51 Transcriptional analysis of selected genes in retinae of *Ndph*$^{y/-}$ knockout (n=5) and wild type (n=5) mice. The average expression value of the wild type group was set to 1. Error bars indicate the confidence interval at a significance level of 95% ($p<0.05$). Quantitative RT-PCR results from p7 retinae for genes that showed increased or decreased expression in the array experiment are depicted in (A) or (B), respectively. **(A)** Expression of Adrenomedullin (*Adm*; 2.7x) and the gene for the Plasmalemma vesicle associated protein (*Plvap*; 4.2x) is significantly increased at p7. **(B)** The neutral amino acid transporter *Slc38a5* (25x), Apolipoprotein D (*ApoD*; 2.4x) and Angiotensin II receptor-like 1 (*Agtrl1*; 2x) show significantly decreased expression at p7. Significant difference in Claudin 5 (*Cldn5*) expression is borderline. *18S / 28S rRNA* were used as endogenous controls.

3.2.4.4 Expression during development

We further investigated expression for the two most differently expressed verified genes, *Plvap* and *Slc38a5*, during postnatal retinal development. In addition to p7, qRT-PCR was conducted on retinal cDNA from p5, p10, p15 and p21 (Figure 52).

Plvap expression in the knockout was significantly increased at every developmental stage in comparison to the wild type. The difference increased about one order of magnitude in later stages (p15/p21) when compared to the earlier stages (p5-p10) (Figure 52a).

Slc38a5 expression was significantly decreased at every developmental stage in the *Ndph* knockout (Figure 52b). Fold-change was about ten times lower at p5 and p15, about twenty-five times lower at p7 and p10 and about three times lower at p21. Since the *Slc38a5* locus is located within 8.6 Mb from the *Ndph* locus, we investigated whether the observed difference was caused by a different genetic background, because the knockout *Ndph* allele is derived from the 129P2 mouse strain, which has then been backcrossed to the C57BL/6 background. We could not exclude a background effect by analysis of a genetic marker inside the *Slc38a5* locus (*rs13483703*), since it indicated the 129P2 allele at this position. Thus, we studied the expression of *Slc38a5* by additional qRT-PCR on p7 retinae of 129P2 wild type males and found similar levels as in the C57BL/6 wild type group (data not shown). Consequently, we excluded an influence of the genetic background on the expressivity of *Slc38a5.*

In summary, these developmental studies, which were performed on array-experiment independent RNA samples, added additional proof to the obtained microarray gene expression data.

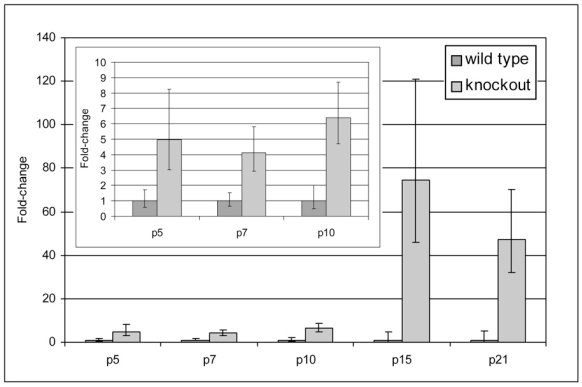

A expression of *Plvap* during development

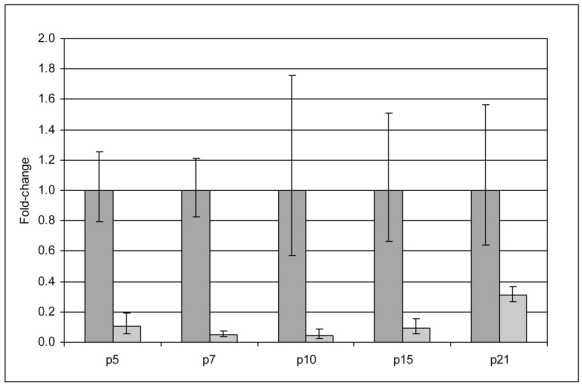

B expression of *Slc38a5* during development

Figure 52 Transcriptional analysis of the two most differently expressed verified genes in retinae of $Ndph^{y/-}$ knockout (n=5) and wild type (n=5) mice. The average expression value of the wild type group was set to 1. Error bars indicate the confidence interval at a significance level of 95% ($p<0.05$). **(A)** *Plvap* expression is significantly increased at every developmental stage from p5 to p21. Difference between wild type and knockout increases about one order of magnitude in later stages (p15/p21) when compared to the earlier stages (p5-p10). Insert shows expression data for p5-p10 in a different scale. **(B)** *Slc38a5* expression is significantly decreased at every developmental stage. Variability of wild type expression is higher in later stages (p10-p21) than in early stages (p5, p7). Following endogenous controls were used: (A): *18S* rRNA (B): *Gapd*

3.2.4.5 Immunohistological staining of Plvap

As gene expression differences do not always reflect consequences at the protein level, immunohistochemistry was also performed for Plvap at all developmental stages that have been investigated on the transcript level (plus p3 in addition). Eye cryosections of *Ndph*$^{y/-}$ and wild type mice were co-immunolabeled with antibodies directed against Plvap, a high specific marker for endothelial cells (MECA-32)[30], and collagen type IV (ColIV) to visualize the vascular beds[23] (Figure 53). In all stages investigated (p3-p21), ColIV staining has been observed in the choroid and the superficial retinal vasculature of both genotypes. Vessels of the inner retina, located in the outer and inner plexiform layers, were detected in later stages in the wild type, but not the knockout retina, as has been described before[13,15].

Plvap was localized similarly to the choroidal vessel system in both wild type and knockout animals at all investigated developmental stages. However, the Plvap staining pattern of the retinal vasculature differed considerably. In the wild type, labeling was very faint at most. Traces were observed in the superficial network at p3, but not in later stages, and the deep vessel system appeared to be slightly stained only at p10 (Figure 53, arrows). In contrast, Plvap staining in the knockout was detected as early as p3, but even more obvious and with increasing intensity at all later stages.

Taken together, these data show that Plvap expression in *Ndph*$^{y/-}$ retinae is increased not only on transcript, but also on protein level, which in particular seems to be confined to the retinal vasculature.

3.2.5 Discussion

3.2.5.1 Norrin and the role of Wnt-signaling

When Norrin has been shown to bind to the Wnt-receptors Frizzled-4 and LRP-5[23], it was suggested that signaling occurs through the canonical Wnt/beta-catenin pathway. Surprisingly, our study suggested only one gene among the most differently transcribed genes besides *Ndph* to be associated with this pathway: Adenomatosis polyposis coli down-regulated 1 (*Apcdd1*). This does not necessarily mean that Norrin is not exerting its function over binding to Wnt-receptors – but it may imply that Norrin does not work primarily as a transcriptional regulator via the canonical Wnt/beta-catenin signaling. However, this conclusion relies heavily on the number of currently known Wnt target genes, and on the assumption that this signaling actually occurs in p7 retinae - so it is still possible that this pathway is more prominent at another developmental stage. Furthermore, since we were not able to detect expression differences of two major angiogenesis-related genes albeit they have been shown to be regulated by Wnt-signaling (*Tie-2/Tek*[31] and *Vegfa*[32]), it is possible that Norrin has a direct role in controlling expression of Wnt-target genes in a spatially and temporally restricted manner which was not detectable by our experimental approach.

On the other hand, we were able to confirm differential expression of five genes that so far were not shown to be Wnt-targets.

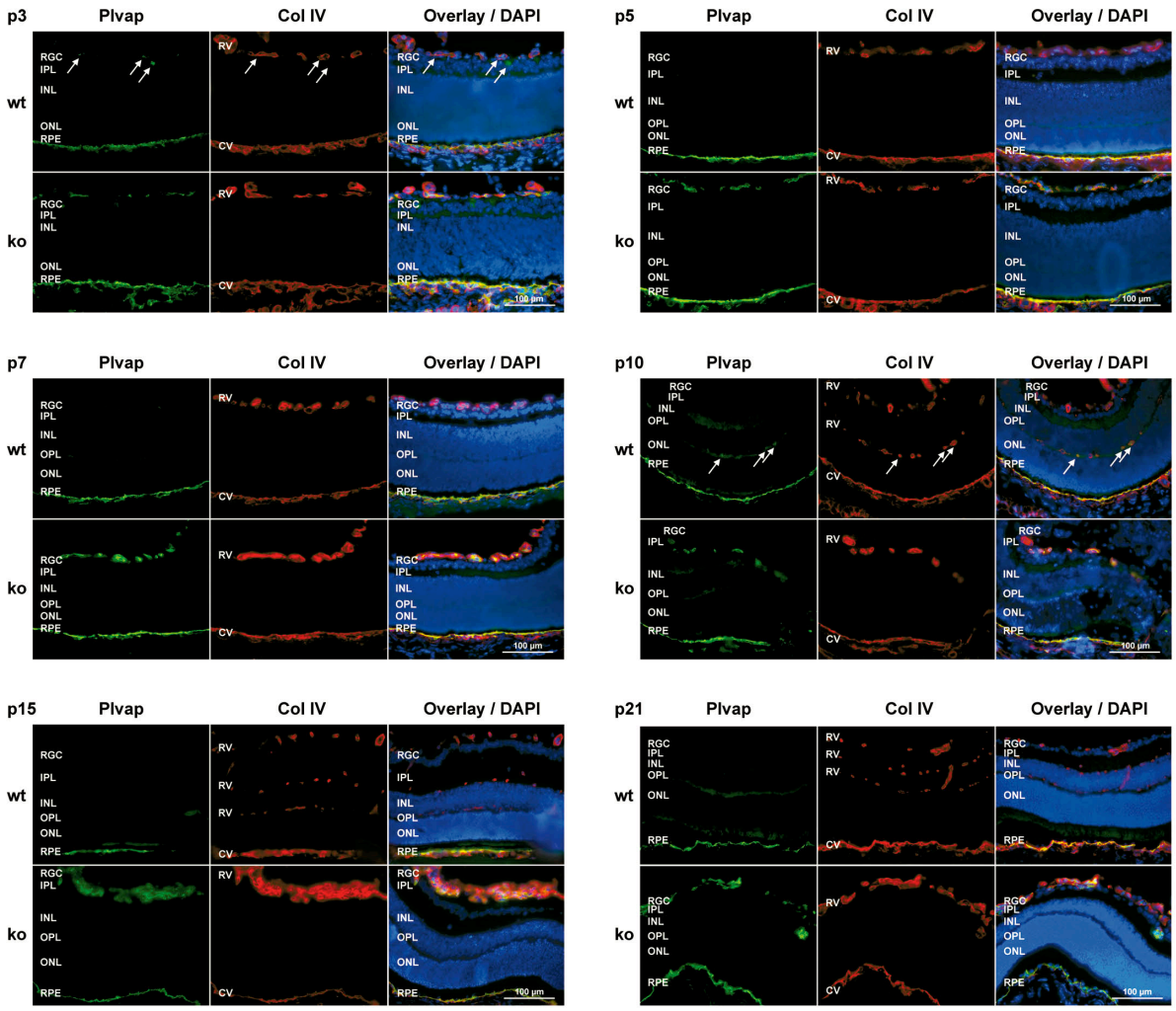

Figure 53 Immunofluorescence images of retinal cryosections of *Ndph*$^{y/-}$ mice in comparison to wild type. For each one of the indicated developmental stages (p3, p5, p7, p10, p15 and p21), co-immunolabeling with antibodies directed against Plvap (AF488; *green*) and Collagen IV (Cy3; *red*) has been performed. Collagen IV localizes to the extracellular matrix of endothelial cells and serves as a marker for blood vessels. In all stages investigated, staining has been observed in the choroid (CV, below the RPE) and the superficial retinal vasculature (RV, inside the RGC/nerve fibre layer). From p10 onwards, blood vessels of the secondary, deep retinal vasculature were detected in the OPL in the wild type, but not the knockout retina. In addition, at p15 and p21, the tertiary, intermediate vessel system in the IPL can be seen in the wild type. Plvap localizes to the choroid vessel system (CV) in both wild type and knockout at all developmental stages. Interestingly, Plvap expression has also been detected in the retinal vasculature (RV) of the knockout animals beginning at p3 and more intense over time. In contrast, the retinal vasculature of the wild type is not, or only very weakly, labeled by the Plvap antibody. In the superficial vessel network, staining in the wild type could only be detected at p3 (arrow), but not in later stages. At p10, slight staining of the deep vessel system was observed (arrows). *RV*: superficial / deep retinal vasculature; *CV*: Choroid; *RGC*: retinal ganglion cell layer; *IPL*: inner plexiform layer; *INL*: inner nuclear layer; *OPL*: outer plexiform layer; *ONL*: outer nuclear layer; *RPE*: retinal pigment epithelium.

3.2.5.2 Plvap as an early indicator for vascular permeability

Our results suggest an early involvement of Plvap (plasmalemma vesicle-associated protein) in the pathogenesis of *NDP*-related retinopathies. We found increased mRNA expression of *Plvap* throughout development (Figure 52a) and also conclusive differences between immuno-stained cryosections of wild type and *Ndph*$^{y/-}$ mice (Figure

53). Plvap is endothelial cell specific, and has been described as integral membrane glycoprotein associated with the stomatal diaphragms of caveolae, transendothelial channels, vesiculo-vacuolar organelles and the diaphragms of endothelial fenestrae[24,33]. Enhanced prevalence of endothelial fenestrae might result in reduced vascular integrity. Both have been observed in retinae of *Ndph*$^{y/-}$ mice as soon as p14[13,15]. Plvap expression further has been shown to be negatively correlated with the differentiation of the blood-brain-barrier[30]. Hence, elevated expression of Plvap may indicate enhanced vascular permeability and break-down of the blood-retina-barrier. It has previously been proposed that blood vessel leakiness is a result of hypoxia-driven VEGF (vascular endothelial growth factor A) upregulation[15] and thus is a secondary effect due to low oxygen supply. Interestingly, *Plvap* itself has been suggested to be a VEGF target[34], rendering a correlation between vessel leakiness and Plvap more likely. Thus, elevated expression of *Plvap* in later developmental stages (p15 onwards; Figure 52a, Figure 53), when a malformed/underdeveloped vasculature causes a pathologic hypoxic condition in the retina, was not surprising. Development of the superficial vessel system, however, is driven by a physiological hypoxia through induction of a periphery-to-center gradient of VEGF[14]. Noteworthy, this hypoxia-driven VEGF expression does not, or only marginally, yield visible Plvap expression in the wild type situation that is detectable by immunohistochemistry. Therefore, we think that an increased Plvap expression in early developmental stages (p3-p10; Figure 52a; Figure 53) of *Ndph*$^{y/-}$ mice is not secondary due to low oxygen supply and subsequent VEGF upregulation, but rather due to a lack of Norrin that may have an important influence on vascular development. This is supported by the observation that *Plvap* upregulation is not solely dependent on hypoxia or VEGF, but is also triggered by other activation of the Erk1/2 MAPK pathway[35]. In addition, also fenestrae induction has been shown to be VEGF-independent, as it is regulated through cytoskeletal remodeling by actin depolymerization[36]. However, we could not detect differences in total- and phosphorylated ERK1/2 MAP-kinase levels on Western blots with retinal protein extracts from p7 *Ndph*$^{y/-}$ wild type and knockout animals so far (data not shown). Additionally, differences in Plvap expression may be due to a mechanism of endothelial cells to compensate the impaired blood vessel development, because evidence has been provided before that Plvap might have a role in angiogenesis[37].

Thus, it remains to be shown whether a possible mode of action for Norrin, besides transcriptional regulation via the Wnt/β-catenin pathway, might be a direct modulation of the microtubule cytoskeleton[38] or Plvap itself. While we are aware of these alternatives, we hypothesize that transient Plvap expression and fenestration occur during maturation of the retinal vasculature and that Norrin signaling is possibly required for its suppression. This might be indicated by the faint staining of the superficial and deep vasculature in the wild type, which was only observed during early development of the respective network (p3 & p10), and the retinal expression pattern in the *Ndph*$^{y/-}$ knockout. Since mRNA and protein levels in the knockout have been higher at each developmental stage examined, Norrin might act as a suppressor of Plvap expression, and thus may be involved in sprouting angiogenesis as well as in the formation and maintenance of the blood-retina- or blood-brain-barrier.

3.2.5.3 Differential gene expression reflects impaired blood vessel development

Besides *Plvap*, we were able to confirm differential expression of four more genes. All but one of them seem to emphasize Norrin's hypothetical role in blood vessel development. *Agtrl1* (angiotensin II receptor-like 1) is a venous marker[39] that has been shown to be important for retinal angiogenesis[40]. Therefore, its two fold reduction correlates well with the observed retinal phenotype of the *Ndph* knockout mouse. However, we cannot exclude that this decreased expression is merely an indicator for the already reduced overall vessel density or, considering the venous/capillary nature of the deep vessel system[14], a lack of development of this particular network. The same applies to the 2.4x reduction of *ApoD* (apolipoprotein D). Nevertheless, *ApoD* could be implicated in the observed angiogenic defect of *Ndph*$^{y/-}$ mice, because it has been reported to stimulate proliferation and migration of vascular smooth muscle cells[41], probably through modulation of the cellular response to Pdgf-bb[42]. *ApoD* expression was suggested to be induced by PDGF-BB itself[43]. Interestingly, *Pdgfb* and *Pdgfrb* expression have been shown to be decreased in *Ndph*$^{y/-}$ mice in early stages (p5/p10) before[15], which could indicate reduced angiogenic activity. Although *Pdgfb* has been shown to be regulated by VEGF[43], *Vegfa* levels were not different at p5 and even higher at p10[15], suggesting an alternative, VEGF-independent transcriptional regulation of *Pdgfb*, and thus *ApoD*, in *Ndph* knockout mice. The possibility of a functional relationship between Norrin and *ApoD* might be supported by the finding of co-expression of these two genes in disease-affected organs. *APOD* has been shown to be upregulated in human endometrium during implantation[44], a process that is disturbed in female homozygous Norrin knockout mice[45]. Further, *ApoD* expression was also reported in the inner ear, another affected organ in Norrie disease patients and mice[46], where it has been suggested to be implicated in cochlear fluid homeostasis[47]. Taken together, Norrin may influence angiogenesis either by direct transcriptional regulation of *ApoD,* or indirectly via Vegfa-independent regulation of Pdgf-β.

Nearly three times elevated transcript levels in the knockout were observed for adrenomedullin (*Adm*) by quantitative RT-PCR. It has been described to be a hypoxia induced vasodilating peptide[48] that might have a vascular protective function[49]. Adm probably exerts its protective role through a reduction of oxidative stress[50] and has further been shown to inhibit vascular remodeling[51]. It is tempting to speculate that elevated expression of *Adm* itself could lead to a developmental defect due to its anti-angiogenic properties, and that improper transcriptional regulation might be the cause for it. Hence, also differential expression of *Adm* correlates well with the *Ndph*$^{y/-}$ phenotype.

Surprisingly, and in contrast to the other genes discussed here, the gene most differently expressed has not directly been linked to angiogenesis. *Slc38a5* (solute carrier familiy 38, member 5), which showed a twenty-five times decreased expression at p7 in *Ndph*$^{y/-}$ mice (Figure 52b), has been reported to be a main glutamine transporter in retinal Müller cells (system N2)[52]. It therefore may play an important role for the neuronal signal transduction through regulation of the glutamate/glutamine household. Its decreased expression in *Ndph*$^{y/-}$ mice may indicate an involvement of Müller glia cells as a target of Norrin signaling. This may be reflected by the reduced synaptic activity that has been observed by ERG measurements in later stages[53] and is consistent with our observation that *Slc38a5* expression is decreased at every developmental stage investigated, including the rather mature p21 (Figure 52b). Besides their importance for neural function, Müller cells also play a role as guidance structures for the developing

deep retinal vasculature[14]. As such, one could speculate that communication between Müller cells and blood vessels might be disturbed in Norrin knockout mice. Interestingly, it has been reported earlier that blood vessels of the ganglion cell layer are frequently not surrounded by glia in p14 *Ndph*$^{y/-}$ mice[13]. However, another possible explanation for reduced *Slc38a5* expression could be a secondary, neuroprotective response of Müller cells to oxidative stress. While this seems to be a likely mechanism at later, hypoxic stages in development (p15/p21), we think a ten-fold decreased expression of *Slc38a5* at p5 is unlikely to be exclusively the result of hypoxia-induced neuroprotection (Figure 52b). Besides this, no evidence for hypoxia at p5 has been provided so far: Western blots for the glial stress marker GFAP and the hypoxia-inducible factor 1-alpha (Hif1a) were shown to be similar up to p15 and p10, respectively, and no significant expression differences could be found for VEGF[15] at this stage. But *Slc38a5* is not only expressed in the retina: it is also abundant in astrocytic end feet in the brain, the highest levels being found in neocortex, hippocampus, striatum and the cerebellum[54].

Thus, differential expression of this molecule might be a hint for a possible pathogenic mechanism also in the brain that could be associated with the mental retardation phenotype of ND. Noteworthy in this context, a microdeletion including *SLC38A5* and the neighboring *FTSJ1* has been found in three brothers with moderate to severe mental retardation[55].

3.2.5.4 Conclusion

Consistent with data obtained from other developmental stages[15], our examination of p7 *Ndph* knockout mice showed insufficient retinal capillarization and lack of deep vessel formation. For the first time, vascular permeability has not been observed only in later, nearly adult stages, but was noted throughout development, as indicated by elevated mRNA and protein expression data for Plvap.

Because of the early developmental stage investigated here and the lack of neovascularization in later stages, we tend to consider a role of VEGF itself in the early pathogenesis of *NDP*-related diseases rather unlikely and ask whether Norrin instead might modulate the cellular response to VEGF. Norrin's hypothetical role as a transcriptional regulator of Wnt/β-catenin target genes is not obvious from the array experiment. However, our recent and previous studies suggest that Norrin is important for retinal angiogenesis. Here, we could identify several genes probably implicated in blood vessel development that may be transcriptionally regulated by Norrin, directly or indirectly. These genes include *Agtrl1*, *ApoD,* and *Adm*, while *Slc38a5* might represent an interesting candidate with regard to future research of aberrant neuronal development and the massive reactive gliosis that may be the basis for the often described pseudogliomas in ND patients[56]. Finally, due its proposed role in angiogenesis and blood vessel integrity[24,37], our findings suggest an important contribution of *Plvap* to the pathogenesis of Norrin-associated diseases.

3.2.6 Acknowledgments

The a-Plvap/MECA-32 monoclonal antibody developed by Eugene C. Butcher was obtained from the Developmental Studies Hybridoma Bank developed under the auspices of the NICHD and maintained by The University of Iowa, Department of Biological Sciences, Iowa City, IA 52242.

We would like to thank Marzanna Künzli from the Functional Genomics Center Zurich for conducting the microarray experiment from reverse transcription to raw data processing.

3.2.7 References

1. Warburg,M. Norrie's disease. A congenital progressive oculo-acoustico-cerebral degeneration. *Acta Ophthalmol (Copenh)*. 1966;Suppl 85:5-147.
2. Berger,W, Meindl,A, van de Pol,TJ et al. Isolation of a candidate gene for Norrie disease by positional cloning. *Nat Genet*. 1992;1:199-203.
3. Chen,ZY, Hendriks,RW, Jobling,MA et al. Isolation and characterization of a candidate gene for Norrie disease. *Nat Genet*. 1992;1:204-208.
4. Berger,W, van de,PD, Warburg,M et al. Mutations in the candidate gene for Norrie disease. *Hum Mol Genet*. 1992;1:461-465.
5. Berger,W. Molecular dissection of Norrie disease. *Acta Anat (Basel)*. 1998;162:95-100.
6. Meindl,A, Berger,W, Meitinger,T et al. Norrie disease is caused by mutations in an extracellular protein resembling C-terminal globular domain of mucins. *Nat Genet*. 1992;2:139-143.
7. Zaremba,J, Feil,S, Juszko,J et al. Intrafamilial variability of the ocular phenotype in a Polish family with a missense mutation (A63D) in the Norrie disease gene. *Ophthalmic Genet*. 1998;19:157-164.
8. Shastry,BS, Hejtmancik,JF, and Trese,MT. Identification of novel missense mutations in the Norrie disease gene associated with one X-linked and four sporadic cases of familial exudative vitreoretinopathy. *Hum Mutat*. 1997;9:396-401.
9. Shastry,BS, Pendergast,SD, Hartzer,MK et al. Identification of missense mutations in the Norrie disease gene associated with advanced retinopathy of prematurity. *Arch Ophthalmol*. 1997;115:651-655.
10. Black,GC, Perveen,R, Bonshek,R et al. Coats' disease of the retina (unilateral retinal telangiectasis) caused by somatic mutation in the NDP gene: a role for norrin in retinal angiogenesis. *Human Molecular Genetics*. 1999;8:2031-2035.
11. Chen,ZY, Battinelli,EM, Fielder,A et al. A mutation in the Norrie disease gene (NDP) associated with X-linked familial exudative vitreoretinopathy. *Nat Genet*. 1993;5:180-183.
12. Berger,W, van de,PD, Bachner,D et al. An animal model for Norrie disease (ND): gene targeting of the mouse ND gene. *Hum Mol Genet*. 1996;5:51-59.
13. Richter,M, Gottanka,J, May,CA et al. Retinal vasculature changes in Norrie disease mice. *Invest Ophthalmol Vis Sci*. 1998;39:2450-2457.
14. Fruttiger,M. Development of the retinal vasculature. *Angiogenesis*. 2007;10:77-88.
15. Luhmann,UF, Lin,J, Acar,N et al. Role of the Norrie Disease Pseudoglioma Gene in Sprouting Angiogenesis during Development of the Retinal Vasculature. *Invest Ophthalmol Vis Sci*. 2005;46:3372-3382.
16. Ohlmann,AV, Adamek,E, Ohlmann,A et al. Norrie Gene Product Is Necessary for Regression of Hyaloid Vessels. *Invest Ophthalmol Vis Sci*. 1-7-2004;45:2384-2390.
17. Masckauchan,TN and Kitajewski,J. Wnt/Frizzled signaling in the vasculature: new angiogenic factors in sight. *Physiology (Bethesda)*. 2006;21:181-188.
18. Feeney,SA, Simpson,DA, Gardiner,TA et al. Role of vascular endothelial growth factor and placental growth factors during retinal vascular development and hyaloid regression. *Invest Ophthalmol Vis Sci*. 2003;44:839-847.
19. Ohlmann,A, Scholz,M, Goldwich,A et al. Ectopic norrin induces growth of ocular capillaries and restores normal retinal angiogenesis in Norrie disease mutant mice. *J Neurosci*. 16-2-2005;25:1701-1710.
20. Robitaille,J, MacDonald,ML, Kaykas,A et al. Mutant frizzled-4 disrupts retinal angiogenesis in familial exudative vitreoretinopathy. *Nat Genet*. 2002;32:326-330.
21. Toomes,C, Bottomley,HM, Jackson,RM et al. Mutations in LRP5 or FZD4 underlie the common familial exudative vitreoretinopathy locus on chromosome 11q. *Am J Hum Genet*. 2004;74:721-730.
22. Wang,Y, Huso,D, Cahill,H et al. Progressive cerebellar, auditory, and esophageal dysfunction caused by targeted disruption of the frizzled-4 gene. *J Neurosci*. 1-7-2001;21:4761-4771.
23. Xu,Q, Wang,Y, Dabdoub,A et al. Vascular development in the retina and inner ear: control by Norrin and Frizzled-4, a high-affinity ligand-receptor pair. *Cell*. 19-3-2004;116:883-895.
24. Stan,RV, Kubitza,M, and Palade,GE. PV-1 is a component of the fenestral and stomatal diaphragms in fenestrated endothelia. *Proc Natl Acad Sci U S A*. 9-11-1999;96:13203-13207.
25. Hubbell,E, Liu,WM, and Mei,R. Robust estimators for expression analysis. *Bioinformatics*. 2002;18:1585-1592.
26. Draghici,S, Khatri,P, Tarca,AL et al. A systems biology approach for pathway level analysis. *Genome Res*. 2007;17:1537-1545.
27. Dennis,G, Jr., Sherman,BT, Hosack,DA et al. DAVID: Database for Annotation, Visualization, and Integrated Discovery. *Genome Biol*. 2003;4:3.

28. Mutch,DM, Berger,A, Mansourian,R et al. The limit fold change model: a practical approach for selecting differentially expressed genes from microarray data. *BMC Bioinformatics*. 21-6-2002;3:17.

29. Luhmann, U. F. Elucidation of Molecular Pathogenic Mechanisms of Norrie Disease (in german) *Freie Universität Berlin*. 2005

30. Hallmann,R, Mayer,DN, Berg,EL et al. Novel mouse endothelial cell surface marker is suppressed during differentiation of the blood brain barrier. *Dev Dyn*. 1995;202:325-332.

31. Masckauchan,TN, Agalliu,D, Vorontchikhina,M et al. Wnt5a Signaling Induces Proliferation and Survival of Endothelial Cells In Vitro and Expression of MMP-1 and Tie-2. *Mol Biol Cell*. 2006;17:5163-5172.

32. Zhang,X, Gaspard,JP, and Chung,DC. Regulation of vascular endothelial growth factor by the Wnt and K-ras pathways in colonic neoplasia. *Cancer Res*. 15-8-2001;61:6050-6054.

33. Niemela,H, Elima,K, Henttinen,T et al. Molecular identification of PAL-E, a widely used endothelial-cell marker. *Blood*. 15-11-2005;106:3405-3409.

34. Strickland,LA, Jubb,AM, Hongo,JA et al. Plasmalemmal vesicle-associated protein (PLVAP) is expressed by tumour endothelium and is upregulated by vascular endothelial growth factor-A (VEGF). *J Pathol*. 2005;206:466-475.

35. Stan,RV, Tkachenko,E, and Niesman,IR. PV1 is a key structural component for the formation of the stomatal and fenestral diaphragms. *Mol Biol Cell*. 2004;15:3615-3630.

36. Ioannidou,S, Deinhardt,K, Miotla,J et al. An in vitro assay reveals a role for the diaphragm protein PV-1 in endothelial fenestra morphogenesis. *Proc Natl Acad Sci U S A*. 7-11-2006;103:16770-16775.

37. Carson-Walter,EB, Hampton,J, Shue,E et al. Plasmalemmal vesicle associated protein-1 is a novel marker implicated in brain tumor angiogenesis. *Clin Cancer Res*. 1-11-2005;11:7643-7650.

38. Salinas,PC. Modulation of the microtubule cytoskeleton: a role for a divergent canonical Wnt pathway. *Trends Cell Biol*. 2007;17:333-342.

39. Saint-Geniez,M, Argence,CB, Knibiehler,B et al. The msr/apj gene encoding the apelin receptor is an early and specific marker of the venous phenotype in the retinal vasculature. *Gene Expr Patterns*. 2003;3:467-472.

40. Kasai,A, Shintani,N, Oda,M et al. Apelin is a novel angiogenic factor in retinal endothelial cells. *Biochem Biophys Res Commun*. 10-12-2004;325:395-400.

41. Leung,WC, Lawrie,A, Demaries,S et al. Apolipoprotein D and platelet-derived growth factor-BB synergism mediates vascular smooth muscle cell migration. *Circ Res*. 23-7-2004;95:179-186.

42. Sarjeant,JM, Lawrie,A, Kinnear,C et al. Apolipoprotein D inhibits platelet-derived growth factor-BB-induced vascular smooth muscle cell proliferated by preventing translocation of phosphorylated extracellular signal regulated kinase 1/2 to the nucleus. *Arterioscler Thromb Vasc Biol*. 2003;23:2172-2177.

43. Witmer,AN, van Blijswijk,BC, van Noorden,CJ et al. In vivo angiogenic phenotype of endothelial cells and pericytes induced by vascular endothelial growth factor-A. *J Histochem Cytochem*. 2004;52:39-52.

44. Kao,LC, Tulac,S, Lobo,S et al. Global gene profiling in human endometrium during the window of implantation. *Endocrinology*. 2002;143:2119-2138.

45. Luhmann,UF, Meunier,D, Shi,W et al. Fetal loss in homozygous mutant Norrie disease mice: A new role of Norrin in reproduction. *Genesis*. 2005;42:253-262.

46. Rehm,HL, Zhang,DS, Brown,MC et al. Vascular Defects and Sensorineural Deafness in a Mouse Model of Norrie Disease. *J Neurosci*. 1-6-2002;22:4286-4292.

47. Hildebrand,MS, de Silva,MG, Klockars,T et al. Expression of the carrier protein apolipoprotein D in the mouse inner ear. *Hear Res*. 2005;200:102-114.

48. Ogita,T, Hashimoto,E, Yamasaki,M et al. Hypoxic induction of adrenomedullin in cultured human umbilical vein endothelial cells. *J Hypertens*. 2001;19:603-608.

49. Ando,K and Fujita,T. Lessons from the adrenomedullin knockout mouse. *Regul Pept*. 15-4-2003;112:185-188.

50. Chini,EN, Chini,CC, Bolliger,C et al. Cytoprotective effects of adrenomedullin in glomerular cell injury: central role of cAMP signaling pathway. *Kidney Int*. 1997;52:917-925.

51. Matsui,H, Shimosawa,T, Itakura,K et al. Adrenomedullin can protect against pulmonary vascular remodeling induced by hypoxia. *Circulation*. 11-5-2004;109:2246-2251.

52. Umapathy,NS, Li,W, Mysona,BA et al. Expression and function of glutamine transporters SN1 (SNAT3) and SN2 (SNAT5) in retinal Muller cells. *Invest Ophthalmol Vis Sci*. 2005;46:3980-3987.

53. Ruether,K, van de,PD, Jaissle,G et al. Retinoschisislike alterations in the mouse eye caused by gene targeting of the Norrie disease gene. *Invest Ophthalmol Vis Sci*. 1997;38:710-718.

54. Cubelos,B, Gonzalez-Gonzalez,IM, Gimenez,C et al. Amino acid transporter SNAT5 localizes to glial cells in the rat brain. *Glia*. 15-1-2005;49:230-244.

55. Froyen,G, Bauters,M, Boyle,J et al. Loss of SLC38A5 and FTSJ1 at Xp11.23 in three brothers with non-syndromic mental retardation due to a microdeletion in an unstable genomic region. *Hum Genet*. 2007;121:539-547.

56. Bringmann,A and Reichenbach,A. Role of Muller cells in retinal degenerations. *Front Biosci*. 1-10-2001;6:E72-E92.

3.2.8 Contributions of authors to the manuscript „Differential gene expression in *Ndph* knockout mice in retinal development"

N.F.S.: Planning and administration of mouse breedings, preparation of animals, preparation of cryosections and flat-mounts, selection of target genes, immunohistochemistry (IHC), morphometric analyses, preparation of RNA, qRT-PCR, Western blots (WB), interpretation of data, writing of the manuscript

U.F.L.: Conceptualization of the experiment, supervision of the initial experiments of the study, editing of the manuscript

S.F.: Technical assistance with mouse genotyping, HE staining, IHC

W.B.: Principal investigator (PI), conceptual planning, design and supervision of the entire study, interpretation of data, editing of the manuscript

M.K.: Technical assistance with the microarray experiment, from reverse transcription to raw data processing

3.3 Further experiments on differential expression in Ndph knockout mice

3.3.1 Whole genome cDNA microarray

In addition to the results published in the IOVS paper (Table 39; Table 40), the complete list of differentially expressed genes without fold-change cut-off and without multiple testing correction at p<0.01 can be found in the appendix (this list was the basis of the pathway analysis referenced in the publication).

3.3.2 Analysis of microarray candidate genes

3.3.2.1 Plasmalemma vesicle associated protein (Plvap)

Retinal mRNA transcripts of the plasmalemma vesicle associated protein (*Plvap*) were increased in the microarray experiment (p7; Table 40), and retinal expression was shown to be increased throughout postnatal retinal development from p5 to p21 (Figure 52 A), especially at more advanced stages. In retinal cryosections, ectopic expression in the retinal vasculature of the *Ndph* ko was detected (Figure 53).

3.3.2.1.1 Western blots from retinal protein extracts

Specificity of the Plvap antibody was supported by Western blots, which did show several bands, but most prominently stained a protein at the expected size between 50-55kDa. These presumptive Plvap protein levels appeared to be higher in the ko than in the wt (Figure 54), but not as high as the transcript levels (Figure 52 A).

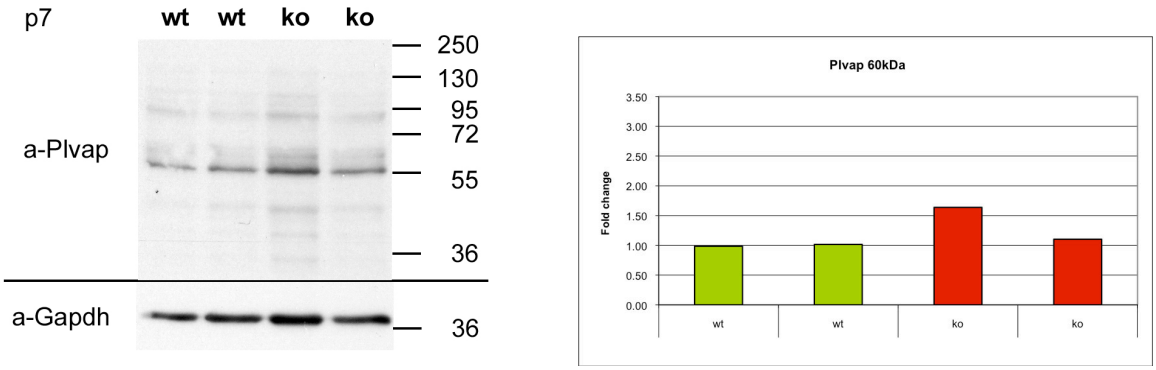

A Plvap Western blot

B Plvap WB quantification

Figure 54 Western blot and corresponding densitometric quantification of 22µg p7 retinal protein extracts of *Ndph* wt and ko mice stained with an antibody against Plvap. For densitometric quantification, density values have been normalized to Gapdh expression and calibrated on the wild type mean. **(A)** The most prominent bands in the Western blot are in the range of the predicted ~50-55 kDa band. Plvap levels in the knockout appear to be marginally higher in the knockout, which could be confirmed by the densitometric analysis **(B)**.

3.3.2.1.2 Immunohistology on retinal flatmounts

In addition to sections, immunohistology was also performed on retinal flatmount preparations (Figure 55). Plvap immunoreactivity was ectopically detected in all blood vessels of the superficial network. Expression was especially prominent in veins, while it appeared reduced in arteries. However, this result could not be confirmed in subsequent experiments.

A Collagen IV **B** Plvap **C** Merge

Figure 55 Retinal flatmount preparation from a p7 *Ndph* ko. (A) An antibody against Collagen IV was used to label the extracellular matrix of the vasculature. (B) Plvap expression was ectopically detected in every retinal blood vessel. (C) The overlay picture reveals predominant Plvap labeling of the capillaries and veins. The major arteries (arrows) appear to be less stained.

3.3.2.2 Solute carrier family 38, member 5 (Slc38a5)

The solute carrier *Slc38a5* was the transcript with the most decreased expression in the microarray experiment (Table 40), and retinal expression was shown to be reduced in norrin ko mice throughout postnatal retinal development from p5 to p21 (Figure 52 B). Slc38a5, a neutral amino acid transporter, has been shown to be an important glutamine transporter in the retina (Umapathy et al., 2005).

3.3.2.2.1 Western blots from retinal protein extracts

To further investigate differential expression, I obtained a custom antibody against the rat *Slc38a5* protein from Francisco Zafra, Madrid (Cubelos et al., 2005). Western blots with p7 retinal protein extracts showed the expected specific staining pattern (Cubelos et al., 2005) and could confirm high specificity of the antiserum also in mouse. Two bands of the predicted size of 50kDa for the monomer and ~200kDa for a possible tetramer were detected (Figure 56). The 200kDa band was higher expressed in the *Ndph* knockout samples. However, densitometric quantification confirmed the impression that protein levels of the 50kDa band were similar in wt and ko.

3.3.2.2.2 Immunohistology of retinal cryosections

Staining of retinal cryosections showed a strong signal in the outer plexiform layer at p7 (Figure 57). Since Slc38a5 has been described as Müller cell specific glutamine-transporter (Umapathy et al., 2005), this localization to a synaptic region was in line with my expectations. However, no differences could be observed between wild type

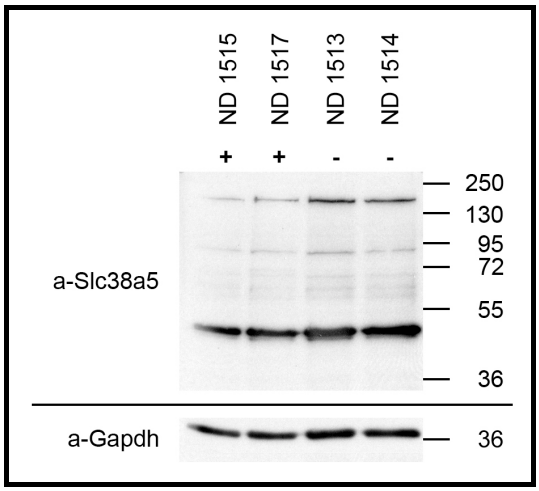

A Slc38a5 Western blot

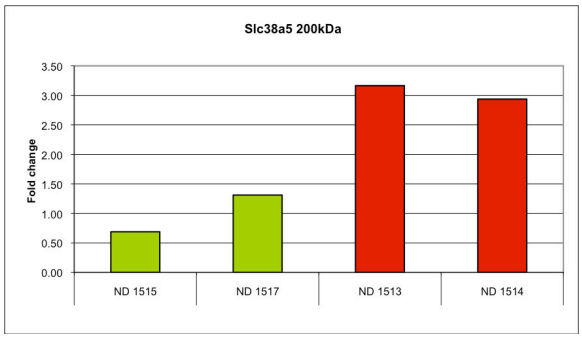

B Slc38a5 WB quantification 200kDa band

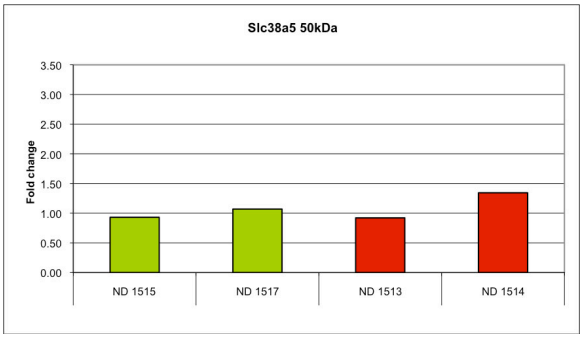

C Slc38a5 WB quantification 50 kDa band

Figure 56 Slc38a5 Western blot and densitometric quantification of 22µg p7 retinal protein extracts of *Ndph* wt (+; *green*) and ko (-; *red*) mice. Density values have been normalized to Gapdh expression and calibrated on the wild type mean. **(A)** Western blot stained with anti-Slc38a5 serum detects two bands of the predicted size of 50kDa for the monomer and ~200kDa for a possible tetramer (Cubelos et al., 2005). **(B)** Densitometric quantification verified stronger expression of the 200kDa band in the knockout samples. **(C)** However, densitometric quantification of the smaller band confirmed the impression that protein levels between wt and ko are comparable.

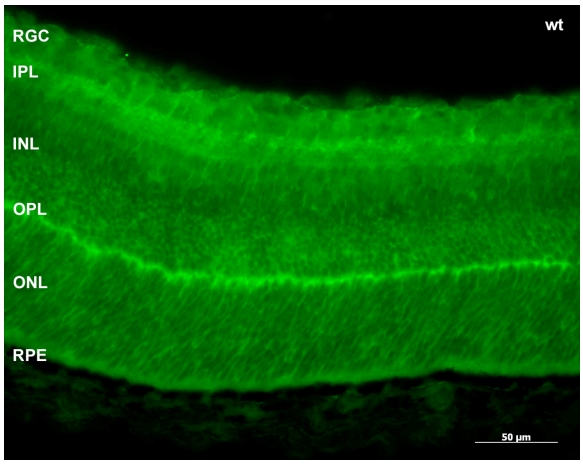

A

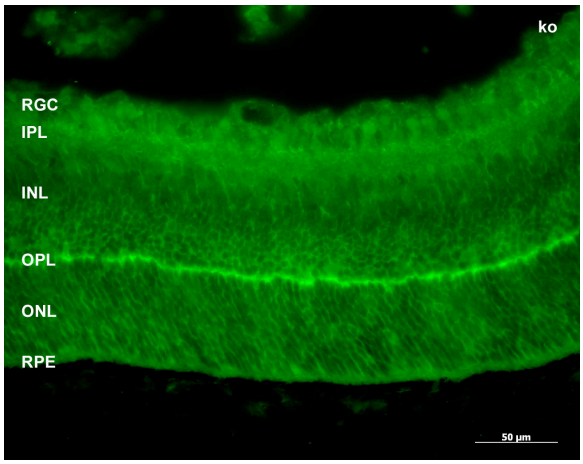

B

Figure 57 Immunofluorescence images of p7 retinal cryosections of *Ndph* wt **(A)** in comparison to knockout mice **(B)**. The antibody against Slc38a5 (detected with a 2nd antibody labeled with AF488; *green*) detects a strong signal in the outer plexiform layer (OPL). No differences between wild type and knockout could be observed. *RGC*: retinal ganglion cell layer; *IPL*: inner plexiform layer; *INL*: inner nuclear layer; *OPL*: outer plexiform layer; *ONL*: outer nuclear layer; *RPE*: retinal pigment epithelium

and knockout specimen, which is in contrast to the significant difference on mRNA level that is about 20-fold lower in the knockout at p7 (Figure 52 B). Since this Slc38a5 antibody has been raised against a rat-peptide, a possible cross-reactivity with other epitopes in the mouse cannot be excluded.

3.3.2.2.3 Expression of Slc38a5 in the cerebellum

Slc38a5 was also found in astrocytes of the cerebellum (Cubelos et al., 2005). If norrin regulates expression of *Slc38a5* in the retina, it is possible that it also controls it in the cerebellum, where *Ndph* is expressed the most among all investigated brain regions (Table 36).

To test this hypothesis, qRT-PCR analyses with RNA extracts from p21 cerebella were conducted by Walther Hänseler (as part of his Masterthesis under my supervision). Indeed, reduced *Slc38a5* expression in the cerebellum of p21 *Ndph* ko mice was found (Figure 58; Hänseler, Masterthesis, 2008).

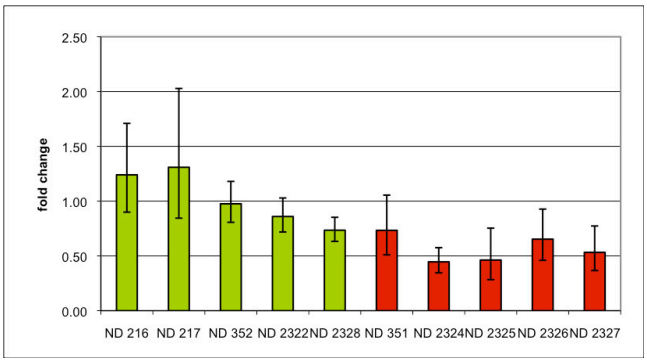

A

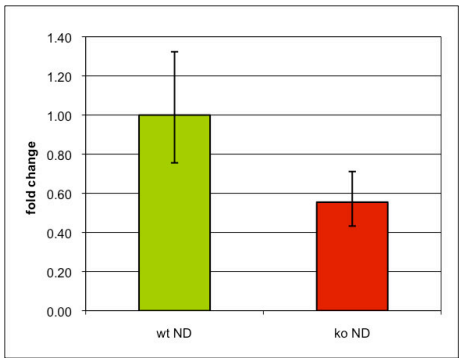

B

Figure 58 Transcriptional analysis of *Slc38a5* in cerebella of p21 *Ndph*$^{y/-}$ knockout (n=5) and wild type (n=5) mice. The average expression value of the wild type group was set to 1. Error bars indicate the confidence interval at a significance level of 95% ($p<0.05$). **(A)** *Slc38a5* mRNA expression of the individual animals. **(B)** Decrease of *Slc38a5* expression is significant when calculated for the biological replicates. *Pol2a* was used as endogenous control. (Source: Masterthesis Hänseler, 2008)

3.3.2.2.4 Immunohistology on cerebellar cryosections

We then also conducted immunohistochemistry with the Slc38a5 antibody on brain sections. Staining intensity was generally weak, but appeared to be stronger in sections from norrin wt mice (Figure 59). In the cerebellum, labeling was most intense around the Purkinje cells.

3.3.2.2.5 Western blots from cerebellar protein extracts

Walther Hänseler also performed a Western blot with cerebellar protein extracts from p21 norrin wt and ko mice. Again, like in the WB with retinal samples, staining was specific, producing the two monomeric and tetrameric bands (Figure 60 A). Densitometric quantification suggested a stronger expression of the 200kDa band in the ko samples, although not as clear as in the retina (Figure 60 B). No differences were observed for the monomeric band (Figure 60 C).

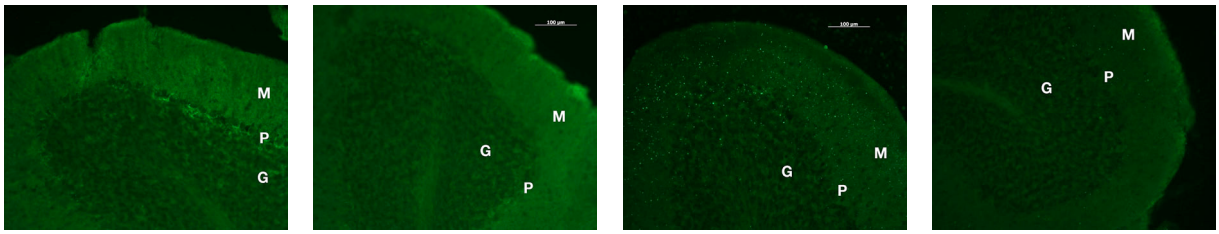

A p21 *Ndph* wt **B** p21 *Ndph* wt **C** p21 *Ndph* ko **D** p21 *Ndph* ko

Figure 59 Cerebellar cryosections stained for Slc38a5. Four p21 animals were examined, 2 wild type **(A,B)** and 2 *Ndph* knockout **(C,D)**. Staining generally appears more intense in the wt samples. Strongest staining was found in (A), labeling areas around the Purkinje cells. *M:* molecular layer; *P:* Purkinje cell layer; *G:* granular cell layer. (Source: Masterthesis Hänseler, 2008)

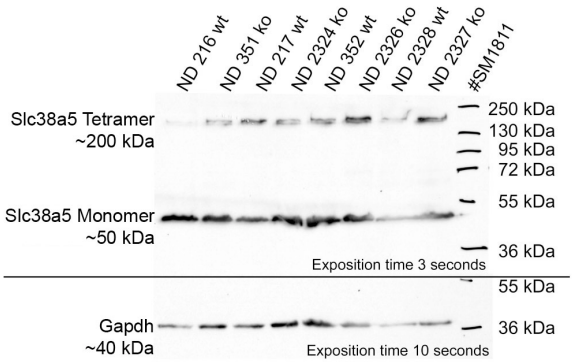

A Slc38a5 Western blot

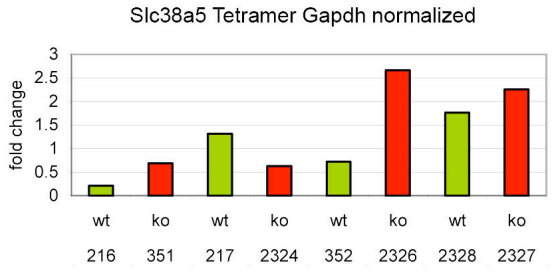

B Slc38a5 WB quantification 200kDa band

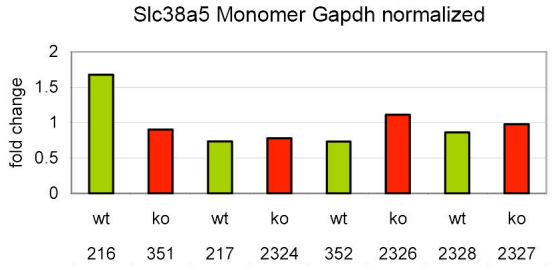

C Slc38a5 WB quantification 50 kDa band

Figure 60 Slc38a5 Western blot and densitometric quantification of p21 cerebellar protein extracts of *Ndph* wt (*green*) and ko (*red*) mice. Density values have been normalized to Gapdh expression and calibrated on the wild type mean. **(A)** Western blot stained with anti-Slc38a5 serum detects two bands of the predicted size of 50kDa for the monomer and ~200kDa for a possible tetramer (Cubelos et al., 2005). **(B)** Densitometric quantification suggests a trend to stronger expression of the 200kDa band in the knockout samples. **(C)** Densitometric quantification of the smaller band confirmed the impression that protein levels between wt and ko are comparable. (Source: Masterthesis Hänseler, 2008)

3.3.2.3 Apolipoprotein D (ApoD)

Retinal mRNA expression of apolipoprotein D (*ApoD*) revealed lower expression in the *Ndph* ko not only at p7 (as published in the IOVS publication), but also at p5 (Figure 61).

3.3.2.3.1 Immunohistology of retinal cryosections

Cryosections treated with an antibody against ApoD resulted in weak labeling of presumably amacrine and horizontal cells, although no differences could be detected between norrin wild type and knockout (Figure 62). No protein at the expected molecular weight of about 21 kDa was labeled on Western blots with p7 retinal protein extracts. Only multiple bands of a different molecular weight were detected, indicating that the antibody probably is unspecific.

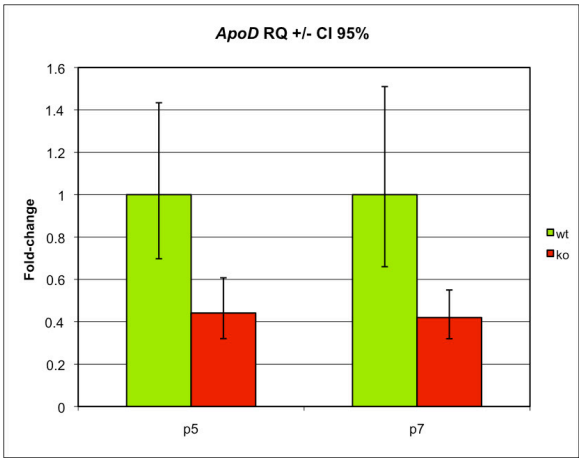

Figure 61 Transcriptional analysis of apolipoprotein D (*ApoD*) in retinae of *Ndph*$^{y/-}$ knockout (n=5; *red*) and wild type (n=5; *green*) mice. Postnatal time points p5 and p7 were investigated. The average expression value of the wild type group was set to 1. Error bars indicate the confidence interval at a significance level of 95% ($p<0.05$). Transcript expression of *ApoD* was significantly lower in the *Ndph* knockout at both p5 (2.3x) and p7 (2.4x) . *18S rRNA* was used as endogenous control.

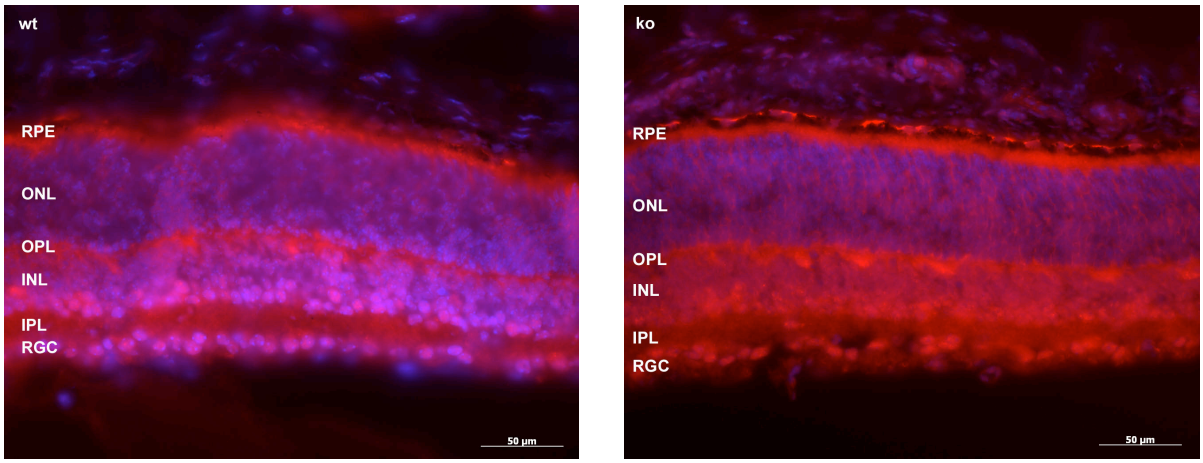

A **B**

Figure 62 Immunofluorescence images of p10 retinal cryosections of *Ndph*$^{y/-}$ mice **(B)** in comparison to wild type **(A)**. The antibody against ApoD (detected with a 2nd antibody labeled with Cy3; *red*) detects

signals in the inner nuclear layer (INL) at the border to the plexiform layers, as well as cells in the retinal ganglion cell layer. These cells could be horizontal (at the border to the OPL) and amacrine cells. Counterstaining with DAPI (*blue*). No differences between wild type and knockout could be observed. *RGC*: retinal ganglion cell layer; *IPL*: inner plexiform layer; *INL*: inner nuclear layer; *OPL*: outer plexiform layer; *ONL*: outer nuclear layer; *RPE*: retinal pigment epithelium

3.3.2.4 Angiotensin receptor-like 1 (Agtrl1)

Transcript analysis of angiotensin receptor-like 1 (*Agtrl1*) revealed significant lower expression in the *Ndph* ko retina at p7 (as published in the IOVS publication), but not at p5 (Figure 63 A), although a trend to lower expression was observed. This was in contrast to my hypothesis: I expected reduced expression of *Agtrl1* also earlier than p7, because it has been shown to be important for retinal angiogenesis (Kasai et al., 2004), the process impaired in the *Ndph* ko mouse retina.

3.3.2.4.1 Immunohistology of retinal cryosections

Unfortunately, no specific staining could be obtained with the antibody against Agtrl1 on eye or brain cryosections, or on Western blots with p7 retinal extracts, which only showed many unspecific bands.

3.3.2.5 Adrenomedullin (Adm)

Adrenomedullin (*Adm*) has been described to be a hypoxia induced vasodilating peptide (Ogita et al., 2001) that might have a vascular protective function (Ando and Fujita, 2003). At p21, hypoxia in the norrin ko retina is evident due to the under-developed retinal vasculature (Luhmann et al, 2005a). Thus, in addition to p7, p21 retina was analyzed by qRT-PCR. Indeed, retinal mRNA expression of *Adm* was elevated even more in the *Ndph* ko at p21 (10x) than at p7 (2.7) (Figure 63 B).

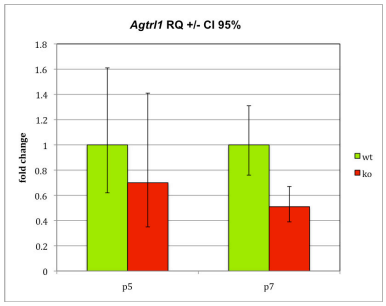

A Retinal *Agtrl1* expression

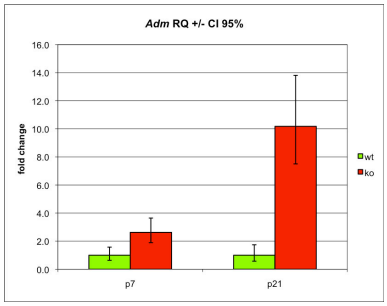

B Retinal *Adm* expression

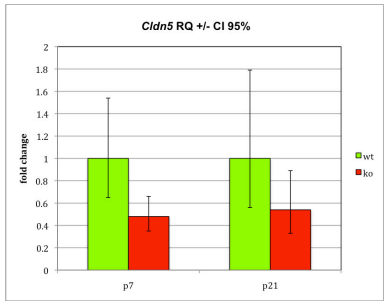

C Retinal *Cldn5* expression

Figure 63 Transcriptional analysis of angiotensin receptor-like 1 (*Agtrl1*), adrenomedullin (*Adm*), and claudin 5 (*Cldn5*) in retinae of *Ndph*$^{y/-}$ knockout (n=5; *red*) and wild type (n=5; *green*) mice. Postnatal time points p5 and p7 (*Agtrl1*) or p7 and p21 (*Adm, Cldn5*) were investigated. The average expression value of the wild type group was set to 1. Error bars indicate the confidence interval at a significance level of 95% ($p<0.05$). **(A)** Transcript expression of *Agtrl1* was significantly lower in the *Ndph* knockout at p7, but not at p5. **(B)** Expression of *Adm* mRNA was significantly higher in the *Ndph* knockout at p7 and especially at p21. **(C)** No significant differences were detected in *Cldn5* expression. However, there is a trend to lower mRNA levels in the *Ndph* ko at both time points, and significance is borderline at p7. *18S rRNA* was used as endogenous control.

3.3.2.6 Claudin 5 (Cldn5)

Significance of claudin 5 (*Cldn5*) transcript expression between *Ndph* wt and ko was only borderline at p7. Since claudin 5 plays a major role in tight junction-specific obliteration of the intercellular space in CNS endothelial cells (Nitta et al., 2003), differential expression of *Cldn5*, in addition to *Plvap*, could explain leakiness of vessels. Thus, *Cldn5* appeared as an attractive candidate gene, and expression was analyzed additionally at p21, when the vasculature in the norrin ko is leaky. However, no significant difference at the transcript level was detected, although the mean expression value was, like in the p7 retina, reduced two fold (Figure 63 C).

3.3.2.7 Abcb1a, Prdm9, and Vwf

ATP-binding cassette, sub-family B (MDR/TAP), member 1A (*Abcb1a*), PR domain containing 9 (*Prdm9*), and von Willebrand factor homolog (*Vwf*) were on the long list of differentially expressed genes, exhibiting a considerable fold-change (see complete list in the appendix), but were excluded through the multiple testing correction procedure from the published table (Table 40). Nonetheless, transcript analysis by qRT-PCR was performed, but no significant expression differences were observed, confirming the microarray results (Figure 64).

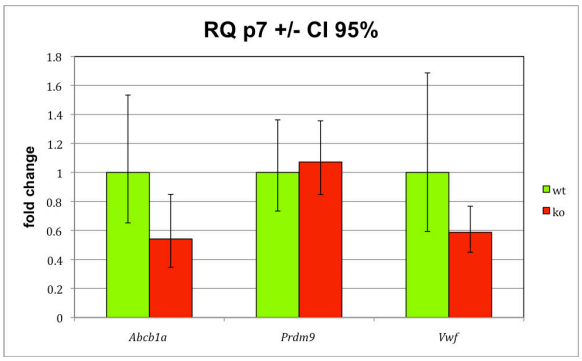

Figure 64 Transcriptional analysis of ATP-binding cassette, sub-family B (MDR/TAP), member 1A (*Abcb1a*), PR domain containing 9 (*Prdm9*), and von Willebrand factor homolog (*Vwf*) in retinae of p7 *Ndph*$^{y/-}$ knockout (n=5; *red*) and wild type (n=5; *green*) mice. The average expression value of the wild type group was set to 1. Error bars indicate the confidence interval at a significance level of 95% ($p<0.05$). No significant differences in gene expression were observed, verifying the microarray results. *18s rRNA* was used as endogenous control.

3.3.2.8 Expression of microarray candidate genes in cerebellum

As part of his Master thesis, Walther Hänseler also performed qRT-PCR analyses with cerebellar mRNA of the target genes I have analyzed in the p7 retina. Besides the p21 results for *Slc38a5*, no significant differences were found for *Abcb1a*, *Aass*, *Adm*, *Agtrl1*, *ApoD*, *Centd3*, *Cldn5*, *Plvap*, *Prdm9*, and *Vwf* expression in either adult or p21 cerebellum. (Masterthesis Hänseler, 2008)

3.3.3 Analysis of mitogen-activated protein kinase (MAPK) activity

It has been shown that *Plvap* expression can be triggered through activation of the extracellular signal-regulated kinase 1/2 (Erk1/2) MAPK pathway (Stan et al., 2004). Since Plvap mRNA and protein levels were increased in the retina of *Ndph* ko mice, I hypothesized that Erk1/2 MAPK levels could be enhanced, too. Thus a Western blot experiment with p7 retinal protein extracts was performed, stained with antibodies against total and phosporylated Erk1/2 MAPKs. Possible differences in MAPK activity would have been visible by a differential ratio of phosphorylated to total Erk1/2 MAP-kinases. However, no genotype-specific differences were detected (Figure 65).

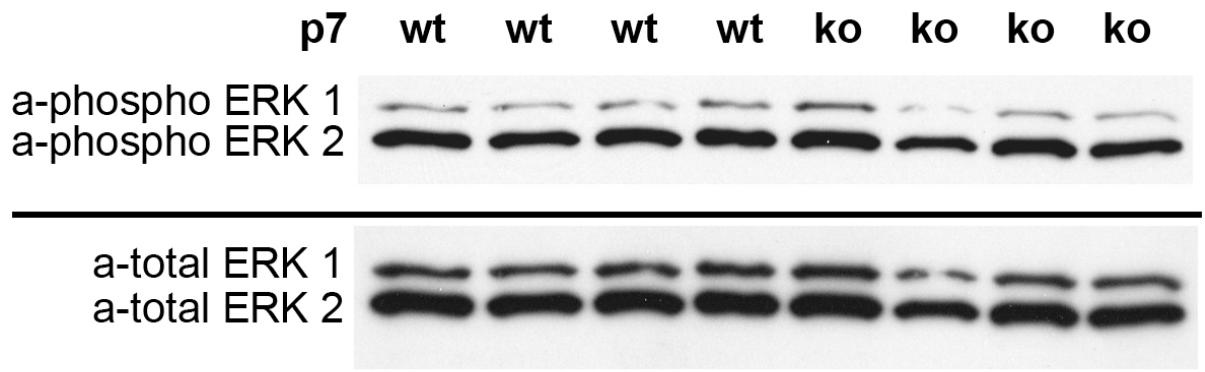

A

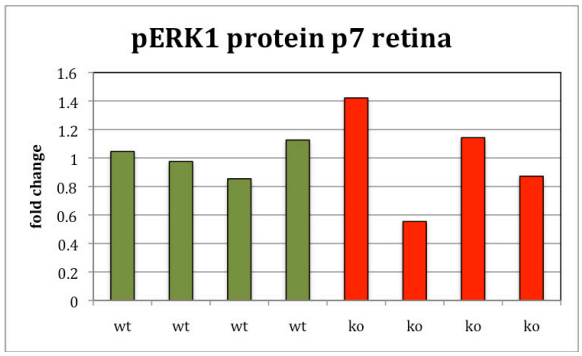

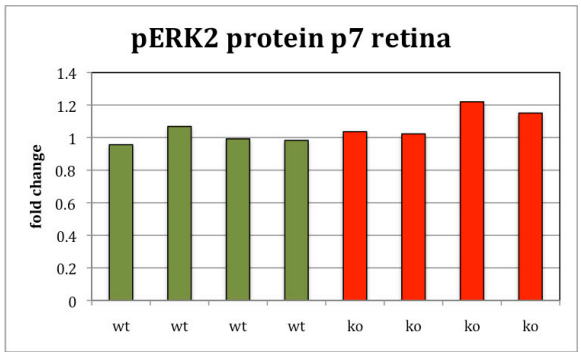

B **C**

Figure 65 Retinal expression of ERK1/2 mitogen-activated protein kinases. **(A)** Western blot with 40µg p7 retinal protein extract (supernatant) loaded in each lane from ND p7 animals. Two prominent bands at ~42kDa and ~44kDa are visible that correspond to the Erk1/2 products. Total MAPK also served as a loading control. No obvious difference between *Ndph* wt and ko bands was noted. **(B)** The densitometric analysis of ERK1 confirmed this impression. Expression of the phosphorylated ERK1 was normalized to total ERK1 expression. The mean of the wt samples was set to 1. Reduced expression of the second ko sample is likely due to an experimental artifact. **(C)** Densitometric analysis of ERK2 analog to (B). Also here, no differences were observed.

3.3.4 Analysis of whole genome microRNA (miRNA) expression

MicroRNAs (miRNAs) are a small RNA species involved in gene suppression (Hamilton and Baulcombe, 1999), and miRNA encoding genes are distributed all over the eukaryotic genome. Their transcripts are cleaved into 60–70 nucleotide microRNA precursors (pre-microRNAs) by a microprocessor complex containing the nuclear RNaseIII Drosha and DiGeorge syndrome critical region 8 protein (Denli et al., 2004; Gregory and Yan et al., 2004; Han and Lee et al., 2004). Pre-microRNAs are then exported from the nucleus and are cleaved by a cytoplasmic RNase III and Dicer. The resulting mature 22bp microRNAs are incorporated into an RNA-induced silencing complex to act as target recognition sequences (Gregory et al., 2005). Many mRNAs contain target sequences for miRNAs and, as a consequence of binding to the silencing complex, can undergo cleavage or translational repression (reviewed in Bartel, 2004).

3.3.4.1 Micro RNAs in angiogenesis and ocular vascular development

Several studies suggest a potential role of microRNAs in angiogenesis. Migration and tube formation of cultured vascular endothelial cells (HUVECs) are reduced by transfection of miR-221/-miR-222 (Poliseno et al., 2006) or global changes in microRNAs induced by knockdown of Dicer (Suárez et al., 2007). Dicer knockout mice die during the embryonic stage because of disruption of the vascular development (Yang et al., 2005), indicating that microRNAs play a critical role in this process. A microarray analysis with ischemic murine retinas (using the *oxygen induced retinopathy (OIR)* technique) revealed 3 miRNAs (miR-31, -150, and -184) that are downregulated during ischemia-induced neovascularization (NV) (Shen et al., 2008). Intraocular injection of pre-miR-31, -150, or -184 significantly reduced ischemia-induced retinal NV, and the authors could further show that miR-31 and -184 are constitutively highly expressed in cornea and lens, two completely avascular tissues.

3.3.4.2 Global miRNA expression in the developing Ndph ko retina

Thus, miRNAs seem to play a crucial role in ocular vascular development. Since we hypothesized that norrin could act as a transcriptional regulator of target genes, and vascular development is impaired in the *Ndph* ko mouse and in ND patients, I also investigated differential miRNA expression in the *Ndph* ko mouse retina.

Two developmental stages were investigated, p5 and p21. Since miRNA microarrays became first available just during the course of my thesis, I wanted to perform the first experiment with a developmental stage that already exhibits large-scale differences between the genotypes. This way, I could expect to see several differentially expressed miRNAs, even if the microarray should turn out to be insensitive. At p21, the *Ndph* ko retina has been shown to be severely hypoxic, just like the retina of the OIR-model Shen et al. used for their experiments. Thus, similar results could be expected. Potential miRNA expression differences at p5 may then be clearly attributable to the *Ndph* knockout genotype, because pathologic retinal hypoxia has not yet developed at this stage.

3.3.4.3 P21 retina

The total number of murine miRNAs known at the time point of the experiment was 547 (human: 706). 40% of them (219) were expressed in the p21 retina. 35 miRNAs were significantly differentially expressed in the *Ndph* ko ($p<0.01$), of which 12 exhibited a fold change over 1.3 (Figure 66). As expected, comparison of my results with the data generated in the OIR model suggested that the *Ndph* ko retina is in a similar (presumably hypoxic) condition as in the OIR model (see discussion; Figure 113).

3.3.4.4 P5 retina

After the miRNA chip has been validated with the p21 experiment, the second run with p5 retinas was performed. Technical requirements (RNA quality, chip readout) were fulfilled: 46% (250) of all known murine miRNAs were expressed in the p5 retina. Expression profiles of the individual samples clustered into two groups. However, no significant differences between *Ndph* wt and ko samples were observed. The samples instead clustered into two groups according to their belonging to one of two litters, with one exception (Figure 67). This exception most likely was due to a confusion. Because both samples were *Ndph* ko, no effect on the comparison between norrin wt and ko had to be assumed. The litter-specific differences were surprising, because all tested animals were offspring of the same parents. The only possible explanation for the significant expression differences between the litters would be a different developmental stage, although both were prepared 5 days after birth.

Increased	Entrez Gene ID	ProbeName
2.15	mmu-miR-322	A_54_P2504
2.09	mmu-miR-210	A_54_P1444
1.75	mmu-miR-126-3p	A_54_P2285
1.53	mmu-miR-27a	A_54_P4385
1.42	mmu-miR-142-3p	A_54_P2308
1.38	mmu-miR-132	A_54_P1054
1.33	mmu-miR-23a	A_54_P1311
1.29	mmu-miR-223	A_54_P2629
1.29	mmu-miR-326	A_54_P1366
1.25	mmu-miR-34c	A_54_P1247
1.22	mmu-miR-34b-5p	A_54_P2446
1.20	mmu-miR-140	A_54_P1075
1.17	mmu-miR-335-3p	A_54_P2691
1.17	mmu-miR-24	A_54_P1143
1.11	mmu-miR-21	A_54_P1307

Decreased	Entrez Gene ID	ProbeName
1.45	mmu-miR-129-3p	A_54_P1337
1.43	mmu-miR-129-5p	A_54_P2343
1.40	mmu-miR-375	A_54_P1511
1.39	mmu-miR-211	A_54_P1466
1.30	mmu-miR-7a	A_54_P2659
1.27	mmu-miR-135b	A_54_P2589
1.25	mmu-miR-33	A_54_P2637
1.19	mmu-miR-149	A_54_P2321
1.18	mmu-miR-218	A_54_P1458
1.15	mmu-miR-137	A_54_P1069
1.14	mmu-miR-30a	A_54_P4363
1.11	mmu-miR-106b	A_54_P1263
1.10	mmu-miR-29c*	A_54_P3467
1.10	mmu-miR-219	A_54_P1459
1.10	mmu-miR-138	A_54_P1073
1.09	mmu-miR-92a	A_54_P2496
1.07	mmu-miR-183*	A_54_P3334
1.07	mmu-miR-361	A_54_P1499
1.05	mmu-miR-376b	A_54_P2716
1.03	mmu-miR-384-5p	A_54_P2696

Figure 66 Global miRNA expression expression analysis of p21 retinas revealed 35 miRNAs that were significantly differentially expressed in the *Ndph* ko ($p<0.01$). Expression of 12 transcripts was different by more than 1.3 fold change: 7 were increased, and 5 were decreased.

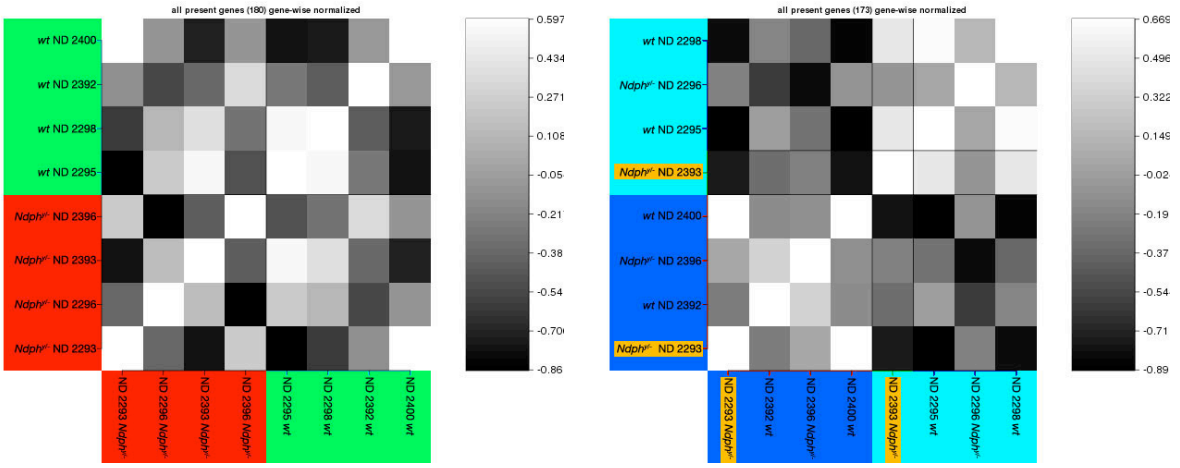

A **B**

Figure 67 Sample correlation plots based on all miRNAs that were present at p5. White color relates to high correlation, black to low correlation of miRNA expression. **(A)** The sample correlation plot was strongly mixed when groups were arranged according to the *Ndph* genotype (*green: Ndph* wt; *red: Ndph* ko). **(B)** However, the samples clearly clustered in two groups. With the exception of samples ND 2293 and ND 2393, the specimens arranged according to their belonging to one of the two litters from which the retinas were prepared. Litter 1 included samples no. ND 2293, 2295, 2296, and 2298 (*light blue*). Litter no. 2 included ND 2392, 2393, 2396, and 2400 (*dark blue*). This clustering suggests that samples ND 2293 and ND 2393 (*orange*) were likely confused with each other, and that differences in miRNA expression at p5 were higher between different litters than between the *Ndph* genotypes.

3.3.4.5 Possible effects on target genes

Nonetheless, since it is evident that miRNAs play an important role in ocular vascular development and remodeling, further studies concentrating on the differentially regulated miRNAs may reveal valuable insight into the molecular pathogenesis of ND. For this purpose, *in silico* analyses regarding the miRNAs already known to affect blood vessel development and those presented in Figure 113 were performed. A database search investigating which targets are recognized by these miRNAs revealed that some could influence expression of angiogenic genes (Table 41). 18 of the 39 representatively selected, putative angiogenesis-related genes harbor a binding site for at least one of these miRNAs. Four genes (*Igf1, Notch3, Dvl3, and Slc38a5*) are recognized by several miRNAs. The miRNA recognizing the most of the selected genes is mmu-miR-27a (5 targets: *Igf1, Cldn5, Dvl2, Notch2, and Notch4*). Interestingly, none of these 39 genes is recognized by the miRNA with the highest differential expression: mmu-miR-322 (2.2x).

3.3.4.6 Synopsis

Taken together, differential expression of miRNAs in the *Ndph* ko retina was detected with the microarray approach at p21, but not at p5. Although this does not exclude differences at p5, it could indicate that differential expression of miRNAs is not a primary event in the pathogenesis of ND, but rather mirrors secondary changes like the establishment of chronic hypoxia. Some of the miRNAs are predicted to regulate angiogenic factors, and it may be interesting to investigate their role in ND.

Target	effect	increased expression							decreased expression					literature				
		mmu-miR-23a	mmu-miR-27a	mmu-miR-126-3p	mmu-miR-132	mmu-miR-142-3p	mmu-miR-210	mmu-miR-322	mmu-miR-7a	mmu-miR-129-3p	mmu-miR-129-5p	mmu-miR-375	mmu-miR-211	mmu-miR-31	mmu-miR-150	mmu-miR-184	mmu-miR-221	mmu-miR-222
Igf1	+/-		x	x							x		x					
Notch3	+								x	x					x			
Dvl3	+/-				x				x									
Slc38a5	-						x							x				x
VegfC	-						x									x		
Angpt2	+										x							
Cldn5	-		x															
Dll4	-				x													
Dvl2	-		x															
Itgav	-					x												
Lrp5	-	x																
Notch2	-		x															
Notch4	-		x															
Nrp-1	+											x						
VegfA	-			x														
VEGFR2/Kdr	+										x							
Fzd4															x			
Tie1														x				
Adm																		
Agtrl1																		
Angpt1																		
ApoD																		
Ctnnb1																		
Dvl1																		
Efnb2																		
EphB4																		
Hif1a																		
Igf2																		
Itgb3																		
Jag1																		
Ndph																		
Notch1																		
Pdgfb																		
PdgfRb																		
Plvap																		
Tie2/Tek																		
VegfB																		
VEGFR1/Flt1																		
VEGFR3/Flt4																		

Table 41 Representative selection of 39 genes that are (likely) involved in blood vessel development. 18 of these genes include a recognition site in the 3'-UTR for at least one of the differentially regulated miRNAs found in p21 *Ndph* retinas, or for the miRNAs already described blood vessel regulating. 4 genes are recognized by more than 1 miRNA. The miRNAs recognizing the most of these selected angiogenesis-related genes are miR-27a (5 targets) and miR-129-5p (3 targets). The miRNA with the highest differential expression (mmu-miR-322) has no predicted target genes amongst this selection. The +/- sign in the „effect" column indicates the impact of differential miRNA expression in p21 *Ndph* ko retina on the target gene. Data have been retrieved from the miRBase hosted by the Sanger institute (microrna.sanger.ac.uk).

3.3.5 Analysis of neuronal markers in the retina

Most data from the analysis of the norrin ko mouse support the hypothesis that impairment of the retinal vascular development is the first pathogenic event, and effects on the neural retina occur only secondarily (Luhmann et al. 2005a; this work). Because of this, Dr. Lucia Galli-Resta from the Institute of Neuroscience at the Consiglio Nazionale delle Ricerche (CNR) in Pisa has approached us with the idea that, if Norrin in the first place is essential for the development of the retinal vasculature, the *Ndph* ko mouse could serve as a model to investigate neuronal development under hypoxic conditions. This is what she was interested in, and so we started a collaboration, where I prepared retinas from the norrin ko breed, and Dr. Galli-Resta and her co-workers, mainly her PhD student Paola Leone, performed a series of immunohistological studies on them. During this collaboration, I had the opportunity to visit Dr. Galli-Resta's lab for a 10-day internship, and worked together with Paola Leone to analyze differential expression of neuronal markers in the *Ndph* ko mouse by immunohistochemistry and confocal microscopy. This set of antibodies contained markers for retinal ganglion cells (Islet-1, beta-tubulin (processes), Neurofilament 150kDa (axons)), amacrine cells (Islet-1, ChAT), bipolar cells (PKC-α (rod bipolars), mGluR6 (ON bipolars)), horizontal cells (calbindin 28kd), Müller cells (vimentin), and synapses (SNAP 25, synaptophysin, mGluR6). Two markers, synaptophysin (Syp) and Islet-1 (Isl-1), were also investigated on the mRNA level after my return.

3.3.5.1 Synaptophysin (Syp)

Synaptophysin (Syp) is, together with synaptobrevin (Syb), the most abundantly expressed protein in synaptic vesicles, and thus is used as a synaptic marker (Calhoun et al., 1996). It probably modifies the release of synaptic vesicles through binding to synaptobrevin, which is central to the exocytotic SNARE complex, and thereby decreases vesicle release (Edelmann et al., 1995). As a marker, it is frequently used for density determination of synapses in brain disorders, as well as for the diagnosis of neuroendocrine, neuroectodermal, and CNS tumours (Morrison & Prayson, 2000; Wick, 2000).

The staining pattern of synaptophysin was different between the *Ndph* wt and ko sections, especially at p21 (Figure 68). A typical pattern of small spots was visible in the plexiform layers of the wild type, indicating numerous synapses. In the knockout, labeling was weaker and more diffuse. Because of unspecific labeling of the secondary anti-mouse IgG antibody, blood vessels were also visible. In the samples from p5 animals, only very faint staining was detected in the wt, and no immunoreactivity for Syp could be observed in the ko.

To further investigate differential expression of Syp, quantitative RT-PCR with 5 wt and 5 ko retinas was performed. At both investigated time points, p5 and p21, no significant differences in mRNA expression could be detected (Student's t-test; $p<0.05$) (Figure 69).

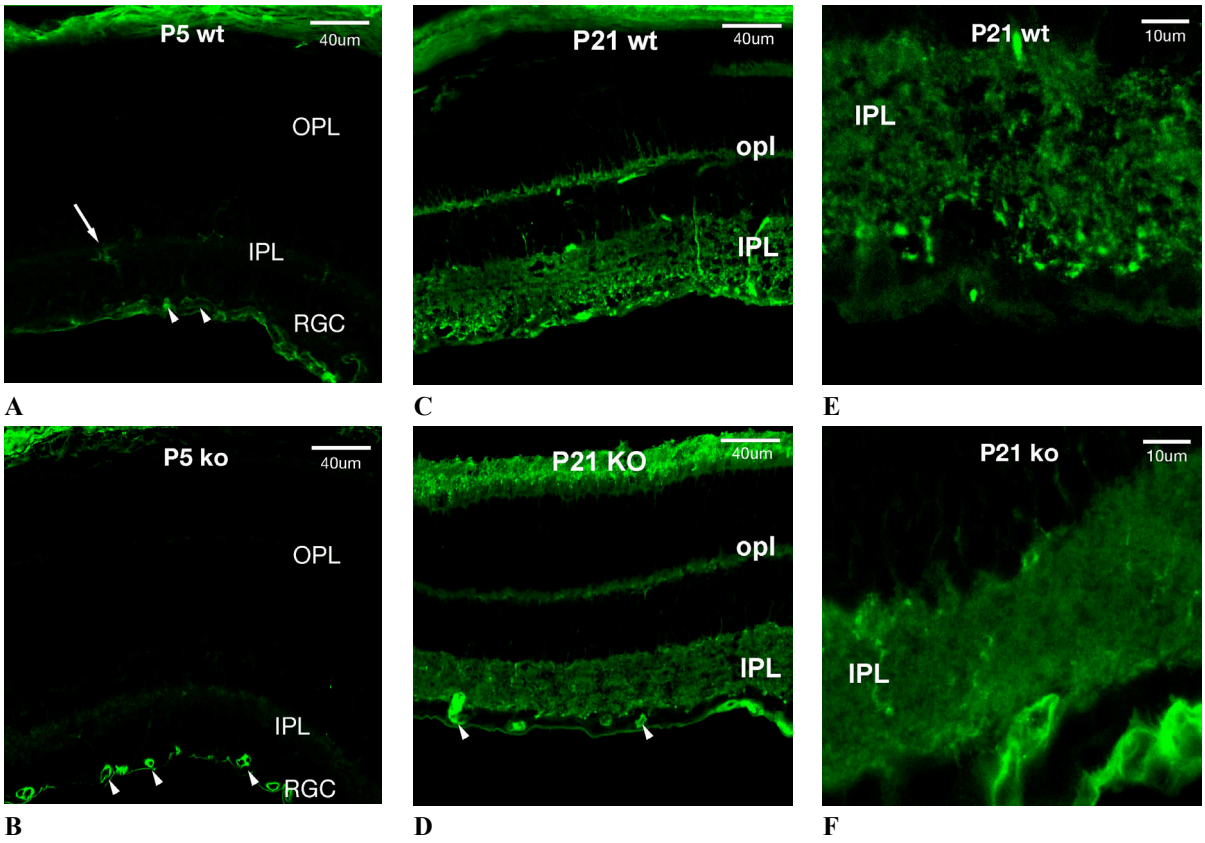

Figure 68 Confocal microscopy images of p5 & p21 retinal cryosections stained with an antibody against synaptophysin (Syp), a synaptic marker. The staining pattern of Syp was different between the *Ndph* wt and ko sections, especially at p21. **(A, B)** At p5, the most prominently labeled structures were blood vessels, which is due to the unspecific labeling by the secondary anti-mouse IgG antibody (arrowheads). Besides very faint staining in the wt (A; arrow), no immunoreactivity for Syp could be observed at p5. **(C)** In the p21 wt a typical pattern of small spots was visible in the plexiform layers. **(D)** A weaker and more uniform labeling was seen in the p21 ko. **(E,F)** Higher magnification images of (C,D) showing the inner plexiform layer of the p21 wt (E) and p21 ko (F). *RGC: retinal ganglion cell layer; IPL: inner plexiform layer; OPL: outer plexiform layer.*

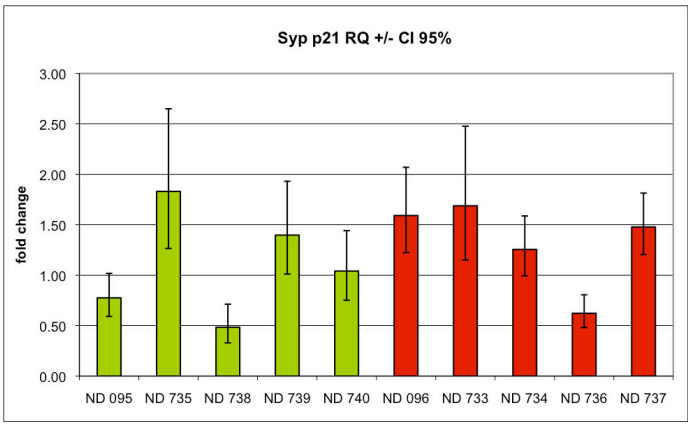

A Syp p21

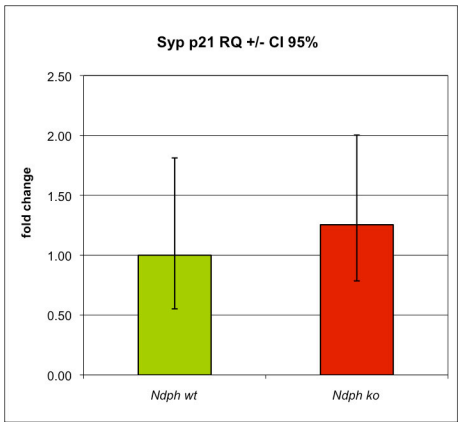

B Syp p21

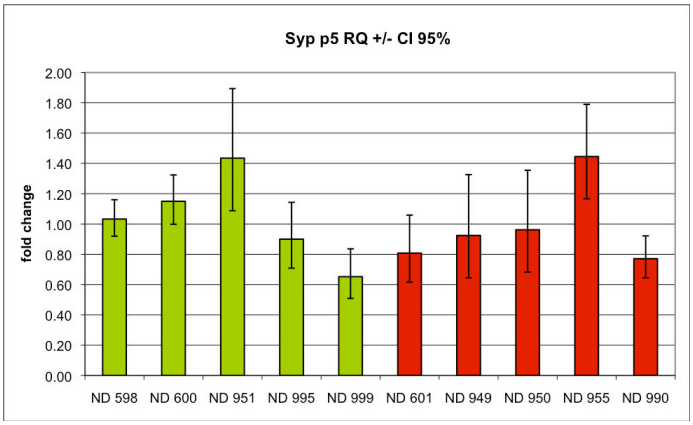

C Syp p5

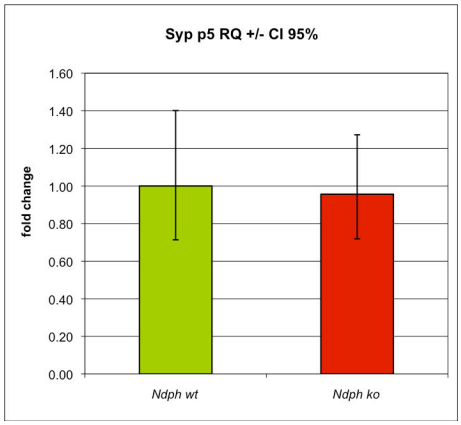

D Syp p5

Figure 69 Transcriptional analysis of synaptophysin (*Syp*) in retinae of *Ndph*$^{y/-}$ knockout (n=5; *red*) and wild type (n=5; *green*) mice. Postnatal time points p5 (C,D) and p21 (A,B) were investigated. The average expression value of the wild type group was set to 1. Error bars indicate the confidence interval at a significance level of 95% ($p<0.05$). **(A)** Quantitative RT-PCR results of the individual p21 samples. **(B)** Mean values of the five wt and 5 ko samples. **(C)** Results of the individual p5 samples. **(D)** Mean values of the p5 samples. No significant differences were found between the wild type and the knockout group. *28S rRNA* was used as endogenous control.

3.3.5.2 Islet-1 (Isl-1)

A subset of RGCs, amacrine, and bipolar cells can be stained with an antibody against the transcription factor islet-1, which has been shown to control the differentiation and maturation of these cell types (Elshatory et al., 2007; Pan et al., 2008).

At p5, immunoreactivity was comparable between *Ndph* wt and ko (Figure 70 A,B). However, the number of amacrine cells appeared to be reduced in the knockout, and the intensity of bipolar cell labeling seemed to be higher. This impression might be due to the exact position of the section, since a clear center-to-periphery gradient was observed in sections from p5 ko specimens for immunoreactive bipolar cells (Figure 71). Multiple sections would have to be analyzed to adequately quantify a possible difference.

Contrary, a clear difference was observed in sections and flatmounts of p21 retinas (Figure 70 C-F). Almost no Isl-1 labeling was detected in the *Ndph* ko. When present, it rather appeared in the cytoplasm than in the cell nucleus (Figure 70 F). Similar to the synaptophysin staining (Figure 68), also here unspecific labeling of blood vessels due to the murine origin of the antibody occured.

Background staining of the plexiform layers appeared to be higher in the ko, possibly due to increased permeability and leakage of the vasculature, and thus presence of IgGs in those areas.

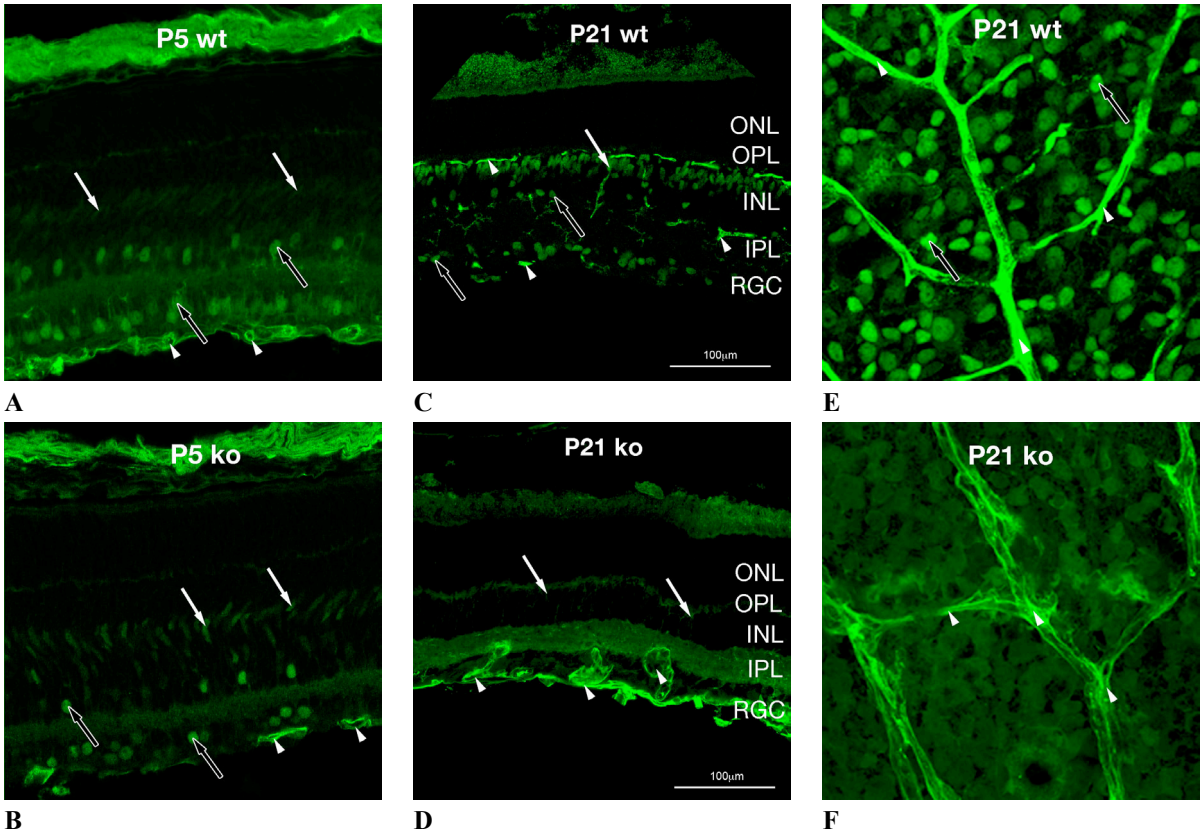

Figure 70 Confocal microscopy images of p5 & p21 retinas stained with an antibody against islet-1, a transcription factor that serves as a marker for bipolar and amacrine cells. The different staining pattern of islet-1 between *Ndph* wt and ko was striking at p21, but not obvious at p5. Unspecific labeling of all 3 blood vessel layers occured due to the specificity of the secondary antibody (arrowheads). **(A, B)** At p5, amacrine (hollow arrows) and bipolar cells (arrows) were labeled in both the *Ndph* wt (A) and the ko (B) sections. However, the number of immunoreactive amacrine cells appeared to be reduced in the ko. **(C)** In p21 wt cryosections, bipolar cells mostly accumulating near the border to the OPL were immunoreactive (arrow). Somata and processi of amacrine cells on both sides of the IPL were labeled as well (hollow arrows). **(D)** In p21 ko cryosections, only the superficial vasculature was present, albeit it appeared to be dilated and was protruding into the retina at some places (arrowheads). Specific staining of islet-1 positive cells was only observed very weakly in the INL (arrows). Virtually no staining of amacrine cells could be detected. Background staining of the plexiform layers appeared to be higher in the ko, possibly due to increased permeability and leakage of the vasculature, and thus presence of IgGs in those areas. **(E)** Wholemounts of wt retinas correlated with the findings made with the cryosections. This confocal image focused on the superficial retina shows specific staining of amacrine cells (hollow arrows) and unspecific labeling of the superficial vessel network (arrowheads). **(F)** No staining (or only diffuse background) of amacrine cells was found in the ko wholemounts. *RGC: retinal ganglion cell layer; IPL: inner plexiform layer; INL: inner nuclear layer; OPL: outer plexiform layer; ONL: outer nuclear layer.*

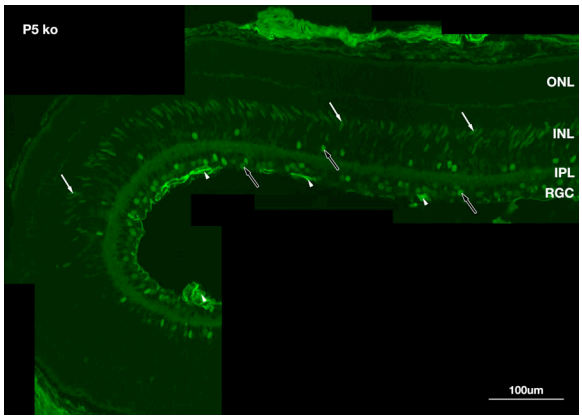

Figure 71 Merged confocal microscopy images of *Ndph* ko p5 retinal sections stained with an antibody against islet-1. Note the center-to-periphery maturation gradient: Staining for bipolar cells (arrows) diminishes with increasing distance to the center (bottom left). Amacrine cells (hollow arrows) and blood vessels (arrowheads) are also immunoreactive. *RGC: retinal ganglion cell layer; IPL: inner plexiform layer; INL: inner nuclear layer; ONL: outer nuclear layer.*

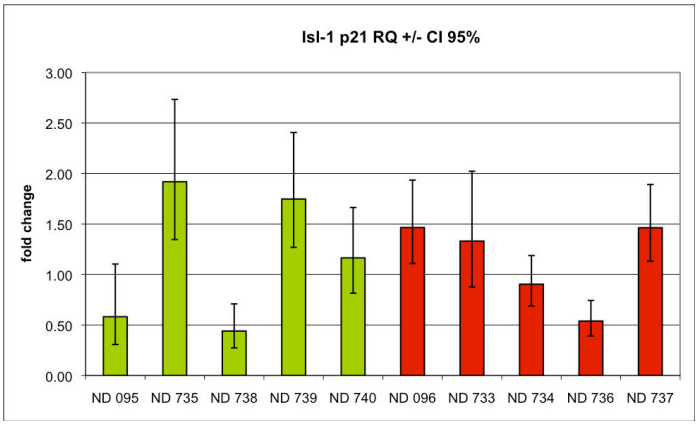

A

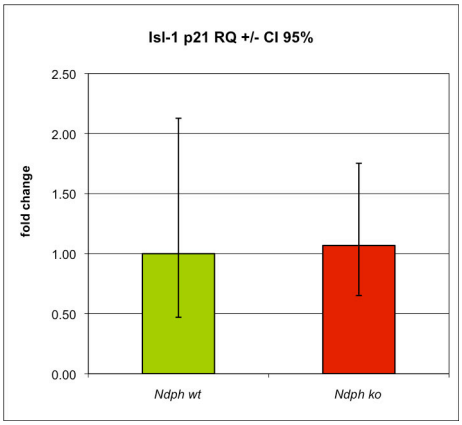

B

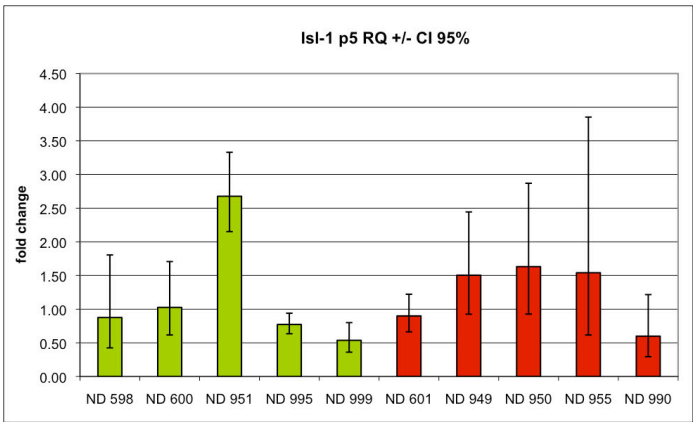

C

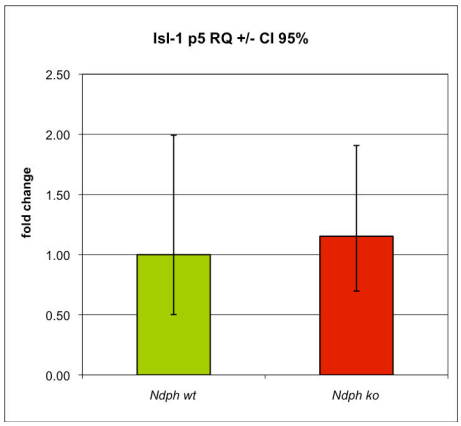

D

Figure 72 Transcriptional analysis of islet-1 (*Isl-1*) in retinae of *Ndph*$^{y/-}$ knockout (n=5; *red*) and wild type (n=5; *green*) mice. Postnatal time points p5 and p21 were investigated. The average expression value of the wild type group was set to 1. Error bars indicate the confidence interval at a significance level of 95% ($p<0.05$). **(A)** Quantitative RT-PCR results of the individual p21 samples. **(B)** Mean values of the five wt and 5 ko samples. **(C)** Results of the individual p5 samples. **(D)** Mean values of the p5 samples. No significant differences were found between the wild type and the knockout group. *28S rRNA* was used as endogenous control.

Differential expression of *Isl-1* was subsequently analyzed by qRT-PCR. No significant differences between *Ndph* wt and ko were found at both investigated time points (p5 & p21; Student's t-test; Figure 72). However, inter-individual expression could differ by factor 4, suggesting substantial individual, but not genotype-related, mRNA differences.

3.3.5.3 Vimentin (Vim), metabotropic glutamate receptor 6 (mGluR6)

Immunohistochemistry with antibodies against vimentin (*Vim*), a Müller cell marker (Lemmon and Rieser, 1983), and metabotropic glutamate receptor 6 (*mGluR6*), labeling ON bipolars (Nomura et al., 1994), did not work, probably because the antibody sera were too old.

3.3.5.4 Neurofilament (NF150)

Neurofilaments (NF) are neuron-specific intermediate filaments (reviewed by Shea, 2000). Based on their molecular weight, different NF families have been defined. In the retina, antibodies against the NFs of medium weight (~150kDa) label axons of ganglion and horizontal cells.

Confocal microscopy revealed no obvious differences between *Ndph* wild type and knockout retinas at p5 and p21 (Figure 73). This suggested the presence of a normal nerve fiber layer in norrin ko mice. Further, also the network of horizontal cell axons was comparable (Figure 73).

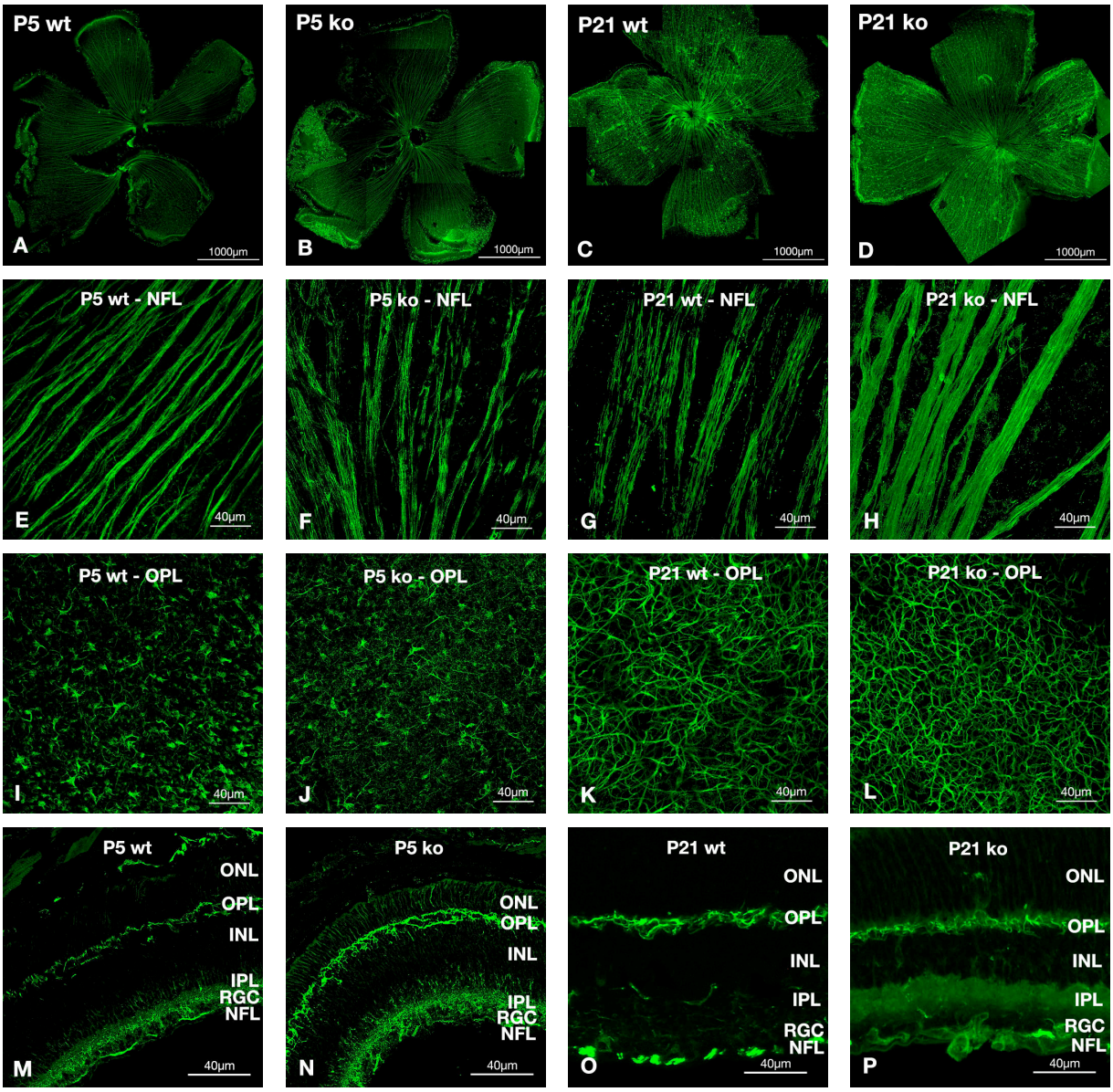

Figure 73 Confocal microscopy images of p5 & p21 retinal flatmount preparations (A-L) and sections (M-P) stained with an antibody against Neurofilament 150kDa, which labeles retinal ganglion cell (RGC) axons and horizontal cells (HC). Flatmount images in **A-D** are composed of several pictures of higher magnifications. **(A)** Retinal flatmount from a p5 *Ndph* wild type. RGC axons are clearly visible as stripes extending radially over the retina, merging at the optic disc. **(B)** Retinal flatmount from a p5 *Ndph* knockout. No obvious differences to the wild type are apparent. On the left side of the image, where the flattened retina is reverted, axons of HCs are visible. **(C)** P21 retinal flatmount from an *Ndph* wt. At this age**,** staining of the RGCs is better visible than at p5. **(D)** P21 retinal flatmount from an *Ndph* ko. Also here, no obvious differences could be detected. **(E-H)** Higher magnification images of A-D, focussed on the nerve fiber layer (NFL). **(E)** In the p5 wt, numerous RGC axon bundles are visible. **(F)** The p5 ko NFL was comparable to the wt. **(G)** Wt p21 NFL morphology appears similar to the p5 samples. **(H)** Also in the p21 *Ndph* ko NFL, no obvious differences to the wt nerve fibers were detected. **(I-L)** Images from the same position as in (E-H), but focussed on the horizontal cells (HC). **(I)** At p5, the outer plexiform layer (OPL) is not developed, as can be seen by the lack of HC axons in the p5 wt. However, HC somata are visible. **(J)** In the p5 ko, no obvious differences were apparent. **(K)** A dense network of HC processi was detected in the p21 wt OPL. **(L)** The p21 ko OPL was similarly stained. **(M-N)** Retinal sections, showing staining of NFL and HCs. **(M)** *Ndph* wt p5 section. **(N)** The *Ndph* ko p5 section showed no differences. **(O)** The p21 wt inner plexiform layer (IPL) appears to be less immunoreactive than at p5. **(P)** The same applies to the p21 ko. In addition, higher background staining in the plexiform layers was noted. *INL: inner nuclear layer; IPL: inner plexiform layer; NFL: nerve fiber layer; ONL: outer nuclear layer; OPL: outer plexiform layer; RGC: retinal ganglion cell layer.*

3.3.5.5 Choline acetyltransferase (ChAT)

Cholinergic acetyltransferase (ChAT) catalyzes the synthesis of the neurotransmitter acetylcholine, through joining Acetyl-CoA to choline. Thus, ChAT can be used as a marker for cholinergic neurons. In the retina, antibodies against ChAT effectively label cholinergic amacrine cells (Galli-Resta, 2002).

Retinal immunohistology analyzed with confocal microscopy revealed two populations of immunoreactive cells: one was located in the inner nuclear layer, and the other formed in the ganglion cell layer. Both were adjacent to the inner plexiform layer and formed two parallel lines of dendritic connections. However, no difference at p5 and p21 could be observed between norrin wt and ko mice (Figure 74), indicating an equal number and distribution of these cells in both genotypes.

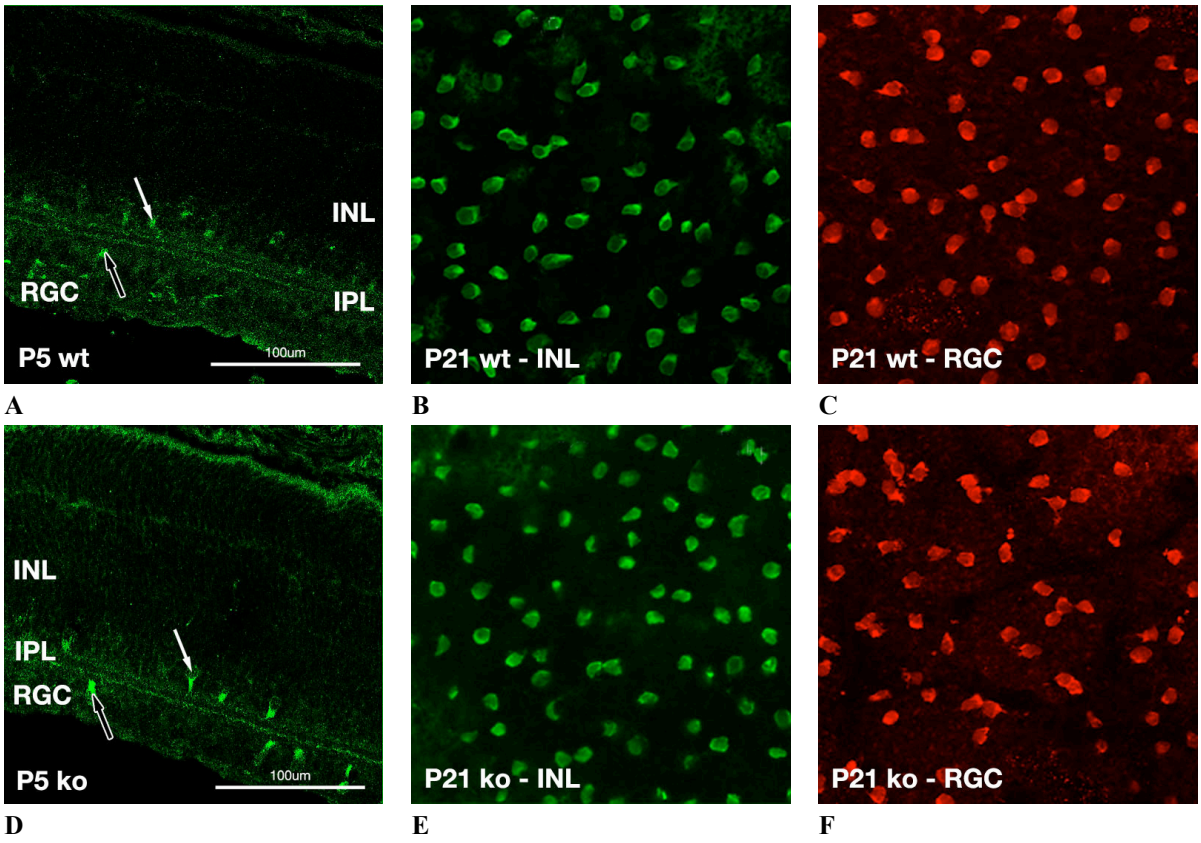

Figure 74 Cholinergic acetyltransferase (ChAT) immunohistology analyzed with confocal microscopy. **(A,D)** Cholinergic amacrine cells located in the inner nuclear layer (INL; arrow) and the retinal ganglion cell layer (RGC; hollow arrow) were clearly visible in p5 sections of *Ndph* wild type **(A)** and knockout **(D)** mice. **(B,C,E,F)** Spacing and immunoreactivity of these two cell layers was also comparable between p21 wt and ko retinal wholemount preparations. **(B)** Amacrine cells in the INL of the wt and **(E)** the ko retina. **(C)** Same position as in (B), but focused on the RGC, showing a second layer of cholinergic amacrine cells. **(F)** Same position as in (E), showing the RGC layer of cholinergic amacrine cells in the ko. *INL: inner nuclear layer; IPL: inner plexiform layer; RGC: retinal ganglion cell layer*

3.3.5.6 Calbindin 28kDa (Calb1)

Calbindin 28kDa is a calcium-binding protein in the nervous system. It is commonly used to label horizontal cells in the retina (Röhrenbeck et al., 1987). But also other neuronal cell types, including subpopulations of amacrine and ganglion cells, express this protein depending on species and developmental stage.

The antibody labeled horizontal, amacrine, and ganglion cells in sections of p5 animals. At p21, horizontal cells were the only immunoreactive cell type. No differences between norrin wt and ko mice were detected at both developmental stages (Figure 75).

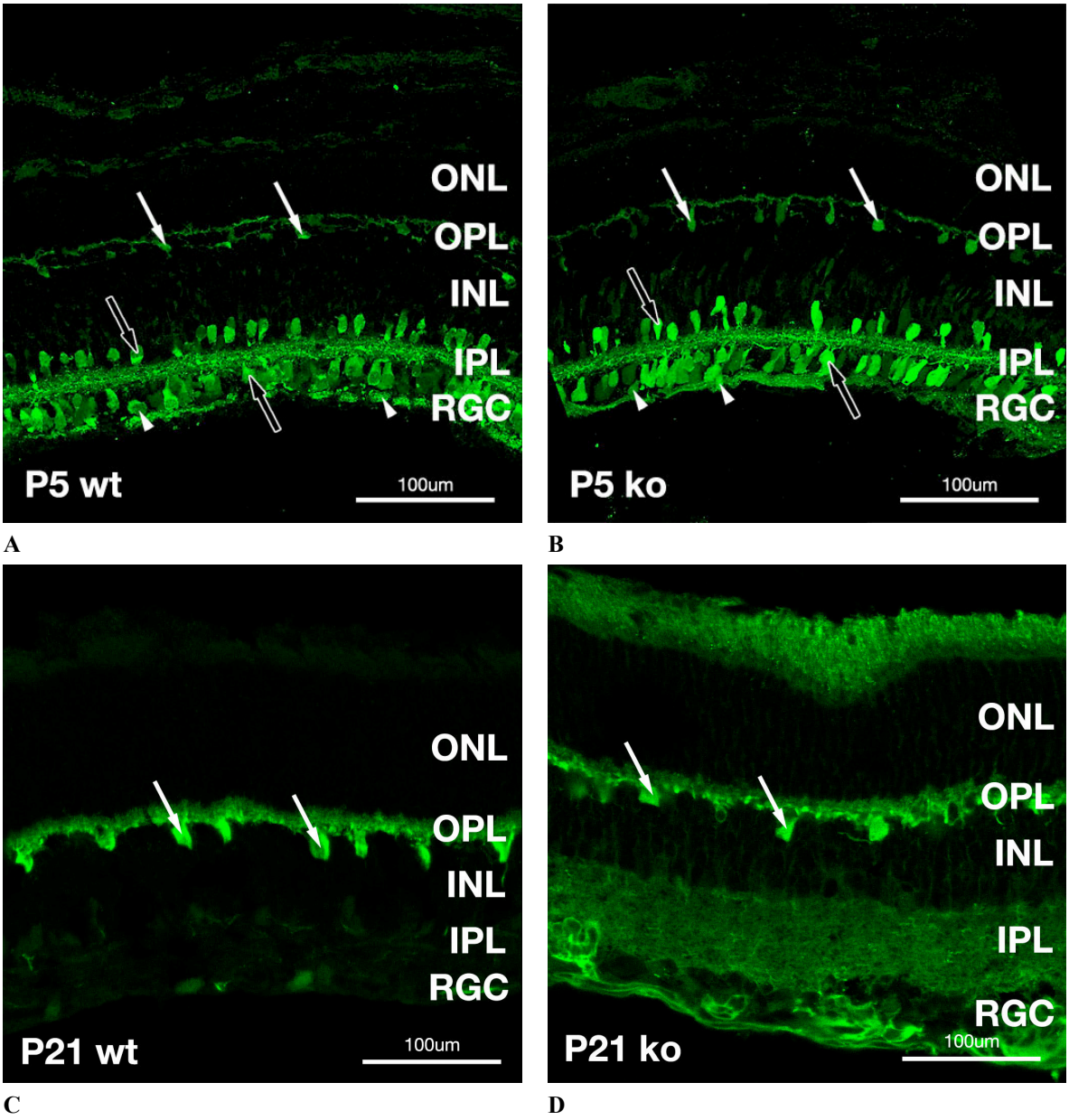

Figure 75 Confocal microscopy images from retinas stained with an antibody against Calbindin 28kDa. **(A,B)** In p5 retinal sections, immunoreactive cells were found in the forming outer plexiform layer (horizontal cells; arrows), framing the inner plexiform layer (amacrine cells; hollow arrows), and in the ganglion cell layer (RGCs; arrowheads). **(A)** Retinal section from a p5 *Ndph* wt. **(B)** Section from a p5 *Ndph* ko. No differences were observed. **(C)** At p21, the antibody only labeled horizontal cells in the wt (arrows). **(D)** In the p21 ko, the only specific staining was also detected in the OPL, and no obvious difference was

detected. However, as has been described before in other immunohistologic experiments, a higher background of unspecific staining occured, especially in the IPL and around the superficial blood vessels. *INL: inner nuclear layer; IPL: inner plexiform layer; NFL: nerve fiber layer; ONL: outer nuclear layer; OPL: outer plexiform layer; RGC: retinal ganglion cell layer*

3.3.5.7 Beta-tubulin, PKC-alpha, SNAP 25

In addition to the already presented neuronal markers, Paola Leone further investigated differential expression of β–tubulin (that labels the IPL, RGCs, and Müller cell processes), protein kinase C alpha (PKCα; marker for rod bipolar cells), and SNAP 25 (one of the SNARE proteins mediating vesicle relase).

The antibody against β-tubulin labeled the radially processing Müller cells, the inner plexiform layer, and also intensely the retinal ganglion cell layer. However, wt and ko sections were not different (Figure 76 A).

PKC-α positive cells, i.e. rod bipolars, were found on both sides of the inner nuclear layer. Also here, wt and ko stainings did not differ, maybe with the exception of a slightly higher background stain in the ko (Figure 76 B). Co-staining with propidium iodide (labeling cell nuclei) showed dislocation of rod bipolar cell terminals in the inner plexiform layer by aberrantly invading vessels (Figure 76 C).

SNAP 25 strongly labeled the outer plexiform layer, with no apparent difference between norrin wt and ko. Also the weaker SNAP 25 staining of the inner plexiform layer (IPL) was comparable between the genotypes (Figure 76 D).

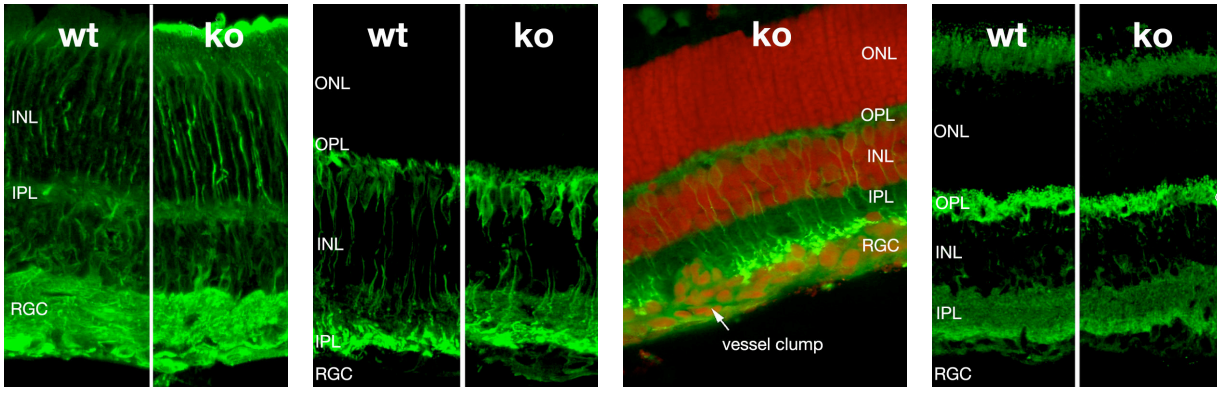

A β-tubulin **B** PKC-α **C** PKC-α **D** SNAP 25

Figure 76 Additional immunostainings of p21 retinal sections performed by Paola Leone. No significant differences between norrin wt and ko samples were detected. **(A)** The antibody against β-tubulin equally labeled the *Ndph* wt and ko sections for Müller cells and, more diffusely, the IPL. Strong response was observed from cells in the RGC. **(B)** Rod bipolars were labeled by an antibody against PKC-α. Unspecific background staining was higher in the ko. **(C)** Co-staining of PKC-α with propidium iodide (*red*). A vessel clump dislocates bipolar cell terminals (*green*) and alters inner retinal morphology. **(D)** Synapses in the plexiform layers were labeled with a SNAP 25 antibody. Staining was stronger in OPL, but *Ndph* wt and ko sections were comparable. *INL: inner nuclear layer; IPL: inner plexiform layer; ONL: outer nuclear layer; OPL: outer plexiform layer; RGC: retinal ganglion cell layer*

3.4 Norrin's role in Wnt/β-catenin signaling

3.4.1 Analysis of known Wnt-signaling mediators and target genes

Upon activation of the canonical Wnt-signaling pathway, β-catenin accumulates in the cytoplasm, translocates into the nucleus and forms a complex with transcription factors of the lymphoid enhancer (*Lef*) or transcription factor (*Tcf*) families to drive target gene expression. (reviewed by Willert and Jones, 2006) Since norrin has been shown to activate this pathway in cell culture (Xu and Wang et al., 2004), mediators and target genes of canonical Wnt-signaling were investigated in the *Ndph* knockout mouse retina. Most of the transcript expression experiments were performed by Bohdan Mikolasek, while I repeated/added some qRT-PCRs, performed β-catenin Western blots, and did the statistical analysis.

3.4.1.1 Beta-catenin (Ctnnb1)

Beta-catenin (*Ctnnb1*) is the central and essential component of the canonical Wnt-signaling cascade (reviewed by Brembeck et al., 2006). It transfers signals through activation of target gene transcription, but also controls cell adhesion at the plasma membrane and mediates the interplay of adherens junction molecules with the actin cytoskeleton. Disturbance of these functions in human disease can lead to loss of cell-cell adhesion and to deregulated transcription of Wnt target genes.

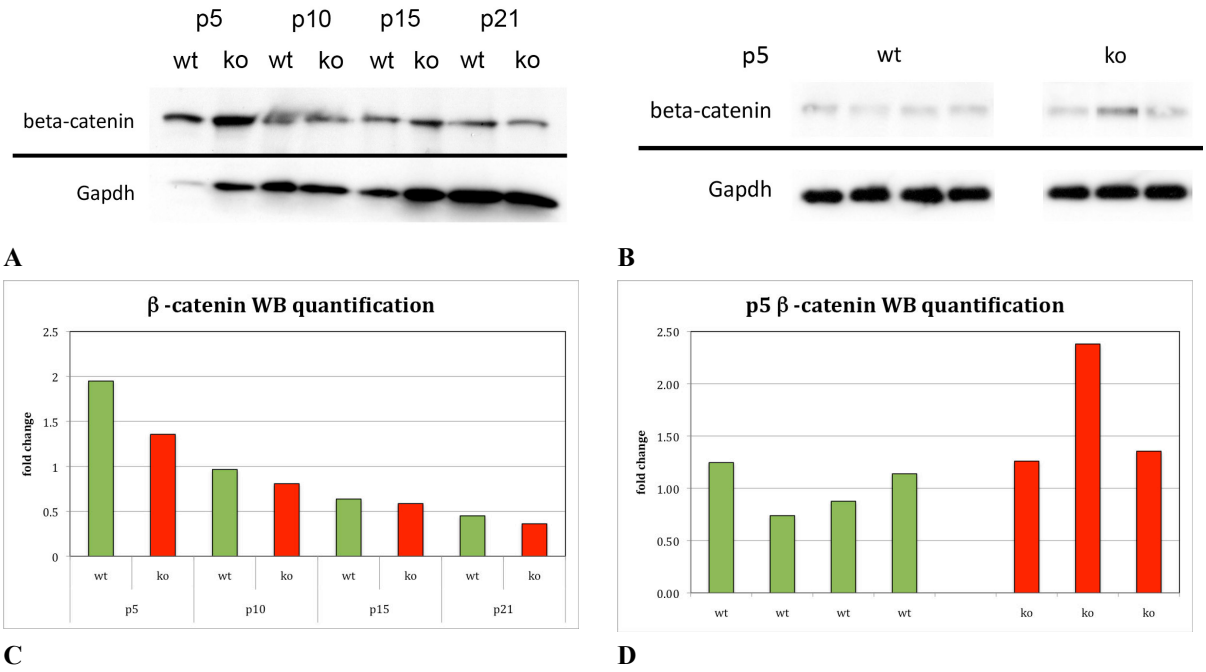

Figure 77 Western blots with retinal protein extracts from *Ndph* wt and ko mice labeled with an antibody against β-catenin. Densitometric quantification values for β-catenin were normalized to Gapdh and calibrated to the wt mean. **(A)** Beta-catenin was strongly expressed at every investigated developmental stage (p5-p21) with no obvious differences between norrin wt and ko. Protein levels of Gapdh increased over time. Gapdh expression appeared to be weak in the first sample (p5 wt). **(B)** When the Western blot was repeated with protein from p5 retinas, no differences between the *Ndph* genotypes could be found (wt: *n=4*; ko: *n=3*). **(C)** Densitometric quantification of the blot presented in (A). Due to normalization of

the β-catenin levels to Gapdh, it appears as if β-catenin protein levels decrease over time. They also seem to be reduced in the *Ndph* ko. **(D)** However, this impression could not be verified for p5. The densitometric analysis of (B) suggests equal, if not higher expression of β-catenin in the norrin ko.

Because norrin activates canonical Wnt-signaling, I hypothesized that β-catenin protein levels should be reduced in norrin-responsive cells in the *Ndph* ko retina. To test this hypothesis, Western blots with retinal protein extracts of norrin wt and ko mice were labeled with an antibody against β-catenin (Figure 77).

Beta-catenin protein levels were strong at every investigated developmental stage (p5-p21). No differences between norrin wt and ko were obvious at first sight, but when normalized to protein levels of Gapdh, β-catenin appeared to be slightly reduced in the ko samples, thus tending to support the hypothesis (Figure 77 C). Since the Gapdh signal of the p5 wt sample was suspiciously low in the first WB (Figure 77 A), a second WB with several norrin wt and ko samples was performed (Figure 77 B,D). Here, no difference in β-catenin protein levels was observed. Due to normalization of β-catenin to Gapdh, it appears as if β-catenin protein levels decrease over time. This would imply that Wnt-signaling is more active during the early phases of retinal development, and declines when the retina matures. However, it is mainly Gapdh expression that increases over time (Figure 77 A), making it difficult to estimate the actual protein levels of β-catenin.

3.4.1.2 Bone morphogenetic protein 4 (Bmp4)

Bmp4, a transforming growth factor-β family member, was shown to be overexpressed in human colon cancer cells in response to oncogene-activated β-catenin expression. (Kim et al., 2002) Thus, this study provided evidence for regulatory interaction of WNT and TGF-β signaling pathways. Since norrin has been described as a growth factor with high homology to TGF-β (Meitinger et al., 1993), and further has been shown to activate canonical Wnt-signaling (Xu and Wang et al., 2004), we chose to investigate *Bmp4* expression in *Ndph* knockout mice.

Expression of *Bmp4* was more than four-fold elevated in the p5 ko retina, and was reduced two-fold at p15 (Figure 78 A). Although differences were not significant at p10 and p21, the data indicated two disease phases: An early phase (including p5 and p10), when expression of *Bmp4* is increased, and a late phase (consisting of p15 and p21), when *Bmp4* expression is reduced. This observation is consistent with the disease phases proposed by Luhmann et al. (Luhmann et al., 2005a).

3.4.1.3 Lymphoid enhancer binding factor 1 (Lef1)

Lymphoid enhancer binding factor 1 *(Lef1)* has been shown to drive the expression of Wnt/β-catenin target genes, while its own expression is negatively regulated by canonical Wnt-signaling, providing a negative feedback loop (Hovanes et al., 2001).

Transcript levels of *Lef1* were significantly reduced in the retina of p15 *Ndph* ko mice by factor 1.8 (Figure 78 B). Expression differences were not statistically significant at the other investiated stages, but the same trend observed for *Bmp4* was also noted for *Lef1*: Higher expression in the ko at p5 and p10, and lower expression at p15 and p21.

3.4.1.4 Transcription factor 3 (Tcf3/Tcf7l1)

Transcription factor 3 (*Tcf3/Tcf7l1*) forms a complex with β-catenin upon Wnt-stimulation and mediates signaling through binding to canonical Tcf DNA motifs of target genes. (Korinek et al., 1998)

In the *Ndph* ko retina, expression of *Tcf3* did not show significant differences at all investigated time points (Figure 78 C).

3.4.1.5 Transcription factor 7-like 2 (Tcf7l2/Tcf4)

Transcription factor 7-like 2 (*Tcf7l2/Tcf4*) is another member of the Tcf family that can act as repressor of Wnt-target genes in the absence of β-catenin, and as activator in its presence. (reviewed by Brantjes et al., 2002)

Like *Tcf3*, *Tcf7l2* mRNA levels were not significantly different in the norrin ko retinas (Figure 78 D).

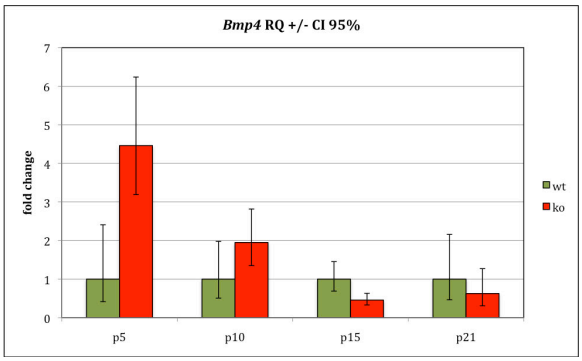

A *Bmp4* expression

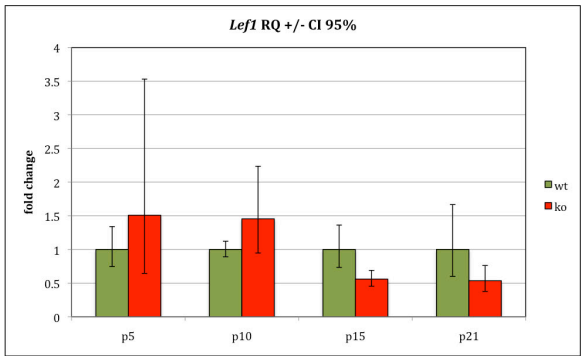

B *Lef1* expression

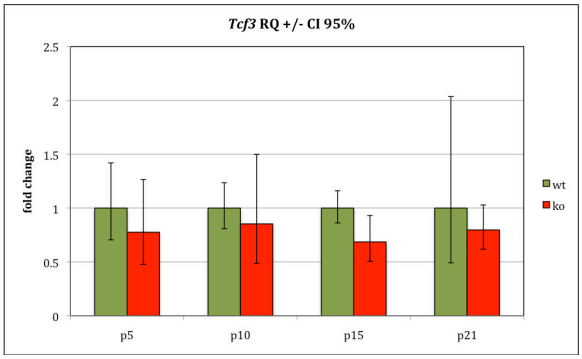

C *Tcf3* expression

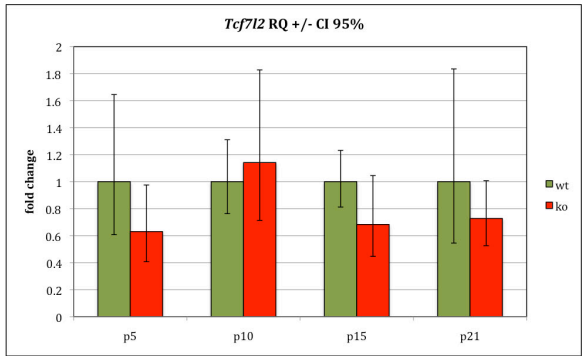

D *Tcf7l2* expression

Figure 78 Transcriptional analysis of Wnt-target genes in retinae of *Ndph*$^{y/-}$ knockout (n=5; *red*) and wild type (n=5; *green*) mice. Postnatal time points p5, p10, p15, and p21 were investigated. The average expression value of each wild type group was set to 1. Error bars indicate the confidence interval at a significance level of 95% ($p<0.05$). *Gapdh* was used as endogenous control. **(A)** *Bmp4* transcript levels were significantly higher in the *Ndph* knockout at p5 (4.5x) and significantly lower at p15 (2.2x). At p5, one wt and one ko sample were determined as outliers and removed from the statistical analysis (wt*: n=4;* ko: *n=4*). **(B)** *Lef1* expression was decreased significantly at p15 (1.8x). As has been observed for *Bmp4* (A), there appears to be a trend of higher transcripts in the ko at p5 and p10, and lower transcripts at p15 and p21 (yet statistically not significant). **(C)** Expression of *Tcf3* was not different in *Ndph* wt and ko samples at all 4 time points. **(D)** The same applies to *Tcf7l2*, were no significant alterations could be observed.

3.4.2 Expression of *SLC38A5* in HEK cells in response to canonical Wnt-signaling

Canonical Wnt-signaling *in vivo* and in cell culture can be activated with lithium chloride (LiCl), which inhibits the enzyme glycogen synthase kinase-3β (GSK-3β) (Klein and Melton, 1996; Hedgepeth et al., 1997). GSK-3β phosphorylates β-catenin in the cytoplasm, targeting it for ubiquitination and degradation. Thus, LiCl increases the amount of β-catenin protein in the cytoplasm, which then translocates into the nucleus, where it regulates Wnt-signaling-induced expression of target genes through binding to transcription factors.

Several candidate genes have been determined by the microarray experiment and subsequent qRT-PCRs. Since *Slc38a5* was so clearly lower expressed at all investigated time points and norrin has been shown to activate Wnt/β-catenin signaling in cell culture (Xu and Wang et. al, 2004), it could be possible that *Slc38a5* is under transcriptional control of canonical Wnt-signaling. To test this hypothesis, human embryonic kidney cells (HEK293T) were treated with either LiCl or NaCl (as negative control), and protein and mRNA expression of SLC38A5 were examined.

3.4.2.1 Expression of β-catenin in LiCl-treated HEK cells

In a first experiment, protein levels of β-catenin were shown to be enhanced in LiCl-treated HEK cells, confirming previous observations (Figure 79).

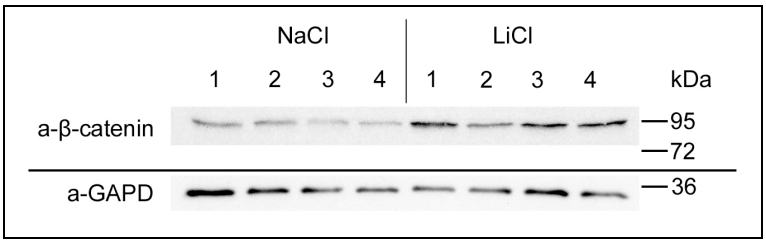

A

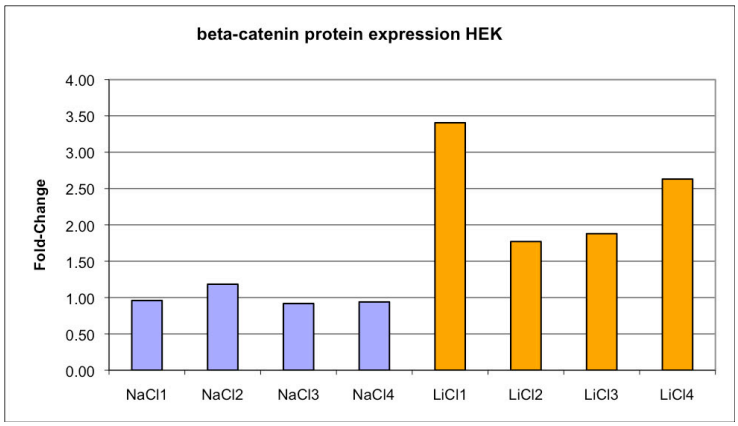

B

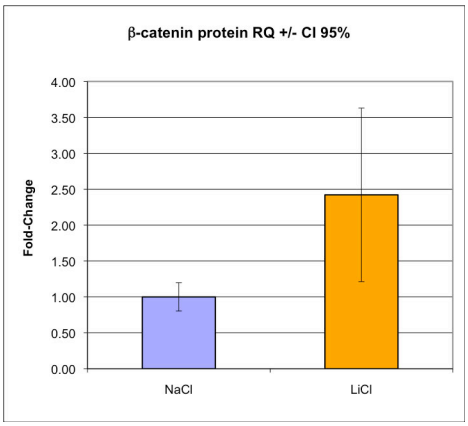

C

Figure 79 Expression of β-catenin is enhanced in LiCl-treated HEK293T cells. **(A)** Western blot with 50µg HEK cell pellet protein extract loaded in each lane. A band at ~92kDa is visible in each of the 8 samples (4 treated with NaCl, 4 treated with LiCl) corresponding to the predicted size of beta-catenin. Bands are stronger in the 4 LiCl-treated samples. **(B,C)** Densitometric quantification of the β-catenin Western blot. Values were normalized to GAPD expression and calibrated to the mean value of the NaCl-treated cells. **(B)** Individual densitometric values of the eight HEK samples. **(C)** The mean β-catenin level of the LiCl-treated cells was significantly higher (2.5x) than that of the control samples (Student's t-test; $p<0.05$).

3.4.2.2 Expression of SLC38A5 in β-catenin-stabilized HEK cells

Expression of *SLC38A5* mRNA was generally low ($C_t \cong 31$ with 10ng cDNA), but technically reproducible (Figure 80 A). It was varying considerably between the separate cell cultures. However, no significant difference was observed between the LiCl- and the NaCl-treated control group (Figure 80).

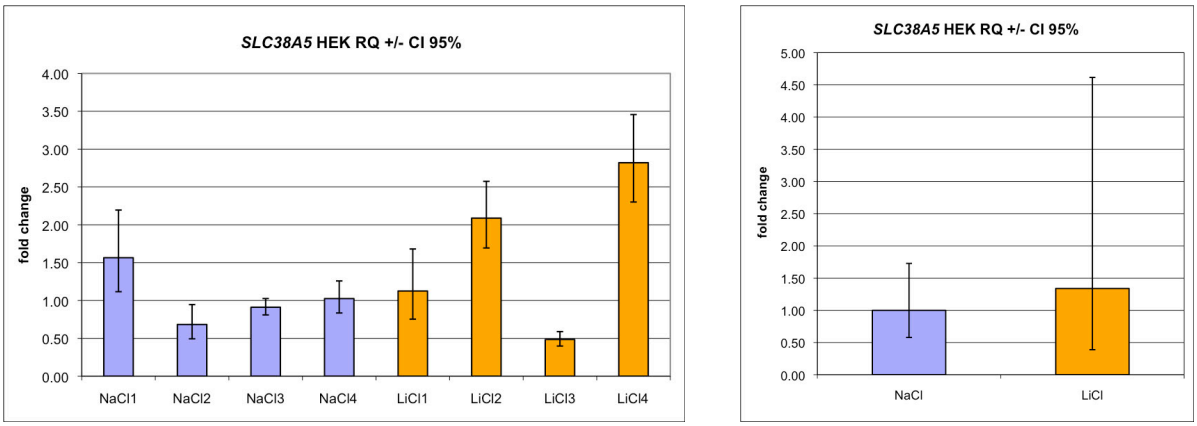

A **B**

Figure 80 Transcriptional analysis of *SLC38A5* in HEK293T cells treated with NaCl (n=4; *blue*) or LiCl (n=4; orange). The average expression value of the NaCl-treated group was set to 1. Error bars indicate the confidence interval at a significance level of 95% ($p<0.05$). **(A)** Quantitative RT-PCR results of the individual HEK cell culture samples. **(B)** Mean values of the NaCl- and LiCl-treated cells. Expression varied significantly between the individual samples, but no significant difference was found between the NaCl- and the LiCl-treated group. *POL2RA* was used as endogenous control.

The picture was a little bit different on the protein level. A Western blot from HEK cultures stained with a rat-antibody against Slc38a5 revealed two distinct bands: one at the predicted molecular weight around 50kDa, and a band around 200kDa, which may resemble a tetramer of the protein (Figure 81 A). Expression of the 50kDa band was similar at first glance, and indicated a slight reduction of Slc38a5 (50kDa) in the LiCl-treated samples only when analyzed by densitometry (down to an average of 0.8 of the control group; Figure 81 B, C).

The tetrameric band appeared to be drastically reduced in 3 out of 4 LiCl-treated samples (Figure 81 D). However, the fourth sample turned out to express Slc38a5 (200kDa) the most, more than every control sample (this resulted in a mean reduction to 0.6 of the NaCl control group, or 0.36 when sample LiCl was excluded; Figure 81 E).

3.4.2.3 Synopsis

Taken together, Slc38a5 expression was not significantly altered in response to LiCl treatment / canonical Wnt-signaling in HEK293T cells. On protein level, a slight reduction in the LiCl-treated samples could be discussed, although it obviously does not fit the hypothesis of norrin positively regulating Slc38a5 expression through canonical Wnt-signaling.

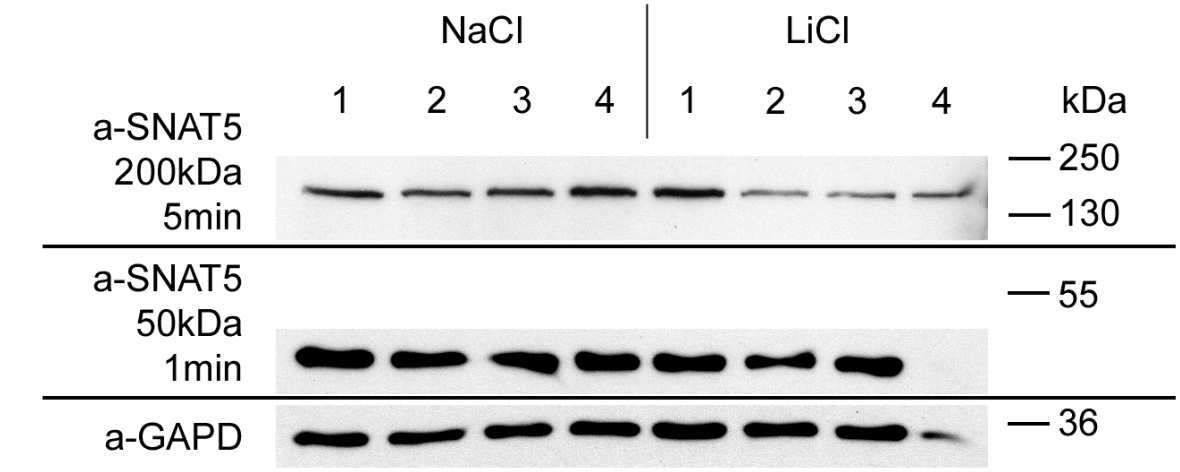

A

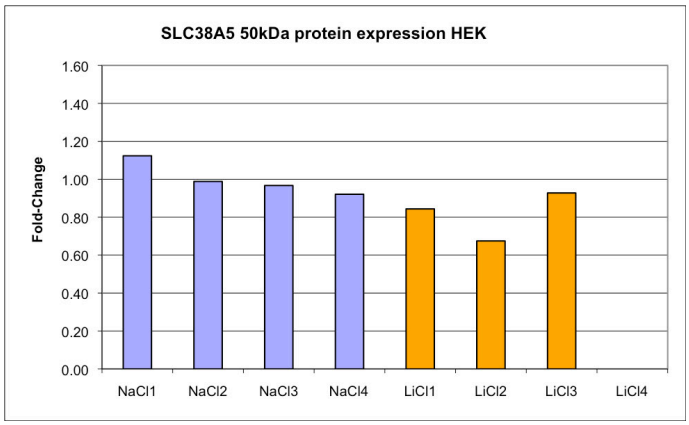

B

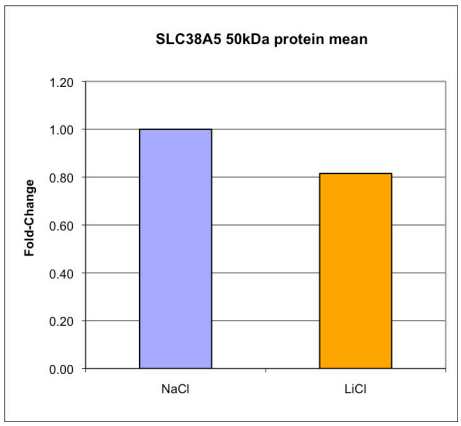

C

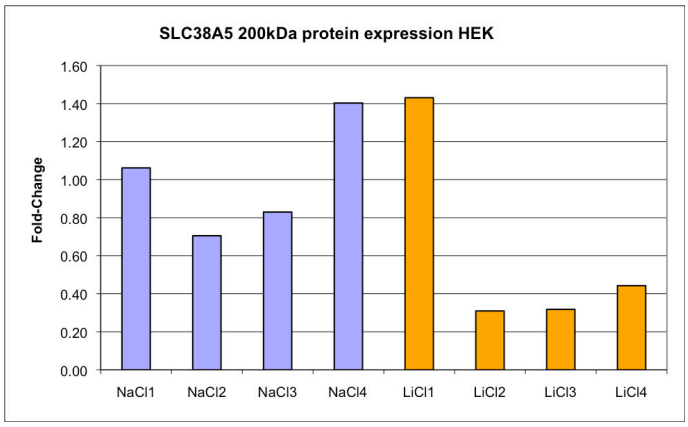

D

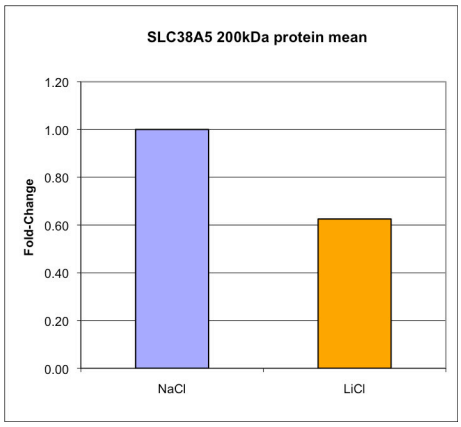

E

Figure 81 Protein expression of SLC38A5 appears to be slightly reduced in LiCl-treated HEK293T cells. **(A)** Western blot with 50µg HEK cell pellet protein extract loaded in each lane. Two prominent bands at ~50kDa and ~200kDa are visible that correspond to the expected mono- and tetramer. Bands at ~50kDa seem to be comparable between NaCl and LiCl treated samples, while bands at ~200kDa seem to be weaker in the LiCl-treated samples. **(B-E)** Densitometric quantification of the SLC38A5 Western blot. Values have been normalized to GAPD expression and calibrated on the NaCl mean. Values for LiCl4 were excluded from the average. **(B)** Individual densitometric values for the 50kDa band. **(C)** The mean protein levels for the 50kDa tetramer band are similar in NaCl- and LiCl-treated cells. **(D)** Individual densitometric values for the 200kDa band. The control protein levels are higher, with the exception of LiCl1, which showed the strongest signal. **(E)** The mean protein level for the 200kDa monomer is lower in the LiCl-treated cells (1.6x; 2.8x without sample LiCl1).

3.4.3 Examination of the Wnt/β-catenin pathway in vivo

It has been shown in cell culture (Xu and Wang et al., 2004) that Norrin can activate transcription via the Wnt/β-catenin signaling pathway. To study the activity of this pathway under the suggested control of Norrin *in vivo* through identification of Norrin-responding cells in the retina and other tissues, I (with the generous help of Ulrich Luhmann) obtained a Wnt-signaling reporter mouse, the so-called BATgal reporter, from Dr. Stefano Piccolo, Padova, Italy. Although this reporter was not used to study Wnt-signaling in the retina, it was successfully used to analayze it in the brain (Maretto et al., 2003). The Norrie Disease mouse line was crossed with this reporter mouse (NDxBATgal), which expresses the bacterial *lacZ* gene under the control of Wnt/β-catenin signaling. Litters of mice aged p5, p7, p10, p15, p21, and also adult, were prepared and eyes and brains were collected. Because these animals were hold under quarantine conditions, which is rather expensive, it was decided to re-establish the line from SPF-conditions in my second PhD year.

3.4.3.1 X-Gal staining of the NDxBATgal retina

Again, litters from the different developmental stages were prepared, and reporter activity in the eye was detected by X-Gal staining, showing reproducible and consistent labeling of the ciliary body (Figure 82). In addition, Wnt-signaling was detected in cells inside the vitreous and adjacent to the lens in *Ndph* wt and ko in early stages (p5: Figure 85; p7: Figure 82, Figure 87) and only in the ko in later stages (p21: Figure 88). These cells highly likely are part of the hyaloid vasculature and the *tunica vasculosa lentis*, which are transient vessel networks during ocular development and nourish the evolving lens. In the wt, these vessels regress after p10, but it has been shown that regression of these systems is delayed in the *Ndph* ko (Richter et al., 1998). Further, hyaloid regression was shown to be Wnt-signaling dependent, and is impaired in *Lrp5* ko mice (Lobov et al., 2005). Thus, X-Gal positive cells could be expected in the hyaloid vasculature, and notably, although regression is impaired in the *Ndph* ko, Wnt-signaling is active in this system.

However, staining of the retina, i.e. in the retinal ganglion cell or inner nuclear layer, only appeared occasionally (Figure 84; Figure 86; Figure 87; Figure 88), contrary to my expectations due to published data of a similar reporter mouse (Liu et al., 2006). Further, staining was not Norrin genotype-specific. Sometimes delineation of X-Gal positive cells in the ganglion cell layer or the vitreous was not clear without ambiguity: *LacZ* staining highly likely located to blood vessels in the section with the most abundant X-Gal labeling I produced during my thesis, although at first glance it appeared to be located inside the ganglion cell layer (Figure 85).These co-localization experiments were performed with an antibody against collagen IV, an extracellular matrix protein of endothelial cells. Co-localization of X-Gal staining and collagen IV immunoreactivity was also observed in the outer plexiform layer of a p21 *Ndph* wt (Figure 86). However, the already cited study that revealed Wnt/β-catenin activity in the retina located it to a subset of retinal ganglion cells, amacrine cells and the ciliary margin (and thereby probably neural progenitor cells), but not to the vasculature (Liu et al. 2006).

Taken together, detection of Wnt-activity in the retina using the Wnt-reporter mouse was, contrary to my expectations, only very weak. This led me to doubt that this experimental approach could facilitate detection of canonical Wnt-signaling at all.

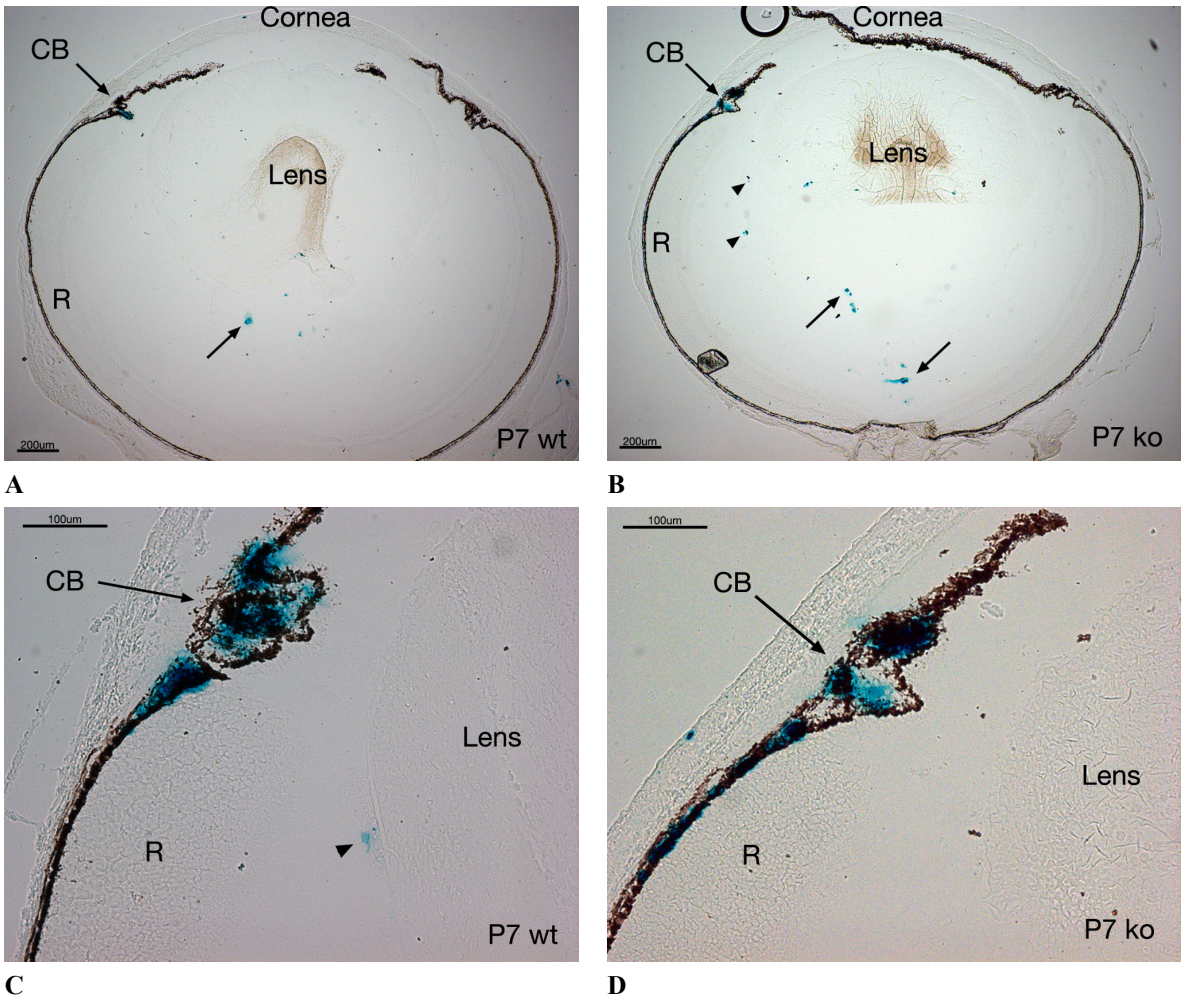

Figure 82 Central ocular sections of p7 *Ndph* wt and ko Wnt-reporter mice. Activity of the reporter *LacZ* gene was detected with X-Gal staining. **(A, B)** Wnt-signaling was detected in cells located in the vitreous (arrows), the cornea, and very strongly inside the ciliary body (CB). It was also found in cells adjacent to the lens, especially in the ko (arrowheads). **(C, D)** The blue staining was masked in some sections because of the pigmentation of the ciliary body, but could be seen always at higher magnifications. *CB: ciliary body; R: retina*

3.4.3.2 X-Gal staining of NDxBATgal brain tissue

In an effort to better visualize reporter gene expression, I tried different protocols (fixation type and time; post-fixation; cryoprotection) without avail and also alternatively detection with a beta-galactosidase antibody. Unfortunately, signals in immunostained cryosections were only unspecific. I therefore decided to re-establish the X-gal staining procedure on brain tissue, because Wnt-activity in the brain is more widespread. And indeed, *LacZ* activity was reproducibly detected with X-gal detection. Brain sections from different postnatal stages were prepared and wild type and knockout littermates were compared (Figure 83). Expression intensity of the reporter

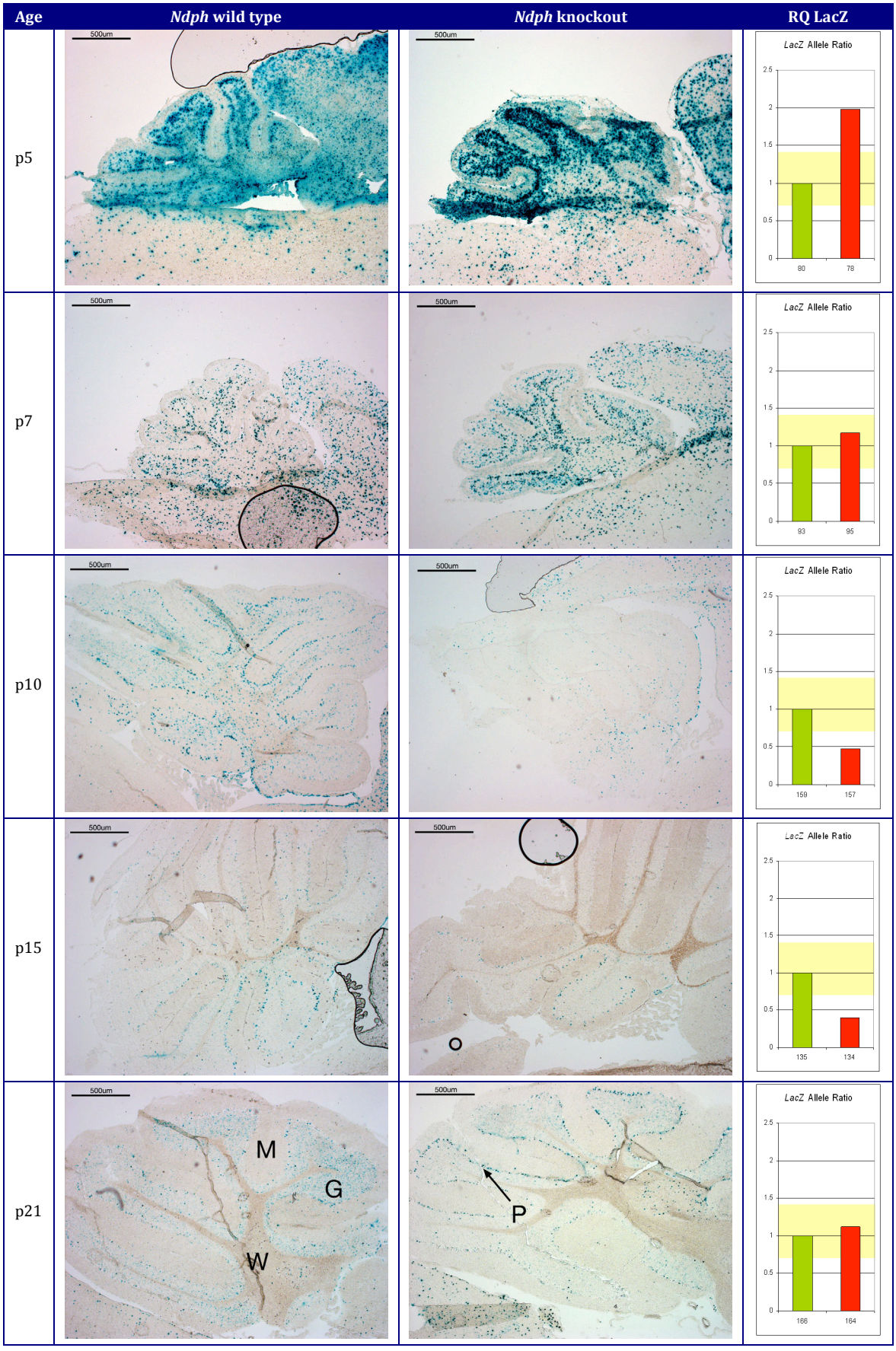

Figure 83 Brain cryosections (8µm) showing the cerebellar region of Norrin wild type and knockout littermates of different developmental stages (p5, p7, p10, p15, p21). All sections were cut sagittally, except for p21, which was cut horizontally. Sections were stained with X-Gal to visualize the Wnt-signaling

reporter. Staining was most prominent at the border between molecular and granular layer, presumably in Purkinje cells, although cells located in the granular layer and white matter were also frequently labeled. Almost no staining has been observed in the molecular layer. Differences in staining intensity correlated with relative genomic abundance of the reporter gene, but not with the *Ndph* genotype. For this purpose, C_t-values of the *LacZ* amplicons were calculated relative to the copy number of the 3rd exon of the *Ndph* gene, which only is present once in each male genome (in wt and in ko). The copy number of the reporter gene allele in the *Ndph* wt was set to 1. The yellow area indicates the technical confidence interval of the qRT-PCR system of 1 ct. *M: Molecular layer, G: Granular layer, P: Purkinje cells, W: White matter*

varied: In one case (p5) it was higher in the knockout, in other cases (p10, p15) in the wild type, and similar in other investigated stages (p7, p21).

This led me to question the validity of this experimental approach. If the hypothesis of norrin regulating canonical Wnt-signaling was valid, I would expect genotype-specific differences of reporter activity. Since the used mice were from an F2 generation, and under the assumption that the transgene integrated just once into the genome, there was a 25% possibility that they received the transgene from both parents. Hence, it was possible that the observed expression differences are due to different copy numbers of the reporter-gene in the different animals, and not due to the presence or absence of norrin. To address this question, a qRT-PCR assay was established to measure the relative quantity of *LacZ*. Indeed, the observed expression differences could be correlated with the relative amount of transgene copies (Figure 83).

3.4.3.3 X-Gal staining of the NDxBATgal retina (revised)

Follwing that experiment, X-Gal staining of ocular cryosections was repeated with eyes from animals with comparable allele frequencies to ensure equal detection of Wnt-signaling. In addition, thicker sections were cut (30µm instead of 8µm) to maximize detetion of *LacZ* positive cells. The examined p7 (Figure 87) and p21 (Figure 88) eyes were from the same animals as the brains displayed in Figure 83. In the p7 sections, X-Gal positive cells were detected in the optic nerve, in cells inside the vitreous, and in cells attached to the posterior border of the lens (Figure 87). The latter two most probably again were cells of the transient hyaloid vasculature. No significant differences between the genotypes were observed. Peripheral sections of the same eyes revealed numerous cells inside the anterior vitreous, close to the ciliary body, which likely represent cells of the hyloidea as well. In the wild type, one single blue cell was observed in the ganglion cell layer. In the p21 sections, two X-Gal positive cells were detected in the inner nuclear layer of the wild type, which otherwise lacked any *LacZ* activity. In the knockout, no cells were stained inside the retina. Instead, Wnt-signaling was detected in remainders of the hyaloid vasculature.

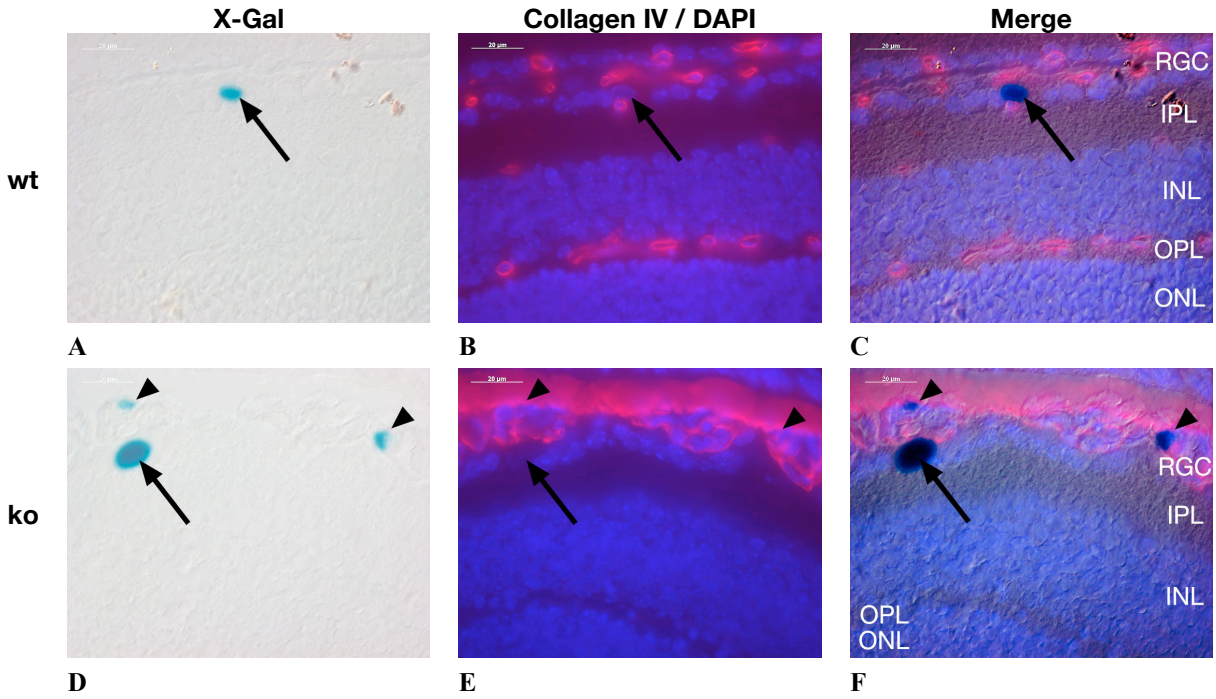

Figure 84 Retinal sections from p10 *Ndph* wt and ko Wnt-reporter mice. Reporter activity was visualized with X-Gal staining (A,D), and blood vessels were labeled with an antibody against collagen IV (B, E). **(A-C)** In the *Ndph* wt, blood vessels were detected in all 3 retinal networks (B). A single cell in the ganglion cell layer was X-Gal positive (A; arrow) that did not co-localize with blood vessels (C; arrow). **(D-E)** The *Ndph* ko presented only with a dilated superficial vasculature (E). X-Gal staining of this section labeled 3 cells (D). One cell (arrow) situated in the ganglion cell layer did not co-localize with blood vessels, while the other two (arrowheads) were located inside the vasculature (F). *INL: inner nuclear layer; IPL: inner plexiform layer; ONL: outer plexiform layer; OPL: outer plexiform layer; RGC: retinal ganglion cell layer*

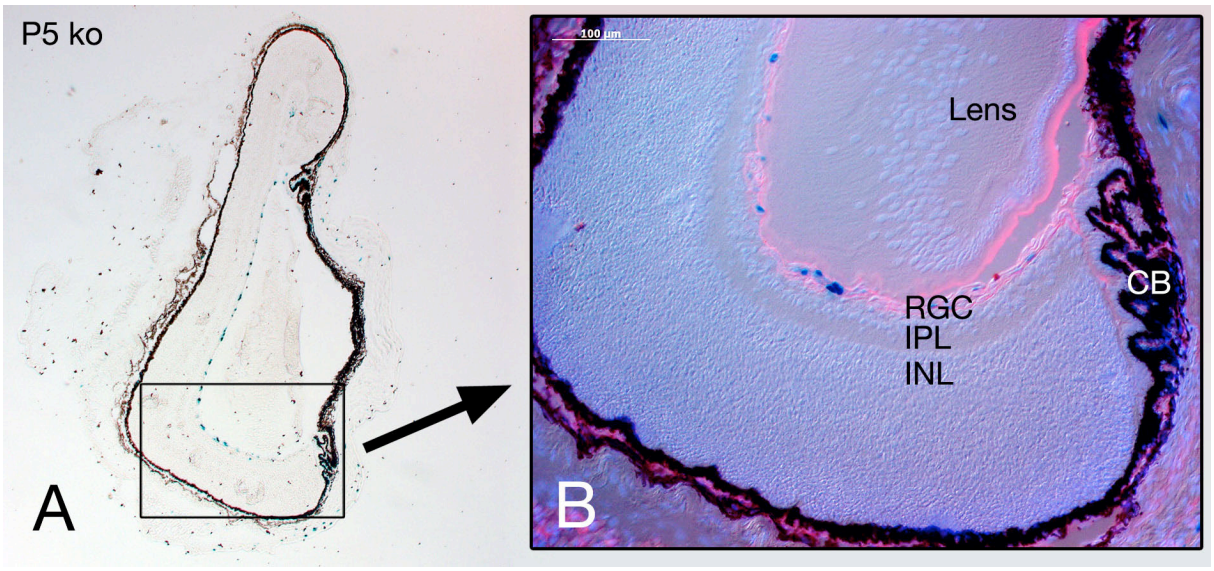

Figure 85 Retinal section from a p5 *Ndph* ko Wnt-reporter mouse. **(A)** This section is the one with the most abundant X-Gal staining I was able to produce during my experiments. At first glance, it appeared that the string-of-pearls like stained cells (*dark blue*) are located inside the retinal ganglion cell layer. **(B)** Co-localization with cells immunoreactive for collagen IV (*red*) suggested that these Wnt-signaling active cells are part of the vasculature. From this section, it is nearly impossible to decide whether the vessels are part of the superficial retinal network or of the hyaloid vasculature, because the lens is located directly adjacent to the retina. This could be a result of the cryoprotection procedure, which likely has drained H_2O from the vitreous. However, the superficial vasculature at p5 is still developing and is not present in the retinal periphery. Thus, vessels adjacent to the retina in this area are likely of hyaloid origin (see right side of the picture, near the ciliary body). *CB: ciliary body; INL: inner nuclear layer; IPL: inner plexiform layer*

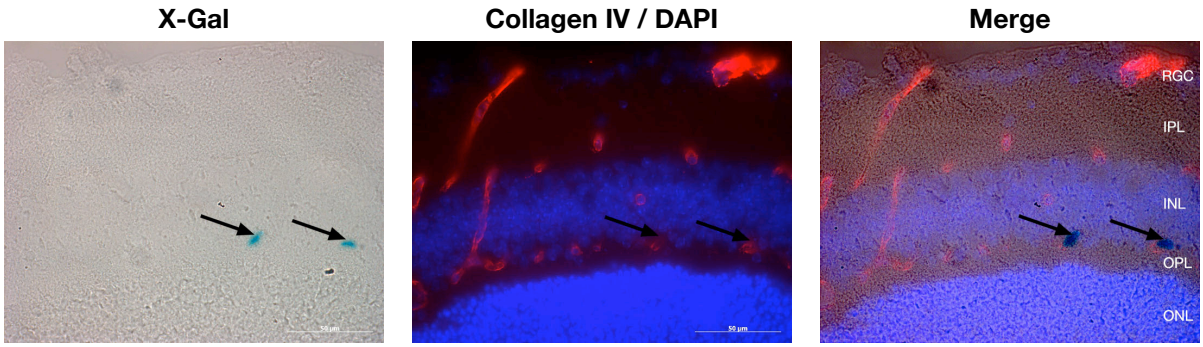

Figure 86 Retinal section from a p21 *Ndph* wt Wnt-reporter mouse. **(A)** Two cells inside the retina were *LacZ* positive. **(B)** Immunostaining with collagen IV labeled all 3 retinal vessel systems. **(C)** The overlay picture revealed co-staining of the two Wnt-signaling active cells with vessels of the deep network, located at the border of the inner nuclear and outer plexiform layers. *INL: inner nuclear layer; IPL: inner plexiform layer; ONL: outer plexiform layer; OPL: outer plexiform layer; RGC: retinal ganglion cell layer*

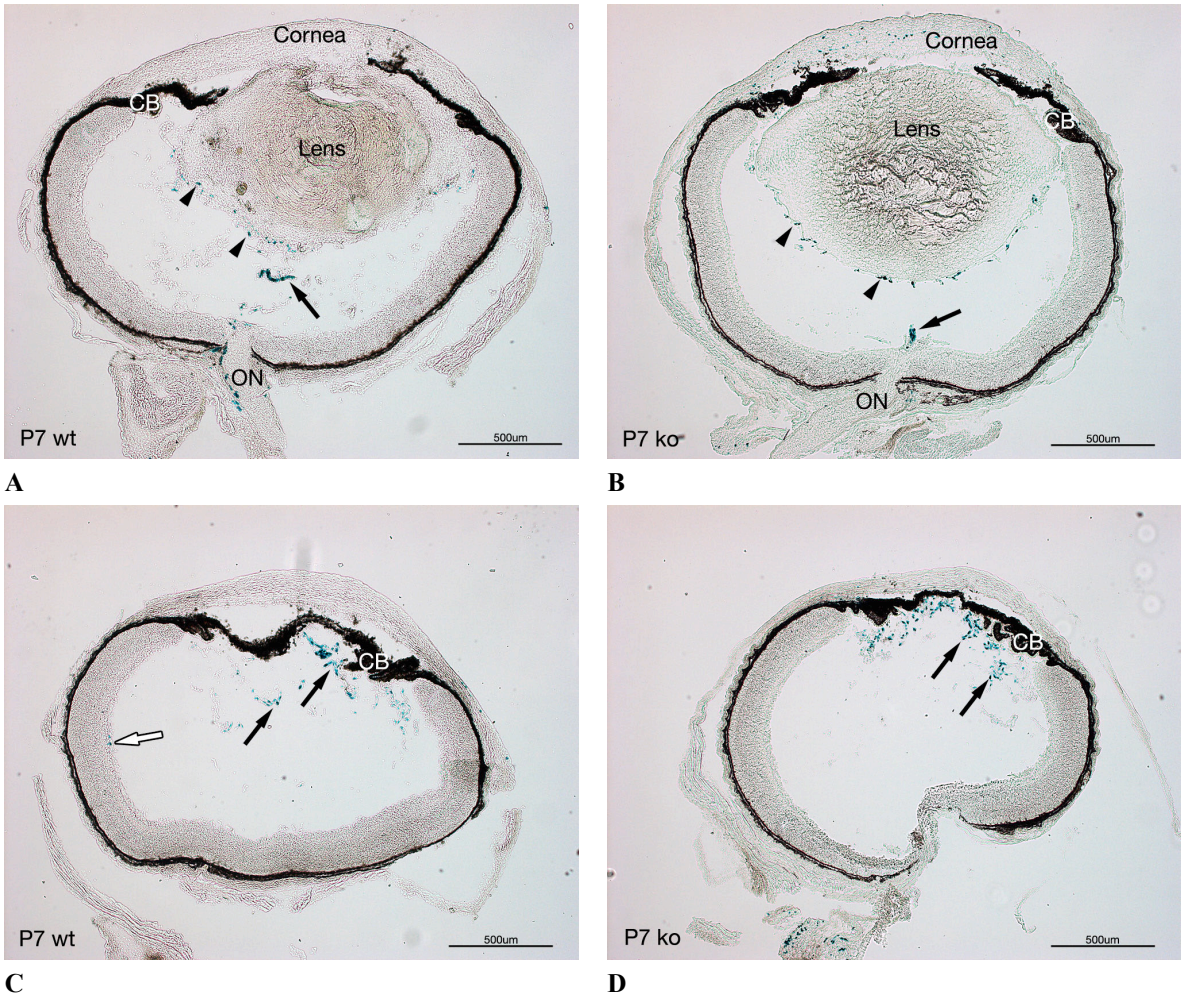

Figure 87 Ocular cryosections (30µm) of p7 *Ndph* wt and ko Wnt-reporter mice were treated with X-Gal to detect activity of Wnt-signaling. No significant differences between the genotypes were observed. **(A)** Central section through an *Ndph* wt eye. X-Gal positive cells (blue) were detected in the optic nerve (ON), in cells inside the vitreous (arrow), and in cells attached to the posterior border of the lens (arrowheads). **(B)** Central section through an *Ndph* ko eye. Similar to the wt staining (A), blue cells were found in the vitreous (arrow; attached to the optic nerve) and adjacent to the lens (arrowheads). In addition, X-Gal positive cells were observed in the cornea. **(C)** Peripheral wt section of the same eye as in (A). Numerous cells inside the anterior vitreous were labeled, close to the ciliary body (arrows). In the retina, one single

blue blue cell was observed in the ganglion cell layer (hollow arrow). **(D)** Peripheral ko section of the eye presented in (B). As in the wt, numerous cells in the anterior part of the vitreous, close to the ciliary body, were labeled (arrows). No staining was observed in the retina. *CB: ciliary body; ON: optic nerve*

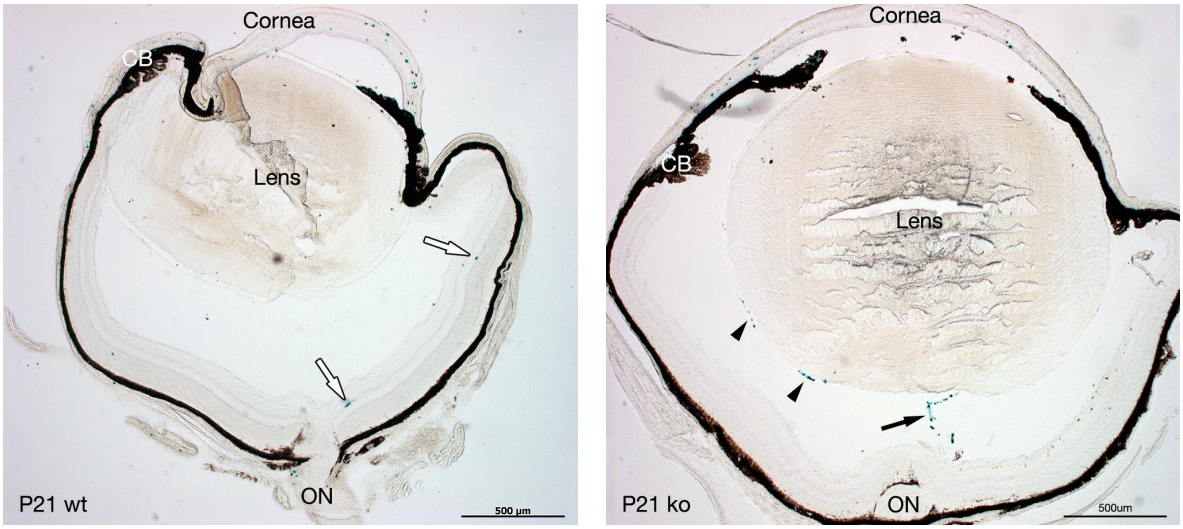

A **B**

Figure 88 Ocular cryosections (30µm) of p21 *Ndph* wt and ko Wnt-reporter mice were treated with X-Gal to detect activity of Wnt-signaling. **(A)** Central section through an *Ndph* wt eye. X-Gal positive cells (blue) were detected in the optic nerve, the cornea, and inside the retina, at the borders of the inner nuclear to the inner and outer plexiform layers (hollow arrows). No cells were labeled inside the vitreous or adjacent to the lens. **(B)** Central section through an *Ndph* ko eye. Stained cells were found in the cornea, the vitreous (arrow), and adjacent to the lens (arrowheads). No X-Gal positive cells were found inside the retina. *CB: ciliary body; ON: optic nerve*

3.4.3.4 Synopsis

After all, detection of retinal Wnt-signaling activity was not successful. Since X-Gal staining did work in other parts of the eye and also in the brain, the results suggest that my experimental procedures were suited to detect *LacZ* activity, but that the used reporter mouse may not allow investigation of Wnt-signaling in the retina. This could not be expected, because a study conducted with a similar reporter mouse did work well (Liu et al., 2006). In addition, the use of this reporter mouse may further not be qualified for quantitative investigation of Wnt-activity, since X-Gal staining intensity varied with the number of *LacZ* alleles present in each animal. This necessitates the establishment of a homozygous breed or the quantification of the *LacZ* copy number in every animal in the experiment.

However, my studies led to some qualitative results: It could be shown that Wnt-signaling was active in the remaining hyaloid vessel system of the norrin ko mouse, although Wnt-signaling usually facilitates the regression of this transient structure (Lobov et al., 2005). Thus, X-Gal positive cells could be expected in the hyaloid vasculature of the wild type, and notably, impaired regression in the *Ndph* ko is not due to a lack of Wnt-signaling in this system.

3.5 Candidate gene screening in patients

3.5.1 Clinical description of patients

A total of 22 patient DNAs referred to our diagnostic division was available for screening of candidate genes (Table 6). Clinical suspicion of Norrie disease was stated 14 times, Coats' disease 6 times, FEVR 3 times, PHPV 2 times, and retinoblastoma was suspected once. For some patients, more than one clinical diagnosis was suggested.

3.5.2 *NDP* screening

All patients mentioned above were screened for mutations in the Norrie disease pseudoglioma (*NDP)* gene in our diagnostic division. All 3 exons were sequenced, including the 5'- and 3'-UTRs (Figure 89).

Figure 89 The *NDP* transcript consists of 1,923 bp coding a 133 aa protein. The gene is located on chromosome Xp11.3, spans 24.82kb and is organized in 3 exons, 2 of them coding. (Source: **www.ensembl.org**)

Five patients (22277, 23081, 25775, 27019, and 27095) were found to harbour mutations in *NDP* prior to this study (Table 6). Since miRNA recognition site mutations in the 3'UTR have been discussed in association with human disease (Abelson et al., 2005; Clop et al., 2006; Sethupathy et al., 2007; Jensen et al., 2008), and the diagnostic routine at the institute did not include sequencing of the 1kb 3'UTR, this region was covered in addition for all patients (excluding 29833). However, no sequence alterations were found.

3.5.3 *FZD4* screening

Frizzled 4 (*FZD4*) was the second gene after *NDP* (Chen et al., 1993) that has been associated with FEVR (Robitaille et al., 2002). In contrast to *NDP*, mutations in *FZD4* follow a dominant mode of inheritance. After the discovery of a similar ocular phenotype in *Ndph* and *Fzd4* ko mice, it has been been shown that *FZD4* acts as a receptor for norrin (Xu and Wang et al., 2004). This common involvement in the same molecular pathway could explain the high phenotypic overlap between patients with mutations in either *NDP* or *FZD4.*

Therefore, patients diagnosed with ND or CD who were negative for mutations in the *NDP* gene were screened for alterations in *FZD4* (Figure 90).

Exon 1 and the coding region of exon 2, as well as the flanking parts of intron 1 were sequenced mainly (12 of 17 patients: 6 females, 7 males, 4 of unknown gender) by Jurian Zürcher as part of his masterthesis.

In addition, two miRNAs (miR-31 and miR-184) that target the 5.5kb 3'UTR of *FZD4* have been shown to inhibit neovascularization (Shen et al., 2008). Since mutations in miRNA recognition sites have been discussed in association with human disease (Abelson et al., 2005; Clop et al., 2006; Sethupathy et al., 2007; Jensen et al., 2008), the two parts of the *FZD4* 3'UTR harboring the recognition sites for miR-31 and miR-184 were also sequenced.

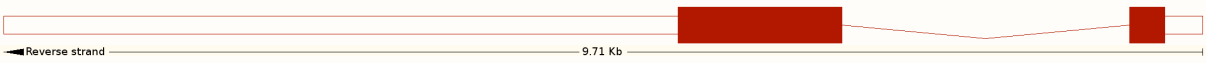

Figure 90 *FZD4* is a 2-exon gene spanning 9.71kb on chromosome 11q14.2. It holds the information for a 7,382 bp transcript, which codes a 537 aa protein. (Source: **www.ensembl.org**)

Three annotated sequence alterations were found in our patient group: A c.1614*2G>T exchange in patient 22439, and the missense mutations c.97C>T (p.P33S) and c.502C>T (p.P168S) in the DNA of patient 27118 (Figure 91). No variations were found in the 3'UTR including the recognition sites for miR-31 and miR-184.

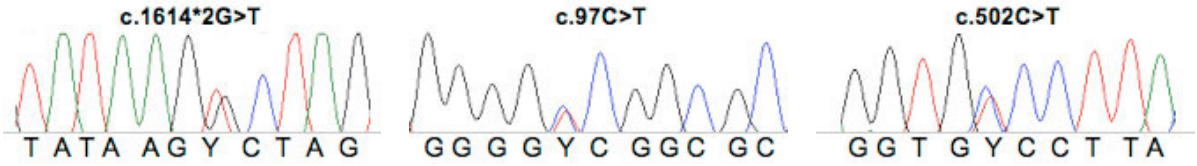

A patient 22439 **B** patient 27118 **C** patient 27118

Figure 91 Electropherograms showing the 3 heterozygous *FZD4* nucleotide variations found in the patient group. **(A)** SNP rs61749246 (c.1614*2G>T) observed in patient 22439. **(B)** The c.97C>T mutation causing the p.P33S substitution in patient 27118. **(C)** The c.502C>T (p.P168S; rs61735303) substitution in patient 27118. (Source: Masterthesis Jurian Zürcher, 2007)

The nucleotide exchange in the 3'-UTR was predicted as a SNP (rs61749246) with an estimated allele frequency of the T allele of 2% in whites (Toomes et al., 2004a). The p.P33S substitution was discussed as pathogenic (CM050619; MacDonald et al., 2006), while the p.P168S substitution (rs61735303) was described as a rare (<0.3%), but benign variant (Toomes et al., 2004).

Patient 27118, harboring the p.P33S and p.P168S variants, is a preterm delivery to opthalmologically healthy parents. She was born with a gestational age of about 30 weeks, a birth weight of 1500g, and received oxygen supplementation for ~6 hours. She had low visual acuity in both eyes since early childhood. At the last examination, she had no light perception on the left, and a visual acuity of 1/25 on her right eye. The left eye presented with microcornea and a shallow anterior chamber. An ophthalmoscopic examination performed by Dr. Charlotte Poloschek, Freiburg, Germany, revealed exudative retinal detachment with massive lipid exudation in both eyes. A vascularized (pseudo-)tumor was present at the 6 o'clock position in the right eye, which has been removed after cryotherapy. Incontinentia pigmentii was excluded by dermatologic examination, and the examining physicians excluded ROP, FEVR, and ND due to the lack of typical temporal dragging, finally diagnosing Coats' disease. Two cousins had retinal detachments. Unfortunately, the patient and her family were not available for further examinations after the molecular diagnosis.

3.5.4 *LRP5* screening

Mutations in the low density lipoprotein receptor-related protein 5 (*LRP5*), the norrin co-receptor to FZD4 (Xu and Wang et al., 2004), have also been associated with FEVR (Toomes et al., 2004). In contrast to *FZD4*, mutations in *LRP5* are mainly inherited recessively, although dominant mutations have been also reported (Gong et al., 2001; Toomes et al., 2004). After mutations in *NDP* and *FZD4* have been excluded, Walther Hänseler performed the screening of the remaining patient DNAs during his masterthesis under my supervision.

All 23 exons and flanking intronic regions of the only known transcript (ENST00000294304; Figure 92) were sequenced from DNAs from 14 patients (5 females, 5 males, and 4 patients with unknown gender).

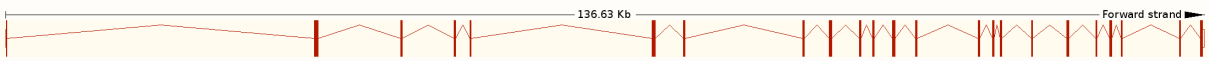

Figure 92 The *LRP5* gene is located on 11q13.2 spanning 136.63kb. The 5,124 bp transcript is organized in 23 exons and codes for a 1,615 aa protein. (Source: **www.ensembl.org**)

Four so far undescribed sequence variants were found. A patient diagnosed with Coats' disease (#28786; Figure 93) was found to harbor a p.T672M (c.2015C>T**;** Figure 94 A) amino acid exchange, which is a position highly conserved among vertebrates.

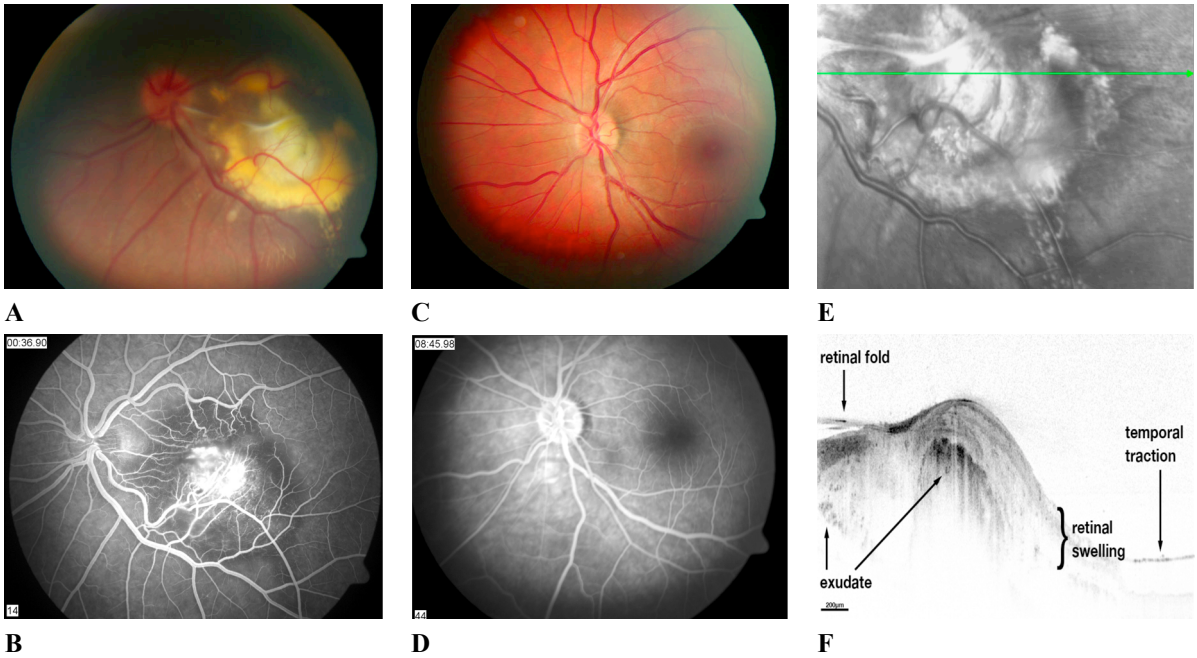

Figure 93 Ocular presentation of patient 28786, a girl diagnosed with CD. **(A)** The left eye was marked by a central lesion surrounded by exudates and retinal folds with papillary adherence. The right eye was clinically unsuspicious. **(B)** Leakage of fluorescein at the macular lesion. **(C, D)** Fundus (C) and fluorescein angiography (FLA; D) of a normal eye of the patient's mother. **(E, F)** Optical coherence tomography (OCT) of the lesion in the patient's left eye revealed an enormous deformation of the retina and extended subretinal exudates. The green line in the funduscopic picture (E) indicates the plane of section of the

corresponding OCT presented in (F). (Pictures taken by Dr. Charlotte Poloschek, Department of Ophthalmology, University of Freiburg, Freiburg, Germany)

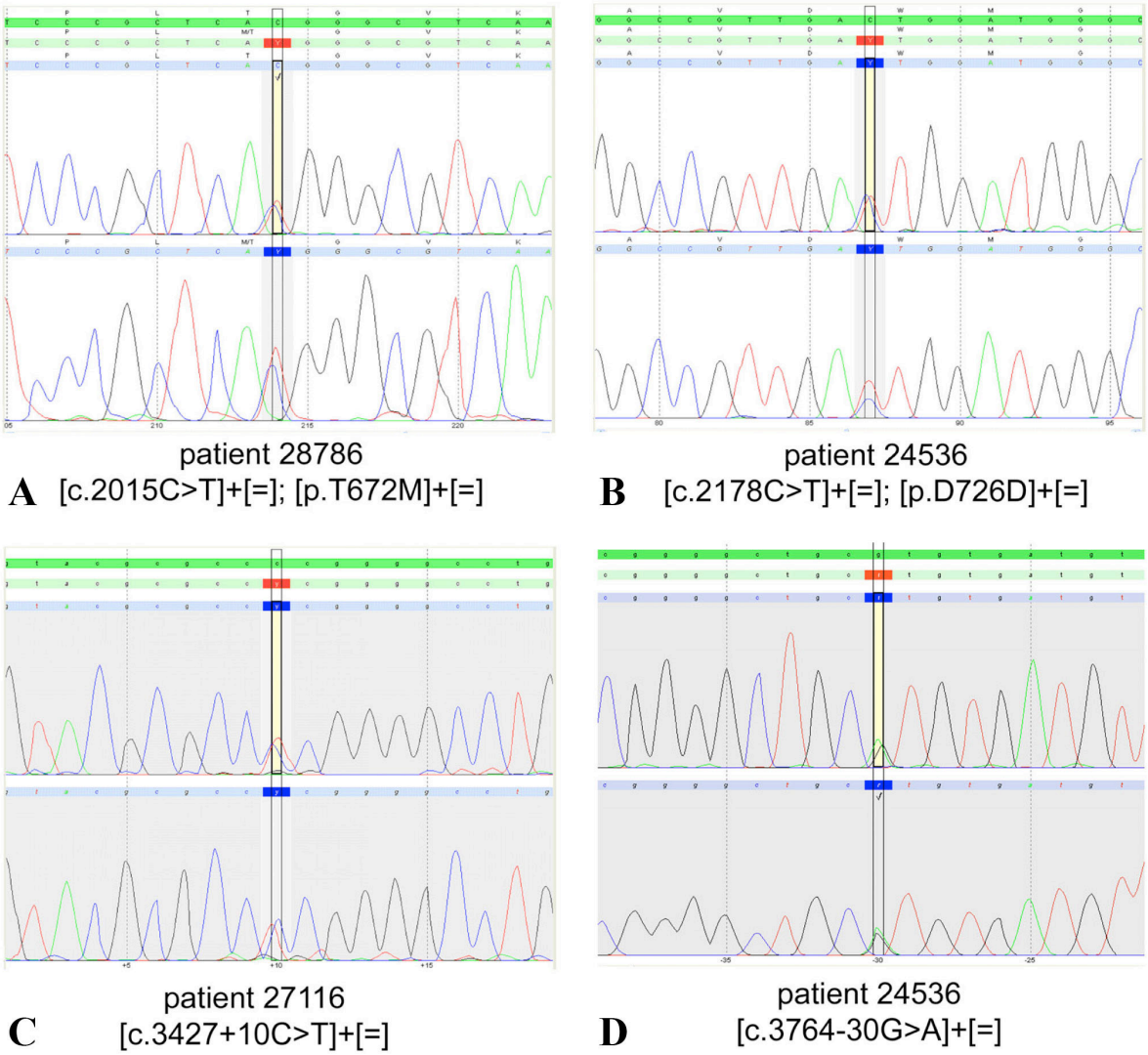

Figure 94 Electropherograms of so far undescribed heterozygous *LRP5* DNA sequence variations in our patient group. **(A)** A c.2015C>T missense mutation (p.T672M) was found in patient 28786. **(B)** A silent mutation in exon 10, c.2178C>T, was found in patient 24536. **(C)** The intronic variation c.3427+10C>T (intron 11) was found in patient 27116. **(D)** A variation in intron 17, c.3764-30G>A, was found in patient 24536. (Source: Masterthesis Hänseler, 2008)

The mutation was absent in 384 control alleles. The amino acid exchange lies in the third β-propeller of the extracellular domain of LRP5 in the binding site of DKK, an endogenous inhibitor of Wnt-signaling (reviewed by Balemans and van Hul, 2007). The mutation thus could imply a functional change of LRP5 that strengthens the affinity to DKK, thereby explaining an *NDP*-related phenotype. Pathogenicity was analyzed *in silico* with the prediction programs SIFT (http://blocks.fhcrc.org/sift/SIFT.html) and PolyPhen (http://coot.embl.de/PolyPhen). SIFT predicted the amino acid exchange to be marginally tolerable, while PolyPhen predicted the p.T672M mutation to be possibly damaging (Masterthesis Hänseler, 2008).

However, the mutation was also found to be heterozygous in the patient's unaffected mother as well as her two so far unaffected younger siblings (Figure 95). This would be consistent with the expected recessive mode of inheritance. Due to the lack of a homozygous mutation in the patient, the clinical picture could be explained with a second, somatic mutation only in the affected eye, similar to the *NDP* mutation described by Black et al., 1999.

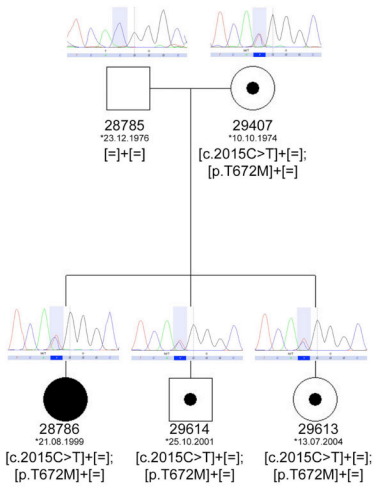

Figure 95 Pedigree of the CD patient 28786, showing the electropherograms for the newly identified c.2015C>T (p.T672M) mutation. The variation is heterozygous in the patient, but as well in her unaffected mother and her two siblings. (Source: Masterthesis Hänseler, 2008)

The three other variations are all silent (Figure 94 B-D). Only one is exonic, the other two lie in intronic regions. Effects on common splice sites could be excluded. Variants c.2178C>T and c.3427+10C>T were not found in 384 control alleles, c.3764-30G>A was found in 3 alleles. (Masterthesis Hänseler, 2008)

The exonic mutation (c.2178C>T; Figure 94 B) was checked *in-silico* for effects on exonic splice enhancers/silencers with the programs ESEfinder (http://rulai.cshl.edu/cgi-bin/tools/ESE3/esefinder.cgi?process=home), PESXs (http://cubweb.biology.columbia.edu/pesx/), and ESRsearch (http://ast.bioinfo.tau.ac.il/ESR.htm). ESRsearch could localize four splicing regulatory motifs involving the C allele that do not recognize the T allele, but also two binding sequences that are present only with the T allele (Figure 96).

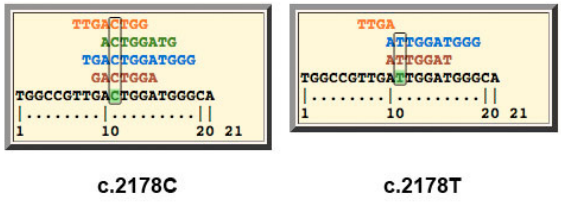

Figure 96 Results from the ESRsearch analysis for exonic splice regulatory elements (ESR). The c.2178 position is framed and the respective allele is highlighted in green. When the c.2178C allele is present, four putative ESR were predicted to bind, while those four would not recognize the c.2178T allele. Instead, two other putative ESR were predicted to recognize the c.2178T allele. (modified after data from **http://ast.bioinfo.tau.ac.il/ESR.htm**)

In addition, eleven known single nucleotide polymorphisms (SNPs) were found (Masterthesis Hänseler, 2008). One of them presented with a significant differential allele frequency in our patient group in comparison to the frequency found in the HAPMAP database (rs4988320; Table 42), suggesting it as risk-factor for the development of an FEVR-like phenotype. However, this conclusion has to be treated with care, because the occurrence of the homozygous risk allele would be several orders of magnitude higher than the occurrence of the disease. Nonetheless, the SNP could modify other genetic or environmental factors (e.g. premature birth) that have an influence on the severity of the disease.

Allele frequency of the *LRP5* SNP							
Exon	SNP	Base substitution	Database	patients	Odds ratio	Lower limit	Upper limit
Ex7	rs4988320	c.1413-50G>A	0.96	0.82	5.33	1.33	21.41

Table 42 Allele frequency for *LRP5* SNP rs4988320. Frequencies are given for the ancestral allele. Frequency data for rs4988320 originates from the CSHL-HAPMAP-CEU cohort (102 alleles). Our patient group consisted of 28 alleles. Data was retrieved from www.ncbi.nlm.nih.gov. Odds ratios were calculated with a web-based tool (http://faculty.vassar.edu/lowry/odds2x2.html). (data taken from: Masterthesis Hänseler, 2008)

3.5.5 *LRP5L* screening

Low density lipoprotein receptor-related protein 5-like (*LRP5L*) first came to my attention during the screening of *LRP5*, because PCR primer pairs designed to amplify fragments of *LRP5* also produced amplicons of *LRP5L* due to its high homology. *LRP5L* is located on chromosome 22q11.23 and encodes for a 252aa protein (Figure 97) that is highly similar to the second β-propeller domain of *LRP5*. Since this a domain where many OPPG mutations cluster (Balemans and van Hul, 2007), I wondered whether mutations in *LRP5L* could contribute to an FEVR-like phenotype. Further indication for a possible role came from a poster presented at the annual ARVO (Association for Research in Vision and Ophthalmology) meeting in 2008 (Gilmour et al., 2009). It described a patient with DiGeorge sequence due to a deletion on chromosome 22q11.2 who in addition presented with an FEVR-like ocular phenotype. At this time point, it was unclear whether the deletion included the *LRP5L* locus, so Walther Hänseler screened the CDS-containing part and flanking intronic regions of this gene as well.

No unknown sequence variants were observed in 13 patients (the same patients who were screened for *LRP5* mutations, but without #29550). Four annotated SNPs were found; for two of them, allele frequency data were available for comparison.

The allele frequency of SNP rs9624807, a silent mutation in exon 2 (c.339C>T), was significantly higher in the patient group, and had a calculated odds ratio of 18.42 (Table 43). Further *in silico* analysis with the ESRsearch tool revealed the creation of a new binding site for a putative exonic splice regulatory element as result of the C>T exchange (Figure 98).

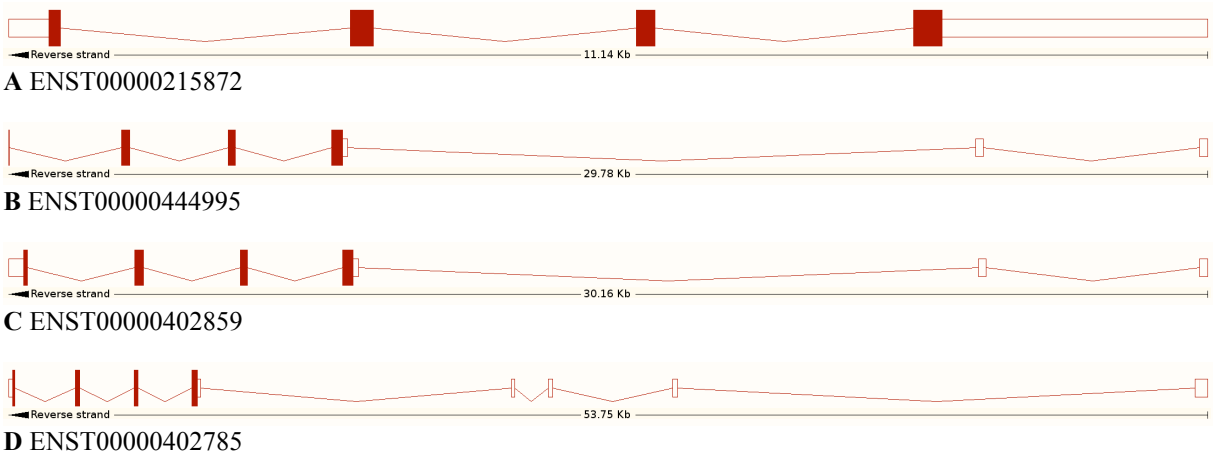

Figure 97 On chromosome 22q11.23, a gene with high homology to *LRP5* is located, termed *LRP5L*. 4 transcripts of the gene are known. **(A)** The longest consists of 3,602 bp, is organized in 4 exons and spans a genomic region of 11.14kb (ENST00000215872). Screening was established to sequence the CDS of these 4 exons. **(B-D)** However, the three other transcripts (ENST00000444995, ENST00000402859, ENST00000402785) span a larger genomic region and include untranslated 5'-exons. All encode a 252 aa protein, with the exception of (B), which encodes a shorter 224 aa product. (Source: **www.ensembl.org**)

Allele frequency of the *LRP5L* SNP							
Exon	SNP	Base substitution	Database	patients	Odds ratio	Lower limit	Upper limit
Ex2	rs9624807	c.339C>T (p.R113R)	0.98	0.73	18.42	3.55	95.56

Table 43 Allele frequencies for the *LRP5L* SNP rs9624807. Frequencies are given for the ancestral allele. Frequency data originates from the CSHL-HAPMAP-CEU cohort (102 alleles). Our patient group consisted of 26 alleles. Data were retrieved from www.ncbi.nlm.nih.gov. Odds ratios were calculated with a web-based tool (http://faculty.vassar.edu/lowry/odds2x2.html). (data taken from: Masterthesis Hänseler, 2008)

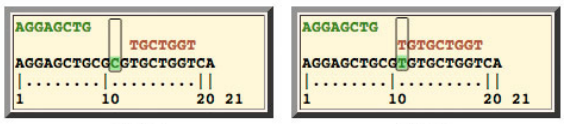

Figure 98 Results from the ESRsearch for exonic splice regulatory sequences. The c.339 position is framed and the respective allele is highlighted in green. When the c.339C allele is present, no putative ESRs bind to the sequence. Instead, a new recognition site for one putative ESR was predicted when the c.339T allele was analyzed. (modified after data from **http://ast.bioinfo.tau.ac.il/ESR.htm**)

3.5.6 *PLVAP* screening

The plasmalemma vesicle associated protein (*PLVAP*) probably is the best characterized and most promising candidate gene of this thesis. Its mRNA expression was increased in the microarray experiment (Table 40), and retinal expression was shown to be increased throughout postnatal retinal development from p5 to p21 (Figure 52 A), especially at the more advanced stages. It likely mediates one of the hallmark features of ND and probably other EVRs: blood vessel leakiness. Since it is differentially expressed already early in development, I hypothesized that it could be a direct target of Norrin (Schäfer et al., 2009). Further, ectopic expression in the retinal vasculature could be shown by immunohistochemistry (Figure 53).

A possible mode of action for Norrin, besides transcriptional regulation via the Wnt/β-catenin pathway, might be a direct modulation of the microtubule cytoskeleton (Salinas, 2007) or Plvap itself. This led me to hypothesize that transient Plvap expression and fenestration occur during maturation of the retinal vasculature and that Norrin signaling is possibly required for its suppression. Mutations in PLVAP thus may affect sprouting angiogenesis as well as the formation and maintenance of the blood-retina- or blood-brain-barrier, and therefore could mimic or modify the ocular effect of *NDP* mutations.

All 6 exons and the flanking intronic regions of the *PLVAP* gene (Figure 99) were sequenced from DNAs of 13 patients (3 females, 6 males, and 4 patients with unknown gender).

No new or unannotated SNPs or mutations were found in the screening.

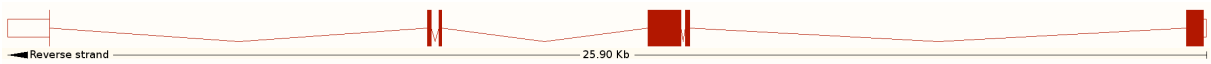

Figure 99 The transcript of the *PLVAP* gene (ENST00000252590) consists of 6 exons and has a length of 2,298bp. The CDS codes for 442aa and starts in exon 1. *PLVAP* is located on chromosome 19p13.11. (Source: **www.ensembl.org**)

However, three silent, annotated SNPs were observed. The first one (rs10417806) is located in exon 1, 44 bases upstream of the ATG in the 5'-UTR. A thymidine is replaced by a guanine. This polymorphism was found heterozygously in patients 25160 and 27110 (Figure 117 in the appendix).

The second SNP (ENSSNP5758645), a guanine to adenosine substitution, is situated 37 nucleotides upstream of exon 6 in intron 5. This sequence variation is present heterozygously in 5 patients: 22439, 24536, 25160, 27110, and 27116 (Figure 118 in the appendix).

The third SNP is rs7259703, which has been found in patients 27113 and 27735. It is a cytosine to thymine substitution and located 329 bp into the 3'-UTR (Figure 119 in the appendix).

A comparison with allele frequency data from the HAPMAP project for rs10417806 and rs7259703 (www.hapmap.org) showed no significant differences with the examined patient group (Table 44). No allele frequencies were available for ENSSNP5758645.

SNP	Nuc Change	AA Change	Exon	Exon position	SNP freq database	Genotype frequencies						
						T/T		T/G		G/G		
						rel.	abs.	rel.	abs.	rel.	abs.	
rs10417806	c.-44T>G	5'-UTR	1	19	CSHL-HAPMAP:HapMap-CEU	0.846	11.0	0.154	2.0	0.000	0.0	patients
						0.793	10.3	0.172	2.2	0.034	0.4	expected
						G/G		G/A		A/A		
						rel.	abs.	rel.	abs.	rel.	abs.	
ENSSNP5758645	c.1322-37G>A	Intron 5	6	-37	none	0.615	8.0	0.385	5	0.000	0.0	patients
						na	na	na	na	na	na	expected
						C/C		C/T		T/T		
						rel.	abs.	rel.	abs.	rel.	abs.	
rs7259703	c.*329C>T	3'-UTR	6	386	CSHL-HAPMAP:HapMap-CEU	0.846	11.0	0.154	2	0.000	0.0	patients
						0.967	12.6	0.033	0.4	0.000	0.0	expected

Table 44 *PLVAP* SNPs found in the patient screening. Genotype frequencies are given in relative and absolute values. No significant differences to frequencies published in databases, when available, were found. dbSNP128. *na:* not available

3.5.7 *LMO2* screening

LIM domain only protein 2, or Rhombotin-2 (*LMO2*), was not on the list of differentially expressed transcripts generated from the microarray experiment, nor was its expression analyzed by other methods in this study. However, some other evidence suggested *LMO2* as promising candidate gene for mutation screening. First, a new locus for ad FEVR has been described on chromosome 11p12-13 (Downey et al., 2001). The linkage interval was determined to a 14cM region, with a maximum LOD score of 6.6, and the locus was termed „EVR3". One of the genes in this interval possibly relevant to FEVR is *LMO2*. It is a transcription factor that affects angiogenesis and is likely involved in Wnt-signaling (Yamada et al., 2000). Like *NDP* and *FZD4*, two of the known FEVR-associated genes, *LMO2* is expressed in the retina and inner ear, two of the organs affected in ND (Deng et al., 2006). Further, *in silico* analysis suggested that *NDP* has a binding site for LMO2 (Katoh and Katoh, 2005). Conservation on transcript level to mouse *Lmo2* is 96% and thus the ko mouse model could be instrumental to the understanding of its function. Lmo2 is a nuclear protein expressed in the erythroid lineage in vivo that is essential for erythroid development in mice. The homozygous *Lmo2* null mutation leads to a failure of yolk sac erythropoiesis and embryonic lethality around E10.5. (Warren et al., 1994). LMO2 has been hypothesized to act as a „bridging" molecule, assembling a DNA-binding complex consisting of different transcription factors (Yamada et al., 2001). Phenotypic variability in EVR patients could thus arise from different constitution of an angiogenesis-specific transcription factor complex.

Besides these considerations, *LMO2* is an attractive candidate gene due to its rather small size. Its largest transcript consists of only 6 exons, has 2,291bp and encodes a 227 aa protein (Figure 100).

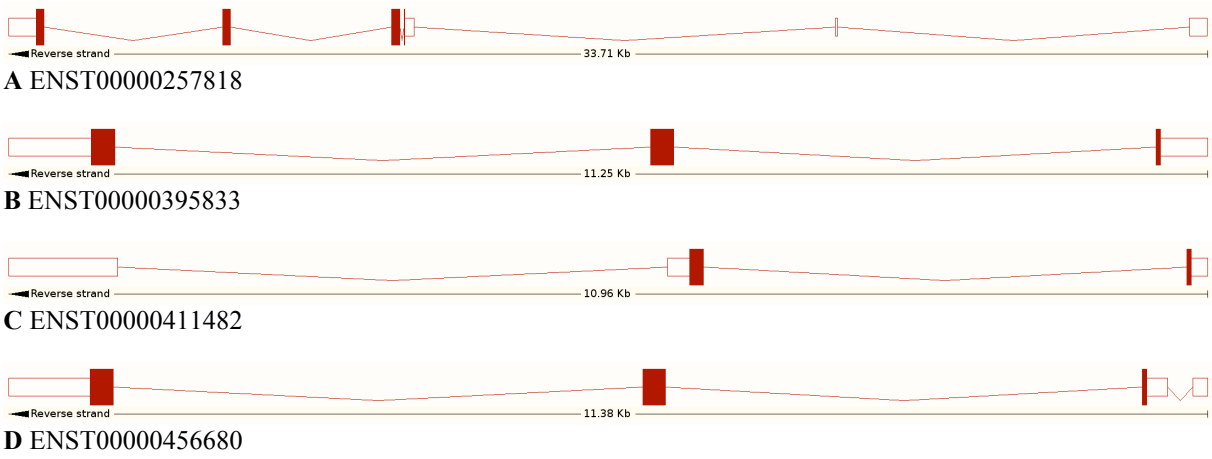

Figure 100 *LMO2*, located on chromosome 11p13, has 4 known transcripts. **(A)** The longest transcript (ENST00000257818) consists of 6 exons and has a length of 2,291bp. The CDS codes for 227aa and starts in exon 4. **(B-D)** The three other transcripts lack at least the first two exons and have a shorter CDS. (Source: **www.ensembl.org**)

All 6 exons and the flanking intronic regions of the *LMO2* gene were sequenced from DNAs from 13 patients (3 females, 6 males, and 4 patients with unknown gender).

Analysis of the sequence data revealed five annotated SNPs (Table 45). The first, rs2273799, is an adenine to guanine substitution in the 5'-UTR (exon 1; c.-796A>G). It was found in a heterozygous state in DNAs from patients 25160, 25649, 27116, and 27735. It was homozygous in patients 22439, 24536, and 27111 (Figure 120 in the appendix). A second one (rs11032432) was found at position c.-425C>G, also in the 5'-UTR. It is located in exon 3, and was present heterozygously in 6 patients: 22439, 25160, 25649, 27111, 27112, and 27188. Patients 24165, 27110, 27116, and 27735 were homozygous (Figure 121 in the appendix). SNP rs2038602, a c.111T>C exchange that has no effect on protein level (p.I37I), was found in 6 patients 22439, 25160, 25659, 27111, 27112, and 27188 in a heterozygous state. 4 patients (24165, 27110, 27116, 27735) were homozygous (Figure 122 in the appendix). Six patients were further heterozygous for another silent SNP, rs3740617, which is a c.363A>G substitution (p.K121K): 22439, 25160, 25649, 27111, 27112, and 27188. The variation was present homozygously in patients 24536, 27113, and 28931 (Figure 123 in the appendix). The last *LMO2* SNP found in the patient group was rs3740616. It is an adenine to thymine exchange in the 3'-UTR (c.*483A>T). Four patients were heterozygous (25649, 27111, 27112, 27116), patient 27110 was homozygous (Figure 124 in the appendix).

For four of the five SNPs, allele frequency data were available. A comparison with frequency data of the patient group (www.hapmap.org) showed no significant differences (Table 45), and all variants appear to be common. No frequency data were available for rs11032432.

No new or unannotated SNP or mutation was found in the screening.

SNP	Nuc Change	AA Change	Exon	Exon position	SNP freq database	Genotype frequencies						
rs2273799	c.-796A>G	5'-UTR	1	269	CSHL-HAPMAP:HapMap-CEU	A/A		A/G		G/G		
						rel.	abs.	rel.	abs.	rel.	abs.	
						0.462	6	0.308	4.0	0.231	3.0	patients
						0.267	3.5	0.500	6.5	0.233	3.0	expected
rs11032432	c.-425C>G	5'-UTR	3	177	none	C/C		C/G		G/G		
						rel.	abs.	rel.	abs.	rel.	abs.	
						0.231	3.0	0.462	6.0	0.308	4.0	patients
						na	na	na	na	na	na	expected
rs2038602	c.111T>C	p.I37I	5	70	CSHL-HAPMAP:HapMap-CEU	T/T		T/C		C/C		
						rel.	abs.	rel.	abs.	rel.	abs.	
						0.231	3.0	0.462	6.0	0.308	4.0	patients
						0.233	3.0	0.533	6.9	0.233	3.0	expected
rs3740617	c.363A>G	p.K121K	6	106	CSHL-HAPMAP:HapMap-CEU	G/G		G/A		A/A		
						rel.	abs.	rel.	abs.	rel.	abs.	
						0.308	4.0	0.462	6.0	0.231	3.0	patients
						0.267	3.5	0.500	6.5	0.233	3.0	expected
rs3740616	c.*483A>T	3'-UTR	6	226	CSHL-HAPMAP:HapMap-CEU	A/A		A/T		T/T		
						rel.	abs.	rel.	abs.	rel.	abs.	
						0.615	8	0.308	4	0.077	1	patients
						0.483	6.3	0.517	6.7	0.017	0.2	expected

Table 45 *LMO2* SNPs found in the patient screening. Genotype frequencies are given in relative and absolute values. dbSNP128. *na:* not available

3.5.8 *SLC38A5* screening

The solute carrier *Slc38a5* was the transcript with the most decreased expression in the microarray experiment (Table 40), and retinal expression was shown to be reduced throughout postnatal retinal development from p5 to p21 (Figure 52 B). It therefore could be a direct target of Norrin. Slc38a5, a neutral amino acid transporter, has been shown to be an important glutamine transporter in the retina (Umapathy et al., 2005), and was also found in astrocytes of the cerebellum (Cubelos et al., 2005). Therefore, it could also mediate norrin function in the brain, and may contribute to the mental retardation phenotype of ND patients. Evidence for this hypothesis came from the report of a microdeletion including *SLC38A5* and the neighboring *FTSJ1* that has been found in three brothers with moderate to severe mental retardation (Froyen et al., 2007). Further experiments lead to the discovery that *Slc38a5* expression is also reduced in the cerebellum of *Ndph* ko mice (Figure 58; Hänseler, Masterthesis, 2008).

Since *NDP* and *SLC38A5* are both located on the X-chromosome and are separated by only 4.5cM (Figure 101), variations in both genes are likely to cosegregate within a familiy. It thus seems possible that *SLC38A5* could act as a modifier for *NDP* mediated function.

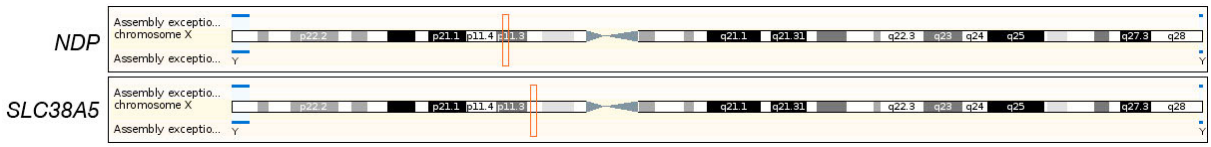

Figure 101 The loci of *NDP* and *SLC38A5* are only separated by 4.5cM on the human X-chromosome. (Source: **www.ensembl.org**)

All 16 exons and the flanking intronic regions of the *SLC38A5* gene (Figure 102) were sequenced from DNAs from a total of 22 patients (8 females, 10 males, and 4 patients with unknown gender). Because it was hypothesized that variations in *SLC38A5* could modify the outcome or severity of the disease, DNAs from patients who already have been diagnosed with mutations in the established genes *NDP* (5), *FZD4* (1), and *LRP5* (1) were included. The screening was performed by Karin Schläpfer under my supervision during her one-month internship at the Institute of Medical Genetics.

Figure 102 The longest transcript of the *SLC38A5* gene (ENST00000376876) consists of 16 exons and has a length of 2,654bp. The CDS codes for 472aa and starts in exon 2. *SLC38A5* is located on chromosome Xp11.23. (Source: **www.ensembl.org**)

Analysis of the sequence data from the 22 patient DNAs revealed two annotated SNPs. The first one (rs2293953) is situated in intron 2, 43 bases upstream of exon 3. A

thymidine is replaced by a cytosine. This polymorphism was found in five patients: Individuals 22777, 24165, 27110 and 28786 are heterozygous for this SNP, whereas 27188 is hemizygous (Figure 125 in the appendix). The second SNP (rs17281188) is located at position 35 of exon 16. Also in this case, there is a cytosine nucleotide instead of a thymidine. As a result, there is a replacement of a methionine residue by a threonine in the protein. This sequence variation is present heterozygously in patients number 22777 and 28786 (Figure 126 in the appendix). A comparison with allele frequency data from the HAPMAP project (www.hapmap.org) showed no significant differences with the examined patient group (Table 46) that would have indicated a possible risk factor.

SNP	Nuc Change	AA Change	Exon	Exon position	SNP freq database	Allele frequencies				
						T		C		
						rel.	abs.	rel.	abs.	
rs2293953	c.-44T>C	Intron 2	2	-43	CSHL-HAPMAP:HapMap-CEU	0.769	20.0	0.231	6.0	patients
						0.809	21.0	0.191	5.0	expected
						T		C		
						rel.	abs.	rel.	abs.	
rs17281188	c.1352T>C	p.M451T	16	35	CSHL-HAPMAP:HapMap-CEU	0.923	24.0	0.077	2.0	patients
						0.942	24.5	0.058	1.5	expected

Table 46 *SLC38A5* SNPs found in the patient screening. Allele frequencies are given in relative and absolute values. Since SLC38A5 is located on the X-chromosome, only allele frequencies are given. A total of 18 patients were examined, 8 females and 10 males (26 alleles). 4 additional patients (27111, 27112, 27113, 27116) were of unknown gender and thus were excluded from the frequency calculation. Allele frequencies were retrieved from the SNP database version dbSNP128 (**www.ensembl.org**).

Besides the two annotated SNPs, one so far not reported change in the sequence of *SLC38A5* was found in a single patient (25649). A guanine residue was replaced hemizygously by an adenine at position 772 of exon 1 (c.-73G>A) (Figure 103).

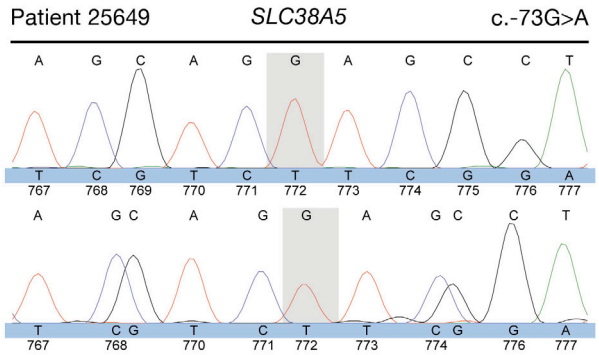

Figure 103 Electropherogram from the sequence analysis of *SLC38A5* from patient 25649. Instead of both a forward and a reverse sequence, the amplicon was sequenced twice in the reverse direction, because the forward read yielded no usable data. Due to this, the c.-73G>A substitution is depicted as an G>T in this electropherogram. Numbers indicate the position inside exon 1, which is upstream of the translation start.

To predict a possible effect of this nucleotide exchange, *in silico* analysis with the ESRsearch tool was performed. The pESR predicted to bind the c.-73G sequence does not recognize the mutatated c.-73A allele. Instead, the base change creates a recognition site for three other pESRs (Figure 104).

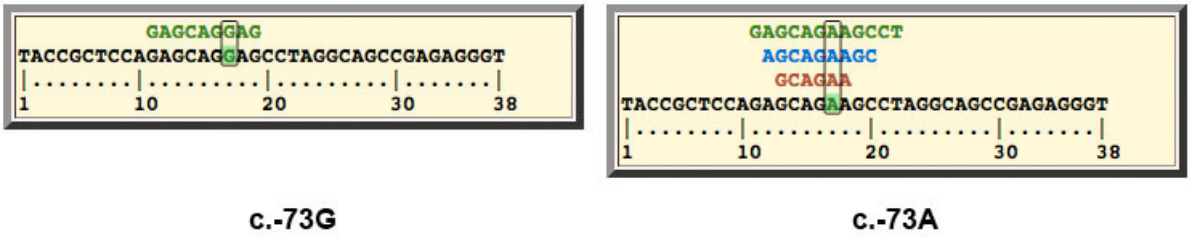

Figure 104 Results from the ESRsearch for exonic splice regulatory sequences. The c.-73 position is framed and the respective allele is highlighted in green. When the c.-73G allele is present, only one putative ESR binds to the sequence. This pESR is not predicted to bind the c.-73A allele. Instead, three other recognition sites for putative ESRs were predicted. (modified after data from **http://ast.bioinfo.tau.ac.il/ESR.htm)**

3.6 Recombinant protein expression in yeast

High amounts of protein are required for functional and structural analyses, typically in the milligrams range. In order to obtain pure protein in sufficient quantity, cell culture systems are used for recombinant protein expression. The bacterium *Escherichia coli* represents an adequate means for fast and cheap expression of high amounts of protein. However, since it is a prokaryotic organism, it lacks the post-translational processing machinery of mammalian cells. Thus it is highly possible that the produced protein is not biologically functional, since e.g. it has not been folded or glycosylated correctly. On the other hand, correct post-translational modification is ensured when mammalian, e.g. HEK293 or COS-7 cell lines are applied. Yet, these cell lines hardly qualify as expression systems for high quantities, and are rather slow and expensive.

One possible intermediate solution is the appliance of a yeast system. The yeast *Pichia pastoris* is comparable to *E. coli* in respect to ease-of-use, speed and costs, but carries eukaryotic features like glycosylation and facilitation of disulphide-bonds, which enables correct protein folding. In the course of my PhD thesis, I used this expression system to generate four different variants of norrin protein and aimed to obtain high quantities in collaboration with Kurt Ballmer, Rolf Jaussi, Suzanne Kronenberg, and Thomas Schleier from the Paul-Scherrer-Institute in Villigen, Switzerland, and my fellow PhD student Lucas Mohn from the Institute of Medical Genetics in Schwerzenbach.

Four different norrin constructs were used: The wild type and a C95R variant, which is a copy of a human pathogenic mutation, with either tags at the N- or C-terminus (Figure 43; Figure 44). The secreted protein should consist of 275/232 amino acids (C-/N-terminal tagged). After secretion into the medium, most of the α-factor signal peptide (89aa) should be cleaved from the protein at the *Kex*2 site, which results into a 186/133 aa (C-/N-terminal tagged) mature NDP protein. The expected molecular weight of the monomer is ~21/17kDa (C-/N-terminal tagged).

3.6.1 Expression control in cultures with a volume of 50ml

Before high quantity production of protein was attempted, an expression control experiment with a medium volume of 50ml was conducted. The yeast cells were grown for 24h and subsequently induced to express recombinant norrin with methanol for 4 days. Every 12 hours a 500µl sample was taken from the cell medium.

To determine the *Pichia* clone which expresses most recombinant protein, a Western blot was performed with 15µl of the cell medium after 4 days of methanol-induction (Figure 105). The proteins were separated on a 12% SDS polyacrylamide gel, and the blot was incubated with a monoclonal anti-c-myc antibody. A double-band in the range of the expected monomeric size (~21kDa) could be detected in the supernatant of all clones with C-terminal tagged constructs. Judging from the intensity of the detected bands, clones no. 223.2 (wt) and 224.2 (C95R) expressed the most protein.

In contrast, a possible monomeric band at ~17kDa could not (or only very marginally) be detected in the supernatants of the clones with N-terminal tagged constructs. However, several other bands of higher molecular weight could be observed. Although

the gel was run under reducing conditions and no polymers were expected, a band at the size of a possible dimer (~34kDa) appeared in all clones.

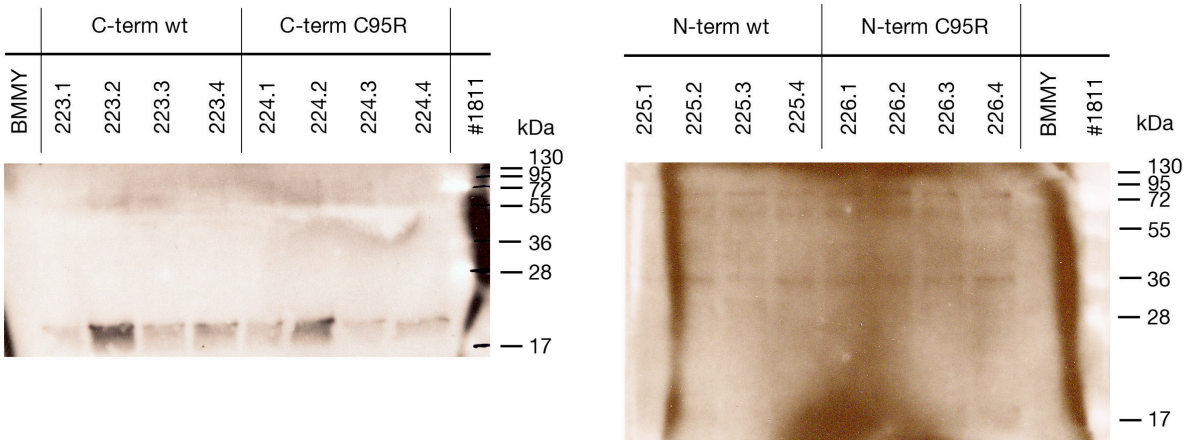

A **B**

Figure 105 Western blots with supernatant from all tested clones after 4d of expression induction (t_4) were stained with c-myc (1:500) and a secondary anti-mouse-IgG-HRP (1:2000) antibody. **(A)** A double-band in the range of the expected size (~21kDa) of the recombinant norrin protein could be detected in the supernatant of all clones with C-terminal tagged constructs. Strongest expression was detected in clones 223.2 (wt) and 224.2 (C95R). **(B)** Many unspecific bands were detected in the supernatant from clones containing the N-terminal tagged constructs. Only a hint of a band could be detected at the expected size of ~17kDa (see clone 226.4). The membrane on the left (A) has been exposed for 30min, the one on the right (B) for 40min. *BMMY*: protein expression medium (negative control); *#1811*: molecular weight ladder.

To determine the optimal culture time, a Western blot was performed with supernatant from 8 different time points after induction (Figure 106). Intensity of the putative norrin band increased over time, reaching a maximum after 4 days (t_4). Thus, it seems advisable to incubate the cultures at least for this period. Further, accumulation of the protein in the medium indicates that it is produced and secreted by the cells as expected. Interestingly, the wt and C95R bands both appeared with a weak smear/double-band on the blot presented in Figure 105. In contrast, there was only a single sharp wt band on the blot in Figure 106, while the C95R variant appeared as a double band on a blot processed at the the same time.

Supernatants (t_4) from the high expressing clones 223.2 (wt) and 224.2 (C95R) were concentrated with filter columns by factor 20. An SDS-PAGE was conducted with 15µl of the concentrated protein, and run under reducing (β-mercaptoethanol) and non-reducing conditions. Since the cysteine at position 95 has been suggested to be responsible for homodimerization of the protein (Meitinger et al., 1993), I expected to see bands at different molecular weights (monomer: ~21kDa; dimer: ~42kDa). However, no difference could be observed (Figure 107). This is in contrast to a similar experiment with recombinant protein from HEK cells (p.55; Masterthesis Lucas Mohn, 2007), where it could be shown that the C95R variant does not form the putative dimer.

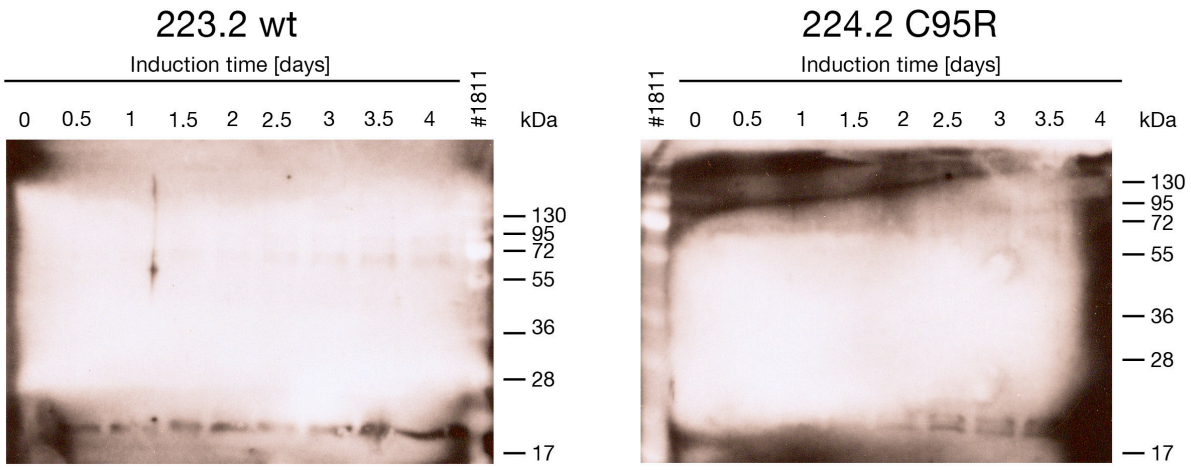

A expected size of the monomer: ~21kDa

B expected size of the monomer: ~21kDa

Figure 106 Western blots with supernatants from the C-terminal tagged clones 223.2 (wt; **A**) and 224.2 (C95R; **B**). Medium samples from 8 different induction time points were loaded. The membranes were stained with c-myc (1:500) and a secondary anti-mouse-IgG-HRP (1:2000) antibody. Intensity of the stained protein bands in the size range of ~21kDa increased over time. Noteworthy, the putative C95R protein appeared as a double-band, whereas the wt variant only produced a single band. *#1811*: molecular weight ladder.

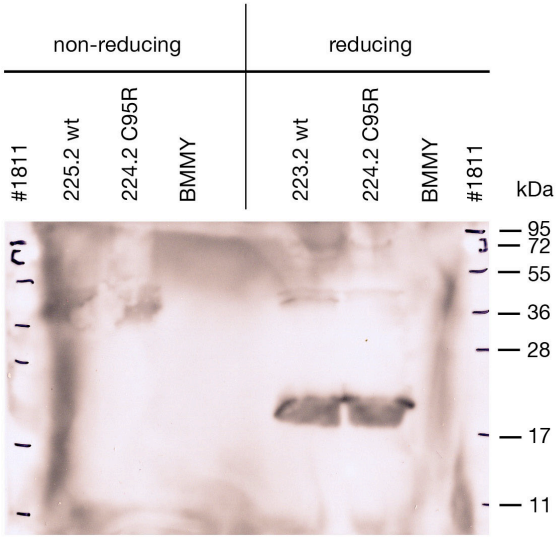

Figure 107 Western blot with concentrated protein from the t_4 supernatants of the C-terminal tagged clones 223.2 (wt) and 224.2 (C95R). The samples were run under reducing (β-mercaptoethanol) and non-reducing conditions. Under reducing conditions, a band at ~21kDa was detected, and a weak double-band of approximately twice the size. Under non-reducing conditions, the double-band at ~42kDa appeared much stronger, and no band at ~21kDa was observed. The banding pattern seemed to be comparable between both norrin variants (wt and C95R). The membrane was stained with c-myc (1:500) and a secondary anti-mouse-IgG-HRP (1:2000) antibody. *BMMY*: protein expression medium (negative control); *#1811*: molecular weight ladder.

3.6.2 Expression in cultures with a volume of 200ml

In a next step, Thomas Schleier conducted expression in a larger, 200ml volume culture at the Paul-Scherrer-Institute. C-terminal tagged clones no. 223.2 (wt) and 224.2 (C95R) were used. Expected size of the recombinant norrin: 21 kDa (30 kDa, if the α-Factor has

not been removed). Per lane, 20µl of 200ml medium were loaded on the SDS-PAGE gel, and silver and Coomassie staining, as well as an α-myc Western Blot were performed.

Distinct bands were visible on both the Coomassie-gel and the Western blot; the longer the MeOH-induction time, the more intensive the bands (Figure 108). This indicates that the detected protein accumulated in the medium over time. Two bands were detected: a double band slightly bigger than 11kDa, and a (double-)band of ~42 kDa. The gels were run under reducing conditions, but arithmetically, this 40kDa band could be a norrin dimer. The smaller, ~11kDa band could be norrin degradation product containing the myc-tag; however, no additional KEX2 recognition site is present in the construct sequence that could explain further cleavage.

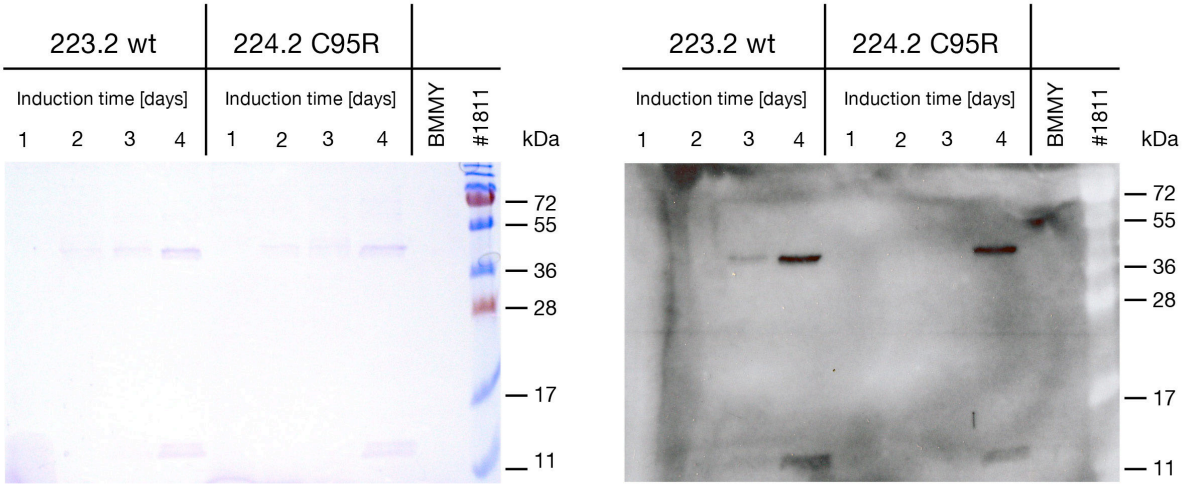

A Coomassie-gel **B** α-myc Western blot

Figure 108 Coomassie-gel **(A)** and corresponding α-myc Western blot **(B)** run under reducing conditions show two bands at >11kDa and ~42kDa that increase with MeOH induction time. C-terminal tagged clones 223.2 (wt) and 224.2 (C95R) were used.

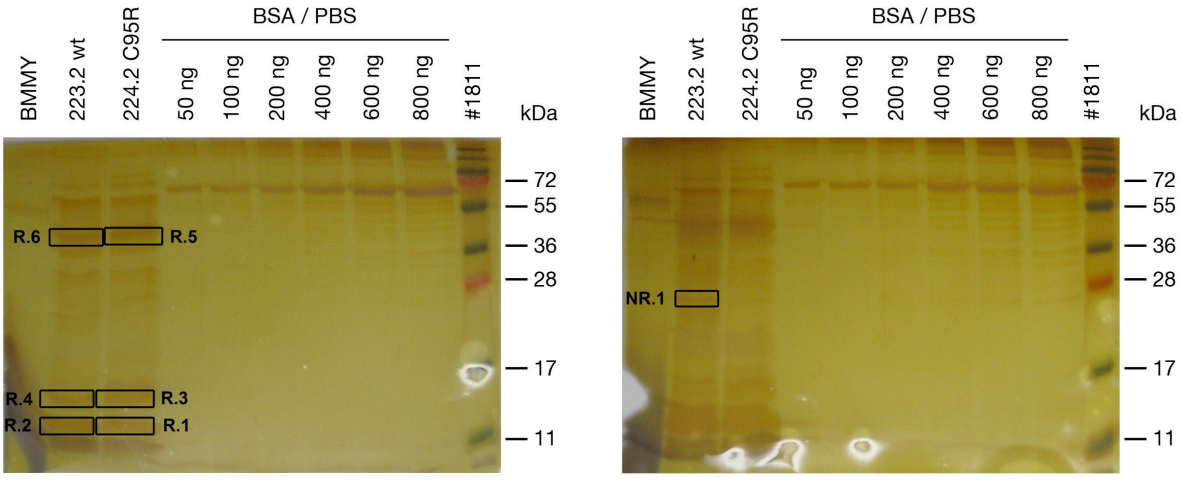

A Silver staining of an SDS-PAGE run under reducing conditions

B Silver staining of an SDS-PAGE run under non reducing conditions

Figure 109 Silver gels and extracted bands that were analyzed by mass spectrometry. Only R.5 and R.6 yielded a sufficient amount for analysis, but were not identical to norrin.

However, the bands visible on the Coomassie-stained gel or the Western blot could not be easily detected by silver staining. Seven bands that could correspond to these bands (highlighted in Figure 109) were isolated; protein was extracted and subsequently analyzed by mass-spectrometry at the protein service lab of the FGCZ. For all bands besides R.5 and R.6 the MS analysis did not allow identification, probably because the sample amount was below the detection limit. Bands R.5 and R.6 are likely due to chitosanase (Q9ALZ1), a protein of bacterial origin. Thus, MS confirmation of norrin could not be achieved so far.

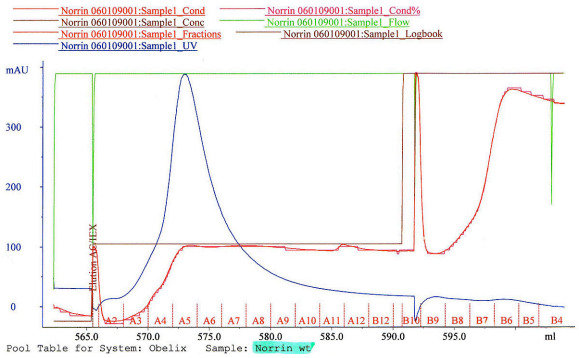

A FPLC chromatogram of IMAC purified 223.2 wt medium

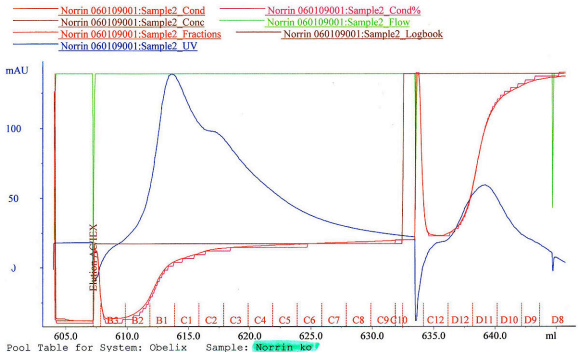

B FPLC chromatogram of IMAC purified 224.2 C95R medium

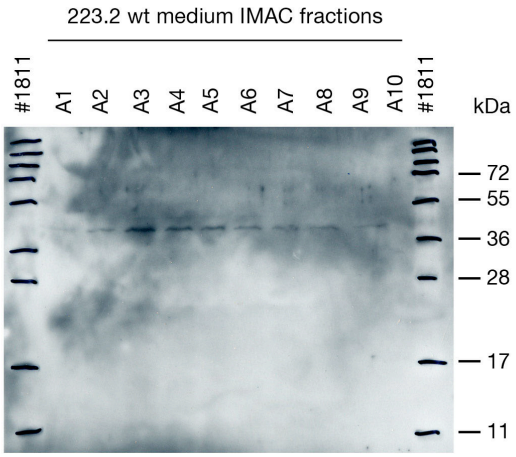

C Western blot against α-myc with 223.2 wt fractions A1-A10 from **(A)**

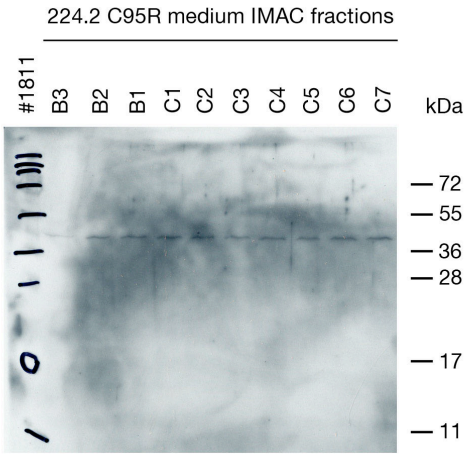

D Western blot against α-myc with 224.2 C95R fractions B3-C7 from **(B)**

Figure 110 FPLC chromatograms of IMAC purified wt **(A)** and C95R **(B)** media and corresponding Western blots under reducing conditions **(C, D)**. FPLC chromatograms provided by Thomas Schleier (PSI). Western blots conducted by Lucas Mohn.

Another 200ml medium from a second expression round conducted at the PSI was IMAC (immobilized metal ion affinity chromatography) purified on nickel columns and FPLC (fast protein liquid chromatography) fractionated in 2ml samples (Figure 110). Ten

fractions for each the wt (223.2) and C95R (224.2) media that cover the respective protein peak (Figure 110 A, B) were separated on an SDS-PAGE and stained with an α-myc antibody (Western blots in Figure 110 C, D). All separated fractions of the wt and the C95R clones yielded a band of ~42kDa, which is the size of a possible norrin dimer. Intensity of these bands correlated with the peak height of the corresponding FPLC chromatogram fractions. No smaller band at >11kDa, which has been observed in the earlier experiments, was visible. If such a product, which may be some form of norrin degradation product, was initially present, it was possibly removed during the purification process due to its small size. Fractions were collected on a 96-well plate and unfortunately, some of them spilled over and mixed with each other. Therefore, it was not possible to allocate the results from the Western blots to the chromatograms with certainty, and worst, wt and C95R protein fractions can not be used for further experiments due to their unknown purity.

Curiously, although both Western blots with protein extracts from the 200ml volume cultures were run under reducing conditions (Figure 108; Figure 110), only the putative norrin dimer bands were detected. In contrast, none of the expected ~21kDa monomeric bands, which have been observed in the 50ml expression control (Figure 105; Figure 106; Figure 107), were visible.

3.7 Revision of the Ndph genotyping strategy

The *Ndph* genotype of the knockout strain was determined using a multiplex PCR (Berger et al., 1996; Table 8). Surprisingly, three instead of the two expected bands were amplified from the ko-allele. Their appearance was noted only occasionally at the beginning of this study, but at present all mice carrying the ko-allele show a three-band-pattern (Figure 111). To investigate the identity of the third band, all PCR products were extracted from the agarose gel and sequenced. In addition to the 133bp product (primers 178 with 180) and the amplicon of 271bp (primers 177 with 179), a third product of 204bp was identified. This additional band was amplified by the primer combination 178 and 180 that also produces the 133bp band (Figure 112). The reason seems to be an insertion of additional 71bp in the ko-allele, which includes an extra binding site for primer 178.

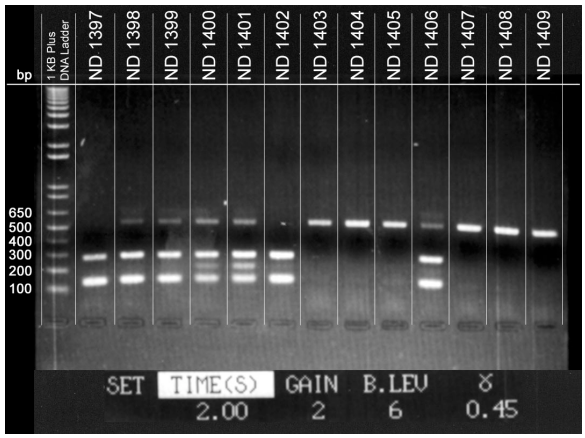

Allele	Primer forward	Primer reverse	Product size
wild type	179	180	527 bp
knockout	179	177	271 bp
knockout	178	180	204 bp
knockout	178	180	133 bp

Figure 111 *Ndph* genotyping PCR. 4 different products can be observed: 1 from the wt allele, and 2 or 3 from the ko allele. All 3 or 4 bands in one sample indicate heterozygosity.

```
...Intron 1...
gacttcatatctcttgtattgcatccatatttcttggtatatatttctgggtaaaatcatttctgatttcattccCTGTGCAGCACATACT
GCTGTGATCGGTTGCAAGTGAAAGAAGCAAGAGAAATTCCTGCATACAAAGGACAATGACAACCAGAAAGCGGCAGCCCTATCCTGCTCTG
GCCTTGAAAGGGACTGGATCCGAACAAACGACCCAACACCCGTGCGTTTTATTCTGTCTTTTTATTGCCGATCCCCTCAGAAGAACTCGTC
AAGAAGGCGATAGAAGGCGATGCGCTGCGAATCGGGAGCGGCGATACCGTAAAGCACGAGGAAGCGGTCAGCCCATTCGCCGCCAAGCTCT
TCAGCAATATCACGGGTAGCCAACGCTATGTCCTGATAGCGGTCCGCCACACCCAGCCGGCCACAGTCGATGAATCCAGAAAAGCGGCCAT
TTTCCACCATGATATTCGGCAAGCAGGCATCGCCATGGGTCACGACGAGATCCTCGCCGTCGGGCATGCGCGCCTTGAGCCTGGCGAACAG
TTCGGCTGGCGCGAGCCCCTGATGCTCTTCGTCCAGATCATCCTGATCGACAAGACCGGCTTCCATCCGAGTACGTGCTCGCTCGATGCGA
TGTTTCGCTTGGTGGTCGAATGGGCAGGTAGCCGGATCAAGCGTATGCAGCCGCCGCATTGCATCAGCCATGATGGATACTTTCTCGGCAG
GAGCAAGGTGAGATGACAGGAGATCCTGCCCCGGCACTTCGCCCAATAGCAGCCAGTCCCTTCCCGCTTCAGTGACAACGTCGAGCACAGC
TGCGCAAGGAACGCCCGTCGTGGCCAGCCACGATAGCCGCGCTGCCTCGTCCTGCAGTTCATTCAGGGCACCGGACAGGTCGGTCTTGACA
AAAAGAACCGGGCGCCCCTGCGCTGACAGCCGGAACACGGCGGCATCAGAGCAGCCGATTGTCTGTTGTGCCCAGTCATAGCCGAATAGCC
TCTCCACCCAAGCGGCCGGAGAACCTGCGTGCAATCCATCTTGTTCAATGGCCGATCCCATATTGGCTGCAGGGTCGCTCGGTGTTCGAGG
CCACACGCGTCACCTTAATATGCGAAGTGGACCTGGGACCGCGCCGCCCCGACTGCATCTGCGTGTTCGAATTCGCCAATGACAAGACGCT
GGGCGGGGTTTGCTCGACATTGGGTGGAAACATTCCAGGCCTGGGTGGAGAGGCTTTTTGCTTCCTCTTGCAAAACCACACTGCTCGACAT
TGGGTGGAAACATTCCAGGCCTGGGTGGAGAGGCTTTTTGCTTCCTCTTGCAAAACCACACTGCTCGAGCTCGAATTCATCGATGATATCA
gataccttctccctcattaatacaagagcagtcatagttccttgtcaggggatggagagctacgaccagagcccaaactggagctctatg
actggcctgcagaacttacaagggaatatttctttagaattttctcactatgcttttccactt
…Intron 2…
```

partial 5'UTR of *NDP* exon 2 | Reverse neomycin cassette | Primer 177 | Primer 178 | Primer 179 | Primer 180

Figure 112 Putative *Ndph*-ko allele. Most of *Ndph* exon 2 (*yellow*), including the entire CDS, has been replaced by a reverse oriented neomycin resistance cassette (*green*; Berger et al., 1996; sequenced only in flanking regions). Primer binding sites for the genotyping PCR are indicated. In contrast to the original sequence, an 71 bp insertion is present.

4. Discussion

In this study, I aimed to identify differences in gene expression in brain and retina of norrin knockout mice, a mouse model for Norrie disease, to further elucidate the sequence of pathogenic events leading to the disease. I further aimed to find supporting evidence for norrin's hypothesized role as transcriptional regulator of so far unknown target genes. Since such downstream genes are ideal candidates for contributing to ND or allelic diseases, a mutation screen was performed in patients who were negative for alterations in the three known, EVR-related genes *NDP*, *FZD4*, and *LRP5*.

4.1 Differential expression in Ndph ko mice

4.1.1 Analyses of the brain

4.1.1.1 Impaired vasculature in the cerebellum

Vascular anomalies and subsequent hypoxia seem to be the common feature in the eye of patients harboring mutations in *NDP*, *FZD4*, and *LRP5*. Since patients with *NDP* and *LRP5* mutations also show neurological symptoms, and brain anomalies were described in the *Fzd4*$^{-/-}$ mouse, the *Ndph* ko mouse was investigated with regard to cerebral vascular defects that might explain the observed mental impairments in patients. Transcript levels of the three EVR-associated genes *Ndph*, *Fzd4*, and *Lrp5*, as well as of three hypoxia-regulated angiogenic factors (*Vegfa*, *Itgrb3*, *Tie1*) were investigated in six different brain regions (cerebellum, cortex, hippocampus, olfactory bulb, pituitary gland and brain stem) of 6-8-month-old *Ndph* wt and ko mice. No significant differences were found between *Ndph* wt and ko mice (Figure 45; Figure 46). Nonetheless, reduced vessel density was found in the white matter of the *Ndph* ko cerebellum (Figure 48; Figure 49). Concordantly, expression of *Ndph* and *Fzd4* was highest in the wt cerebellum (Figure 45), substantiating that an Ndph/Fzd4-mediated signal involved in vascular development of the cerebellum could be associated with mental impairment in patients.

Interestingly, while no ND patients were reported with cerebral vascular anomalies, reduced development of the CNS deep venous system in favor of a prominent superficial venous plexus was described in a Coats' patient (Robitaille et al., 1996). However, in contrast to the *Fzd4*$^{-/-}$ mouse (Wang et al., 2001), no reduction of Purkinje or granular cells was noted in the *Ndph* ko (Figure 47). The more severe phenotype in the *Fzd4*$^{-/-}$ ko could indicate that ligands other than norrin might also be involved in the development of the cerebellar vasculature, which can in part compensate the loss of *Ndph* in the ko. Such a compensatory action of Wnt-ligands has been suggested for axonal growth and synaptogenesis of cerebellar mossy fibers as they find their granule cell targets (Lucas and Salinas, 1997; Hall et al., 2000). The lack of mental impairment in patients harboring *FZD4* mutations (typically diagnosed as ad-FEVR patients) might be due to their dominant nature in humans. So far, only one homozygous *FZD4* case was reported, but in contrast to the mouse model, no extraocular symptoms were observed (Kondo et al., 2007; Kondo, personal communication), maybe because the *FZD4* mutation (p.R417Q) is only hypomorphic, and not a complete loss-of-function as in the ko mouse.

4.1.1.2 Differential cerebellar expression of the glutamine transporter Slc38a5

After global transcript analysis of the *Ndph* ko retina revealed the glial amino acid transporter *Slc38a5* to be lower expressed (Figure 52), mRNA levels were also investigated in the brain, where it has already been found abundantly in astrocytic end feet (Cubelos et al., 2005). No differences were detected in adult brains, but reduced expression of *Slc38a5* was found in the cerebellum of p21 *Ndph* ko mice (Figure 58; Hänseler, Masterthesis, 2008), the region where *Ndph* is expressed the most among all investigated wt brain regions (Table 36). Antibody-staining of cryosections appeared to be stronger in sections from norrin wt mice, and was most intense around the Purkinje cells (Figure 59). This correlates with the finding that Slc38a5 has been located to Bergmann glia (Cubelos et al., 2005). Their cell somata are located in the Purkinje cell layer, and their processes expand into the molecular layer, ensheating parallel fiber cell terminals and synapses of Purkinje cells with climbing fibers. Both climbing fibers and parallel fibers excitate Purkinje cells using glutamate (or aspartate) as neurotransmitter. Since Slc38a5 has been reported as an important glutamine transporter (Umapathy et al., 2005), reduced expression in the *Ndph* ko cerebellum could hint to another possible pathogenic mechanism in the brain that could explain the mental impairments in ND patients. Based on the published localization of Slc38a5 in Bergmann glia and our own observations, it is tempting to speculate that Norrin induces expression of *Slc38a5* in the retina and cerebellum, and that lack of norrin leads to reduced levels of the glutamine transporter in these tissues. Glutamate/glutamine homeostasis would be disturbed, and excitatory signaling of granule cells and climbing fibers on Purkinje cells would be impaired. Since this neuronal network is primarily involved in fine-tuning of motor control and learning, altered signaling could induce a cerebellar ataxia-like phenotype similar to that reported in *Fzd4*$^{-/-}$ mice. Cerebellar anomalies, however, are harder to associate with the mental disabilities typically seen in ND patients, like autistic features, cognitive impairment (low IQ to severe MR), seizures, or developmental delay. Nonetheless, cerebellar ataxia has been described in several CD patients (Tolmie et al., 1988; Révész et al., 1992; Goutieres et al., 1999).

4.1.1.3 Synopsis

In summary, investigation of the *Ndph* ko brain added further evidence to the hypothesis that the unifying feature of all observed symptoms in eye, ear, brain, female reproductive system, and peripheral venous system is a defect in angiogenesis. In addition, differential expression of a glutamine transporter in cerebellar glia cells could indicate impaired synaptic transmission in and function of cerebellar motor circuits.

4.1.2 Analyses of the retina

Consistent with data obtained from other developmental stages (Luhmann et al., 2005a), examination of the p7 *Ndph* knockout mice showed insufficient retinal capillarization and lack of deep vessel formation. Vascular permeability has not been observed only in later, nearly adult stages, but was noted throughout development, as indicated by elevated mRNA and protein expression data for Plvap. Although norrin's hypothetical role as a transcriptional regulator of Wnt/β-catenin target genes was not obvious from the array experiment, I was able to substantiate the finding that Norrin is important for retinal angiogenesis. Several genes probably implicated in blood vessel development that may be transcriptionally regulated by Norrin were identified.

4.1.2.1 Possible implications of microarray-detected differentially expressed genes

Differential expression of five genes that were conspicuous in the microarray experiment could be confirmed by qRT-PCR. Since the role of these five genes has been discussed extensively in the IOVS publication, I just want to give a short summary in the following paragraph, extended by a few additional arguments.

Three genes showed a decreased expression in the ko: the neutral amino acid transporter *Slc38a5* (24x less), apolipoprotein D (*ApoD*; 2.4x less), and angiotensin II receptor-like 1 (*Agtrl1*; 2x less). Increased expression was found for the plasmalemma vesicle associated protein (*Plvap*; 4.2x higher) and adrenomedullin (*Adm*; 2.7x higher). *Slc38a5* and *Plvap* mRNA expression in addition was shown to be significantly different not only at p7, but also at p5, p10, p15, and p21. Differences were especially apparent in the retinal cryosections stained with an antibody against Plvap.

4.1.2.1.1 Plasmalemma vesicle associated protein (*Plvap*)

The experimental results suggested an early involvement of plasmalemma vesicle-associated protein (*Plvap*) in the pathogenesis of *NDP*-related retinopathies. It remains to be shown whether a possible mode of action for Norrin, besides transcriptional regulation via the Wnt/β-catenin pathway, might be a direct modulation of the microtubule cytoskeleton (Salinas, 2007) or Plvap itself. Regardless the exact molecular function, I hypothesized that transient Plvap expression and fenestration occur during maturation of the retinal vasculature and that Norrin signaling is possibly required for its suppression. Norrin thus may be involved in sprouting angiogenesis as well as in the formation and maintenance of the blood-retina- or blood-brain-barrier. Interestingly, Plvap expression appeared especially prominent in veins (Figure 55), which correlates with the finding that deeper networks start to develop from veins and capillaries, but not arteries (Fruttiger, 2007).

4.1.2.1.2 Solute carrier family 38, member 5 (*Slc38a5*)

The role of solute carrier family 38, member 5 (*Slc38a5*) is less clear. Slc38a5 has been reported to be a main glutamine transporter in retinal Müller cells (system N2) (Umapathy et al., 2005), and therefore may play an important role in neuronal signal transduction through regulation of the glutamate/glutamine household. Its decreased expression in *Ndph*$^{y/-}$ mice (Figure 52) may indicate an involvement of Norrin in neuronal differentiation or synaptogenesis, which would correlate with the reduced ERG activity found in the inner retina (Berger et al., 1996; Rüther et al., 1997). Another role could be impaired communication between Müller cells and developing retinal vessels, for which they serve as guidance structures (Fruttiger, 2007).

4.1.2.1.3 Angiotensin II receptor-like 1 (*Agtrl1*)

Angiotensin II receptor-like 1 (*Agtrl1*), or apelin receptor (*APLNR*), has been described as venous marker (Saint-Geniez et al., 2003) that is important for retinal angiogenesis (Kasai et al., 2004). The 2-fold decreased expression in the p7 *Ndph* ko retina (Figure 63 A) coincides with the observed impaired vascular development, but could merely reflect reduced vessel density or, considering the venous/capillary nature of the deep vessel system (Fruttiger, 2007), a lack of development of this particular network. The last consideration probably is more likely, because no significant expression differences were found in the p5 retina. Upon binding of its ligand apelin, Agtrl1 signals via the ERK1/2 MAPK-pathway (Bai et al., 2008). Like *FZD4* and *LRP5*, *AGTRL1* is located on the proximal part of the long arm of chromosome 11 (11q12).

4.1.2.1.4 Apolipoprotein D (*ApoD*)

In contrast, transcript levels of apolipoprotein D (*ApoD*) were not only reduced at p7, but also at p5 (Figure 61). It could be implicated in the observed angiogenic defect of *Ndph*$^{y/-}$ mice, because ApoD has been reported to stimulate proliferation and migration of vascular smooth muscle cells (Leung et al., 2004), probably through suppression of Pdgf-bb-mediated proliferation through inhibition of ERK1/2 nuclear translocation (Sarjeant et al., 2003). A possible functional relationship between norrin and *ApoD* could further be indicated by co-expression of these two genes in disease-affected organs. Besides the retina, *APOD* has been shown to be upregulated in human endometrium during implantation (Kao et al., 2002), a process that is disturbed in female homozygous norrin knockout mice (Luhmann et al., 2005b). Further, *ApoD* expression was also reported in the inner ear, another affected organ in Norrie disease patients and mice (Rehm et al., 2002), where it has been suggested to be implicated in cochlear fluid homeostasis (Hildebrand et al., 2005).

4.1.2.1.5 Adrenomedullin (*Adm*)

Adrenomedullin (*Adm*) is a hypoxia induced vasodilating peptide (Ogita et al., 2001) that has been suggested to be vascular protective (Ando and Fujita, 2003). In addition to p7, *Adm* transcript expression was elevated even more in the *Ndph* ko retina at p21 (Figure 63 B). This finding correlates with the observation that adrenomedullin inhibits vascular remodeling (Matsui et al., 2004). Although high *Adm* levels at p21 could be a result of retinal hypoxia, it is tempting to speculate that norrin-mediated enhanced expression of *Adm* causes the defects in retinal vascularization due to its anti-angiogenic properties. Like Agtrl1, ApoD, and Plvap, Adm seems to be involved in MAPK-signaling, because it has been found to act as a survival factor in osteoblastic cells via a CGRP1 receptor/MEK-ERK pathway (Uzan et al., 2008). The genes for the CGRP1-receptor (*CALCA*) and *ADM* itself are located on chromosome 11p15.

4.1.2.2 Further genes possibly involved in the pathogenesis of ND

The microarray experiment provided additional candidate genes that could be involved in ND pathogenesis. They appeared on the list of differentially expressed transcripts (Table 40) or at least on the complete list without multiple testing correction (appendix), but could not be verified by qRT-PCR. The discrepancy between the microarray and the qRT-PCR results most likely has various reasons. Besides the technical differences of the experimental setup, microarray calculation procedures that transform raw data into expression estimates are distinct and vary depending on the platform, laboratory, and researchers involved (Gyorffy et al., 2009). Background correction, normalization, and summarization of multiple probes are typically combined in a preprocessing algorithm that is intended to standardize analyses. But each algorithm is based on its own set of assumptions, and no gold standard can be formulated for experimental research. The same, maybe in a lesser extent, applies to the analysis of qRT-PCR data (Skern et al., 2005). Here, in addition, selection of the appropriate reference gene is of critical importance (Radonić et al., 2004). Depending on the nature of the expected data, each researcher has to decide which analysis method might be best suited for his/her experimental setup. Thus, conclusions from gene expression experiments are substantially influenced by the chosen set of algorithms. To make biological sense out of a set of numbers, it is good practice to use two different methods to estimate the significance of an experimental finding (Imbeaud et al., 2005).

For this reason, I aimed to validate the microarray findings by qRT-PCR. Data that could be confirmed was treated as more reliable, but that does not exclude biological significance for genes that only emerged in one experiment. Thus, it might be interesting to analyze their role in future research.

4.1.2.2.1 Claudin 5 (*Cldn5*)

Claudin 5 (*Cldn5*) plays a major role in tight junction-specific obliteration of the intercellular space in CNS endothelial cells (Nitta et al., 2003). Thus, reduced expression of *Cldn5*, in addition to elevated expression of *Plvap*, could explain leakiness of vessels in the *Ndph* ko. However, differences at the transcript level as determined by qRT-PCR were not significant, although a trend to reduced expression could be observed (Figure 63 C).

4.1.2.2.2 ATP-binding cassette, sub-family B (MDR/TAP), member 1A (*Abcb1a*)

Differential expression of ATP-binding cassette, sub-family B (MDR/TAP), member 1A (*Abcb1a*) could not be confirmed by qRT-PCR (Figure 64), but it was the second-lowest differentially expressed gene in the microarray experiment (down 4.9x). It has been shown to be Wnt-regulated (Wielenga et al., 1999). It is a cell-surface glycoprotein involved in cell-cell interactions, cell adhesion and migration, plays a major role in the blood-brain barrier and permeability for certain drugs (Schinkel et al., 1994), can bind to matrix metalloproteinases, and is involved in tumour development (Comerford et al., 2002). Thus, reduced expression in the *Ndph* ko retina would be consistent with a possible Wnt-mediated regulation through norrin, which could be involved in enhanced vascular permeability and reduced angiogenic activity.

4.1.2.2.3 Von Willebrand factor (*Vwf*)

Von Willebrand factor homolog (*Vwf*) is expressed in platelets that could induce capillary sprouting of microvascular endothelial cells (Rhee et al., 2004). Reduced expression in the *Ndph* ko retina could indicate reduced amounts of platelets in the retinal vasculature, or the missing ability of platelets to bind to angiogenic sprouting tips (Kisucka et al., 2006), and thus account for reduced vascular development in the *Ndph* ko mouse. However, the indicated reduced expression could not be confirmed by qRT-PCR (Figure 64).

4.1.2.3 Analysis of neuronal markers in the retina

Most data from the analysis of the norrin ko mouse support the hypothesis that impairment of the retinal vascular development is the first pathogenic event, and effects on the neural retina occur only secondarily (Luhmann et al. 2005a; this work). If Norrin in the first place is essential for the development of the retinal vasculature, the *Ndph* ko mouse could serve as a model to investigate neuronal development under hypoxic conditions. However, norrin has also been suggested to have a direct neurotrophic effect (Ohlmann et al., 2005). Therefore, if further data would indicate early involvement of norrin in neuronal differentiation, maturation, or migration, the hypothesis of an initially impaired vessel development would have to be reevaluated.

Based on the analyses of several neuronal markers (Islet-1, beta-tubulin, neurofilament 150kDa, ChAT, PKC-α, calbindin 28kd, SNAP 25, synaptophysin), no differences were found in the p5 *Ndph* ko retina, supporting the hypothesis that neuronal changes occur secondarily to vascular changes. At later stages, alterations of the retinal morphology,

especially in the ganglion cell layer, seemed to correlate with tissue invasion by pathognomonic retinal vessels (Figure 76 C) in accordance with previously reported findings (Berger et al., 1996). Background staining of the plexiform layers appeared to be higher in the ko retinas, possibly due to increased permeability and leakage of the vasculature, and thus presence of IgGs in those areas. We observed a trend to reduced numbers of ganglion cells, similar to previous observations (Richter et al., 1998). Neuronal damage was indicated by a reduced protein level of the RGC marker islet-1 (*Isl-1*) at p21, and an altered protein expression of synaptophysin (*Syp*) (Figure 68; Figure 70). However, these changes were not present on mRNA level (Figure 69; Figure 72). In contrast, mRNA transcript levels of the solute carrier *Slc38a5* were reduced in the ko during the whole postnatal retinal development (Figure 52), but no differences were found in immunohistochemically stained cryosections (Figure 57).

4.1.2.3.1 Islet-1 (*Isl-1*)

Islet-1 (*Isl-1*) is a transcription factor under the control of Wnt/β-catenin signaling that has been shown to be involved in proliferation and survival of cardiac progenitor cells (Lin et al., 2007). It is also indispensable for retinal neuron differentiation, as a conditional loss of *Isl-1* led to significant reductions of mature ON- and OFF-bipolar (>76%), cholinergic amacrine (93%), and ganglion (71%) cells (Elshatory et al., 2007). Thus, it could be hypothesized that *Isl-1* is under transcriptional control of *Ndph*/*Fzd4*/*Lrp5*-signaling, and that lack of this signaling in ND patients leads to impaired maturation of bipolar and amacrince cells, as well as reduced viability of retinal ganglion cells. Lack of Isl-1 immunoreactivity in the retina of p21 *Ndph* ko mice supports this hypothesis, as well as the possibly reduced staining in p5 *Ndph* ko bipolar cells, hinting to a function of norrin in the differentiation and survival of neuronal cells in agreement with its proposed neurotrophic function (Ohlmann et al., 2005). However, the detected staining differences at p5 could be only due to the center-to-periphery gradient of retinal neuronal differentiation, or a slightly different developmental stage of the investigated animals. Also opposing the possible involvement of *Isl-1* in the pathogenesis of ND is the finding of similar expression in wt and ko on the transcript level at p5 and p21 (Figure 72).

4.1.2.3.2 Synaptophysin (*Syp*)

Synaptophysin (*Syp*) is one of the most abundantly expressed proteins in synaptic vesicles (Calhoun et al., 1996), and is thought to negatively modify the release of synaptic vesicles through binding to synaptobrevin (*Syb*) (Edelmann et al., 1995). The retinal staining pattern of synaptophysin differed between *Ndph* wt and ko, especially at p21 (Figure 68). A typical pattern of small spots was visible in the plexiform layers of the wild type, indicating numerous synapses. In the knockout, labeling was weaker and more diffuse. In the samples from p5 animals, only very faint staining was detected in the wt, and no immunoreactivity for Syp could be observed in the ko. However, no significant differences in mRNA expression could be detected at either p5 or p21 (Figure 69). Analysis of a *Syp* knockout mouse revealed that behavior and appearance of mice lacking *Syp* was indistinguishable from that of their wild type litter mates and that synaptic transmission was normal with no detectable changes in synaptic plasticity or the probability of release (McMahon et al., 1996). This implied that the function of synaptophysin is redundant or has only a subtle effect on synpatic vesicle release.

Nonetheless, synaptophysin was upregulated 198-fold in the rat retina after optic nerve transection (Piri et al., 2006), and has recently been associated with mild mental retardation and occasional seizures (Tarpey et al., 2009). Besides its role in the CNS, synaptophysin has been suggested to be involved in intracellular transport and the release of hormones in the gastrointestinal tract, e.g. in serotonin-producing enterochromaffin cells (Portela-Gomes et al., 1999). Since *SYP* is located on the short arm of the X chromosome (Xp11.23-p11.22), only about 5cM from the *NDP* locus, mutations are likely to co-segregate with *NDP* mutations and could contribute to some of the interfamilial differences with regard to the severity of ND.

Taken together, the cellular composition of the neural retina seems to be mainly unaffected in the *Ndph* ko mouse. All investigated cell types were similarly present in the ko retina, only the number of ganglion cells appears to decrease at p21, as has been previously reported (Richter et al., 1998). Evidence was provided that their function could be impaired, as demonstrated by an aberrant protein expression of islet-1 and synaptophysin, and different mRNA transcript levels for the glutamine-transporter *Slc38a5*. However, a conclusive statement about their role in ND and allelic diseases remains elusive. Future research could detect hypoxia-induced impairment in synaptic transmission, which would correlate with the reduced ERG-activity of the inner retina found in *Ndph* ko mice (Berger et al., 1996; Rüther et al., 1997). On the other side, based on the presented results, I would not exclude a primary role for Wnt-signaling controlled decreased or ectopic expression of *Isl-1* that could lead to a maturation defect and reduced viability of retinal neurons, or an important role of dysregulated *Syp* expression in the control of vascular development through impaired neuronal secretion of angiogenic factors.

4.1.2.4 Differences in retinal miRNA expression

Micro RNAs, in addition to messenger RNAs, present another level of gene activity regulation, which has been investigated only very limited so far. Recently, several miRNAs were found to be differently expressed in the retina under hypoxic conditions (Shen et al., 2008). Specifically, miR-31, miR-150, and miR-184 were lower expressed, and injection of pre-miR-31, pre-miR-150, or pre-miR-184 reduced ischemia-induced retinal neovascularization. Thus, the reported data suggested a crucial role for miRNAs in ocular vascular development.

Since norrin is required for early angiogenic sprouting and the formation of deep retinal capillary networks, probably through transcriptional regulation of target genes via the Wnt/β-catenin pathway, I investigated if lack of Norrin had an influence on the transcription of miRNAs that could be involved in retinal blood vessel development.

Two developmental stages were investigated, p5 and p21. No differences in global miRNA expression were found in the *Ndph* ko p5 retina. At p21, 12 miRNAs exhibited a fold change over 1.3 (Figure 66). Eight (66.6%) of the 12 miRNAs with a fold change greater than 1.3 were also described as differentially expressed in the hypoxic OIR retina in the study by Shen et al. (Figure 113), although their fold change differences were generally higher (e.g. expression of the most decrased miRNA mmu-miR-184 was 11.3x down). One of those miRNAs (mmu-miR-211) was present in the opposite group, however (i.e. 1.4-fold reduced expression in the *Ndph* ko, but 2-fold increased expression in the OIR model). As expected, comparison of these data suggests that the

Ndph ko retina is in a similar (presumably hypoxic) condition as in the OIR model. None of the three miRNAs that Shen et al. could prove to inhibit blood vessel development (mmu-miR-31, -150, -184) was differentially expressed in the p21 *Ndph* ko retina, nor were mmu-miR-221/-222, which were reported to inhibit HUVEC migration and tube formation (Poliseno et al., 2006).

The fact that litter-specific differences in p5 retinal miRNA expression were bigger than *Ndph* genotype-specific differences implies that we could not detect a direct influence of norrin on the expression of miRNAs that could account for the impaired retinal development. Expression changes of miRNAs in later stages are probably the result of the hypoxic environment, as indicated by the high similarity of differentially expressed miRNAs in the p21 norrin ko and the hypoxic OIR retina.

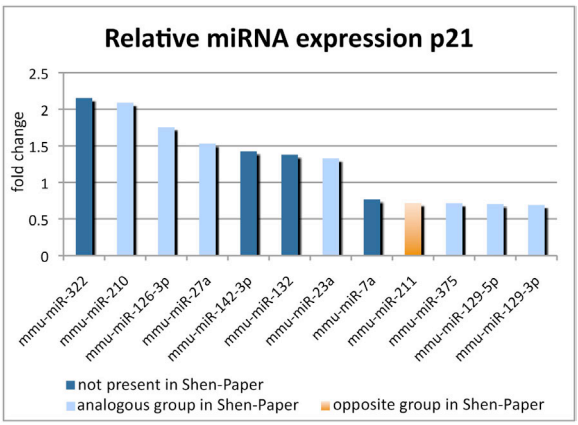

Figure 113 Comparison between the 12 most differentially expressed miRNAs of the p21 *Ndph* ko retina with the hypoxic retina described by Shen et al., 2008. Expression of 7 miRNAs was also different in their study (*light blue*), and one miRNA (miR-211) was differentially expressed in the opposite direction: lower in the *Ndph* ko, but higher in their study (*orange*). The remaining 4 differentially expressed miRNAs were not mentioned in their study (*dark blue*).

4.1.2.4.1 Possible effects on target genes

A database search on 39 representatively selected, putative angiogenesis-related genes revealed that 18 harbor a binding site for at least one of the miRNAs differentially expressed in the p21 *Ndph* ko retina (Table 41). Four genes (*Igf1, Notch3, Dvl3, and Slc38a5*) are recognized by several miRNAs. The miRNA recognizing the most of the selected genes is mmu-miR-27a (5 targets: *Igf1, Cldn5, Dvl2, Notch2, and Notch4*).

Interestingly, none of these 39 genes is recognized by the miRNA with the highest differential expression: mmu-miR-322 (2.2x). However, it is predicted to bind to 880 genes such as *Chat, Dll1, Efna5, Epha7, Fgf8, Fgfr1, Icam1, Ifng, Igf1r, Lrp6, Pecam1,* and *Timp4.* The gene encoding the precursor of mmu-miR-322 is situated 34Mb from the *Ndph* locus on chromosome X, which roughly correlates to a meiotic recombination rate of 17%. Therefore, it is possible that two different mmu-miR-322 alleles with varying expressivity simply co-segregate with the *Ndph* wt and ko alleles, and the expression difference is the result of a different genetic background (*wt:* C57Bl/6 vs. *ko:* 129P2).

Differential expression of miRNAs correlates to some extent with observed expression differences of target genes: For example, *Angpt2* and *Kdr* (VEGFR2) both have been

described to be higher expressed in the p21 *Ndph* ko retina (Luhmann et al., 2005a), and both are targeted by mmu-miR-129-5p, which is lower expressed in the norrin ko. Additionally, *Nrp1*, the co-receptor for Kdr, is also recognized by a miRNA with reduced expression (mmu-miR-375), which favors its increased expression. Angpt2, Kdr, and Nrp-1 all act simultaneously in angiogenic remodeling – a process that is impaired in the norrin ko (reviewed in Penn et al., 2008). On the other side, expression of *Vegfa* and *Itgav* has been shown to be increased in the *Ndph* ko, but the corresponding miRNAs (mmu-miR-126-3p and -142-3p, respectively) are also higher expressed. Thus, I would have expected them to have a negative effect on their target genes. *Igf1* and *Dvl3* are recognized both by miRNAs that are decreased and increased, making it difficult to predict a transcriptional effect.

An interesting target gene is *Slc38a5*. Its expression has been shown to be significantly decreased in the norrin ko mouse by the microarray experiment (Table 40) and following qRT-PCRs (3-fold at p21; Figure 52). Strikingly, the recognizing miRNA miR-210 is increased at p21 (Figure 66), and thus could account for the reduced transcript amounts of *Slc38a5*. In addition, *Slc38a5* has predicted recognition sites for miR-31 and -222. These miRNAs have been shown to reduce neovascularisation and tube formation, respectively, and thus deliver another hint that *Slc38a5* could be involved in angiogenesis.

4.1.2.4.2 Synopsis

Taken together, differential expression of miRNAs in the *Ndph* ko retina was detected with the microarray approach at p21, but not at p5. Although this does not exclude differences at p5 (insufficient sensitivity of the approach, dilution effect through employment of a whole tissue, not a single cell type), it could indicate that differential expression of miRNAs is not a primary event in the pathogenesis of ND, but rather mirrors secondary changes like the establishment of chronic hypoxia. This conclusion is supported by the finding that eight (66.6%) of the 12 miRNAs with a fold change greater than 1.3 were also described as differentially expressed in the hypoxic retina of the OIR model (Shen et al., 2008). One of those miRNAs, mmu-miR-211, was differentially expressed in the opposite direction (Figure 113), and thus represents an interesting candidate that might explain differences between the hypoxic retinas of the OIR and *Ndph* ko mouse models. Transcript expression differences of some angiogenic factors (*Slc38a5*, *Angpt2*, and *Kdr*) could be correlated with differences in miRNA expression, while expression of others (*Vegfa* and *Itgav*) was opposite to what could be expected from differential expression of recognizing miRNAs. Nonetheless, experimental manipulation of e.g. miR-27a could lead to further interesting insights into the molecular pathogenesis of ND, since it recognizes many angiogenic transcripts.

4.2 Norrin in pathways and pathogenesis

The microarray experiment suggested that all pathways that appear to be affected in the *Ndph* knockout p7 retina (Table 39) are involved in angiogenesis: MAPK signaling, focal adhesion, Ca^{2+} signaling, tight junction, and Wnt-signaling.

4.2.1 MAPK-signaling

The MAP-Kinase pathway, which has been suggested to be the main VEGF-mediating signaling cascade, and the phosphatidylinositol 3-kinase (PI3K)/Akt pathway are thought to induce endothelial cell survival and proliferation, mediate vascular permeability and vasodilation through nitric oxide (NO) generation and elevation of cytosolic Ca^{2+}, and control angiogenesis through upregulation of matrix metalloproteinases and activation of focal adhesion kinase (Zachary and Gliki, 2001; Wu et al., 1999). Further, a crosstalk to different Wnt-signaling pathways involves either transcription of angiogenesis-relevant genes such as VEGF (Zhang et al., 2001) or TEK (Masckauchan et al., 2006) or directly modifies the cytoskeleton, e.g. through PKC- and Ca^{2+}-dependent regulation of tight junctions (Harhai and Antonetti, 2004). Thus, the MAPK-pathway seems to involve all signaling systems apparently affected in the norrin ko retina, and emphasizes a role for norrin in blood vessel development. Although 4 of the 5 verified differentially expressed genes presented in the IOVS publication (page 114) appear to be involved in MAPK-signaling (*Adm*, *Agtrl1*, *ApoD*, and *Plvap*), no difference in phosphorylation of the ERK1/2 MAPK (and thus differential activity of a main MAPK-pathway) was found in the p7 *Ndph* ko retina (Figure 65). Therefore, additional experiments are required to test the hypothesis. Because of the early developmental stage investigated here and the lack of neovascularization in later stages, I tend to consider a role of VEGF itself in the early pathogenesis of *NDP*-related diseases rather unlikely and hypothesize whether Norrin instead might modulate the cellular response to VEGF.

4.2.2 Wnt-signaling

4.2.2.1 Wnt-signaling in the retina and brain of $Ndph^{y/-}$ ko mice

Norrin's hypothetical role as a transcriptional regulator of Wnt/β-catenin target genes was not obvious from the array experiment. The pathway analysis suggested involvement of Wnt-signaling only at the 5th position (Table 39), and only one of the 34 genes (besides *Ndph* itself) listed among the most differentially regulated has been associated with it: adenomatosis polyposis coli downregulated 1 (*Apcdd1*) (Table 40) (Takahashi et al., 2002). This does not necessarily mean that Norrin is not exerting its function over binding to Wnt-receptors – but it may imply that Norrin does not work primarily as a transcriptional regulator via the canonical Wnt/β-catenin signaling. However, this conclusion relies heavily on the number of currently known Wnt target genes, and on the assumption that this signaling actually occurs in p7 retinae. Further, as two major angiogenesis-related genes have been shown to be transcriptionally regulated by Wnt-signaling, *Tie-2/Tek* (Masckauchan et al., 2006) and *Vegfa* (Zhang et

al., 2001), it is possible that Norrin has a direct role in controlling expression of these genes in a spatially and temporally restricted manner which was not detectable by the microarray approach. This also applies to expression of the norrin receptors *Fzd4* and *Lrp5*, which was shown to be elevated in the *Ndph* ko retina at p15 and p21, but not at p5 or p10 (Luhmann et al., 2005a). Besides transcriptional regulation, activation of Wnt-signaling has been shown to also stabilize the microtubule cytoskeleton through a transcription-independent pathway, as it becomes resistant to depolymerization through inhibition of Gsk3β (Ciani et al., 2004; Salinas et al., 2007). If Norrin acts as an activator of Wnt-signaling, lack of Norrin could promote a higher susceptibility to depolymerization of the microtubule cytoskeleton and therefore might have a direct influence on cell migration.

In addition to the published results, Wnt-signaling was investigated in further experiments. The gene most differentially transcribed in the microarray experiment was *Slc38a5*. To test the hypothesis that its reduced expression is caused by a lack of norrin and subsequently lack of canonical Wnt-signaling, I investigated *SLC38A5* expression in HEK-cells in response to LiCl treatment, a potent activator of Wnt/β-catenin signaling. No significant effect was found on mRNA level (Figure 80), but an interesting and reproducible finding was made on Western blots. The Slc38a5 antibody labeled two bands, one band corresponding to the molecular weight of the monomer, and one band corresponding to a possible tetramer. Levels of the monomeric band were similar in protein extracts from treated and untreated HEK-cells (Figure 81) as well as from *Ndph* wt and ko retina (Figure 56) and cerebellum (Figure 60). However, the tetrameric band appeared to be more intense in the absence of *Ndph* (Figure 56; Figure 60), and weaker in LiCl-treated, Wnt-signaling activated cells (Figure 81). This observation is in contrast to the reduced mRNA levels in the retina and cerebellum of *Ndph* ko mice, and does not explain the different appearance of the tetrameric band. Since *Slc38a5* is strongly expressed in glia in the CNS, it may be worthwile to repeat the experiment in a cell-line of neuronal origin, where expression and regulation probably are more closely resembling the *in vivo* situation than HEK-cells, which are derived from embryonic kidney tissue.

The molecule central to canonical Wnt-signaling, β-catenin, was not differently active in the p7 *Ndph*$^{y/-}$ retina (Figure 77), as determined by Western blots. Further, the Wnt-specific transcription factors *Tcf3* and *Tcf4* were not differentially expressed in the ko during retinal development (Figure 78).

Expression of the lymphoid enhancer binding factor 1 *(Lef1)* was significantly reduced in the p15 *Ndph* ko retina (Figure 78 B). It has been described as transcription factor in canonical Wnt-signaling, whereas itself is negatively regulated by the same pathway in a negative feedback loop (Hovanes et al., 2001). This could be hinting at higher Wnt-signaling activitiy at p15 in the *Ndph* ko retina. Differences at p5, p10, and p21 were not significant. Nonetheless, a trend could be observed of higher expression in the early stages (p5 and p10), and lower expression in the later stages (p15 and p21).

The same trend was observed for *Bmp4*, a transforming growth factor-β family member. Expression of *Bmp4* was more than four-fold elevated in the p5 ko retina, and was reduced two-fold at p15 (Figure 78 A). Although differences were not significant at p10 and p21, these data also indicated two disease phases. This observation is consistent with the disease phases proposed by Luhmann et al. (Luhmann et al., 2005a). Since *Bmp4* was shown to be upregulated in response to β-catenin (Kim et al., 2002), in

contrast to negative feedback on *Lef1*, it is not possible to draw a definite conclusion about Wnt-signaling activity in the *Ndph* ko retina. While the *Lef1* expression profile suggests reduced Wnt-signaling activity in the early phase, and enhanced activity in the late phase, it is exactly the opposite in regard to *Bmp4* expression. However, it has been shown that up- or downregulation of canonical Wnt-target genes depends on the type of transcription factors and the position of their binding sites (Logan and Nusse, 2004). Thus, it is possible that β-catenin activity is uniformly shifted in the *Ndph* ko retina, but that different transcription factors mediate an opposite effect on the two investigated target genes. Further, *Bmp4* regulation through β-catenin provided a link between WNT and TGF-β signaling pathways (Kim et al., 2002). My experimental data now add further support for WNT/TGF-β crosstalk, because norrin has initially been described as a growth factor with high homology to TGF-β (Meitinger et al., 1993) and apparently affects *Bmp4* expression via canonical Wnt-signaling.

4.2.2.2 The role of Wnt-signaling in the regression of hyaloid vessels

In this thesis, I also aimed to demonstrate altered Wnt-signaling in *Ndph* ko mice *in vivo*. However, the used Wnt-reporter mouse proved to be inadequate to detect Wnt-signaling in the retina. In contrast, intense Wnt-signaling was detected in the remaining hyaloid vasculature of *Ndph*$^{y/-}$ mice (Figure 82; Figure 87). This is of particular interest, because it has been shown that macrophage-mediated apoptosis of hyaloid vessels in the *Lrp5*$^{-/-}$ mouse failed (Kato et al., 2002), and that this defect correlates with missing Wnt-signaling activity in hyaloid endothelial cells (Lobov et al., 2005). Persistent hyloid vessels and reduced levels of cell death were also found in *Lef1* deficient mice, further substantiating involvement of canonical Wnt-signaling (Lobov et al., 2005). This report initially lead me to the hypothesis that hyaloid regression is dependent on norrin-induced canonical Wnt-signaling in endothelial cells through binding to Lrp5. However, two facts contradict this hypothesis: For one, macrophage-associated Wnt7b was shown to be the necessary Lrp5-ligand for Wnt-induced regression of the hyaloid vessels (Lobov et al., 2005). And second, canonical Wnt-signaling appeared to be active in the hyaloid vasculature of norrin-deficient mice (Figure 82; Figure 87). But since hyaloid vessels persist in the *Ndph* ko, these data suggest that norrin is necessary for the regression of the hyaloid vasculature, but not via canonical Wnt-signaling in hyaloid endothelial cells. One possible mode of function could be that norrin effects hyaloid vessels via a non-canonical Wnt-pathway, or that it has no direct function on the transient vitreal vasculature at all, causing the failed regression only indirectly through impaired development of the retinal vasculature. It would be interesting to further investigate norrin's role in hyaloid regression, e.g. through transciptional analysis of *Wnt7b* and *Lrp5* in the *Ndph* ko vitreous.

4.2.2.3 Valproic acid: a modifier of Wnt-signaling

In one family with a mutation in *FZD4* (p.I114T), the mother of two boys suffering from a severe form of FEVR has been treated with valproic acid (VPA) during pregnancy (Robitaille et al., 2009). VPA is an epigenetic anticancer drug that targets chromatin through inhibition of histone deacetylases and DNA methyltransferases, and therefore unspecifically acts on most tumor types. Treatment with VPA evokes differential expression of hundreds of genes belonging to multiple pathways, and in high doses has

been associated with neural tube defects and other major congenital malformations. Since it was also shown to up-regulate genes involved in the Wnt-pathway (Duenas-Gonzales et al., 2008), it was speculated that valproic acid could be a modifier for mutations in *FZD4* and might account for the more severe phenotype (Robitaille et al., 2009).

4.2.2.4 Wnt-signaling in bone synthesis

Reduced bone mass in *Lrp5*$^{-/-}$ mice has been found to be caused by a lack of osteoblast cells, which account for bone synthesis (Kato et al., 2002). Since *Lrp5* is expressed in osteoblasts and further has been shown to be involved in Wnt/β-catenin signaling (Xu and Wang et al., 2004), it was hypothesized that *Lrp5* mutants cause impaired Wnt-signaling in these cells, and OPPG and HBM were considered Wnt-related diseases (Krishnan et al., 2006). However, osteoblast-specific loss- or gain-of-function mutations in β-catenin did not affect bone formation (Glass et al., 2005). Concordantly, isolated *Lrp5*$^{-/-}$ osteoblasts proliferated well ex vivo, indicating that Wnt-signaling in osteoblasts is not the cause for the bone phenotype in *Lrp5*$^{-/-}$ mice and OPPG patients (Yadav et al., 2008). Based on these findings, Yadav and colleagues could show that LRP5 instead controls bone formation by inhibiting serotonin synthesis in the duodenum (Figure 114) (Yadav et al., 2008).

4.2.2.5 Thoughts about Wnt-related candidate genes for future investigations

The presence of several genes involved in blinding disorders on the proximal portion of chromosome 11q (*FZD4*, *LRP5*, *BEST1*) might indicate a hotspot for genes that are evolutionary and functionally linked, and it can be speculated about the emergence of further disease-associated genes in this region. One such candidate would be *WNT11*, which has been shown to be important for eye development, and to interact with LRP5 and Wnt-signaling (Cavodeassi et al., 2005). Another one could be matrix metalloproteinase-7 (*MMP7*), which has been shown to be positively regulated by Wnt/β-catenin signaling and is involved in degradation of the extracellular matrix during angiogenic remodeling and in cell migration (Brabletz et al., 1999; Crawford et al., 1999). It is also situated on the long arm of chromosome 11, but a little bit more distal (11q22).

Hypomorphic *Wnt7b* mutants were reported to display a PFV phenotype (Lobov et al., 2005), whereas *Wnt7b* null-mutants die embryonically (Shu et al., 2002). In addition, homozygous *Wnt7b* hypomorphic mutans are infertile due to a defect in placental development (Parr et al., 2001), in agreement with the phenotype observed in *Ndph* ko mice (Luhmann et al., 2005b). Wnt7a/Wnt7b further have been shown to be essential for CNS vasculature development (Stenman et al., 2008). Thus, mutations in *Wnt7b* cause angiogenic defects in the same organs that are affected in *Ndph* ko mice, and represents another interesting candidate gene for future research. *Wnt7b* is located on 22q13 (outside the DiGeorge-critical region).

Vimentin (*Vim*) is a GFAP-binding member of the intermediate filament family and is widely used as Müller cell marker (Lemmon and Rieser, 1983). It has been proposed as direct target of β-catenin/TCF (Gilles et al., 2003), although another report suggests it is involved in cell migration not via the canonical pathway (Katoh, 2008). Further,

mutations in *VIM* cause dominant, pulverant cataract (Müller et al., 2009), although *Vim* ko mice lack an obvious phenotype (Colucci-Guyon et al., 1994). Unfortunately, staining of retinal cryosections gave no results, probably because the available antibody was no longer working. It's role in *NDP*-related diseases should nonetheless be investigated.

4.2.2.6 Synopsis

The hypothesized involvement of norrin in canonical Wnt-signaling was not obvious from the global expression analysis (Table 39), nor was the activity of the most central molecule, β-catenin (Figure 77), different in p7 *Ndph* ko retinas. Further, two Wnt-specific transcription factors (*Tcf3, Tcf4*) were not differentially expressed during retinal development (Figure 78). Differential expression of *Lef1* and *Bmp4* suggested two diseases phases, an early (p5, p10) and a late (p15, p21) one (Figure 78) in accordance with the previously proposed model (Luhmann et al., 2005a). However, although both genes were lower expressed at p15, *Lef1* has been reported to be repressed by Wnt-signaling, whereas *Bmp4* has been found to be enhanced. Thus, a uniform conclusion about different activity of canonical Wnt-signaling cannot be made. In contrast to my expectations, Wnt-signaling was active in the hyaloid vasculature of *Ndph* ko mice (Figure 82; Figure 87), suggesting that vessel regression is not dependent on norrin-induced Wnt-signaling. However, differential Wnt-activity in the retina, which could have elucidated norrin's role *in vivo*, could not be investigated with the reporter mouse employed. Further genes involved in Wnt-signaling and angiogenesis should be investigated in subsequent experiments.

A recent report suggested that LRP5-controlled repression of systemic serotonin levels appears to be the key to the bone phenotypes in OPPG and HBM (Yadav et al., 2008). It remains to be shown whether this control is mediated via the canonical Wnt-pathway, and whether serotonin is also crucial for the development of the ocular phenotype of ND/FEVR/OPPG.

4.2.3 Serotonin-mediated signaling

Serotonin (5-HT; 5-hydroxytryptamine) is a monoamine neurotransmitter that is produced in enterochromaffin cells in the gut (80%-90% of total 5-HT), and to a minor extent in serotonergic neurons in the CNS. Because 5-HT does not pass the blood-brain-barrier, two different functions and places of action have been postulated: one inside the CNS, and one outside. In the CNS, serotonin is involved in the control of mood and anger, and in the gut, it has been associated with the control of intestinal movements, amongst others (Purves, 2004).

Interestingly, high serotonin levels have frequently been observed in patients with osteoporosis and autism (Hediger et al., 2008), and patients with mood disorders chronically taking selective serotonin reuptake inhibitors (SSRIs) have been found to develop osteoporosis as well (Richards et al., 2007). Now recently, *Lrp5* expressed in enterochromaffin cells of the duodenum was shown to inhibit expression of tryptophan hydroxylase 1 (*Tph1*), the rate-limiting enzyme involved in serotonin synthesis (Figure 114) (Yadav et al., 2008). Serotonin secreted in the blood can bind to osteoblasts through its receptor Htr1b, which inhibits intracellular Creb and thus also proliferation of osteoblasts via reduced expression of *CycD1*. Although no bone phenotype has been reported in patients with mutations in *NDP* or *FZD4*, nor in the respective mouse

models, it may be worthwile to investigate the role of serotonin with regard to the development of the vascular anomalies and other symptoms found in EVR-related diseases. While *Lrp5* in the gut is probably activated by another ligand than norrin, it cannot be excluded that norrin has an influence on serotonin homeostasis in the local retinal vasculature or in the CNS, although the authors state that the CNS analogue of *Tph1*, *Tph2*, is not differentially expressed in the CNS of *Lrp5*$^{-/-}$ mice. However, differential protein expression of synaptophysin (*Syp*) was found in inner retinal neurons of the *Ndph* ko (Figure 68). Since this protein has been suggested to be involved in the release of hormones, such as serotonin, in the gastrointestinal tract (Portela-Gomes et al., 1999), it is tempting to speculate whether it excerts this function also in the retina.

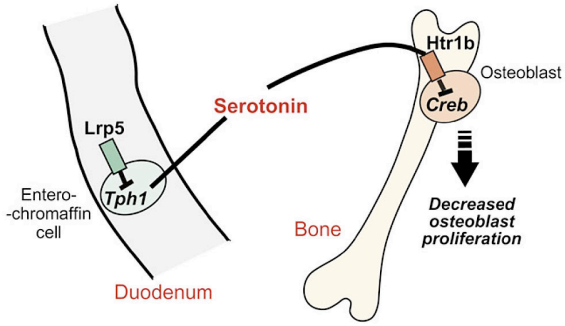

Figure 114 Model of the proposed function of LRP5 in bone formation. Lrp5 facilitates bone mass accrual through inhibition of expression of *Tph1*, the rate-limiting enzyme for serotonin synthesis in the duodenum. Serotonin has been shown to reduce *CycD1* expression in and proliferation of osteoblasts through Htr1b mediated inhibition of Creb. (Source: Yadav et al., 2008)

High serotonin levels caused by therapeutic drugs (SSRIs, MAO-inhibitors) cause a wide spectrum of symptoms (reviewed by Boyer and Shannon, 2005). Some of these symptoms may also be found in ND/OPPG-related diseases, if investigated properly. Among them are, in addition to osteoporosis, myoclonic seizures, which have often been reported in conjunction with ND patients, and disseminated intravascular coagulation (DIC). DIC describes a condition where coagulation processes are pathologically activated. Small blood clods form inside the blood vessels, resulting in impaired organ perfusion (e.g. through microvascular thrombosis) and subsequent ischemia, while hemorrhages may be due to the consumption of all available coagulation proteins and platelets. Misbalance in the coagulation/fibrinolysis system may further activate the complement and kinin systems, contributing to increased vascular permeability.

It has been shown that serotonin has no effect on healthy adult retinal blood vessels in monkeys, but that it elicits vasospasms in artherosclerotic vessels, leading to temporary complete occlusion or impaired blood flow (reviewed by Hayreh, 1999). Thus, it is tempting to speculate that increased serum serotonin levels not only affect injured, but also developing vessels, and that 5-HT may also be related to the vascular anomalies found in patients harboring *LRP5* mutations, or even those with mutations in *NDP* or *FZD4*. In addition, serotonin has been shown to cause transient cataracts in the rat eye, probably through decreased production of aqueous (Boerrigter et al., 1992), which resembles another symptom often described in ND/OPPG patients. An interesting sidenote may be the close genetic localization of *NDP* and the *MAO* genes, since *MAOA* catalyzes the breakdown of serotonin. Thus, co-segregating mutations in *MAOA* may also

lead to increased 5-HT levels, further contributing to the severity of homeostatic misbalance. Systemic and significant reduction in the activity of both *MAO* genes has been found in ND patients with an X-chromosomal deletion, presumably including *NDP*, *MAOA* and *MAOB* (Murphy et al., 1990). This correlated with markedly increased 5-HT levels in the plasma and cerebrospinal fluid of ND microdeletion patients (Collins et al., 1992). Interestingly, MAOA not only preferentially deaminates 5-HT, but also norepinephrine (NE). However, no changes in NE plasma levels were observed (Collins et al., 1992), which could be indicative of another cause for the elevated 5-HT levels, e.g. lack of or mutations in *NDP*. In addition, it already has been proposed that an imbalance between 5-HT activity and the activity of other neurotransmitters could account for cataplexy and REM sleep disturbances in ND patients (Vossler et al., 1996). However, no altered serotonin levels have been reported from ND patients with point mutations in the *NDP* gene so far.

4.2.3.1 Synopsis

Taken together, it has been shown that elevated serotonin serum levels account for the osteoporosis phenotype in the *Lrp5*$^{-/-}$ mouse (Yadav et al., 2008), and may also contribute to some neuronal phenotypes in ND patients (cataplexy, sleep disturbances) (Vossler et al., 1996). Althouh no bone phenotype has been reported in conjunction with *NDP* or *FZD4* mutations, it seems very promising to me to investigate serotonin-mediated signaling also in the *Ndph* knockout mice as well as in patients, especially because of the reported vascular effects of high serotonin levels. In contrast to the *Lrp5*$^{-/-}$ mouse, I expect that systemic 5-HT blood levels are not conspicuously altered, since no bone phenotype has been observed, but that local serotonin levels in the retina are elevated, possibly contributing to the developmental anomalies. If so, elevated 5-HT levels could be reduced by a tryptophan-less diet or the administration of parachlorophenylalanine (pCPA) during ocular development (Yadav et al., 2008; Kubera et al., 2000). Interestingly, the gene for tryptophane hydroxylase 1 (*TPH1*), the serotonin-synthesis rate limiting enzyme, is located on 11p15.3-14, only ~4cM outside the genomic region designated as EVR3 (11p3; Downey et al., 2001), and thus could present another candidate gene for future mutation screenings.

4.3 Production of recombinant norrin protein

Production efforts of recombinant norrin in yeast cells resulted in a single 40 kDa band in 200ml expression control setups that could correlate with a putative norrin dimer (Figure 108). The 21 kDa monomeric band was only visible after 50ml expression controls (Figure 106; Figure 107), maybe due to differences in cultivation conditions at the Institute of Medical Genetics and the Paul-Scherrer-Institute. Nonetheless, high amounts of recombinant norrin protein that could be used for functional assays or structural analyses should be easily obtained through additional expression rounds. However, the engineered protein still has to be confirmed by mass spectrometry and functional tests. The latter may be of special importance, because although *Pichia pastoris* carries eukaryotic features like glycosylation and facilitation of disulphide-bonds, it remains to be shown that the recombinant human protein is glycosylated and folded correctly. Such functional tests would include proliferation, migration, and endothelial-tube-formation assays, as well as pathway assays which include activation of luciferase reporters like the Wnt-signaling-controlled Super TOP-FLASH (Xu and Wang et al., 2004).

4.4 Gene screening in patients

A total of 22 patients with ND/FEVR-like clinical presentation were screened for mutations in *NDP*, *FZD4*, and *LRP5*, and subsequently for mutations in the candidate genes *LRP5L*, *LMO2*, *PLVAP*, and *SLC38A5*. Different medical terms were used to describe the respective clinical entity, and for some patients, more than one diagnosis was suggested. In this respect, I like to cite Ulrich Kellner, who proposed: "When no genetic basis for the disease could be identified, the diagnosis should be „unclassified vitreoretinopathy (with or without syndromic features)", rather than an enforced, but maybe misleading or wrong allocation to ND or a similar disease" (Kellner et al., 2004).

In order to determine whether an annotated SNP found in the patient group is more or less frequent than it is in the average population, the frequency of the ancestral allele among the patients was calculated and compared with the allele frequency in the Caucasian European population (HapMap-CEU database, dbSNP128, www.ensembl.org). It was assumed that most of our patients belong to this population, although ethnic origin of most individuals was unknown, and it cannot be excluded that some are members of other ethnic groups. This consideration should be kept in mind, because it may lead to false prediction of genetic risk factors. For most SNPs, only a minor difference was determined. Therefore, neither potential risk-alleles nor protective alleles for Norrie disease were found. However, the size of our patient group is probably not sufficient to make statistically significant predictions concerning risk-alleles or protective alleles. Therefore, even when a considerable difference between patients and average population was found, this could have occurred by chance. Of course, also the opposite is true: the existence of risk-alleles and protective alleles for ND/EVR-like phenotypes cannot be completely excluded, since allele frequencies could be similar due to coincidence.

4.4.1 *NDP* screening

No variations in addition to the five mutations detected prior to this study were found in the *NDP* gene, including its 5'- and 3'-UTRs. This implies that 16 out of 22 patients analyzed in this study were negative for mutations in *NDP* despite being clinically diagnosed as ND or CD patients (one patient was diagnosed with Eales' Disease). Regarding the variety of other diseases with similar ocular phenotypes and the relative rarity of the disease, it could be possible that false diagnosis is common. On the other hand, in the case of familial occurrence of the disease, involvement of other genes, especially of the already associated *FZD4* and *LRP5*, is highly likely. I was speculating that mutations in the 3'-UTR could also contribute to the disease, because this part of the gene was not routinely tested in our diagnostic division, and miRNA recognition site mutations in the 3'UTR have been discussed in association with human disease (Abelson et al., 2005; Clop et al., 2006; Sethupathy et al., 2007; Jensen et al., 2008). However, it appears that no mutations in *NDP* have been missed in our patient group, and no evidence for involvement of miRNAs in the regulation of *NDP*-associated diseases could be found.

4.4.2 *FZD4* screening

Exon 1 and the coding region of exon 2 were screened by Jurian Zürcher as part of his masterthesis (Masterthesis Zürcher, 2007). Since two miRNAs shown to inhibit neovascularization (Shen et al., 2008) are predicted to bind to the FZD4 3'-UTR, the two parts harboring the recognition sites were sequenced additionally. However, no alterations were found in these regions of the 3'-UTR, leaving a possible involvement of miR-31- and miR-184-mediated regulation of *FZD4* in the pathogenesis of ND/EVR open.

Two already described single nucleotide substitutions, c.97C>T (p.P33S; CM050619) and c.502C>T (p.P168S), were found in patient 27118 (Masterthesis Zürcher, 2007). Although *in silico* analyses suggested a possibly pathogenic effect of the p.P168S variation, it has been described as a SNP before (Toomes et al., 2004). However, the particular control proband was not examined by fluorescein angiography, and could be an asymptomatic carrier. Both parents of patient 27118 were reported to be asymptomatic, and since mutations in *FZD4* have been described to follow a dominant mode of inheritance (Robitaille et al., 2009), incomplete penetrance has to be assumed in the parent who inherited the p.P33S mutation.

A haplotype analysis of the two sequence variants p.P33S and p.P168S revealed that they are located on different chromosomes (Masterthesis Zürcher, 2007), suggesting that they have been inherited from both parents. This facilitates the alternative hypothesis of compound heterozygousity in the patient and a recessive mode of inheritance. However, p.P33S and p.P168S have recently been found in several FEVR patients on the same allele that did not co-segregate with FEVR (Boonstra et al., 2009).

More family members of patient 27118 should be examined to prove or reject the hypothesis of a recessive or dominant mode (with incomplete penetrance) of inheritance of these *FZD4* mutations. Unfortunately, none of the family members was available for further examinations.

This patient is a good example for the variety of diagnoses that are made in an attempt to describe the clinical entity. She was diagnosed with Coats' disease, although both eyes were affected, and had a history of preterm birth, which would have qualified for ROP. ND was considered, but rejected because of her gender, and our molecular analysis finally pointed to FEVR.

4.4.3 *LRP5 screening*

An amino acid exchange at position p.T672M (c.2015C>T**;** Figure 94 A) was found in a CD patient (Masterthesis Hänseler, 2008). The position is highly conserved among vertebrates, and the mutation was absent in 374 control alleles. The amino acid exchange is located in the third β-propeller of the extracellular domain of LRP5 in the binding site of DKK, an endogenous inhibitor of Wnt-signaling. The mutation thus could imply a functional change of LRP5 that strengthens the affinity to DKK, thereby explaining an *NDP*-related ocular phenotype. Bone anomalies typical for OPPG were not observed in the patient and her family. However, no determination of bone density has been performed.

The fact that the p.T672M mutation was also found to be heterozygous in the patient's unaffected mother as well as her two so far unaffected younger siblings (Figure 95)

excludes a dominant phenotype of this mutation and leaves the clinical presentation of the patient unexplained. Most probably, a second somatic mutation in the affected eye, as it has been described for an *NDP* mutation found in a CD patient (Black et al., 1999), accounts for the clinical presentation.

To clarify the pathogenic relevance of this mutation, screening of *NDP*, *FZD4*, and *LRP5* should be repeated with DNA from the affected eye, if it became available. This would be the first time that a case of Coats' disease is associated with a mutation in *LRP5*.

In addition to this amino acid exchange, one silent mutation (c.2178C>T) was found in patient 24536. *In silico* analysis suggested a possible effect on splicing (Figure 96) that should be investigated when RNA became available. Splice variants, which can also be affected by mutations in the intron, especially the exon flanking regions, are often expressed in a tissue specific manner. A mutation could favour the formation of a transcript normally not or only marginally expressed in a tissue that is otherwise specific for another isoform, or vice versa, abolish or diminish expression of a certain transcript. As a result, the ratios between different splice products would be affected, which might influence clinical phenotypes, such as those characteristic for Norrie disease.

Further, one SNP in the patient group (rs4988320) showed a significantly different allele frequency in comparison to the HAPMAP database, suggesting it as a risk-factor for the development of an CD-like phenotype. This hypothesis would have to be supported by additional sequencing of patients, and should be tested also by differential splicing experiments.

So far, almost only exonic mutations have been found in *LRP5*. Regarding the genomic size (136.63kb) and exon structure of *LRP5* (23 exons), it appears promising to investigate the intronic regions through deep or next-generation sequencing in future studies, and analyse differential splicing in RNA samples, since only one transcript has been annotated in the public databases of NCBI and Ensembl so far.

4.4.4 *LRP5L screening / 22q11 deletion syndromes*

Since no mutations have been observed in the *LRP5L* gene, no evidence for an association with ND/EVR was found. However, i*n silico* analysis of a silent variation in exon 2 (c.339C>T; rs9624807) revealed the creation of a new binding site for a putative splice regulatory element (Figure 98), which in addition to the significant higher allele frequency in the patient group (odds-ratio 18.42) indicates a possible risk-factor. As has been discussed above, the pathogenic potential of this variation has to be confirmed by screening of additional patients, and investigation of differential splicing (if RNA was available).

Recently, the case of the DiGeorge patient who presented with an FEVR-like ocular phenotype, which was presented at the ARVO annual meeting in 2008, was published (Gilmour et al., 2009). The authors adressed my hypothesis, and investigated *LRP5L* as possible candidate gene for FEVR. Allele loss studies demonstrated that it is situated >2.5Mb from the deletion on chromosome 22 that was linked to DiGeorge sequence. Although not deleted itself, there could be positional effects of regulatory elements in the proximity of *LRP5L* that might have been deleted. However, the authors point out

that the longest range reported in a position effect mutation to date is 1 Mb, making this possibility rather unlikely (Kleinjan et al., 2005).

On the other hand, another DiGeorge sequence case report has been published before, describing a patient with Coats' disease-like phenotype (Scholz et al., 1997), who also harbors a chromosome 22q11 deletion (although of unreported extent). This case could support the hypothesis that among the ~40 known genes typically involved in 22q11 deletions (reviewed by Shprintzen, 2008), one gene contributes to an ND/FEVR phenotype.

With regard to *LRP5/LRP5L* and ND/OPPG, I think it is noteworthy that DiGeorge patients often suffer from skeletal anomalies, mental retardation, and hearing disabilities (Shprintzen, 2008). However, about 180 phenotypes for the typical 3Mb 22q11 deletion have been described so far, and it is difficult to associate single clinical presentations with a certain gene. Several attempts have been made, the most noticable maybe concerning T-box 1 (*TBX1*), a gene coding for a transcription factor involved in developmental processes that is always involved in 22q11 deletion syndromes. It has been shown that Tbx1 interacts with Vegfa, and thus may represent an additional link to ND and allelic diseases (Stalmans et al., 2003).

4.4.5 *PLVAP* screening

No mutations or not annotated SNPs were found in the patient group, leaving a possible implication of *PLVAP* in ND or similar diseases open. Allele frequencies of the three annotated SNPs were in the expected range of the control population (Table 44). Since *Plvap* was higher expressed in the absence of functional norrin, it is difficult to speculate about possible pathogenic consequences of *PLVAP* mutations. A mere loss-of-function through deletions, frameshift, or nonsense mutations would result in lack of PLVAP protein, which has been shown to be important for the structure and development of endothelial fenestrae diaphragms (Figure 115) (Stan et al., 1999). Endothelial fenestrae do not always contain a diaphragm, as has been shown in muscle capillaries, (Bearer and Orci, 1985) but it is responsible for fenestrated capillary permeability.

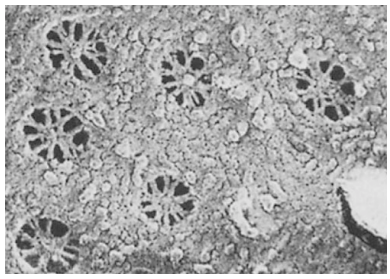

Figure 115 Electron microscopic image (120'000x) of fenestral diaphragms on the etched surface of peritubular capillaries in the rat kidney cortex (luminal surface view). Plvap is thought to be the main constituent of the intertwining fibrils that compose the diaphragm (Stan et al., 1999). (Source: Bearer and Orci, 1995).

Thus, loss-of-function mutations do probably not lead to an ND-like ocular phenotype, because the development of vessel leakiness should be impaired. However, as was

discussed in the IOVS publication, transient expression of Plvap and fenestration of capillaries may be important for proper remodeling of the retinal vasculature. Therefore, lack of Plvap could contribute to impaired angiogenesis, and thus may be involved in the pathogenesis of the disease. Gain-of-function mutations or mutations leading to increased expression of *PLVAP* would mirror the situation found in the *Ndph* ko mouse, and in my opinion are more likely to induce a ND-like phenotype. Therefore, it may be worthwhile to identify potential upstream regulatory regions of *PLVAP*, and to sequence those regions in our patient group.

4.4.6 *SLC38A5* screening

Two annotated SNPs with allele frequencies similar to the control population have been found in the *SLC38A5* screening, but no pathogenic amino acid exchanges. However, one new sequence variation was found in the 5'-UTR. Patient 25649 harbors a c.-73G>A exchange that is not affecting the coding sequence. Instead, the base change could have occurred in a promoter element or a regulatory sequence, or affect the splice pattern. *In silico* analysis predicted a change in putative exonic regulatory elements that can bind to the sequence (Figure 104). Thus, the variation could affect splicing that should be investigated when RNA became available.

Among the investigated genes, *SLC38A5* would be of particular interest, because it is only located 4.5 cM from the *NDP* locus on the short arm of the X-chromosome (Figure 116), and variations in both genes would co-segregate with a high probability. This could explain some of the (interfamilial) phenotypic variability of the disease.

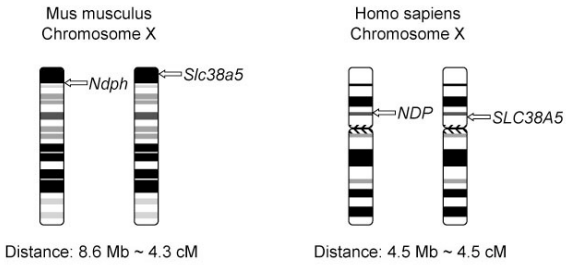

Figure 116 The loci of *Ndph*/*NDP* and *Slc38a5*/*SLC38A5* are only separated by 4.3cM and 4.5cM on the murine and human X-chromosome, respectively. Thus, cosegregation of the two alleles is highly likely.

4.4.7 *LMO2* screening

Although differential expression of *LMO2* was not investigated in this study, I selected it for patient screening for several reasons. For one, it is located in the linkage interval for EVR3 on chromosome 11p12-13 (Downey et al., 2001). Two, it has been associated with angiogenesis and Wnt-signaling (Yamada et al., 2000). Three, it is expressed in retina and inner ear, two of the organs affected in ND (Deng et al., 2006). Four, *in silico* analyses predicted a binding site for *NDP* (Katoh and Katoh, 2005).

However, after sequencing of all six exons and flanking intronic regions, no mutations were found in the patient group. Allele frequencies for four of the five SNPs observed were similar to the database values, and for one SNP (rs11032432), no frequency data

was available. This information should be retrieved by sequencing a cohort of control DNAs.

4.4.8 Promising candidate genes for future genetic screening of ND/EVR patients

In addition to genes that were shown to be differentially expressed or have been discussed above (*MAOA*, *MMP7*, *TPH1*, *WNT7B*, *WNT11*), following candidates should be considered for future research:

4.4.8.1 Tissue inhibitor of metalloproteinases 1 (TIMP1)

This gene is located within intron 6 of the synapsin I gene and is transcribed in the opposite direction at Xp11.3 (~5 cM from *NDP*). TIMP1 was shown to inhibit matrix metalloproteinase (MMP) activity and thereby suppresses angiogenesis in vitro and in vivo (Johnson et al., 1994). Although two patients with ND and a submicroscopic deletion of Xp11.3-11.2 were found to retain the *TIMP1* gene (Gal et al., 1986), it should not be excluded as candidate, since two genes closely located two each other may interact functionally and can contribute to the same disease, as has been demonstrated by the adjacent genes *FZD4* and *LRP5* on chromosome 11q.

4.4.8.2 NF-κ-B essential modulator gene (NEMO/IKBKG)

The NF-kappa-B essential modulator gene (*NEMO/IKBKG*) has been shown to cause incontinentia pigmenti (IP), which has an ocular phenotype very similar to ND (Smahi et al., 2000). Usually, familial mutations in *NEMO/IKBKG* cause extra-ocular symptoms, especially and maybe best visible in the skin. But in the case of somatic mutations that only affect the eyes, mutations in *NEMO/IKBKG* could account for an ND-like phenotype. Thus, *NEMO/IKBKG* should be considered as candidate gene for screening in ND/FEVR patients without mutations in *NDP*.

4.4.8.3 Insulin-like growth factor 1 (IGF-1)

Insulin-like growth factor 1 (*IGF-1*) has been shown to be necessary for ocular vascular development (Hellström et al., 2002), and low serum levels have been associated with ROP (Hellström et al., 2003). Further, growth failure, sensorineural deafness, and mental retardation were observed (Woods et al., 1996; Bonapace et al., 2003). In one family, a mutation in *IGF-1* (p.V44M) additionally presented with bilateral cataract, shallow anterior chamber, and varying degrees of reduced bone density up to osteoporosis, all clinical features reminiscent of ND/OPPG (Walenkamp et al., 2005). However, no significant differences were found on transcript level in the *Ndph* ko retina (Luhmann et al., 2005a).

4.4.8.4 Angiopoietin 2 (ANGPT-2)

Angiopoietin 2 is necessary for angiogenesis and vessel regression (Fruttiger, 2007). Transcript levels are elevated during neovascularization and can also be found in the *Ndph* ko retina at p15 and p21 (Luhmann et al., 2005a). High levels have further been observed in the vitreous of patients diagnosed with proliferative diabetic retinopathy (Watanabe et al., 2005). The *Angpt-2* ko mouse is an ocular phenocopy of the *Ndph* ko mouse, presenting with delayed and incomplete development of the superficial retinal vasculature, lack of deep and intermediate networks, and lack of hyaloid vessel regression (Hackett et al., 2002).

4.4.8.5 Endothelial-specific receptor tyrosine kinase (TEK/TIE2)

TEK is a key protein for angiogenesis (Fruttiger, 2007) that has been shown to be regulated by Wnt5a (Masckauchan et al., 2006) via non-canonical Wnt-signaling. Since expression of the *Tie-2* mRNA in the p5 *Ndph* ko retina is significantly reduced (Luhmann et al., 2005a), it is tempting to speculate if norrin might be involved in its regulation as well.

4.4.8.6 Dickkopf 2 (DKK2)

Dickkopf 2 (*Dkk2*) is an inhibitor of canonical Wnt-signaling that has been shown to be a key regulator in corneal fate determination of the ocular surface epithelium (Mukhopadhyay et al., 2006). *Dkk2* ko mice present with opaque corneas, another feature frequently observed in ND patients. Mutations in *DKK2* could affect norrin/FZD4/LRP5 signaling in the eye, and thus contribute to the severity of the disease.

4.4.9 Synopsis

Five of our 22 patients were previously found to harbor mutations in *NDP* (p.M1V, p.R74C, p.C110S, p.C128X, c.174+1G>T) (Table 6). Of the remaining 17 patients, one had a mutation in *FZD4* (p.P33S), and one had a new heterozygous mutation in *LRP5* (p.T672M). 15 patients had no mutations in these three genes, but sequence analyses of *LRP5L*, *LMO2*, *PLVAP*, and *SLC38A5* revealed no additional pathogenic variants. In the patient group, significant different allele frequencies were found for one SNP in *LRP5* (rs4988320) and one in *LRP5L* (rs9624807), which should be confirmed through additional screening of patients and analyzed with regard to differential splicing activity. One new sequence variant was found in exon 1 of *SLC38A5*, which has been predicted to possibly affect splicing also (c.-73G>A). The absence of mutations in *LRP5L*, *LMO2*, *PLVAP*, and *SLC38A5* in 15 patients does not implicate that these genes are not of importance for the pathogenesis of ND/EVR-like diseases, and thus should nonetheless be considered as candidates for future screening efforts. In addition, several other genes should be included, such as *ANGPT2, DKK2, IGF-1, ISL1, IKBKG, MAOA, MMP7, SYP, TEK, TIMP1, TPH1, WNT7B,* and *WNT11.*

5. Acknowledgements

First of all I am indebted to Prof. Dr. Wolfgang Berger, who gave me the opportunity to do my thesis in his lab. His constant support and guidance were essential, and all that was achieved is based on this relation.

Then I would like to thank all my colleagues in the Berger lab in Schwerzenbach, who undoubtedly were the people I have spent the most time with in the last four years. They were not only co-workers, but also friends, buddys, good listeners, helpful advisers, and even some kind of family to me. Special thanks go to my co-workers and collaborators on the Norrie disease project:

Ulrich Luhmann, who introduced me to the topic and to numerous biological techniques, as well as becoming a scientist in general. Thank you so much for being a great supervisor during the first year of my thesis! I'll never forget your help and support!

Lucas Mohn and Jurian Zürcher progressed from students in a practical course under my supervision to irreplacable team Norrie PhD buddies. Gentlemen, it was a pleasure for me to share my work space and office, thoughts and ideas, ups & downs with you! Thank you for all the help, motivation, good mood, beers, and stupid powerpoint slides!

Walther Hänseler, who spend a whole year of his life as my first diploma student to mainly work on ideas and experiments I came up with - without ever complaining! I truly hope that you haven't carried away any lasting damages!

Karin Schläpfer did an internship under my supervision and was super-smart, super-quick, super-friendly, super-collaborating, but also super-fast gone again!

Silke Feil was a constant support in mastering the tedious, but necessary laboratory work that often is taken for granted, but mustn't be underestimated.

I also want to thank Sandra Brunner, Gaby Tanner, István Magyar, and Fabian Schmid, who were my other fellow PhD students in the lab, for sharing my experiences, the good and the not-so-good ones!

Then, leaving the lab, I would like to thank Dr. Lucia Galli-Resta and Paola Leone from the Istituto di Neuroscience, CNR, Pisa, Italy, who were great hosts during my visit to their lab, and, like Italians do, gave me the opportunity to be part of their family. Grazie per tutto!

Further thanks go to Andrea Patrignani, Marzanna Künzli, Ulrich Wagner, and Hubert Rehrauer from the Functional Genomics Center Zurich, who provided me with invaluable help on the microarray experiments - thank you for making it possible!

I also owe thanks to Rolf Jaussi, Suzanne Kronenberg, Thomas Schleier, and Kurt Ballmer from the Paul-Scherrer-Institute in Villigen, who collaborated with me on the production of recombinant norrin.

A special thanks to Drs. Charlotte Poloschek and Christina Pieh from the University Clinic in Freiburg, Germany, and Bernd Wissinger and Susanne Kohl from the University in Tübingen, Germany, who provided me with DNAs from their patients and shared their insights from clinical examinations.

And then, last but not least, my friends and family, who always believed in me, who always understood me, who always gave me constant support during this special time. Oma, Papa, Kathrin - ohne Euch wäre das nicht gegangen! Markus, thank you for making it possible every single time! And finally my wholehearted thanks to Ines for being so patient and loving all the time, even when it was hard!

Thank all of you!!!

In memory of the more than 2,000 mice that lived and died to make this thesis possible.

6. References

Abelson, J., Kwan, K., O'Roak, B., Baek, D., Stillman, A., Morgan, T., et al. (2005). Sequence variants in SLITRK1 are associated with Tourette's syndrome. *Science , 310* (5746), 317-20.

Adams, R., & Alitalo, K. (2007). Molecular regulation of angiogenesis and lymphangiogenesis. *Nature Reviews Molecular Cell Biology , 8* (6), 464-78.

Ai, M., Heeger, S., Bartels, C., Schelling, D., & Osteoporosis-Pseudoglioma Collaborative Group. (2005). Clinical and molecular findings in osteoporosis-pseudoglioma syndrome. *American Journal of Human Genetics , 77* (5), 741-53.

Ai, M., Holmen, S., Van Hul, W., Williams, B., & Warman, M. (2005). Reduced affinity to and inhibition by DKK1 form a common mechanism by which high bone mass-associated missense mutations in LRP5 affect canonical Wnt signaling. *Molecular and Cellular Biology , 25* (12), 4946-55.

Akiyama, T., & Kawasaki, Y. (2006). Wnt signalling and the actin cytoskeleton. *Oncogene , 25* (57), 7538-7544.

Alitalo, K., Tammela, T., & Petrova, T. (2005). Lymphangiogenesis in development and human disease. *Nature , 438* (7070), 946-53.

Allen, R., Russell, S., Streb, L., Alsheikheh, A., & Stone, E. (2006). Phenotypic heterogeneity associated with a novel mutation (Gly112Glu) in the Norrie disease protein. *Eye , 20* (2), 234-41.

Alsheikheh, A., Lieb, W., & Grehn, F. (2004). [Criswick-Schepens syndrome -- familial exudative vitreoretinopathy. Report of six cases in two consanguineous families]. *Der Ophthalmologe , 101* (9), 914-8.

Amos, C. (2007). Successful design and conduct of genome-wide association studies. *Human Molecular Genetics , 16 Spec No. 2*, R220-5.

Ando, K., & Fujita, T. (2003). Lessons from the adrenomedullin knockout mouse. *Regulatory Peptides , 112* (1-3), 185-8.

Antonetti, D., Barber, A., Hollinger, L., Wolpert, E., & Gardner, T. (1999). Vascular endothelial growth factor induces rapid phosphorylation of tight junction proteins occludin and zonula occluden 1. A potential mechanism for vascular permeability in diabetic retinopathy and tumors. *The Journal of Biological Chemistry , 274* (33), 23463-7.

Aponte, E., Pulido, J., Ellison, J., Quiram, P., & Mohney, B. (2009). A novel NDP mutation in an infant with unilateral persistent fetal vasculature and retinal vasculopathy. *Ophthalmic Genetics , 30* (2), 99-102.

Arandjelovic, S., Van Sant, C., & Gonias, S. (2006). Limited mutations in full-length tetrameric human alpha2-macroglobulin abrogate binding of platelet-derived growth factor-BB and transforming growth factor-beta1. *The Journal of Biological Chemistry , 281* (25), 17061-8.

Asai-Coakwell, M., French, C., Ye, M., Garcha, K., Bigot, K., Perera, A., et al. (2009). Incomplete penetrance and phenotypic variability characterize Gdf6-attributable oculo-skeletal phenotypes. *Human Molecular Genetics , 18* (6), 1110-21.

Ashburner, M., Ball, C., Blake, J., Botstein, D., Butler, H., Cherry, J., et al. (2000). Gene ontology: tool for the unification of biology. The Gene Ontology Consortium. *Nature Genetics , 25* (1), 25-9.

Ashton, N., Ward, B., & Serpell, G. (1954). Effect of oxygen on developing retinal vessels with particular reference to the problem of retrolental fibroplasia. *The British Journal of Ophthalmology , 38* (7), 397-432.

Ashton, N., Ward, B., & Serpell, G. (1953). Role of oxygen in the genesis of retrolental fibroplasia; a preliminary report. *The British Journal of Ophthalmology , 37* (9), 513-20.

Bányász, I., Bokodi, G., Vannay, A., Szebeni, B., Treszl, A., Vásárhelyi, B., et al. (2006). Genetic polymorphisms of vascular endothelial growth factor and angiopoietin 2 in retinopathy of prematurity. *Current Eye Research , 31* (7-8), 685-90.

Badea, T., & Nathans, J. (2004). Quantitative analysis of neuronal morphologies in the mouse retina visualized by using a genetically directed reporter. *The Journal of Comparative Neurology , 480* (4), 331-51.

Bai, B., Tang, J., Liu, H., Chen, J., Li, Y., & Song, W. (2008). Apelin-13 induces ERK1/2 but not p38 MAPK activation through coupling of the human apelin receptor to the Gi2 pathway. *Acta Biochimica et Biophysica Sinica , 40* (4), 311-8.

Bainbridge, J., Smith, A., Barker, S., Robbie, S., Henderson, R., Balaggan, K., et al. (2008). Effect of gene therapy on visual function in Leber's congenital amaurosis. *The New England Journal of Medicine , 358* (21), 2231-9.

Balemans, W., & Van Hul, W. (2007). The genetics of low-density lipoprotein receptor-related protein 5 in bone: a story of extremes. *Endocrinology , 148* (6), 2622-9.

Balemans, W., Devogelaer, J.-P., Cleiren, E., Piters, E., Caussin, E., & Van Hul, W. (2007). Novel LRP5 missense mutation in a patient with a high bone mass phenotype results in decreased DKK1-mediated inhibition of Wnt signaling. *Journal of Bone and Mineral Research , 22* (5), 708-16.

Bamashmus, M., Downey, L., Inglehearn, C., Gupta, S., & Mansfield, D. (2000). Genetic heterogeneity in familial exudative vitreoretinopathy; exclusion of the EVR1 locus on chromosome 11q in a large autosomal dominant pedigree. *British Journal of Ophthalmology , 84* (4), 358-63.

Banin, E., Dorrell, M., Aguilar, E., Ritter, M., Aderman, C., Smith, A., et al. (2006). T2-TrpRS inhibits preretinal neovascularization and enhances physiological vascular regrowth in OIR as assessed by a new method of quantification. *Investigative Ophthalmology & Visual Science , 47* (5), 2125-34.

Barber, A., & Antonetti, D. (2003). Mapping the blood vessels with paracellular permeability in the retinas of diabetic rats. *Investigative Ophthalmology & Visual Science , 44* (12), 5410-6.

Barber, A., Antonetti, D., Kern, T., Reiter, C., Soans, R., Krady, J., et al. (2005). The Ins2Akita mouse as a model of early retinal complications in diabetes. *Investigative Ophthalmology & Visual Science , 46* (6), 2210-8.

Barrios-Rodiles, M., Brown, K., Ozdamar, B., Bose, R., Liu, Z., Donovan, R., et al. (2005). High-throughput mapping of a dynamic signaling network in mammalian cells. *Science , 307* (5715), 1621-5.

Barros, E., Dias da Silva, M., Kunii, I., & Lazaretti-Castro, M. (2008). Three years follow-up of pamidronate therapy in two brothers with osteoporosis-pseudoglioma syndrome (OPPG) carrying an LRP5 mutation. *Journal of pediatric endocrinology & metabolism : JPEM , 21* (8), 811-8.

Barros, E., Dias da Silva, M., Kunii, I., Hauache, O., & Lazaretti-Castro, M. (2007). A novel mutation in the LRP5 gene is associated with osteoporosis-pseudoglioma syndrome. *Osteoporosis International , 18* (7), 1017-8.

Bartel, D. (2004). MicroRNAs: genomics, biogenesis, mechanism, and function. *Cell , 116* (2), 281-97.

Bateman, J. (1992). Linkage analysis of Norrie disease with X-chromosomal ornithine aminotransferase. *Transactions of the American Ophthalmological Society , 90*, 405-79.

Bateman, J., Kojis, T., Cantor, R., Heinzmann, C., Ngo, J., Spence, M., et al. (1993). Linkage analysis of Norrie disease with an X-chromosomal ornithine aminotransferase locus. *Transactions of the American Ophthalmological Society , 91*, 299-307; discussion 307-8.

Battinelli, E., Boyd, Y., Craig, I., Breakefield, X., & Chen, Z.-Y. (1996). Characterization and mapping of the mouse NDP (Norrie disease) locus (Ndp). *Mammalian Genome , 7* (2), 93-7.

Bearer, E., & Orci, L. (1985). Endothelial fenestral diaphragms: a quick-freeze, deep-etch study. *The Journal of Cell Biology , 100* (2), 418-28.

Bechmann, I., Galea, I., & Perry, V. (2007). What is the blood-brain barrier (not)? *Trends in Immunology , 28* (1), 5-11.

Beier, M., Franke, A., Paunel-Görgülü, A., Scheerer, N., & Dünker, N. (2006). Transforming growth factor beta mediates apoptosis in the ganglion cell layer during all programmed cell death periods of the developing murine retina. *Neuroscience Research , 56* (2), 193-203.

Bergen, A., Wapenaar, M., Schuurman, E., Diergaarde, P., Lerach, H., Monaco, A., et al. (1993). Detection of a new submicroscopic Norrie disease deletion interval with a novel DNA probe isolated by differential Alu PCR fingerprint cloning. *Cytogenetics and Cell Genetics , 62* (4), 231-5.

Berger, M., Muraro, M., Fagioli, F., & Ferrari, S. (2008). Osteosarcoma derived from donor stem cells carrying the Norrie's disease gene. *The New England Journal of Medicine , 359* (23), 2502-4.

Berger, W. (1998). Molecular dissection of Norrie disease. *Acta Anatomica , 162* (2-3), 95-100.

Berger, W. (2008). Mouse Models of Norrie Disease. *Eye, Retina, and Visual System of the Mouse. Edited by Leo M. Chalupa and Robert W. Williams. MIT Press, Cambridge, MA, USA , 1* (1), 527-537.

Berger, W., & Ropers, H.-H. (2001). Norrie Disease. *The Metabolic and Molecular Basis of Inherited Disease , chapter 239, part 29, eye* (8th edition), 5977-5985.

Berger, W., Meindl, A., de Leeuw, B., de Roos, A., van de Pol, T., Meitinger, T., et al. (1992). Generation and characterization of radiation reduced cell hybrids and isolation of probes from the proximal short arm of the human X chromosome. *Human Genetics , 90* (3), 243-6.

Berger, W., Meindl, A., van de Pol, T., Cremers, F., Ropers, H., Döerner, C., et al. (1992). Isolation of a candidate gene for Norrie disease by positional cloning. *Nature Genetics , 2* (1), 84.

Berger, W., Meindl, A., van de Pol, T., Cremers, F., Ropers, H.-H., Döerner, C., et al. (1992). Isolation of a candidate gene for Norrie disease by positional cloning. *Nature Genetics , 1* (3), 199-203.

Berger, W., van de Pol, D., Bächner, D., Oerlemans, F., Winkens, H., Hameister, H., et al. (1996). An animal model for Norrie disease (ND): gene targeting of the mouse ND gene. *Human Molecular Genetics , 5* (1), 51-9.

Berger, W., van de Pol, D., Warburg, M., Gal, A., Bleeker-Wagemakers, L., de Silva, H., et al. (1992). Mutations in the candidate gene for Norrie disease. *Human Molecular Genetics , 1* (7), 461-5.

Berinstein, D., Hiraoka, M., Trese, M., & Shastry, B. (2001). Coats' disease and congenital retinoschisis in a single eye: a case report and DNA analysis. *Ophthalmologica , 215* (2), 132-5.

Bernstein, S., & Wong, P. (1998). Regional expression of disease-related genes in human and monkey retina. *Molecular Vision , 4*, 24.

Bhat, B., Allen, K., Liu, W., Graham, J., Morales, A., Anisowicz, A., et al. (2007). Structure-based mutation analysis shows the importance of LRP5 beta-propeller 1 in modulating Dkk1-mediated inhibition of Wnt signaling. *Gene , 391* (1-2), 103-12.

Bianchine, J., Briard-Guillemot, M., Marcteaux, P., Frezal, J., & Harrison, H. (1972). Generalized osteoporosis with bilateral pseudoglioma - an autosomal recessive disorder of connective tissue. *American Journal of Human Genetics , 24*, 34a.

Biccas Neto, L., Mesquita, A., & Louro, I. (2009). Familial exudative vitreoretinopathy (FEVR) associated with infantile osteoporosis: case report. *Arquivos brasileiros de oftalmologia , 72* (2), 257-60.

Biswas, J., Sharma, T., Gopal, L., Madhavan, H., Sulochana, K., & Ramakrishnan, S. (2002). Eales disease--an update. *Survey of Ophthalmology , 47* (3), 197-214.

Björklund, P., Åkerström, G., & Westin, G. (2007). An LRP5 receptor with internal deletion in hyperparathyroid tumors with implications for deregulated WNT/beta-catenin signaling. *PLoS Medicine , 4* (11), e328.

Black, G., Coleman, M., Chen, Z.-Y., Nemeth, A., Davies, K., & Craig, I. (1995). A bidirectional YAC walk from the Norrie disease (NDP) locus. *Genomics , 25* (3), 644-9.

Black, G., Perveen, R., Bonshek, R., Cahill, M., Clayton-Smith, J., Lloyd, I., et al. (1999). Coats' disease of the retina (unilateral retinal telangiectasis) caused by somatic mutation in the NDP gene: a role for norrin in retinal angiogenesis. *Human Molecular Genetics , 8* (11), 2031-5.

Bleeker-Wagemakers, E., Zweije-Hofman, I., & Gal, A. (1988). Norrie disease as part of a complex syndrome explained by a submicroscopic deletion of the X chromosome. *Ophthalmic Paediatrics and Genetics , 9* (3), 137-42.

Bleeker-Wagemakers, L., Friedrich, U., Gal, A., Wienker, T., Warburg, M., & Ropers, H. (1985). Close linkage between Norrie disease, a cloned DNA sequence from the proximal short arm, and the centromere of the X chromosome. *Human Genetics , 71* (3), 211-4.

Bloch, B. (1926). Eigentümliche bisher nicht beschriebene Pigmentaffektion (Incontinentia pigmenti). *Schweiz. Med. Wschr. , 7*, 404.

Blum, M., Alexandridis, E., & Rating, D. (1994). [Cerebral tuberous sclerosis and Coats disease]. *Der Ophthalmologe : Zeitschrift der Deutschen Ophthalmologischen Gesellschaft , 91* (3), 377-9.

Bodine, P., Billiard, J., Moran, R., Ponce-De-Leon, H., Mclarney, S., Mangine, A., et al. (2005). The Wnt antagonist secreted frizzled-related protein-1 controls osteoblast and osteocyte apoptosis. *Journal of Cellular Biochemistry , 96* (6), 1212-30.

Boerrigter, R., Siertsema, J., & Kema, I. (1992). Serotonin (5-HT) and the rat's eye. Some pilot studies. *Documenta ophthalmologica Advances in ophthalmology , 82* (1-2), 141-50.

Boltshauser, E. (2004). Cerebellum-small brain but large confusion: a review of selected cerebellar malformations and disruptions. *American journal of medical genetics Part A , 126A* (4), 376-85.

Bomberger, J., Parameswaran, N., Hall, C., Aiyar, N., & Spielman, W. (2005). Novel function for receptor activity-modifying proteins (RAMPs) in post-endocytic receptor trafficking. *The Journal of Biological Chemistry , 280* (10), 9297-307.

Bonapace, G., Concolino, D., Formicola, S., & Strisciuglio, P. (2003). A novel mutation in a patient with insulin-like growth factor 1 (IGF1) deficiency. *Journal of Medical Genetics , 40* (12), 913-7.

Bondjers, C., He, L., Takemoto, M., Norlin, J., Asker, N., Hellström, M., et al. (2006). Microarray analysis of blood microvessels from PDGF-B and PDGF-Rbeta mutant mice identifies novel markers for brain pericytes. *The FASEB Journal , 20* (10), 1703-5.

Boonstra, N., van Nouhuys, E., Schuil, J., de Wijs, I., van der Donk, K., Nikopoulos, K., et al. (25. Mar 2009). Clinical and molecular evaluation of probands and family members with familial exudative vitreoretinopathy (FEVR). *Investigative Ophthalmology & Visual Science* .

Bottomley, H., Downey, L., Inglehearn, C., & Toomes, C. (2006). Comment on 'cosegregation of two unlinked mutant alleles in some cases of autosomal dominant familial exudative vitreoretinopathy'. *European Journal of Human Genetics , 14* (1), 6-7; author reply 7-8.

Boulland, J.-L., Osen, K., Levy, L., Danbolt, N., Edwards, R., Storm-Mathisen, J., et al. (2002). Cell-specific expression of the glutamine transporter SN1 suggests differences in dependence on the glutamine cycle. *The European Journal of Neuroscience , 15* (10), 1615-31.

Boyden, L., Mao, J., Belsky, J., Mitzner, L., Farhi, A., Mitnick, M., et al. (2002). High bone density due to a mutation in LDL-receptor-related protein 5. *The New England Journal of Medicine , 346* (20), 1513-21.

Boyer, E., & Shannon, M. (2005). The serotonin syndrome. *The New England Journal of Medicine , 352* (11), 1112-20.

Brabletz, T., Jung, A., Dag, S., Hlubek, F., & Kirchner, T. (1999). beta-catenin regulates the expression of the matrix metalloproteinase-7 in human colorectal cancer. *The American Journal of Pathology , 155* (4), 1033-8.

Bradl, M., & Hohlfeld, R. (2003). Molecular pathogenesis of neuroinflammation. *Journal of Neurology, Neurosurgery & Psychiatry , 74* (10), 1364-70.

Braet, F., & Wisse, E. (2002). Structural and functional aspects of liver sinusoidal endothelial cell fenestrae: a review. *Comparative Hepatology , 1* (1), 1.

Brankin, B., Campbell, M., Canning, P., Gardiner, T., & Stitt, A. (2005). Endostatin modulates VEGF-mediated barrier dysfunction in the retinal microvascular endothelium. *Experimental Eye Research , 81* (1), 22-31.

Brannon, M., Gomperts, M., Sumoy, L., Moon, R., & Kimelman, D. (1997). A beta-catenin/XTcf-3 complex binds to the siamois promoter to regulate dorsal axis specification in Xenopus. *Genes & Development , 11* (18), 2359-70.

Brantjes, H., Barker, N., van Es, J., & Clevers, H. (2002). TCF: Lady Justice casting the final verdict on the outcome of Wnt signalling. *Biological Chemistry , 383* (2), 255-61.

Brembeck, F., Rosário, M., & Birchmeier, W. (2006). Balancing cell adhesion and Wnt signaling, the key role of beta-catenin. *Current Opinion in Genetics & Development , 16* (1), 51-9.

Bringmann, A., & Reichenbach, A. (2001). Role of Muller cells in retinal degenerations. *Frontiers in Bioscience: A Journal and Virtual Library , 6*, E72-92.

Bringmann, A., Pannicke, T., Grosche, J., Francke, M., Wiedemann, P., Skatchkov, S., et al. (2006). Müller cells in the healthy and diseased retina. *Progress in Retinal and Eye Research , 25* (4), 397-424.

Brown, A. (2005). Canonical Wnt signaling: high-throughput RNAi widens the path. *Genome Biology , 6* (9), 231.

Bryja, V., Andersson, E., Schambony, A., Esner, M., Bryjová, L., Biris, K., et al. (2009). The extracellular domain of Lrp5/6 inhibits noncanonical Wnt signaling in vivo. *Molecular Biology of the Cell , 20* (3), 924-36.

Burch, J., Leveille, A., & Morse, P. (1980). Ichthyosis hystrix (epidermal nevus syndrome) and Coats' disease. *American Journal of Ophthalmology , 89* (1), 25-30.

Byrne, C., Tainsky, M., & Fuchs, E. (1994). Programming gene expression in developing epidermis. *Development , 120* (9), 2369-83.

Caballero, M., Veske, A., Rodriguez, J., Lugo, N., Schroeder, B., Hesse, L., et al. (1996). Two novel mutations in the Norrie disease gene associated with the classical ocular phenotype. *Ophthalmic Genetics , 17* (4), 187-91.

Cadoret, A., Ovejero, C., Terris, B., Souil, E., Lévy, L., Lamers, W., et al. (2002). New targets of beta-catenin signaling in the liver are involved in the glutamine metabolism. *Oncogene , 21* (54), 8293-301.

Calhoun, M., Jucker, M., Martin, L., Thinakaran, G., Price, D., & Mouton, P. (1996). Comparative evaluation of synaptophysin-based methods for quantification of synapses. *Journal of neurocytology , 25* (12), 821-8.

Canny, C., & Oliver, G. (1976). Fluorescein angiographic findings in familial exudative vitreoretinopathy. *Archives of Ophthalmology , 94* (7), 1114-20.

Carmeliet, P. (2003). Angiogenesis in health and disease. *Nature Medicine , 9* (6), 653-60.

Carmeliet, P. (2005). Angiogenesis in life, disease and medicine. *Nature , 438* (7070), 932-6.

Carmeliet, P. (2000). Mechanisms of angiogenesis and arteriogenesis. *Nature Medicine , 6* (4), 389-95.

Carmeliet, P. (2000). VEGF gene therapy: stimulating angiogenesis or angioma-genesis? *Nature Medicine , 6* (10), 1102-3.

Carmeliet, P., & Tessier-Lavigne, M. (2005). Common mechanisms of nerve and blood vessel wiring. *Nature , 436* (7048), 193-200.

Carmeliet, P., Moons, L., Luttun, A., Vincenti, V., Compernolle, V., De Mol, M., et al. (2001). Synergism between vascular endothelial growth factor and placental growth factor contributes to angiogenesis and plasma extravasation in pathological conditions. *Nature Medicine , 7* (5), 575-83.

Carney, R. (1976). Incontinentia pigmenti. A world statistical analysis. *Archives of dermatology , 112* (4), 535-42.

Carninci, P., Kasukawa, T., Katayama, S., Gough, J., Frith, M., Maeda, N., et al. (2005). The transcriptional landscape of the mammalian genome. *Science , 309* (5740), 1559-63.

Carson-Walter, E., Hampton, J., Shue, E., Geynisman, D., Pillai, P., Sathanoori, R., et al. (2005). Plasmalemmal vesicle associated protein-1 is a novel marker implicated in brain tumor angiogenesis. *Clinical Cancer Research , 11* (21), 7643-50.

Catalano, R. (1990). Incontinentia pigmenti. *American Journal of Ophthalmology , 110* (6), 696-700.

Cavodeassi, F., Carreira-Barbosa, F., Young, R., Concha, M., Allende, M., Houart, C., et al. (2005). Early stages of zebrafish eye formation require the coordinated activity of Wnt11, Fz5, and the Wnt/beta-catenin pathway. *Neuron , 47* (1), 43-56.

Cébe-Suarez, S., Zehnder-Fjällman, A., & Ballmer-Hofer, K. (2006). The role of VEGF receptors in angiogenesis; complex partnerships. *Cellular and Molecular Life Sciences , 63* (5), 601-15.

Chandel, N., McClintock, D., Feliciano, C., Wood, T., Melendez, J., Rodriguez, A., et al. (2000). Reactive oxygen species generated at mitochondrial complex III stabilize hypoxia-inducible factor-1alpha during hypoxia: a mechanism of O2 sensing. *The Journal of Biological Chemistry , 275* (33), 25130-8.

Chang, B., Smith, R., Peters, M., Savinova, O., Hawes, N., Zabaleta, A., et al. (2001). Haploinsufficient Bmp4 ocular phenotypes include anterior segment dysgenesis with elevated intraocular pressure. *BMC Genetics , 2*, 18.

Checchin, D., Sennlaub, F., Levavasseur, E., Leduc, M., & Chemtob, S. (2006). Potential role of microglia in retinal blood vessel formation. *Investigative Ophthalmology & Visual Science , 47* (8), 3595-602.

Chen, J., & Smith, L. (2007). Retinopathy of prematurity. *Angiogenesis , 10* (2), 133-40.

Chen, J., Somanath, P., Razorenova, O., Chen, W., Hay, N., Bornstein, P., et al. (2005). Akt1 regulates pathological angiogenesis, vascular maturation and permeability in vivo. *Nature Medicine , 11* (11), 1188-96.

Chen, Y., Hu, Y., Lu, K., Flannery, J., & Ma, J.-X. (2007). Very low density lipoprotein receptor, a negative regulator of the wnt signaling pathway and choroidal neovascularization. *The Journal of Biological Chemistry , 282* (47), 34420-8.

Chen, Z.-Y., Battinelli, E., Woodruff, G., Young, I., Breakefield, X., & Craig, I. (1993). Characterization of a mutation within the NDP gene in a family with a manifesting female carrier. *Human Molecular Genetics , 2* (10), 1727-9.

Chen, Z.-Y., Battinelli, E., Fielder, A., Bundey, S., Sims, K., Breakefield, X., et al. (1993). A mutation in the Norrie disease gene (NDP) associated with X-linked familial exudative vitreoretinopathy. *Nature Genetics, 5* (2), 180-3.

Chen, Z.-Y., Battinelli, E., Hendriks, R., Powell, J., Middleton-Price, H., Sims, K., et al. (1993). Norrie disease gene: characterization of deletions and possible function. *Genomics, 16* (2), 533-5.

Chen, Z.-Y., Denney, R., & Breakefield, X. (1995). Norrie disease and MAO genes: nearest neighbors. *Human Molecular Genetics , 4 Spec No*, 1729-37.

Chen, Z.-Y., Hendriks, R., Jobling, M., Powell, J., Breakefield, X., Sims, K., et al. (1992). Isolation and characterization of a candidate gene for Norrie disease. *Nature Genetics, 1* (3), 204-8.

Chen, Z.-Y., Sims, K., Coleman, M., Donnai, D., Monaco, A., Breakefield, X., et al. (1992). Characterization of a YAC containing part or all of the Norrie disease locus. *Human Molecular Genetics, 1* (3), 161-4.

Cheng, N., Brantley, D., Liu, H., Lin, Q., Enriquez, M., Gale, N., et al. (2002). Blockade of EphA receptor tyrosine kinase activation inhibits vascular endothelial cell growth factor-induced angiogenesis. *Molecular Cancer Research, 1* (1), 2-11.

Cheung, W., Jin, L., Smith, D., Cheung, P., Kwan, E., Low, L., et al. (2006). A family with osteoporosis pseudoglioma syndrome due to compound heterozygosity of two novel mutations in the LRP5 gene. *Bone, 39* (3), 470-6.

Chini, E., Chini, C., Bolliger, C., Jougasaki, M., Grande, J., Burnett, J., et al. (1997). Cytoprotective effects of adrenomedullin in glomerular cell injury: central role of cAMP signaling pathway. *Kidney international, 52* (4), 917-25.

Chow, J., Yen, Z., Ziesche, S., & Brown, C. (2005). Silencing of the mammalian X chromosome. *Annual Review of Genomics and Human Genetics, 6*, 69-92.

Christensen, R., Fujikawa, K., Madore, R., Oettgen, P., & Varticovski, L. (2002). NERF2, a member of the Ets family of transcription factors, is increased in response to hypoxia and angiopoietin-1: a potential mechanism for Tie2 regulation during hypoxia. *Journal of Cellular Biochemistry, 85* (3), 505-15.

Chrzanowska-Wodnicka, M., Kraus, A., Gale, D., White, G., & Vansluys, J. (2008). Defective angiogenesis, endothelial migration, proliferation, and MAPK signaling in Rap1b-deficient mice. *Blood, 111* (5), 2647-56.

Chung, B., Kayserili, H., Ai, M., Freudenberg, J., Uzümcü, A., Uyguner, O., et al. (28. Jan 2009). A mutation in the signal sequence of LRP5 in a family with an osteoporosis-pseudoglioma syndrome (OPPG)-like phenotype indicates a novel disease mechanism for trinucleotide repeats. *Human Mutation*.

Chynn, E., Walton, D., Hahn, L., & Dryja, T. (1996). Norrie disease. Diagnosis of a simplex case by DNA analysis. *Archives of Ophthalmology, 114* (9), 1136-8.

Ciani, L. (2004). A divergent canonical WNT-signaling pathway regulates microtubule dynamics: Dishevelled signals locally to stabilize microtubules. *The Journal of Cell Biology, 164* (2), 243-253.

Ciani, L., & Salinas, P. (2005). WNTs in the vertebrate nervous system: from patterning to neuronal connectivity. *Nature Reviews Neuroscience, 6* (5), 351-62.

Claxton, S., & Fruttiger, M. (2005). Oxygen modifies artery differentiation and network morphogenesis in the retinal vasculature. *Developmental Dynamics , 233* (3), 822-8.

Clément-Lacroix, P., Ai, M., Morvan, F., Roman-Roman, S., Vayssière, B., Belleville, C., et al. (2005). Lrp5-independent activation of Wnt signaling by lithium chloride increases bone formation and bone mass in mice. *Proceedings of the National Academy of Sciences of the United States of America , 102* (48), 17406-11.

Clevers, H. (2004). Wnt signaling: Ig-norrin the dogma. *Current Biology , 14* (11), R436-7.

Clop, A., Marcq, F., Takeda, H., Pirottin, D., Tordoir, X., Bibé, B., et al. (2006). A mutation creating a potential illegitimate microRNA target site in the myostatin gene affects muscularity in sheep. *Nature Genetics , 38* (7), 813-8.

Coats, G. (1908). Forms of retinal disease with massive exudation. *Roy London Ophthalmol Hosp Rep , 17*, 440-525.

Cofer, S., & Ross, S. (1996). The murine gene encoding apolipoprotein D exhibits a unique expression pattern as compared to other species. *Gene , 171* (2), 261-3.

Cole, J., & Cole, H. (1959). Incontinentia pigmenti associated with changes in the posterior chamber of the eye. *American Journal of Ophthalmology , 47* (3), 321-8.

Collins, F., Murphy, D., Reiss, A., Sims, K., Lewis, J., Freund, L., et al. (1992). Clinical, biochemical, and neuropsychiatric evaluation of a patient with a contiguous gene syndrome due to a microdeletion Xp11.3 including the Norrie disease locus and monoamine oxidase (MAOA and MAOB) genes. *American Journal of Medical Genetics , 42* (1), 127-34.

Colucci-Guyon, E., Portier, M., Dunia, I., Paulin, D., Pournin, S., & Babinet, C. (1994). Mice lacking vimentin develop and reproduce without an obvious phenotype. *Cell , 79* (4), 679-94.

Comerford, K., Wallace, T., Karhausen, J., Louis, N., Montalto, M., & Colgan, S. (2002). Hypoxia-inducible factor-1-dependent regulation of the multidrug resistance (MDR1) gene. *Cancer Research , 62* (12), 3387-94.

Constância, M., Angiolini, E., Sandovici, I., Smith, P., Smith, R., Kelsey, G., et al. (2005). Adaptation of nutrient supply to fetal demand in the mouse involves interaction between the Igf2 gene and placental transporter systems. *Proceedings of the National Academy of Sciences of the United States of America , 102* (52), 19219-24.

Cooney, R., Hynes, S., Duffy, A., Sharif, F., & O'Brien, T. (2006). Adenoviral-mediated gene transfer of nitric oxide synthase isoforms and vascular cell proliferation. *Journal of Vascular Research , 43* (5), 462-72.

Cottet, S. (2006). Biological characterization of gene response in Rpe65-/- mouse model of Leber's congenital amaurosis during progression of the disease. *The FASEB Journal , 20* (12), 2036-2049.

Coultas, L., Chawengsaksophak, K., & Rossant, J. (2005). Endothelial cells and VEGF in vascular development. *Nature , 438* (7070), 937-45.

Cowden Dahl, K., Robertson, S., Weaver, V., & Simon, M. (2005). Hypoxia-inducible factor regulates alphavbeta3 integrin cell surface expression. *Molecular Biology of the Cell , 16* (4), 1901-12.

Crabbe, P., Balemans, W., Willaert, A., Van Pottelbergh, I., Cleiren, E., Coucke, P., et al. (2005). Missense mutations in LRP5 are not a common cause of idiopathic osteoporosis in adult men. *Journal of Bone and Mineral Research , 20* (11), 1951-9.

Crackower, M., Sarao, R., Oudit, G., Yagil, C., Kozieradzki, I., Scanga, S., et al. (2002). Angiotensin-converting enzyme 2 is an essential regulator of heart function. *Nature , 417* (6891), 822-8.

Crawford, H., Fingleton, B., Rudolph-Owen, L., Goss, K., Rubinfeld, B., Polakis, P., et al. (1999). The metalloproteinase matrilysin is a target of beta-catenin transactivation in intestinal tumors. *Oncogene , 18* (18), 2883-91.

Crawford, S., Stellmach, V., Murphy-Ullrich, J., Ribeiro, S., Lawler, J., Hynes, R., et al. (1998). Thrombospondin-1 is a major activator of TGF-beta1 in vivo. *Cell , 93* (7), 1159-70.

Criswick, V., & Schepens, C. (1969). Familial exudative vitreoretinopathy. *American Journal of Ophthalmology , 68* (4), 578-94.

Cubelos, B., González-González, I., Giménez, C., & Zafra, F. (2005). Amino acid transporter SNAT5 localizes to glial cells in the rat brain. *Glia , 49* (2), 230-44.

Cui, Z., Tuladhar, R., Hart, S., Marber, M., Pearson, J., & Baydoun, A. (2005). Rate of transport of l-arginine is independent of the expression of inducible nitric oxide synthase in HEK 293 cells. *Nitric Oxide : Biology and Chemistry , 12* (1), 21-30.

Curtis, D., Blank, C., Parsons, M., & Hughes, H. (1989). Carrier detection and prenatal diagnosis in Norrie disease. *Prenatal Diagnosis , 9* (10), 735-40.

Dabdoub, A., & Kelley, M. (2005). Planar cell polarity and a potential role for a Wnt morphogen gradient in stereociliary bundle orientation in the mammalian inner ear. *Journal of Neurobiology , 64* (4), 446-57.

Davidson, G., Wu, W., Shen, J., Bilic, J., Fenger, U., Stannek, P., et al. (2005). Casein kinase 1 gamma couples Wnt receptor activation to cytoplasmic signal transduction. *Nature , 438* (7069), 867-72.

Davis, R. (1993). The mitogen-activated protein kinase signal transduction pathway. *The Journal of Biological Chemistry , 268* (20), 14553-6.

de Iongh, R., Abud, H., & Hime, G. (2006). WNT/Frizzled signaling in eye development and disease. *Frontiers in Bioscience: A Journal and Virtual Library , 11*, 2442-64.

de Juan Jr., E., Farr, A., & Noorily, S. (2001). *Retinal Detachment in Infants* (Bd. 3).

Deng, M., Pan, L., Xie, X., & Gan, L. (2006). Differential expression of LIM domain-only (LMO) genes in the developing mouse inner ear. *Gene Expression Patterns , 6* (8), 857-63.

Denis, C., Methia, N., Frenette, P., Rayburn, H., Ullman-Culleré, M., Hynes, R., et al. (1998). A mouse model of severe von Willebrand disease: defects in hemostasis and thrombosis. *Proceedings of the National Academy of Sciences of the United States of America , 95* (16), 9524-9.

Denli, A., Tops, B., Plasterk, R., Ketting, R., & Hannon, G. (2004). Processing of primary microRNAs by the Microprocessor complex. *Nature , 432* (7014), 231-5.

Dennis, G., Sherman, B., Hosack, D., Yang, J., Gao, W., Lane, H., et al. (2003). DAVID: Database for Annotation, Visualization, and Integrated Discovery. *Genome Biology , 4* (5), P3.

Deroanne, C., Vouret-Craviari, V., Wang, B., & Pouysségur, J. (2003). EphrinA1 inactivates integrin-mediated vascular smooth muscle cell spreading via the Rac/PAK pathway. *Journal of Cell Science , 116* (Pt 7), 1367-76.

Dheda, K., Huggett, J., Bustin, S., Johnson, M., Rook, G., & Zumla, A. (2004). Validation of housekeeping genes for normalizing RNA expression in real-time PCR. *BioTechniques, 37* (1), 112-4, 116, 118-9.

Dhingra, S. (2006). Advanced bilateral persistent fetal vasculature associated with a novel mutation in the Norrie gene. *British Journal of Ophthalmology , 90* (10), 1324-1325.

Dickinson, J., Sale, M., Passmore, A., Fitzgerald, L., Wheatley, C., Burdon, K., et al. (2006). Mutations in the NDP gene: contribution to Norrie disease, familial exudative vitreoretinopathy and retinopathy of prematurity. *Clinical & Experimental Ophthalmology , 34* (7), 682-8.

Diergaarde, P., Wieringa, B., Bleeker-Wagemakers, E., Sims, K., Breakefield, X., & Ropers, H. (1989). Physical fine-mapping of a deletion spanning the Norrie gene. *Human Genetics , 84* (1), 22-6.

Donnai, D., Mountford, R., & Read, A. (1988). Norrie disease resulting from a gene deletion: clinical features and DNA studies. *Journal of Medical Genetics , 25* (2), 73-8.

Dorrell, M., & Friedlander, M. (2006). Mechanisms of endothelial cell guidance and vascular patterning in the developing mouse retina. *Progress in Retinal and Eye Research , 25* (3), 277-95.

Dorrell, M., Aguilar, E., & Friedlander, M. (2002). Retinal vascular development is mediated by endothelial filopodia, a preexisting astrocytic template and specific R-cadherin adhesion. *Investigative Ophthalmology & Visual Science , 43* (11), 3500-10.

Dorrell, M., Aguilar, E., Weber, C., & Friedlander, M. (2004). Global gene expression analysis of the developing postnatal mouse retina. *Investigative Ophthalmology & Visual Science , 45* (3), 1009-19.

Dorrell, M., Uusitalo-Jarvinen, H., Aguilar, E., & Friedlander, M. (2007). Ocular neovascularization: basic mechanisms and therapeutic advances. *Survey of Ophthalmology , 52 Suppl 1*, S3-19.

Downey, L., Bottomley, H., Sheridan, E., Ahmed, M., Gilmour, D., Inglehearn, C., et al. (2006). Reduced bone mineral density and hyaloid vasculature remnants in a consanguineous recessive FEVR family with a mutation in LRP5. *British Journal of Ophthalmology , 90* (9), 1163-7.

Downey, L., Keen, T., Roberts, E., Mansfield, D., Bamashmus, M., & Inglehearn, C. (2001). A new locus for autosomal dominant familial exudative vitreoretinopathy maps to chromosome 11p12-13. *American Journal of Human Genetics 68* (3), 778-81.

Draghici, S., Khatri, P., Bhavsar, P., Shah, A., Krawetz, S., & Tainsky, M. (2003). Onto-Tools, the toolkit of the modern biologist: Onto-Express, Onto-Compare, Onto-Design and Onto-Translate. *Nucleic Acids Research , 31* (13), 3775-81.

Draghici, S., Khatri, P., Tarca, A., Amin, K., Done, A., Voichita, C., et al. (2007). A systems biology approach for pathway level analysis. *Genome Research , 17* (10), 1537-45.

Drenser, K., & Trese, M. (2007). Familial exudative vitreoretinopathy and osteoporosis-pseudoglioma syndrome caused by a mutation in the LRP5 gene. *Archives of Ophthalmology, 125* (3), 431-2.

Drescher, U. (2005). A no-Wnt situation: SFRPs as axon guidance molecules. *Nature Neuroscience , 8* (10), 1281-2.

Duenas-Gonzalez, A., Candelaria, M., Perez-Plascencia, C., Perez-Cardenas, E., de la Cruz-Hernandez, E., & Herrera, L. (2008). Valproic acid as epigenetic cancer drug: preclinical, clinical and transcriptional effects on solid tumors. *Cancer treatment reviews , 34* (3), 206-22.

Dufourcq, P., Leroux, L., Ezan, J., Descamps, B., Lamazière, J.-M., Costet, P., et al. (2008). Regulation of endothelial cell cytoskeletal reorganization by a secreted frizzled-related protein-1 and frizzled 4- and frizzled 7-dependent pathway: role in neovessel formation. *The American Journal of Pathology , 172* (1), 37-49.

Dvoriantchikova, G., Ivanov, D., Panchin, Y., & Shestopalov, V. (2006). Expression of pannexin family of proteins in the retina. *FEBS Letters , 580* (9), 2178-82.

Eales, H. (1880). Cases of retinal hemorrhage associated with epistaxis and constipation. *Birmingham Med. Rev. , 9*, 262.

Edelmann, L., Hanson, P., Chapman, E., & Jahn, R. (1995). Synaptobrevin binding to synaptophysin: a potential mechanism for controlling the exocytotic fusion machine. *The EMBO Journal , 14* (2), 224-31.

Eichler, W., Yafai, Y., Wiedemann, P., & Reichenbach, A. (2004). Angiogenesis-related factors derived from retinal glial (Müller) cells in hypoxia. *NeuroReport , 15* (10), 1633-7.

Eichmann, A., Makinen, T., & Alitalo, K. (2005). Neural guidance molecules regulate vascular remodeling and vessel navigation. *Genes & Development , 19* (9), 1013-21.

Eklund, L., & Olsen, B. (2006). Tie receptors and their angiopoietin ligands are context-dependent regulators of vascular remodeling. *Experimental Cell Research , 312* (5), 630-41.

Elshatory, Y., Everhart, D., Deng, M., Xie, X., Barlow, R., & Gan, L. (2007). Islet-1 controls the differentiation of retinal bipolar and cholinergic amacrine cells. *The Journal of Neuroscience , 27* (46), 12707-20.

Esser, S., Wolburg, K., Wolburg, H., Breier, G., Kurzchalia, T., & Risau, W. (1998). Vascular endothelial growth factor induces endothelial fenestrations in vitro. *The Journal of Cell Biology , 140* (4), 947-59.

Fard, A., & Goldberg, M. (1998). Persistence of fetal vasculature in the eyes of patients with incontinentia pigment. *Archives of Ophthalmology , 116* (5), 682-4.

Feeney, S., Simpson, D., Gardiner, T., Boyle, C., Jamison, P., & Stitt, A. (2003). Role of vascular endothelial growth factor

and placental growth factors during retinal vascular development and hyaloid regression. *Investigative Ophthalmology & Visual Science , 44* (2), 839-47.

Feit-Leichman, R., Kinouchi, R., Takeda, M., Fan, Z., Mohr, S., Kern, T., et al. (2005). Vascular damage in a mouse model of diabetic retinopathy: relation to neuronal and glial changes. *Investigative Ophthalmology & Visual Science , 46* (11), 4281-7.

Feng, Y., vom Hagen, F., Pfister, F., Djokic, S., Hoffmann, S., Back, W., et al. (2007). Impaired pericyte recruitment and abnormal retinal angiogenesis as a result of angiopoietin-2 overexpression. *Thrombosis and Haemostasis , 97* (1), 99-108.

Fernandez-Lopez, A., Garrido-Martin, E., Sanz-Rodriguez, F., Pericacho, M., Rodriguez-Barbero, A., Eleno, N., et al. (2007). Gene expression fingerprinting for human hereditary hemorrhagic telangiectasia. *Human Molecular Genetics , 16* (13), 1515-33.

Ferrara, N., & Kerbel, R. (2005). Angiogenesis as a therapeutic target. *Nature , 438* (7070), 967-74.

Ferrari, S., Deutsch, S., Choudhury, U., Chevalley, T., Bonjour, J.-P., Dermitzakis, E., et al. (2004). Polymorphisms in the low-density lipoprotein receptor-related protein 5 (LRP5) gene are associated with variation in vertebral bone mass, vertebral bone size, and stature in whites. *American Journal of Human Genetics , 74* (5), 866-75.

Fiedler, U., Reiss, Y., Scharpfenecker, M., Grunow, V., Koidl, S., Thurston, G., et al. (2006). Angiopoietin-2 sensitizes endothelial cells to TNF-alpha and has a crucial role in the induction of inflammation. *Nature Medicine , 12* (2), 235-9.

Flower, R. (1985). Perinatal retinal vascular physiology. *Silverman, WA, and Flynn, JT, eds: Retinopathy of prematurity. Boston, Blackwell Scientific Publishers* .

Flynn, J., & Chan-Ling, T. (2006). Retinopathy of prematurity: two distinct mechanisms that underlie zone 1 and zone 2 disease. *American Journal of Ophthalmology , 142* (1), 46-59.

Folk, J., Genovese, F., & Biglan, A. (1981). Coats' disease in a patient with Cornelia de Lange syndrome. *American Journal of Ophthalmology , 91* (5), 607-10.

François, J. (1984). Incontinentia pigmenti (Bloch-Sulzberger syndrome) and retinal changes. *The British Journal of Ophthalmology , 68* (1), 19-25.

Franze, K., Grosche, J., Skatchkov, S., Schinkinger, S., Foja, C., Schild, D., et al. (2007). Muller cells are living optical fibers in the vertebrate retina. *Proceedings of the National Academy of Sciences of the United States of America , 104* (20), 8287-92.

Fretz, J., Zella, L., Kim, S., Shevde, N., & Pike, J. (2006). 1,25-Dihydroxyvitamin D3 regulates the expression of low-density lipoprotein receptor-related protein 5 via deoxyribonucleic acid sequence elements located downstream of the start site of transcription. *Molecular Endocrinology , 20* (9), 2215-30.

Friedlander, M. (2007). Fibrosis and diseases of the eye. *Journal of Clinical Investigation , 117* (3), 576-86.

Froyen, G., Bauters, M., Boyle, J., Van Esch, H., Govaerts, K., van Bokhoven, H., et al. (2007). Loss of SLC38A5 and FTSJ1 at Xp11.23 in three brothers with non-syndromic mental retardation due to a microdeletion in an unstable genomic region. *Human Genetics , 121* (5), 539-47.

Fruttiger, M. (2002). Development of the mouse retinal vasculature: angiogenesis versus vasculogenesis. *Investigative Ophthalmology & Visual Science , 43* (2), 522-7.

Fruttiger, M. (2007). Development of the retinal vasculature. *Angiogenesis , 10* (2), 77-88.

Fuchs, S., Kellner, U., Wedemann, H., & Gal, A. (1995). Missense mutation (Arg121Trp) in the Norrie disease gene associated with x-linked exudative vitreoretinopathy. *Human Mutation , 6* (3), 257-9.

Fuchs, S., van de Pol, D., Beudt, U., Kellner, U., Meire, F., Berger, W., et al. (1996). Three novel and two recurrent mutations of the Norrie disease gene in patients with Norrie syndrome. *Human Mutation , 8* (1), 85-8.

Fuchs, S., Xu, S., Caballero, M., Salcedo, M., La O, A., Wedemann, H., et al. (1994). A missense point mutation (Leu13Arg) of the Norrie disease gene in a large Cuban kindred with Norrie disease. *Human Molecular Genetics , 3* (4), 655-6.

Fuentes, J., Volpini, V., Fernández-Toral, F., Coto, E., & Estivill, X. (1993). Identification of two new missense mutations (K58N and R121Q) in the Norrie disease (ND) gene in two Spanish families. *Human Molecular Genetics , 2* (11), 1953-5.

Fujino, T., Asaba, H., Kang, M.-J., Ikeda, Y., Sone, H., Takada, S., et al. (2003). Low-density lipoprotein receptor-related protein 5 (LRP5) is essential for normal cholesterol metabolism and glucose-induced insulin secretion. *Proceedings of the National Academy of Sciences of the United States of America , 100* (1), 229-34.

Gal, A., Schinzel, A., Orth, U., Fraser, N., Mollica, F., Craig, I., et al. (1989). Gene of X-chromosomal congenital stationary night blindness is closely linked to DXS7 on Xp. *Human Genetics , 81* (4), 315-8.

Gal, A., Uhlhaas, S., Glaser, D., & Grimm, T. (1988). Prenatal exclusion of Norrie disease with flanking DNA markers. *American Journal of Medical Genetics , 31* (2), 449-53.

Gal, A., Veske, A., Jojart, G., Grammatico, B., Huber, B., Gu, S., et al. (1996). Norrie-Warburg syndrome: two novel mutations in patients with classical clinical phenotype. *Acta Ophthalmologica Scandinavica* (219), 13-6.

Gal, A., Wieringa, B., Smeets, D., Bleeker-Wagemakers, L., & Ropers, H. (1986). Submicroscopic interstitial deletion of the X chromosome explains a complex genetic syndrome dominated by Norrie disease. *Cytogenetics and Cell Genetics , 42* (4), 219-24.

Gale, N., Thurston, G., Hackett, S., Renard, R., Wang, Q., McClain, J., et al. (2002). Angiopoietin-2 is required for postnatal angiogenesis and lymphatic patterning, and only the latter role is rescued by Angiopoietin-1. *Developmental Cell , 3* (3), 411-23.

Galea, I., Bechmann, I., & Perry, V. (2007). What is immune privilege (not)? *Trends in Immunology , 28* (1), 12-8.

Galli-Resta, L. (2002). Putting neurons in the right places: local interactions in the genesis of retinal architecture. *Trends in Neurosciences , 25* (12), 638-43.

Gariano, R., & Gardner, T. (2005). Retinal angiogenesis in development and disease. *Nature , 438* (7070), 960-6.

Gariano, R., Hu, D., & Helms, J. (2006). Expression of angiogenesis-related genes during retinal development. *Gene Expression Patterns , 6* (2), 187-92.

Gass, J., Harbin, T., & Del Piero, E. (1991). Exudative stellate neuroretinopathy and Coats' syndrome in patients with progressive hemifacial atrophy. *European Journal of Ophthalmology , 1* (1), 2-10.

Gassler, N., & Lommatzsch, P. (1995). [Clinicopathologic study of 817 enucleations]. *Klinische Monatsblätter für Augenheilkunde , 207* (5), 295-301.

Gerber, H., Hillan, K., Ryan, A., Kowalski, J., Keller, G., Rangell, L., et al. (1999). VEGF is required for growth and survival in neonatal mice. *Development , 126* (6), 1149-59.

Gerhardt, H., Golding, M., Fruttiger, M., Ruhrberg, C., Lundkvist, A., Abramsson, A., et al. (2003). VEGF guides angiogenic sprouting utilizing endothelial tip cell filopodia. *The Journal of Cell Biology , 161* (6), 1163-77.

Gerhardt, H., Ruhrberg, C., Abramsson, A., Fujisawa, H., Shima, D., & Betsholtz, C. (2004). Neuropilin-1 is required for endothelial tip cell guidance in the developing central nervous system. *Developmental Dynamics , 231* (3), 503-9.

Ghiasvand, N., Kanis, A., Helms, C., Sheffield, V., Stone, E., & Donis-Keller, H. (2000). Nonsyndromic congenital retinal nonattachment gene maps to human chromosome band 10q21. *American Journal of Medical Genetics , 90* (2), 165-8.

Gieser, S., & Murphy, R. (2001). Eales' disease. *Retina, 3rd edition. Vol. II: Medical Retina. Edited by Stephen J. Ryan and Andrew P. Schachat , 2* (3), 1504-1508.

Gilgenkrantz, S., Tridon, P., Pinel-Briquel, N., Beurey, J., & Weber, M. (1985). Translocation (X;9)(p11;q34) in a girl with incontinentia pigmenti (IP): implications for the regional assignment of the IP locus to Xp11? *Annales de génétique , 28* (2), 90-2.

Gilles, C., Polette, M., Mestdagt, M., Nawrocki-Raby, B., Ruggeri, P., Birembaut, P., et al. (2003). Transactivation of vimentin by beta-catenin in human breast cancer cells. *Cancer Research , 63* (10), 2658-64.

Gilmour, D., Downey, L., Sheridan, E., Long, V., Bradbury, J., Inglehearn, C., et al. (2009). Familial Exudative Vitreoretinopathy and DiGeorge Syndrome A New Locus for Familial Exudative Vitreoretinopathy on Chromosome 22q11.2? *Ophthalmology* . E-pub ahead of print

Giordano, F. (2005). Oxygen, oxidative stress, hypoxia, and heart failure. *Journal of Clinical Investigation , 115* (3), 500-8.

Glass, D., Bialek, P., Ahn, J., Starbuck, M., Patel, M., Clevers, H., et al. (2005). Canonical Wnt signaling in differentiated osteoblasts controls osteoclast differentiation. *Developmental Cell , 8* (5), 751-64.

Godel, V., & Goodman, R. (1981). X-linked recessive primary retinal dysplasia: clinical findings in affected males and carrier females. *Clinical Genetics , 20* (4), 260-6.

Goldberg, M. (1997). Persistent fetal vasculature (PFV): an integrated interpretation of signs and symptoms associated with persistent hyperplastic primary vitreous (PHPV). LIV Edward Jackson Memorial Lecture. *American Journal of Ophthalmology , 124* (5), 587-626.

Gong, Y., Slee, R., Fukai, N., Rawadi, G., Roman-Roman, S., Reginato, A., et al. (2001). LDL receptor-related protein 5 (LRP5) affects bone accrual and eye development. *Cell , 107* (4), 513-23.

Gong, Y., Vikkula, M., Boon, L., Liu, J., Beighton, P., Ramesar, R., et al. (1996). Osteoporosis-pseudoglioma syndrome, a disorder affecting skeletal strength and vision, is assigned to chromosome region 11q12-13. *American Journal of Human Genetics , 59* (1), 146-51.

Good, W., & Gendron, R. (2007). Genomics and proteomics of retinopathy of prematurity: DNA-based prevention and treatment. *The British Journal of Ophthalmology , 91* (12), 1577.

Goodwin, A., & D'Amore, P. (2002). Wnt signaling in the vasculature. *Angiogenesis , 5* (1-2), 1-9.

Goodwin, A., Sullivan, K., & D'Amore, P. (2006). Cultured endothelial cells display endogenous activation of the canonical Wnt signaling pathway and express multiple ligands, receptors, and secreted modulators of Wnt signaling. *Developmental Dynamics , 235* (11), 3110-20.

Goutières, F., Dollfus, H., Becquet, F., & Dufier, J. (1999). Extensive brain calcification in two children with bilateral Coats' disease. *Neuropediatrics , 30* (1), 19-21.

Greenberg, D., & Jin, K. (2005). From angiogenesis to neuropathology. *Nature , 438* (7070), 954-9.

Gregory, R., Chendrimada, T., Cooch, N., & Shiekhattar, R. (2005). Human RISC couples microRNA biogenesis and posttranscriptional gene silencing. *Cell , 123* (4), 631-40.

Gregory, R., Yan, K.-P., Amuthan, G., Chendrimada, T., Doratotaj, B., Cooch, N., et al. (2004). The Microprocessor complex mediates the genesis of microRNAs. *Nature , 432* (7014), 235-40.

Gu, C., Yoshida, Y., Livet, J., Reimert, D., Mann, F., Merte, J., et al. (2005). Semaphorin 3E and plexin-D1 control vascular pattern independently of neuropilins. *Science , 307* (5707), 265-8.

Gu, W., Sander, T., Heils, A., Lenzen, K., & Steinlein, O. (2005). A new EF-hand containing gene EFHC2 on Xp11.4: tentative evidence for association with juvenile myoclonic epilepsy. *Epilepsy Research , 66* (1-3), 91-8.

Gupta, S., Zhu, H., Zon, L., & Evans, T. (2006). BMP signaling restricts hemato-vascular development from lateral mesoderm during somitogenesis. *Development , 133* (11), 2177-87.

Gustavson, M., Crawford, H., Fingleton, B., & Matrisian, L. (2004). Tcf binding sequence and position determines beta-catenin and Lef-1 responsiveness of MMP-7 promoters. *Molecular Carcinogenesis , 41* (3), 125-39.

Guyton, K., Liu, Y., Gorospe, M., Xu, Q., & Holbrook, N. (1996). Activation of mitogen-activated protein kinase by H_2O_2. Role in cell survival following oxidant injury. *The Journal of Biological Chemistry , 271* (8), 4138-42.

Gyorffy, B., Molnar, B., Lage, H., Szallasi, Z., & Eklund, A. (2009). Evaluation of microarray preprocessing algorithms based on concordance with RT-PCR in clinical samples. *PLoS ONE , 4* (5), e5645.

Hüttenhofer, A., Schattner, P., & Polacek, N. (2005). Non-coding RNAs: hope or hype? *Trends in Genetics , 21* (5), 289-97.

Hänseler, W. (2008). LRP5 and LRP5L mutation screening in patients with Norrie disease pseudoglioma-related phenotypes & Expression analysis of potential Norrin targets in Norrin knockout mouse cerebellum. *Masterthesis, University of Zurich* .

Hackett, S., Wiegand, S., Yancopoulos, G., & Campochiaro, P. (2002). Angiopoietin-2 plays an important role in retinal angiogenesis. *Journal of Cellular Physiology , 192* (2), 182-7.

Hallmann, R., Mayer, D., Berg, E., Broermann, R., & Butcher, E. (1995). Novel mouse endothelial cell surface marker is suppressed during differentiation of the blood brain barrier. *Developmental Dynamics , 202* (4), 325-32.

Halpin, C., & Sims, K. (2008). Twenty years of audiology in a patient with Norrie disease. *International Journal of Pediatric Otorhinolaryngology , 72* (11), 1705-10.

Halpin, C., Owen, G., Gutiérrez-Espeleta, G., Sims, K., & Rehm, H. (2005). Audiologic features of Norrie disease. *The Annals of Otology, Rhinology, and Laryngology , 114* (7), 533-8.

Hamilton, A., & Baulcombe, D. (1999). A species of small antisense RNA in posttranscriptional gene silencing in plants. *Science , 286* (5441), 950-2.

Han, J., Lee, Y., Yeom, K.-H., Kim, Y.-K., Jin, H., & Kim, V. (2004). The Drosha-DGCR8 complex in primary microRNA processing. *Genes & Development , 18* (24), 3016-27.

Hardin, J., & King, R. (2008). The long and the short of Wnt signaling in C. elegans. *Current Opinion in Genetics & Development , 18* (4), 362-7.

Harhaj, N., & Antonetti, D. (2004). Regulation of tight junctions and loss of barrier function in pathophysiology. *The International Journal of Biochemistry & Cell Biology , 36* (7), 1206-37.

Hartikka, H., Mäkitie, O., Männikkö, M., Doria, A., Daneman, A., Cole, W., et al. (2005). Heterozygous mutations in the LDL receptor-related protein 5 (LRP5) gene are associated with primary osteoporosis in children. *Journal of Bone and Mineral Research , 20* (5), 783-9.

Hartzer, M., Cheng, M., Liu, X., & Shastry, B. (1999). Localization of the Norrie disease gene mRNA by in situ hybridization. *Brain Research Bulletin , 49* (5), 355-8.

Hashimoto, T., Kihara, M., Ishida, J., Imai, N., Yoshida, S.-i., Toya, Y., et al. (2006). Apelin stimulates myosin light chain phosphorylation in vascular smooth muscle cells. *Arteriosclerosis, Thrombosis, and Vascular Biology , 26* (6), 1267-72.

Hatsukawa, Y., Nakao, T., Yamagishi, T., Okamoto, N., & Isashiki, Y. (2002). Novel nonsense mutation (Tyr44stop) of the Norrie disease gene in a Japanese family. *The British Journal of Ophthalmology , 86* (12), 1452-3.

Hay, E., Faucheu, C., Suc-Royer, I., Touitou, R., Stiot, V., Vayssière, B., et al. (2005). Interaction between LRP5 and Frat1 mediates the activation of the Wnt canonical pathway. *The Journal of Biological Chemistry , 280* (14), 13616-23.

Hayreh, S. (1999). Retinal and optic nerve head ischemic disorders and atherosclerosis: role of serotonin. *Progress in Retinal and Eye Research , 18* (2), 191-221.

Hedgepeth, C., Conrad, L., Zhang, J., Huang, H., Lee, V., & Klein, P. (1997). Activation of the Wnt signaling pathway: a molecular mechanism for lithium action. *Developmental Biology , 185* (1), 82-91.

Hediger, M., England, L., Molloy, C., Yu, K., Manning-Courtney, P., & Mills, J. (2008). Reduced bone cortical thickness in boys with autism or autism spectrum disorder. *Journal of Autism and Developmental Disorders , 38* (5), 848-56.

Hellström, A., Carlsson, B., Niklasson, A., Segnestam, K., Boguszewski, M., de Lacerda, L., et al. (2002). IGF-I is critical for normal vascularization of the human retina. *The Journal of Clinical Endocrinology and Metabolism , 87* (7), 3413-6.

Hellström, A., Engström, E., Hård, A.-L., Albertsson Wikland, K., Carlsson, B., Niklasson, A., et al. (2003). Postnatal serum insulin-like growth factor I deficiency is associated with retinopathy of prematurity and other complications of premature birth. *Pediatrics , 112* (5), 1016-20.

Hellström, M., Gerhardt, H., Kalén, M., Li, X., Eriksson, U., Wolburg, H., et al. (2001). Lack of pericytes leads to endothelial hyperplasia and abnormal vascular morphogenesis. *The Journal of Cell Biology , 153* (3), 543-53.

Hey, P., Twells, R., Phillips, M., Yusuke Nakagawa, Brown, S., Kawaguchi, Y., et al. (1998). Cloning of a novel member of the low-density lipoprotein receptor family. *Gene , 216* (1), 103-11.

Hildebrand, M., de Silva, M., Klockars, T., Solares, C., Hirose, K., Smith, J., et al. (2005). Expression of the carrier protein apolipoprotein D in the mouse inner ear. *Hearing Research , 200* (1-2), 102-14.

Hiraoka, M., Berinstein, D., Trese, M., & Shastry, B. (2001). Insertion and deletion mutations in the dinucleotide repeat region of the Norrie disease gene in patients with advanced retinopathy of prematurity. *Journal of Human Genetics , 46* (4), 178-81.

Hirschi, K., & D'Amore, P. (1996). Pericytes in the microvasculature. *Cardiovascular Research , 32* (4), 687-98.

Hnasko, R., Carter, J., Medina, F., Frank, P., & Lisanti, M. (2006). PV-1 labels trans-cellular openings in mouse endothelial cells and is negatively regulated by VEGF. *Cell Cycle , 5* (17), 2021-8.

Hnasko, R., Frank, P., Ben-Jonathan, N., & Lisanti, M. (2006). PV-1 is negatively regulated by VEGF in the lung of caveolin-1, but not caveolin-2, null mice. *Cell Cycle , 5* (17), 2012-20.

Hodgson, S., Neville, B., Jones, R., Fear, C., & Bobrow, M. (1985). Two cases of X/autosome translocation in females with incontinentia pigmenti. *Human Genetics , 71* (3), 231-4.

Hoeben, A., Landuyt, B., Highley, M., Wildiers, H., Van Oosterom, A., & De Bruijn, E. (2004). Vascular endothelial growth factor and angiogenesis. *Pharmacological Reviews , 56* (4), 549-80.

Hoefsloot, L., Nillesen, W., & Mariman, E. (2000). Gene symbol: NDP. Disease: Norrie disease. *Human Genetics , 106*, 258.

Hohlfeld, R., Kerschensteiner, M., Stadelmann, C., Lassmann, H., & Wekerle, H. (2006). The neuroprotective effect of inflammation: implications for the therapy of multiple sclerosis. *Neurological Sciences , 27 Suppl 1*, S1-7.

Holmen, S., Robertson, S., Zylstra, C., & Williams, B. (2005). Wnt-independent activation of beta-catenin mediated by a Dkk1-Fz5 fusion protein. *Biochemical and Biophysical Research Communications , 328* (2), 533-9.

Holmström, G., van Wijngaarden, P., Coster, D., & Williams, K. (2007). Genetic susceptibility to retinopathy of prematurity: the evidence from clinical and experimental animal studies. *The British Journal of Ophthalmology , 91* (12), 1704-8.

Honjo, Y., Nagineni, C., Larsson, J., Nandula, S., Hooks, J., Chan, C.-C., et al. (2007). Neuron-specific TGF-beta signaling

deficiency results in retinal detachment and cataracts in mice. *Biochemical and Biophysical Research Communications , 352* (2), 418-22.

Horndasch, M., Lienkamp, S., Springer, E., Schmitt, A., Pavenstädt, H., Walz, G., et al. (2006). The C/EBP homologous protein CHOP (GADD153) is an inhibitor of Wnt/TCF signals. *Oncogene , 25* (24), 3397-407.

Hosoya, M., Kawamata, Y., Fukusumi, S., Fujii, R., Habata, Y., Hinuma, S., et al. (2000). Molecular and functional characteristics of APJ. Tissue distribution of mRNA and interaction with the endogenous ligand apelin. *The Journal of Biological Chemistry , 275* (28), 21061-7.

Hovanes, K., Li, T., Munguia, J., Truong, T., Milovanovic, T., Lawrence Marsh, J., et al. (2001). Beta-catenin-sensitive isoforms of lymphoid enhancer factor-1 are selectively expressed in colon cancer. *Nature Genetics , 28* (1), 53-7.

Hsieh, M., Boerboom, D., Shimada, M., Lo, Y., Parlow, A., Luhmann, U., et al. (2005). Mice null for Frizzled4 (Fzd4-/-) are infertile and exhibit impaired corpora lutea formation and function. *Biology of Reproduction , 73* (6), 1135-46.

Huang, H.-C., & Klein, P. (2004). The Frizzled family: receptors for multiple signal transduction pathways. *Genome Biology , 5* (7), 234.

Hubbell, E., Liu, W.-M., & Mei, R. (2002). Robust estimators for expression analysis. *Bioinformatics , 18* (12), 1585-92.

Hughes, S., Yang, H., & Chan-Ling, T. (2000). Vascularization of the human fetal retina: roles of vasculogenesis and angiogenesis. *Investigative Ophthalmology & Visual Science , 41* (5), 1217-28.

Hutcheson, K., Paluru, P., Bernstein, S., Koh, J., Rappaport, E., Leach, R., et al. (2005). Norrie disease gene sequence variants in an ethnically diverse population with retinopathy of prematurity. *Molecular Vision , 11*, 501-8.

I, S., Nie, Z., Stewart, A., Najdovska, M., Hall, N., He, H., et al. (2004). ARAP3 is transiently tyrosine phosphorylated in cells attaching to fibronectin and inhibits cell spreading in a RhoGAP-dependent manner. *Journal of Cell Science , 117* (Pt 25), 6071-84.

Imbeaud, S., & Auffray, C. (2005). 'The 39 steps' in gene expression profiling: critical issues and proposed best practices for microarray experiments. *Drug Discovery Today , 10* (17), 1175-82.

Ioannidou, S., Deinhardt, K., Miotla, J., Bradley, J., Cheung, E., Samuelsson, S., et al. (2006). An in vitro assay reveals a role for the diaphragm protein PV-1 in endothelial fenestra morphogenesis. *Proceedings of the National Academy of Sciences of the United States of America , 103* (45), 16770-5.

Isashiki, Y., Ohba, N., Yanagita, T., Hokita, N., Doi, N., Nakagawa, M., et al. (1995). Novel mutation at the initiation codon in the Norrie disease gene in two Japanese families. *Human Genetics , 95* (1), 105-8.

Isashiki, Y., Ohba, N., Yanagita, T., Hokita, N., Hotta, Y., Hayakawa, M., et al. (1995). Mutations in the Norrie disease gene: a new mutation in a Japanese family. *British Journal of Ophthalmology , 79* (7), 703-4.

Ishida, J., Hashimoto, T., Hashimoto, Y., Nishiwaki, S., Iguchi, T., Harada, S., et al. (2004). Regulatory roles for APJ, a seven-transmembrane receptor related to angiotensin-type 1 receptor in blood pressure in vivo. *The Journal of Biological Chemistry , 279* (25), 26274-9.

Ishida, S., Yamashiro, K., Usui, T., Kaji, Y., Ogura, Y., Hida, T., et al. (2003). Leukocytes mediate retinal vascular remodeling during development and vaso-obliteration in disease. *Nature Medicine , 9* (6), 781-8.

Itäranta, P., Chi, L., Seppänen, T., Niku, M., Tuukkanen, J., Peltoketo, H., et al. (2006). Wnt-4 signaling is involved in the control of smooth muscle cell fate via Bmp-4 in the medullary stroma of the developing kidney. *Developmental Biology , 293* (2), 473-83.

Ivanov, D., Dvoriantchikova, G., Nathanson, L., McKinnon, S., & Shestopalov, V. (2006). Microarray analysis of gene expression in adult retinal ganglion cells. *FEBS Letters , 580* (1), 331-5.

Iwig, M. (1969). [Retinal dysplasia. Morphological identity of the retinal dysplasia syndrome (Reese) and D (13-15) trisomy syndrome (Patau)]. *Zentralblatt für allgemeine Pathologie und pathologische Anatomie , 112* (5), 492-504.

Jain, R., & Willetts, G. (1978). Fundus changes in incontinentia pigmenti (Bloch-Sulzberger syndrome): a case report. *The British Journal of Ophthalmology , 62* (9), 622-6.

Jensen, K., Covault, J., Conner, T., Tennen, H., Kranzler, H., & Furneaux, H. (2009). A common polymorphism in serotonin receptor 1B mRNA moderates regulation by miR-96 and associates with aggressive human behaviors. *Molecular psychiatry , 14* (4), 381-9.

Jeon, C., Strettoi, E., & Masland, R. (1998). The major cell populations of the mouse retina. *The Journal of Neuroscience , 18* (21), 8936-46.

Jiao, X., Ventruto, V., Trese, M., Shastry, B., & Hejtmancik, J. (2004). Autosomal recessive familial exudative vitreoretinopathy is associated with mutations in LRP5. *American Journal of Human Genetics , 75* (5), 878-84.

Johnsen, S., Tarby, T., Lewis, K., Bird, R., & Prenger, E. (2002). Cerebellar infarction: an unrecognized complication of very low birthweight. *Journal of child neurology , 17* (5), 320-4.

Johnson, K., Mintz-Hittner, H., Conley, Y., & Ferrell, R. (1996). X-linked exudative vitreoretinopathy caused by an arginine to leucine substitution (R121L) in the Norrie disease protein. *Clinical Genetics , 50* (3), 113-5.

Johnson, M., Kim, H., Chesler, L., Tsao-Wu, G., Bouck, N., & Polverini, P. (1994). Inhibition of angiogenesis by tissue inhibitor of metalloproteinase. *Journal of Cellular Physiology , 160* (1), 194-202.

Jones, C., & Li, D. (2007). Common cues regulate neural and vascular patterning. *Current Opinion in Genetics & Development , 17* (4), 332-6.

Joos, K., Kimura, A., Vandenburgh, K., Bartley, J., & Stone, E. (1994). Ocular findings associated with a Cys39Arg mutation in the Norrie disease gene. *Archives of Ophthalmology , 112* (12), 1574-9.

Joy, J., Poglod, R., Murphy, D., Sims, K., de la Chapelle, A., Sankila, E., et al. (1991). Abnormal protein in the cerebrospinal fluid of patients with a submicroscopic X-chromosomal deletion associated with Norrie disease: preliminary report. *Applied and Theoretical Electrophoresis : The Official Journal of the International Electrophoresis Society , 2* (1), 3-5.

Jukkola, T., Sinjushina, N., & Partanen, J. (2004). Drapc1 expression during mouse embryonic development. *Gene Expression Patterns , 4* (6), 755-62.

Körner, J., Uhlhaas, S., Neugebauer, M., & Gal, A. (1989). [Norrie syndrome: identification of carriers by segregation analysis with flanking DNA markers]. *Fortschritte der Ophthalmologie: Zeitschrift der Deutschen Ophthalmologischen Gesellschaft , 86* (1), 78-81.

Kaemmerer, W., Reddy, R., Warlick, C., Hartung, S., McIvor, R., & Low, W. (2000). In vivo transduction of cerebellar Purkinje cells using adeno-associated virus vectors. *Molecular Therapy , 2* (5), 446-57.

Kajtár, P., & Méhes, K. (1994). Bilateral coats retinopathy associated with aplastic anaemia and mild dyskeratotic signs. *American Journal of Medical Genetics , 49* (4), 374-7.

Kanda, S., Miyata, Y., & Kanetake, H. (2005). T-cell factor-4-dependent up-regulation of fibronectin is involved in fibroblast growth factor-2-induced tube formation by endothelial cells. *Journal of Cellular Biochemistry , 94* (4), 835-47.

Kane, R., Godson, C., & O'Brien, C. (2008). Chordin-like 1, a bone morphogenetic protein-4 antagonist, is upregulated by hypoxia in human retinal pericytes and plays a role in regulating angiogenesis. *Molecular Vision , 14*, 1138-48.

Kao, L., Tulac, S., Lobo, S., Imani, B., Yang, J., Germeyer, A., et al. (2002). Global gene profiling in human endometrium during the window of implantation. *Endocrinology , 143* (6), 2119-38.

Karali, M., Peluso, I., Marigo, V., & Banfi, S. (2007). Identification and characterization of microRNAs expressed in the mouse eye. *Investigative Ophthalmology & Visual Science , 48* (2), 509-15.

Kasai, A., Shintani, N., Oda, M., Kakuda, M., Hashimoto, H., Matsuda, T., et al. (2004). Apelin is a novel angiogenic factor in retinal endothelial cells. *Biochemical and Biophysical Research Communications , 325* (2), 395-400.

Kato, M., Patel, M., Levasseur, R., Lobov, I., Chang, B.-J., Glass, D., et al. (2002). Cbfa1-independent decrease in osteoblast proliferation, osteopenia, and persistent embryonic eye vascularization in mice deficient in Lrp5, a Wnt coreceptor. *The Journal of Cell Biology , 157* (2), 303-14.

Katoh, M. (2008). WNT signaling in stem cell biology and regenerative medicine. *Current drug targets , 9* (7), 565-70.

Katoh, M., & Katoh, M. (2005). Comparative genomics on Norrie disease gene. *International Journal of Molecular Medicine , 15* (5), 885-9.

Kellner, U., Fuchs, S., Bornfeld, N., Foerster, M., & Gal, A. (1996). Ocular phenotypes associated with two mutations (R121W, C126X) in the Norrie disease gene. *Ophthalmic Genetics , 17* (2), 67-74.

Kellner, U., Renner, A., & Tillack, H. (2004). [Hereditary retinochoroidal dystrophies. Part 2: differential diagnosis]. *Der Ophthalmologe , 101* (4), 397-412; quiz 413-4.

Kellner, U., Tillack, H., & Renner, A. (2004). [Hereditary retinochoroidal dystrophies. Part 1: Pathogenesis, diagnosis, therapy and patient counselling]. *Der Ophthalmologe , 101* (3), 307-19; quiz 320.

Kenyon, J., & Craig, I. (1999). Analysis of the 5' regulatory region of the human Norrie's disease gene: evidence that a non-translated CT dinucleotide repeat in exon one has a role in controlling expression. *Gene , 227* (2), 181-8.

Khaliq, S., Hameed, A., Ismail, M., Anwar, K., Leroy, B., Payne, A., et al. (2001). Locus for autosomal recessive nonsyndromic persistent hyperplastic primary vitreous. *Investigative Ophthalmology & Visual Science , 42* (10), 2225-8.

Khan, A., Shamsi, F., Al-Saif, A., & Kambouris, M. (2004). A novel missense Norrie disease mutation associated with a severe ocular phenotype. *Journal of pediatric ophthalmology and strabismus , 41* (6), 361-3.

Khatri, P., Sellamuthu, S., Malhotra, P., Amin, K., Done, A., & Draghici, S. (2005). Recent additions and improvements to the Onto-Tools. *Nucleic Acids Research , 33* (Web Server issue), W762-5.

Kim, C., Kuehn, M., Clark, A., & Kwon, Y. (2006). Gene expression profile of the adult human retinal ganglion cell layer. *Molecular Vision , 12*, 1640-8.

Kim, H., & Kim, T.-Y. (2005). Regulation of vascular endothelial growth factor expression by insulin-like growth factor-II in human keratinocytes, differential involvement of mitogen-activated protein kinases and feedback inhibition of protein kinase C. *The British Journal of Dermatology , 152* (3), 418-25.

Kim, J., Yu, Y., Kim, J., & Park, S. (2002). Mutations of the Norrie gene in Korean ROP infants. *Korean Journal of Ophthalmology , 16* (2), 93-6.

Kim, J.-S., Crooks, H., Dracheva, T., Nishanian, T., Singh, B., Jen, J., et al. (2002). Oncogenic beta-catenin is required for bone morphogenetic protein 4 expression in human cancer cells. *Cancer Research , 62* (10), 2744-8.

Kim, J.-Y., Yim, J.-H., Cho, J.-H., Kim, J.-H., Ko, J.-H., Kim, S.-M., et al. (2006). Adrenomedullin regulates cellular glutathione content via modulation of gamma-glutamate-cysteine ligase catalytic subunit expression. *Endocrinology , 147* (3), 1357-64.

Kim, Y.-M., Hwang, S., Pyun, B.-J., Kim, T.-Y., Lee, S.-T., Gho, Y., et al. (2002). Endostatin blocks vascular endothelial growth factor-mediated signaling via direct interaction with KDR/Flk-1. *The Journal of Biological Chemistry , 277* (31), 27872-9.

Kisucka, J., Butterfield, C., Duda, D., Eichenberger, S., Saffaripour, S., Ware, J., et al. (2006). Platelets and platelet adhesion support angiogenesis while preventing excessive hemorrhage. *Proceedings of the National Academy of Sciences of the United States of America , 103* (4), 855-60.

Klagsbrun, M., & Eichmann, A. (2005). A role for axon guidance receptors and ligands in blood vessel development and tumor angiogenesis. *Cytokine & Growth Factor Reviews , 16* (4-5), 535-48.

Klein, P., & Melton, D. (1996). A molecular mechanism for the effect of lithium on development. *Proceedings of the National Academy of Sciences of the United States of America , 93* (16), 8455-9.

Kleinjan, D., & van Heyningen, V. (2005). Long-range control of gene expression: emerging mechanisms and disruption in disease. *American Journal of Human Genetics , 76* (1), 8-32.

Kolb, H. (2003). How the Retina Works. *American Scientist, 91* (January-February), 28-35.

Kondo, H., Hayashi, H., Oshima, K., Tahira, T., & Hayashi, K. (2003). Frizzled 4 gene (FZD4) mutations in patients with familial exudative vitreoretinopathy with variable

expressivity. *The British Journal of Ophthalmology , 87* (10), 1291-5.

Kondo, H., Qin, M., Kusaka, S., Tahira, T., Hasebe, H., Hayashi, H., et al. (2007). Novel mutations in Norrie disease gene in Japanese patients with Norrie disease and familial exudative vitreoretinopathy. *Investigative Ophthalmology & Visual Science , 48* (3), 1276-82.

Kondo, H., Qin, M., Tahira, T., Uchio, E., & Hayashi, K. (2007). Severe form of familial exudative vitreoretinopathy caused by homozygous R417Q mutation in frizzled-4 gene. *Ophthalmic Genetics , 28* (4), 220-3.

Korinek, V., Barker, N., Willert, K., Molenaar, M., Roose, J., Wagenaar, G., et al. (1998). Two members of the Tcf family implicated in Wnt/beta-catenin signaling during embryogenesis in the mouse. *Molecular and Cellular Biology , 18* (3), 1248-56.

Koshibu, A., Uyama, M., & Matoba, H. (1978). Two cases of retinitis pigmentosa associated with retinal vasculopathy. *Japanese Journal of Clinical Ophthalmology , 33*, 1523-1532.

Krishnan, V., Bryant, H., & MacDougald, O. (2006). Regulation of bone mass by Wnt signaling. *Journal of Clinical Investigation , 116* (5), 1202-9.

Kubista, M., Andrade, J., Bengtsson, M., Forootan, A., Jonák, J., Lind, K., et al. (2006). The real-time polymerase chain reaction. *Molecular Aspects of Medicine , 27* (2-3), 95-125.

Kubo, F., Takeichi, M., & Nakagawa, S. (2003). Wnt2b controls retinal cell differentiation at the ciliary marginal zone. *Development , 130* (3), 587-98.

Kulikov, R., Boehme, K., & Blattner, C. (2005). Glycogen synthase kinase 3-dependent phosphorylation of Mdm2 regulates p53 abundance. *Molecular and Cellular Biology , 25* (16), 7170-80.

Kvanta, A. (2006). Ocular angiogenesis: the role of growth factors. *Acta Ophthalmologica Scandinavica , 84* (3), 282-8.

Kwee, M., Balemans, W., Cleiren, E., Gille, J., Van Der Blij, F., Sepers, J., et al. (2005). An autosomal dominant high bone mass phenotype in association with craniosynostosis in an extended family is caused by an LRP5 missense mutation. *Journal of Bone and Mineral Research , 20* (7), 1254-60.

Lad, N., Cheshier, S., & Kalani, Y. (2008). Wnt Signaling in Retinal Development and Disease. *Stem Cells and Development* .

Lai, T., Wong, V., & Lam, D. (2006). Asymmetrical ocular involvement and persistent fetal vasculature in an adult with osteoporosis-pseudoglioma syndrome. *Archives of Ophthalmology , 124* (3), 422-3.

LaMarre, J., Wollenberg, G., Gonias, S., & Hayes, M. (1991). Cytokine binding and clearance properties of proteinase-activated alpha 2-macroglobulins. *Laboratory Investigation: A Journal of Technical Methods and Pathology , 65* (1), 3-14.

Lamba, D., Karl, M., Ware, C., & Reh, T. (2006). Efficient generation of retinal progenitor cells from human embryonic stem cells. *Proceedings of the National Academy of Sciences of the United States of America , 103* (34), 12769-74.

Lammert, E., Gu, G., McLaughlin, M., Brown, D., Brekken, R., Murtaugh, L., et al. (2003). Role of VEGF-A in vascularization of pancreatic islets. *Current Biology , 13* (12), 1070-4.

Lamont, R., & Childs, S. (2006). MAPping out arteries and veins. *Science's STKE , 2006* (355), pe39.

Lan, N., Heinzmann, C., Gal, A., Klisak, I., Orth, U., Lai, E., et al. (1989). Human monoamine oxidase A and B genes map to Xp 11.23 and are deleted in a patient with Norrie disease. *Genomics , 4* (4), 552-9.

Lang, G., Rott, H., & Naumann, G. (1991). [Keratotorus in Norrie disease]. *Klinische Monatsblätter für Augenheilkunde , 199* (2), 110-3.

Lang, R., Lustig, M., Francois, F., Sellinger, M., & Plesken, H. (1994). Apoptosis during macrophage-dependent ocular tissue remodelling. *Development , 120* (12), 3395-403.

Laqua, H. (1980). Familial exudative vitreoretinopathy. *Albrecht von Graefes Archiv für klinische und experimentelle Ophthalmologie Albrecht von Graefe's archive for clinical and experimental ophthalmology , 213* (2), 121-33.

Lee, B.-H., Bae, J., Park, R., Kim, J.-E., Park, J., & Kim, I.-S. (2006). betaig-h3 triggers signaling pathways mediating adhesion and migration of vascular smooth muscle cells through alphavbeta5 integrin. *Experimental & Molecular Medicine , 38* (2), 153-61.

Lee, W., Bookstein, R., Hong, F., Young, L., Shew, J., & Lee, E. (1987). Human retinoblastoma susceptibility gene: cloning, identification, and sequence. *Science , 235* (4794), 1394-9.

Leiper, J., Nandi, M., Torondel, B., Murray-Rust, J., Malaki, M., O'hara, B., et al. (2007). Disruption of methylarginine metabolism impairs vascular homeostasis. *Nature Medicine , 13* (2), 198-203.

Lemmon, V., & Rieser, G. (1983). The development distribution of vimentin in the chick retina. *Brain Research , 313* (2), 191-7.

Lenders, J., Eisenhofer, G., Abeling, N., Berger, W., Murphy, D., Konings, C., et al. (1996). Specific genetic deficiencies of the A and B isoenzymes of monoamine oxidase are characterized by distinct neurochemical and clinical phenotypes. *Journal of Clinical Investigation , 97* (4), 1010-9.

Lenzner, S., Prietz, S., Feil, S., Nuber, U., Ropers, H.-H., & Berger, W. (2002). Global gene expression analysis in a mouse model for Norrie disease: late involvement of photoreceptor cells. *Investigative Ophthalmology & Visual Science , 43* (9), 2825-33.

Leung, W., Lawrie, A., Demaries, S., Massaeli, H., Burry, A., Yablonsky, S., et al. (2004). Apolipoprotein D and platelet-derived growth factor-BB synergism mediates vascular smooth muscle cell migration. *Circulation Research , 95* (2), 179-86.

Lev, D., Binson, I., Foldes, A., Watemberg, N., & Lerman-Sagie, T. (2003). Decreased bone density in carriers and patients of an Israeli family with the osteoporosis-pseudoglioma syndrome. *The Israel Medical Association Journal , 5* (6), 419-21.

Lev, D., Weigl, Y., Hasan, M., Gak, E., Davidovich, M., Vinkler, C., et al. (2007). A novel missense mutation in the NDP gene in a child with Norrie disease and severe neurological involvement including infantile spasms. *American Journal of Medical Genetics , 143A* (9), 921-4.

Levasseur, R., Lacombe, D., & de Vernejoul, M. (2005). LRP5 mutations in osteoporosis-pseudoglioma syndrome and high-bone-mass disorders. *Joint, Bone, Spine: Revue du Rhumatisme , 72* (3), 207-14.

Levy, E., Powell, J., Buckle, V., Hsu, Y., Breakefield, X., & Craig, I. (1989). Localization of human monoamine oxidase-A gene to Xp11.23-11.4 by in situ hybridization: implications for Norrie disease. *Genomics , 5* (2), 368-70.

Lewandowski, N., & Small, S. (2005). Brain microarray: finding needles in molecular haystacks. *The Journal of Neuroscience , 25* (45), 10341-6.

Li, Y., Fuhrmann, C., Schwinger, E., Gal, A., & Laqua, H. (1992). The gene for autosomal dominant familial exudative vitreoretinopathy (Criswick-Schepens) on the long arm of chromosome 11. *American Journal of Ophthalmology , 113* (6), 712-3.

Lin, L., Cui, L., Zhou, W., Dufort, D., Zhang, X., Cai, C.-L., et al. (2007). Beta-catenin directly regulates Islet1 expression in cardiovascular progenitors and is required for multiple aspects of cardiogenesis. *Proceedings of the National Academy of Sciences of the United States of America , 104* (22), 9313-8.

Little, R., Carulli, J., Del Mastro, R., Dupuis, J., Osborne, M., Folz, C., et al. (2002). A mutation in the LDL receptor-related protein 5 gene results in the autosomal dominant high-bone-mass trait. *American Journal of Human Genetics , 70* (1), 11-9.

Liu, C., & Nathans, J. (2008). An essential role for frizzled 5 in mammalian ocular development. *Development , 135* (21), 3567-76.

Liu, H., Mohamed, O., Dufort, D., & Wallace, V. (2003). Characterization of Wnt signaling components and activation of the Wnt canonical pathway in the murine retina. *Developmental Dynamics , 227* (3), 323-34.

Liu, X., Rubin, J., & Kimmel, A. (2005). Rapid, Wnt-induced changes in GSK3beta associations that regulate beta-catenin stabilization are mediated by Galpha proteins. *Current Biology , 15* (22), 1989-97.

Liu, X.-Z., Yuan, Y., Yan, D., Ding, E., Ouyang, X., Fei, Y., et al. (2009). Digenic inheritance of non-syndromic deafness caused by mutations at the gap junction proteins Cx26 and Cx31. *Human Genetics , 125* (1), 53-62.

Liu, Y., Shi, J., Lu, C.-C., Wang, Z.-B., Lyuksyutova, A., Song, X.-J., et al. (2005). Ryk-mediated Wnt repulsion regulates posterior-directed growth of corticospinal tract. *Nature Neuroscience , 8* (9), 1151-9.

Liu, Z., Tang, Y., Qiu, T., Cao, X., & Clemens, T. (2006). A dishevelled-1/Smad1 interaction couples WNT and bone morphogenetic protein signaling pathways in uncommitted bone marrow stromal cells. *The Journal of Biological Chemistry , 281* (25), 17156-63.

Liu, Z.-J., Shirakawa, T., Li, Y., Soma, A., Oka, M., Dotto, G., et al. (2003). Regulation of Notch1 and Dll4 by vascular endothelial growth factor in arterial endothelial cells: implications for modulating arteriogenesis and angiogenesis. *Molecular and Cellular Biology , 23* (1), 14-25.

Ljubimov, A., Caballero, S., Aoki, A., Pinna, L., Grant, M., & Castellon, R. (2004). Involvement of protein kinase CK2 in angiogenesis and retinal neovascularization. *Investigative Ophthalmology & Visual Science , 45* (12), 4583-91.

Lobov, I., Rao, S., Carroll, T., Vallance, J., Ito, M., Ondr, J., et al. (2005). WNT7b mediates macrophage-induced programmed cell death in patterning of the vasculature. *Nature , 437* (7057), 417-21.

Lobov, I., Renard, R., Papadopoulos, N., Gale, N., Thurston, G., Yancopoulos, G., et al. (2007). Delta-like ligand 4 (Dll4) is induced by VEGF as a negative regulator of angiogenic sprouting. *Proceedings of the National Academy of Sciences of the United States of America , 104* (9), 3219-24.

Logan, C., & Nusse, R. (2004). The Wnt signaling pathway in development and disease. *Annual Review of Cell and Developmental Biology , 20*, 781-810.

Longo, K., Kennell, J., Ochocinska, M., Ross, S., Wright, W., & MacDougald, O. (2002). Wnt signaling protects 3T3-L1 preadipocytes from apoptosis through induction of insulin-like growth factors. *The Journal of Biological Chemistry , 277* (41), 38239-44.

Love, J., Scholes, P., Gilpin, B., Savill, M., Lin, S., & Samuel, L. (2006). Evaluation of uncertainty in quantitative real-time PCR. *Journal of Microbiological Methods , 67* (2), 349-56.

Luhmann, U. (2005). Aufklärung molekularer Pathogenesemechanismen des Norrie-Syndroms. *PhD Thesis, Freie Universität Berlin* , 1-204.

Luhmann, U., Lin, J., Acar, N., Lammel, S., Feil, S., Grimm, C., et al. (2005a). Role of the Norrie disease pseudoglioma gene in sprouting angiogenesis during development of the retinal vasculature. *Investigative Ophthalmology & Visual Science , 46* (9), 3372-82.

Luhmann, U., Meunier, D., Shi, W., Lüttges, A., Pfarrer, C., Fundele, R., et al. (2005b). Fetal loss in homozygous mutant Norrie disease mice: a new role of Norrin in reproduction. *Genesis , 42* (4), 253-62.

Luhmann, U., Neidhardt, J., Kloeckener-Gruissem, B., Schäfer, N., Glaus, E., Feil, S., et al. (2008). Vascular changes in the cerebellum of Norrin/Ndph knockout mice correlate with high expression of Norrin and Frizzled-4. *The European Journal of Neuroscience , 27* (10), 2619-28.

Lutty, G., & McLeod, D. (2003). Retinal vascular development and oxygen-induced retinopathy: a role for adenosine. *Progress in Retinal and Eye Research , 22* (1), 95-111.

Lutz, M., & Knaus, P. (2002). Integration of the TGF-beta pathway into the cellular signalling network. *Cellular Signalling , 14* (12), 977-88.

Müller, G., Behrens, J., Nussbaumer, U., Böhlen, P., & Birchmeier, W. (1987). Inhibitory action of transforming growth factor beta on endothelial cells. *Proceedings of the National Academy of Sciences of the United States of America , 84* (16), 5600-4.

Müller, M., Bhattacharya, S., Moore, T., Prescott, Q., Wedig, T., Herrmann, H., et al. (2009). Dominant cataract formation in association with a vimentin assembly disrupting mutation. *Human Molecular Genetics , 18* (6), 1052-7.

Müller, M., Kusserow, C., Orth, U., Klär-Dissars, U., Laqua, H., & Gal, A. (2008). [Mutations of the frizzled-4 gene. Their impact on medical care of patients with autosomal dominant exudative vitreoretinopathy]. *Der Ophthalmologe , 105* (3), 262-8.

MacDonald, M., Goldberg, Y., Macfarlane, J., Samuels, M., Trese, M., & Shastry, B. (2005). Genetic variants of frizzled-4 gene in familial exudative vitreoretinopathy and advanced retinopathy of prematurity. *Clinical Genetics , 67* (4), 363-6.

Mao, B., Wu, W., Li, Y., Hoppe, D., Stannek, P., Glinka, A., et al. (2001). LDL-receptor-related protein 6 is a receptor for Dickkopf proteins. *Nature , 411* (6835), 321-5.

Maretto, S., Cordenonsi, M., Dupont, S., Braghetta, P., Broccoli, V., Hassan, A., et al. (2003). Mapping Wnt/beta-catenin signaling during mouse development and in colorectal tumors. *Proceedings of the National Academy of Sciences of the United States of America , 100* (6), 3299-304.

Markel, P., Shu, P., Ebeling, C., Carlson, G., Nagle, D., Smutko, J., et al. (1997). Theoretical and empirical issues for marker-assisted breeding of congenic mouse strains. *Nature Genetics, 17* (3), 280-4.

Masckauchán, T., Agalliu, D., Vorontchikhina, M., Ahn, A., Parmalee, N., Li, C.-M., et al. (2006). Wnt5a signaling induces proliferation and survival of endothelial cells in vitro and expression of MMP-1 and Tie-2. *Molecular Biology of the Cell, 17* (12), 5163-72.

Matsui, H., Shimosawa, T., Itakura, K., Guanqun, X., Ando, K., & Fujita, T. (2004). Adrenomedullin can protect against pulmonary vascular remodeling induced by hypoxia. *Circulation , 109* (18), 2246-51.

Matsuzaka, T., Sakuragawa, N., Terasawa, K., & Kuwabara, H. (1986). Facioscapulohumeral dystrophy associated with mental retardation, hearing loss, and tortuosity of retinal arterioles. *Journal of child neurology , 1* (3), 218-23.

Mazuruk, K., Schoen, T., Chader, G., & Rodriguez, I. (1995). Structural organization and expression of the human phosphatidylinositol-specific phospholipase C beta-3 gene. *Biochemical and Biophysical Research Communications , 212* (1), 190-5.

McDonald, N., & Hendrickson, W. (1993). A structural superfamily of growth factors containing a cystine knot motif. *Cell , 73* (3), 421-4.

McMahon, H., Bolshakov, V., Janz, R., Hammer, R., Siegelbaum, S., & Südhof, T. (1996). Synaptophysin, a major synaptic vesicle protein, is not essential for neurotransmitter release. *Proceedings of the National Academy of Sciences of the United States of America , 93* (10), 4760-4.

McMahon, H., Missler, M., Li, C., & Südhof, T. (1995). Complexins: cytosolic proteins that regulate SNAP receptor function. *Cell , 83* (1), 111-9.

Mechoulam, H., & Pierce, E. (2003). Retinopathy of prematurity: molecular pathology and therapeutic strategies. *American Journal of Pharmacogenomics : Genomics-related Research in Drug Development and Clinical Practice, 3* (4), 261-77.

Meier, P., Sterker, I., & Tegetmeyer, H. (2006). [Leucocoria in childhood]. *Klinische Monatsblätter für Augenheilkunde , 223* (6), 521-7.

Meindl, A., Berger, W., Meitinger, T., van de Pol, D., Achatz, H., Döerner, C., et al. (1992). Norrie disease is caused by mutations in an extracellular protein resembling C-terminal globular domain of mucins. *Nature Genetics , 2* (2), 139-43.

Meindl, A., Lorenz, B., Achatz, H., Hellebrand, H., Schmitz-Valckenberg, P., & Meitinger, T. (1995). Missense mutations in the NDP gene in patients with a less severe course of Norrie disease. *Human Molecular Genetics , 4* (3), 489-90.

Meire, F., Lafaut, B., Speleman, F., & Hanssens, M. (1998). Isolated Norrie disease in a female caused by a balanced translocation t(X,6). *Ophthalmic Genetics, 19* (4), 203-7.

Meitinger, T., Meindl, A., Bork, P., Rost, B., Sander, C., Haasemann, M., et al. (1993). Molecular modelling of the Norrie disease protein predicts a cystine knot growth factor tertiary structure. *Nature Genetics , 5* (4), 376-80.

Mencía, A., Modamio-Høybjør, S., Redshaw, N., Morín, M., Mayo-Merino, F., Olavarrieta, L., et al. (2009). Mutations in the seed region of human miR-96 are responsible for nonsyndromic progressive hearing loss. *Nature Genetics, 41* (5), 609-13.

Mensheha-Manhart, O., Rodrigues, M., Shields, J., Shannon, G., & Mirabelli, R. (1975). Retinal pigment epithelium in incontinentia pigmenti. *American Journal of Ophthalmology, 79* (4), 571-7.

Michaelides, M., Luthert, P., Cooling, R., Firth, H., & Moore, A. (2004). Norrie disease and peripheral venous insufficiency. *British Journal of Ophthalmology , 88* (11), 1475.

Mikels, A., & Nusse, R. (2006). Purified Wnt5a protein activates or inhibits beta-catenin-TCF signaling depending on receptor context. *PLoS Biology , 4* (4), e115.

Minami, T., Donovan, D., Tsai, J., Rosenberg, R., & Aird, W. (2002). Differential regulation of the von Willebrand factor and Flt-1 promoters in the endothelium of hypoxanthine phosphoribosyltransferase-targeted mice. *Blood , 100* (12), 4019-25.

Mintz-Hittner, H., Ferrell, R., Sims, K., Fernandez, K., Gemmell, B., Satriano, D., et al. (1996). Peripheral retinopathy in offspring of carriers of Norrie disease gene mutations. Possible transplacental effect of abnormal Norrin. *Ophthalmology , 103* (12), 2128-34.

Mitchell, C., Risau, W., & Drexler, H. (1998). Regression of vessels in the tunica vasculosa lentis is initiated by coordinated endothelial apoptosis: a role for vascular endothelial growth factor as a survival factor for endothelium. *Developmental Dynamics , 213* (3), 322-33.

Mohamed, S., Schaa, K., Cooper, M., Ahrens, E., Alvarado, A., Colaizy, T., et al. (2009). Genetic contributions to the development of retinopathy of prematurity. *Pediatric Research , 65* (2), 193-7.

Mohn, L. (2007). Expression of Norrin towards the understanding of its role in retinal angiogenesis. *Masterthesis, University of Zurich*.

Morecroft, I., Dempsie, Y., Bader, M., Walther, D., Kotnik, K., Loughlin, L., et al. (2007). Effect of tryptophan hydroxylase 1 deficiency on the development of hypoxia-induced pulmonary hypertension. *Hypertension , 49* (1), 232-6.

Morris, P., Dunmore, B., & Brindle, N. (2006). Mutant Tie2 causing venous malformation signals through Shc. *Biochemical and Biophysical Research Communications , 346* (1), 335-8.

Morrison, C., & Prayson, R. (2000). Immunohistochemistry in the diagnosis of neoplasms of the central nervous system. *Seminars in diagnostic pathology , 17* (3), 204-15.

Mu, X., Fu, X., Sun, H., Liang, S., Maeda, H., Frishman, L., et al. (2005). Ganglion cells are required for normal progenitor-cell proliferation but not cell-fate determination or patterning in the developing mouse retina. *Current Biology, 15* (6), 525-30.

Mudhar, H., Pollock, R., Wang, C., Stiles, C., & Richardson, W. (1993). PDGF and its receptors in the developing rodent retina and optic nerve. *Development , 118* (2), 539-52.

Mukhopadhyay, M., Gorivodsky, M., Shtrom, S., Grinberg, A., Niehrs, C., Morasso, M., et al. (2006). Dkk2 plays an essential role in the corneal fate of the ocular surface epithelium. *Development, 133* (11), 2149-54.

Muletarow, J., Paditz, E., Petersen, H., & Kreuz, F. (2004). Coats' disease in conjunction with other disorders. *Monatsschrift Kinderheilkunde, 152* (4), 403-412.

Mullis, K., Faloona, F., Scharf, S., Saiki, R., Horn, G., & Erlich, H. (1986). Specific Enzymatic Amplification of DNA In Vitro: The Polymerase Chain Reaction. *Cold Spring Harbor Symposia on Quantitative Biology , 51*, 263-273.

Murohara, T., Horowitz, J., Silver, M., Tsurumi, Y., Chen, D., Sullivan, A., et al. (1998). Vascular endothelial growth factor/vascular permeability factor enhances vascular permeability via nitric oxide and prostacyclin. *Circulation , 97* (1), 99-107.

Murphy, D., Sims, K., Eisenhofer, G., Greenberg, B., George, T., Berlin, F., et al. (1998). Are MAO-A deficiency states in the general population and in putative high-risk populations highly uncommon? *Journal of Neural Transmission: Supplementum , 52*, 29-38.

Murphy, D., Sims, K., Karoum, F., de la Chapelle, A., Norio, R., Sankila, E., et al. (1990). Marked amine and amine metabolite changes in Norrie disease patients with an X-chromosomal deletion affecting monoamine oxidase. *Journal of Neurochemistry , 54* (1), 242-7.

Murphy, D., Sims, K., Karoum, F., Garrick, N., de la Chapelle, A., Sankila, E., et al. (1991). Plasma amine oxidase activities in Norrie disease patients with an X-chromosomal deletion affecting monoamine oxidase. *Journal of Neural Transmission: General Section , 83* (1-2), 1-12.

Mutch, D., Berger, A., Mansourian, R., Rytz, A., & Roberts, M.-A. (2002). The limit fold change model: a practical approach for selecting differentially expressed genes from microarray data. *BMC Bioinformatics , 3*, 17.

Nagineni, C., Samuel, W., Nagineni, S., Pardhasaradhi, K., Wiggert, B., Detrick, B., et al. (2003). Transforming growth factor-beta induces expression of vascular endothelial growth factor in human retinal pigment epithelial cells: involvement of mitogen-activated protein kinases. *Journal of Cellular Physiology , 197* (3), 453-62.

Nakanishi, T., Sugawara, M., Huang, W., Martindale, R., Leibach, F., Ganapathy, M., et al. (2001). Structure, function, and tissue expression pattern of human SN2, a subtype of the amino acid transport system N. *Biochemical and Biophysical Research Communications , 281* (5), 1343-8.

Nallathambi, J., Shukla, D., Rajendran, A., Namperumalsamy, P., Muthulakshmi, R., & Sundaresan, P. (2006). Identification of novel FZD4 mutations in Indian patients with familial exudative vitreoretinopathy. *Molecular Vision , 12*, 1086-92.

Nam, J.-O., Kim, J.-E., Jeong, H.-W., Lee, S.-J., Lee, B.-H., Choi, J.-Y., et al. (2003). Identification of the alphavbeta3 integrin-interacting motif of betaig-h3 and its anti-angiogenic effect. *The Journal of Biological Chemistry , 278* (28), 25902-9.

Nance, W., Hara, S., Hansen, A., Elliott, J., Lewis, M., & Chown, B. (1969). Genetic linkage studies in a Negro kindred with Norrie's disease. *American Journal of Human Genetics , 21* (5), 423-9.

Naskar, R., & Thanos, S. (2006). Retinal gene profiling in a hereditary rodent model of elevated intraocular pressure. *Molecular Vision , 12*, 1199-210.

Nelson, W., & Nusse, R. (2004). Convergence of Wnt, beta-catenin, and cadherin pathways. *Science, 303* (5663), 1483-7.

Newton, C., Graham, A., Heptinstall, L., Powell, S., Summers, C., Kalsheker, N., et al. (1989). Analysis of any point mutation in DNA. The amplification refractory mutation system (ARMS). *Nucleic Acids Research , 17* (7), 2503-16.

Ngo, J., Bateman, J., Cortessis, V., Sparkes, R., Mohandas, T., Inana, G., et al. (1989). Norrie disease: linkage analysis using a 4.2-kb RFLP detected by a human ornithine aminotransferase cDNA probe. *Genomics , 4* (4), 539-45.

Ngo, J., Spence, M., Cortessis, V., Bateman, J., & Sparkes, R. (1989). Duplicate report crossing over in Norrie disease family. *American Journal of Medical Genetics , 33* (2), 286.

Niehrs, C. (2001). Developmental biology. Solving a sticky problem. *Nature , 413* (6858), 787-8.

Niehrs, C. (2004). Norrin and frizzled; a new vein for the eye. *Developmental Cell , 6* (4), 453-4.

Niemelä, H., Elima, K., Henttinen, T., Irjala, H., Salmi, M., & Jalkanen, S. (2005). Molecular identification of PAL-E, a widely used endothelial-cell marker. *Blood, 106* (10), 3405-9.

Nitta, T., Hata, M., Gotoh, S., Seo, Y., Sasaki, H., Hashimoto, N., et al. (2003). Size-selective loosening of the blood-brain barrier in claudin-5-deficient mice. *The Journal of Cell Biology, 161* (3), 653-60.

Nocito, A., Dahm, F., Jochum, W., Jang, J., Georgiev, P., Bader, M., et al. (2008). Serotonin regulates macrophage-mediated angiogenesis in a mouse model of colon cancer allografts. *Cancer Research , 68* (13), 5152-8.

Nomura, A., Shigemoto, R., Nakamura, Y., Okamoto, N., Mizuno, N., & Nakanishi, S. (1994). Developmentally regulated postsynaptic localization of a metabotropic glutamate receptor in rat rod bipolar cells. *Cell, 77* (3), 361-9.

Norrie, G. (1927). Causes of blindness in children. *Acta Ophthalmol. (Copenhagen) , 5*, 357-386.

Novelli, G., de Luca, A., Torrente, I., Mangino, M., Castellan, C., & Dallapiccola, B. (1999). Gene symbol: NDP. Disease: Norrie disease. *Human Genetics , 105*, 374.

Ogita, T., Hashimoto, E., Yamasaki, M., Nakaoka, T., Matsuoka, R., Kira, Y., et al. (2001). Hypoxic induction of adrenomedullin in cultured human umbilical vein endothelial cells. *Journal of Hypertension , 19* (3 Pt 2), 603-8.

Ohlmann, A., Adamek, E., Ohlmann, A., & Lütjen-Drecoll, E. (2004). Norrie gene product is necessary for regression of hyaloid vessels. *Investigative Ophthalmology & Visual Science , 45* (7), 2384-90.

Ohlmann, A., Scholz, M., Goldwich, A., Chauhan, B., Hudl, K., Ohlmann, A., et al. (2005). Ectopic norrin induces growth of ocular capillaries and restores normal retinal angiogenesis in Norrie disease mutant mice. *The Journal of Neuroscience , 25* (7), 1701-10.

Ojima, T., Takagi, H., Suzuma, K., Oh, H., Suzuma, I., Ohashi, H., et al. (2006). EphrinA1 inhibits vascular endothelial growth factor-induced intracellular signaling and suppresses retinal neovascularization and blood-retinal barrier breakdown. *The American Journal of Pathology , 168* (1), 331-9.

Okamoto, N. (1998). [Norrie disease]. *Ryōikibetsu Shōkōgun Shirīzu* (19 Pt 2), 627-9.

Olney, J. (1968). An electron microscopic study of synapse formation, receptor outer segment development, and other aspects of developing mouse retina. *Investigative Ophthalmology , 7* (3), 250-68.

Omoto, S., Hayashi, T., Kitahara, K., Takeuchi, T., & Ueoka, Y. (2004). Autosomal dominant familial exudative vitreoretinopathy in two Japanese families with FZD4 mutations (H69Y and C181R). *Ophthalmic Genetics , 25* (2), 81-90.

Orkin, S. (1995). Hematopoiesis: how does it happen? *Current Opinion in Cell Biology , 7* (6), 870-7.

Oshima, Y., Oshima, S., Nambu, H., Kachi, S., Takahashi, K., Umeda, N., et al. (2005). Different effects of angiopoietin-2 in different vascular beds: new vessels are most sensitive. *The FASEB Journal , 19* (8), 963-5.

Ott, S., Patel, R., Appukuttan, B., Wang, X., & Stout, J. (2000). A novel mutation in the Norrie disease gene. *Journal of AAPOS: The official publication of the American Association for Pediatric Ophthalmology and Strabismus , 4* (2), 125-6.

Palmer, E., Flynn, J., Hardy, R., Phelps, D., Phillips, C., Schaffer, D., et al. (1991). Incidence and early course of retinopathy of prematurity. The Cryotherapy for Retinopathy of Prematurity Cooperative Group. *Ophthalmology , 98* (11), 1628-40.

Palmer, E., Patz, A., Phelps, D., & Spencer, R. (2001). *Retinopathy of Prematurity* (Bd. 2).

Pan, L., Deng, M., Xie, X., & Gan, L. (2008). ISL1 and BRN3B co-regulate the differentiation of murine retinal ganglion cells. *Development , 135* (11), 1981-90.

Parkes, J. (1999). Genetic factors in human sleep disorders with special reference to Norrie disease, Prader-Willi syndrome and Moebius syndrome. *Journal of Sleep Research , 8 Suppl 1*, 14-22.

Parr, B., Cornish, V., Cybulsky, M., & McMahon, A. (2001). Wnt7b regulates placental development in mice. *Developmental Biology , 237* (2), 324-32.

Parsons, M., Curtis, D., Blank, C., Hughes, H., & McCartney, A. (1992). The ocular pathology of Norrie disease in a fetus of 11 weeks' gestational age. *Graefe's Archive for Clinical and Experimental Ophthalmology = Albrecht von Graefes Archiv für klinische und experimentelle Ophthalmologie, 230* (3), 248-51.

Paxinos, G., & B. J. Franklin, K. (2001). *The Mouse Brain In Stereotaxic Coordinates.* Academic Press.

Pedram, A., Razandi, M., & Levin, E. (1998). Extracellular signal-regulated protein kinase/Jun kinase cross-talk underlies vascular endothelial cell growth factor-induced endothelial cell proliferation. *The Journal of Biological Chemistry , 273* (41), 26722-8.

Pendergast, S., Trese, M., Liu, X., & Shastry, B. (1998). Study of the Norrie disease gene in 2 patients with bilateral persistent hyperplastic primary vitreous. *Archives of Ophthalmology , 116* (3), 381-2.

Penn, J., Madan, A., Caldwell, R., Bartoli, M., Caldwell, R., & Hartnett, M. (2008). Vascular endothelial growth factor in eye disease. *Progress in Retinal and Eye Research , 27* (4), 331-71.

Perez-Vilar, J., & Hill, R. (1997). Norrie disease protein (norrin) forms disulfide-linked oligomers associated with the extracellular matrix. *The Journal of Biological Chemistry , 272* (52), 33410-5.

Pettenati, M., Rao, P., Weaver, R., Thomas, I., & McMahan, M. (1993). Inversion (X)(p11.4q22) associated with Norrie disease in a four generation family. *American Journal of Medical Genetics , 45* (5), 577-80.

Piri, N., Kwong, J., Song, M., Elashoff, D., & Caprioli, J. (2006). Gene expression changes in the retina following optic nerve transection. *Molecular Vision , 12*, 1660-73.

Planutis, K., Planutiene, M., Moyer, M., Nguyen, A., Pérez, C., & Holcombe, R. (2007). Regulation of norrin receptor frizzled-4 by Wnt2 in colon-derived cells. *BMC Cell Biology , 8*, 12.

Polakis, P. (2002). Casein kinase 1: a Wnt'er of disconnect. *Current Biology , 12* (14), R499-R501.

Poliseno, L., Tuccoli, A., Mariani, L., Evangelista, M., Citti, L., Woods, K., et al. (2006). MicroRNAs modulate the angiogenic properties of HUVECs. *Blood , 108* (9), 3068-71.

Portela-Gomes, G., Stridsberg, M., Johansson, H., & Grimelius, L. (1999). Co-localization of synaptophysin with different neuroendocrine hormones in the human gastrointestinal tract. *Histochemistry and cell biology , 111* (1), 49-54.

Prasad, S., Howley, S., & Murphy, K. (2008). Candidate genes and the behavioral phenotype in 22q11.2 deletion syndrome. *Developmental disabilities research reviews , 14* (1), 26-34.

Purves, D., Augustine, G., Fitzpatrick, D., Hall, W., LaMantia, A., MacNamara, J., et al. (2004). *Neuroscience.* Sinauer Associates.

Qi, X., Li, T.-G., Hao, J., Hu, J., Wang, J., Simmons, H., et al. (2004). BMP4 supports self-renewal of embryonic stem cells by inhibiting mitogen-activated protein kinase pathways. *Proceedings of the National Academy of Sciences of the United States of America , 101* (16), 6027-32.

Qin, M., Hayashi, H., Oshima, K., Tahira, T., Hayashi, K., & Kondo, H. (2005). Complexity of the genotype-phenotype correlation in familial exudative vitreoretinopathy with mutations in the LRP5 and/or FZD4 genes. *Human Mutation , 26* (2), 104-12.

Qin, M., Kondo, H., Tahira, T., & Hayashi, K. (2008). Moderate reduction of Norrin signaling activity associated with the causative missense mutations identified in patients with familial exudative vitreoretinopathy. *Human Genetics , 122* (6), 615-23.

Qiu, W., Andersen, T., Bollerslev, J., Mandrup, S., Abdallah, B., & Kassem, M. (2007). Patients with high bone mass phenotype exhibit enhanced osteoblast differentiation and inhibition of adipogenesis of human mesenchymal stem cells. *Journal of Bone and Mineral Research , 22* (11), 1720-31.

Röhrenbeck, J., Wässle, H., & Heizmann, C. (1987). Immunocytochemical labelling of horizontal cells in mammalian retina using antibodies against calcium-binding proteins. *Neuroscience letters , 77* (3), 255-60.

Radonić, A., Thulke, S., Mackay, I., Landt, O., Siegert, W., & Nitsche, A. (2004). Guideline to reference gene selection for quantitative real-time PCR. *Biochemical and Biophysical Research Communications , 313* (4), 856-62.

Ramakrishnan, S., Rajesh, M., & Sulochana, K. (2007). Eales' disease: oxidant stress and weak antioxidant defence. *Indian journal of ophthalmology , 55* (2), 95-102.

Ramsauer, M., & D'Amore, P. (2007). Contextual role for angiopoietins and TGFbeta1 in blood vessel stabilization. *Journal of Cell Science , 120* (Pt 10), 1810-7.

Ravia, Y., Braier-Goldstein, O., Bat-Miriam, K., Erlich, S., Barkai, G., & Goldman, B. (1993). X-linked recessive primary retinal dysplasia is linked to the Norrie disease locus. *Human Molecular Genetics , 2* (8), 1295-7.

Redmond, R., Vaughan, J., Jay, M., & Jay, B. (1993). In-utero diagnosis of Norrie disease by ultrasonography. *Ophthalmic Paediatrics and Genetics , 14* (1), 1-3.

Reed, M., Koike, T., Sadoun, E., Sage, E., & Puolakkainen, P. (2003). Inhibition of TIMP1 enhances angiogenesis in vivo and cell migration in vitro. *Microvascular Research , 65* (1), 9-17.

Reese, A., & Straatsma, B. (1958). Retinal dysplasia. *American Journal of Ophthalmology , 45* (4, Part 2), 199-211.

Rehm, H., Gutiérrez-Espeleta, G., Garcia, R., Jiménez, G., Khetarpal, U., Priest, J., et al. (1997). Norrie disease gene mutation in a large Costa Rican kindred with a novel phenotype including venous insufficiency. *Human Mutation , 9* (5), 402-8.

Rehm, H., Zhang, D.-S., Brown, M., Burgess, B., Halpin, C., Berger, W., et al. (2002). Vascular defects and sensorineural deafness in a mouse model of Norrie disease. *The Journal of Neuroscience , 22* (11), 4286-92.

Ren, X., Du, Q., Huang, Y., Ao, S., Mei, L., & Xiong, W. (2001). Regulation of CDC42 GTPase by proline-rich tyrosine kinase 2 interacting with PSGAP, a novel pleckstrin homology and Src homology 3 domain containing rhoGAP protein. *The Journal of Cell Biology , 152* (5), 971-84.

Revesz, T., Fletcher, S., al-Gazali, L., & DeBuse, P. (1992). Bilateral retinopathy, aplastic anaemia, and central nervous system abnormalities: a new syndrome? *Journal of Medical Genetics , 29* (9), 673-5.

Rhee, J.-S., Black, M., Schubert, U., Fischer, S., Morgenstern, E., Hammes, H.-P., et al. (2004). The functional role of blood platelet components in angiogenesis. *Thrombosis and Haemostasis , 92* (2), 394-402.

Richard-Parpaillon, L., Héligon, C., Chesnel, F., Boujard, D., & Philpott, A. (2002). The IGF pathway regulates head formation by inhibiting Wnt signaling in Xenopus. *Developmental Biology , 244* (2), 407-17.

Richards, J., Papaioannou, A., Adachi, J., Joseph, L., Whitson, H., Prior, J., et al. (2007). Effect of selective serotonin reuptake inhibitors on the risk of fracture. *Archives of internal medicine , 167* (2), 188-94.

Richter, M., Gottanka, J., May, C., Welge-Lüssen, U., Berger, W., & Lütjen-Drecoll, E. (1998). Retinal vasculature changes in Norrie disease mice. *Investigative Ophthalmology & Visual Science , 39* (12), 2450-7.

Rickels, M., Zhang, X., Mumm, S., & Whyte, M. (2005). Oropharyngeal skeletal disease accompanying high bone mass and novel LRP5 mutation. *Journal of Bone and Mineral Research , 20* (5), 878-85.

Ritter, M., Banin, E., Moreno, S., Aguilar, E., Dorrell, M., & Friedlander, M. (2006). Myeloid progenitors differentiate into microglia and promote vascular repair in a model of ischemic retinopathy. *Journal of Clinical Investigation , 116* (12), 3266-76.

Riveiro-Alvarez, R., Cantalapiedra, D., Vallespin, E., Aguirre-Lamban, J., Avila-Fernandez, A., Gimenez, A., et al. (2008). Gene symbol: NDP. Disease: Norrie disease. *Human Genetics , 124* (3), 308.

Riveiro-Alvarez, R., Trujillo-Tiebas, M., Gimenez-Pardo, A., Garcia-Hoyos, M., Cantalapiedra, D., Lorda-Sanchez, I., et al. (2005). Genotype-phenotype variations in five Spanish families with Norrie disease or X-linked FEVR. *Molecular Vision , 11*, 705-12.

Rivera-Vega, M., Chiñas-Lopez, S., Vaca, A., Arenas-Sordo, M., Kofman-Alfaro, S., Messina-Baas, O., et al. (2005). Molecular analysis of the NDP gene in two families with Norrie disease. *Acta Ophthalmologica Scandinavica , 83* (2), 210-4.

Robitaille, J., Macdonald, M., Kaykas, A., Sheldahl, L., Zeisler, J., Dubé, M.-P., et al. (2002). Mutant frizzled-4 disrupts retinal angiogenesis in familial exudative vitreoretinopathy. *Nature Genetics , 32* (2), 326-30.

Robitaille, J., Monsein, L., & Traboulsi, E. (1996). Coats' disease and central nervous system venous malformation. *Ophthalmic Genetics , 17* (4), 215-8.

Robitaille, J., Wallace, K., Zheng, B., Beis, M., Samuels, M., Hoskin-Mott, A., et al. (2009). Phenotypic overlap of familial exudative vitreoretinopathy (FEVR) with persistent fetal vasculature (PFV) caused by FZD4 mutations in two distinct pedigrees. *Ophthalmic Genetics , 30* (1), 23-30.

Rossazza, C., Guerois, M., Yesou, C., & Gouriou, J. (1983). [Association of Leber-Coats disease and Fahr syndrome]. *Bulletin des sociétés d'ophtalmologie de France , 83* (6-7), 891-3.

Royer, G., Hanein, S., Raclin, V., Gigarel, N., Rozet, J.-M., Munnich, A., et al. (2003). NDP gene mutations in 14 French families with Norrie disease. *Human Mutation , 22* (6), 499.

Ruether, K., van de Pol, D., Jaissle, G., Berger, W., Tornow, R., & Zrenner, E. (1997). Retinoschisislike alterations in the mouse eye caused by gene targeting of the Norrie disease gene. *Investigative Ophthalmology & Visual Science , 38* (3), 710-8.

Ruggiero, D., Lecomte, M., Michoud, E., Lagarde, M., & Wiernsperger, N. (1997). Involvement of cell-cell interactions in the pathogenesis of diabetic retinopathy. *Diabetes & Metabolism , 23* (1), 30-42.

Ryan, D., Oliveira-Fernandes, M., & Lavker, R. (2006). MicroRNAs of the mammalian eye display distinct and overlapping tissue specificity. *Molecular Vision , 12*, 1175-84.

Sánchez, D., Ganfornina, M., & Martínez, S. (2002). Expression pattern of the lipocalin apolipoprotein D during mouse embryogenesis. *Mechanisms of Development , 110* (1-2), 225-9.

Saiki, R., Gelfand, D., Stoffel, S., Scharf, S., Higuchi, R., Horn, G., et al. (1988). Primer-directed enzymatic amplification of DNA with a thermostable DNA polymerase. *Science, 239* (4839), 487-491.

Saint-Geniez, M., & D'Amore, P. (2004). Development and pathology of the hyaloid, choroidal and retinal vasculature. *The International Journal of Developmental Biology, 48* (8-9), 1045-58.

Saint-Geniez, M., Argence, C., Knibiehler, B., & Audigier, Y. (2003). The msr/apj gene encoding the apelin receptor is an early and specific marker of the venous phenotype in the retinal vasculature. *Gene Expression Patterns, 3* (4), 467-72.

Saint-Geniez, M., Masri, B., Malecaze, F., Knibiehler, B., & Audigier, Y. (2002). Expression of the murine msr/apj receptor and its ligand apelin is upregulated during formation of the retinal vessels. *Mechanisms of Development , 110* (1-2), 183-6.

Salinas, P. (2007). Modulation of the microtubule cytoskeleton: a role for a divergent canonical Wnt pathway. *Trends in Cell Biology, 17* (7), 333-42.

Salinas, P. (2005). Signaling at the vertebrate synapse: new roles for embryonic morphogens? *Journal of Neurobiology , 64* (4), 435-45.

Sambrook, J., Maniatis, T., & Fritsch, E. (1989). *Molecular Cloning: A Laboratory Manual* (Bd. 1). Cold Spring Harbor Laboratory Press.

Sanchez, D., López-Arias, B., Torroja, L., Canal, I., Wang, X., Bastiani, M., et al. (2006). Loss of glial lazarillo, a homolog of apolipoprotein D, reduces lifespan and stress resistance in Drosophila. *Current Biology , 16* (7), 680-6.

Sanders Strickland, L., & Koeppen, H. (2006). Comments on plasmalemmal vesicle associated protein-1 as a novel marker implicated in brain tumor angiogenesis. *Clinical Cancer Research , 12* (8), 2649; 2649-50.

Sanger, F., Nicklen, S., & Coulson, A. (1977). DNA sequencing with chain-terminating inhibitors. *Proceedings of the National Academy of Sciences of the United States of America, 74* (12), 5463-7.

Sarjeant, J., Lawrie, A., Kinnear, C., Yablonsky, S., Leung, W., Massaeli, H., et al. (2003). Apolipoprotein D inhibits platelet-derived growth factor-BB-induced vascular smooth muscle cell proliferated by preventing translocation of phosphorylated extracellular signal regulated kinase 1/2 to the nucleus. *Arteriosclerosis, Thrombosis, and Vascular Biology , 23* (12), 2172-7.

Sato, M., Umetsu, D., Murakami, S., Yasugi, T., & Tabata, T. (2006). DWnt4 regulates the dorsoventral specificity of retinal projections in the Drosophila melanogaster visual system. *Nature Neuroscience , 9* (1), 67-75.

Sauer, C., Gehrig, A., Warneke-Wittstock, R., Marquardt, A., Ewing, C., Gibson, A., et al. (1997). Positional cloning of the gene associated with X-linked juvenile retinoschisis. *Nature Genetics , 17* (2), 164-70.

Schüller, U., & Rowitch, D. (2007). Beta-catenin function is required for cerebellar morphogenesis. *Brain Research, 1140*, 161-9.

Schäfer, N., Luhmann, U., Feil, S., & Berger, W. (2009). Differential gene expression in Ndph-knockout mice in retinal development. *Investigative Ophthalmology & Visual Science , 50* (2), 906-16.

Scheef, E., Wang, S., Sorenson, C., & Sheibani, N. (2005). Isolation and characterization of murine retinal astrocytes. *Molecular Vision , 11*, 613-24.

Schinkel, A., Smit, J., van Tellingen, O., Beijnen, J., Wagenaar, E., van Deemter, L., et al. (1994). Disruption of the mouse mdr1a P-glycoprotein gene leads to a deficiency in the blood-brain barrier and to increased sensitivity to drugs. *Cell , 77* (4), 491-502.

Schmitz-Valckenberg, P., & Scholz, W. (1977). [Norrie syndrome (author's transl)]. *Klinische Monatsblätter für Augenheilkunde , 171* (4), 562-7.

Scholz, M., Salamon-Looijen, M., Pfau, B., Kujat, C., Hille, K., & Graf, N. (1997). Morbus Coats bei einem Jungen mit DiGeorge-Syndrom. *Monatsschr Kinderheilkd, 145* (10), 1061-1065.

Schroeder, B., Hesse, L., Brück, W., & Gal, A. (1997). Histopathological and immunohistochemical findings associated with a null mutation in the Norrie disease gene. *Ophthalmic Genetics, 18* (2), 71-7.

Schroedl, C., McClintock, D., Budinger, G., & Chandel, N. (2002). Hypoxic but not anoxic stabilization of HIF-1alpha requires mitochondrial reactive oxygen species. *American Journal of Physiology Lung Cellular and Molecular Physiology , 283* (5), L922-31.

Schuback, D., Chen, Z.-Y., Craig, I., Breakefield, X., & Sims, K. (1995). Mutations in the Norrie disease gene. *Human Mutation , 5* (4), 285-92.

Seifert, J., & Mlodzik, M. (2007). Frizzled/PCP signalling: a conserved mechanism regulating cell polarity and directed motility. *Nature Reviews Genetics , 8* (2), 126-38.

Selbach, M., Schwanhäusser, B., Thierfelder, N., Fang, Z., Khanin, R., & Rajewsky, N. (2008). Widespread changes in protein synthesis induced by microRNAs. *Nature , 455* (7209), 58-63.

Seller, M., Pal, K., Horsley, S., Davies, A., Berry, A., Meredith, R., et al. (1995). A fetus with an X;1 balanced reciprocal translocation and eye disease. *Journal of Medical Genetics , 32* (7), 557-60.

Semenov, M., & He, X. (2006). LRP5 mutations linked to high bone mass diseases cause reduced LRP5 binding and inhibition by SOST. *The Journal of Biological Chemistry , 281* (50), 38276-84.

Sethi, C., Lewis, G., Fisher, S., Leitner, W., Mann, D., Luthert, P., et al. (2005). Glial remodeling and neural plasticity in human retinal detachment with proliferative vitreoretinopathy. *Investigative Ophthalmology & Visual Science , 46* (1), 329-42.

Sethupathy, P., Borel, C., Gagnebin, M., Grant, G., Deutsch, S., Elton, T., et al. (2007). Human microRNA-155 on chromosome 21 differentially interacts with its polymorphic target in the AGTR1 3' untranslated region: a mechanism for functional single-nucleotide polymorphisms related to phenotypes. *American Journal of Human Genetics, 81* (2), 405-13.

Shah, G., Summers, C., Walsh, A., & Neely, K. (1997). Optic nerve neovascularization in incontinentia pigmenti. *American Journal of Ophthalmology , 124* (3), 410-2.

Shastry, B., & Trese, M. (2004). Cosegregation of two unlinked mutant alleles in some cases of autosomal dominant familial exudative vitreoretinopathy. *European Journal of Human Genetics, 12* (1), 79-82.

Shastry, B., & Trese, M. (2003). Overproduction and partial purification of the Norrie disease gene product, norrin, from a recombinant baculovirus. *Biochemical and Biophysical Research Communications, 312* (1), 229-34.

Shastry, B., Hejtmancik, J., & Trese, M. (1997). Identification of novel missense mutations in the Norrie disease gene associated with one X-linked and four sporadic cases of familial exudative vitreoretinopathy. *Human Mutation , 9* (5), 396-401.

Shastry, B., Hejtmancik, J., Plager, D., Hartzer, M., & Trese, M. (1995). Linkage and candidate gene analysis of X-linked familial exudative vitreoretinopathy. *Genomics, 27* (2), 341-4.

Shastry, B., Hiraoka, M., Trese, D., & Trese, M. (1999). Norrie disease and exudative vitreoretinopathy in families with affected female carriers. *European Journal of Ophthalmology, 9* (3), 238-42.

Shastry, B., Liu, X., Hejtmancik, J., Plager, D., & Trese, M. (1997). Evidence for genetic heterogeneity in X-linked familial exudative vitreoretinopathy. *Genomics, 44* (2), 247-8.

Shastry, B., Pendergast, S., Hartzer, M., Liu, X., & Trese, M. (1997). Identification of missense mutations in the Norrie disease gene associated with advanced retinopathy of prematurity. *Archives of Ophthalmology , 115* (5), 651-5.

Shea, T. (2000). Microtubule motors, phosphorylation and axonal transport of neurofilaments. *Journal of neurocytology , 29* (11-12), 873-87.

Shen, J., Yang, X., Xie, B., Chen, Y., Swaim, M., Hackett, S., et al. (2008). MicroRNAs regulate ocular neovascularization. *Molecular Therapy, 16* (7), 1208-16.

Shibuya, M. (2006). Differential roles of vascular endothelial growth factor receptor-1 and receptor-2 in angiogenesis. *Journal of Biochemistry and Molecular Biology, 39* (5), 469-78.

Shima, C., Kusaka, S., Kondo, H., Hasebe, H., Fujikado, T., & Tano, Y. (2009). Lens-sparing vitrectomy effective for reattachment of newly developed falciform retinal detachment in a patient with Norrie disease. *Archives of Ophthalmology, 127* (4), 579-80.

Shprintzen, R. (2008). Velo-cardio-facial syndrome: 30 Years of study. *Developmental disabilities research reviews, 14* (1), 3-10.

Shu, W., Jiang, Y., Lu, M., & Morrisey, E. (2002). Wnt7b regulates mesenchymal proliferation and vascular development in the lung. *Development, 129* (20), 4831-42.

Sieweke, M., & Graf, T. (1998). A transcription factor party during blood cell differentiation. *Current Opinion in Genetics & Development, 8* (5), 545-51.

Silverman, W., & Flynn, J. (1985). *Retinopathy of Prematurity*. 303.

Simpanya, M., Wistow, G., Gao, J., David, L., Giblin, F., & Mitton, K. (2008). Expressed sequence tag analysis of guinea pig (Cavia porcellus) eye tissues for NEIBank. *Molecular Vision , 14*, 2413-27.

Sims, K., de la Chapelle, A., Norio, R., Sankila, E., Hsu, Y., Rinehart, W., et al. (1989). Monoamine oxidase deficiency in males with an X chromosome deletion. *Neuron, 2* (1), 1069-76.

Sims, K., Irvine, A., & Good, W. (1997). Norrie disease in a family with a manifesting female carrier. *Archives of Ophthalmology , 115* (4), 517-9.

Sims, K., Lebo, R., Benson, G., Shalish, C., Schuback, D., Chen, Z.-Y., et al. (1992). The Norrie disease gene maps to a 150 kb region on chromosome Xp11.3. *Human Molecular Genetics , 1* (2), 83-9.

Sims, K., Ozelius, L., Corey, T., Rinehart, W., Liberfarb, R., Haines, J., et al. (1989). Norrie disease gene is distinct from the monoamine oxidase genes. *American Journal of Human Genetics , 45* (3), 424-34.

Skern, R., Frost, P., & Nilsen, F. (2005). Relative transcript quantification by quantitative PCR: roughly right or precisely wrong? *BMC Molecular Biology , 6* (1), 10.

Skevas, A., Kastanioudakis, I., Daniilidis, B., & Exarchakos, G. (1992). [Norrie-Warburg syndrome]. *Laryngorhinootologie , 71* (10), 534-6.

Skuta, G., France, T., Stevens, T., & Laxova, R. (1987). Apparent Coats' disease and pericentric inversion of chromosome 3. *American Journal of Ophthalmology , 104* (1), 84-6.

Smahi, A., Courtois, G., Vabres, P., Yamaoka, S., Heuertz, S., Munnich, A., et al. (2000). Genomic rearrangement in NEMO impairs NF-kappaB activation and is a cause of incontinentia pigmenti. The International Incontinentia Pigmenti (IP) Consortium. *Nature , 405* (6785), 466-72.

Small, R. (1968). Coats' disease and muscular dystrophy. *Transactions - American Academy of Ophthalmology and Otolaryngology American Academy of Ophthalmology and Otolaryngology , 72* (2), 225-31.

Smallwood, P., Williams, J., Xu, Q., Leahy, D., & Nathans, J. (2007). Mutational analysis of Norrin-Frizzled4 recognition. *The Journal of Biological Chemistry , 282* (6), 4057-68.

Smit, L., Lammers, G., & Catsman-Berrevoets, C. (2006). Cataplexy leading to the diagnosis of Niemann-Pick disease type C. *Pediatric Neurology , 35* (1), 82-4.

Smithen, L., Brown, G., Brucker, A., Yannuzzi, L., Klais, C., & Spaide, R. (2005). Coats' disease diagnosed in adulthood. *Ophthalmology , 112* (6), 1072-8.

Spitznas, M., Meyer-Schwickerath, G., & Stephan, B. (1975). The clinical picture of Eales' disease. *Albrecht von Graefes Archiv für klinische und experimentelle Ophthalmologie Albrecht von Graefe's archive for clinical and experimental ophthalmology , 194* (2), 73-85.

Stalmans, I., Lambrechts, D., De Smet, F., Jansen, S., Wang, J., Maity, S., et al. (2003). VEGF: a modifier of the del22q11 (DiGeorge) syndrome? *Nature Medicine, 9* (2), 173-82.

Stalmans, I., Ng, Y.-S., Rohan, R., Fruttiger, M., Bouché, A., Yuce, A., et al. (2002). Arteriolar and venular patterning in retinas of mice selectively expressing VEGF isoforms. *Journal of Clinical Investigation , 109* (3), 327-36.

Stan, R., Kubitza, M., & Palade, G. (1999). PV-1 is a component of the fenestral and stomatal diaphragms in fenestrated endothelia. *Proceedings of the National Academy of Sciences of the United States of America , 96* (23), 13203-7.

Stan, R.-V. (2004). Multiple PV1 dimers reside in the same stomatal or fenestral diaphragm. *American Journal of Physiology Heart and Circulatory Physiology, 286* (4), H1347-53.

Stan, R.-V., Arden, K., & Palade, G. (2001). cDNA and protein sequence, genomic organization, and analysis of cis regulatory elements of mouse and human PLVAP genes. *Genomics , 72* (3), 304-13.

Stan, R.-V., Tkachenko, E., & Niesman, I. (2004). PV1 is a key structural component for the formation of the stomatal and fenestral diaphragms. *Molecular Biology of the Cell , 15* (8), 3615-30.

Steinbach, K., Volkmer, H., & Schlosshauer, B. (2002). Semaphorin 3E/collapsin-5 inhibits growing retinal axons. *Experimental Cell Research , 279* (1), 52-61.

Steinhoff, C., & Vingron, M. (2006). Normalization and quantification of differential expression in gene expression microarrays. *Briefings in Bioinformatics, 7* (2), 166-77.

Stenman, J., Rajagopal, J., Carroll, T., Ishibashi, M., McMahon, J., & McMahon, A. (2008). Canonical Wnt signaling regulates organ-specific assembly and differentiation of CNS vasculature. *Science , 322* (5905), 1247-50.

Stocks, S., Taylor, S., & Shiels, I. (2001). Transforming growth factor-beta1 induces alpha-smooth muscle actin expression and fibronectin synthesis in cultured human retinal pigment epithelial cells. *Clinical & Experimental Ophthalmology , 29* (1), 33-7.

Stone, J., & Maslim, J. (1997). Mechanisms of Retinal Angiogenesis. *Progress in Retinal and Eye Research , 16* (2), 157-181.

Stone, J., Itin, A., Alon, T., Pe'er, J., Gnessin, H., Chan-Ling, T., et al. (1995). Development of retinal vasculature is mediated by hypoxia-induced vascular endothelial growth factor (VEGF) expression by neuroglia. *The Journal of Neuroscience , 15* (7 Pt 1), 4738-47.

Strasberg, P., Liede, H., Stein, T., Warren, I., Sutherland, J., & Ray, P. (1995). A novel mutation in the Norrie disease gene predicted to disrupt the cystine knot growth factor motif. *Human Molecular Genetics , 4* (11), 2179-80.

Streeten, E., McBride, D., Puffenberger, E., Hoffman, M., Pollin, T., Donnelly, P., et al. (2008). Osteoporosis-pseudoglioma syndrome: description of 9 new cases and beneficial response to bisphosphonates. *Bone , 43* (3), 584-90.

Strickland, D., Ashcom, J., Williams, S., Burgess, W., Migliorini, M., & Argraves, W. (1990). Sequence identity between the alpha 2-macroglobulin receptor and low density lipoprotein receptor-related protein suggests that this molecule is a multifunctional receptor. *The Journal of Biological Chemistry , 265* (29), 17401-4.

Strickland, L., Jubb, A., Hongo, J.-A., Zhong, F., Burwick, J., Fu, L., et al. (2005). Plasmalemmal vesicle-associated protein (PLVAP) is expressed by tumour endothelium and is upregulated by vascular endothelial growth factor-A (VEGF). *The Journal of Pathology , 206* (4), 466-75.

Suárez, Y., Fernández-Hernando, C., Pober, J., & Sessa, W. (2007). Dicer dependent microRNAs regulate gene expression and functions in human endothelial cells. *Circulation Research , 100* (8), 1164-73.

Suárez-Merino, B., Bye, J., McDowall, J., Ross, M., & Craig, I. (2001). Sequence analysis and transcript identification within 1.5 MB of DNA deleted together with the NDP and MAO genes in atypical Norrie disease patients presenting with a profound phenotype. *Human Mutation , 17* (6), 523.

Sulzberger, M. (1927). Über eine bisher nicht beschriebene congenitale Pigmentanomalie (Incontinentia pigmenti). *Arch. Derm. Syph. , 154*, 19-32.

Sun, Y., Jain, A., & Moshfeghi, D. (2007). Elevated vascular endothelial growth factor levels in Coats disease: rapid response to pegaptanib sodium. *Graefe's Archive for Clinical and Experimental Ophthalmology = Albrecht von Graefes Archiv für klinische und experimentelle Ophthalmologie , 245* (9), 1387-8.

Surace, E., Balaggan, K., Tessitore, A., Mussolino, C., Cotugno, G., Bonetti, C., et al. (2006). Inhibition of ocular neovascularization by hedgehog blockade. *Molecular Therapy , 13* (3), 573-9.

Sybert, V. (1994). Incontinentia pigmenti nomenclature. *American Journal of Human Genetics , 55* (1), 209-11.

Takahashi, M., Fujita, M., Furukawa, Y., Hamamoto, R., Shimokawa, T., Miwa, N., et al. (2002). Isolation of a novel human gene, APCDD1, as a direct target of the beta-Catenin/T-cell factor 4 complex with probable involvement in colorectal carcinogenesis. *Cancer Research, 62* (20), 5651-6.

Talks, S., Ebenezer, N., Hykin, P., Adams, G., Yang, F., Schulenberg, E., et al. (2001). De novo mutations in the 5' regulatory region of the Norrie disease gene in retinopathy of prematurity. *Journal of Medical Genetics , 38* (12), E46.

Tarpey, P., Smith, R., Pleasance, E., Whibley, A., Edkins, S., Hardy, C., et al. (2009). A systematic, large-scale resequencing screen of X-chromosome coding exons in mental retardation. *Nature Genetics , 41* (5), 535-43.

Taylor, P., Coates, T., & Newhouse, M. (1959). Episkopi blindness; hereditary blindness in a Greek Cypriot family. *The British Journal of Ophthalmology, 43* (6), 340-4.

Terry, T. (1942). Extreme prematurity and fibroblastic overgrowth of persistent vascular sheath behind each crystalline lens. I. Preliminary report. *American Journal of Ophthalmology , 25*, 203-204.

Terry, T. (1944). Retrolental Fibroplasia in the Premature Infant: V. Further Studies on Fibroplastic Overgrowth of the Persistent Tunica Vasculosa Lentis. *Transactions of the American Ophthalmological Society , 42*, 383-96.

Thapa, N., Kang, K.-B., & Kim, I.-S. (2005). Beta ig-h3 mediates osteoblast adhesion and inhibits differentiation. *Bone , 36* (2), 232-42.

Thaung, C., West, K., Clark, B., McKie, L., Morgan, J., Arnold, K., et al. (2002). Novel ENU-induced eye mutations in the mouse: models for human eye disease. *Human Molecular Genetics , 11* (7), 755-67.

Therese, K., Deepa, P., Therese, J., Bagyalakshmi, R., Biswas, J., & Madhavan, H. (2007). Association of mycobacteria with Eales' disease. *The Indian journal of medical research , 126* (1), 56-62.

Thurston, G. (2003). Role of Angiopoietins and Tie receptor tyrosine kinases in angiogenesis and lymphangiogenesis. *Cell and Tissue Research , 314* (1), 61-8.

Thurston, G., Wang, Q., Baffert, F., Rudge, J., Papadopoulos, N., Jean-Guillaume, D., et al. (2005). Angiopoietin 1 causes vessel enlargement, without angiogenic sprouting, during a critical developmental period. *Development , 132* (14), 3317-26.

Tian, Q., Jin, H., Cui, Y., Guo, C., & Lu, X. (2005). Regulation of Wnt gene expression. *Development, Growth & Differentiation , 47* (5), 273-81.

Tolmie, J., Browne, B., McGettrick, P., & Stephenson, J. (1988). A familial syndrome with coats' reaction retinal angiomas, hair and nail defects and intracranial calcification. *Eye, 2 (Pt 3)*, 297-303.

Toma, I., Kang, J., Sipos, A., Vargas, S., Bansal, E., Hanner, F., et al. (2008). Succinate receptor GPR91 provides a direct link between high glucose levels and renin release in murine and rabbit kidney. *Journal of Clinical Investigation , 118* (7), 2526-34.

Tomasek, J., Haaksma, C., Schwartz, R., Vuong, D., Zhang, S., Ash, J., et al. (2006). Deletion of smooth muscle alpha-actin

alters blood-retina barrier permeability and retinal function. *Investigative Ophthalmology & Visual Science , 47* (6), 2693-700.

Toomes, C., Bottomley, H., Jackson, R., Towns, K., Scott, S., Mackey, D., et al. (2004). Mutations in LRP5 or FZD4 underlie the common familial exudative vitreoretinopathy locus on chromosome 11q. *American Journal of Human Genetics , 74* (4), 721-30.

Toomes, C., Bottomley, H., Scott, S., Mackey, D., Craig, J., Appukuttan, B., et al. (2004). Spectrum and frequency of FZD4 mutations in familial exudative vitreoretinopathy. *Investigative Ophthalmology & Visual Science , 45* (7), 2083-90.

Toomes, C., Downey, L., Bottomley, H., Mintz-Hittner, H., & Inglehearn, C. (2005). Further evidence of genetic heterogeneity in familial exudative vitreoretinopathy; exclusion of EVR1, EVR3, and EVR4 in a large autosomal dominant pedigree. *British Journal of Ophthalmology , 89* (2), 194-7.

Toomes, C., Downey, L., Bottomley, H., Scott, S., Woodruff, G., Trembath, R., et al. (2004). Identification of a fourth locus (EVR4) for familial exudative vitreoretinopathy (FEVR). *Molecular Vision , 10*, 37-42.

Torrente, I., Mangino, M., Gennarelli, M., Novelli, G., Giannotti, A., Vadalà, P., et al. (1997). Two new missense mutations (A105T and C110G) in the norrin gene in two Italian families with Norrie disease and familial exudative vitreoretinopathy. *American Journal of Medical Genetics , 72* (2), 242-4.

Tretiach, M., van Driel, D., & Gillies, M. (2003). Transendothelial electrical resistance of bovine retinal capillary endothelial cells is influenced by cell growth patterns: an ultrastructural study. *Clinical & Experimental Ophthalmology , 31* (4), 348-53.

Turner, B., Bhaskar, K., Hadzopoulou-Cladaras, M., & LaMont, J. (1999). Cysteine-rich regions of pig gastric mucin contain von willebrand factor and cystine knot domains at the carboxyl terminal(1). *Biochimica et Biophysica Acta , 1447* (1), 77-92.

Uehara, F., Sameshima, M., Yanagita, T., Iwakiri, N., & Ohba, N. (1996). Lectin-histochemical study of O-linked glycoconjugates in dysplastic retina of Norrie disease. *Japanese Journal of Ophthalmology , 40* (2), 251-4.

Uemura, A., Kusuhara, S., Katsuta, H., & Nishikawa, S.-I. (2006). Angiogenesis in the mouse retina: a model system for experimental manipulation. *Experimental Cell Research , 312* (5), 676-83.

Umapathy, N., Dun, Y., Martin, P., Duplantier, J., Roon, P., Prasad, P., et al. (2008). Expression and function of system N glutamine transporters (SN1/SN2 or SNAT3/SNAT5) in retinal ganglion cells. *Investigative Ophthalmology & Visual Science , 49* (11), 5151-60.

Umapathy, N., Li, W., Mysona, B., Smith, S., & Ganapathy, V. (2005). Expression and function of glutamine transporters SN1 (SNAT3) and SN2 (SNAT5) in retinal Müller cells. *Investigative Ophthalmology & Visual Science, 46* (11), 3980-7.

Uzan, B., Villemin, A., Garel, J.-M., & Cressent, M. (2008). Adrenomedullin is anti-apoptotic in osteoblasts through CGRP1 receptors and MEK-ERK pathway. *Journal of Cellular Physiology , 215* (1), 122-8.

van Amerongen, R., & Berns, A. (2006). Knockout mouse models to study Wnt signal transduction. *Trends in Genetics , 22* (12), 678-89.

Van Wesenbeeck, L., Cleiren, E., Gram, J., Beals, R., Bénichou, O., Scopelliti, D., et al. (2003). Six novel missense mutations in the LDL receptor-related protein 5 (LRP5) gene in different conditions with an increased bone density. *American Journal of Human Genetics , 72* (3), 763-71.

Veeman, M., Axelrod, J., & Moon, R. (2003). A second canon. Functions and mechanisms of beta-catenin-independent Wnt signaling. *Developmental Cell , 5* (3), 367-77.

Veeramachaneni, V., & Fielder, P. (2001). Index of suspicion. Case 2. Diagnosis: Norrie disease. *Pediatrics in Review , 22* (6), 211-5.

Vierck, J., Bryne, K., & Dodson, M. (2000). Evaluating dot and Western blots using image analysis and pixel quantification of electronic images. *Methods in Cell Science , 22* (4), 313-8.

Vitt, U., Hsu, S., & Hsueh, A. (2001). Evolution and classification of cystine knot-containing hormones and related extracellular signaling molecules. *Molecular Endocrinology , 15* (5), 681-94.

Vogel, C., Bauer, A., Wiesnet, M., Preissner, K., Schaper, W., Marti, H., et al. (2007). Flt-1, but not Flk-1 mediates hyperpermeability through activation of the PI3-K/Akt pathway. *Journal of Cellular Physiology , 212* (1), 236-43.

Vogt, R., Unda, R., Yeh, L.-C., Vidro, E., Lee, J., & Tsin, A. (2006). Bone morphogenetic protein-4 enhances vascular endothelial growth factor secretion by human retinal pigment epithelial cells. *Journal of Cellular Biochemistry , 98* (5), 1196-202.

von Tell, D., Armulik, A., & Betsholtz, C. (2006). Pericytes and vascular stability. *Experimental Cell Research , 312* (5), 623-9.

Vossler, D., Wyler, A., Wilkus, R., Gardner-Walker, G., & Vlcek, B. (1996). Cataplexy and monoamine oxidase deficiency in Norrie disease. *Neurology, 46* (5), 1258-61.

Votin, V., Nelson, W., & Barth, A. (2005). Neurite outgrowth involves adenomatous polyposis coli protein and beta-catenin. *Journal of Cell Science, 118* (Pt 24), 5699-708.

Wadman, I., Osada, H., Grütz, G., Agulnick, A., Westphal, H., Forster, A., et al. (1997). The LIM-only protein Lmo2 is a bridging molecule assembling an erythroid, DNA-binding complex which includes the TAL1, E47, GATA-1 and Ldb1/NLI proteins. *The EMBO Journal, 16* (11), 3145-57.

Walenkamp, M., Karperien, M., Pereira, A., Hilhorst-Hofstee, Y., van Doorn, J., Chen, J., et al. (2005). Homozygous and heterozygous expression of a novel insulin-like growth factor-I mutation. *The Journal of Clinical Endocrinology and Metabolism , 90* (5), 2855-64.

Walker, J., Dixon, J., Fenton, C., Hungerford, J., Lynch, S., Stenhouses, S., et al. (1997). Two new mutations in exon 3 of the NDP gene: S73X and S101F associated with severe and less severe ocular phenotype, respectively. *Human Mutation, 9* (1), 53-6.

Wan, M., & Cao, X. (2005). BMP signaling in skeletal development. *Biochemical and Biophysical Research Communications , 328* (3), 651-7.

Wang, B., Weidenfeld, J., Lu, M., Maika, S., Kuziel, W., Morrisey, E., et al. (2004). Foxp1 regulates cardiac outflow tract, endocardial cushion morphogenesis and myocyte

proliferation and maturation. *Development, 131* (18), 4477-87.

Wang, Y., Huso, D., Cahill, H., Ryugo, D., & Nathans, J. (2001). Progressive cerebellar, auditory, and esophageal dysfunction caused by targeted disruption of the frizzled-4 gene. *The Journal of Neuroscience , 21* (13), 4761-71.

Warburg, M. (1963). Norrie's disease (atrofia bulborum hereditaria). *Acta Ophthalmol. (Copenhagen), 41*, 134-146.

Warburg, M. (1968). Norrie's disease. *Journal of mental deficiency research, 12*, 247-251.

Warburg, M. (1966). Norrie's disease. A congenital progressive oculo-acoustico-cerebral degeneration. *Acta Ophthalmol. (Copenhagen) Suppl., 89*, 1-47.

Warburg, M. (1961). Norrie's disease: A new hereditary bilateral pseudotumour of the retina. *Acta Ophthalmol. (Copenhagen), 39*, 757-772.

Warren, A., Colledge, W., Carlton, M., Evans, M., Smith, A., & Rabbitts, T. (1994). The oncogenic cysteine-rich LIM domain protein rbtn2 is essential for erythroid development. *Cell , 78* (1), 45-57.

Watanabe, D., Suzuma, K., Suzuma, I., Ohashi, H., Ojima, T., Kurimoto, M., et al. (2005). Vitreous levels of angiopoietin 2 and vascular endothelial growth factor in patients with proliferative diabetic retinopathy. *American Journal of Ophthalmology , 139* (3), 476-81.

Waterman, M. (2004). Lymphoid enhancer factor/T cell factor expression in colorectal cancer. *Cancer Metastasis Reviews , 23* (1-2), 41-52.

Watzke, R., Stevens, T., & Carney, R. (1976). Retinal vascular changes of incontinentia pigmenti. *Archives of Ophthalmology, 94* (5), 743-6.

Weis, S., & Cheresh, D. (2005). Pathophysiological consequences of VEGF-induced vascular permeability. *Nature , 437* (7058), 497-504.

Whitney, E., Kemper, T., Rosene, D., Bauman, M., & Blatt, G. (2008). Calbindin-D28k is a more reliable marker of human Purkinje cells than standard Nissl stains: a stereological experiment. *Journal of Neuroscience Methods , 168* (1), 42-7.

Whyte, M., Reinus, W., & Mumm, S. (2004). High-bone-mass disease and LRP5. *The New England Journal of Medicine , 350* (20), 2096-9; author reply 2096-9.

Wick, M. (2000). Immunohistology of neuroendocrine and neuroectodermal tumors. *Seminars in diagnostic pathology , 17* (3), 194-203.

Widelitz, R. (2005). Wnt signaling through canonical and non-canonical pathways: recent progress. *Growth Factors, 23* (2), 111-6.

Wielenga, V., Smits, R., Korinek, V., Smit, L., Kielman, M., Fodde, R., et al. (1999). Expression of CD44 in Apc and Tcf mutant mice implies regulation by the WNT pathway. *The American Journal of Pathology , 154* (2), 515-23.

Wilensky, J., Goldberg, M., Ziyai, F., & Wong, P. (1976). Infantile cataracts, Coats' disease, and ketotic hypoglycemia. *Journal of pediatric ophthalmology, 13* (2), 75-9.

Wilkinson, D., Neale, G., Mao, S., Naeve, C., & Goorha, R. (1997). Elf-2, a rhombotin-2 binding ets transcription factor: discovery and potential role in T cell leukemia. *Leukemia , 11* (1), 86-96.

Wilkinson-Berka, J., Jones, D., Taylor, G., Jaworski, K., Kelly, D., Ludbrook, S., et al. (2006). SB-267268, a nonpeptidic antagonist of alpha(v)beta3 and alpha(v)beta5 integrins, reduces angiogenesis and VEGF expression in a mouse model of retinopathy of prematurity. *Investigative Ophthalmology & Visual Science , 47* (4), 1600-5.

Willert, J., Epping, M., Pollack, J., Brown, P., & Nusse, R. (2002). A transcriptional response to Wnt protein in human embryonic carcinoma cells. *BMC Developmental Biology , 2*, 8.

Willert, K., & Jones, K. (2006). Wnt signaling: is the party in the nucleus? *Genes & Development , 20* (11), 1394-404.

Willert, K., Brown, J., Danenberg, E., Duncan, A., Weissman, I., Reya, T., et al. (2003). Wnt proteins are lipid-modified and can act as stem cell growth factors. *Nature , 423* (6938), 448-52.

Williams, C., Li, J.-L., Murga, M., Harris, A., & Tosato, G. (2006). Up-regulation of the Notch ligand Delta-like 4 inhibits VEGF-induced endothelial cell function. *Blood , 107* (3), 931-9.

Witmer, A., van Blijswijk, B., van Noorden, C., Vrensen, G., & Schlingemann, R. (2004). In vivo angiogenic phenotype of endothelial cells and pericytes induced by vascular endothelial growth factor-A. *The Journal of Histochemistry and Cytochemistry , 52* (1), 39-52.

Witschel, H. (1974). [Retinopathia pigmentosa and "Morbus Coats" (author's transl)]. *Klinische Monatsblätter für Augenheilkunde , 164* (3), 405-11.

Wolff, G., Mayerová, A., Wienker, T., Atalianis, P., Ioannou, P., & Warburg, M. (1992). Clinical reinvestigation and linkage analysis in the family with Episkopi blindness (Norrie disease). *Journal of Medical Genetics , 29* (11), 816-9.

Wollmann, G., Lenzner, S., Berger, W., Rosenthal, R., Karl, M., & Strauss, O. (2006). Voltage-dependent ion channels in the mouse RPE: comparison with Norrie disease mice. *Vision Research , 46* (5), 688-98.

Wong, F., Goldberg, M., & Hao, Y. (1993). Identification of a nonsense mutation at codon 128 of the Norrie's disease gene in a male infant. *Archives of Ophthalmology, 111* (11), 1553-7.

Wong, P., MacDonald, I., Sood, R., Smith, C., Pilon, R., & Tenniswood, M. (1993). Identification and partial characterization of a candidate gene for X-linked retinopathies using a lateral approach. *Genomics , 15* (3), 467-71.

Wong, W., Ou, X.-M., Chen, K., & Shih, J. (2002). Activation of human monoamine oxidase B gene expression by a protein kinase C MAPK signal transduction pathway involves c-Jun and Egr-1. *The Journal of Biological Chemistry , 277* (25), 22222-30.

Woodruff, G., Newbury-Ecob, R., Plaha, D., & Young, I. (1993). Manifesting heterozygosity in Norrie's disease? *The British Journal of Ophthalmology , 77* (12), 813-4.

Woods, K., Camacho-Hübner, C., Savage, M., & Clark, A. (1996). Intrauterine growth retardation and postnatal growth failure associated with deletion of the insulin-like growth factor I gene. *The New England Journal of Medicine, 335* (18), 1363-7.

Wu, H., Yuan, Y., Zawieja, D., Tinsley, J., & Granger, H. (1999). Role of phospholipase C, protein kinase C, and calcium in VEGF-induced venular hyperpermeability. *The American Journal of Physiology, 276* (2 Pt 2), H535-42.

Wu, W.-C., Drenser, K., Trese, M., Capone, A., & Dailey, W. (2007). Retinal phenotype-genotype correlation of pediatric patients expressing mutations in the Norrie disease gene. *Archives of Ophthalmology , 125* (2), 225-30.

Xia, C.-H., Liu, H., Cheung, D., Wang, M., Cheng, C., Du, X., et al. (2008). A model for familial exudative vitreoretinopathy caused by LPR5 mutations. *Human Molecular Genetics , 17* (11), 1605-12.

Xiong, D.-H., Shen, H., Zhao, L.-J., Xiao, P., Yang, T.-L., Guo, Y., et al. (2006). Robust and comprehensive analysis of 20 osteoporosis candidate genes by very high-density single-nucleotide polymorphism screen among 405 white nuclear families identified significant association and gene-gene interaction. *Journal of Bone and Mineral Research , 21* (11), 1678-95.

Xu, Q., Qaum, T., & Adamis, A. (2001). Sensitive blood-retinal barrier breakdown quantitation using Evans blue. *Investigative Ophthalmology & Visual Science , 42* (3), 789-94.

Xu, Q., Wang, Y., Dabdoub, A., Smallwood, P., Williams, J., Woods, C., Nathans, J., et al. (2004). Vascular development in the retina and inner ear: control by Norrin and Frizzled-4, a high-affinity ligand-receptor pair. *Cell, 116* (6), 883-95.

Xu, S., Witmer, P., Lumayag, S., Kovacs, B., & Valle, D. (2007). MicroRNA (miRNA) transcriptome of mouse retina and identification of a sensory organ-specific miRNA cluster. *The Journal of Biological Chemistry, 282* (34), 25053-66.

Yadav, V., Ryu, J.-H., Suda, N., Tanaka, K., Gingrich, J., Schütz, G., et al. (2008). Lrp5 controls bone formation by inhibiting serotonin synthesis in the duodenum. *Cell , 135* (5), 825-37.

Yamada, K., Limprasert, P., Ratanasukon, M., Tengtrisorn, S., Yingchareonpukdee, J., Vasiknanonte, P., et al. (2001). Two Thai families with Norrie disease (ND): association of two novel missense mutations with severe ND phenotype, seizures, and a manifesting carrier. *American Journal of Medical Genetics , 100* (1), 52-5.

Yamada, Y., Pannell, R., Forster, A., & Rabbitts, T. (2000). The oncogenic LIM-only transcription factor Lmo2 regulates angiogenesis but not vasculogenesis in mice. *Proceedings of the National Academy of Sciences of the United States of America , 97* (1), 320-4.

Yang, W., Yang, D., Na, S., Sandusky, G., Zhang, Q., & Zhao, G. (2005). Dicer is required for embryonic angiogenesis during mouse development. *The Journal of Biological Chemistry , 280* (10), 9330-5.

Yasumoto, K.-i., Takeda, K., Saito, H., Watanabe, K.-i., Takahashi, K., & Shibahara, S. (2002). Microphthalmia-associated transcription factor interacts with LEF-1, a mediator of Wnt signaling. *The EMBO Journal , 21* (11), 2703-14.

Yoshida, S., Arita, R.-I., Yoshida, A., Tada, H., Emori, A., Noda, Y., et al. (2004). Novel mutation in FZD4 gene in a Japanese pedigree with familial exudative vitreoretinopathy. *American Journal of Ophthalmology , 138* (4), 670-1.

Yu, D.-Y., & Cringle, S. (2001). Oxygen distribution and consumption within the retina in vascularised and avascular retinas and in animal models of retinal disease. *Progress in Retinal and Eye Research , 20* (2), 175-208.

Yuan, J., Reed, A., Chen, F., & Stewart, C. (2006). Statistical analysis of real-time PCR data. *BMC Bioinformatics , 7*, 85.

Zürcher, J. (2007). Promoter analysis of NDP, FZD4 and LRP5 & Mutation analysis of FZD4. *Masterthesis, University of Zurich* , 1-102.

Zachary, I., & Gliki, G. (2001). Signaling transduction mechanisms mediating biological actions of the vascular endothelial growth factor family. *Cardiovascular Research , 49* (3), 568-81.

Zachary, I., Mathur, A., Yla-Herttuala, S., & Martin, J. (2000). Vascular protection: A novel nonangiogenic cardiovascular role for vascular endothelial growth factor. *Arteriosclerosis, Thrombosis, and Vascular Biology , 20* (6), 1512-20.

Zaremba, J., Feil, S., Juszko, J., Myga, W., van Duijnhoven, G., & Berger, W. (1998). Intrafamilial variability of the ocular phenotype in a Polish family with a missense mutation (A63D) in the Norrie disease gene. *Ophthalmic Genetics, 19* (3), 157-64.

Zeng, Y., & Verheyen, E. (2004). Nemo is an inducible antagonist of Wingless signaling during Drosophila wing development. *Development , 131* (12), 2911-20.

Zenibayashi, M., Miyake, K., Horikawa, Y., Hirota, Y., Teranishi, T., Kouyama, K., et al. (2008). Lack of association of LRP5 and LRP6 polymorphisms with type 2 diabetes mellitus in the Japanese population. *Endocrine Journal , 55* (4), 699-707.

Zergollern, L., & Cupak, K. (1986). Norrie-Warburg syndrome. *Acta Medica Iugoslavica , 40* (4), 263-73.

Zerlin, M., Julius, M., & Kitajewski, J. (2008). Wnt/Frizzled signaling in angiogenesis. *Angiogenesis , 11* (1), 63-9.

Zhang, G., Fahmy, R., diGirolamo, N., & Khachigian, L. (2006). JUN siRNA regulates matrix metalloproteinase-2 expression, microvascular endothelial growth and retinal neovascularisation. *Journal of Cell Science , 119* (Pt 15), 3219-26.

Zhang, S., & Ma, J.-X. (2007). Ocular neovascularization: Implication of endogenous angiogenic inhibitors and potential therapy. *Progress in Retinal and Eye Research , 26* (1), 1-37.

Zhang, X., Gaspard, J., & Chung, D. (2001). Regulation of vascular endothelial growth factor by the Wnt and K-ras pathways in colonic neoplasia. *Cancer Research , 61* (16), 6050-4.

Zhang, Y., Wang, Y., Li, X., Zhang, J., Mao, J., Li, Z., et al. (2004). The LRP5 high-bone-mass G171V mutation disrupts LRP5 interaction with Mesd. *Molecular and Cellular Biology , 24* (11), 4677-84.

Zhu, D., & Hussels Maumenee, I. (1994). Mutation analysis of the Norrie disease gene in eleven families. *Investigative Ophthalmology & Visual Science, 35* (4), 1265.

Zhu, D., & Hussels Maumenee, I. (1993). Mutations in the ND gene in families with Norrie disease. *American Journal of Human Genetics , 53* (3, Supplement), 1260.

Zhu, D., Antonarakis, S., Schmeckpeper, B., Diergaarde, P., Greb, A., & Hussels Maumenee, I. (1989). Microdeletion in the X-chromosome and prenatal diagnosis in a family with Norrie disease. *American Journal of Medical Genetics , 33* (4), 485-8.

Appendix

Primer sequences used in this work

ID	Name	Sequence 5´- 3´
54	LacZ1L20	GAT TTC CAT GTT GCC ACT CG
55	LacZ1U20	TCG TCT GCT CAT CCA TGA CC
56	M13 -20tg	GTA AAA CGA CGG CCA GTG
57	M13 rev	GGA AAC AGC TAT GAC CAT G
177	SL105	CTA TCG CCT TCT TGA CGA GTT
178	SL106	GGC CTG GGT GGA GAG GCT TTT T
179	SL107	GTA TTG CAT CCA TAT TTC TTG G
180	SL108	CTC TCC ATC CCC TGA CAA GGA
188	Sry fwd1	TTC AGC CCT ACA GCC ACA TGA
189	Sry rev1	ATG TGG GTT CCT GTC CCA CTG
196	GAPD fwd	GAC CAC AGT CCA TGC CAT CAC T
197	GAPD rev	TCC ACC ACC CTG TTG CTG TAG
198	Slc38a5 fwd	CGA CCT TTG GAT ACC TCA CCT T
199	Slc38a5 rev	TGG GTG TAC ATT TCC AGC ATC T
200	Mdm2 Int6 fwd	AAG ACA GGC TCT CAC TAT TAG CTA TGG
201	Mdm2 Int6 rev	TGG GAG TTA AAG GTC TGC CTG AT
202	mm 28S rRNA for1	TTG AAA ATC CGC GGG AGA G
203	mm 28S rRNA rev 1	ACA TTG TTC CAA CAT GCC AG
204	mm Gapd for1	AAC GAC CCC TTC ATT GAC
205	mm Gapd rev1	TCC ACG ACA TAC TCA GCA C
206	mm Ppia fwd1	CAG ACG CCA CTG TCG CTT
207	mm Ppia rev1	TGT CTT TGC GAA CTT TGT CTG CAA
210	mmTcf7 for1	TAC TCT GCC TTC AAT CTG CTC ATG
211	mmTcf7 rev1	GTG GAC TGC TGA AAT GTT CGT AGA
212	mmTcf3 for1	GCG CAC CTA CCT ACA GAT GAA AT
213	mmTcf3 rev1	CAG CGG GTG CAT GTG ATG
214	mmTcf7l2 for1	GTC CTC GCT GGT CAA TGA ATC
215	mmTcf7l2 rev1	GCT TCC TGC TTG GAC ATC AAG
216	mmTcf7l2 for2	GAA GCC TCC AGA GCA GAC AAA C
217	mmTcf7l2 rev2	GCG TGA GTG GGT GGA CAT G
218	mm Lef1 for1	GAG AGC GAA TGT CGT AGC TGA GT
219	mm Lef1 rev1	TTT CCG TGC TAG TTC ATA GTA TTT GG
220	mmBmp4 for1	AGG GAA CCG GGC TTG AGT AC
221	mmBmp4 rev1	GGA TGC TGC TGA GGT TGA AGA
222	mmCdkn2a for1	ACA TGT TGT TGA GGC TAG AGA GGA T
223	mmCdkn2a rev1	TTG AGC AGA AGA GCT GCT ACG T
230	LacZ fwd	ACA CAA ATC AGC GAT TTC CAT GT

ID	Name	Sequence 5´- 3´
231	LacZ rev	TCT GAA CTT CAG CCT CCA GTA CAG
232	DXMit136 fwd	ATT TTG ATT ACA GCA TGT CCC C
233	DXMit136 rev	ACG GAA ACA CTC TTA TGT GCG
234	Gata1 fwd	CAG AAA ACA AGG AGG CGA AGG
235	Gata1 rev	CTC CCT CTG ACT CCC AGT GC
275	mSlc38a5 fwd2	GCC TGT GAA GTG CTT GGT TTG ATT
276	mSlc38a5 rev2	CCA GAG CTG TGG ATG GAC AGA CAT
277	1120 attB1 NDP f1	GGG GAC AAG TTT GTA CAA AAA AGC AGG CTT CCT GGT GCC GCG CGG CAG CAA AAC GGA CAG CTC ATT CAT AAT GG
278	1121 attB2 NDP r1	GGG GAC CAC TTT GTA CAA GAA AGC TGG GTC GGA TCC GCG CGG CAC CAG GGA ATT GCA TTC CTC GCA GTG AC
279	1124 NDP-NT f1	AGG ATC TGC ACC ATC ACC ATC ACC ATC TGG TGC CGC GCG GCA GCA AAA CGG ACA GCT CAT TCA TAA TGG
280	1125 NDP-NT r1	GGG GAC CAC TTT GTA CAA GAA AGC TGG GTC GGA TCC GCG CGG CAC CAG CTA TCA GGA ATT GCA TTC CTC GCA GTG AC
281	1126 NDP-NT f2	GGG GAC AAG TTT GTA CAA AAA AGC AGG CTT CGA ACA AAA ACT CAT CTC AGA AGA GGA TCT GCA CCA TCA CCA TCA C
282	AOX 5'	GAC TGG TTC CAA TTG ACA AGC
283	AOX 3'	GCA AAT GGC ATT CTG ACA TCC
284	mm Isl-1 5' Exon 2	AGG GAT GGG AAA ACC TAC TGT AAA
285	mm Isl-1 3' Exon 3	AGT CGT TCT TGC TGA AGC CTA TG
286	mm Syp 5' Exon 3	GAG TGC CCT CAA CAT CGA AGT C
287	mm Syp 3' Exon 4	GCA GGA GGG TGC ATC AAA GT
289	LRP5 Exon1 fwd	GCC TCA GTT TCC CCA CTC ATA GAG G
290	LRP5 Exon1 rev	TCG CCA AGT CGC TTC CGA GA
291	LRP5 Exon2 fwd	TAG GGG TGG GAG GAA GGA ACT G
292	LRP5 Exon2 rev	GGC TCA TGC AAA TTC GAG AGA GAG
293	LRP5 Exon3 fwd	GAA GGG AAG GTG CCC AGA ATT TAC T
294	LRP5 Exon3 rev	TTC AAG GGC TGG TGG CAA A
295	LRP5 Exon4 fwd	AAA GAA ATT AAT TGG GTC AGC AGC A
296	LRP5 Exon4 rev	TGC AGC AGG TAC CCC TTT AGA GAG
297	LRP5 Exon5 rev	AGT GGA AAA TAT CTG GGG CAA AAA T
298	LRP5 Exon5 fwd	CAG CGA TGA GGC AGG TGG AA
299	LRP5 Exon6 fwd (PCR)	CGT GCA TAA CCT CTC AGT GCT TCA
300	LRP5 Exon6 rev	CCG GTG TTT TAA CAA GCC CTC CT

ID	Name	Sequence 5´- 3´
301	LRP5 Exon7 fwd	ACC GAC ATT TAC GAG CAC CGA CAT
302	LRP5 Exon7 rev	AGG CAC CTG GCC GAA TGA TAA C
303	LRP5 Exon8 fwd	TAA AGT TGC GGC TCT TGG GCA
304	LRP5 Exon8 rev	ACT TAT GCC CAG GCA TGG ACC C
305	LRP5 Exon9 fwd (PCR)	CCC GCA CTG CTG TTA CTG ATA CCC TT
306	LRP5 Exon9 rev	CTT TGA GGC AGG AAC AGA GGC A
307	LRP5 Exon10 fwd	CCT GTA ATC CCC ACC TAC TT
308	LRP5 Exon10 rev	AGC TCT AAT CAC CGA GGG CCA C
309	LRP5 Exon11 fwd	CTT CCT GCG CGT GGC TTT CT
310	LRP5 Exon11 rev	GAG CCT CTC CCG ACA TAA CTG C
311	LRP5 Exon12 fwd	ACT TTA AGG CAT TCA TGT GGT CGC
312	LRP5 Exon12 rev	CAG TGC ACA ACC TAC CCA ACC ATC
313	LRP5 Exon13 fwd	AAT TCC CCA TAG CGC ACC CC
314	LRP5 Exon13 rev	CAT CCT CTG TTT CCT CCC TCT GCT A
315	LRP5 Exon14 fwd	CGG GGG TCT CCG CCA GTG
316	LRP5 Exon14 rev	TCC TGG AGG GGC TGT GAA AGA G
317	LRP5 Exon15 fwd	ATA GAA TGT GAC CTG TCA GCC TCG G
318	LRP5 Exon15 rev	TTT TCT GCC TCT GCC CTG TGG
319	LRP5 Exon16 fwd	TCC CTG GCA GTC CTG TCA ACC T
320	LRP5 Exon16 rev	CGC TGT TCG TGG TGA TTT GTT CT
321	LRP5 Exon17 fwd	GTT CTC ATT TGG CCC CTA CCC T
322	LRP5 Exon17 rev	GGA AAA TTC ATA GCA CCG A
323	LRP5 Exon18 fwd	CCG TAC AGC AGG GAT GCC AA
324	LRP5 Exon18 rev	GTG GGA CAG GAT GGG TGG AAC T
325	LRP5 Exon19 fwd	CAC TCC CCG CTG GTC CTA GAA A
326	LRP5 Exon19 rev	AGG CAC GTC TCC TCC CCT AAA CT
327	LRP5 Exon20 fwd	GGC AAA GCC AGC CCC TTC AG
328	LRP5 Exon20 rev	CAC AGG CTC AGT GGG AAA GGC T
329	LRP5 Exon21 fwd	CTG GTC TGA GTC TCG TGG GTA GTG G
330	LRP5 Exon21 rev	AAG GGA AGA AAG CAA GCA TGC C
331	LRP5 Exon22 fwd	CGC CTT CAC AGC CCA GCA TCT
332	LRP5 Exon22 rev	CCC AGA ATA CCT CCC CTC ATC AGT
333	LRP5 Exon23 fwd	AAG TGA TGA GCC CTG GCG ACA
334	LRP5 Exon23 rev	TGC AGG AGG ACT CTC ATG GTG G
335	LRP5 Exon1 fwd (Seq)	CTC CTC CCC GTC GTC CTG GT
336	LRP5 Exon6 fwd (Seq)	GTG CGT GTC ACC TAA CAT CAC CAG
337	LRP5 Exon6 fwd (Seq)	GTG CTG CAG GTG GAC GAC ATC
338	LRP5 Exon6 rev (Seq)	GTG TCG GTC CAG TAG AGG GTT TCG
339	LRP5 Exon9 fwd (Seq)	ACG GCA GCA TTC ATT GTG TGG

ID	Name	Sequence 5´- 3´
340	LRP5 Exon23 fwd	CCG ACG TGT GTG ACA GCG ACT AC
341	LRP5 Exon23 rev	CCC ACC CCA TCA CAG TTC ACA T
342	LRP5 Exon10 fwd	ACT CCA GGC TGG GCA AGA AGA
343	LRP5 Exon14 rev	GGA GAG ACC CCC ACA CCA ATA CTG
344	LRP5 Exon10 fwd	GCA TGT GCC TGT AAT CCC CAC CTA
345	LRP5 Exon10 rev	CAG TAC AGC TCT AAT CAC CGA GGG C
346	LRP5 Exon1 fwd	TCC GTG CCT CAG TTT CCC CAC TCA TAG A
347	LRP5 Exon1 rev	CCC AAC TCG CTC CCA ACT CGC C
348	LRP5 Ex1 fwd Toomes	TTC CGC TCC CGC GCG CCC AGC T
349	LRP5 Ex1 rev Toomes	GCG GGG CCG CCC GGG CCA TT
350	LRP5 Ex10 fwd (Seq)	AAG ATG CTG GTT CCT AAA ATG TG
351	Pola2 Exon6 fwd	TCC CAG AAA TAC ACC TCC AGA A
352	Pola2 Exon6 rev	ACC TTC AGA CTG ACG CTT CCA
353	LRP5 Exon1 fwd	GGC TCC ACA GGT GAC ACA C
354	LRP5 Exon1 rev	CAA GTC GCT TCC GAG ACG
355	LRP5 Exon1 fwd	CCA GCT CCC TCC TCC CCG TCG TC
356	LRP5 Exon1 rev	CGC CCC AAC TCG CTC CCA ACT C
357	LRP5 Exon1 fwd LR	ACA GAG CCA GCA CGT TCC AGC CT
358	LRP5 Exon1 rev LR	CTC ACT GGC CCC AGG ACA GCC
359	LRP5 Exon1 fwd NE	TCC CTC CTC CCC GTC GTC CTG GTC C
360	LRP5 Exon1 rev NE	CTC GCC AAG TCG CTT CCG AGA CGG
362	LRP5L Exon1 fwd	CGG TAG ACG GAC CAA TGG AGG
363	LRP5L Exon1 rev	CCA GGT TCT GAT GCA AGA CAG TGT T
364	LRP5L Exon2 fwd	TGC CGA TAT TTA CTG ACC CCA ACA
365	LRP5L Exon2 rev	CCA CCT CAG TCT CCA AGT AGC TGT GA
366	LRP5L Exon3 fwd	CAG CAC CCC TGG AGA GCC GT
367	LRP5L Exon3 rev	GGC ACC CCA GCT CAA CAC TTA TG
368	LRP5L Exon4 fwd	TTG AGC CTG GCC ATG GGA AT
369	LRP5L Exon4 rev	TTG AGG CAG GTA CAG AGG GAA GG
428	FZD4-1-fwd	CTG CTA CCC CCG ATG CTG
429	FZD4-1-rev	GGA TGA TCA ACT TGG CAT GG
430	FZD4-2a-fwd	CTG GAA GCA TTC AAC TCA GC
431	FZD4-2a-rev	TTG GTT CCC ACA GAG TGA CA
432	FZD4-2b-fwd	GTG CCC TTA CCT CAC AAA ACC
433	FZD4-2b-rev	CAG GAT ATC CTT TCC CGG CC
434	FZD4-2c-fwd	CGC CCC ATC ATA TTT CTC AG
435	FZD4-2c-rev	CAC AAG CCA GTC AGT TCA TC
436	FZD4-2d-fwd	CAT CCC CGC AGT GAA AAC CA
437	FZD4-2d-rev	GGA ATC ATC TGC AGA ATA CCG

ID	Name	Sequence 5´- 3´
438	FZD4-2e-fwd	GTT CCT GCA ACG TGT GTG AT
439	FZD4-2e-rev	CGG GGG TCA CTT AAT TGT TG
442	FZD4-2a-rev V1	AGT TCA GGC TCC TTT TCA CC
443	FZD4-2b-fwd V1	TGG GAA CCA ATT CTG ATC AG
444	FZD4-2b-rev V1	GAG TGT CAG AAT AAC CCA CC
445	FZD4-2c-fwd V1	CTT AAG AAC ACA GGA TGT GC
446	FZD4-2e-fwd V1	GAC TGA TGG TCA AGA TTG GG
447	FZD4-2c-rev V1	CAG GCA ATC ACA CAC GTT GC
450	FZD4-2a-rev V2	GTA TAA GCC AGC ATC ATA GC
451	FZD4-1-fwd V1	GGG GTG TCT GCC AGA GCA GCC
465	FZD4-1-fwd v2	CAA ACT GGG GGT GTC TGC CAG
476	27118 fwd	GCC CAC ACA GCC ATC CAG AT
477	27118 rev	GCG CCC CCG TGC AAA CT
478	MacDonald-fwd	CGG GAC GTC TAA AAT CCC ACA CAG TCG
479	MacDonald-rev	GAT ATC CTT TCC CGG CCT ACA GTC AGC
492	LRP5L Exon2 rev (Seq)	GGT GCC TTG GTG ATA CGT ATG TCA
526	hGAPDH-fwd	CAG CCT CAA GAT CAT CAG CAA T
527	hGAPDH-rev	GAG GGG CCA TCC ACA GTC
534	LRP5L Exon4 rev (Seq)	CGA GAG CAG GAT GGC CAC ATC
539	LRP5L Exon3 fwd (Seq)	GAA GTT GAG GCT CCT GGG TGT TG
540	LRP5L Exon3 fwd (Seq)	CCC TGG CCC ATC CAG ACC T
541	mm 18S rRNA fwd	CGG CTA CCA CAT CCA AGG AA
542	mm 18S rRNA rev	GCT GGA ATT ACC GCG GCT
543	mm beta-actin Ex3-Ex4 fwd	GGC CAA CCG TGA AAA GAT GA
544	mm beta-actin Ex3-Ex4 rev	CAC AGC CTG GAT GGC TAC GT
545	PLVAP Ex1.1 fwd	AGG AGC CAG GCA GAG GAA GT
546	PLVAP Ex1.1 rev	TGC AGG TTG GAC TCT GTG CT
547	PLVAP Ex1.2 fwd	GCC ATG GAG CAC GGA GG
548	PLVAP Ex1.2 rev	GAA ACT CAG GCT CAG AGA GGT GA
549	PLVAP Ex2 fwd	CAG GGT GCT CGA TCT GGG T
550	PLVAP Ex2 rev	GGA AAA CAG GAC CAG GAG ACC
551	PLVAP Ex3.1 fwd	TCC CTG CCC AGT GCT CTC
552	PLVAP Ex3.1 rev	GAG TTC TCG CGG GCC AC
553	PLVAP Ex3.2 fwd	GCC TCC ATC CGC AGA GC
554	PLVAP Ex3.2 rev	ACC CAA CCT AGA CCA GGA AGC
555	PLVAP Ex4-5 fwd	GGC AGA GTT TGC AAT GAG CC
556	PLVAP Ex4-5 rev	CTC CAC CCT CAG TCC TGG TC
557	PLVAP Ex6.1 fwd	GCC CAG GGT GGT AGG AGG
558	PLVAP Ex6.1 rev	ATG CCA TCG CCG CGT
559	PLVAP Ex6.2 fwd	ACG CGG CGA TGG CAT
560	PLVAP Ex6.2 rev	ACA GGC GTG AGC CAG CAT
561	NDP Ex3.1 fwd	TCT CCT GTC ACT GCG AGG AAT
562	NDP Ex3.1 rev	GCA GCA ATG GCA ACC TTA GAC
563	NDP Ex3.2 fwd	CAA TGC TGT TTG GGT TTC CA
564	NDP Ex3.2 rev	GGA ACC CCA TTT CTG TCT CCT T
565	LMO2 Ex1 fwd	GGG AGA GGG AGC TAT GTG TGA AC
566	LMO2 Ex1 rev	TCA CCA CTT CTT CTG GCT CCT T
567	LMO2 Ex2 fwd	CCC ACC CGT CAC GCT ATC
568	LMO2 Ex2 rev	TGC CCA GGA TTA AAT CCA AGA G
569	LMO2 Ex3 fwd	CTC TCC CCG TCC CCG AC
570	LMO2 Ex3 rev	GCG CAG CCT GGC TCC
571	LMO2 Ex4 fwd	CCG GAG AGA GAC GCA CGG T
572	LMO2 Ex4 rev	GGG GGC CGC ACT TAC TCT GAA
573	LMO2 Ex5 fwd	CAA AAC GAT CTC GGA CCC TC
574	LMO2 Ex5 rev	TCT ATA GGT GGT GTC CGA GCC T
575	LMO2 Ex6.1 fwd	CGG CCT CCT TTC TAG GGC T
576	LMO2 Ex6.1 rev	CGC CTG CTT GCC CCT AA
577	LMO2 Ex6.2 fwd	TGG GTA TCA AGA CAT AGC ATC CA
578	LMO2 Ex6.2 rev	AGA GCA TTT CCC CGC CAT
581	NDP PCR_1 fwd (1)	TGG CAT TCC CAT TTG CTA GT
582	NDP PCR_1 rev (2)	AGG ATG AAA TGC TCG GTT TG
583	NDP PCR_2 fwd (3)	TGG GTT CCA TTA GTG GTT CTG
584	NDP PCR_2 rev (4)	TTC TCC ATC CCC TGA CAA AG
585	NDP PCR_3 fwd (5)	GCA ACG AGT GTG AGG GTC TT
586	NDP PCR_3 rev (6)	AGA GTC CCG GGA GAA TTG TT
587	NDP PCR_1 fwd (7)	GTC GCT TAA ACA ACA GTC CTA
588	LMO2 Ex3-4 fwd	TCC TTC TAT TGT ATT TGA ATC GTG A
589	LMO2 Ex3-4 rev	GAA TCA CCC GGG AGG AAG
590	NDP Ex3.2 rev2	AGG AGA TGC TCA AGC ACT AGC
591	PLVAP Ex4-5 fwd2	TCC TAC CAA CCT CCC TCC AT
594	hsFZD4-Ex2-fwd1	AGT AGG CCA CAA GGA CAT GG
595	hsFZD4-Ex2-rev1	CCA GAA AGG AGG TTG GAC AG
596	hsFZD4-Ex2-fwd2	AAA TGT GAA CTC CCT GTG CTG
597	hsFZD4-Ex2-rev2	TGC CTT GGT CAC ACA ATC AC
598	mm Gpr91-fwd	ACA GAA GCC GAC AGC AGA ATG

ID	Name	Sequence 5´- 3´
599	mm Gpr91-rev	CCC AAG CAG TCC AAA AAT GAA C
600	LMO2 Ex5 fwd2	AGT CAG GTG AGA TGC CCT GT
601	LMO2 Ex5 rev2	ACA CAC CGA CTG CAG ATG TC
602	hsPOLR2A fwd	TGT GGA GAT CTT CAC GGT GCT
603	hsPOLR2A rev	CAT AAG CAC GTC CAC CGT TTC
604	hsSLC38A5 Ex1A fwd	TTT GCG GAC AGT GTG AGT TC
605	hsSLC38A5 Ex1A rev	GAG GAG GGG ATG CTA GGG
606	hsSLC38A5 Ex1B fwd	TGG TGT GTC TGG TCC TAC CC
607	hsSLC38A5 Ex1B rev	CCA CTT GGA GGG AGA CAG C
608	hsSLC38A5 Ex1C fwd	TCT CCT ACT CTC TCT CTG TCT CCT C
609	hsSLC38A5 Ex1C rev	GCT AAA ATG TCT CCA AGG AAC C
610	hsSLC38A5 Ex2-3 fwd	CCC CTG CCT TGT CTC TTT CT
611	hsSLC38A5 Ex2-3 rev	GAG GGG AGC GAC CAA GTA GT
612	hsSLC38A5 Ex4-5 fwd	CTC TCC TTG GCT TCT CTC CA
613	hsSLC38A5 Ex4-5 rev	GGG GTC CAA GGT CTG TGT T
614	hsSLC38A5 Ex6-7 fwd	ACT GCT TAA CCC CCA CCT TC
615	hsSLC38A5 Ex6-7 rev	TCT GGA AGT CAG CTG CAC AC
616	hsSLC38A5 Ex8 fwd	ACC CTA TTG TGC CGT TTG TC
617	hsSLC38A5 Ex8 rev	TCT GTT CAA GCC CAC ATC AA
618	hsSLC38A5 Ex9-10 fwd	GCT GGT CTC GAA CTC CTG A
619	hsSLC38A5 Ex9-10 rev	CCA ATA TCC AGC TCC ACT CTG
620	hsSLC38A5 Ex11 fwd	TCA TAT GGT GCA TCC TGC TC
621	hsSLC38A5 Ex11 rev	CCC TCC CAT GAC ACA ACC TA
622	hsSLC38A5 Ex12 fwd	CAT GTG TGC CAG CTG AAT G
623	hsSLC38A5 Ex12 rev	GCC CCA GAA ACC CAT ACA TA
624	hsSLC38A5 Ex13 fwd	CAG AAG GTG TGC CTC ACT TG
625	hsSLC38A5 Ex13 rev	TTG CCA TCT CTG TCC ATC TG
626	hsSLC38A5 Ex14-15 fwd	GCA GGG TGG AGC CAT AGA TA
627	hsSLC38A5 Ex14-15 rev	ATG CAT GTC CCT TTC ACC TC
628	hsSLC38A5 Ex16A fwd	GTG GAA GGA CTC GCA GAA AG
629	hsSLC38A5 Ex16A rev	GGG TTG GGG TTG GGA TTA G
630	hsSLC38A5 Ex16B fwd	CCG CAT GTC TGG ACA CTG AT
631	hsSLC38A5 Ex16B rev	CAC TCG CAG GGC TTC AGT T
632	hsSLC38A5 Ex9-10 fwd2	TTA GTA GAG ATG GGG CTT TGC
633	hsSLC38A5 Ex9-10 rev2	AAT GTC CAA TAT CCA GCT CCA

Results from the whole genome cDNA microarray (p <0.01)

Increased	Symbol	Name	Affymetrix ID
3.06	*Mdm2*	Transformed mouse 3T3 cell double minute 2	1457929_at
2.79	*Wdr67*	WD repeat domain 67	1442286_at
2.47	*Seh1l*	SEH1-like (S. cerevisiae)	1441857_x_at
2.30	*Fndc3a*	fibronectin type III domain containing 3A	1444482_at
2.16	*Prdm9*	PR domain containing 9	1426107_at
2.04	*E330034G19Rik*	RIKEN cDNA E330034G19 gene	1433798_a_at
2.03	*Adm*	adrenomedullin	1447839_x_at
2.00	*Ifnb1*	Interferon beta, fibroblast	1422305_at
2.00	*Lilrb4*	leukocyte immunoglobulin-like receptor, subfamily B, member 4	1420394_s_at
1.95	*Arhgap10*	Rho GTPase activating protein 10	1442967_at
1.88	*Iqsec2*	IQ motif and Sec7 domain 2	1448063_at
1.87	*Lenep*	lens epithelial protein	1422309_a_at
1.86	*Plvap*	plasmalemma vesicle associated protein	1418090_at
1.84	*Foxp1*	forkhead box P1	1446280_at
1.81	*Sc4mol*	sterol-C4-methyl oxidase-like	1459627_at
1.81	*A2m*	alpha-2-macroglobulin	1434719_at
1.80	*Klhl7*	kelch-like 7 (Drosophila)	1459477_at
1.80	*Emp1*	epithelial membrane protein 1	1416529_at
1.79	*Spsb1*	splA/ryanodine receptor domain and SOCS box containing 1	1421474_a_at
1.76	*Sync*	syncoilin	1432350_at
1.67	*Acta2*	actin, alpha 2, smooth muscle, aorta	1416454_s_at
1.66		Mus musculus transcribed sequences	1457729_at
1.65	*Gfra2*	glial cell line derived neurotrophic factor family receptor alpha 2	1459847_x_at
1.65	*Ganab*	alpha glucosidase 2, alpha neutral subunit	1437812_x_at
1.65	*Dync1li1*	dynein cytoplasmic 1 light intermediate chain 1	1425953_at
1.65	*Car12*	carbonic anyhydrase 12	1428485_at
1.63	*Maob*	monoamine oxidase B	1434354_at
1.59	*Ms4a6b*	membrane-spanning 4-domains, subfamily A, member 6B	1418826_at
1.58	*Prkag1*	protein kinase, AMP-activated, gamma 1 non-catalytic subunit	1457803_at
1.56	*St13*	suppression of tumorigenicity 13	1416851_at
1.55	*Xist*	inactive X specific transcripts	1436936_s_at
1.55	*Ndufa4l2*	NADH dehydrogenase (ubiquinone) 1 alpha subcomplex, 4-like 2	1434905_at
1.54	*Thrsp*	thyroid hormone responsive SPOT14 homolog (Rattus)	1422973_a_at
1.52	*Arpp21*	cyclic AMP-regulated phosphoprotein, 21	1442121_at
1.52	*Nr2c2*	nuclear receptor subfamily 2, group C, member 2	1433379_at
1.49	*Kif26b*	kinesin family member 26B	1440990_at
1.49	*Hk2*	hexokinase 2	1422612_at
1.48	*Ppfia2*	protein tyrosine phosphatase, receptor type, f polypeptide (PTPRF), interacting protein (liprin), alpha 2	1445766_at
1.47	*2700054A10Rik*	Mus musculus 11 days embryo whole body cDNA, RIKEN full-length enriched library, clone:2700054A10 product:unknown EST, full insert sequence	1431223_at
1.47	*Tgfbi*	transforming growth factor, beta induced	1437463_x_at
1.47	*Ptchd2*	patched domain containing 2	1440288_at
1.46	*D12Ertd647e*	ISG12a protein	1452956_a_at
1.45	*Rere*	arginine glutamic acid dipeptide (RE) repeats	1439159_at
1.44	*Mrpl15*	mitochondrial ribosomal protein L15	1458612_at
1.44	*Map2k5*	mitogen activated protein kinase kinase 5	1430180_at
1.44	*Obfc2a*	oligonucleotide/oligosaccharide-binding fold containing 2A	1460521_a_at
1.44	*RP23-376N23.4*	predicted gene, OTTMUSG00000016611	1420318_at
1.43	*Myst2*	MYST histone acetyltransferase 2	1447631_at
1.43	*Fbxw9*	F-box and WD-40 domain protein 9	1425857_at

1.42	*Ednrb*	endothelin receptor type B	1423594_a_at
1.42	*Ints7*	integrator complex subunit 7	1443045_at
1.42	*Lsp1*	lymphocyte specific 1	1417756_a_at
1.40	*Mt1*	metallothionein 1	1422557_s_at
1.40	*Pfkp*	phosphofructokinase, platelet	1437759_at
1.38	*Slc25a40*	solute carrier family 25, member 40	1458031_at
1.38	*Bnip3*	BCL2/adenovirus E1B 19kDa-interacting protein 1, NIP3	1422470_at
1.38	*Trappc6a*	trafficking protein particle complex 6A	1460054_at
1.36	*AI452102*	expressed sequence AI452102	1458459_a_at
1.36	*Gnl3*	guanine nucleotide binding protein-like 3 (nucleolar)	1440766_at
1.36	*Kcnj3*	potassium inwardly-rectifying channel, subfamily J, member 3	1421468_at
1.36	*Amot*	angiomotin	1425907_s_at
1.35	*Tacstd1*	tumor-associated calcium signal transducer 1	1447899_x_at
1.35	*Sfrp4*	secreted frizzled-related sequence protein 4	1451031_at
1.35	*Chst14*	carbohydrate (N-acetylgalactosamine 4-0) sulfotransferase 14	1426866_at
1.34	*Arih2*	ariadne homolog 2 (Drosophila)	1445934_at
1.34	*Sufu*	suppressor of fused homolog (Drosophila)	1420848_at
1.33	*H19*	H19 fetal liver mRNA	1448194_a_at
1.32	*Pfkp*	phosphofructokinase, platelet	1416069_at
1.30	*A930016P21Rik*	RIKEN cDNA A930016P21 gene	1444686_at
1.29	*Slc19a2*	solute carrier family 19 (thiamine transproter), member 2	1426117_a_at
1.29	*Pdk1*	3-phosphoinositide dependent protein kinase-1	1423748_at
1.28	*Flrt1*	fibronectin leucine rich transmembrane protein 1	1460041_at
1.28	*Ppp1r10*	protein phosphatase 1, regulatory subunit 10	1430560_at
1.27	*Cops6*	COP9 (constitutive photomorphogenic) homolog, subunit 6 (Arabidopsis thaliana)	1451367_at
1.27	*H2-Q7*	histocompatibility 2, Q region locus 7	1418536_at
1.27	*Dmrtc1a*	DMRT-like family C1a	1431360_s_at
1.26	*Sirt1*	sirtuin 1 (silent mating type information regulation 2, homolog) 1 (S. cerevisiae)	1458538_at
1.26	*Cenpo*	centromere protein O	1418542_s_at
1.26	*Mrps5*	mitochondrial ribosomal protein S5	1435563_at
1.26	*Akap8l*	neighbor of A-kinase anchoring protein 95	1428814_at
1.25	*Ppih*	peptidyl prolyl isomerase H	1429832_at
1.25	*AL807384.5*	RIKEN cDNA 1700030G11 gene	1439592_at
1.25	*Ptpdc1*	protein tyrosine phosphatase domain containing 1	1435107_at
1.24	*Sec24d*	Sec24 related gene family, member D (S. cerevisiae)	1426972_at
1.24	*Zfp13*	zinc finger protein 13	1435131_at
1.24	*Igf2*	insulin-like growth factor 2	1448152_at
1.24	*Lrrc8d*	leucine rich repeat containing 8D	1447491_at
1.24	*Hnrpdl*	heterogeneous nuclear ribonucleoprotein D-like	1428225_s_at
1.23	*Loxl2*	lysyl oxidase-like 2	1431004_at
1.23		Mus musculus transcribed sequences	1458798_at
1.23	*0610037D15Rik*	RIKEN cDNA 0610037D15 gene	1453639_s_at
1.23	*2310056P07Rik*	family with sequence similarity 162, member A	1451385_at
1.23	*Pi4kb*	phosphatidylinositol 4-kinase, catalytic, beta polypeptide	1447950_at
1.23	*Vps13d*	vacuolar protein sorting 13 D (yeast)	1439187_at
1.22	*Atp9b*	ATPase, class II, type 9B	1460099_at
1.21	*Ndel1*	nuclear distribution gene E-like homolog 1 (A. nidulans)	1424893_at
1.20	*Rasal2*	RAS protein activator like 2	1436910_at
1.20	*Selenbp2*	selenium binding protein 2	1417580_s_at
1.20	*Gpi1*	phosphatidylinositol glycan anchor biosynthesis, class Q	1456909_at
1.19	*Gins3*	GINS complex subunit 3 (Psf3 homolog)	1429149_at
1.18	*Pnpla8*	patatin-like phospholipase domain containing 8	1442416_at
1.18	*Lba1*	lupus brain antigen 1	1429276_at
1.18	*Ccnt2*	cyclin T2	1427088_at

1.16	*Siat9*	sialyltransferase 9 (CMP-NeuAc:lactosylceramide alpha-2,3-sialyltransferase)	1449198_a_at
1.15	*EG245190*	predicted gene, EG245190	1455739_at
1.15	*Seh1l*	SEH1-like (S. cerevisiae)	1420386_at
1.15	*Xrcc1*	X-ray repair complementing defective repair in Chinese hamster cells 1	1416587_a_at
1.15	*Elmo2*	engulfment and cell motility 2, ced-12 homolog (C. elegans)	1436011_at
1.14	*Pgk1*	phosphoglycerate kinase 1	1417864_at
1.13	*Zfp50*	zinc finger protein 50	1453175_at
1.12	*Nedd4l*	neural precursor cell expressed, developmentally down-regulated gene 4-like	1423269_a_at
1.11	*Pomgnt1*	protein O-linked mannose beta1,2-N-acetylglucosaminyltransferase	1426618_a_at
1.08	*Ift172*	intraflagellar transport 172 homolog (Chlamydomonas)	1423068_at

Decreased	Symbol	Name	Affymetrix ID
14.03	*Slc38a5*	SN2; C81234	1454622_at
4.88	*Abcb1a*	ATP-binding cassette, sub-family B (MDR/TAP), member 1A	1419758_at
2.82	*Rps10*	ribosomal protein S10	1439374_x_at
2.72	*4833411O04Rik*	4833411O04Rik	1447914_x_at
2.57		Mus musculus 10 day old male pancreas cDNA, RIKEN full-length enriched library, clone:1810021B22 product:unknown EST, full insert sequence	1440350_at
2.44	*Mfsd2*	major facilitator superfamily domain containing 2	1428223_at
2.24	*Nutf2*	nuclear transport factor 2	1447440_at
2.13	*Aass*	aminoadipate-semialdehyde synthase	1423523_at
2.06	*Apod*	apolipoprotein D	1416371_at
2.05	*Centd3*	centaurin, delta 3	1419833_s_at
2.03	*Cldn5*	claudin 5	1417839_at
2.02	*Vwf*	Von Willebrand factor homolog	1435386_at
2.01	*Ndph*	Norrie disease homolog	1449251_at
1.92	*Agtrl1*	angiotensin receptor-like 1	1438651_a_at
1.89	*6230424C14Rik*	Mus musculus adult male cecum cDNA, RIKEN full-length enriched library, clone:9130410H17 product:unknown EST, full insert sequence	1441972_at
1.88	*2310015A05Rik*	RIKEN cDNA 2310015A05 gene	1436104_a_at
1.85	*6330409D20Rik*	RIKEN cDNA 6330409D20 gene	1430098_at
1.85	*Plekhh1*	pleckstrin homology domain containing, family H (with MyTH4 domain) member 1	1435053_s_at
1.79	*6720489N17Rik*	RIKEN cDNA 6720489N17 gene	1440869_x_at
1.76	*Zf206*	Mus musculus similar to zinc finger protein 206 (LOC332221), mRNA	1438787_at
1.74	*Abcc9*	ATP-binding cassette, sub-family C (CFTR/MRP), member 9	1435752_s_at
1.72	*Eltd1*	EGF, latrophilin seven transmembrane domain containing 1	1418059_at
1.67	*Ets1*	E26 avian leukemia oncogene 1, 5' domain	1452163_at
1.67	*Vwa1*	von Willebrand factor A domain containing 1	1426399_at
1.66	*Apcdd1*	adenomatosis polyposis coli down-regulated 1	1418383_at
1.66		Mus musculus transcribed sequences	1443322_at
1.62	*Slc7a1*	Solute carrier family 7 (cationic amino acid transporter, y+ system), member 1	1454992_at
1.61	*Gpr123*	G protein-coupled receptor 123 (Secretin family)	1459750_s_at
1.60	*9630027E11*	Mus musculus 16 days neonate cerebellum cDNA, RIKEN full-length enriched library, clone:9630027E11 product:unknown EST, full insert sequence	1440177_at
1.60	*Osmr*	oncostatin M receptor	1418674_at
1.59	*AI851453*	Mus musculus adult male diencephalon cDNA, RIKEN full-length enriched library, clone:9330115I17 product:unclassifiable, full insert sequence	1441815_at
1.56	*5330430P22Rik*	RIKEN cDNA 2310066I18 gene	1453832_at
1.56	*Gpr23*	G protein-coupled receptor 23	1439665_at
1.55	*Gpr22*	G protein-coupled receptor 22	1434673_at
1.55	*Sema3e*	sema domain, immunoglobulin domain (Ig), short basic domain, secreted, (semaphorin) 3E	1419717_at
1.55	*Ccl9*	chemokine (C-C motif) ligand 9	1417936_at
1.54	*A930033C23Rik*	RIKEN cDNA A930033C23 gene	1431490_at
1.53	*Mobkl2c*	MOB1, Mps One Binder kinase activator-like 2C (yeast)	1459919_a_at
1.52	*Alox5ap*	arachidonate 5-lipoxygenase activating protein	1452016_at

1.52	*5730508B09Rik*	RIKEN cDNA 5730508B09 gene	1447100_s_at
1.51	*Serpinb6a*	serine (or cysteine) proteinase inhibitor, clade B, member 6a	1436189_at
1.51	*Mmp15*	matrix metalloproteinase 15	1437462_x_at
1.51	*Col25a1*	collagen, type XXV, alpha 1	1438540_at
1.51	*Lect1*	leukocyte cell derived chemotaxin 1	1460258_at
1.50	*Cit*	citron kinase	1455609_at
1.50	*1500009L16Rik*	Mus musculus adult male cerebellum cDNA, RIKEN full-length enriched library, clone:1500009L16 product:hypothetical protein, full insert sequence	1452840_at
1.49		Mus musculus transcribed sequence with strong similarity to protein sp:P00722 (E. coli) BGAL_ECOLI Beta-galactosidase (Lactase)	1447922_at
1.48	*Kirrel3*	kin of IRRE like 3 (Drosophila)	1431402_at
1.48	*Cyhr1*	cysteine and histidine rich 1	1419284_at
1.47	*Tacr3*	tachykinin receptor 3	1450278_at
1.47	*Agtrl1*	angiotensin receptor-like 1	1423037_at
1.46	*Slco2b1*	solute carrier organic anion transporter family, member 2b1	1433933_s_at
1.46	*BC022687*	Uncharacterized protein C14orf79 homolog	1451533_at
1.46	*Myo1b*	myosin IB	1447364_x_at
1.45	*Sh3d1B*	SH3 domain protein 1B	1446735_at
1.45	*Paxip1*	PAX interacting (with transcription-activation domain) protein 1	1434363_x_at
1.45		Mus musculus transcribed sequence with strong similarity to protein sp:P00722 (E. coli) BGAL_ECOLI Beta-galactosidase (Lactase)	1440271_at
1.44		Mus musculus transcribed sequences	1439816_at
1.44	*Pigc*	phosphatidylinositol glycan, classC	1424190_at
1.44	*Mff*	mitochondrial fission factor	1457371_at
1.44		Mus musculus LOC386430 (LOC386430), mRNA	1443871_at
1.43	*Rnaseh2c*	ribonuclease H2, subunit C	1435733_x_at
1.43	*9030624J02Rik*	RIKEN cDNA 9030624J02 gene	1426695_at
1.43	*Adcy7*	adenylate cyclase 7	1450065_at
1.42	*Gimap8*	GTPase, IMAP family member 8	1456061_at
1.42	*1700012H17Rik*	family with sequence similarity 110, member B	1440359_at
1.42	*Ramp2*	receptor (calcitonin) activity modifying protein 2	1418187_at
1.42	*Pdlim5*	PDZ and LIM domain 5	1422862_at
1.42	*Itm2a*	integral membrane protein 2A	1423608_at
1.41	*B430007K19Rik*	Mus musculus 16 days neonate heart cDNA, RIKEN full-length enriched library, clone:D830033F17 product:unknown EST, full insert sequence	1440038_at
1.41	*Apcdd1*	adenomatosis polyposis coli down-regulated 1	1454822_x_at
1.41	*Dnase2a*	deoxyribonuclease II alpha	1448986_x_at
1.41	*Wee1*	wee 1 homolog (S. pombe)	1416774_at
1.40	*Zbtb33*	zinc finger and BTB domain containing 33	1456596_at
1.40	*Sepp1*	selenoprotein P, plasma, 1	1452141_a_at
1.40	*Phf2*	PHD finger protein 2	1421067_a_at
1.39		Mus musculus, Similar to sodium channel, voltage-gated, type I, alpha polypeptide, clone IMAGE:5361050, mRNA	1441728_at
1.39	*Eltd1*	EGF, latrophilin seven transmembrane domain containing 1	1418058_at
1.38	*Atp5g1*	ATP synthase, H+ transporting, mitochondrial F0 complex, subunit c (subunit 9), isoform 1	1444874_at
1.38	*Myt1*	myelin transcription factor 1	1439365_at
1.38	*Cyb5r3*	cytochrome b5 reductase 3	1456554_at
1.38	*Pgr*	progesterone receptor	1439527_at
1.38	*Aifm2*	apoptosis-inducing factor, mitochondrion-associated 2	1431143_x_at
1.37	*H2afz*	H2A histone family, member Z	1456032_x_at
1.37		Mus musculus transcribed sequence with weak similarity to protein ref:NP_081764.1 (M.musculus) RIKEN cDNA 5730493B19 [Mus musculus]	1442387_at
1.36	*Eraf*	erythroid associated factor	1449077_at
1.36	*Traf3ip3*	TRAF3 interacting protein 3	1457267_at
1.36	*Dpyd*	dihydropyrimidine dehydrogenase	1427946_s_at
1.36	*Tha1*	threonine aldolase 1	1428780_at
1.35	*4930404N11Rik*	Mus musculus similar to hypothetical protein MGC20700 (LOC216175), mRNA	1434263_at

1.35	*Magel2*	melanoma antigen, family L, 2	1417217_at
1.35	*2410002O22Rik*	RIKEN cDNA 2410002O22 gene	1453332_at
1.34	*Rag1*	recombination activating gene 1	1450680_at
1.34	*Mettl7a1*	methyltransferase like 7A1	1434151_at
1.34	*Smad7*	MAD homolog 7 (Drosophila)	1423389_at
1.34	*Tmem168*	transmembrane protein 168	1451133_s_at
1.34	*Bcl11a*	B-cell CLL/lymphoma 11A (zinc finger protein)	1426552_a_at
1.34	*Tmhs*	tetraspan transmembrane protein, hair cell stereocilia	1429266_at
1.34	*Slc7a1*	solute carrier family 7	1454991_at
1.34	*Taok2*	TAO kinase 2	1438208_at
1.33	*Mrps24*	mitochondrial ribosomal protein S24	1438563_s_at
1.33	*Egfr*	epidermal growth factor receptor	1424932_at
1.33	*Pard6b*	par-6 (partitioning defective 6) homolog beta (C. elegans)	1423174_a_at
1.32	*Spin2*	spindlin family, member 2	1455297_at
1.32	*Zfp148*	zinc finger protein 148	1436217_at
1.32	*Dhx30*	DEAH (Asp-Glu-Ala-His) box polypeptide 30	1438832_x_at
1.32	*Ppm1a*	protein phosphatase 1A, magnesium dependent, alpha isoform	1417221_at
1.32	*2810410L24Rik*	Mus musculus 10, 11 days embryo whole body cDNA, RIKEN full-length enriched library, clone:2810410L24 product:unknown EST, full insert sequence	1429510_at
1.32	*Suv39h2*	suppressor of variegation 3-9 homolog 2 (Drosophila)	1433996_at
1.32	*Sdk2*	sidekick homolog 2 (chicken)	1457333_at
1.31		Mus musculus transcribed sequences	1458920_at
1.31	*Chchd7*	coiled-coil-helix-coiled-coil-helix domain containing 7	1454640_at
1.31	*Pkn1*	protein kinase C-like 1	1436851_at
1.31	*3830431G21Rik*	hypothetical protein 3830431G21	1436035_at
1.31	*Alg1*	asparagine-linked glycosylation 1 homolog (yeast, beta-1,4-mannosyltransferase)	1451368_at
1.31	*AI447490*	RIKEN cDNA A130022J15 gene	1433671_at
1.31	*Cart*	cocaine and amphetamine regulated transcript	1422825_at
1.31	*Nfkbia*	nuclear factor of kappa light chain gene enhancer in B-cells inhibitor, alpha	1449731_s_at
1.31	*Fkbp1b*	FK506 binding protein 1b	1449429_at
1.30	*Epha3*	Eph receptor A3	1425575_at
1.30	*D430047L21Rik*	Mus musculus transcribed sequences	1435590_at
1.30	*Gpr124*	G protein-coupled receptor 124	1418379_s_at
1.30	*Zbtb8a*	zinc finger and BTB domain containing 8a	1452063_at
1.30	*Rad51ap1*	RAD51 associated protein 1	1448899_s_at
1.30	*Lrrc4*	leucine rich repeat containing 4	1435832_at
1.30	*Gart*	phosphoribosylglycinamide formyltransferase	1424436_at
1.30	*Rfc4*	replication factor C (activator 1) 4	1424321_at
1.30		Mus musculus transcribed sequences	1455147_at
1.30	*2410003K15Rik*	RIKEN cDNA 2410003K15 gene	1428495_at
1.30	*Lsm5*	LSM5 homolog, U6 small nuclear RNA associated (S. cerevisiae)	1418656_at
1.30	*1700066J24Rik*	RIKEN cDNA 1700066J24 gene	1436150_at
1.29	*Smpd4*	sphingomyelin phosphodiesterase 4	1429530_a_at
1.29	*Rbpms*	RNA binding protein gene with multiple splicing	1429359_s_at
1.29	*Dgkz*	diacylglycerol kinase zeta	1426738_at
1.29	*Nptx1*	neuronal pentraxin 1	1434877_at
1.29	*Clmn*	calmin	1439117_at
1.29	*Sema4a*	sema domain, immunoglobulin domain (Ig), transmembrane domain (TM) and short cytoplasmic domain, (semaphorin) 4A	1438934_x_at
1.29	*Zfp580*	zinc finger protein 580	1429634_at
1.29	*Smarcd1*	SWI/SNF related, matrix associated, actin dependent regulator of chromatin, subfamily d, member 1	1448913_at
1.29	*Atp5sl*	ATP5S-like	1416775_at
1.28	*9430008C03Rik*	RIKEN cDNA 9430008C03 gene	1434574_at
1.28	*4632433K11Rik*	RIKEN cDNA 4632433K11 gene	1438689_at

1.28	*Slc40a1*	solute carrier family 40 (iron-regulated transporter), member 1	1448566_at
1.28	*Rgmb*	RGM domain family, member B	1442811_at
1.28	*1110038B12Rik*	RIKEN cDNA 1110038B12 gene	1441081_a_at
1.28	*Ddx1*	DEAD (Asp-Glu-Ala-Asp) box polypeptide 1	1440816_x_at
1.28	*4930471M23Rik*	RIKEN cDNA 4930471M23 gene	1426220_at
1.28	*Mtrr*	5-methyltetrahydrofolate-homocysteine methyltransferase reductase	1452110_at
1.28	*Chchd6*	coiled-coil-helix-coiled-coil-helix domain containing 6	1438659_x_at
1.28	*Suclg2*	succinate-Coenzyme A ligase, GDP-forming, beta subunit	1435841_s_at
1.28	*Foxk2*	forkhead box K2	1428353_at
1.27		Mus musculus transcribed sequences	1440378_at
1.27	*Riok2*	RIO kinase 2 (yeast)	1436684_a_at
1.27	*Tmem51*	transmembrane protein 51	1424383_at
1.27	*Tcfap2e*	transcription factor AP-2, epsilon	1435205_at
1.27	*Glul*	glutamate-ammonia ligase (glutamine synthase)	1426236_a_at
1.27	*3300001P08Rik*	RIKEN cDNA 3300001P08	1444677_at
1.27	*Cep68*	centrosomal protein 68	1441340_at
1.27	*Nrsn2*	neurensin 2	1434640_at
1.27	*Zic3*	zinc finger protein of the cerebellum 3	1423424_at
1.27	*Stmn3*	stathmin-like 3	1460181_at
1.27	*Ccdc45*	coiled-coil domain containing 45	1436620_at
1.27	*Rab11fip4*	RAB11 family interacting protein 4 (class II)	1434156_at
1.27	*Nup210*	nucleoporin 210	1417585_at
1.27	*Nmd3*	NMD3 homolog (S. cerevisiae)	1448133_at
1.27	*Ano8*	anoctamin 8	1437895_at
1.27	*Slain2*	SLAIN motif family, member 2	1427024_at
1.27	*9430016H08Rik*	RIKEN cDNA 9430016H08 gene	1424075_at
1.26	*Nmnat*	NMN adenylyltransferase; nicotinamide mononucleotide adenylyl transferase	1429819_at
1.26	*Osbpl1a*	oxysterol binding protein-like 1A	1416823_a_at
1.26	*Rnf138*	ring finger protein 138	1419368_a_at
1.26	*Strn4*	striatin, calmodulin binding protein 4	1426209_at
1.26	*Cd2ap*	CD2-associated protein	1455310_at
1.26	*Blzf1*	basic leucine zipper nuclear factor 1	1442164_at
1.26	*Ccdc123*	coiled-coil domain containing 123	1421949_a_at
1.26	*Rab14*	RAB14, member RAS oncogene family	1419244_a_at
1.26	*Rex3*	reduced expression 3	1448595_a_at
1.26	*Rab11b*	RAB11B, member RAS oncogene family	1439508_at
1.25	*Slc25a20*	solute carrier family 25 (mitochondrial carnitine/acylcarnitine translocase), member 20	1423109_s_at
1.25	*Rab4a*	RAB4A, member RAS oncogene family	1418341_at
1.25	*Zc3h10*	zinc finger CCCH type containing 10	1417833_at
1.25	*AW121567*	Transmembrane protein FAM155A	1435138_at
1.25	*Zfp191*	zinc finger protein 191	1430651_s_at
1.25	*Tmem185b*	transmembrane protein 185B	1452093_at
1.25	*Myo18a*	myosin XVIIIa	1451422_at
1.25	*Dusp4*	dual specificity phosphatase 4	1428834_at
1.25	*Crlz1*	charged amino acid rich leucine zipper 1	1417583_a_at
1.25	*Tmco7*	transmembrane and coiled-coil domains 7	1458249_at
1.25	*Sfrs15*	splicing factor, arginine/serine-rich 15	1427333_s_at
1.25	*D11Bwg0517e*	Fox-1 homolog C	1456149_at
1.25	*1700012H17Rik*	family with sequence similarity 110, member B	1437150_at
1.24	*Rhbdd3*	rhomboid domain containing 3	1454719_at
1.24	*5730437N04Rik*	RIKEN cDNA 4933402O15 gene	1453591_at
1.24	*Hdac9*	histone deacetylase 9	1434572_at
1.24	*Tcof1*	Treacher Collins Franceschetti syndrome 1, homolog	1423601_s_at
1.24	*Shfdg1*	split hand/foot deleted gene 1	1418574_a_at
1.24	*Kdelc2*	KDEL (Lys-Asp-Glu-Leu) containing 2	1453071_s_at

1.24	*Shisa2*	shisa homolog 2 (Xenopus laevis)	1423852_at
1.24	*Ipo9*	importin 9	1439481_at
1.24	*6530403A03Rik*	RIKEN cDNA 6530403A03 gene	1425319_s_at
1.23	*Tanc2*	tetratricopeptide repeat, ankyrin repeat and coiled-coil containing 2	1435078_at
1.23	*Sh3bp5*	calpain 7	1421923_at
1.23	*Ppp1r14a*	protein phosphatase 1, regulatory (inhibitor) subunit 14A	1418086_at
1.23	*Ablim3*	actin binding LIM protein family, member 3	1434013_at
1.23	*Zfp354a*	zinc finger protein 354A	1420390_s_at
1.23	*Mrpl9*	mitochondrial ribosomal protein L9	1437749_s_at
1.23	*4921537I17Rik*	Mus musculus adult male testis cDNA, RIKEN full-length enriched library, clone:4921537I17 product:unknown EST, full insert sequence	1431259_at
1.23	*Evi5l*	ecotropic viral integration site 5 like	1430510_at
1.23	*Otop3*	otopetrin 3	1429036_at
1.23	*0610010K14Rik*	RIKEN cDNA 0610010K14 gene	1428679_s_at
1.23	*Commd1*	COMM domain containing 1	1424121_at
1.23	*Grb14*	growth factor receptor bound protein 14	1417673_at
1.23	*Fxc1*	fractured callus expressed transcript 1	1448887_x_at
1.23	*4921504N20Rik*	---	1440778_x_at
1.23	*Mrpl52*	mitochondrial ribosomal protein L52	1415762_x_at
1.22	*6720467C03Rik*	RIKEN cDNA 6720467C03 gene	1451570_a_at
1.22	*Syt7*	synaptotagmin VII	1439633_at
1.22	*Mtdh*	Metadherin	1434882_at
1.22	*Pprc1*	peroxisome proliferative activated receptor, gamma, coactivator-related 1	1426381_at
1.22	*Arpp19*	cAMP-regulated phosphoprotein 19	1422608_at
1.22	*Dhx9*	DEAH (Asp-Glu-Ala-His) box polypeptide 9	1451770_s_at
1.22	*Ash1l*	ash1 (absent, small, or homeotic)-like (Drosophila)	1450072_at
1.22	*Pfdn1*	prefoldin 1	1417026_at
1.22	*Tomm20*	translocase of outer mitochondrial membrane 20 homolog (yeast)	1455357_x_at
1.22	*Sec62*	SEC62 homolog (S. cerevisiae)	1454697_at
1.22	*Evi2a*	ecotropic viral integration site 2a	1450241_a_at
1.22	*2310009B15Rik*	Mus musculus adult male tongue cDNA, RIKEN full-length enriched library, clone:2310009B15 product:unknown EST, full insert sequence	1435776_at
1.22	*Sept6*	septin 6	1420877_at
1.22	*Cdh13*	cadherin 13	1454015_a_at
1.22	*Lmbr1l*	limb region 1 like	1451165_at
1.22	*Daam1*	dishevelled associated activator of morphogenesis 1	1458662_at
1.22	*Wtap*	Wilms' tumour 1-associating protein	1454805_at
1.22	*Atpaf1*	ATP synthase mitochondrial F1 complex assembly factor 1	1434934_at
1.22	*Ndufb6*	NADH dehydrogenase (ubiquinone) 1 beta subcomplex, 6	1434056_a_at
1.22	*Arrdc4*	arrestin domain containing 4	1424759_at
1.22	*Srp14*	signal recognition particle 14	1454615_x_at
1.22	*Cdc42ep3*	CDC42 effector protein (Rho GTPase binding) 3	1450700_at
1.22	*Psmg2*	proteasome (prosome, macropain) assembly chaperone 2	1448212_at
1.22	*Rex3*	reduced expression 3	1428209_at
1.22		Mus musculus transcribed sequences	1457141_at
1.22	*Rpl27*	ribosomal protein L27	1448217_a_at
1.22	*Efna2*	ephrin A2	1444606_at
1.22	*Dkc1*	dyskeratosis congenita 1, dyskerin homolog (human)	1438016_at
1.22	*B4galt6*	UDP-Gal:betaGlcNAc beta 1,4-galactosyltransferase, polypeptide 6	1435758_at
1.22	*Cmc1*	COX assembly mitochondrial protein homolog (S. cerevisiae)	1431510_s_at
1.22	*Trim8*	tripartite motif protein 8	1418577_at
1.21	*Zrf2*	zuotin related factor 2	1448794_s_at
1.21	*Psmc3ip*	proteasome (prosome, macropain) 26S subunit, ATPase 3, interacting protein	1425271_at
1.21	*Mrps36*	mitochondrial ribosomal protein S36	1423242_at
1.21	*Slc35a4*	solute carrier family 35, member A4	1456013_x_at
1.21	*Rps24*	ribosomal protein S24	1453362_x_at

1.21	*Usp6nl*	USP6 N-terminal like	1440883_at
1.21	*Pan3*	PAN3 polyA specific ribonuclease subunit homolog (S. cerevisiae)	1428768_at
1.21	*Sat1*	spermidine/spermine N1-acetyl transferase 1	1420502_at
1.21	*1500019G21Rik*	RIKEN cDNA 1500019G21 gene	1416894_at
1.21	*Ppfibp1*	PTPRF interacting protein, binding protein 1 (liprin beta 1)	1452759_s_at
1.21	*4930430E16Rik*	family with sequence similarity 161, member A	1443569_at
1.21	*Bms1l*	BMS1-like, ribosome assembly protein (yeast)	1433636_at
1.21	*Ndufs5*	NADH dehydrogenase (ubiquinone) Fe-S protein 5	1416495_s_at
1.21	*Fkbp8*	FK506 binding protein 8	1416113_at
1.21	*Tbca*	tubulin cofactor a	1456205_x_at
1.21	*Angel2*	angel homolog 2 (Drosophila)	1448360_s_at
1.21	*Cox17*	cytochrome c oxidase, subunit XVII assembly protein homolog (yeast)	1434435_s_at
1.21	*2810002O09Rik*	family with sequence similarity 123, member B	1439565_at
1.21	*Cog1*	component of oligomeric golgi complex 1	1433774_x_at
1.21	*Tctex1*	t-complex testis expressed 1	1428116_a_at
1.21	*3110009E18Rik*	RIKEN cDNA 3110009E18 gene	1428023_at
1.21	*Nef3*	neurofilament 3, medium	1422520_at
1.21	*Shfdg1*	split hand/foot deleted gene 1	1418575_at
1.21	*Cetn3*	centrin 3	1417239_at
1.20	*A230106M20Rik*	RIKEN cDNA A230106M20 gene	1458997_at
1.20	*1200016B10Rik*	RIKEN cDNA 1200016B10 gene	1452859_at
1.20	*Rpl37*	ribosomal protein L37	1438291_x_at
1.20	*D11Bwg0517e*	Fox-1 homolog C	1436450_at
1.20	*Vav3*	vav 3 oncogene	1417123_at
1.20	*Snrpe*	small nuclear ribonucleoprotein E	1451294_s_at
1.20	*Tspan2*	tetraspanin 2	1424567_at
1.20	*Wdr31*	WD repeat domain 31	1459664_at
1.20	*Giyd2*	GIY-YIG domain containing 2	1454082_a_at
1.20	*Hdac2*	histone deacetylase 2	1449080_at
1.20	*Scamp2*	secretory carrier membrane protein 2	1448404_at
1.20	*Stx1a*	syntaxin 1A (brain)	1437390_x_at
1.20	*D2Bwg1335e*	DNL-type zinc finger protein	1435528_at
1.20	*Abl1*	c-abl oncogene 1, receptor tyrosine kinase	1423999_at
1.20	*Ndufb5*	NADH dehydrogenase (ubiquinone) 1 beta subcomplex, 5	1417102_a_at
1.20	*Mrpl12*	mitochondrial ribosomal protein L12	1452048_at
1.20	*Gtf3c5*	general transcription factor IIIC, polypeptide 5	1423998_at
1.20	*Epc1*	enhancer of polycomb homolog 1 (Drosophila)	1440742_at
1.20	*Rpl37*	ribosomal protein L37	1434872_x_at
1.20	*2310005N03Rik*	RIKEN cDNA 2310005N03 gene	1428619_at
1.20	*Csnk1e*	casein kinase 1, epsilon	1417175_at
1.20	*Dcun1d5*	DCN1, defective in cullin neddylation 1, domain containing 5 (S. cerevisiae)	1432271_a_at
1.20	*6330416L07Rik*	RIKEN cDNA 6330416L07 gene	1425085_at
1.20	*Cdk4*	cyclin-dependent kinase 4	1422439_a_at
1.20	*Rpl22*	ribosomal protein L22	1416603_at
1.20	*Ncl*	nucleolin	1415772_at
1.20	*A130090K04Rik*	RIKEN cDNA A130090K04 gene	1439808_at
1.20	*4930420K17Rik*	RIKEN cDNA 4930420K17 gene	1436337_at
1.20	*Dut*	deoxyuridine triphosphatase	1419270_a_at
1.20	*Rps12*	ribosomal protein S12	1416453_x_at
1.19	*Rgl1*	ral guanine nucleotide dissociation stimulator,-like 1	1449124_at
1.19	*Irak1*	interleukin-1 receptor-associated kinase 1	1448668_a_at
1.19	*Pawr*	PRKC, apoptosis, WT1, regulator	1426910_at
1.19	*Atp6ap2*	ATPase, H+ transporting, lysosomal accessory protein 2	1423662_at
1.19	*Crmp1*	collapsin response mediator protein 1	1448289_at
1.19	*Tmem85*	transmembrane protein 85 Gene	1438369_x_at

1.19	*Saps1*	SAPS domain family, member 1	1436306_at
1.19	*Thtpa*	thiamine triphosphatase	1433436_s_at
1.19	*Rbm18*	RIKEN cDNA 2010004P11 gene	1420608_at
1.19	*Kdelr1*	KDEL (Lys-Asp-Glu-Leu) endoplasmic reticulum protein retention receptor 1	1460211_a_at
1.19	*Ubxn2b*	UBX domain protein 2B	1449122_at
1.19	*Wdr9*	WD repeat domain 9	1433955_at
1.19	*Tmco1*	transmembrane and coiled-coil domains 1	1423759_a_at
1.19	*5530601H04Rik*	Mus musculus 0 day neonate kidney cDNA, RIKEN full-length enriched library, clone:D630033M22 product:hypothetical protein, full insert sequence	1452750_at
1.19	*Rps24*	ribosomal protein S24	1428530_x_at
1.19	*Srd5a2l*	steroid 5 alpha-reductase 2-like	1423574_s_at
1.19	*Cycs*	cytochrome c, somatic	1422484_at
1.19	*Cnot6*	CCR4-NOT transcription complex, subunit 6	1418273_a_at
1.19	*Snrpd1*	small nuclear ribonucleoprotein D1	1416336_s_at
1.19	*Dbi*	diazepam binding inhibitor	1455976_x_at
1.19	*Wdr77*	WD repeat domain 77	1434552_at
1.19	*2810002N01Rik*	RIKEN cDNA 2810002N01 gene	1429248_at
1.19	*Crym*	crystallin, mu	1416776_at
1.19	*1110003E01Rik*	RIKEN cDNA 1110003E01 gene	1416767_a_at
1.19	*6430571L13Rik*	RIKEN cDNA 6430571L13 gene	1458456_x_at
1.19	*2810002D19Rik*	RIKEN cDNA 2810002D19 gene	1452312_at
1.19	*A630054L15Rik*	family with sequence similarity 116, member A	1451568_at
1.19	*Ebf1*	early B-cell factor 1	1448293_at
1.19	*Rps7*	ribosomal protein S7	1435593_x_at
1.19	*Smo*	smoothened homolog (Drosophila)	1427049_s_at
1.19	*Klhdc2*	kelch domain containing 2	1460678_at
1.19	*Zdhhc24*	zinc finger, DHHC domain containing 24	1452719_at
1.19	*Mdc1*	mediator of DNA damage checkpoint 1	1434837_at
1.19	*AI428479*	Mus musculus transcribed sequences	1434422_at
1.19	*Pkia*	protein kinase inhibitor, alpha	1420859_at
1.19	*Mbd3*	methyl-CpG binding domain protein 3	1417728_at
1.18	*Ppil6*	sphingomyelin phosphodiesterase 2, neutral	1453310_at
1.18	*Fbxl10*	F-box and leucine-rich repeat protein 10	1452198_at
1.18	*Sesn1*	sestrin 1	1433711_s_at
1.18	*2310022M17Rik*	RIKEN cDNA 2310022M17 gene	1428293_at
1.18	*Zfp91*	zinc finger protein 91	1426326_at
1.18	*Nsmce1*	non-SMC element 1 homolog (S. cerevisiae)	1455927_x_at
1.18	*Vps29*	vacuolar protein sorting 29 (S. pombe)	1417660_s_at
1.18	*Stoml1*	stomatin-like 1	1452738_at
1.18	*Rps27l*	ribosomal protein S27-like	1435429_x_at
1.18	*Sec63*	SEC63-like (S. cerevisiae)	1424924_at
1.18	*Rbbp7*	Mus musculus transcribed sequences	1456227_x_at
1.18	*Pmvk*	phosphomevalonate kinase	1427893_a_at
1.18	*Hint1*	histidine triad nucleotide binding protein	1424018_at
1.18	*Brp44*	brain protein 44	1423833_a_at
1.18	*Nfe2l2*	nuclear, factor, erythroid derived 2, like 2	1416543_at
1.18	*Magoh*	mago-nashi homolog, proliferation-associated (Drosophila)	1416212_at
1.18	*Ell*	elongation factor RNA polymerase II	1460643_at
1.18	*Cacnb3*	calcium channel, voltage-dependent, beta 3 subunit	1448656_at
1.18	*1110054O05Rik*	RIKEN cDNA 1110054O05 gene	1429242_at
1.18	*Mark2*	MAP/microtubule affinity-regulating kinase 2	1415952_at
1.18	*Gabpa*	GA repeat binding protein, alpha	1450664_at
1.18	*Enoph1*	enolase-phosphatase 1	1423705_at
1.18	*Cobra1*	cofactor of BRCA1	1421292_a_at
1.18	*Mast1*	RIKEN cDNA 9430008B02 gene	1449423_at
1.18	*Mrpl44*	mitochondrial ribosomal protein L44	1437391_x_at

1.18	*Sdccag33*	serologically defined colon cancer antigen 33	1427233_at
1.18	*2900092E17Rik*	RIKEN cDNA 2900092E17 gene	1424014_at
1.18	*Siat7d*	sialyltransferase 7 ((alpha-N-acetylneuraminyl 2,3-betagalactosyl-1,3)-N-acetyl galactosaminide alpha-2,6-sialyltransferase) D	1418074_at
1.18	*Nfia*	nuclear factor I/A	1456087_at
1.18	*Rdbp*	RD RNA-binding protein	1450705_at
1.18	*Ube2f*	predicted gene, EG432649	1450275_x_at
1.18	*1110002B05Rik*	RIKEN cDNA 1110002B05 gene	1448388_a_at
1.18	*Prickle4*	prickle homolog 4 (Drosophila)	1437336_x_at
1.18	*St5*	suppression of tumorigenicity 5	1428372_at
1.18	*Stk24*	FERM, RhoGEF (Arhgef) and pleckstrin domain protein 1 (chondrocyte-derived)	1426248_at
1.17	*Nfib*	nuclear factor I/B	1454834_at
1.17	*Sort1*	sortilin 1	1423363_at
1.17	*Ihpk1*	inositol hexaphosphate kinase 1	1422969_s_at
1.17	*Dirc2*	disrupted in renal carcinoma 2 (human)	1454654_at
1.17	*Tarsl2*	threonyl-tRNA synthetase-like 2	1434738_at
1.17	*AC139040.8*	40S ribosomal protein S12	1433432_x_at
1.17	*Ube2e2*	ubiquitin-conjugating enzyme E2E 2 (UBC4/5 homolog, yeast)	1424358_at
1.17	*Gp1bb*	glycoprotein Ib, beta polypeptide	1422977_at
1.17	*Zfp36l1*	zinc finger protein 36, C3H type-like 1	1422528_a_at
1.17	*Khdrbs1*	KH domain containing, RNA binding, signal transduction associated 1	1418629_a_at
1.17	*Ctbp1*	C-terminal binding protein 1	1415702_a_at
1.17	*Ly6e*	lymphocyte antigen 6 complex, locus E	1453304_s_at
1.17	*Aptx*	aprataxin	1450921_at
1.17	*Mafb*	v-maf musculoaponeurotic fibrosarcoma oncogene family, protein B (avian)	1435335_a_at
1.17	*Med9*	mediator of RNA polymerase II transcription, subunit 9 homolog (yeast)	1419377_at
1.17	*Sox2*	SRY-box containing gene 2	1416967_at
1.17	*Rps10*	ribosomal protein S10	1438723_a_at
1.17	*Ankrd17*	ankyrin repeat domain 17	1436775_a_at
1.17	*BC017158*	UPF0420 protein C16orf58 homolog	1424812_at
1.17	*Cdc26*	cell division cycle 26	1423987_at
1.17	*Tfpt*	transmembrane channel-like gene family 4	1418064_at
1.17	*Spin*	spindlin	1415794_a_at
1.17	*Sf3a2*	splicing factor 3a, subunit 2	1455546_s_at
1.17	*U2af1-rs2*	U2 small nuclear ribonucleoprotein auxiliary factor (U2AF) 1, related sequence 2	1442154_at
1.17	*Zfp513*	zinc finger protein 513	1437483_at
1.17	*Gpkow*	G patch domain and KOW motifs	1434344_at
1.17	*Ccdc90b*	coiled-coil domain containing 90B	1428505_at
1.17	*Rbm28*	RNA binding motif protein 28	1426513_at
1.17	*Rpl21*	ribosomal protein L21	1455767_x_at
1.17	*1500001M20Rik*	RIKEN cDNA 1500001M20 gene	1428684_at
1.17	*Eif1b*	eukaryotic translation initiation factor 1B	1428272_at
1.17	*Rabl4*	RAB, member of RAS oncogene family-like 4	1424648_at
1.17	*Znhit2*	zinc finger, HIT domain containing 2	1416651_at
1.17	*Psma6*	proteasome (prosome, macropain) subunit, alpha type 6	1416506_at
1.17	*Gcsh*	glycine cleavage system protein H (aminomethyl carrier)	1432164_a_at
1.17	*Tysnd1*	trypsin domain containing 1	1428689_at
1.17	*Gatc*	glutamyl-tRNA(Gln) amidotransferase, subunit C homolog (bacterial)	1425211_at
1.17	*Echdc1*	enoyl Coenzyme A hydratase domain containing 1	1425001_at
1.17	*Nck2*	non-catalytic region of tyrosine kinase adaptor protein 2	1416796_at
1.16	*Jund1*	Jun proto-oncogene related gene d1	1449117_at
1.16	*Wdr48*	WD repeat domain 48	1443836_x_at
1.16	*Hsdl2*	hydroxysteroid dehydrogenase like 2	1426856_at
1.16	*Ddx26*	DEAD/H (Asp-Glu-Ala-Asp/His) box polypeptide 26	1423275_at
1.16	*Yy1*	YY1 transcription factor	1422570_at

1.16	*Ssb*	Sjogren syndrome antigen B	1416421_a_at
1.16	*L3mbtl3*	l(3)mbt-like 3 (Drosophila)	1454882_at
1.16	*Ube2a*	ubiquitin-conjugating enzyme E2A, RAD6 homolog (S. cerevisiae)	1417609_at
1.16	*Rpl22*	ribosomal protein L22	1453118_s_at
1.16	*Wdr32*	WD repeat domain 32	1438727_at
1.16	*AI316807*	Uncharacterized protein C8orf40 homolog	1438199_at
1.16	*Vapb*	vesicle-associated membrane protein, associated protein B and C	1436079_s_at
1.16	*Rps10*	ribosomal protein S10	1434854_a_at
1.16	*Kif16b*	kinesin family member 16B	1429062_at
1.16	*Ptch1*	patched homolog 1	1428853_at
1.16	*Prr6*	proline-rich polypeptide 6	1428706_at
1.16	*Lrrc42*	leucine rich repeat containing 42	1424049_at
1.16	*E130012K09*	hypothetical protein E130012K09	1457737_at
1.16	*Hint1*	histidine triad nucleotide binding protein	1424017_a_at
1.16	*AC121926.3*	Mitochondrial import inner membrane translocase subunit Tim16 (Mitochondria-associated granulocyte macrophage CSF-signaling molecule)	1416765_s_at
1.16	*Rragc*	Ras-related GTP binding C	1415749_a_at
1.16	*Ndufv2*	NADH dehydrogenase (ubiquinone) flavoprotein 2	1452692_a_at
1.16	*Ube2v1*	ubiquitin-conjugating enzyme E2 variant 1	1444523_s_at
1.16	*Gats*	opposite strand transcription unit to Stag3	1437252_at
1.16	*Rab11b*	RAB11B, member RAS oncogene family	1435253_at
1.16	*Bclaf1*	BCL2-associated transcription factor 1	1428844_a_at
1.16	*Ndufa1*	NADH dehydrogenase (ubiquinone) 1 alpha subcomplex, 1	1422241_a_at
1.16	*Mkrn2*	makorin, ring finger protein, 2	1417935_at
1.16	*Mosc2*	MOCO sulphurase C-terminal domain containing 2	1416766_at
1.16	*Txn1*	thioredoxin 1	1416119_at
1.16	*Znhit1*	zinc finger, HIT domain containing 1	1451745_a_at
1.16	*Rab9*	RAB9, member RAS oncogene family	1448391_at
1.16	*Ncoa6*	nuclear receptor coactivator 6	1423374_at
1.16	*Yeats4*	YEATS domain containing 4	1423105_a_at
1.15	*Poldip3*	polymerase (DNA-directed), delta interacting protein 3	1437335_x_at
1.15	*Arhgap21*	Rho GTPase activating protein 21	1428369_s_at
1.15	*Tomm7*	translocase of outer mitochondrial membrane 7 homolog (yeast)	1428214_at
1.15	*Myst4*	MYST histone acetyltransferase (monocytic leukemia) 4	1423508_at
1.15	*Ubxn1*	UBX domain protein 1	1436342_a_at
1.15	*Rps21*	ribosomal protein S21	1430288_x_at
1.15	*Zipro1*	zinc finger proliferation 1	1420095_s_at
1.15	*Rps20*	ribosomal protein S20	1456436_x_at
1.15	*Cox5a*	cytochrome c oxidase, subunit Va	1448153_at
1.15	*Ndufs6*	NADH dehydrogenase (ubiquinone) Fe-S protein 6	1433603_at
1.15	*Sfrs10*	splicing factor, arginine/serine-rich 10 (transformer 2 homolog, Drosophila)	1427432_a_at
1.15	*Gcn5l2*	GCN5 general control of amino acid synthesis-like 2 (yeast)	1426783_at
1.15	*Sui1-rs1*	suppressor of initiator codon mutations, related sequence 1 (S. cerevisiae)	1423799_at
1.15	*Rnf220*	ring finger protein 220	1415717_at
1.15	*Ube2a*	ubiquitin-conjugating enzyme E2A, RAD6 homolog (S. cerevisiae)	1448772_at
1.15	*Mfhas1*	malignant fibrous histiocytoma amplified sequence 1	1429005_at
1.15	*Ndufb10*	NADH dehydrogenase (ubiquinone) 1 beta subcomplex, 10	1428322_a_at
1.15	*Tcf12*	transcription factor 12	1427670_a_at
1.15	*Ssbp3*	single-stranded DNA binding protein 3	1425940_a_at
1.15	*Hagh*	hydroxyacyl glutathione hydrolase	1424172_at
1.15	*Ndufb9*	NADH dehydrogenase (ubiquinone) 1 beta subcomplex, 9	1452184_at
1.15	*Prss12*	protease, serine, 12 neurotrypsin (motopsin)	1447896_s_at
1.15	*BC023814*	UPF0431 protein C1orf66 homolog	1433961_at
1.15	*Phip*	pleckstrin homology domain interacting protein	1429004_at
1.15	*6330403K07Rik*	RIKEN cDNA 6330403K07 gene	1426766_at
1.15	*Setd8*	SET domain containing (lysine methyltransferase) 8	1426406_at

1.15	*Cnp1*	cyclic nucleotide phosphodiesterase 1	1418980_a_at
1.15	*Mrpl52*	mitochondrial ribosomal protein L52	1460701_a_at
1.15	*Ndufb6*	NADH dehydrogenase (ubiquinone) 1 beta subcomplex, 6	1434057_at
1.15	*6430548M08Rik*	RIKEN cDNA 6430548M08 gene	1425637_at
1.15	*Myo1c*	myosin IC	1419649_s_at
1.15	*Zfyve20*	zinc finger, FYVE domain containing 20	1456754_at
1.15	*Ndufb2*	NADH dehydrogenase (ubiquinone) 1 beta subcomplex, 2	1448483_a_at
1.15	*Hmgcs1*	3-hydroxy-3-methylglutaryl-Coenzyme A synthase 1	1433445_x_at
1.15	*Rps10*	ribosomal protein S10	1456497_x_at
1.15	*Zfp715*	zinc finger protein 715	1434461_at
1.15	*March5*	membrane-associated ring finger (C3HC4) 5	1428843_at
1.15	*Polr2i*	polymerase (RNA) II (DNA directed) polypeptide I	1428494_a_at
1.15	*Sdbcag84*	serologically defined breast cancer antigen 84	1423548_s_at
1.15	*Ptprf*	protein tyrosine phosphatase, receptor type, F	1420842_at
1.14	*Bcap37*	B-cell receptor-associated protein 37	1455713_x_at
1.14	*Pi4k2a*	phosphatidylinositol 4-kinase type 2 alpha	1454605_a_at
1.14	*Rpl18*	Mus musculus transcribed sequence with weak similarity to protein ref:NP_000970.1 (H.sapiens) ribosomal protein L18; 60S ribosomal protein L18 [Homo sapiens]	1436699_x_at
1.14	*Ube1dc1*	ubiquitin-activating enzyme E1-domain containing 1	1435247_at
1.14	*Skiip*	SKI interacting protein	1429002_at
1.14	*Mrpl30*	mitochondrial ribosomal protein L30	1423857_at
1.14	*Ranbp9*	RAN binding protein 9	1422736_at
1.14	*Tnpo3*	transportin 3	1419950_s_at
1.14	*Gkap1*	G kinase anchoring protein 1	1417594_at
1.14	*Rab6*	RAB6, member RAS oncogene family	1448304_a_at
1.14	*Eif4el3*	eukaryotic translation initiation factor 4E like 3	1435803_a_at
1.14	*Apoe*	apolipoprotein E	1432466_a_at
1.14	*1600027N09Rik*	RIKEN cDNA 1600027N09 gene	1428366_at
1.14	*Acsl5*	fatty acid Coenzyme A ligase, long chain 5	1428082_at
1.14	*Syap1*	synapse associated protein 1	1416472_at
1.14	*Mtch1*	mitochondrial carrier homolog 1 (C. elegans)	1460718_s_at
1.14	*Socs7*	Nck, Ash and phospholipase C binding protein	1455402_at
1.14	*Thoc7*	THO complex 7 homolog (Drosophila)	1448461_a_at
1.14	*Med10*	mediator of RNA polymerase II transcription, subunit 10 homolog (NUT2, S. cerevisiae)	1448295_at
1.14	*Limch1*	LIM and calponin homology domains 1	1435106_at
1.14	*Dlat*	dihydrolipoamide S-acetyltransferase (E2 component of pyruvate dehydrogenase complex)	1426264_at
1.14	*Blcap*	bladder cancer associated protein homolog (human)	1420631_a_at
1.14	*Faim*	Fas apoptotic inhibitory molecule	1418029_at
1.14	*Chmp4b*	chromatin modifying protein 4B	1451988_s_at
1.14	*Ppp1r2*	protein phosphatase 1, regulatory (inhibitor) subunit 2	1448684_at
1.14	*Kpnb1*	karyopherin (importin) beta 1	1448526_at
1.14	*Ppp2r2c*	protein phosphatase 2 (formerly 2A), regulatory subunit B (PR 52), gamma isoform	1438671_at
1.14	*Sept2*	septin 2	1435985_at
1.14	*Kif3c*	kinesin family member 3C	1434947_at
1.14	*Eif2ak1*	eukaryotic translation initiation factor 2 alpha kinase 1	1421901_at
1.14	*Tubg1*	tubulin, gamma 1	1417144_at
1.14	*Atp5j2*	ATP synthase, H+ transporting, mitochondrial F0 complex, subunit f, isoform 2	1416269_at
1.14	*Mdm4*	transformed mouse 3T3 cell double minute 4	1460542_s_at
1.14	*Rbm27*	RNA binding motif protein 27	1456058_at
1.14	*Serbp1*	Serpine1 mRNA binding protein 1	1441501_at
1.14	*Samhd1*	SAM domain and HD domain, 1	1434438_at
1.14	*1600002H07Rik*	RIKEN cDNA 1600002H07 gene	1428832_at
1.14	*Tmem70*	transmembrane protein 70	1424541_at

1.14	*Cygb*	cytoglobin	1423630_at
1.14	*Tce4*	T-complex expressed gene 4	1420326_s_at
1.14	*Rpl36*	ribosomal protein L36	1416519_at
1.14	*Tubb3*	tubulin, beta 3	1415978_at
1.14	*Podxl2*	podocalyxin-like 2	1455622_at
1.14	*Cxxc5*	RIKEN cDNA 4930415K17 gene	1448960_at
1.14	*Igfbp4*	insulin-like growth factor binding protein 4	1437405_a_at
1.14	*Rpl13a*	ribosomal protein L13a	1435873_a_at
1.14	*Nutf2*	nuclear transport factor 2	1434367_s_at
1.14	*Ndufs7*	NADH dehydrogenase (ubiquinone) Fe-S protein 7	1424313_a_at
1.14	*Ncbp2*	nuclear cap binding protein subunit 2	1423045_at
1.14	*Dia1*	diaphorase 1 (NADH)	1422186_s_at
1.14	*Mettl9*	methyltransferase like 9	1417710_at
1.14	*Qser1*	glutamine and serine rich 1	1452331_s_at
1.14	*Ptdss2*	phosphatidylserine synthase 2	1450354_a_at
1.14	*Neurod4*	neurogenic differentiation 4	1436694_s_at
1.14	*Ssbp3*	single-stranded DNA binding protein 3	1427917_s_at
1.14	*Fads1*	fatty acid desaturase 1	1423680_at
1.14	*Ube2l3*	ubiquitin-conjugating enzyme E2L 3	1417908_s_at
1.14	*Atp5j*	ATP synthase, H+ transporting, mitochondrial F0 complex, subunit F	1416143_at
1.14	*1700029F09Rik*	RIKEN cDNA 1700029F09 gene	1428593_at
1.14	*Dnajc9*	DnaJ (Hsp40) homolog, subfamily C, member 9	1426473_at
1.13	*Drap1*	Dr1 associated protein 1 (negative cofactor 2 alpha)	1451676_at
1.13	*Kcnh2*	potassium voltage-gated channel, subfamily H (eag-related), member 2	1449544_a_at
1.13	*Clp1*	cardiac lineage protein 1	1419359_at
1.13	*Fbxo8*	F-box only protein 8	1418510_s_at
1.13	*Rabac1*	Rab acceptor 1 (prenylated)	1427773_a_at
1.13	*Grcc10*	gene rich cluster, C10 gene	1416522_a_at
1.13	*Nipsnap3a*	nipsnap homolog 3A (C. elegans)	1448967_at
1.13	*Ndufb5*	NADH dehydrogenase (ubiquinone) 1 beta subcomplex, 5	1448589_at
1.13	*Lysmd2*	LysM, putative peptidoglycan-binding, domain containing 2	1428626_at
1.13	*1810063B07Rik*	RIKEN cDNA 1810063B07 gene	1427905_at
1.13	*Dnajc14*	DnaJ (Hsp40) homolog, subfamily C, member 14	1426553_at
1.13	*Wbscr18*	Williams-Beuren syndrome chromosome region 18 homolog (human)	1418081_at
1.13	*Msh6*	mutS homolog 6 (E. coli)	1416915_at
1.13	*Rnf153*	membrane-associated ring finger (C3HC4) 5	1452925_a_at
1.13	*Atp5k*	ATP synthase, H+ transporting, mitochondrial F1F0 complex, subunit e	1434053_x_at
1.13	*Caml*	calcium modulating ligand	1417842_at
1.13	*Rpl35a*	ribosomal protein L35a	1417317_s_at
1.13	*Tm4sf8*	transmembrane 4 superfamily member 8	1416009_at
1.13	*2610204K03Rik*	Sec24 related gene family, member C (S. cerevisiae)	1452147_at
1.13	*Tomm7*	translocase of outer mitochondrial membrane 7 homolog (yeast)	1428215_x_at
1.13	*Hnrpr*	heterogeneous nuclear ribonucleoprotein R	1427129_a_at
1.13	*Ube2m*	ubiquitin C, related sequence 2	1424345_s_at
1.13	*Thy1*	thymus cell antigen 1, theta	1423135_at
1.13	*Banf1*	barrier to autointegration factor 1	1421082_s_at
1.13	*Tce1*	T-complex expressed gene 1	1417891_at
1.13	*Stat3*	signal transducer and activator of transcription 3	1460700_at
1.13	*Sf3b2*	splicing factor 3b, subunit 2	1433461_at
1.13	*Calm2*	calmodulin 3	1422414_a_at
1.13	*6330500D04Rik*	RIKEN cDNA 6330500D04 gene	1460555_at
1.13	*Tctn2*	tectonic family member 2	1423224_at
1.13	*Ptp4a2*	protein tyrosine phosphatase 4a2	1420613_at
1.13	*Ccdc12*	coiled-coil domain containing 12	1419803_s_at
1.13	*Ppm1g*	protein phosphatase 1G (formerly 2C), magnesium-dependent, gamma isoform	1416792_at

1.12	*AC140307.3*	NAT11_MOUSE Isoform 2 of Q8VE10	1452120_at
1.12	*Ppp3cb*	protein phosphatase 3, catalytic subunit, beta isoform	1428473_at
1.12	*Fbxo3*	F-box only protein 3	1423491_at
1.12	*Ptbp2*	polypyrimidine tract binding protein 2	1423470_at
1.12	*Sca10*	spinocerebellar ataxia 10 homolog (human)	1422576_at
1.12	*Hras1*	Harvey rat sarcoma virus oncogene 1	1422407_s_at
1.12	*Dek*	DEK oncogene (DNA binding)	1452659_at
1.12	*Nnp1*	novel nuclear protein 1	1427720_a_at
1.12	*Trib2*	tribbles homolog 2 (Drosophila)	1426640_s_at
1.12	*Xpo7*	exportin 7	1415682_at
1.12	*Trpc4ap*	transient receptor potential cation channel, subfamily C, member 4 associated protein	1460720_at
1.12	*Clta*	clathrin, light polypeptide (Lca)	1434540_a_at
1.12	*C230096C10Rik*	RIKEN cDNA C230096C10 gene	1434021_at
1.12	*Lrrc47*	leucine rich repeat containing 47	1428451_at
1.12	*Smn*	survival motor neuron	1426596_a_at
1.12	*Hpcal1*	hippocalcin-like 1	1448812_at
1.12	*Hnrpab*	heterogeneous nuclear ribonucleoprotein A/B	1448144_at
1.12	*Rnps1*	ribonucleic acid binding protein S1	1438267_x_at
1.12	*Brsk2*	BR serine/threonine kinase 2	1431826_a_at
1.12	*Rtn1*	reticulon 1	1429761_at
1.12	*Dus3l*	dihydrouridine synthase 3-like (S. cerevisiae)	1424066_at
1.12	*Acas2*	acetyl-Coenzyme A synthetase 2 (ADP forming)	1422479_at
1.12	*Fbxo13*	F-box only protein 13	1452860_at
1.12	*Limk2*	LIM motif-containing protein kinase 2	1452060_a_at
1.12	*Rps8*	ribosomal protein S8	1437610_x_at
1.12	*Actr1b*	ARP1 actin-related protein 1 homolog B (yeast)	1426403_at
1.12	*Hspa9a*	heat shock protein, A	1418504_at
1.12	*Tmem132a*	transmembrane protein 132A	1416845_at
1.12	*Rps16*	ribosomal protein S16	1416404_s_at
1.12	*Npdc1*	neural proliferation, differentiation and control gene 1	1415919_at
1.12	*Fkbp1a*	FK506 binding protein 1a	1448184_at
1.12	*D030012E24Rik*	RIKEN cDNA D030012E24 gene	1436747_at
1.12	*Dgkd*	diacylglycerol kinase, delta	1433564_at
1.12	*Chmp2a*	chromatin modifying protein 2A	1425591_a_at
1.12	*Dnaja2*	DnaJ (Hsp40) homolog, subfamily A, member 2	1417183_at
1.12	*Rps8*	ribosomal protein S8	1455319_x_at
1.12	*Map1lc3a*	microtubule-associated protein 1 light chain 3 alpha	1451290_at
1.12	*Pdcd2l*	programmed cell death 2-like	1426845_at
1.12	*Odag*	GATA zinc finger domain containing 1	1425599_a_at
1.12	*Bax*	Bcl2-associated X protein	1416837_at
1.12	*Npm1*	nucleophosmin 1	1415839_a_at
1.12	*Rps6*	ribosomal protein S6	1454620_x_at
1.12	*Ctdp1*	CTD (carboxy-terminal domain, RNA polymerase II, polypeptide A) phosphatase, subunit 1	1452697_at
1.12	*Kctd3*	potassium channel tetramerisation domain containing 3	1436811_at
1.12	*Mll5*	serine/arginine-rich protein specific kinase 2	1434704_at
1.12	*Ube2d2*	ubiquitin-conjugating enzyme E2D 2	1416477_at
1.12	*Hmgb3*	high mobility group box 3	1416155_at
1.11	*Wbscr1*	Williams-Beuren syndrome chromosome region 1 homolog (human)	1438554_x_at
1.11	*Ppp1r1a*	protein phosphatase 1, regulatory (inhibitor) subunit 1A	1422605_at
1.11	*Rpl35*	ribosomal protein L35	1455950_x_at
1.11	*Nutf2*	nuclear transport factor 2	1449017_at
1.11	*Rpl14*	ribosomal protein L14	1436688_x_at
1.11	*Rpl14*	ribosomal protein L14	1433688_x_at
1.11	*Rpl21*	ribosomal protein L21	1429077_x_at

1.11	*Gnaq*	guanine nucleotide binding protein, alpha q polypeptide	1428938_at
1.11	*Ppp4r1*	protein phosphatase 4, regulatory subunit 1	1424294_at
1.11	*Ddx39*	DEAD (Asp-Glu-Ala-Asp) box polypeptide 39	1455814_x_at
1.11	*Psma3*	proteasome (prosome, macropain) subunit, alpha type 3	1448442_a_at
1.11	*Cs*	citrate synthase	1450667_a_at
1.11	*Atp5a1*	ATP synthase, H+ transporting, mitochondrial F1 complex, alpha subunit, isoform 1	1449710_s_at
1.11	*Bat1a*	HLA-B-associated transcript 1A	1448221_at
1.11	*Prdx1*	peroxiredoxin 1	1436691_x_at
1.11	*Nat5*	N-acetyltransferase 5 (ARD1 homolog, S. cerevisiae)	1418244_at
1.11	*Dnajc12*	DnaJ (Hsp40) homolog, subfamily C, member 12	1417441_at
1.11	*Cdc42ep4*	CDC42 effector protein (Rho GTPase binding) 4	1416511_a_at
1.11	*Smad1*	MAD homolog 1 (Drosophila)	1459843_s_at
1.11	*Ndufa12*	NADH dehydrogenase (ubiquinone) 1 alpha subcomplex, 12	1455806_x_at
1.11	*Pcbp4*	poly(rC) binding protein 4	1449055_x_at
1.11	*Tceb2*	serine/arginine repetitive matrix 2	1436949_a_at
1.11	*Rpl17*	ribosomal protein L17	1435791_x_at
1.11	*Srm*	spermidine synthase	1421260_a_at
1.11	*Snx25*	sorting nexin 25	1455020_at
1.11	*Pcnxl3*	pecanex-like 3 (Drosophila)	1451328_at
1.11	*Rpl36al*	ribosomal protein L36a-like	1448697_s_at
1.11	*AC132435.3*	coiled-coil domain containing 6	1428311_at
1.11	*Aof2*	amine oxidase (flavin containing) domain 2	1426762_s_at
1.11	*Bnip2*	BCL2/adenovirus E1B 19kDa-interacting protein 1, NIP2	1422490_at
1.11	*Sin3a*	transcriptional regulator, SIN3A (yeast)	1419101_at
1.11	*Wdr5*	WD repeat domain 5	1416581_at
1.11	*Sgta*	small glutamine-rich tetratricopeptide repeat (TPR)-containing, alpha	1451067_at
1.11	*Arhgef12*	Rho guanine nucleotide exchange factor (GEF) 12	1423902_s_at
1.11	*Snx3*	sorting nexin 3	1422480_at
1.11	*Maged1*	melanoma antigen, family D, 1	1450062_a_at
1.11	*Cox4i1*	cytochrome c oxidase subunit IV isoform 1	1448322_a_at
1.11	*Rpl31*	ribosomal protein L31	1436924_x_at
1.11	*Pak1ip1*	glycerophosphodiester phosphodiesterase domain containing 1	1423766_at
1.10	*Vps26b*	vacuolar protein sorting 26 homolog B (yeast)	1453762_at
1.10	*Dbi*	diazepam binding inhibitor	1433991_x_at
1.10	*Ran*	Mus musculus transcribed sequence with strong similarity to protein pdb:1I2M (H.sapiens) A Chain A, Ran-Rcc1-So4 Complex	1433569_x_at
1.10	*Chgb*	chromogranin B	1415885_at
1.10	*Ncl*	nucleolin	1415771_at
1.10	*Ndufv2*	NADH dehydrogenase (ubiquinone) flavoprotein 2	1438159_x_at
1.10	*Egflam*	EGF-like, fibronectin type III and laminin G domains	1434647_at
1.10	*Ptgr2*	prostaglandin reductase 2	1433503_at
1.10	*Tceb1*	transcription elongation factor B (SIII), polypeptide 1	1427914_a_at
1.10	*Fbxo9*	f-box only protein 9	1417480_at
1.10	*Ubl1*	ubiquitin-like 1	1456349_x_at
1.10	*Copb2*	coatomer protein complex, subunit beta 2 (beta prime)	1456175_a_at
1.10	*Cbx5*	chromobox homolog 5 (Drosophila HP1a)	1454636_at
1.10	*Fkbp3*	FK506 binding protein 3	1416859_at
1.10	*Trappc1*	trafficking protein particle complex 1	1436019_a_at
1.10	*Tssc4*	tumor-suppressing subchromosomal transferable fragment 4	1427661_a_at
1.10	*Fh1*	fumarate hydratase 1	1424828_a_at
1.10	*Rpl35*	ribosomal protein L35	1454856_x_at
1.10	*2700081O15Rik*	RIKEN cDNA 2700081O15 gene	1437291_at
1.10	*BC002199*	cDNA sequence BC002199	1426234_s_at
1.10	*B230219D22Rik*	RIKEN cDNA B230219D22 gene	1424005_at
1.10	*Actr10*	ARP10 actin-related protein 10 homolog (S. cerevisiae)	1417157_at

1.10	*D330038O06Rik*	RIKEN cDNA D330038O06 gene	1455334_at
1.10	*Sfrs4*	splicing factor, arginine/serine-rich 4 (SRp75)	1448778_at
1.10	*Centg2*	centaurin, gamma 2	1437394_at
1.10	*Cln3*	ceroid lipofuscinosis, neuronal 3, juvenile (Batten, Spielmeyer-Vogt disease)	1417551_at
1.10	*Trspap1*	tRNA selenocysteine associated protein 1	1428747_at
1.10	*Mapt*	microtubule-associated protein tau	1424719_a_at
1.10	*Prdx2*	peroxiredoxin 2	1418506_a_at
1.10	*Vdac3*	voltage-dependent anion channel 3	1416175_a_at
1.10	*Lrrc40*	leucine rich repeat containing 40	1448720_at
1.10	*2900010M23Rik*	RIKEN cDNA 2900010M23 gene	1448685_at
1.10	*Snrpb*	small nuclear ribonucleoprotein B	1437193_s_at
1.10	*Sdccag8*	serologically defined colon cancer antigen 8	1435260_at
1.10	*Pnrc1*	proline-rich nuclear receptor coactivator 1	1433668_at
1.10	*6720456B07Rik*	RIKEN cDNA 6720456B07 gene	1423188_a_at
1.09	*Np15*	nuclear protein 15.6	1455911_x_at
1.09	*Rpl29*	ribosomal protein L29	1454627_a_at
1.09	*Rpl18*	ribosomal protein L18	1437005_a_at
1.09	*Akirin2*	akirin 2	1428237_at
1.09	*Pofut2*	protein O-fucosyltransferase 2	1416573_at
1.09	*Ppp1ca*	protein phosphatase 1, catalytic subunit, alpha isoform	1460165_at
1.09	*Sltm*	SAFB-like, transcription modulator	1424452_at
1.09	*Rbmxrt*	RNA binding motif protein, X chromosome retrogene	1416177_at
1.09	*Usp7*	ubiquitin specific protease 7	1454948_at
1.09	*Gcap14*	granule cell antiserum positive 14	1452223_s_at
1.09	*Fliih*	flightless I homolog (Drosophila)	1448189_a_at
1.09	*Ndufa12*	NADH dehydrogenase (ubiquinone) 1 alpha subcomplex, 12	1433513_x_at
1.09	*Unc45a*	unc-45 homolog A (C. elegans)	1415866_at
1.09	*Actr3*	ARP3 actin-related protein 3 homolog (yeast)	1452051_at
1.09	*Tprgl*	transformation related protein 63 regulated like	1451172_at
1.09	*Wdr61*	WD repeat domain 61	1448102_a_at
1.09	*Ubqln4*	ubiquilin 4	1448691_at
1.09	*Thap4*	THAP domain containing 4	1424052_at
1.09	*Gosr2*	golgi SNAP receptor complex member 2	1419371_s_at
1.09	*Ifrg15*	interferon alpha responsive gene	1418115_s_at
1.09	*Rpl24*	ribosomal protein L24	1460201_a_at
1.09	*Zfp90*	zinc finger protein 90	1449126_at
1.08	*Leo1*	Leo1, Paf1/RNA polymerase II complex component, homolog (S. cerevisiae)	1455293_at
1.08	*Gnb2*	guanine nucleotide binding protein, beta 2	1450623_at
1.08	*Mast2*	microtubule associated testis specific serine/threonine protein kinase	1417324_at
1.08	*Atp5k*	ATP synthase, H+ transporting, mitochondrial F1F0 complex, subunit e	1422525_at
1.08	*Rps6kb1*	ribosomal protein S6 kinase, polypeptide 1	1460705_at
1.08	*Ttll1*	tubulin tyrosine ligase-like 1	1426427_at
1.08	*Akt1*	thymoma viral proto-oncogene 1	1425711_a_at
1.08	*Rpl19*	ribosomal protein L19	1416219_at
1.08	*Bms1l*	BMS1 homolog, ribosome assembly protein (yeast)	1447679_s_at
1.08	*Tmem178*	transmembrane protein 178	1429175_at
1.08	*Prr13*	proline rich 13	1423686_a_at
1.08	*Wbp5*	WW domain binding protein 5	1451230_a_at
1.08	*2700060E02Rik*	RIKEN cDNA 2700060E02 gene	1448238_at
1.08	*Cops7a*	COP9 (constitutive photomorphogenic) homolog, subunit 7a (Arabidopsis thaliana)	1429078_a_at
1.08	*Gpsn2*	short coiled-coil protein	1416352_s_at
1.08	*Larp5*	La ribonucleoprotein domain family, member 5	1434597_at
1.07	*Klhdc3*	kelch domain containing 3	1454747_a_at
1.07	*Htatip*	HIV-1 tat interactive protein, homolog (human)	1433980_at
1.07	*Eif4g2*	eukaryotic translation initiation factor 4, gamma 2	1428362_at

1.07	*Rpl31*	ribosomal protein L31	1428212_x_at
1.07	*Dhx15*	DEAH (Asp-Glu-Ala-His) box polypeptide 15	1416145_at
1.07	*Ndst1*	N-deacetylase/N-sulfotransferase (heparan glucosaminyl) 1	1460436_at
1.07	*Secisbp2*	SECIS binding protein 2	1428497_at
1.07	*Slc39a6*	solute carrier family 39 (metal ion transporter), member 6	1424674_at
1.07	*Actr8*	ARP8 actin-related protein 8 homolog (S. cerevisiae)	1423385_at
1.07	*Rab14*	RAB14, member RAS oncogene family	1415686_at
1.07	*D0HXS9928E*	DNA segment, human DXS9928E	1419516_at
1.06	*Kctd20*	potassium channel tetramerisation domain containing 20	1416323_at
1.06	*Stox2*	storkhead box 2	1447624_s_at
1.06	*Chn1*	chimerin (chimaerin) 1	1420545_a_at
1.06	*Acin1*	apoptotic chromatin condensation inducer in the nucleus	1416568_a_at
1.06	*Clns1a*	chloride channel, nucleotide-sensitive, 1A	1436935_x_at
1.06	*Gtf2i*	general transcription factor II I	1425628_a_at
1.05	*Prkrir*	protein-kinase, interferon-inducible double stranded RNA dependent inhibitor, repressor of (P58 repressor)	1426482_at

Electropherograms

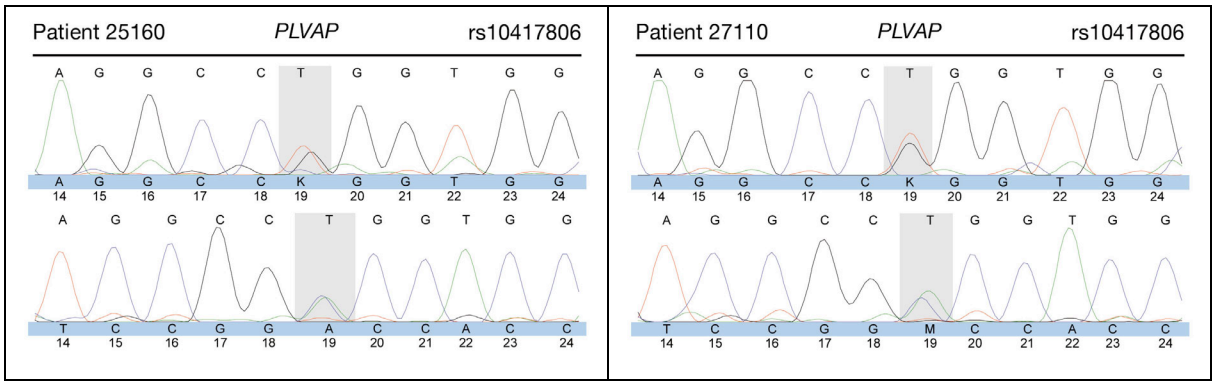

Figure 117 Electropherograms from the *PLVAP* sequence analysis showing SNP rs10417806, which is a heterozygous c.-44T>G substitution in patients 25160 and 27110.

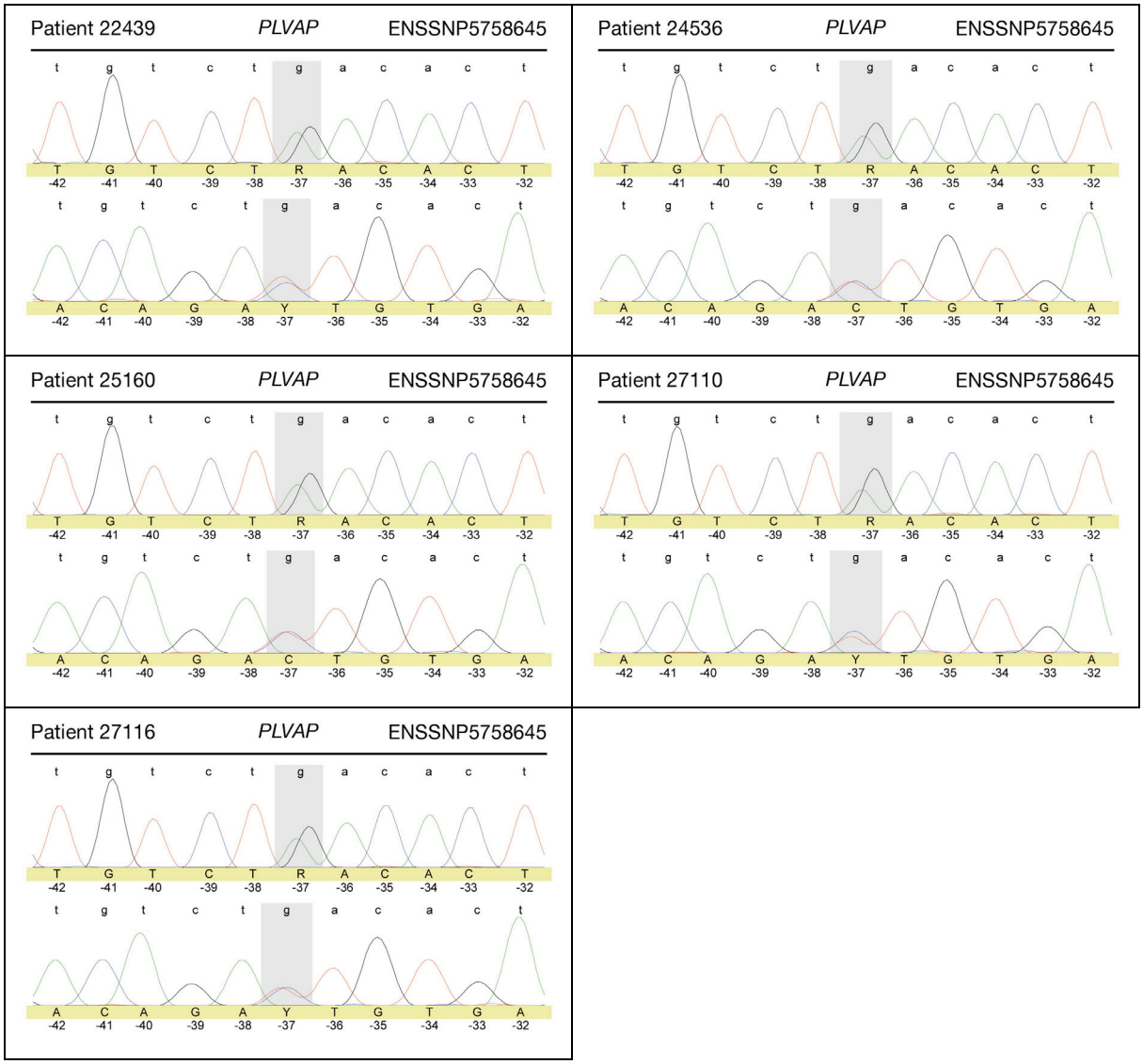

Figure 118 Electropherograms from the *PLVAP* sequence analysis showing SNP ENSSNP5758645. Patients 22439, 24536, 25160, 27110, and 27116 are heterozygous for the c.1322-37G>A exchange.

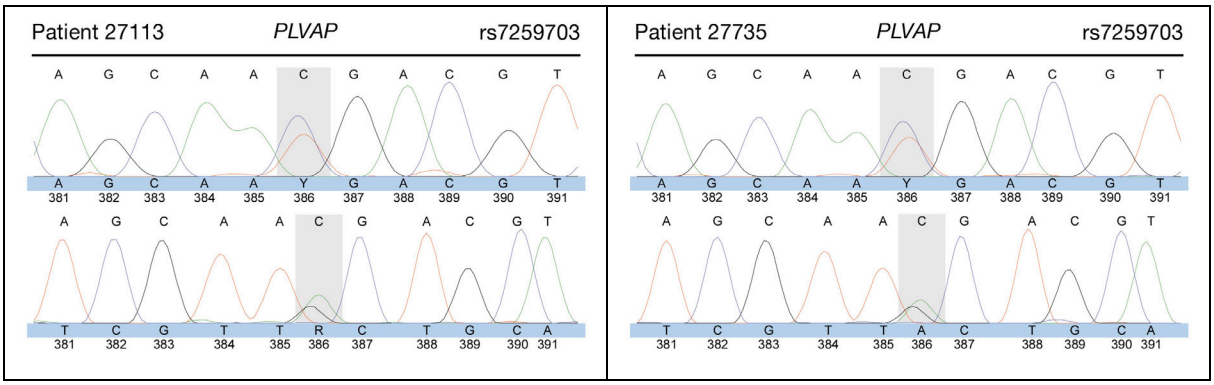

Figure 119 Electropherogram of the rs7259703 SNP located in the 3'-UTR of *PLVAP*. Patients 27113 and 27735 were found to have this c.*329C>T substitution heterozygously.

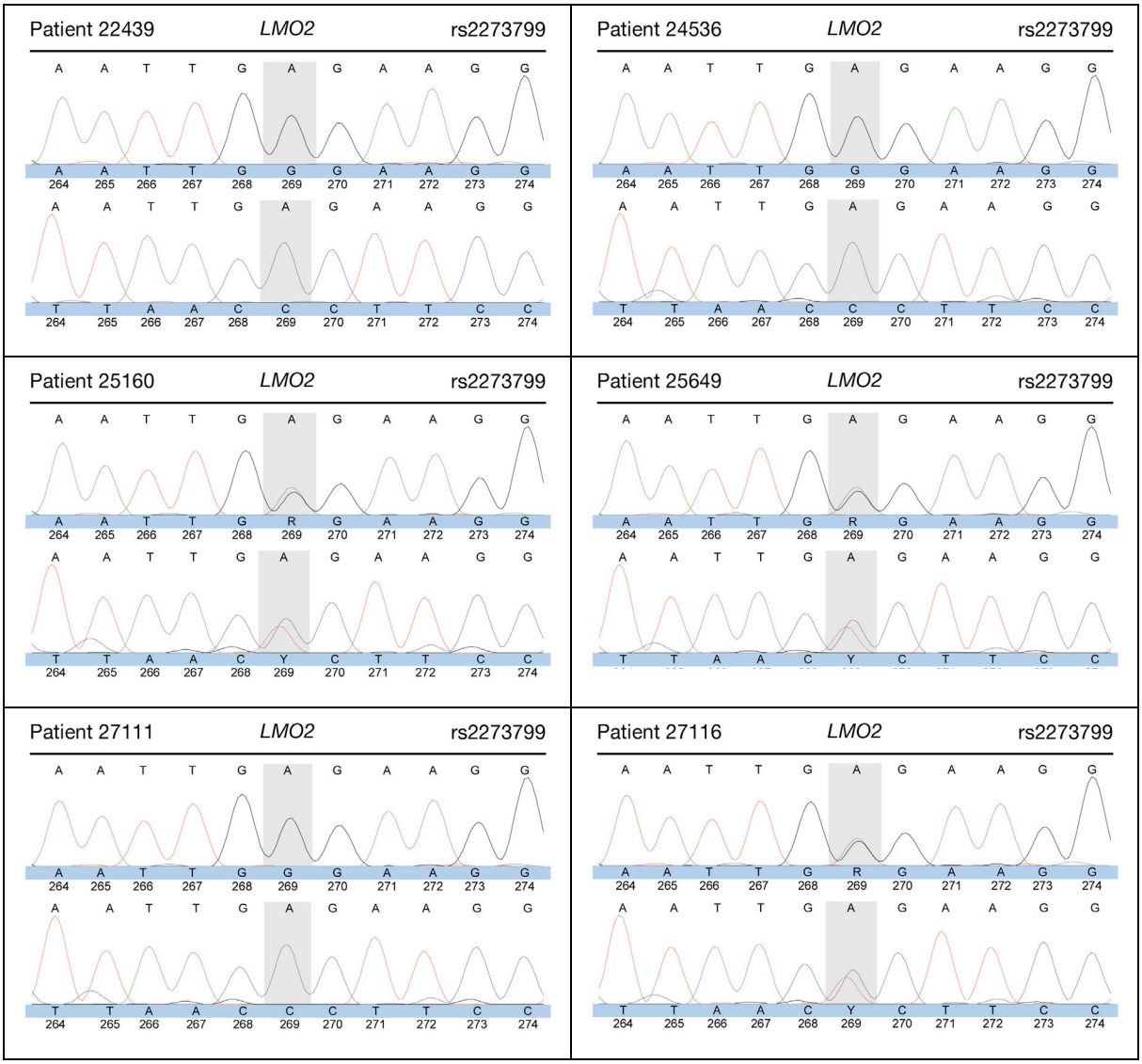

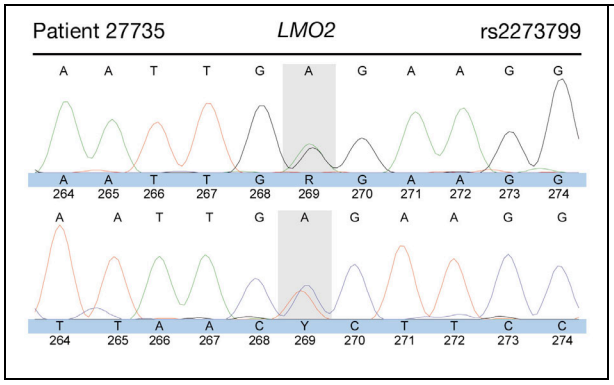

Figure 120 Electropherograms from the *LMO2* sequence analysis showing SNP rs2273799. Patients 25160, 25649, 27116, and 27735 are heterozygous, patient 22439, 24536 and 27111 are homozygous for the c.-796A>G exchange.

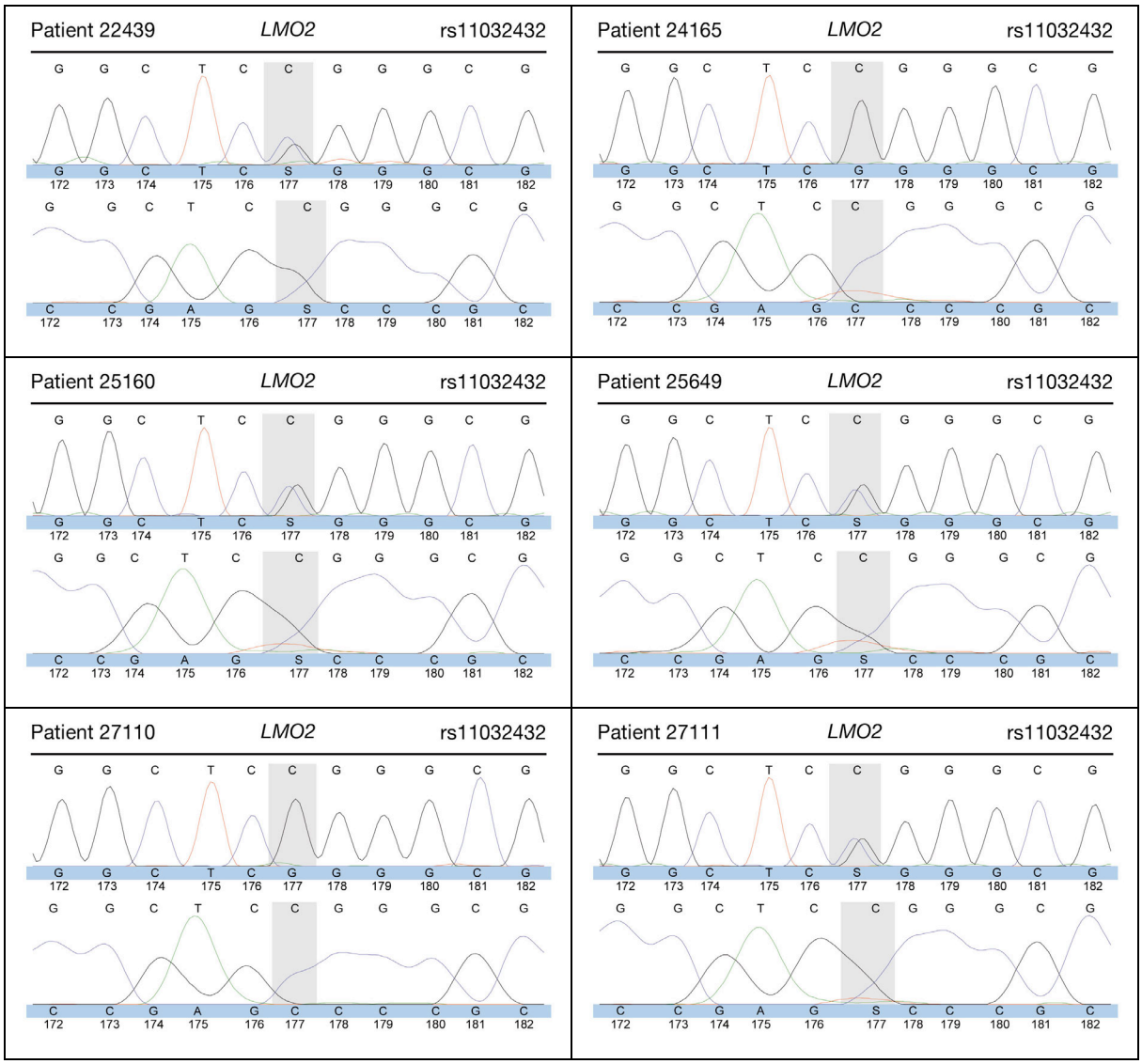

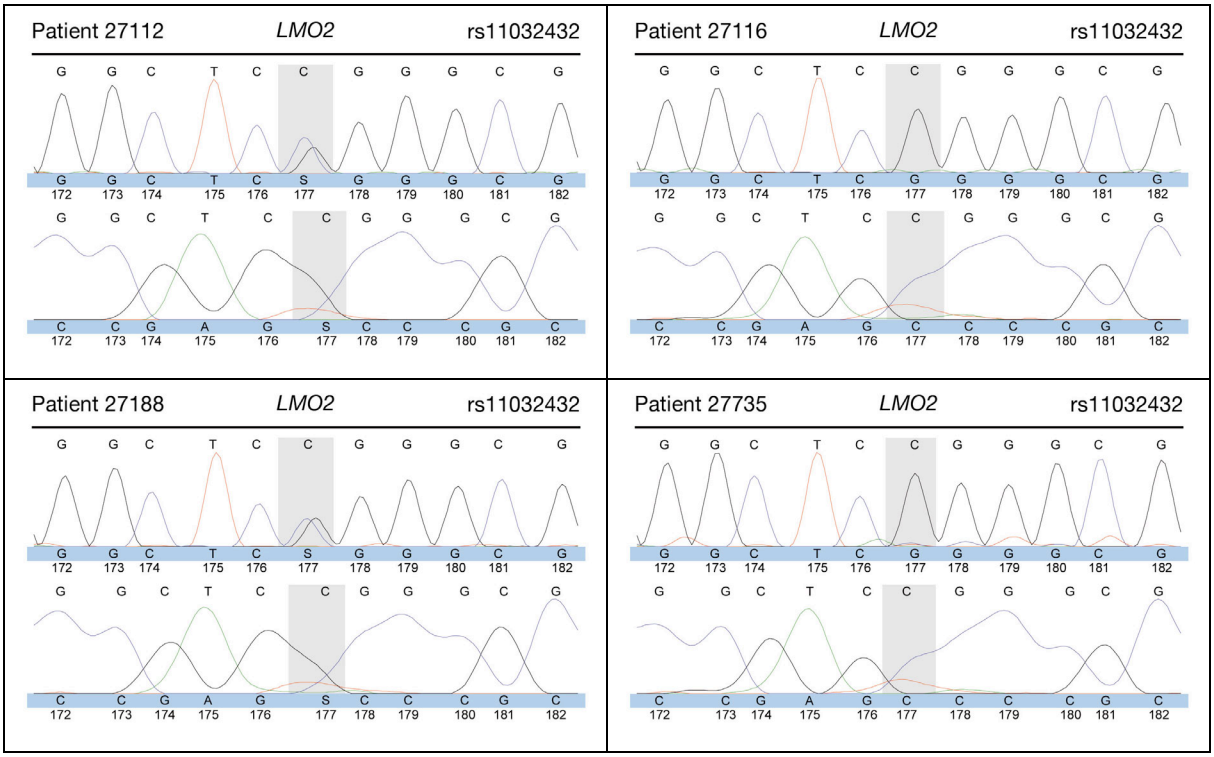

Figure 121 Electropherograms showing SNP rs11032432 in the *LMO2* gene. Patients 22439, 25160, 25649, 27111, 27112, and 27188 are heterozygous for the c.-425C>G substitution, patients 24165, 27110, 27116, and 27735 are homozygous.

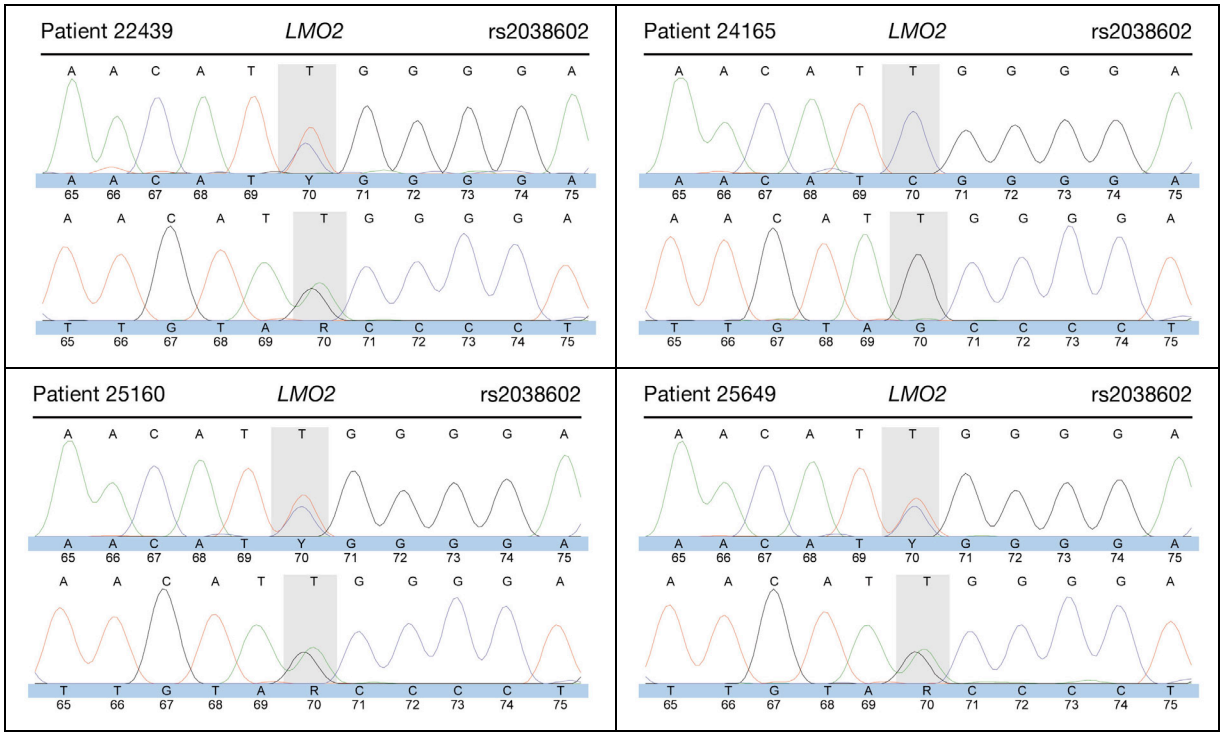

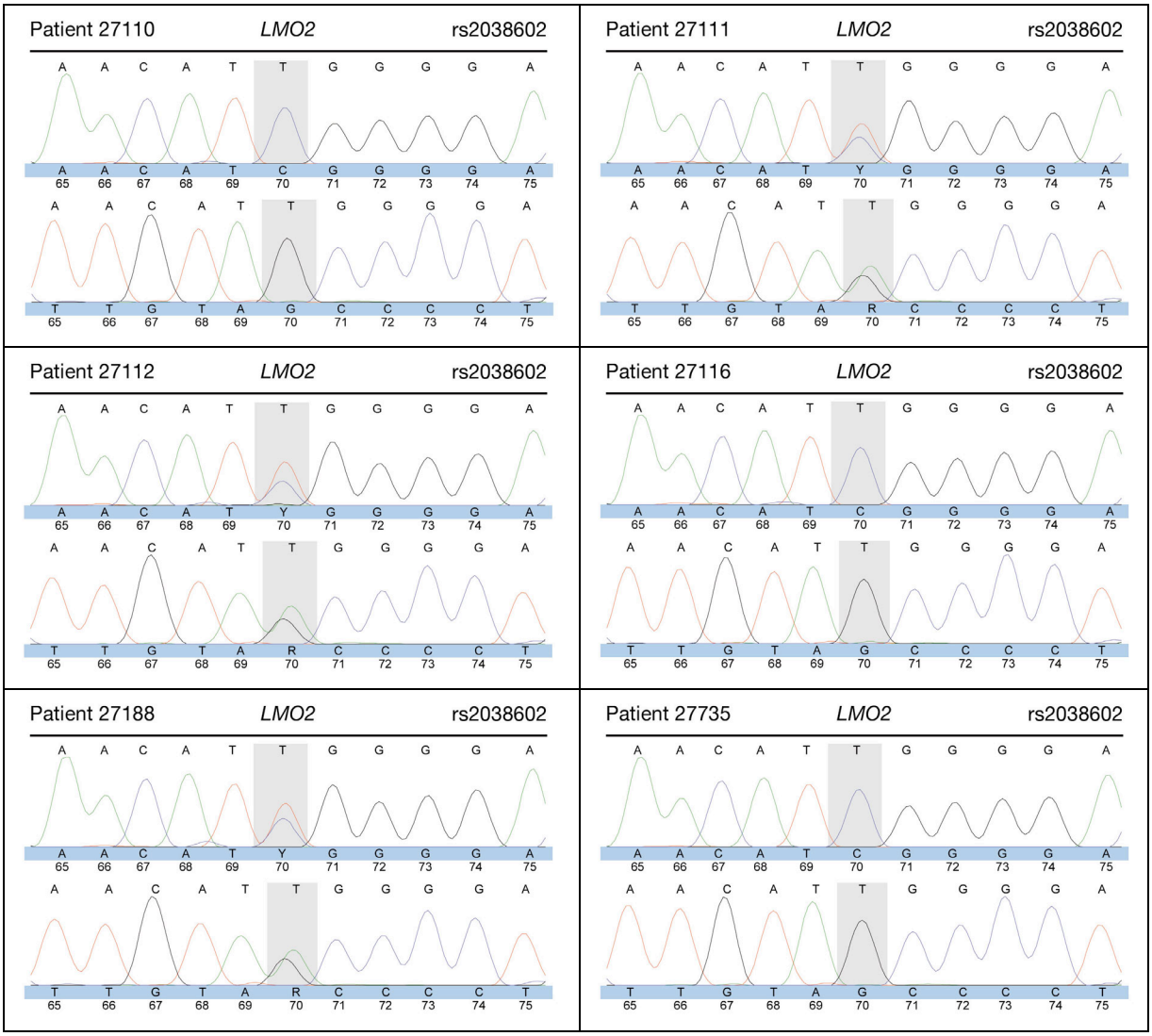

Figure 122 Electropherograms from the *LMO2* sequence analysis showing SNP rs2038602. Six patients are heterozygous for the c.111T>C (p.I37I) substitution (22439, 25160, 25659, 27111, 27112, 27188), four patients are homozygous (24165, 27110, 27116, 27735).

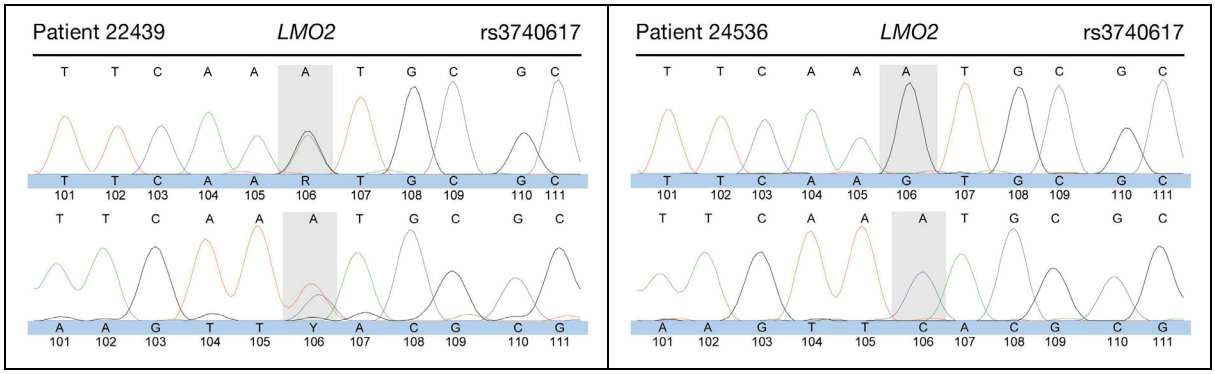

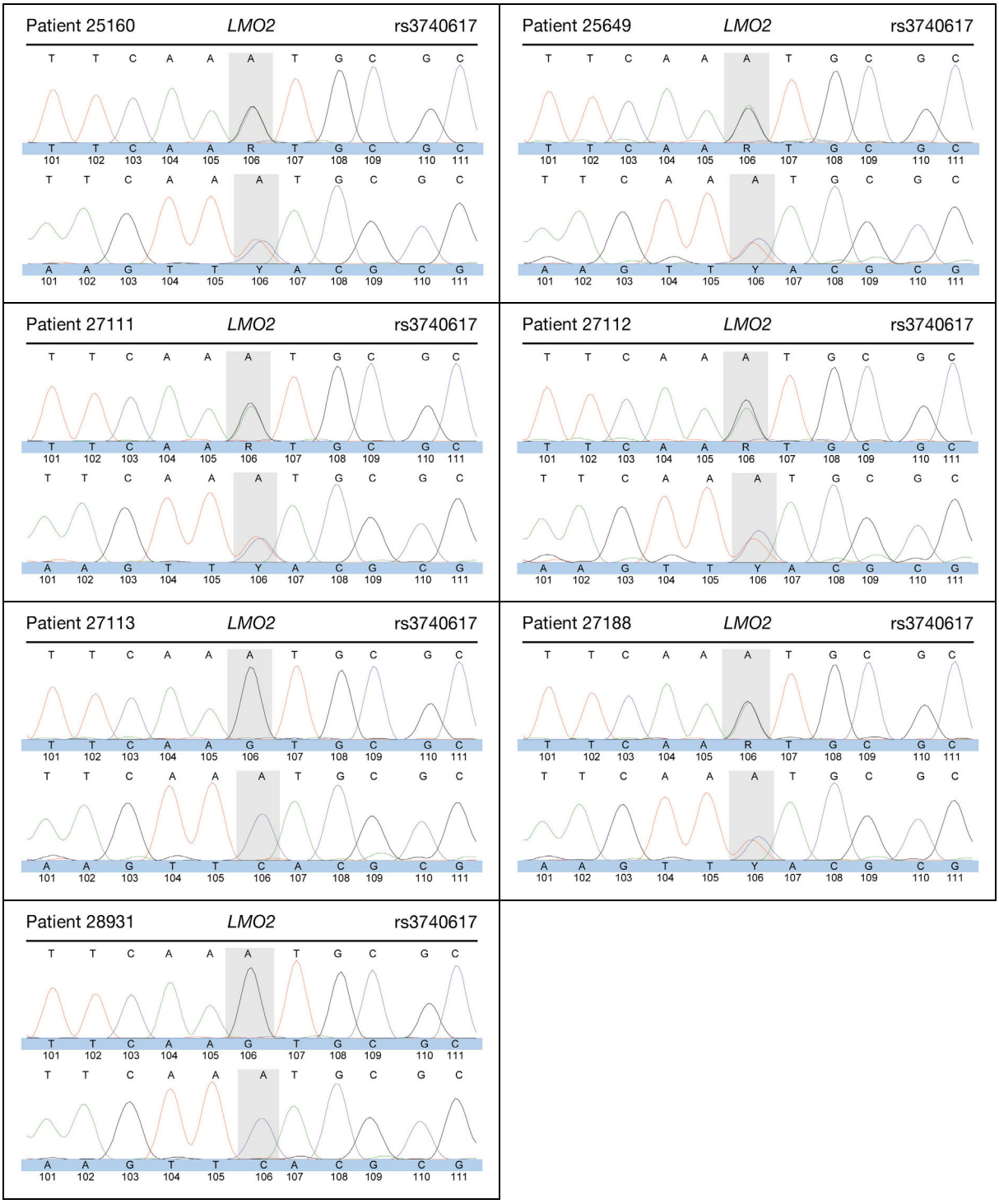

Figure 123 *LMO2* electropherograms revealed patients 22439, 25160, 25649, 27111, 27112, and 27188 harbor the SNP rs3740617 in a heterozygous fashion, patients 24536, 27113, and 28931 are homozygous gor this c.363A>G (p.K121K) variation.

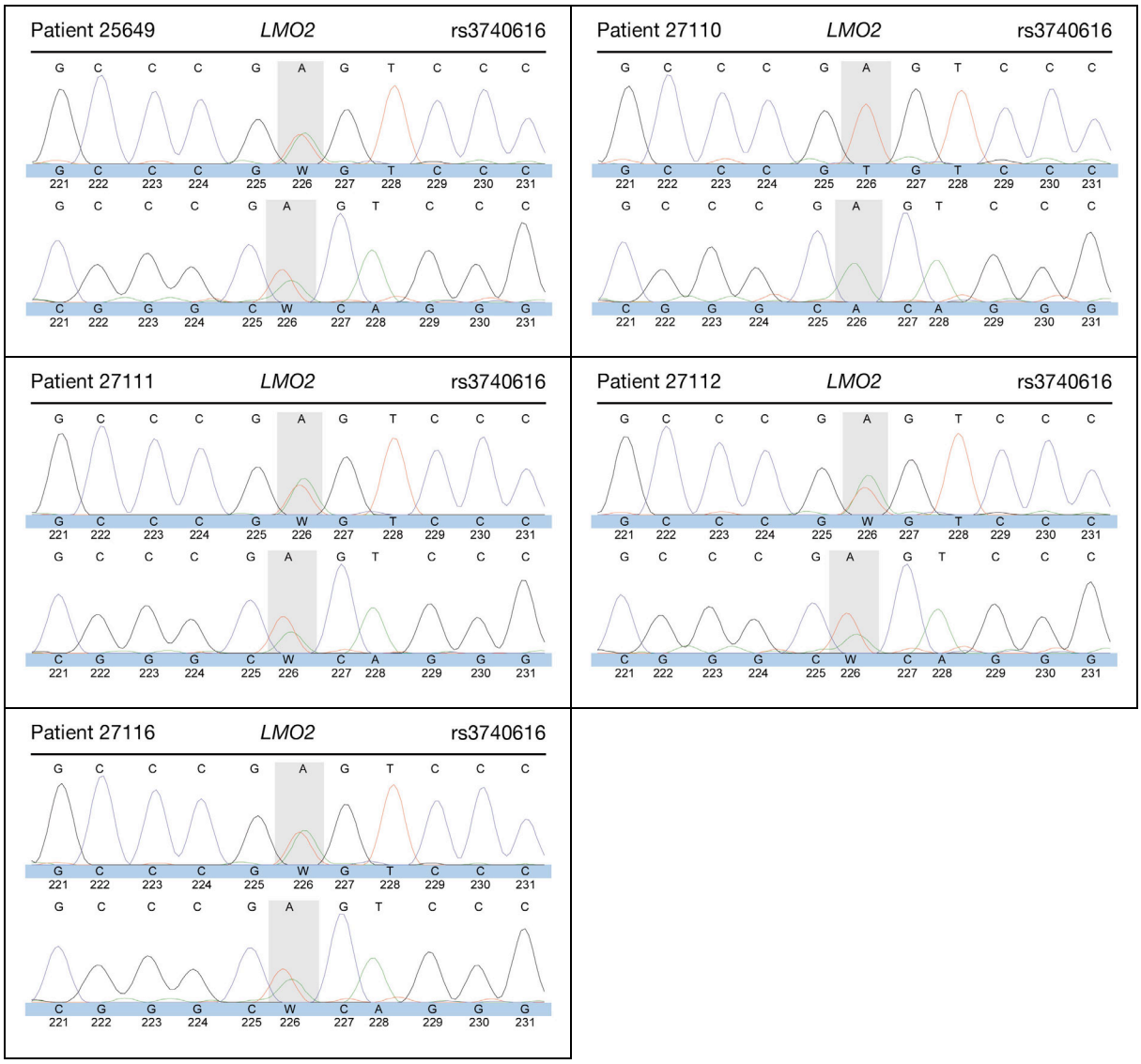

Figure 124 Electropherograms from the *LMO2* sequence analysis showed heterozygous occurence of SNP rs3740616 in patients 25649, 27111, 27112, and 27116, while patient 27110 is homozygous for the c.*483A>T substitution.

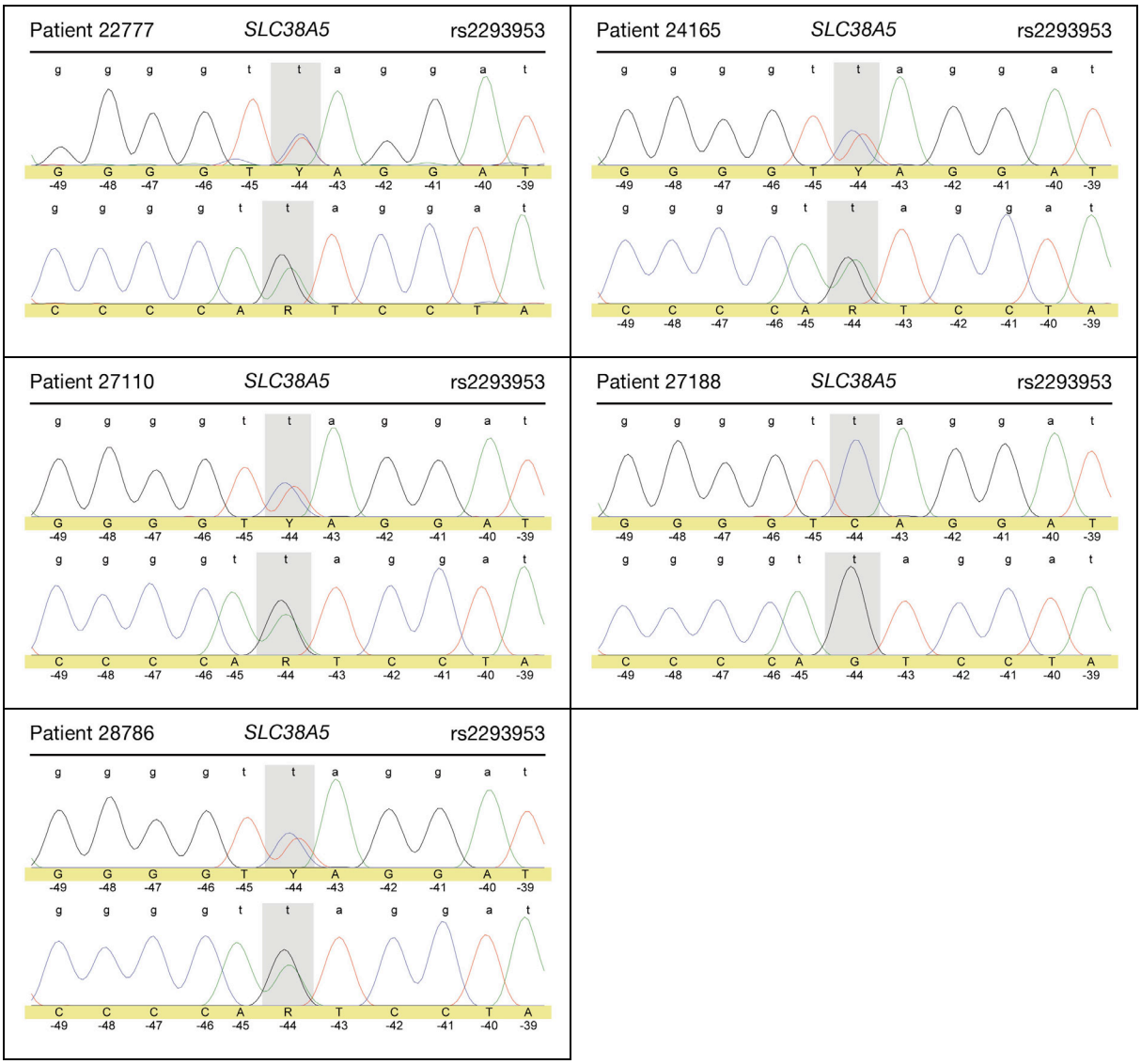

Figure 125 Electropherograms from the *SLC38A5* sequence analysis showing SNP rs2293953. Patients 22777, 24165, 27110, and 28786 are heterozygous, patient 27188 is hemizygous for the c.-44T>C exchange.

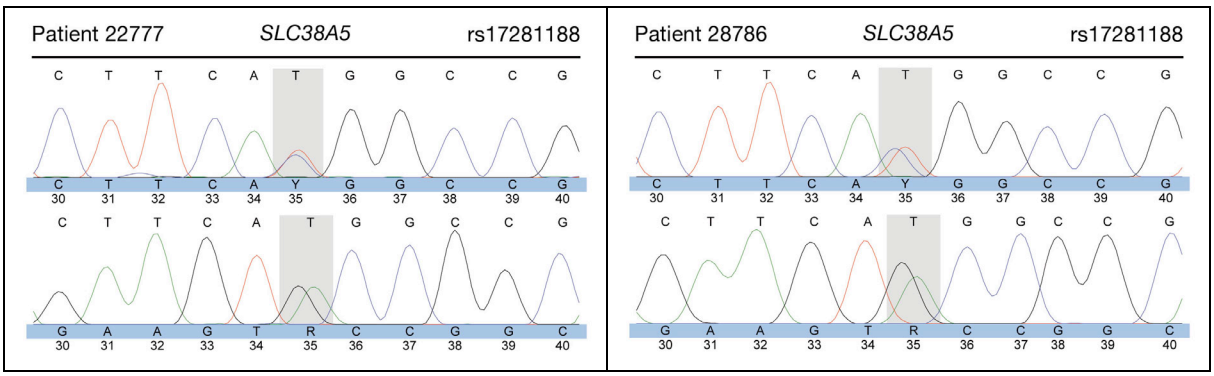

Figure 126 Electropherograms from the *SLC38A5* sequence analysis showing SNP rs17281188. Patients 22777 and 28786 are heterozygous for the c.1352T>C exchange. Numbers indicate position in exon 16.

Curriculum vitae

Name:	Nikolaus Fritz Schäfer
Date of birth:	April 27th, 1977
Place of birth:	Munich, Germany
Citizenship:	German

Education

Dr. sc. nat.	PhD student at the Institute of Medical Genetics, University of Zurich, and the Center for Neuroscience, University / ETH Zurich, Switzerland. Title of the PhD thesis: *„Norrin signaling in Norrie disease and allelic disorders"*	07/2005 - to date
Dipl.-Biol.	Study of biology at the University of Düsseldorf, Germany, and the University of Jena, Germany. Title of the diploma thesis: *„Isolation of Eph-Genes from the oriental fire-bellied toad Bombina orientalis"*	09/1997 - 11/2004
Abitur	Dietrich-Bonhoeffer-Gymnasium and Geschwister-Scholl-Gymnasium, Ratingen, Germany	08/1987 - 07/1996

Working Experience

Sales representative, Gravis Computers, Munich	04/2005 - 05/2005
Scientific associate at the Institute of Zoology and Animal Physiology, University of Jena, Germany	09/2002 - 11/2004
Emergency Medical Technician at Malteser Hilfsdienst, Ratingen, Germany	09/1996 - 10/1997

Publications

Schäfer, N., Luhmann, U., Feil, S., Berger, W. (2009). *Differential gene expression in Ndph-knockout mice in retinal development.* Investigative Ophthalmology & Visual Science, 50 (2), 906-16.	2009
Luhmann, U., Neidhardt, J., Kloeckener-Gruissem, B., **Schäfer, N.**, Glaus, E., Feil, S., Berger, W. (2008). *Vascular changes in the cerebellum of Norrin/Ndph knockout mice correlate with high expression of Norrin and Frizzled-4.* The European Journal of Neuroscience, 27 (10), 2619-28.	2008

Conferences / Scientific Meetings

Talks:

Swiss Eye Research Meeting, Biel, Switzerland 2009

„Genetic analyses of exudative vitreoretinopathies“ - Award for best presentation of a junior researcher

ZNZ Symposium, Zürich, Switzerland (short talk/Data-Blitz) 2007

„Gene expression profiling in Norrin deficient mice”

Swiss Eye Research Meeting, Brunnen, Switzerland 2007

„Gene expression in Norrin deficient mice - a model for vaso-proliferative human eye diseases“

PhD Retreat of the Center of Neuroscience (ZNZ) Uni/ETH Zürich, Valens, Switzerland 2006

„Norrin signaling in Norrie Disease and allelic disorders“

Poster presentations:

The German Societies for Human Genetics (GfH) Annual Meeting, Aachen, Germany 2009

Schäfer, N., Hänseler, W., Zürcher, J., Feil, S., Kohl, S., Wissinger, B., Poloschek, C., Berger, W. (2009) *„Screening of candidate genes for familial exudative vitreo-retinopathy (FEVR) and related vasoproliferative ocular disorders“*

The Association for Research in Vision and Ophthalmology (ARVO) Annual Meeting, Fort Lauderdale, FL, USA 2008

Schäfer, N., Luhmann, U., Feil, S., Berger, W. (2008) *“Differential Gene Expression in Ndph Knockout Mice in Retinal Development”*

TeleThon Scientific Convention, Salsomaggiore Terme, Italy 2007

Galli-Resta, L., Leone, P., Resta, V., Luhmann, U., **Schäfer, N.**, Berger, W. (2007) *„Neuro-vascular interactions in the developing retina: exploring the cellular etiology of Norrie disease and testing the rationale for experimental therapeutic approaches in animal models“*

ProRetina Research Colloquium, Potsdam, Germany 2006, 2007, 2008

Schäfer, N., Luhmann, U., Feil, S., Berger, W. (2008) *“Plasmalemma vesicle-associated protein (Plvap), a major component of vascular fenestrae, is overexpressed in Norrin deficient mice“*

Schäfer, N., Luhmann, U., Berger, W. (2007) *“Gene expression profiling in Norrin deficient mice”*

Schäfer, N., Mikolasek, B., Luhmann, U., Berger, W. (2006) *„Analysis of Wnt/beta-catenin signaling in the retina of a mouse model for Norrie disease”*

Luhmann, U., Neidhardt, J., Kloeckener-Gruissem, B., **Schäfer, N.**, Glaus, E., Feil, S., Berger, W. (2006) *"Differential expression of the Norrie disease pseudoglioma homolog gene in brain regions and evaluation of vascular changes in Ndph knockout mice"*

ZNZ Symposium, Zürich, Switzerland — 2006, 2007

Schäfer, N., Luhmann, U., Feil, S., Berger, W. (2007) *"New insights on angiogenesis from a mouse model for impaired retinal vascular development"*

Schäfer, N., Luhmann, U., Feil, S., Berger, W. (2006) *"Gene expression profiling in Norrin deficient mice"*